TISSUE STEM CELLS DURING TRAUMA: FROM BASIC BIOLOGY TO TRANSLATIONAL MEDICINE

EDITED BY: Guohui Liu, Guozhi Xiao, Ren Xu, Jiacan Su and Zhidao Xia
PUBLISHED IN: Frontiers in Cell and Developmental Biology and
Frontiers in Genetics

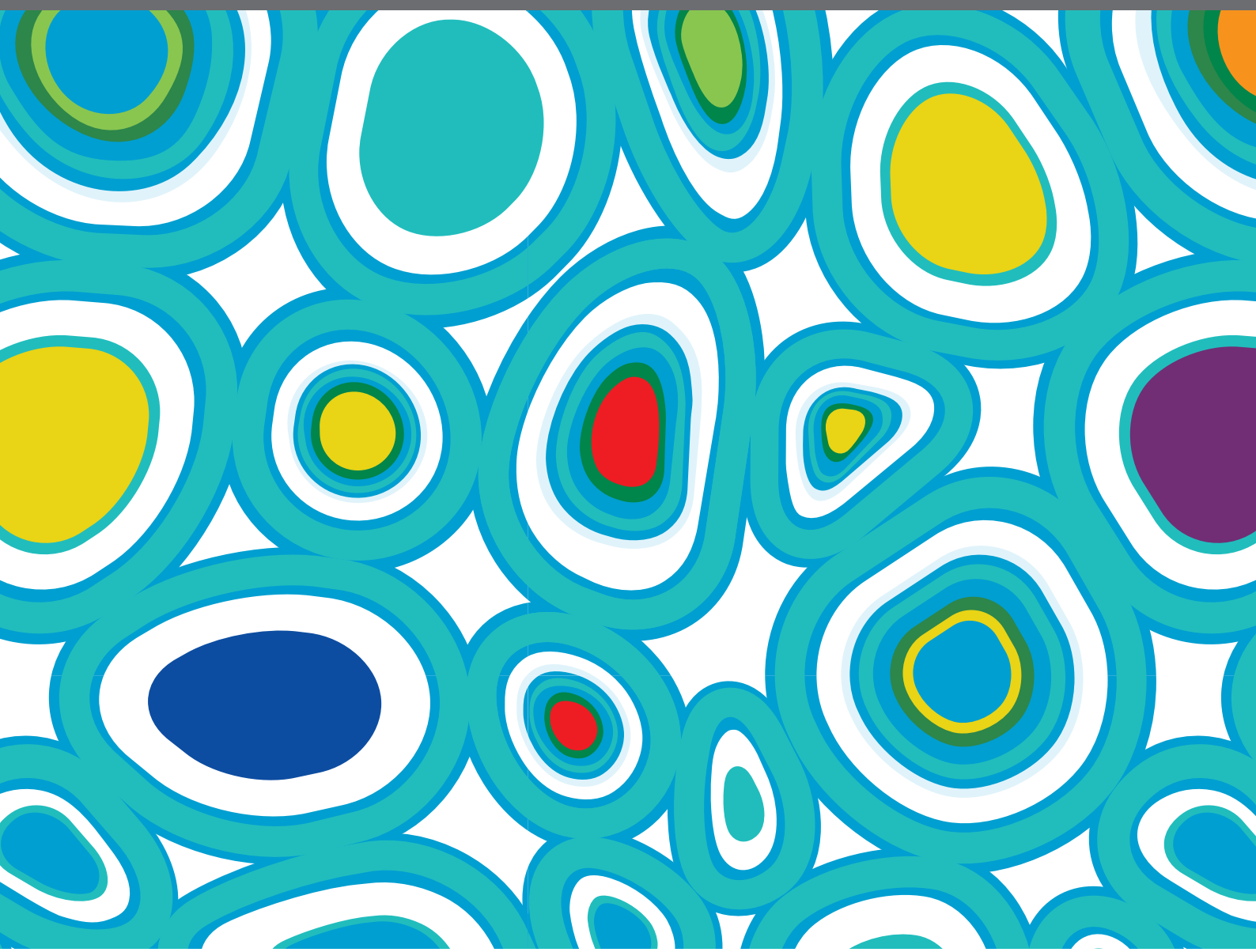

frontiers Research Topics

frontiers

ISSN 1664-8714
ISBN 978-2-88976-385-6
DOI 10.3389/978-2-88976-385-6

About Frontiers

Frontiers is more than just an open-access publisher of scholarly articles: it is a pioneering approach to the world of academia, radically improving the way scholarly research is managed. The grand vision of Frontiers is a world where all people have an equal opportunity to seek, share and generate knowledge. Frontiers provides immediate and permanent online open access to all its publications, but this alone is not enough to realize our grand goals.

Frontiers Journal Series

The Frontiers Journal Series is a multi-tier and interdisciplinary set of open-access, online journals, promising a paradigm shift from the current review, selection and dissemination processes in academic publishing. All Frontiers journals are driven by researchers for researchers; therefore, they constitute a service to the scholarly community. At the same time, the Frontiers Journal Series operates on a revolutionary invention, the tiered publishing system, initially addressing specific communities of scholars, and gradually climbing up to broader public understanding, thus serving the interests of the lay society, too.

Dedication to Quality

Each Frontiers article is a landmark of the highest quality, thanks to genuinely collaborative interactions between authors and review editors, who include some of the world's best academicians. Research must be certified by peers before entering a stream of knowledge that may eventually reach the public - and shape society; therefore, Frontiers only applies the most rigorous and unbiased reviews.
Frontiers revolutionizes research publishing by freely delivering the most outstanding research, evaluated with no bias from both the academic and social point of view. By applying the most advanced information technologies, Frontiers is catapulting scholarly publishing into a new generation.

What are Frontiers Research Topics?

Frontiers Research Topics are very popular trademarks of the Frontiers Journals Series: they are collections of at least ten articles, all centered on a particular subject. With their unique mix of varied contributions from Original Research to Review Articles, Frontiers Research Topics unify the most influential researchers, the latest key findings and historical advances in a hot research area! Find out more on how to host your own Frontiers Research Topic or contribute to one as an author by contacting the Frontiers Editorial Office: frontiersin.org/about/contact

TISSUE STEM CELLS DURING TRAUMA: FROM BASIC BIOLOGY TO TRANSLATIONAL MEDICINE

Topic Editors:
Guohui Liu, Huazhong University of Science and Technology, China
Guozhi Xiao, Southern University of Science and Technology, China
Ren Xu, Xiamen University, China
Jiacan Su, Second Military Medical University, China
Zhidao Xia, Swansea University, United Kingdom

Citation: Liu, G., Xiao, G., Xu, R., Su, J., Xia, Z., eds. (2022). Tissue Stem Cells During Trauma: From Basic Biology to Translational Medicine. Lausanne: Frontiers Media SA. doi: 10.3389/978-2-88976-385-6

Table of Contents

frontiers | Frontiers in Cell and Developmental Biology

EDITORIAL
published: 26 May 2022
doi: 10.3389/fcell.2022.914582

Editorial: Tissue Stem Cells During Trauma: From Basic Biology to Translational Medicine

Guohui Liu[1]*, *Guozhi Xiao*[2]*, *Jiacan Su*[3]*, *Ren Xu*[4]* and *Zhidao Xia*[5]*

[1]Department of Orthopedics, Union Hospital, Tongji Medical College, Huazhong University of Science and Technology, Wuhan, China, [2]Guangdong Provincial Key Laboratory of Cell Microenvironment and Disease Research, Shenzhen Key Laboratory of Cell Microenvironment, Department of Biochemistry, School of Medicine, Southern University of Science and Technology, Shenzhen, China, [3]Department of Orthopedics Trauma, Shanghai Changhai Hospital, Second Military Medical University, Shanghai, China, [4]State Key Laboratory of Cellular Stress Biology, School of Medicine, Xiamen University, Xiamen, China, [5]Institute of Life Science, College of Medicine, Swansea University, Swansea, United Kingdom

OPEN ACCESS

Edited by:
Atsushi Asakura,
University of Minnesota Twin Cities,
United States

Reviewed by:
Marco Tatullo,
University of Bari Medical School, Italy
Pradyumna Kumar Mishra,
ICMR-National Institute for Research in Environmental Health, India

***Correspondence:**
Guohui Liu
liuguohui@hust.edu.cn
Guozhi Xiao
xiaogz@sustech.edu.cn
Jiacan Su
drsujiacan@163.com
Ren Xu
xuren526@xmu.edu.cn
Zhidao Xia
z.xia@swansea.ac.uk

Specialty section:
This article was submitted to Stem Cell Research, a section of the journal Frontiers in Cell and Developmental Biology

Received: 07 April 2022
Accepted: 11 May 2022
Published: 26 May 2022

Citation:
Liu G, Xiao G, Su J, Xu R and Xia Z (2022) Editorial: Tissue Stem Cells During Trauma: From Basic Biology to Translational Medicine. Front. Cell Dev. Biol. 10:914582. doi: 10.3389/fcell.2022.914582

Keywords: stem cells, translational medicine, osteoporosis, drugs, biophysical stimuli

Editorial on the Research Topic

Tissue Stem Cells During Trauma: From Basic Biology to Translational Medicine

Bone is a metabolically active organ that undergoes regular and ongoing remodeling throughout the lifespan, which is crucial for the maintenance of mineral metabolism and normal skeletal structure (Salhotra et al., 2020). The dynamic balance between bone formation and bone resorption is essential to maintain normal bone homeostasis. It is generally accepted that osteoporosis is attributed to an imbalance between bone formation and resorption during bone reconstruction under certain conditions, such as senescence, estrogen deficiency and use of glucocorticoid, whereby the rate of bone absorption is greater than that of bone formation, resulting in accelerated bone turnover and rapid bone loss.

Osteogenic differentiation is the key process in bone formation, and the decreased osteogenic differentiation ability of mesenchymal stem cells (MSCs) leads to decreased bone formation, which has been proven to be responsible for multiple bone disorders, including osteonecrosis of the femoral head and osteoporosis. Multiple clinical trials and animal experiments have demonstrated the beneficial effects of MSCs in preventing bone loss (Wang et al., 2021). Thus, MSCs may provide a therapeutic approach for patients suffering from osteoporosis, potentially contributing to promoting osteogenic differentiation, enhancing bone formation, and influencing the progression of bone remodeling (Jiang et al., 2021). However, current available therapies have some side effects, including muscle cramps, increased serum or urine calcium, etc, which may lead to decreased treatment compliance. Therefore, the continuous search for novel, effective drugs with low side effects has become a commitment to humanity.

Lin et al. found that polydatin (POL) may have a promising therapeutic effect in osteoporosis by bioinformatic analyses, and POL treatment exhibited an increase in the ALP-positive area, the alizarin red-positive area and levels of osteogenic gens, including collagen type I alpha 1 (COL1A1), alkaline phospatase (ALP), osteocalcin (OCN) and Runx2, through MAPK signaling pathway *in vitro* Lin et al., 2021 Another studies supplemented that POL could improve osteogenic differentiation of MSCs potentially via BMP2-Wnt/β-catenin signaling pathway (Shen et al., 2020), Nrf2 signaling (Chen et al., 2016) and regulating osteoprotegerin (OPG) and RANKL levels *in vivo* and *in vitro* (Zhou et al., 2016). These results demonstrated that POL treatment could increase bone mass *via* activation of multiple signaling molecules, but the side effects and the strength of the effect are unknown compared the current available drugs. This can only be clarified by a large randomized trial.

Hesperidin, a flavanone glycoside highly abundant in citrus fruits, has exhibited a protective role in osteoporosis through enhancing osteogenic differentiation and inhibition of osteoclastogenesis (Liu et al., 2019; Miguez et al., 2021; Zhang et al., 2021), but little is known about the role of hesperidin in the dexamethasone-induced osteoporosis. Zhang et al. indicated that hesperidin showed enhanced osteogenic differentiation and partially reversed dexamethasone-induced inhibition of osteogenic differentiation by p53 signaling pathway *in vitro*, suggesting the compound may be a promising candidate against dexamethasone-induced osteoporosis (Zhang et al., 2021). However, hesperidin in combination with calcium supplementation appears to have better effect in preserving bone in postmenopausal women compared with hesperidin (Martin et al., 2016). Given that hesperidin was widely found in vegetables and fruits, the study by Zhang et al. may provide evidence to support that food therapy could treatment or prevent dexamethasone-induced osteoporosis to some extent, but the effective dose of the compound is needed to be identify.

Xie et al. demonstrated that SHIP1 activator AQX-1125 not only simulated differentiation of bone mesenchymal stem cells (BMSCs) into osteoblasts and osteoblast matrix mineralization, but inhibited osteoclast formation and function in a dose-dependent manner, and subsequently reversed estrogen deficiency-induced bone loss. AQX-1125 is first-in-class, oral SHIP1 activator in clinic, and a clinical trial regarding the effect of the SHIP1 activator AQX-1125 reported that it was well tolerated and low side effect (Nickel et al., 2016). Therefore, AQX-1125, maybe have some unique advantages compared with current available therapies, such as few side effects, easily accessibility and dual effects between osteogenesis and osteoclastogensis. The short-term efficacy of AQX-1125 may be excellent in rescuing bone loss, but the long-term administration may lead to low bone turnover, resulting in high bone strength but increased bone fragility.

A combination of biophysical stimuli and drugs therapy may be a future direction in treatment osteoporosis. Given the inefficiency of current biomaterials and bioactive molecules, biophysical stimulation for MSCs osteogenesis, including internal structural stimulation, external mechanical stimulation and electromagnetic stimulation, showed promising potential to prevent and treat osteoporosis, although specific osteoinductive mechanisms remains unclear (Hao et al.; Zhang et al., 2021). Furthermore, application of biophysical stimuli might augment the therapeutic benefit and reduce drugs dose, subsequently reducing the side effects. Therefore, it appears to be an ideal adjunct on top of antiosteoporosis drugs.

In summary, the Research Topic indicated that the efficacy of these therapies and its mechanism against osteoporosis, highlighting the fact that strategies for enhanced osteogenic differentiation of MSCs in osteoporosis are effective. As researchers come round to the understanding that bone is a mechanosensitive tissue, biophysical stimulations offer some unique advantages for enhancing osteogenic differentiation of MSCs. Furthermore, drugs therapy in combination with biophysical stimuli may be as a first line therapy in the future. We predict that this Research Topic will continue to rapidly evolve and attract more researches to develop more antiosteoporosis therapies with few side effects.

AUTHOR CONTRIBUTIONS

All authors listed have made a substantial, direct, and intellectual contribution to the work and approved it for publication.

FUNDING

This work was supported by the National Science Foundation of China (Nos 82002313 and 82072444), The National Key Research & Development Program of China (Nos 2018YFC2001502 and 2018YFB1105705), The Hubei Province Key Laboratory of Oral and Maxillofacial Development and Regeneration (No. 2020kqhm008), and the Wuhan Union Hospital "Pharmaceutical Technology nursing" special fund (No. 2019xhyn021).

ACKNOWLEDGMENTS

We thank all the authors, reviewers, and editors for their contributions to the Research Topic.

REFERENCES

Chen, M., Hou, Y., and Lin, D. (2016). Polydatin Protects Bone Marrow Stem Cells against Oxidative Injury: Involvement of Nrf 2/ARE Pathways. *Stem Cells Int.* 2016, 9394150. doi:10.1155/2016/9394150

Jiang, Y., Zhang, P., Zhang, X., Lv, L., and Zhou, Y. (2021). Advances in Mesenchymal Stem Cell Transplantation for the Treatment of Osteoporosis. *Cell. Prolif.* 54, e12956. doi:10.1111/cpr.12956

Liu, H., Dong, Y., Gao, Y., Zhao, L., Cai, C., Qi, D., et al. (2019). Hesperetin Suppresses RANKL-induced Osteoclastogenesis and Ameliorates Lipopolysaccharide-induced Bone Loss. *J. Cell. Physiology* 234, 11009–11022. doi:10.1002/jcp.27924

Martin, B. R., McCabe, G. P., McCabe, L., Jackson, G. S., Horcajada, M. N., Offord-Cavin, E., et al. (2016). Effect of Hesperidin with and without a Calcium (Calcilock) Supplement on Bone Health in Postmenopausal Women. *J. Clin. Endocrinol. Metabolism* 101, 923–927. doi:10.1210/jc.2015-3767

Miguez, P. A., Tuin, S. A., Robinson, A. G., Belcher, J., Jongwattanapisan, P., Perley, K., et al. (2021). Hesperidin Promotes Osteogenesis and Modulates Collagen Matrix Organization and Mineralization *In Vitro* and *In Vivo*. *Int. J. Mol. Sci.* 22, 3223. doi:10.3390/ijms22063223

Nickel, J. C., Egerdie, B., Davis, E., Evans, R., Mackenzie, L., and Shrewsbury, S. B. (2016). A Phase II Study of the Efficacy and Safety of the Novel Oral SHIP1 Activator AQX-1125 in Subjects with Moderate to Severe Interstitial Cystitis/Bladder Pain Syndrome. *J. Urology* 196, 747–754. doi:10.1016/j.juro.2016.03.003

Salhotra, A., Shah, H. N., Levi, B., and Longaker, M. T. (2020). Mechanisms of Bone Development and Repair. *Nat. Rev. Mol. Cell. Biol.* 21, 696–711. doi:10.1038/s41580-020-00279-w

Shen, Y.-S., Chen, X.-J., Wuri, S.-N., Yang, F., Pang, F.-X., Xu, L.-L., et al. (2020). Polydatin Improves Osteogenic Differentiation of Human Bone Mesenchymal Stem Cells by Stimulating TAZ Expression via BMP2-Wnt/β-Catenin Signaling Pathway. *Stem Cell. Res. Ther.* 11, 204. doi:10.1186/s13287-020-01705-8

Wang, P., Wang, M., Zhuo, T., Li, Y., Lin, W., Ding, L., et al. (2021). Hydroxysafflor Yellow A Promotes Osteogenesis and Bone Development via Epigenetically Regulating β-catenin and Prevents Ovariectomy-Induced Bone Loss. *Int. J. Biochem. Cell. Biol.* 137, 106033. doi:10.1016/j.biocel.2021.106033

Zhang, Q., Song, X., Chen, X., Jiang, R., Peng, K., Tang, X., et al. (2021). Antiosteoporotic Effect of Hesperidin against Ovariectomy-Induced Osteoporosis in Rats via Reduction of Oxidative Stress and Inflammation. *J. Biochem. Mol. Toxicol.* 35, e22832. doi:10.1002/jbt.22832

Zhou, Q.-L., Qin, R.-Z., Yang, Y.-X., Huang, K.-B., and Yang, X.-W. (2016). Polydatin Possesses Notable Anti-osteoporotic Activity via Regulation of OPG, RANKL and β-catenin. *Mol. Med. Rep.* 14, 1865–1869. doi:10.3892/mmr.2016.5432

Conflict of Interest: The authors declare that the research was conducted in the absence of any commercial or financial relationships that could be construed as a potential conflict of interest.

Publisher's Note: All claims expressed in this article are solely those of the authors and do not necessarily represent those of their affiliated organizations, or those of the publisher, the editors and the reviewers. Any product that may be evaluated in this article, or claim that may be made by its manufacturer, is not guaranteed or endorsed by the publisher.

frontiers in Cell and Developmental Biology

ORIGINAL RESEARCH
published: 29 September 2021
doi: 10.3389/fcell.2021.730362

Polydatin Ameliorates Osteoporosis via Suppression of the Mitogen-Activated Protein Kinase Signaling Pathway

Ze Lin[1,2†], Yuan Xiong[1,2†], Yiqiang Hu[1,2†], Lang Chen[1,2], Adriana C. Panayi[3], Hang Xue[1,2], Wu Zhou[1,2], Chenchen Yan[1,2], Liangcong Hu[1,2], Xudong Xie[1,2], Yun Sun[1], Bobin Mi[1,2]* and Guohui Liu[1,2]**

[1] Department of Orthopedics, Union Hospital, Tongji Medical College, Huazhong University of Science and Technology, Wuhan, China, [2] Hubei Province Key Laboratory of Oral and Maxillofacial Development and Regeneration, Wuhan, China, [3] Division of Plastic Surgery, Brigham and Women's Hospital, Harvard Medical School, Boston, MA, United States

OPEN ACCESS

Edited by:
Ming Li,
Osaka University, Japan

Reviewed by:
Adel Abdel Moneim,
Beni-Suef University, Egypt
Qiaobing Huang,
Southern Medical University, China

***Correspondence:**
Guohui Liu
liuguohui@hust.edu.cn
Bobin Mi
mibobin@hust.edu.cn
Yun Sun
627224540@qq.com

† These authors have contributed equally to this work and share first authorship

Specialty section:
This article was submitted to Stem Cell Research, a section of the journal Frontiers in Cell and Developmental Biology

Received: 24 June 2021
Accepted: 06 September 2021
Published: 29 September 2021

Citation:
Lin Z, Xiong Y, Hu Y, Chen L, Panayi AC, Xue H, Zhou W, Yan C, Hu L, Xie X, Sun Y, Mi B and Liu G (2021) Polydatin Ameliorates Osteoporosis via Suppression of the Mitogen-Activated Protein Kinase Signaling Pathway. Front. Cell Dev. Biol. 9:730362. doi: 10.3389/fcell.2021.730362

Purpose: Polydatin (POL) is a natural active compound found in *Polygonum multiflorum* with reported anti-oxidant and antiviral effects. With the aging population there has been a stark increase in the prevalence of osteoporosis (OP), rendering it an imposing public health issue. The potential effect of POL as a therapy for OP remains unclear. Therefore, we sought to investigate the therapeutic effect of POL in OP and to elucidate the underlying signaling mechanisms in its regulatory process.

Methods: The POL-targeted genes interaction network was constructed using the Search Tool for Interacting Chemicals (STITCH) database, and the shared Kyoto Encyclopedia of Genes and Genomes (KEGG). Pathways involved in OP and POL-targeted genes were identified. Quantitative real-time PCR (qRT-PCR) and enzyme-linked immunosorbent assay (ELISA) were performed to evaluate the osteogenic genes and the phosphorylation level in pre-osteoblastic cells. In addition, ALP and alizarin red staining was used to test the effect of POL on extracellular matrix mineralization.

Results: Twenty-seven KEGG pathways shared between POL-related genes and OP were identified. *MAPK* signaling was identified as a potential key mechanism. *In vitro* results highlighted a definitive anti-OP effect of POL. The phosphorylation levels of *MAPK* signaling, including *p38α*, *ERK1/2*, and *JNK*, were significantly decreased in this regulatory process.

Conclusion: Our results suggest that POL has a promising therapeutic effect in OP. *MAPK* signaling may be the underlying mechanism in this effect, providing a novel sight in discovering new drugs for OP.

Keywords: MAPK, gene, osteoporosis, polydatin, KEGG pathway

Abbreviations: OP, osteoporosis; POL, polydatin; MAPK, mitogen-activated protein kinase; STITCH, Search Tool for Interacting Chemicals; KEGG, Kyoto Encyclopedia of Genes and Genomes; ELISA, enzyme-linked immunosorbent assay.

INTRODUCTION

Osteoporosis (OP), a condition characterized by thin and brittle bones, compromises bone strength and predisposes bones to fractures, especially the bones in the hip, spine, and wrist (Cummings and Melton, 2002; Compston et al., 2019). The prevalence of OP is on the rise, owing to the aging population, with millions of people worldwide either already having OP or being at high risk due to low bone mass (Black and Rosen, 2016; Compston et al., 2019). Studies have suggested that approximately one in two women and up to one in four men aged 50 and older will suffer a bone fracture due to OP (Sambrook and Cooper, 2006; Rachner et al., 2011; Compston et al., 2019). Although immense strides have been made in drug development, the incidence of OP is growing exponentially (Rachner et al., 2011; Compston et al., 2019). Design and development of effective drugs that can delay the pathological progress of OP have the potential to revolutionize healthcare provision.

Owing to their low toxicity, natural active compounds of a plant origin are attracting attention (Zhu et al., 2018; Suroowan and Mahomoodally, 2019). Polydatin (POL, 3, 4, 5-trihydroxystibene-3-β-mono-D-glucoside), a stilbenoid compound obtained from the root of *Polygonum cuspidatum*, has a long history of use as a Chinese traditional medicine in a wide array of diseases (Chen et al., 2013; Jiang et al., 2013; Huang et al., 2015; Mele et al., 2018). Polydatin (POL) has been reported to enhance the anti-oxidant ability of bone marrow stromal cells (BMSCs) and to induce bone remodeling (Chen et al., 2019). A recent study reported that POL has anti-OP activity in ovariectomized mice (Shen et al., 2020). However, to the best of our knowledge, the mechanism of POL's anti-OP activity remains elusive and requires further investigation.

Bioinformatic analyses have been widely applied in the elucidation of potential molecular mechanisms underlying diseases (Agarwal and Searls, 2009; Zampieri et al., 2017). In the current study, we employ a set of bioinformatic tools to identify the target genes and Kyoto Encyclopedia of Genes and Genomes (KEGG) pathways involved in POL's mechanism of anti-OP activity. Our primary aim was to identify the potential molecular and cellular mechanism of POL in OP. We analyzed the shared KEGG pathways between POL-targeted genes and OP, and performed *in vitro* assays to validate our hypothesis.

MATERIALS AND METHODS

Reagents

Polydatin was purchased from MedChemExpress LLC (NJ, United States), the quantitative real-time PCR (qRT-PCR) kit was purchased from Thermo Fisher Scientific Co. (Boston, MA, United States). The enzyme-linked immunosorbent assay (ELISA) kits were purchased from R&D SYSTEMS Co. (p-p38α and p-ERK1/2, Emeryville, CA, United States), and Shanghai Jianglai Ltd. (p-JNK, Shanghai, China).

Culture of MC3T3-E1 Cells

Murine pre-osteoblasts (MC3T3-E1 cells) were kindly donated by the Shanghai University of Medicine & Health Sciences (Shanghai, China). The medium used for cell culture is α-MEM containing 10% FBS, and 1% penicillin and streptomycin. The cells were grown at 37°C with 5% CO_2 at 95% humidity and were used for up to five passages. To induce a cellular OP model the MC3T3-E1 cells were treated with 100 μM dexamethasone (DXM) for 7 days.

TABLE 1 | mRNA primer sequences.

microRNA or gene names	Primer sequence (5′–3′)
Mmu-Col-1a1-Forward	CTGACTGGAAGAGCGGAGAG
Mmu-Col-1a1-Reverse	CGGCTGAGTAGGGAACACAC
Mmu-ALP-Forward	TGACTACCACTCGGGTGAACC
Mmu-ALP-Reverse	TGATATGCGATGTCCTTGCAG
Mmu-OCN-Forward	TTCTGCTCACTCTGCTGACCC
Mmu-OCN-Reverse	CTGATAGCTCGTCACAAGCAGG
Mmu-Runx2-Forward	CGCCACCACTCACTACCACAC
Mmu-Runx2-Reverse	TGGATTTAATAGCGTGCTGCC
Mmu-GAPDH-Forward	TGAAGGGTGGAGCCAAAAG
Mmu-GAPDH-Reverse	AGTCTTCTGGGTGGCAGTGAT

Quantitative Real-Time PCR Analysis

TRIzol was used for RNA extraction, according to the manufacturer's protocol. cDNA was generated with a one-step Prime Script miRNA cDNA synthesis kit, and amplification of equivalent cDNA amounts was performed by SYBR Premix Ex TaqII. The qPCR analysis was performed by using a Thermal Cycler C-1000 Touch system. The reverse transcription-quantitative polymerase chain reaction messenger RNA quality of each gene was calculated using the $2^{-\Delta\Delta Ct}$ method and normalized to GAPDH. The primer sequences of the genes are displayed in **Table 1**.

Enzyme-Linked Immunosorbent Assay

MC3T3-E1 were incubated serum-free medium for a 48-h period. The concentration of proteins was measured by ELISA. Before the ELISA assay, the number of cells in each culture well was counted to ensure that the cell numbers were same. The concentration of phospho-p38α, phospho-ERK1/2 and phospho-JNK were calculated based on the standard curve.

ALP Staining

An ALP staining was performed by using the color-development kit based on the provided guidance to evaluate ALP staining results. Briefly, MC3T3-E1 cells were fixed in 10% formalin for 15 min after washing the cells twice with PBS. The BCIP/NBT liquid substrate was used to stain cells for 24 h. Absorbance was measured at 405 nm.

Alizarin Red Staining

Cells were grown in six-well plates in a special osteogenic media (#HUXMA-90021, Cyagen, United States) for 21 days to promote osteogenesis. Briefly, cells were washed twice with PBS, followed by fixation in 10% formalin for 15 min. The cells were stained with 0.5% Alizarin-Red solution at room temperature for 15

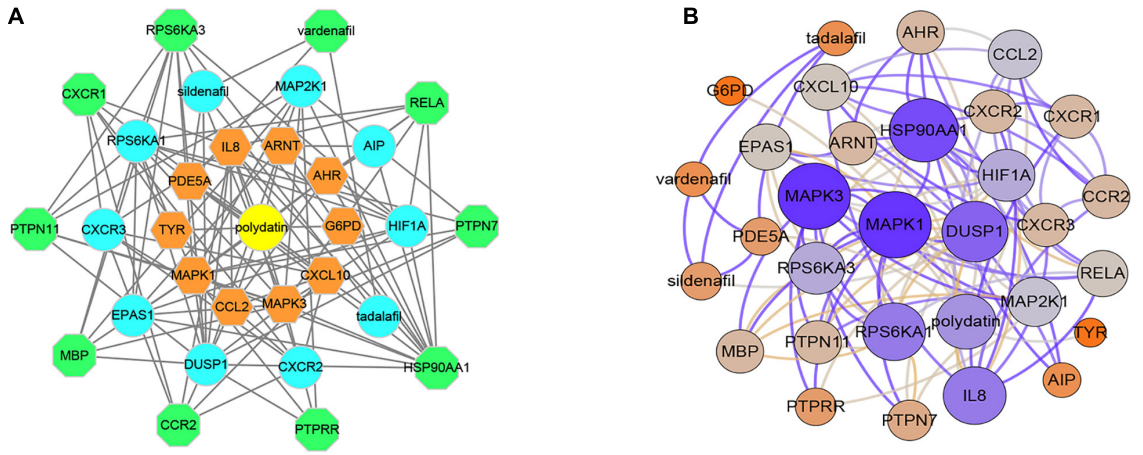

FIGURE 1 | Interaction networks of polydatin-targeted genes. **(A)** Interaction network constructed by Cytoscape. **(B)** Weighted interaction network.

minutes, then rinsed with distilled water for 5 min. A charge-coupled device microscope was used to analyzed red mineralized nodules. Absorbance was measured at 570 nm.

Retrieval of Polydatin-Related Genes and Compounds

The Search Tool for Interacting Chemicals (STITCH) database[1] was used to search for POL-related genes and compounds. STITCH is a database of known and predicted interactions between chemicals and proteins (Szklarczyk et al., 2016). POL-related genes and compounds were obtained using the following settings: the maximum number of interactions in each shell was 10, three shells were retrieved, and the intermediate confidence score was 0.4. The data were imported into Cytoscape 3.8.0 to construct a POL-related gene relationship network and to calculate the degree, betweenness, and closeness of each gene in the network. A weighted network was constructed according to the degree of genes in Cytoscape (Shannon et al., 2003).

Enrichment Analysis of Genes and Kyoto Encyclopedia of Genes and Genomes Pathways

The database for Annotation, Visualization, and Integrated Discovery (DAVID) database was used to search POL-related KEGG pathway. The DAVID knowledge base contains millions of identifiers from thousands of species allowing agglomeration of a diverse array of functional and sequence annotation, greatly enriching the level of biological information available for each gene (Huang et al., 2009; Jiao et al., 2012).

Shared Kyoto Encyclopedia of Genes and Genomes Pathways

The miRwalk2.0 database was used to search for KEGG pathway related to OP (Dweep and Gretz, 2015). POL targeted gene related KEGG pathways were also identified ($q \leq 0.05$). The shared KEGG pathways were established with a Venn Diagram (Venny 2.1[2]).

Identification of the Hub Genes

Gplot, an R package that visually combines expression data with functional analysis, was used to present the enrichment information of the top five KEGG pathways (Walter et al., 2015). The genes included in the top five KEGG pathways were considered hub genes. The specific information and chromosomal position of all genes in the network were presented using the circlize R package (Gu et al., 2014).

[1]http://stitch.embl.de/

[2]http://bioinfogp.cnb.csic.es/tools/venny/index.html

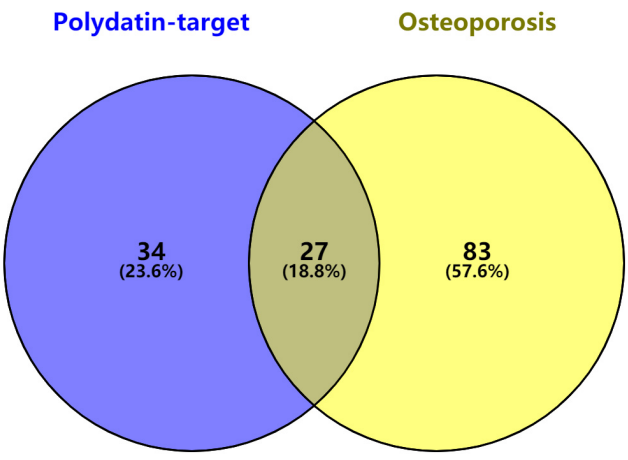

FIGURE 2 | Identification of KEGG pathways shared between polydatin-targeted genes and osteoporosis. Sixty-one polydatin-targeted genes related KEGG pathways, and 110 osteoporosis related KEGG pathways were found; 27 (18.8%) shared KEGG pathways were identified.

Retrieval of the Kyoto Encyclopedia of Genes and Genomes Pathway

The top five shared KEGG pathways with the smallest *q*-values were selected and the KEGG pathways were established using the KEGG database.[3]

[3]https://www.kegg.jp/

Statistical Analysis

All analyses were conducted by GraphPad Prism 8.0; the presentation of data is mean ± SD. The data of two groups were compared with Student's *t*-test, whereas one-way analysis of variance with Tukey's textitpost-hoc test was used to compare groups of 3 or more. $P < 0.05$ was considered to be statistically significant. All experiments were repeated in triplicate.

TABLE 2 | Top five KEGG pathway and related genes.

Term	KEGG pathway	Polydatin-targeted genes	q-value
hsa04062	Chemokine signaling pathway	CXCL10, MAP2K1, CXCL8, CXCR1, CXCR3, CXCR2, MAPK1, CCL2, RELA, CCR2, MAPK3	9.52E-09
hsa05211	Renal cell carcinoma	MAP2K1, EPAS1, ARNT, MAPK1, PTPN11, HIF1A, MAPK3	1.90E-06
hsa04010	MAPK signaling pathway	RPS6KA3, MAP2K1, PTPRR, DUSP1, RPS6KA1, MAPK1, PTPN7, RELA, MAPK3	1.57E-05
hsa04722	Neurotrophin signaling pathway	RPS6KA3, MAP2K1, RPS6KA1, MAPK1, PTPN11, RELA, MAPK3	2.72E-05
hsa05200	Pathways in cancer	MAP2K1, HSP90AA1, CXCL8, EPAS1, ARNT, MAPK1, HIF1A, RELA, MAPK3	1.52E-04

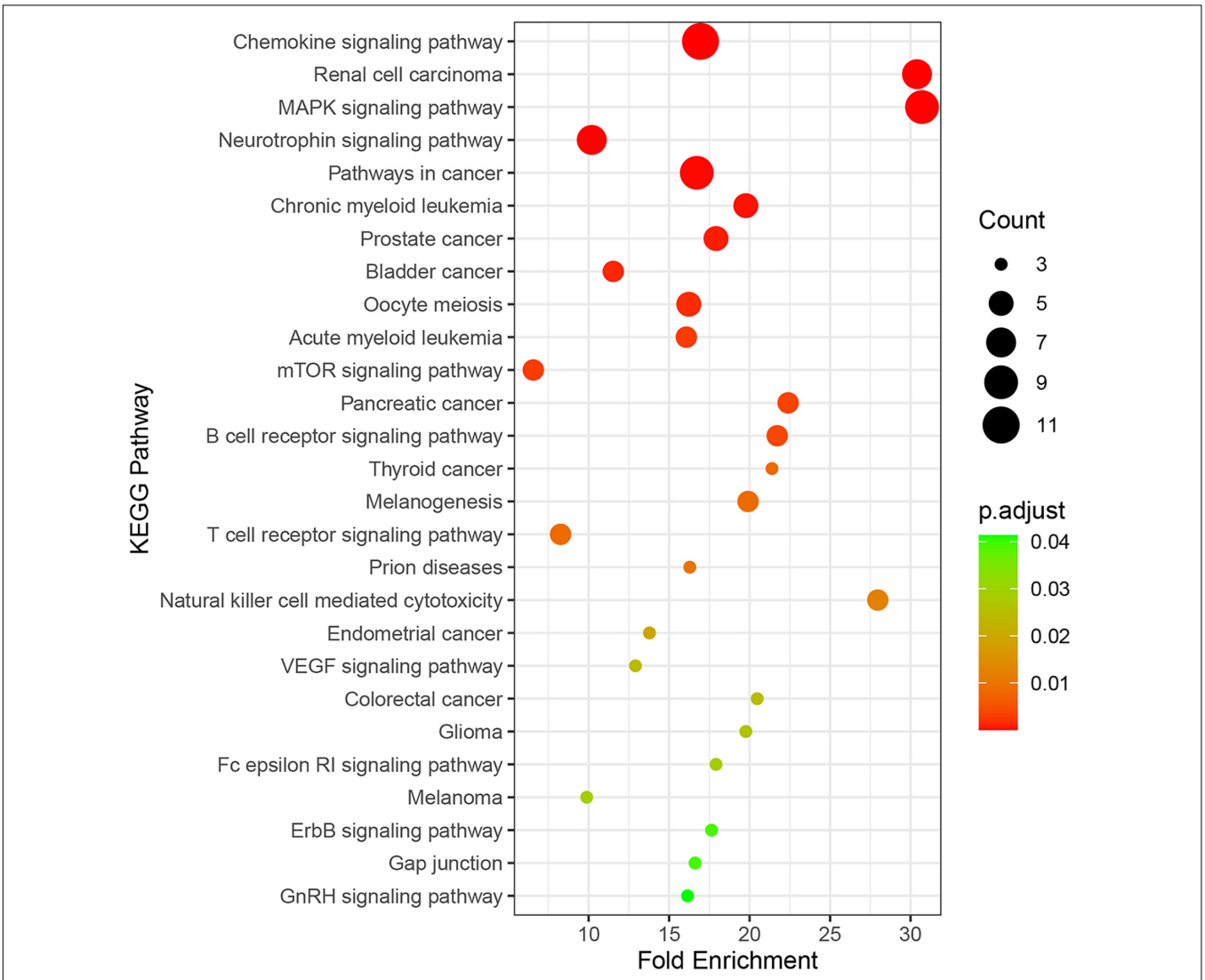

FIGURE 3 | Enrichment information of KEGG pathways with *p*.adjust < 0.05. Top five KEGG pathways were the Chemokine signaling pathway (hsa04062), Renal cell carcinoma (hsa05211), the MAPK signaling pathway (hsa04010), the Neurotrophin signaling pathway (hsa04722), and Pathways in cancer (hsa052009).

RESULTS

Polydatin-Related Genes and Interaction Network

In total, 30 POL genes and compounds were obtained in STITCH using a limit of three shells. The interaction network was constructed in Cytoscape (**Figure 1A**). IL8, ARNT, AHR, G6PD, CXCL10, MAPK3, CCL2, MAPK1, TYR, and PDE5A were involved in the first shell. Sildenafil, MAP2K1, AIPm HIF1A, tadalafil, CXCR2, DUSP1, EPAS1, CXCR3, and RPS6KA1 were involved in the second shell. RPS6KA3, vardenafil, RELA, PTPN7, HSP90AA1, PTPRR, CCR2, MBP, PTPN11, and CXCR1 were involved in the third shell. A weighted network was constructed (**Figure 1B**). MAPK1 and MAPK3 had the highest weight.

DAVID database was used to obtain 69 polydatin-related KEGG pathways and 61 KEGG pathways with q-value < 0.05 were selected. And the miRwalk database was used to obtain 110 osteoporosis-related KEGG pathways.

Enrichment Analysis of Genes and Kyoto Encyclopedia of Genes and Genomes Pathway

Twenty-seven KEGG pathways shared between POL-related genes and OP were identified using a Venn Diagram (**Figure 2**). According to the above analysis, the top five KEGG pathways were Chemokine signaling pathway, Renal cell carcinoma, MAPK signaling pathway, Neurotrophin signaling pathway, and Pathways in cancer (**Table 2**). According to the information in the table, MAPK1, MAPK3, and MAP2K1 are found in all top five KEGG pathways. Therefore, these genes are regarded as hub genes. The enrichment information of the KEGG pathways with p.adjust < 0.05 is shown in **Figure 3**. The gene enrichment analysis results are shown in **Figure 4**. The specific information

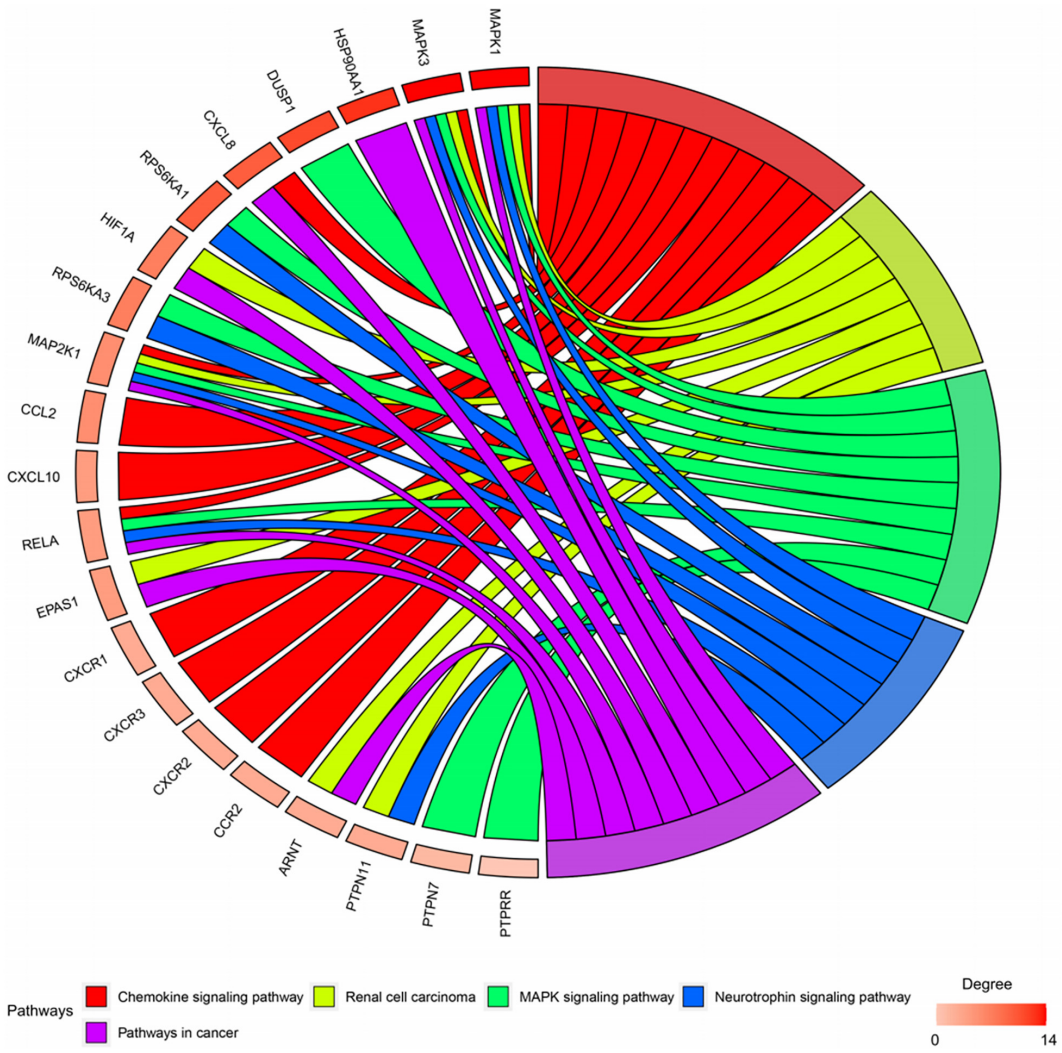

FIGURE 4 | Gene enrichment analysis. MAP2K1, MAPK1, and MAPK3 were involved in all five pathways. The sub genes by degree were MAPK1, MAPK3, and MAP2K1.

and the chromosomal position of all genes in the network are shown in **Figure 5**.

Retrieval of the Kyoto Encyclopedia of Genes and Genomes Pathway

The top five shared KEGG pathways with the smallest q-values are shown in **Figure 6**. These pathways are involved in proliferation, invasion, differentiation, inflammation, and cell survival. The MAPK signaling pathway is found in all the top five shared KEGG pathways.

Polydatin Reverses Osteoporosis *in vitro*

A cellular OP model was created using DXM. The MC3T3-E1 cells were treated with POL in different concentrations (20, 40, and 80 μM), the total RNA was extracted and the levels of osteogenic genes, including Col-1a1, ALP, OCN, and Runx2 were measured using qRT-PCR analysis. Our results showed that the DXM treatment could significantly decreased the bone turnover markers in MC3T3-E1 cells, and POL could partially reverse this effect in a dose-dependent manner (**Figures 7A–D**). Additionally, ALP staining was performed to visualize the extracellular matrix mineralization among the different groups. Similarly, POL could partially rescue the impaired mineralization induced by the DXM treatment (**Figures 7E–H**).

MAPK Signaling Pathway Involved in the Regulation of POL

As shown in **Figure 8**, in the POL-treated groups, the relative expression of p-JNK, p-P38, and p-ERK was decreased compared to the control group (PBS treatment) in a dose-dependent manner. Thus, it can be assumed that the *MAPK* signaling pathway is involved in the regulation of POL.

DISCUSSION

Polydatin, a stilbenoid compound obtained from the root of *P. cuspidatum*, is believed to possess anti-osteoporotic activity (Chen et al., 2016, 2019; Zhou et al., 2016). BMSCs have the ability of self-renewal and multidirectional differentiation. They

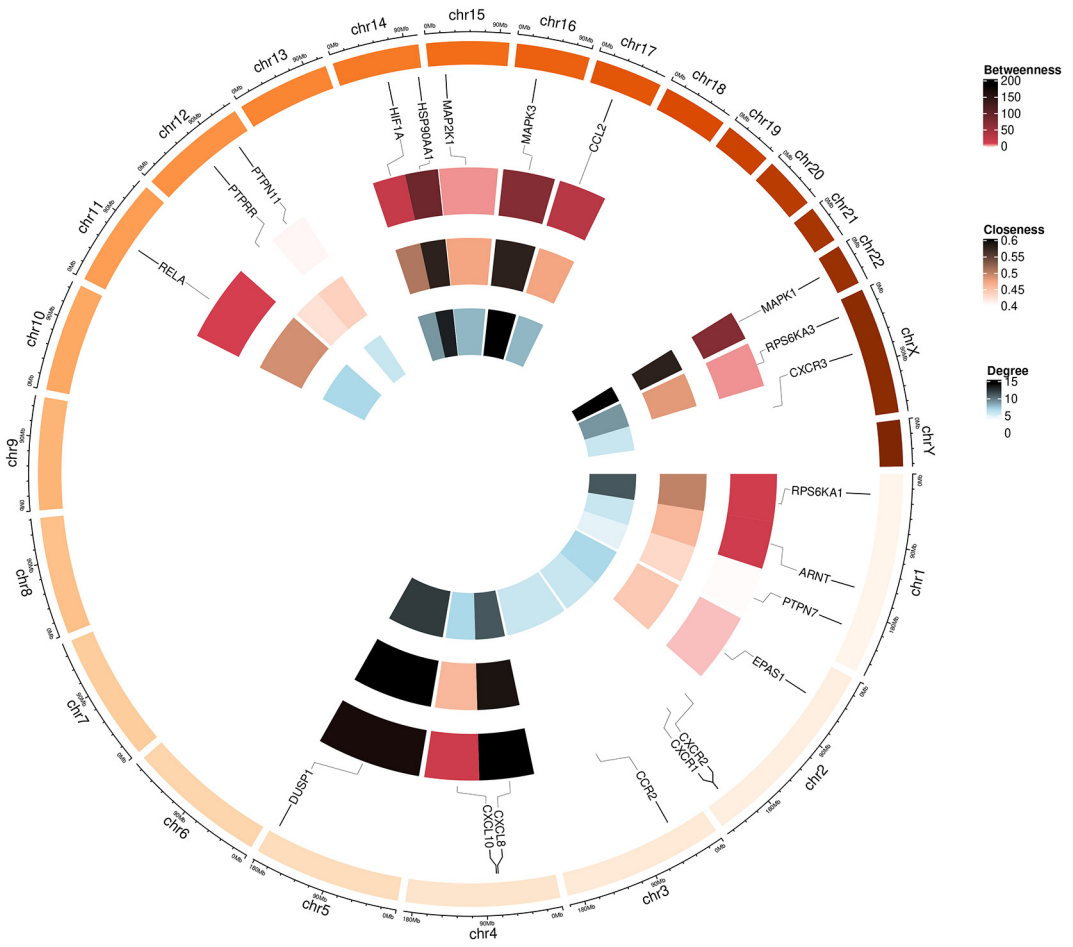

FIGURE 5 | Circular visualization of the chromosomal positions and connectivity of polydatin-targeted genes. Gene names are shown in the outer circle. In the outer heatmap, deep color represents high betweenness, in the middle heatmap, deep color represents high closeness, and in the inner heatmap, deep color represents high degree. Lines extend from each gene point to its specific chromosomal locatio on the chromosomal circle.

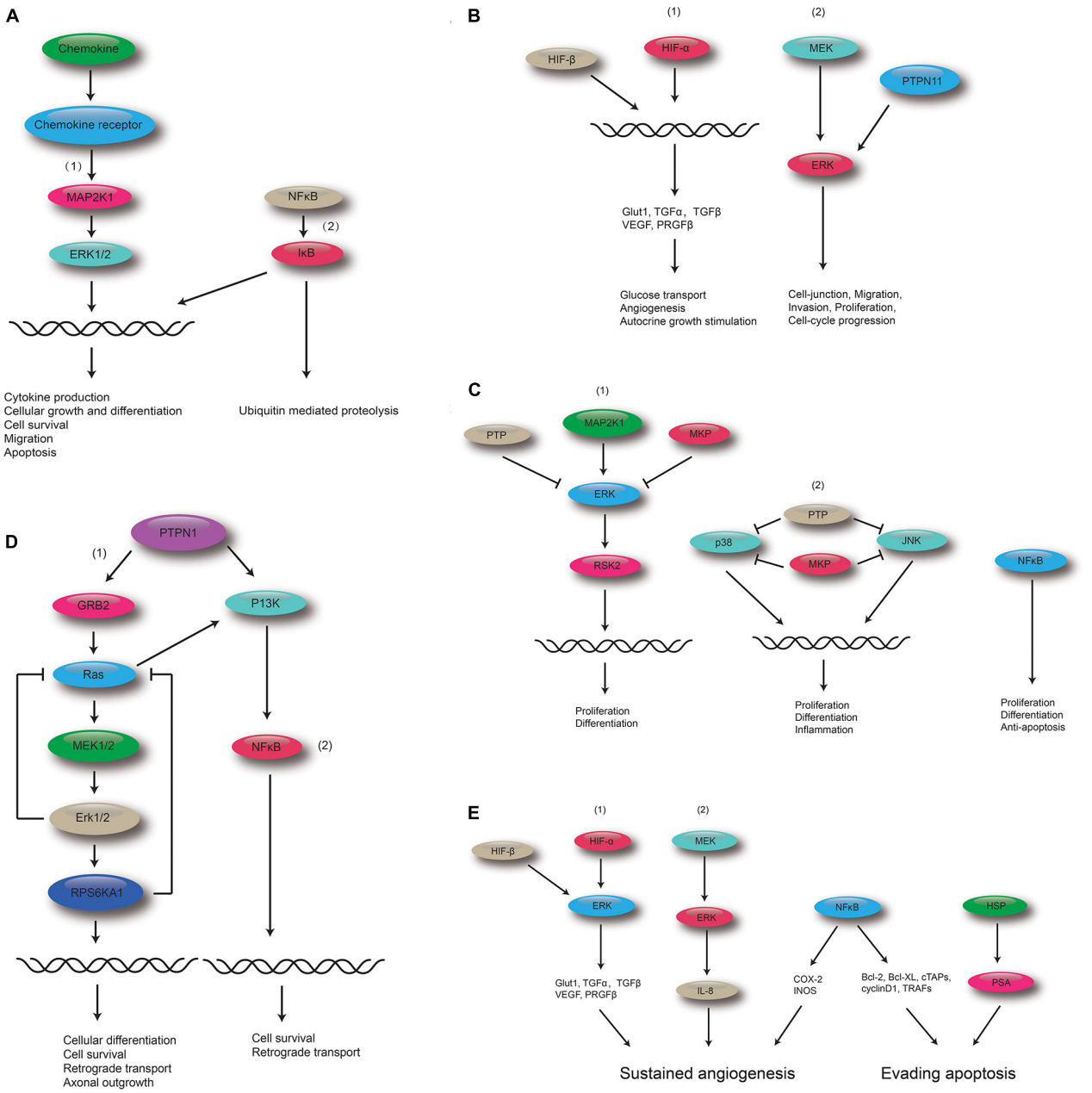

FIGURE 6 | Polydatin-targeted genes related to the top five shared KEGG pathways. **(A)** Polydatin-targeted genes related to the Chemokine signaling pathway: (1) MAPK signaling pathway and (2) NF-kB. **(B)** Polydatin-targeted genes related to Renal cell carcinoma: (1) HIF-1 signaling pathway, and (2) MAPK signaling pathway. **(C)** Polydatin-targeted genes related to the MAPK signaling pathway:(1) Classical MAP kinase pathway, (2) JUK and p38 MAP kinase pathway, and (3) NFκB. **(D)** Polydatin-targeted genes related to the Neurotrophin signaling pathway: (1) MAPK signaling pathway, and (2) NFκB. **(E)** Polydatin-targeted genes related to Pathways in cancer: (1) HIF-1 signaling pathway, (2) MAKP signaling pathway, (3) NFκB, and (4) HSP.

can potentially differentiate into adipocytes, osteoblasts, and chondrocytes (Yim et al., 2014; Ruiz et al., 2016). Therefore, BMSCs play a key role in the treatment of OP. As shown in previous study, POL can protect from oxidative stress and promote BMSCs migration (Chen et al., 2019). POL has also been shown to possess notable anti-OP activity via regulation of OPG, RANKL, and β-catenin (Zhou et al., 2016). In addition, a study suggested that POL may promote BMSC migration via the ERK 1/2 signaling pathways (Chen et al., 2016). However, the precise mechanism of POL's anti-OP activity has yet to be investigated.

In this study, we identified 27 KEGG pathway shared between POL-targeted genes and OP. The top five KEGG pathways with the smallest q-values were Chemokine signaling pathway, Renal cell carcinoma, MAPK signaling pathway, Neurotrophin signaling pathway, and Pathways in cancer. The hub genes of the five signaling pathway were MAPK1, MAPK3, and MAP2K1.

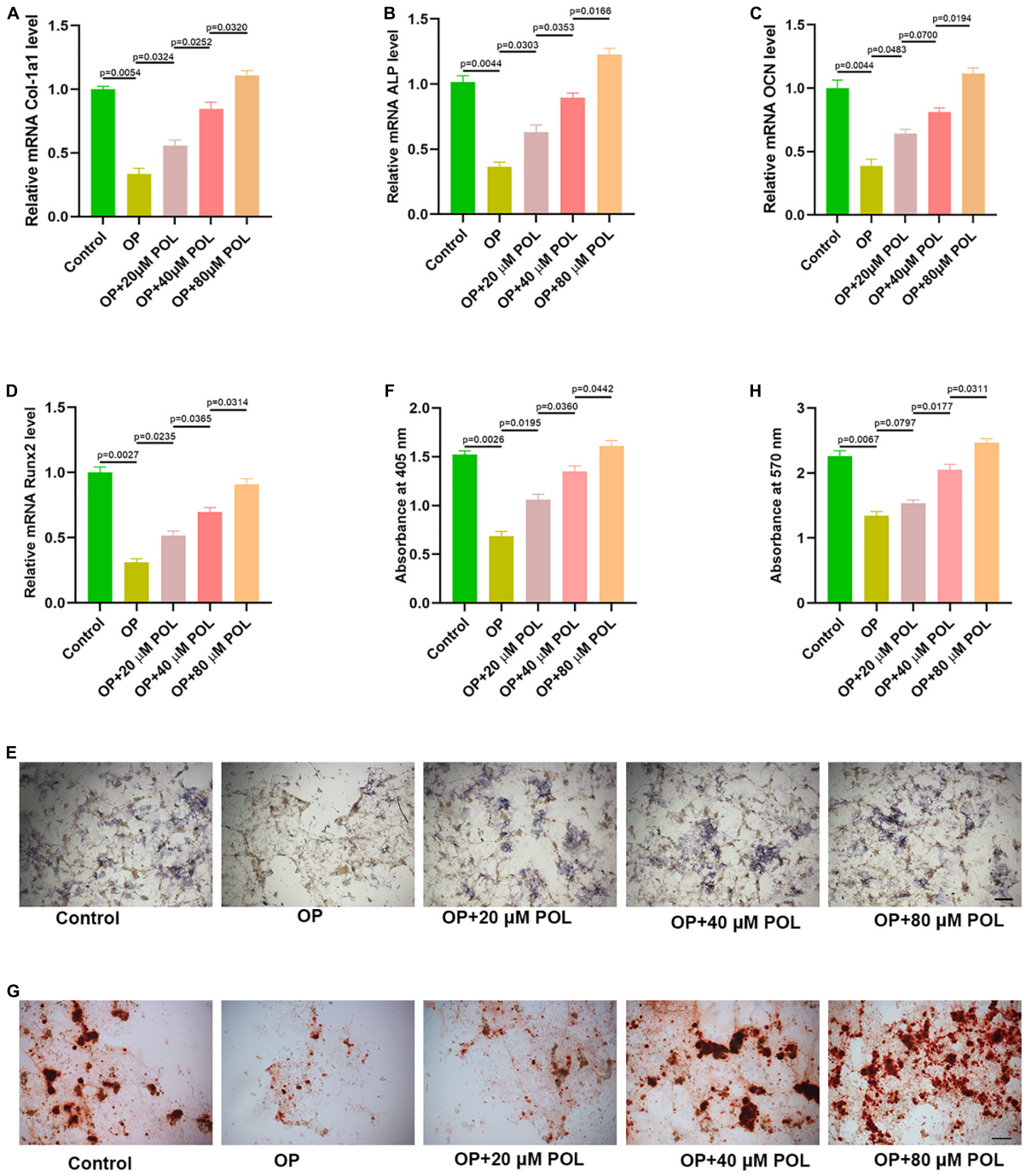

FIGURE 7 | Polydatin (POL) reverses OP *in vitro*. **(A–D)** The expression of Col-1a1, ALP, OCN, and Runx2 in the different groups [Control(PBS); OP; OP + 20μM POL; OP + 40μM POL; OP + 80μM POL] was measured using a qRT-PCR analysis. The cellular OP model was performed using DXM; **(E,F)** ALP staining in MC3T3-E1 following different treatments; **(G,H)** Alizarin red- calcium staining in MC3T3-E1 following different treatments.

By mapping the KEGG pathways related to target genes, we found that POL exerts its biological effects through regulating Classical *MAP* kinase pathway, *JNK*, and *p38 MAP* kinase pathway. POL-targeted genes *ERK (MAPK1, MAPK3), MEK1 (MAP2K1)* were involved in the above pathways. And the identified POL-targeted genes are associated with proliferation, differentiation, inflammation, cellular growth and differentiation, and cytokine production.

As is known, there are three major subfamilies of MAPK: the extracellular-signal-regulated kinases (ERK MAPK, Ras/Raf1/MEK/ERK), the c-Jun N-terminal or stress-activated protein kinases (JNK, SAPK), and p38

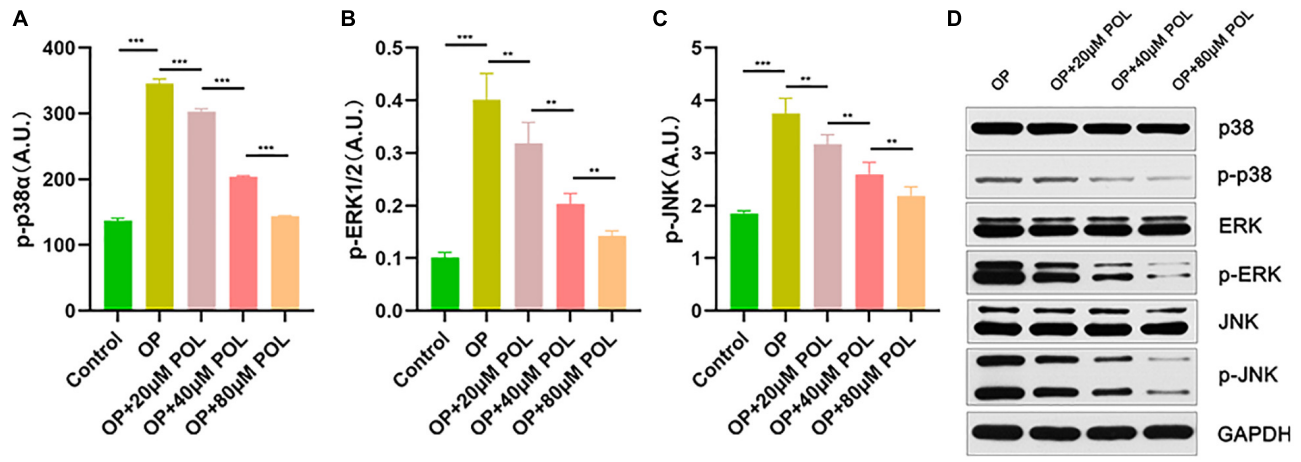

FIGURE 8 | Involvement of the MAPK signaling pathway in the regulation of POL. The relative expression of **(A)** p-P38, **(B)** p-ERK, and **(C)** p-JNK in the different groups [Control (PBS); OP; OP + 20μM POL; OP + 40μM POL; OP + 80μM POL] by ELISA is shown (**$P < 0.05$, ***$P < 0.001$). **(D)** The cellular OP models were treated with different concentrations of POL. Western blotting results of p38, p-p38, ERK, p-ERK, JNK, and p-JNK protein levels in BMSCs.

(Fang and Richardson, 2005; Cargnello and Roux, 2011). JNK and p38 have similar functions and are related to inflammation, apoptosis, and growth (Wagner and Nebreda, 2009). ERK is responsible for basic cell processes, including cell proliferation and differentiation (Guo et al., 2020). Several studies have suggested that the ERK-MAPK pathway can positively regulate bone development (Radio et al., 2006; Ge et al., 2007; Shim et al., 2013). At the same time, studies have shown that the p38 MAPK pathway is essential for bone production and bone homeostasis (Greenblatt et al., 2010; Weske et al., 2018). In addition, osteoclast formation and survival can be inhibited through the attenuation of JNK/c-jun and NFκB signaling (Abe et al., 2003; Krum et al., 2010).

Protein phosphorylation (PP) is a common regulatory mode in organism and plays an important role in the process of cell signal transduction (Kummer and Ban, 2021). It was widely demonstrated that PP is the most basic, universal and important mechanism for regulating and controlling protein activity and function (Jiang et al., 2021). To validate our bioinformatic results, the phosphorylation level of MAPK signaling pathway was detected. Our results indicated that POL reduced the phosphorylation levels of ERK1/2, p38α and JNK in MC3T3-E1, suggesting *MAPK* signaling pathway involved in the regulation of POL, which is high incidence with the bioinformatic results. In the current study, we proved that POL induces osteoblastic differentiation via suppressing the *MAPK* signaling pathway, and further signaling pathways involved in the protective functions of POL on OP will be verified in future studies.

Like other bioinformatic analysis, some limitations could be found in the study. On the one hand, the effect of activation or suppression of *MAPK* signaling on osteoblasitc differentiation was not explored in the present research. On the other hand, animal osteoporotic model was not constructed and the beneficial effect of POL on OP was nor demonstrated *in vivo*.

However, it is worth noting, that previous researches has identified POL as a potential activator of the Sirtuin family, which is involved in specific biological functions, including regulation of transcription, cell cycle, cell differentiation, apoptosis, anti-oxidation, and genomic stabilization (Chen and Lan, 2017; Sun et al., 2021). Sirtuins, which is highly conserved NAD+ dependent deacetylases, exist in most organisms and play a key role in promoting the health and survival (Sinclair and Guarente, 2006; Haigis and Sinclair, 2010). According to previous studies, sirtuins can regulate the lifespan of lower organisms and age-related diseases in mammals (Imai and Guarente, 2014). A study has shown that sirtuin might play an important role in the treatment of mitochondrial dysfunction, aging, and metabolic diseases (Westphal et al., 2007). As an activator of sirtuin, resveratrol can reduce oxidative stress and inflammation by acting on Akt and MAPK signaling pathways (Shin et al., 2012). A related study has reported that sirituin affects the MAPK pathway by regulating the phosphorylation of p38, JNK, and ERK (Becatti et al., 2012). Therefore, this evidence taken together with our results, allows for speculation that polydatin might alleviates osteoporosis by acting on the Sirtuin family and regulating biological processes and MAPK signaling. This highlights a potential path for subsequent research.

CONCLUSION

Our study determined that POL exhibited protective effects in OP, as evidenced by a suppression of *MAPK* signaling *in vitro*. This study identifies a promising potential candidate for the treatment of OP.

DATA AVAILABILITY STATEMENT

The original contributions presented in the study are included in the article/supplementary material, further inquiries can be directed to the corresponding authors.

AUTHOR CONTRIBUTIONS

GL conceived and designed the study. BM and YS supervised the study. ZL, YX, and YH performed the bioinformatics analysis and experiments and wrote the manuscript. LC, WZ, and HX analyzed the data. LH and AP provided advice and technical assistance. CY and XX revised the figures and tables. All authors approved the final manuscript.

FUNDING

This study was supported by the National Key Research and Development Program of China (2018YFB1105700), the National Science Foundation of China (No.31600754 and NO.81472144), Healthy Commission Key Project of Hubei Province (No. WJ2019Z009), and Healthy Commission General Project of Hubei Province (No. WJ2019M023).

REFERENCES

Abe, E., Marians, R. C., Yu, W., Wu, X. B., Ando, T., Li, Y., et al. (2003). TSH is a negative regulator of skeletal remodeling. *Cell* 115, 151–162.

Agarwal, P., and Searls, D. B. (2009). Can literature analysis identify innovation drivers in drug discovery? *Nature Rev. Drug Discov.* 8, 865–878. doi: 10.1038/nrd2973

Becatti, M., Taddei, N., Cecchi, C., Nassi, N., Nassi, P. A., and Fiorillo, C. (2012). SIRT1 modulates MAPK pathways in ischemic-reperfused cardiomyocytes. *Cell. Mol. Life Sci. CMLS* 69, 2245–2260. doi: 10.1007/s00018-012-0925-5

Black, D. M., and Rosen, C. J. (2016). Clinical practice. Postmenopausal osteoporosis. *N. Engl. J. Med.* 374, 254–262. doi: 10.1056/NEJMcp1513724

Cargnello, M., and Roux, P. P. (2011). Activation and function of the MAPKs and their substrates, the MAPK-activated protein kinases. *Microbiol. Mol. Biol. Rev.* 75, 50–83. doi: 10.1128/MMBR.00031-10

Chen, L., and Lan, Z. (2017). Polydatin attenuates potassium oxonate-induced hyperuricemia and kidney inflammation by inhibiting NF-κB/NLRP3 inflammasome activation via the AMPK/SIRT1 pathway. *Food Funct.* 8, 1785–1792. doi: 10.1039/c6fo01561a

Chen, L., Lan, Z., Lin, Q., Mi, X., He, Y., Wei, L., et al. (2013). Polydatin ameliorates renal injury by attenuating oxidative stress-related inflammatory responses in fructose-induced urate nephropathic mice. *Food Chem. Toxicol.* 52, 28–35. doi: 10.1016/j.fct.2012.10.037

Chen, X.-J., Shen, Y.-S., He, M.-C., Yang, F., Yang, P., Pang, F.-X., et al. (2019). Polydatin promotes the osteogenic differentiation of human bone mesenchymal stem cells by activating the BMP2-Wnt/β-catenin signaling pathway. *Biomed. Pharmacother.* 112:108746. doi: 10.1016/j.biopha.2019.108746

Chen, Z., Wei, Q., Hong, G., Chen, D., Liang, J., He, W., et al. (2016). Polydatin induces bone marrow stromal cells migration by activation of ERK1/2. *Biomed. Pharmacother.* 82, 49–53. doi: 10.1016/j.biopha.2016.04.059

Compston, J. E., McClung, M. R., and Leslie, W. D. (2019). Osteoporosis. *Lancet (London, England)* 393, 364–376. doi: 10.1016/S0140-6736(18)32112-3

Cummings, S. R., and Melton, L. J. (2002). Epidemiology and outcomes of osteoporotic fractures. *Lancet (London, England)* 359, 1761–1767.

Dweep, H., and Gretz, N. (2015). miRWalk2.0: a comprehensive atlas of microRNA-target interactions. *Nat. Methods* 12:697. doi: 10.1038/nmeth.3485

Fang, J. Y., and Richardson, B. C. (2005). The MAPK signalling pathways and colorectal cancer. *Lancet Oncol.* 6, 322–327. doi: 10.1016/s1470-2045(05)70168-6

Ge, C., Xiao, G., Jiang, D., and Franceschi, R. T. (2007). Critical role of the extracellular signal-regulated kinase-MAPK pathway in osteoblast differentiation and skeletal development. *J. Cell Biol.* 176, 709–718. doi: 10.1083/jcb.200610046

Greenblatt, M. B., Shim, J. H., Zou, W., Sitara, D., Schweitzer, M., Hu, D., et al. (2010). The p38 MAPK pathway is essential for skeletogenesis and bone homeostasis in mice. *J. Clin. Invest.* 120, 2457–2473. doi: 10.1172/JCI42285

Gu, Z., Gu, L., Eils, R., Schlesner, M., and Brors, B. (2014). circlize Implements and enhances circular visualization in R. *Bioinformatics* 30, 2811–2812. doi: 10.1093/bioinformatics/btu393

Guo, Y. J., Pan, W. W., Liu, S. B., Shen, Z. F., Xu, Y., and Hu, L. L. (2020). ERK/MAPK signalling pathway and tumorigenesis. *Exp. Ther. Med.* 19, 1997–2007. doi: 10.3892/etm.2020.8454

Haigis, M. C., and Sinclair, D. A. (2010). Mammalian sirtuins: biological insights and disease relevance. *Annu. Rev. Pathol.* 5, 253–295. doi: 10.1146/annurev.pathol.4.110807.092250

Huang, D. W., Sherman, B. T., and Lempicki, R. A. (2009). Systematic and integrative analysis of large gene lists using DAVID bioinformatics resources. *Nat. Protoc.* 4, 44–57. doi: 10.1038/nprot.2008.211

Huang, K., Chen, C., Hao, J., Huang, J., Wang, S., Liu, P., et al. (2015). Polydatin promotes Nrf2-ARE anti-oxidative pathway through activating Sirt1 to resist AGEs-induced upregulation of fibronetin and transforming growth factor-β1 in rat glomerular messangial cells. *Mol. Cell. Endocrinol.* 399, 178–189. doi: 10.1016/j.mce.2014.08.014

Imai, S.-I., and Guarente, L. (2014). NAD+ and sirtuins in aging and disease. *Trends Cell Biol.* 24, 464–471. doi: 10.1016/j.tcb.2014.04.002

Jiang, X., Liu, W., Deng, J., Lan, L., Xue, X., Zhang, C., et al. (2013). Polydatin protects cardiac function against burn injury by inhibiting sarcoplasmic reticulum Ca2+ leak by reducing oxidative modification of ryanodine receptors. *Free Radic. Biol. Med.* 60, 292–299. doi: 10.1016/j.freeradbiomed.2013.02.030

Jiang, Y., Dong, Y., Luo, Y., Jiang, S., Meng, F.-L., Tan, M., et al. (2021). AMPK-mediated phosphorylation on 53BP1 promotes c-NHEJ. *Cell Rep.* 34:108713. doi: 10.1016/j.celrep.2021.108713

Jiao, X., Sherman, B. T., Huang da, W., Stephens, R., Baseler, M. W., Lane, H. C., et al. (2012). DAVID-WS: a stateful web service to facilitate gene/protein list analysis. *Bioinformatics* 28, 1805–1806. doi: 10.1093/bioinformatics/bts251

Krum, S. A., Chang, J., Miranda-Carboni, G., and Wang, C. Y. (2010). Novel functions for NFkappaB: inhibition of bone formation. *Nat. Rev. Rheumatol.* 6, 607–611. doi: 10.1038/nrrheum.2010.133

Kummer, E., and Ban, N. (2021). Mechanisms and regulation of protein synthesis in mitochondria. *Nat. Rev. Mol. Cell Biol.* 22, 307–325. doi: 10.1038/s41580-021-00332-2

Mele, L., Paino, F., Papaccio, F., Regad, T., Boocock, D., Stiuso, P., et al. (2018). A new inhibitor of glucose-6-phosphate dehydrogenase blocks pentose phosphate pathway and suppresses malignant proliferation and metastasis in vivo. *Cell Death Dis.* 9:572. doi: 10.1038/s41419-018-0635-5

Rachner, T. D., Khosla, S., and Hofbauer, L. C. (2011). Osteoporosis: now and the future. *Lancet (London, England)* 377, 1276–1287. doi: 10.1016/S0140-6736(10)62349-5

Radio, N. M., Doctor, J. S., and Witt-Enderby, P. A. (2006). Melatonin enhances alkaline phosphatase activity in differentiating human adult mesenchymal stem cells grown in osteogenic medium via MT2 melatonin receptors and the MEK/ERK (1/2) signaling cascade. *J. Pineal Res.* 40, 332–342.

Ruiz, M., Cosenza, S., Maumus, M., Jorgensen, C., and Noël, D. (2016). Therapeutic application of mesenchymal stem cells in osteoarthritis. *Expert Opin. Biol. Ther.* 16, 33–42. doi: 10.1517/14712598.2016.1093108

Sambrook, P., and Cooper, C. (2006). Osteoporosis. *Lancet (London, England)* 367, 2010–2018.

Shannon, P., Markiel, A., Ozier, O., Baliga, N. S., Wang, J. T., Ramage, D., et al. (2003). Cytoscape: a software environment for integrated models of biomolecular interaction networks. *Genome Res.* 13, 2498–2504. doi: 10.1101/gr.1239303

Shen, Y.-S., Chen, X.-J., Wuri, S.-N., Yang, F., Pang, F.-X., Xu, L.-L., et al. (2020). Polydatin improves osteogenic differentiation of human bone mesenchymal stem cells by stimulating TAZ expression via BMP2-Wnt/β-catenin signaling pathway. *Stem Cell Res. Ther.* 11:204. doi: 10.1186/s13287-020-01705-8

Shim, J. H., Greenblatt, M. B., Zou, W., Huang, Z., Wein, M. N., Brady, N., et al. (2013). Schnurri-3 regulates ERK downstream of WNT signaling in osteoblasts. *J. Clin. Invest.* 123, 4010–4022. doi: 10.1172/JCI69443

Shin, J. A., Lee, K.-E., Kim, H.-S., and Park, E.-M. (2012). Acute resveratrol treatment modulates multiple signaling pathways in the ischemic brain. *Neurochem. Res.* 37, 2686–2696. doi: 10.1007/s11064-012-0858-2

Sinclair, D. A., and Guarente, L. (2006). Unlocking the secrets of longevity genes. *Sci. Am.* 294, 48–51, 54–57.

Sun, Z., Wang, X., and Xu, Z. (2021). SIRT1 provides new pharmacological targets for polydatin through its role as a metabolic sensor. *Biomed. Pharmacother.* 139:111549. doi: 10.1016/j.biopha.2021.111549

Suroowan, S., and Mahomoodally, M. F. (2019). Herbal medicine of the 21st century: a focus on the chemistry, pharmacokinetics and toxicity of five widely advocated phytotherapies. *Curr. Top. Med. Chem.* 19, 2718–2738. doi: 10.2174/1568026619666191112121330

Szklarczyk, D., Santos, A., von Mering, C., Jensen, L. J., Bork, P., and Kuhn, M. (2016). STITCH 5: augmenting protein-chemical interaction networks with tissue and affinity data. *Nucleic Acids Res.* 44, D380–D384.

Wagner, E. F., and Nebreda, A. R. (2009). Signal integration by JNK and p38 MAPK pathways in cancer development. *Nat. Rev. Cancer* 9, 537–549. doi: 10.1038/nrc2694

Walter, W., Sanchez-Cabo, F., and Ricote, M. (2015). GOplot: an R package for visually combining expression data with functional analysis. *Bioinformatics* 31, 2912–2914. doi: 10.1093/bioinformatics/btv300

Weske, S., Vaidya, M., Reese, A., von Wnuck Lipinski, K., Keul, P., Bayer, J. K., et al. (2018). Targeting sphingosine-1-phosphate lyase as an anabolic therapy for bone loss. *Nat. Med* 24, 667–678. doi: 10.1038/s41591-018-0005-y

Westphal, C. H., Dipp, M. A., and Guarente, L. (2007). A therapeutic role for sirtuins in diseases of aging? *Trends Biochem. Sci.* 32, 555–560.

Yim, R. L.-H., Lee, J. T.-Y., Bow, C. H., Meij, B., Leung, V., Cheung, K. M. C., et al. (2014). A systematic review of the safety and efficacy of mesenchymal stem cells for disc degeneration: insights and future directions for regenerative therapeutics. *Stem Cells Dev.* 23, 2553–2567. doi: 10.1089/scd.2014.0203

Zampieri, M., Sekar, K., Zamboni, N., and Sauer, U. (2017). Frontiers of high-throughput metabolomics. *Curr. Opin. Chem. Biol.* 36, 15–23. doi: 10.1016/j.cbpa.2016.12.006

Zhou, Q. L., Qin, R. Z., Yang, Y. X., Huang, K. B., and Yang, X. W. (2016). Polydatin possesses notable antiosteoporotic activity via regulation of OPG, RANKL and betacatenin. *Mol. Med. Rep.* 14, 1865–1869. doi: 10.3892/mmr.2016.5432

Zhu, Y. Z., Wu, W., Zhu, Q., and Liu, X. (2018). Discovery of Leonuri and therapeutical applications: from bench to bedside. *Pharmacol. Therap.* 188, 26–35. doi: 10.1016/j.pharmthera.2018.01.006

Conflict of Interest: The authors declare that the research was conducted in the absence of any commercial or financial relationships that could be construed as a potential conflict of interest.

Publisher's Note: All claims expressed in this article are solely those of the authors and do not necessarily represent those of their affiliated organizations, or those of the publisher, the editors and the reviewers. Any product that may be evaluated in this article, or claim that may be made by its manufacturer, is not guaranteed or endorsed by the publisher.

frontiers in Cell and Developmental Biology

ORIGINAL RESEARCH
published: 14 October 2021
doi: 10.3389/fcell.2021.757830

Mesenchymal Stem Cells and NF-κB Sensing Interleukin-4 Over-Expressing Mesenchymal Stem Cells Are Equally Effective in Mitigating Particle-Associated Chronic Inflammatory Bone Loss in Mice

Ning Zhang[1†], Takeshi Utsunomiya[1†], Tzuhua Lin[1], Yusuke Kohno[1], Masaya Ueno[1], Masahiro Maruyama[1], Ejun Huang[1], Claire Rhee[1], Zhenyu Yao[1] and Stuart B. Goodman[1,2]*

[1] Department of Orthopaedic Surgery, Stanford University, Stanford, CA, United States, [2] Department of Bioengineering, Stanford University, Stanford, CA, United States

Wear particles from total joint arthroplasties (TJAs) induce chronic inflammation, macrophage infiltration and lead to bone loss by promoting bone destruction and inhibiting bone formation. Inhibition of particle-associated chronic inflammation and the associated bone loss is critical to the success and survivorship of TJAs. The purpose of this study is to test the hypothesis that polyethylene particle induced chronic inflammatory bone loss could be suppressed by local injection of NF-κB sensing Interleukin-4 (IL-4) over-expressing MSCs using the murine continuous polyethylene particle infusion model. The animal model was generated with continuous infusion of polyethylene particles into the intramedullary space of the femur for 6 weeks. Cells were locally injected into the intramedullary space 3 weeks after the primary surgery. Femurs were collected 6 weeks after the primary surgery. Micro-computational tomography (μCT), histochemical and immunohistochemical analyses were performed. Particle-infusion resulted in a prolonged pro-inflammatory M1 macrophage dominated phenotype and a decrease of the anti-inflammatory M2 macrophage phenotype, an increase in TRAP positive osteoclasts, and lower alkaline phosphatase staining area and bone mineral density, indicating chronic particle-associated inflammatory bone loss. Local injection of MSCs or NF-κB sensing IL-4 over-expressing MSCs reversed the particle-associated chronic inflammatory bone loss and facilitated bone healing. These results demonstrated that local inflammatory bone loss can be effectively modulated via MSC-based treatments, which could be an efficacious therapeutic strategy for periprosthetic osteolysis.

Keywords: wear particles, chronic inflammation, bone loss, mesenchymal stem cells, macrophages

OPEN ACCESS

Edited by:
Ren Xu,
Xiamen University, China

Reviewed by:
Fangming Song,
Guangxi Medical University, China
Anton G. Kutikhin,
Research Institute of Complex Problems of Cardiovascular Disease Russian Academy of Medical Sciences, Russia

****Correspondence:***
Stuart B. Goodman
goodbone@stanford.edu

† These authors have contributed equally to this work

Specialty section:
This article was submitted to Stem Cell Research, a section of the journal Frontiers in Cell and Developmental Biology

Received: *12 August 2021*
Accepted: *27 September 2021*
Published: *14 October 2021*

Citation:
Zhang N, Utsunomiya T, Lin T, Kohno Y, Ueno M, Maruyama M, Huang E, Rhee C, Yao Z and Goodman SB (2021) Mesenchymal Stem Cells and NF-κB Sensing Interleukin-4 Over-Expressing Mesenchymal Stem Cells Are Equally Effective in Mitigating Particle-Associated Chronic Inflammatory Bone Loss in Mice. Front. Cell Dev. Biol. 9:757830. doi: 10.3389/fcell.2021.757830

INTRODUCTION

Wear particles from total joint arthroplasties (TJAs) incite a persistent macrophage-mediated chronic inflammatory reaction resulting in the release of cytokines, chemokines, and other molecules (Bi et al., 2001; Xu et al., 2009; Abu-Amer, 2013) and, stimulate key paracrine and autocrine cell interactions (Goodman et al., 2013). This reaction promotes bone resorption and impedes bone formation, leading to periprosthetic osteolysis and eventually, loss of mechanical support for the implant (Goodman, 2007; Goodman et al., 2014; Qiu et al., 2020). Revision surgery for osteolysis is technically demanding, with higher costs and poorer outcomes than primary arthroplasty (Kurtz et al., 2014). Although modern bearing couples and alloys have been developed to reduce wear, new strategies for reducing particle-induced osteolysis are needed to improve the durability of TJAs.

Mesenchymal stem cells (MSCs) have shown great potential in skeletal tissue regeneration (Caplan, 1991; Zhang et al., 2021). Previously we showed an intervention using unaltered MSCs during the chronic inflammatory phase could mitigate the adverse effects of contaminated particles on bone (Utsunomiya et al., 2021a). Furthermore, specific properties of MSCs, such as differentiation capability and immunomodulation potential can be further refined by genetic modification to optimize MSC-based therapy (Wei et al., 2018; Zhang et al., 2021). Whether local delivery of genetically modified MSCs could abrogate the adverse effects of particles on bone *in vivo*, using the murine continuous femoral infusion model is unknown. Interleukin-4 over expression by genetically modified MSCs mitigates inflammation by converting pro-inflammatory M1 macrophages to an anti-inflammatory M2 phenotype (Lin et al., 2017b); modulation of macrophage phenotype at an appropriate time can optimize osteogenic differentiation of MSCs (Lin et al., 2019) and enhance bone regeneration (Chow et al., 2019; Niu et al., 2021). An *in vitro* study showed that genetically modified MSCs over-secreting IL-4 trigged by NF-κB activation could mitigate the proinflammatory response of macrophages exposed to wear particle (Lin et al., 2018). In the present study, we injected NF-κB sensing IL-4 over-expressing MSCs locally in the murine continuous femoral particle infusion model. We test whether NF-κB sensing IL-4 over-expressing MSC treatment is a more efficacious therapeutic strategy than unaltered MSCs for particle induced chronic inflammatory bone loss in this model.

MATERIALS AND METHODS

Cells

Male BALB/c murine bone marrow derived MSCs were isolated and characterized as previously described (Lin et al., 2015). Briefly, 8–10- week-old BALB/c male mice were used to collect the bone marrow from femurs and tibias. The bone marrow with cells was filtered through 70 μm cell strainer, spun down and resuspended using α-minimal essential medium (α-MEM, Thermo Fisher Scientific, Waltham, MA United States) supplied with 10% certified fetal bovine serum (FBS, Invitrogen, Thermo Fisher Scientific, Waltham, MA United States) and antibiotic-antimycotic solution (100 units of penicillin, 100 μg of streptomycin and 0.25 μg of amphotericin B per milliliter, Hyclone, Thermo Fisher Scientific, Waltham, MA United States). Unattached cells were removed by replacing medium the next day (passage 1). Flow cytometry (LSRII, Stanford Shared FACS Facility, Stanford, CA, United States) was used to characterize the immunophenotype of isolated MSCs at passage 4: spinocerebellar ataxia type 1 ($Sca1^+$)/$CD105^+$ /$CD44^+$ /$CD34^-$/$CD45^-$/$CD11b^-$. Identified MSCs passages 4–8 were used in the experiments. This protocol has been approved by Stanford's Administrative Panel on Laboratory Animal Care (APLAC).

Generation of Genetically Modified Mesenchymal Stem Cells

The lentiviral vector preparation was performed as previously described (Pajarinen et al., 2015). Human embryonic kidney 293T cells (ATCC, Manassas, VA, United States) were used to transfect the control lentivirus vector the mouse IL-4 secreting pCDH-NF-κB-mIL-4-copGFP expressing lentivirus vector (Lin et al., 2017b) together with psPAX2 packaging vector and pMD2G VSV-G envelope vector using the calcium phosphate transfection kit (Clontech, Mountain View, CA, United States) with 25 μM chloroquine. The virus was diluted in MSC culture medium supplemented with 6 μg/ml of polybrene (Sigma Aldrich, St. Louis, MO, United States), and infected to murine MSCs at multiplicity of infection (MOI) = 100. At 3 days post-infection, the infected cells were GPF positive confirmed by fluorescence microscope (Keyence, Itasca, IL, United States).

Enzyme-Linked Immunosorbent Assay

ELISA kits for mouse IL-4 (R&D system, Minneapolis, MN, United States) were used to quantify IL-4 expression by the genetically modified MSCs exposed to 1 μg/ml LPS (Sigma Aldrich, St. Louis, MO) or left untreated for 24 h culture. The manufacturers' protocols were carefully followed. The optical densities were determined using SpectraMax M2e Microplate Readers (Molecular Devices, San Jose, CA, United States) set at 450 nm with wavelength correction set to 540 nm.

Ultra-High Molecular Weight Polyethylene Particles

The polyethylene particles were processed as previously described (Lin et al., 2018, 2019). Briefly, Ceridust 3,610 polyethylene particles (Clariant Corporation, CA, United States) were washed by ethanol and filtered using a 20 μm pore membrane. A particle size of 4.62 ± 3.76 μm was verified by an electron microscopy (Cell Science Image Facility at Stanford University). The filtered particles were vacuum dried for 3 days then resuspended using Phosphate-Buffered Saline (PBS) containing 5% Bovine Serum Albumin (BSA, Thermo Fisher Scientific). The concentration of the resuspended particles was approximately 3.1×10^{10} particles/ml. 10 ng/ml of lipopolysaccharides (LPS, Sigma-Aldrich St. Louis, MO, United States) was used to generate the contaminated particles (cPE) (Greenfield et al., 2010). The

endpoint chromogenic Limulus Amebocyte Lysate assay (Lonza, Portsmouth, NH, United States) was used to confirm the sterility of the particles.

Continuous Femoral Infusion Murine Model

The animal experiment was approved by the Institutional APLAC at Stanford University (Protocol number: 17566). Institutional Guidelines for the Care and Use of Laboratory Animals were followed in all aspects of this project. Eleven to twelve-week-old BALB/c male mice were used to generate the murine continuous femoral infusion model as previously described (Ma et al., 2008; Ren et al., 2011; Gibon et al., 2012; Sato et al., 2015, 2016; Lin et al., 2016; Nabeshima et al., 2017; Pajarinen et al., 2017; Goodman et al., 2019). The surgery was conducted on mice under preoperative analgesia by subcutaneously injection of 0.1 mg/kg of buprenorphine, and inhalation anesthesia using 1 L/min flow of 2% isoflurane in 100% oxygen on small animal surgery station at 37°C. The right distal femur was exposed after patellar dislocation via a lateral parapatellar incision. 25 gauges, 23 gauges, and 22 gauges needles were used sequentially to pierce through the intercondylar notch into the medullary cavity. A hollow titanium rod (6 mm long, 23 gauge) (**Figures 1A–D**, part III) was then press-fit into the distal canal of the femur. An osmotic pump (**Figures 1A–D**, part I) containing 10% BSA/PBS with or without contaminated polyethylene particles (cPE, 1.25% of polyethylene particles and 10 ng/ml of LPS) was implanted into dorsal side of mouse subcutaneously through a second incision around the right shoulder girdle; the pump was connected to the implanted rod via subcutaneous vinyl catheter tubing (**Figures 1A–D**, part II). Skin incisions were closed using 5–0 Ethilon sutures (J&J Medical Devices) after all the procedures. No infection was observed in any of the mice and all mice appeared to ambulate relatively normally several days after the surgical procedure. Three weeks after primary surgery, pumps (**Figures 1A–D**, part I) and connected tubing (**Figures 1A–D**, part II) were removed. 10 μl PBS with 0.5×10^6 MSCs or NF-κB sensing IL-4 over-expressing MSCs were injected through the rod into the femur (**Figures 1A–D**, part III), then pumps and tubes were changed to new ones containing 10% BSA/PBS with/without cPE, which was infused for 3 more weeks (**Figure 1E**).

Thus, there were 6 groups with/without cPE and with/without different MSCs as follows: (1) control without cPE (cPE- control group), (2) MSCs injection at 3 weeks after primary surgery without cPE (cPE- MSCs group), (3) NF-κB sensing IL-4 over-expressing MSCs injection at 3 weeks after primary surgery without cPE (cPE- IL-4 MSCs group), (4) control with cPE (cPE + control group), (5) MSCs injection at 3 weeks after primary surgery with cPE (cPE + MSCs group), (6) NF-κB sensing IL-4 over-expressing MSCs injection at 3 weeks after primary surgery with cPE (cPE + IL-4 MSCs group).

Micro-Computational Tomography

Mice were euthanized 6 weeks after the primary surgery (**Figure 1E**) and the titanium rod was removed from the distal femur. μCT scans were performed using TriFoil Imaging CT120 (TriFoil Imaging, Chatsworth, CA, United States) with 49 μm resolution. A 4 mm × 4 mm × 3 mm three-dimension (3D) region of interest (ROI) was created within the distal femur which began 3 mm from the distal end of the femur and proceeded proximally (**Figures 1C**, **2A**; Lin et al., 2016; Nabeshima et al., 2017). The threshold bone mineral density (BMD, mg/mm^3) was quantified by using GEMS MicroView software (threshold: 700 HU).

Tissue Processing and Histological Staining

Isolated femurs were fixed with 4% paraformaldehyde overnight and decalcified with 0.5 M ethylenediamine tetra acetic acid (EDTA, pH 7.4). After dehydration, the specimens were embedded in optimal cutting temperature (OCT) compounds. The ROI (**Figure 1C**) located 3 mm from the distal end of femur was cut into transverse sections with 10 μm-thickness for subsequent staining (Lin et al., 2016). Hematoxylin and Eosin (H&E) staining and immunohistochemistry were performed for general tissue morphological assessment and morphometry.

Immunohistochemistry for Macrophage Phenotype Analysis

To identify the macrophages by immunohistochemistry, the sections were covered by blocking buffer (5% BSA) for 30 min at room temperature followed by primary and secondary antibody incubation for 1 h each at room temperature. Macrophages were identified by immunofluorescence staining with rat anti-mouse F4/80 monoclonal antibody (CI: A3-1, Bio-Rad) followed by Alexa Fluor® 594 conjugated goat anti-rat IgG (Invitrogen, CA, United States). M1 pro-inflammatory macrophages were further identified by rabbit anti-mouse inducible nitric oxide synthase (iNOS) polyclonal antibody (Abcam, Cambridge, MA, United States) followed by Alexa Fluor® 488 conjugated goat anti-rabbit IgG (Invitrogen, CA, United States). M2 anti-inflammatory macrophages were identified by rabbit anti-mouse liver Arginase (Arg1) polyclonal antibody (Abcam, Cambridge, MA, United States) followed by Alexa Fluor® 488 conjugated goat anti-rabbit IgG (Invitrogen, CA, United States). ProLong Gold Antifade Mount with DAPI (Life Technologies, Grand Island, NY, United States) was used to mount the slides. A fluorescence microscope (Digital Microscope, Keyence, IL, United States) was used to detect the immunohistochemistry staining. Finally, the cells were manually counted in 3 randomly selected fields of view by Image J software (National Institutes of Health, United States).

Osteoclast-Like Cells and Osteoblast-Like Cells Detection

Osteoblast-like and osteoclast-like cells were identified as previously described (Goodman et al., 2013; Sato et al., 2015; Miron et al., 2016; Brooks et al., 2019). The tartrate resistant acid phosphatase (TRAP) staining kit (Sigma-Aldrich, St. Louis, MO, United States) was used to identify osteoclast-like cells; multi-nucleated TRAP positive cells located on the bone perimeter within the resorption lacunae were defined as osteoclast-like

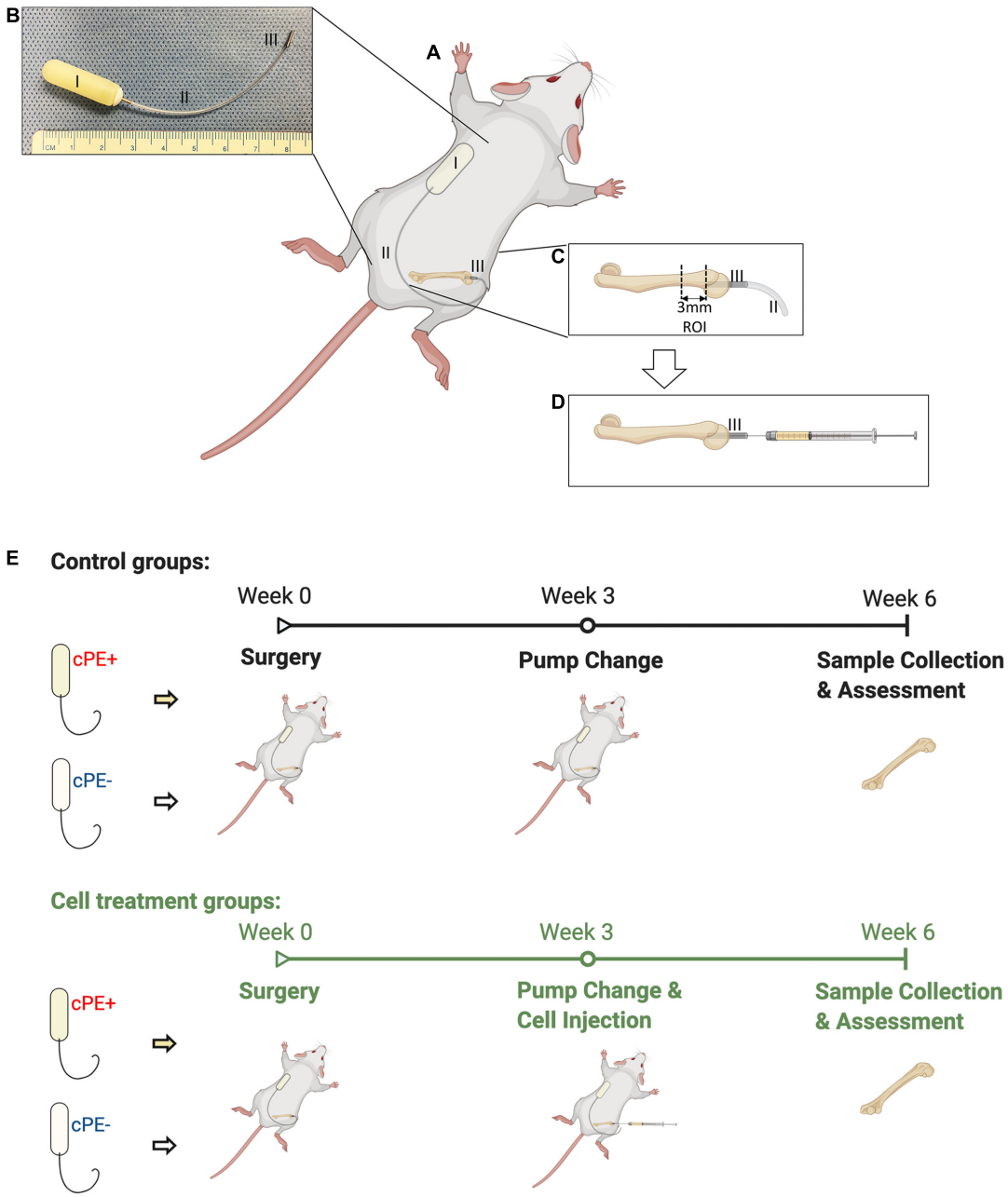

FIGURE 1 | Continuous femoral infusion murine model generation and experimental design based on the treatments. **(A)** The murine continuous femoral infusion model. **(B)** Infusion system. I: osmotic pump; II: connected tube; III: hollow titanium rod. **(C)** Rod press-fit into the distal femoral canal and the selected ROI for assessments. **(D)** Cell injection at 2nd surgery. **(E)** Summary of the treatments and experimental design.

cells. For the detection of osteoblast-like cells, anti-alkaline phosphatase staining (1-stepTM NBT/BCIP Substrate Solution, Thermo Fisher Scientific, Rockford, IL) was used. The TRAP positive cell number of 6 randomly selected areas in each section and the percentage of ALP positive area of the entire area of each section were quantified using Image J software (National Institutes of Health, United States) according to our previous protocol (Utsunomiya et al., 2021a). The color threshold of each parameter was determined by consensus of three of the investigators. Double-blinded quantitative analysis was conducted by two of the investigators.

Statistical Analysis

The statistical analysis was conducted using Prism 8 (GraphPad Software, San Diego, CA, United States). Data were expressed as median with interquartile range. Mann-Whitney *U*-test was performed to evaluate the difference between the control group with and without cPE. The Kruskal-Wallis test with Dunn's

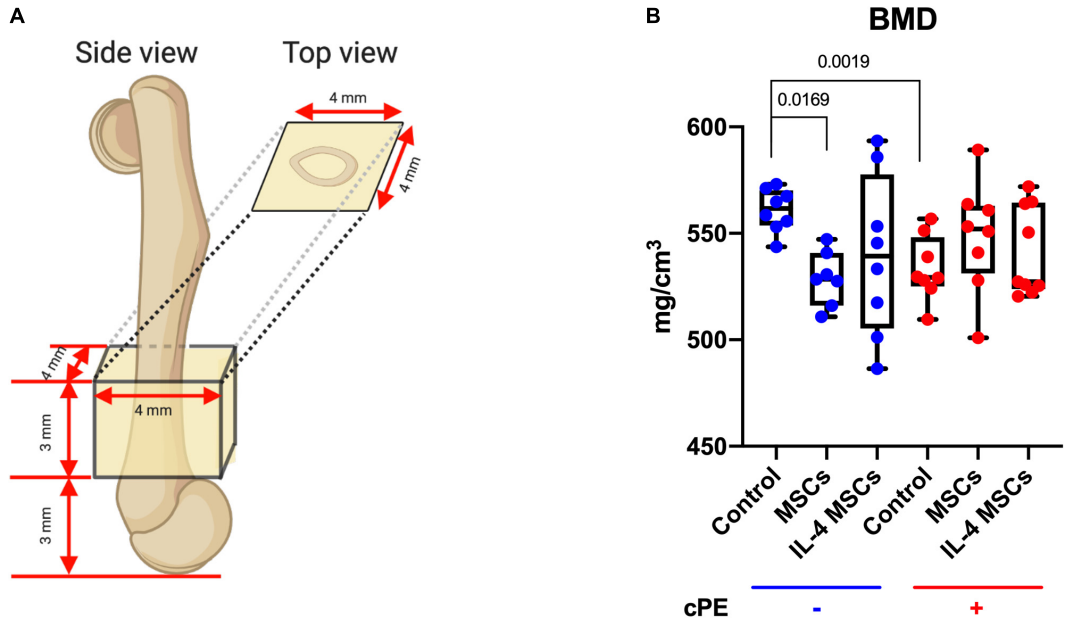

FIGURE 2 | Bone Mineral Density (BMD) within the ROI for all groups. **(A)** The 3D ROI was defined as a 4 mm × 4 mm × 3 mm box and started 3 mm from the distal femur end. **(B)** Quantitative assessments of BMD within the region of interest for all groups. (cPE- control group: $n = 8$; cPE- MSCs group: $n = 7$; cPE- IL-4 MSCs group: $n = 8$; cPE + control group: $n = 8$; cPE + MSCs group: $n = 8$; cPE + IL-4 MSCs group: $n = 9$).

multiple comparisons was used to compare data with 3 or more groups. $p < 0.05$ was regarded as statistically significant.

RESULTS

NF-κB Sensing Interleukin-4 Over-Expressing Mesenchymal Stem Cells Generation and Characterization

Murine MSCs were successfully infected by empty lentiviral vectors (Vector MSCs) and NF-κB sensing IL-4 expressing lentiviral vectors (IL-4 MSCs). GFP positive MSCs were also produced successfully (**Figure 3A**). The IL-4 secretion in the unaltered MSC group and Vector MSC group was below the detectable range by ELISA with or without 1 μg/ml LPS treatment (Lin et al., 2017b). The current LPS concentration (1 μg/ml) was used according to the protocols of previous studies investigating the effect of LPS on MSCs with the goal of reliably inducing NF-κB activation rather than modeling any specific disease state (Pevsner-Fischer et al., 2007; Wang et al., 2009; Ti et al., 2015). IL-4 secretion in the IL-4 MSCs group was significantly upregulated by 1 μg/ml LPS treatment for 24 h (from 97.75 ± 11.29 pg/ml to 1832.55 ± 105.19 pg/ml, **Figure 3B**).

Local Injection of Cells Decreased M1 Macrophage and Increased M2 Macrophage Proportions in the Presence of Contaminated Particles

The proportion of M1 pro-inflammatory macrophages (iNOS+, F4/80+) in cPE + control group was significantly increased compared with that in cPE- control group ($p = 0.0002$) (**Figures 4A,B**). Local injection of MSCs significantly decreased the proportion of M1 macrophages when comparing cPE + MSCs group with cPE + control group ($p = 0.0297$). Local injection of NF-κB sensing IL-4 over-expressing MSCs also significantly decreased the proportion of M1 macrophages when comparing cPE + IL-4 MSCs group with cPE + control group ($p = 0.0029$) (**Figures 4A,B**). The M2 anti-inflammatory macrophage (Arg1+, F4/80+) proportion in cPE + control group was significantly decreased compared with that in cPE- control group ($P = 0.0001$) (**Figures 4C,D**). Local injection of MSCs and NF-κB sensing IL-4 over-expressing MSCs significantly increased the proportion of M2 macrophages when comparing cPE + MSCs group with cPE + control group ($p = 0.0001$) and comparing cPE + IL-4 MSCs group with cPE + control group ($p = 0.0112$) (**Figures 4C,D**).

Local Injection of Cells Reduced the Osteoclast-Like Cell Number Induced by Contaminated Particles

The TRAP staining positive cell number in cPE + control group was significantly increased compared with that in the cPE- control group ($p = 0.0041$) (**Figures 5A,B**). Local injection of cells including MSCs and NF-κB sensing IL-4 over-expressing MSCs significantly reduced the TRAP positive cell number in cPE + MSCs group and cPE + IL-4 MSCs group when compared with the cPE + control group ($p = 0.00209$, $p = 0.0491$, respectively). No differences were observed among cPE- groups with or without injection of cells (**Figures 5A,B**).

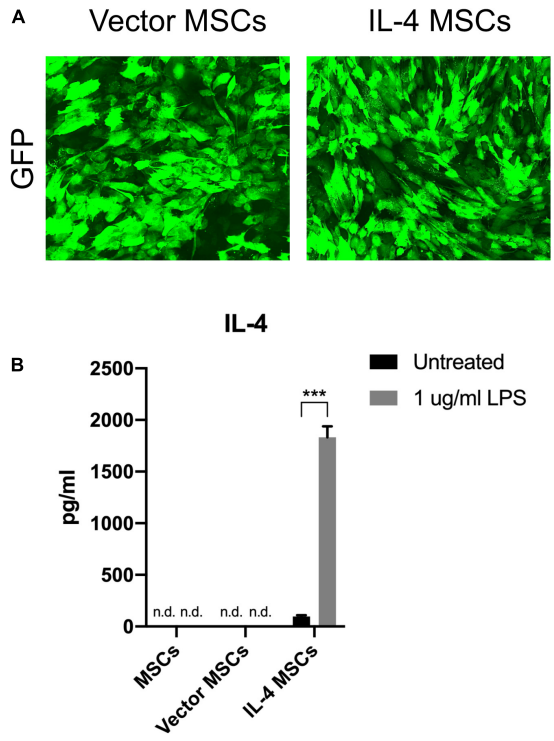

FIGURE 3 | Characterization of MSCs and genetically modified MSCs. **(A)** Representative fluorescence microscopy images of genetically modified MSCs. **(B)** IL-4 secreting levels detected by ELISA in the culture media with or without 1 μg/ml LPS treatment for 24 h (n.d.: cannot be detected by ELISA; ***: $p < 0.001$). Note the high levels of IL-4 protein produced by the IL-4 MSCs exposed to LPS.

Local Injection of Cells Increased the Positive Staining Area of Osteoblast-Like Cells

The percentage of ALP positive area in cPE + control group showed decreased staining compared with that in the cPE- control group, but the decrease did not reach statistical significance (**Figures 6A,B**). The percentage of ALP positive area in cPE + MSCs group was significantly ($p = 0.0198$) increased compared with that in the cPE + control groups (**Figure 6B**) and the percentage of ALP positive area in the cPE + IL-4 MSCs group exhibited a strong trend ($p = 0.0679$) when compared with that in the cPE + control group (**Figure 6B**). The percentage of ALP positive area in the cPE- MSCs group increased significantly compared with that in the cPE- control group ($p = 0.0204$). The percentage of ALP positive area in the cPE- IL-4 MSCs group demonstrated a dramatic increase ($p = 0.00091$) compared with that in the cPE- control group (**Figure 6B**).

Local Injection of Mesenchymal Stem Cells Mitigates Contaminated Particles-Induced Bone Loss in Chronic Inflammation

The BMD in the ROI (**Figure 2A**) of the cPE + control group was significantly reduced compared with the BMD of the cPE- control group ($p = 0.0019$). Local injection of MSCs and NF-κB sensing IL-4 over-expressing MSCs in the presence of cPE increased the BMD compared with the cPE + control group although no significant differences were detected. Interestingly, after local injection of MSCs in the cPE- groups, the cPE- MSCs group showed significantly lower BMD compared with the cPE- control group ($p = 0.0169$). The cPE- IL-4 MSCs group also showed slightly lower BMD compared with the cPE- control group, but no significant difference was detected (**Figure 2B**).

DISCUSSION

Chronic inflammation around implants due to byproducts of wear or other causes (e.g., instability, low grade infection etc.) is still a major an unsolved problem. We have demonstrated that local delivery of contaminated polyethylene particles (cPE) can induce acute or chronic inflammation and polarize macrophages to a pro-inflammatory M1 rather than an anti-inflammatory M2 macrophage phenotype in different *in vitro* and *in vivo* models (Utsunomiya et al., 2021a,b). Macrophages are the characteristic cell type involved in chronic inflammation (Allison et al., 1978; Maruyama et al., 2020); furthermore modulation of macrophage phenotype at an appropriate time can optimize osteogenic differentiation of MSCs (Lin et al., 2019) and the enhancement of the bone regeneration (Chow et al., 2019; Niu et al., 2021). The increased pro-inflammatory M1 macrophage proportion and the decreased anti-inflammatory M2 macrophage proportion caused by cPE over a 3-week period was subsequently reduced by the local injection of MSCs and NF-κB sensing IL-4 over-expressing MSCs at harvest 3 weeks later. The increased TRAP positive osteoclast-like cell number, the lower ALP positive osteoblast-like area and BMD trend in the presence of cPE infusion further confirmed that the cPE could induce bone loss (Lin et al., 2016, 2017a; Pajarinen et al., 2017; Utsunomiya et al., 2021a,b). The injection of MSCs and NF-κB sensing IL-4 over-expressing MSCs reversed these findings in part.

The results of TRAP staining (**Figure 5**) showed significant differences between control groups with and without cPE. However, only a trend was noted when assessing ALP staining comparing cPE- control group with cPE + control group. Similar results concerning the TRAP and ALP staining were observed in other reports using the murine continuous infusion model with polyethylene particles (Lin et al., 2016, 2017a). This suggests that the cPE might selectively affect the regulation of osteoclastogenesis more than osteoblastogenesis. Therapeutic strategies targeting the regulation of osteoclastogenesis could be a promising approach to limit the bone loss due to wear particles. Interestingly, similar efficacy was observed between controls vs. the MSCs or IL-4 MSCs group in the presence of cPE, respectively. It would appear that unaltered MSCs are sufficiently activated to downregulate the chronic inflammation induced by cPE.

The presence of cPE significantly reduced BMD in the control groups. Previous reports showed that injection of MSCs and preconditioning of MSCs during the chronic inflammation stage could increase the BMD in the presence of cPE (Utsunomiya et al., 2021a). In the current study, local injection of MSCs and

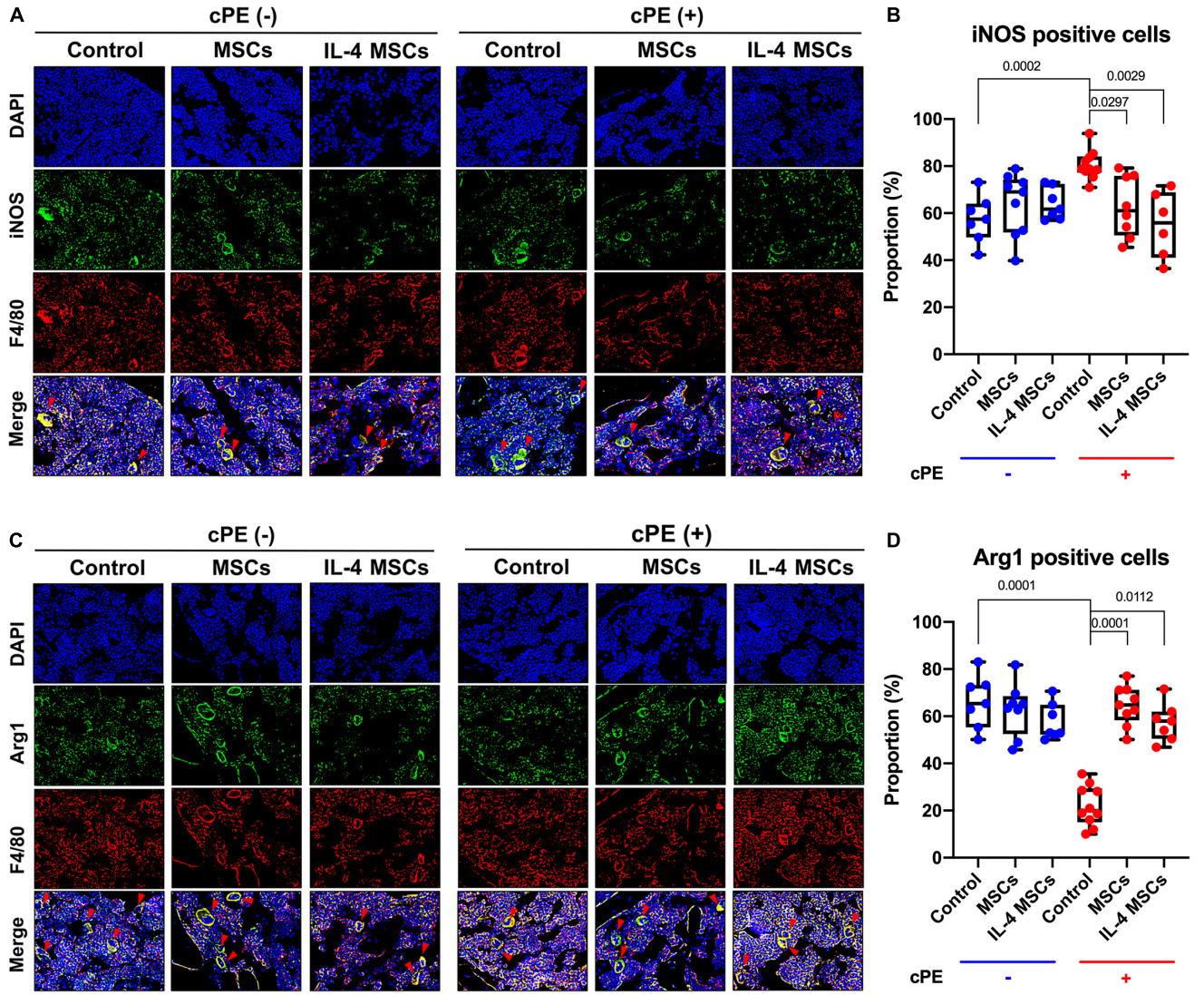

FIGURE 4 | Immunohistochemistry and quantitative analysis for M1 and M2 macrophages in all groups. **(A)** Representative images of immunohistochemistry for M1 macrophages (iNOS + , F4/80 + , red arrows). **(B)** Quantitative analysis for iNOS positive cell proportion (cPE- control group: $n = 7$; cPE- MSCs group: $n = 9$; cPE- IL-4 MSCs group: $n = 7$; cPE + control group: $n = 10$; cPE + MSCs group: $n = 8$; cPE + IL-4 MSCs group: $n = 6$). **(C)** Representative images of immunohistochemistry for M2 macrophages (Arg1 + , F4/80 + red arrows). **(D)** Quantitative analysis for Arg1 positive cell proportion (cPE- control group: $n = 7$; cPE- MSCs group: $n = 8$; cPE- IL-4 MSCs group: $n = 7$; cPE + control group: $n = 10$; cPE + MSCs group: $n = 9$; cPE + IL-4 MSCs group: $n = 7$).

NF-κB sensing IL-4 over-expressing MSCs also tended to increase BMD in the presence of cPE. Surprisingly, local injection of MSCs reduced the BMD without cPE. The possible reasons for these observations may be that this is a shorter-term model of a complex process, and BMD may be less sensitive than other methods of analysis to determine efficacy using the parameters chosen for this experiment. In fact, we observed confirmatory differences in the histological and immunohistological results, which are consistent with our previous *in vitro* studies. Possible reasons for the lack of difference in BMD may be the specific shorter-term model used, the particle load chosen, the well-established and efficacious immunomodulatory properties of MSCs alone and the production of IL-4 by the MSCs. A longer time period for particle infusion and resultant bone loss, and for subsequent cell delivery may further highlight the potential efficiency of MSCs and NF-κB sensing IL-4 over-expressing MSCs in the murine cPE infusion model.

Nuclear factor kappa-light-chain- enhancer of activated B cells (NF-κB) is the key transcription factor associated with chronic inflammation and osteolysis (Xu et al., 2009; Abu-Amer, 2013; Zuo et al., 2018). Previous studies have shown that suppression of NF-κB by its decoy oligodeoxynucleotides (ODNs) could enhance osteogenesis in MSCs exposed to polyethylene particles *in vitro* (Lin et al., 2015) and mitigate the *in vivo* particle induced chronic inflammatory osteolysis (Lin et al., 2016, 2017a; Utsunomiya et al., 2021b). In the current study, NF-κB sensing

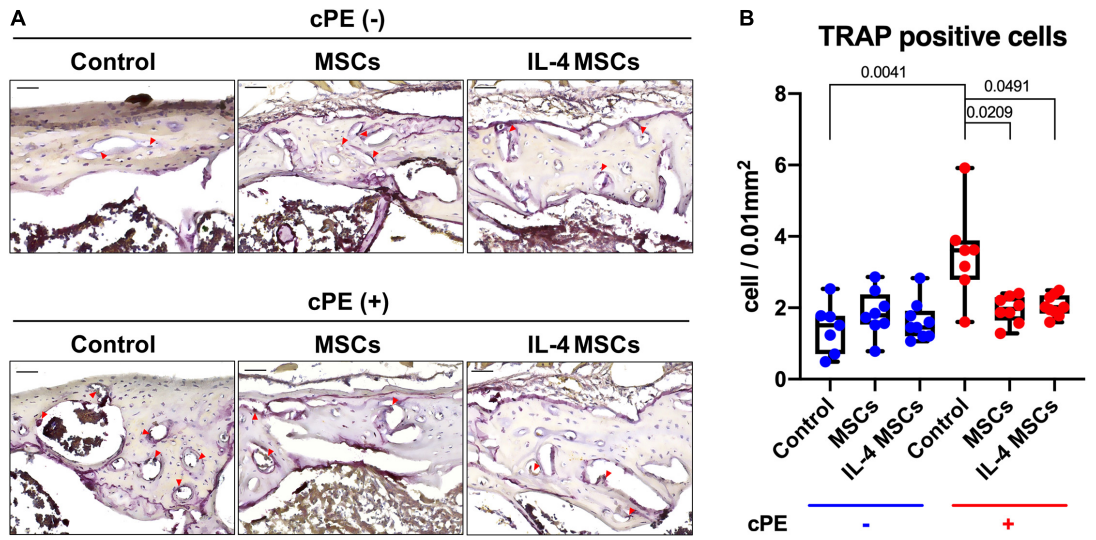

FIGURE 5 | TRAP staining of all the groups. **(A)** Representative images of TRAP staining, red arrows point the TRAP positive cells. **(B)** Quantitative analysis of TRAP positive cells number. (cPE- control group: *n* = 7; cPE- MSCs group: *n* = 8; cPE- IL-4 MSCs group: *n* = 9; cPE + control group: *n* = 7; cPE + MSCs group: *n* = 8; cPE + IL-4 MSCs group: *n* = 9).

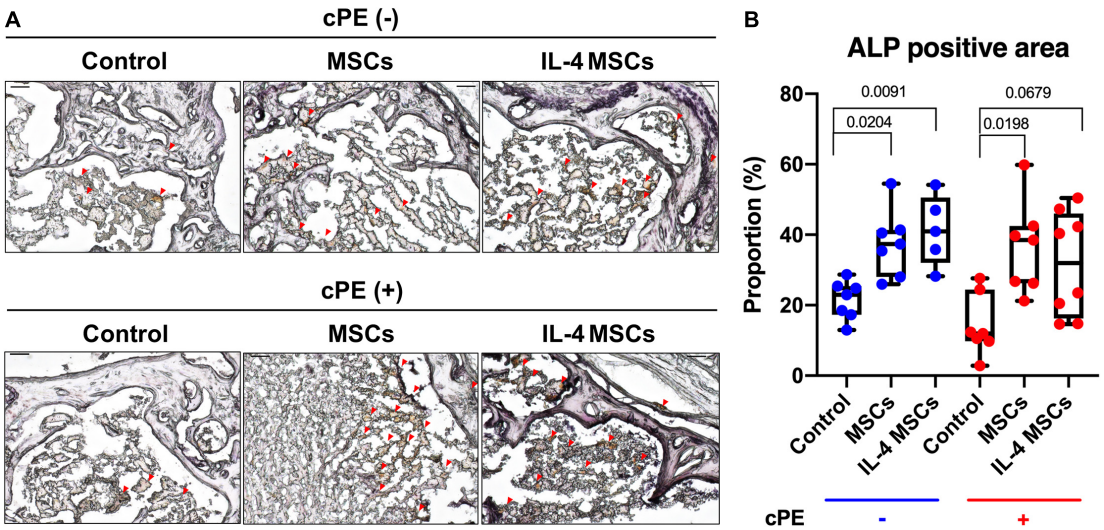

FIGURE 6 | ALP staining of all the groups. **(A)** Representative images of ALP staining, red arrows point the ALP positive area. **(B)** Quantitative analysis of ALP positive proportion. (cPE- control group: *n* = 7; cPE- MSCs group: *n* = 7; cPE- IL-4 MSCs group: *n* = 5; cPE + control group: *n* = 7; cPE + MSCs group: *n* = 7; cPE + IL-4 MSCs group: *n* = 8).

IL-4 secreting MSCs produced IL-4 when the NF-κB pathway was activated by inflammatory signals; IL-4 production ceased when the inflammatory activation signal was withdrawn (Lin et al., 2017b). IL-4 was only expressed by the genetically modified MSCs during the ongoing chronic inflammation period, limiting potential adverse effects caused by excessive IL-4 expression (Lin et al., 2017b; Zhang et al., 2021). This feedback mechanism would be potentially useful in other inflammatory conditions in other organ systems.

Surprisingly, the unaltered MSCs were as effective as the NF-κB sensing IL-4 over-expressing MSCs in reversing the adverse effects of cPE on bone. This may be due to the specific animal model chosen, and the duration and particle load delivered. The efficacious immunomodulatory properties of MSCs by themselves with/without the over-production of IL-4 may be the potential reason for this comparable effectiveness. More prolonged and intense inflammatory stimuli may demonstrate an augmented utility of NF-κB sensing IL-4 over-expressing MSCs in chronic inflammation.

The current study has some limitations. Unaltered MSCs were locally injected rather than MSCs infected with an empty vector (vector-MSCs) to investigate the efficacy of naïve

MSCs. Six weeks of continuous cPE infusion is a relatively shorter-term time period compared to the longer-term process associated with periprosthetic osteolysis in clinical scenarios. Only one time point at week 6 analysis was conducted; multiple time points for analysis would be more informative about this process. The generation of MSCs with combinations of co-expressing cytokines, growth factors, or chemokines to enhance the bone regeneration (Nabeshima et al., 2017; Zhang et al., 2020, 2021) in the presence of wear particles might be more efficient in mitigating the particle induced chronic inflammatory bone loss.

In summary, continuous infusion of cPE into the femur increased the pro-inflammatory M1 macrophage phenotype and decreased the anti-inflammatory M2 macrophage phenotype. Also, cPE increased osteoclastogenesis and lowered BMD. Local delivery of either MSCs or NF-κB sensing IL-4 over-expressing MSCs is a potential therapeutic intervention in mitigating particle-associated chronic inflammatory bone loss.

DATA AVAILABILITY STATEMENT

The raw data supporting the conclusions of this article will be made available by the authors, without undue reservation.

ETHICS STATEMENT

The animal study was reviewed and approved by the Stanford's Administrative Panel on Laboratory Animal Care (APLAC).

AUTHOR CONTRIBUTIONS

NZ and TU contributed to the study design, acquisition, analysis and interpretation of data, drafting and revision of the manuscript. TL, YK, MU, MM, EH, and CR contributed to the acquisition and analysis and interpretation of data. ZY contributed to the study design and interpretation of data. SG contributed to the study conceptualization and design, interpretation of data, and critical revision of the manuscript. All authors approved the submission of the manuscript.

FUNDING

This work was supported by the NIH grants R01AR073145 and R01AR063717 from NIAMS and the Ellenburg Chair in Surgery at Stanford University.

REFERENCES

Abu-Amer, Y. (2013). NF-kappaB signaling and bone resorption. *Osteoporos. Int.* 24, 2377–2386. doi: 10.1007/s00198-013-2313-x

Allison, A. C., Ferluga, J., Prydz, H., and Schorlemmer, H. U. (1978). The role of macrophage activation in chronic inflammation. *Agents Actions* 8, 27–35. doi: 10.1007/bf01972398

Bi, Y., Seabold, J. M., Kaar, S. G., Ragab, A. A., Goldberg, V. M., Anderson, J. M., et al. (2001). Adherent endotoxin on orthopedic wear particles stimulates cytokine production and osteoclast differentiation. *J. Bone Miner. Res.* 16, 2082–2091. doi: 10.1359/jbmr.2001.16.11.2082

Brooks, P. J., Glogauer, M., and McCulloch, C. A. (2019). An overview of the derivation and function of multinucleated giant cells and their role in pathologic processes. *Am. J. Pathol.* 189, 1145–1158. doi: 10.1016/j.ajpath.2019.02.006

Caplan, A. I. (1991). Mesenchymal stem cells. *J. Orthop. Res.* 9, 641–650.

Chow, S. K., Chim, Y. N., Wang, J., Zhang, N., Wong, R. M., Tang, N., et al. (2019). Vibration treatment modulates macrophage polarisation and enhances early inflammatory response in oestrogen-deficient osteoporotic-fracture healing. *Eur. Cell. Mater.* 38, 228–245. doi: 10.22203/ecm.v038a16

Gibon, E., Batke, B., Jawad, M. U., Fritton, K., Rao, A., Yao, Z., et al. (2012). MC3T3-E1 osteoprogenitor cells systemically migrate to a bone defect and enhance bone healing. *Tissue Eng. Part A* 18, 968–973. doi: 10.1089/ten.tea.2011.0545

Goodman, S. B. (2007). Wear particles, periprosthetic osteolysis and the immune system. *Biomaterials* 28, 5044–5048. doi: 10.1016/j.biomaterials.2007.06.035

Goodman, S. B., Gibon, E., Pajarinen, J., Lin, T. H., Keeney, M., Ren, P. G., et al. (2014). Novel biological strategies for treatment of wear particle-induced periprosthetic osteolysis of orthopaedic implants for joint replacement. *J. R. Soc. Interface* 11:20130962. doi: 10.1098/rsif.2013.0962

Goodman, S. B., Gibon, E., and Yao, Z. (2013). The basic science of periprosthetic osteolysis. *Instr. Course Lect.* 62, 201–206.

Goodman, S. B., Pajarinen, J., Yao, Z., and Lin, T. (2019). Inflammation and bone repair: from particle disease to tissue regeneration. *Front. Bioeng. Biotechnol.* 7:230. doi: 10.3389/fbioe.2019.00230

Greenfield, E. M., Beidelschies, M. A., Tatro, J. M., Goldberg, V. M., and Hise, A. G. (2010). Bacterial pathogen-associated molecular patterns stimulate biological activity of orthopaedic wear particles by activating cognate Toll-like receptors. *J. Biol. Chem.* 285, 32378–32384. doi: 10.1074/jbc.m110.136895

Kurtz, S. M., Ong, K. L., Lau, E., and Bozic, K. J. (2014). Impact of the economic downturn on total joint replacement demand in the United States: updated projections to 2021. *J. Bone Joint Surg. Am.* 96, 624–630. doi: 10.2106/jbjs.m.00285

Lin, T., Kohno, Y., Huang, J. F., Romero-Lopez, M., Maruyama, M., Ueno, M., et al. (2019). Preconditioned or IL4-Secreting mesenchymal stem cells enhanced osteogenesis at different stages. *Tissue Eng. Part A* 25, 1096–1103. doi: 10.1089/ten.tea.2018.0292

Lin, T., Kohno, Y., Huang, J. F., Romero-Lopez, M., Pajarinen, J., Maruyama, M., et al. (2018). NFkappaB sensing IL-4 secreting mesenchymal stem cells mitigate the proinflammatory response of macrophages exposed to polyethylene wear particles. *J. Biomed. Mater. Res. A* 106, 2744–2752. doi: 10.1002/jbm.a.36504

Lin, T., Pajarinen, J., Nabeshima, A., Lu, L., Nathan, K., Yao, Z., et al. (2017b). Establishment of NF-κB sensing and interleukin-4 secreting mesenchymal stromal cells as an "on-demand" drug delivery system to modulate inflammation. *Cytotherapy* 19, 1025–1034. doi: 10.1016/j.jcyt.2017.06.008

Lin, T., Pajarinen, J., Nabeshima, A., Córdova, L. A., Loi, F., Gibon, E., et al. (2017a). Orthopaedic wear particle-induced bone loss and exogenous macrophage infiltration is mitigated by local infusion of NF-κB decoy oligodeoxynucleotide. *J. Biomed. Mater. Res. Part A* 105, 3169–3175. doi: 10.1002/jbm.a.36169

Lin, T. H., Pajarinen, J., Sato, T., Loi, F., Fan, C., Cordova, L. A., et al. (2016). NF-kappaB decoy oligodeoxynucleotide mitigates wear particle-associated bone loss in the murine continuous infusion model. *Acta Biomater.* 41, 273–281. doi: 10.1016/j.actbio.2016.05.038

Lin, T. H., Sato, T., Barcay, K. R., Waters, H., Loi, F., Zhang, R., et al. (2015). NF-kappaB decoy oligodeoxynucleotide enhanced osteogenesis in mesenchymal stem cells exposed to polyethylene particle. *Tissue Eng. Part A* 21, 875–883. doi: 10.1089/ten.tea.2014.0144

Ma, T., Huang, Z., Ren, P. G., McCally, R., Lindsey, D., Smith, R. L., et al. (2008). An in vivo murine model of continuous intramedullary infusion of polyethylene particles. *Biomaterials* 29, 3738–3742. doi: 10.1016/j.biomaterials.2008.05.031

Maruyama, M., Rhee, C., Utsunomiya, T., Zhang, N., Ueno, M., Yao, Z., et al. (2020). Modulation of the inflammatory response and bone healing. *Front. Endocrinol. (Lausanne)* 11:386. doi: 10.3389/fendo.2020.00386

Miron, R. J., Zohdi, H., Fujioka-Kobayashi, M., and Bosshardt, D. D. (2016). Giant cells around bone biomaterials: osteoclasts or multi-nucleated giant cells? *Acta Biomater.* 46, 15–28. doi: 10.1016/j.actbio.2016.09.029

Nabeshima, A., Pajarinen, J., Lin, T. H., Jiang, X., Gibon, E., Cordova, L. A., et al. (2017). Mutant CCL2 protein coating mitigates wear particle-induced bone loss in a murine continuous polyethylene infusion model. *Biomaterials* 117, 1–9.

Niu, Y., Wang, Z., Shi, Y., Dong, L., and Wang, C. (2021). Modulating macrophage activities to promote endogenous bone regeneration: biological mechanisms and engineering approaches. *Bioact. Mater.* 6, 244–261. doi: 10.1016/j.bioactmat.2020.08.012

Pajarinen, J., Lin, T. H., Sato, T., Loi, F., Yao, Z., Konttinen, Y. T., et al. (2015). Establishment of green fluorescent protein and firefly luciferase expressing mouse primary macrophages for in vivo bioluminescence imaging. *PLoS One* 10:e0142736. doi: 10.1371/journal.pone.0142736

Pajarinen, J., Nabeshima, A., Lin, T. H., Sato, T., Gibon, E., Jamsen, E., et al. (2017). Murine model of progressive orthopedic wear particle-induced chronic inflammation and osteolysis. *Tissue Eng. Part C Methods* 23, 1003–1011. doi: 10.1089/ten.tec.2017.0166

Pevsner-Fischer, M., Morad, V., Cohen-Sfady, M., Rousso-Noori, L., Zanin-Zhorov, A., Cohen, S., et al. (2007). Toll-like receptors and their ligands control mesenchymal stem cell functions. *Blood* 109, 1422–1432. doi: 10.1182/blood-2006-06-028704

Qiu, J., Peng, P., Xin, M., Wen, Z., Chen, Z., Lin, S., et al. (2020). ZBTB20-mediated titanium particle-induced peri-implant osteolysis by promoting macrophage inflammatory responses. *Biomater. Sci.* 8, 3147–3163. doi: 10.1039/d0bm00147c

Ren, P. G., Irani, A., Huang, Z., Ma, T., Biswal, S., and Goodman, S. B. (2011). Continuous infusion of UHMWPE particles induces increased bone macrophages and osteolysis. *Clin. Orthop. Relat. Res.* 469, 113–122. doi: 10.1007/s11999-010-1645-5

Sato, T., Pajarinen, J., Behn, A., Jiang, X., Lin, T. H., Loi, F., et al. (2016). The effect of local IL-4 delivery or CCL2 blockade on implant fixation and bone structural properties in a mouse model of wear particle induced osteolysis. *J. Biomed. Mater. Res. A* 104, 2255–2262. doi: 10.1002/jbm.a.35759

Sato, T., Pajarinen, J., Lin, T. H., Tamaki, Y., Loi, F., Egashira, K., et al. (2015). NF-kappaB decoy oligodeoxynucleotide inhibits wear particle-induced inflammation in a murine calvarial model. *J. Biomed. Mater. Res. A* 103, 3872–3878. doi: 10.1002/jbm.a.35532

Ti, D., Hao, H., Tong, C., Liu, J., Dong, L., Zheng, J., et al. (2015). LPS-preconditioned mesenchymal stromal cells modify macrophage polarization for resolution of chronic inflammation via exosome-shuttled let-7b. *J. Transl. Med.* 13:308.

Utsunomiya, T., Zhang, N., Lin, T., Kohno, Y., Ueno, M., Maruyama, M., et al. (2021a). Different effects of intramedullary injection of mesenchymal stem cells during the acute vs. chronic inflammatory phase on bone healing in the murine continuous polyethylene particle infusion model. *Front. Cell Dev. Biol.* 9:631063. doi: 10.3389/fcell.2021.631063

Utsunomiya, T., Zhang, N., Lin, T., Kohno, Y., Ueno, M., Maruyama, M., et al. (2021b). Suppression of NF-kappaB-induced chronic inflammation mitigates inflammatory osteolysis in the murine continuous polyethylene particle infusion model. *J. Biomed. Mater. Res. A* 109, 1828–1839. doi: 10.1002/jbm.a.37175

Wang, Z. J., Zhang, F. M., Wang, L. S., Yao, Y. W., Zhao, Q., and Gao, X. (2009). Lipopolysaccharides can protect mesenchymal stem cells (MSCs) from oxidative stress-induced apoptosis and enhance proliferation of MSCs via Toll-like receptor(TLR)-4 and PI3K/Akt. *Cell Biol. Int.* 33, 665–674. doi: 10.1016/j.cellbi.2009.03.006

Wei, W., Huang, Y., Li, D., Gou, H. F., and Wang, W. (2018). Improved therapeutic potential of MSCs by genetic modification. *Gene Ther.* 25, 538–547. doi: 10.1038/s41434-018-0041-8

Xu, J., Wu, H. F., Ang, E. S., Yip, K., Woloszyn, M., Zheng, M. H., et al. (2009). NF-kappaB modulators in osteolytic bone diseases. *Cytokine Growth Factor Rev.* 20, 7–17. doi: 10.1016/j.cytogfr.2008.11.007

Zhang, N., Chim, Y. N., Wang, J., Wong, R. M. Y., Chow, S. K. H., and Cheung, W. H. (2020). Impaired fracture healing in sarco-osteoporotic mice can be rescued by vibration treatment through myostatin suppression. *J. Orthop. Res.* 38, 277–287. doi: 10.1002/jor.24477

Zhang, N., Lo, C. W., Utsunomiya, T., Maruyama, M., Huang, E., Rhee, C., et al. (2021). PDGF-BB and IL-4 co-overexpression is a potential strategy to enhance mesenchymal stem cell-based bone regeneration. *Stem Cell Res. Ther.* 12:40.

Zuo, C., Zhao, X., Shi, Y., Wu, W., Zhang, N., Xu, J., et al. (2018). TNF-alpha inhibits SATB2 expression and osteoblast differentiation through NF-kappaB and MAPK pathways. *Oncotarget* 9, 4833–4850. doi: 10.18632/oncotarget.23373

Conflict of Interest: The authors declare that the research was conducted in the absence of any commercial or financial relationships that could be construed as a potential conflict of interest.

Publisher's Note: All claims expressed in this article are solely those of the authors and do not necessarily represent those of their affiliated organizations, or those of the publisher, the editors and the reviewers. Any product that may be evaluated in this article, or claim that may be made by its manufacturer, is not guaranteed or endorsed by the publisher.

frontiers in Cell and Developmental Biology

REVIEW
published: 09 November 2021
doi: 10.3389/fcell.2021.790050

Biophysical Stimuli as the Fourth Pillar of Bone Tissue Engineering

Zhuowen Hao[1†], Zhenhua Xu[1†], Xuan Wang[1†], Yi Wang[1], Hanke Li[1], Tianhong Chen[1], Yingkun Hu[1], Renxin Chen[1], Kegang Huang[2], Chao Chen[3,4] and Jingfeng Li[1]**

[1]Department of Orthopedics, Zhongnan Hospital of Wuhan University, Wuhan, China, [2]Wuhan Institute of Proactive Health Management Science, Wuhan, China, [3]Department of Orthopedics, Union Hospital, Tongji Medical College, Huazhong University of Science and Technology, Wuhan, China, [4]Department of Orthopedics, Hefeng Central Hospital, Enshi, China

The repair of critical bone defects remains challenging worldwide. Three canonical pillars (biomaterial scaffolds, bioactive molecules, and stem cells) of bone tissue engineering have been widely used for bone regeneration in separate or combined strategies, but the delivery of bioactive molecules has several obvious drawbacks. Biophysical stimuli have great potential to become the fourth pillar of bone tissue engineering, which can be categorized into three groups depending on their physical properties: internal structural stimuli, external mechanical stimuli, and electromagnetic stimuli. In this review, distinctive biophysical stimuli coupled with their osteoinductive windows or parameters are initially presented to induce the osteogenesis of mesenchymal stem cells (MSCs). Then, osteoinductive mechanisms of biophysical transduction (a combination of mechanotransduction and electrocoupling) are reviewed to direct the osteogenic differentiation of MSCs. These mechanisms include biophysical sensing, transmission, and regulation. Furthermore, distinctive application strategies of biophysical stimuli are presented for bone tissue engineering, including predesigned biomaterials, tissue-engineered bone grafts, and postoperative biophysical stimuli loading strategies. Finally, ongoing challenges and future perspectives are discussed.

Keywords: biophysical stimuli, mesenchymal stem cells, osteoinductive mechanisms, biophysical transduction, osteogenesis

OPEN ACCESS

Edited by:
Guohui Liu,
Huazhong University of Science and Technology, China

Reviewed by:
Zhong Wu,
Tongji University, China
Min Nie,
Cornell University, United States

****Correspondence:***
Chao Chen
chenchao027@163.com
Jingfeng Li
jingfengli@whu.edu.cn

†These authors have contributed equally to this work

Specialty section:
This article was submitted to Stem Cell Research, a section of the journal Frontiers in Cell and Developmental Biology

Received: *06 October 2021*
Accepted: *26 October 2021*
Published: *09 November 2021*

Citation:
Hao Z, Xu Z, Wang X, Wang Y, Li H, Chen T, Hu Y, Chen R, Huang K, Chen C and Li J (2021) Biophysical Stimuli as the Fourth Pillar of Bone Tissue Engineering. Front. Cell Dev. Biol. 9:790050. doi: 10.3389/fcell.2021.790050

1 INTRODUCTION

After trauma, bone tissue shows self-healing property, but this ability is limited for critical bone defects (average diameter over 2 cm in humans) caused by serious injury, tumor excision, or other orthopedic diseases (Lopes et al., 2018). Bone healing failure, which occurs in 5–10% of all patients with bone fracture, generally causes delayed union (healing process over 3 months) or non-union (healing process over 9 months without obvious bone regeneration in the first 3 months) (Zura et al., 2016; Wojda and Donahue, 2018). Autologous bone grafting is currently the gold standard for the healing of critical bone defects because it provides three critical components: an osteoconductive substrate, osteoinducive signals, and preosteoblastic cells (Yong et al., 2020). However, the strategy fails to meet clinical requirements because of limited autografts, potential donor site complications (such as infections, chronic pain, and bleeding), and the risk of graft failure (Roseti et al., 2017; Yang et al., 2018).

Bone tissue engineering has been becoming an ideal strategy to replace autologous bone grafting, and it is composed of three pillars to emulate the basic components of autografts: biomaterial scaffolds, bioactive molecules, and stem cells (Huang et al., 2020). Bioactive molecules are generally

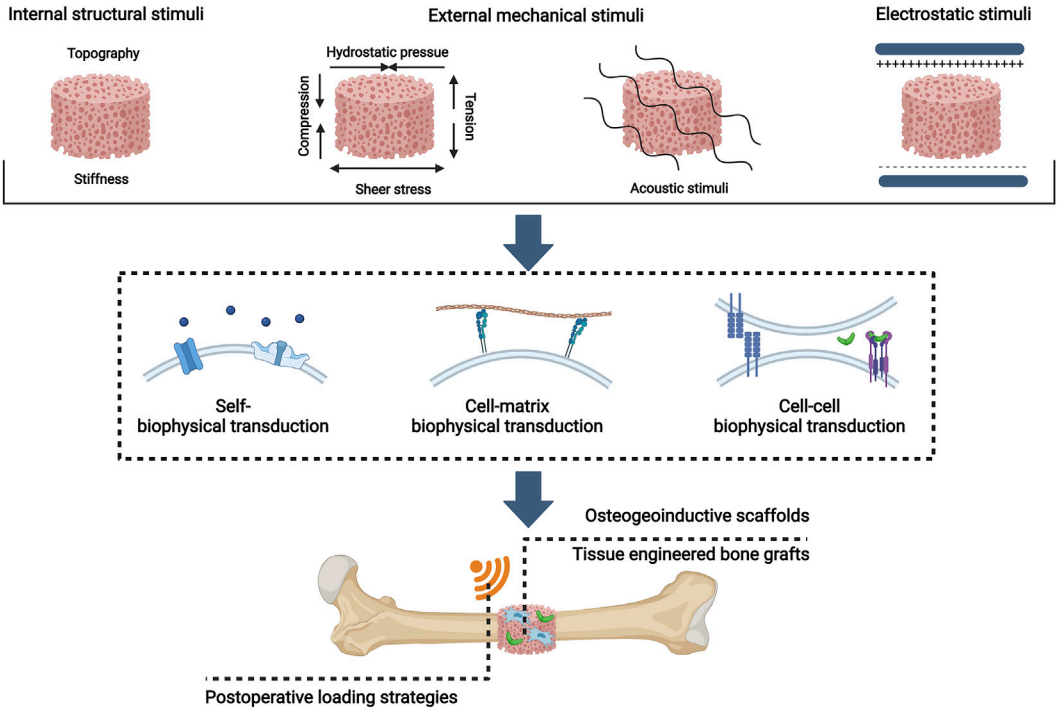

FIGURE 1 | Overview of biophysical stimuli for bone tissue engineering: distinctive patterns, osteoinductive mechanisms, and bone tissue engineering applications. Created with BioRender.com.

in the form of recombinant growth factors or small molecular bioactive peptides to provide osteoinductive properties (Yang et al., 2018). But the delivery of bioactive molecules shows some limitations: 1) initial burst release, 2) declined biological activity, 3) high therapeutic dosage, and 4) potential side effects (Krishnan et al., 2017; Bertrand et al., 2020). Therefore, another pillar showing osteoinductive properties needs to be incorporated into bone tissue engineering for bone regeneration or bone healing.

Biophysical stimuli have attracted great attention for bone regeneration because of their great promise as the fourth pillar of bone tissue engineering. From Wolff's law to Frost's "mechanostat theory", a plethora of evidence verifies that bone is a mechanosensitive tissue (Tyrovola 2015; Haffner-Luntzer et al., 2016; Qin E. C. et al., 2020). Multiple bone cells that respond to biophysical stimuli include osteocytes, osteoblasts, osteoclasts, bone lining cells, and mesenchymal stem cells (MSCs) (Steward and Kelly, 2015; Stewart et al., 2020). In bone tissue engineering, the osteogenic differentiation of MSCs is the most important process. Therefore, this review focuses on the osteoinductive effects of biophysical stimuli toward MSCs. Biophysical stimuli with osteoinductive properties can be categorized into three groups depending on their physical properties: internal structural stimuli, external mechanical stimuli, and electromagnetic stimuli.

External mechanical stimuli were proposed as the fourth pillar of bone regeneration by Lopes et al. (2018). Here we suggest that the concept can cover even more comprehensive forms of biophysical stimuli. In this review, we first update the fourth pillar of bone tissue engineering as biophysical stimuli and summarize distinctive biophysical stimuli with their osteoinductive windows for MSC osteogenesis, including internal structural stimuli, external mechanical stimuli, and electromagnetic stimuli. Then, a novel concept of biophysical transduction (a process of sensing, transmission, and regulation) that incorporates mechanotransduction and electrocoupling is proposed to interpret the osteoinductive mechanisms of biophysical stimuli for the osteogenic differentiation of MSCs. And biophysical stimuli, depending on sensing mechanisms, can be divided into self-biophysical transduction, cell-matrix transduction, and cell-cell biophysical transduction. Moreover, the application strategies of biophysical stimuli as the fourth pillar of bone tissue engineering are presented, which include preconstructed scaffolds with osteoinductive properties, tissue engineered bone grafts (TEBGs), and postoperative biophysical stimuli loading strategies. (**Figure 1**). This review aims to propose a novel and comprehensive concept that biophysical stimuli show potential to be used as the fourth pillar of bone tissue engineering.

2 DISTINCTIVE BIOPHYSICAL STIMULI FOR BONE TISSUE ENGINEERING

MSCs can be obtained from various tissues, including bone marrow-derived MSCs (BMSCs), periosteum-derived stem cells (PDSCs), adipose-derived stem cells (ADSCs), and periodontal

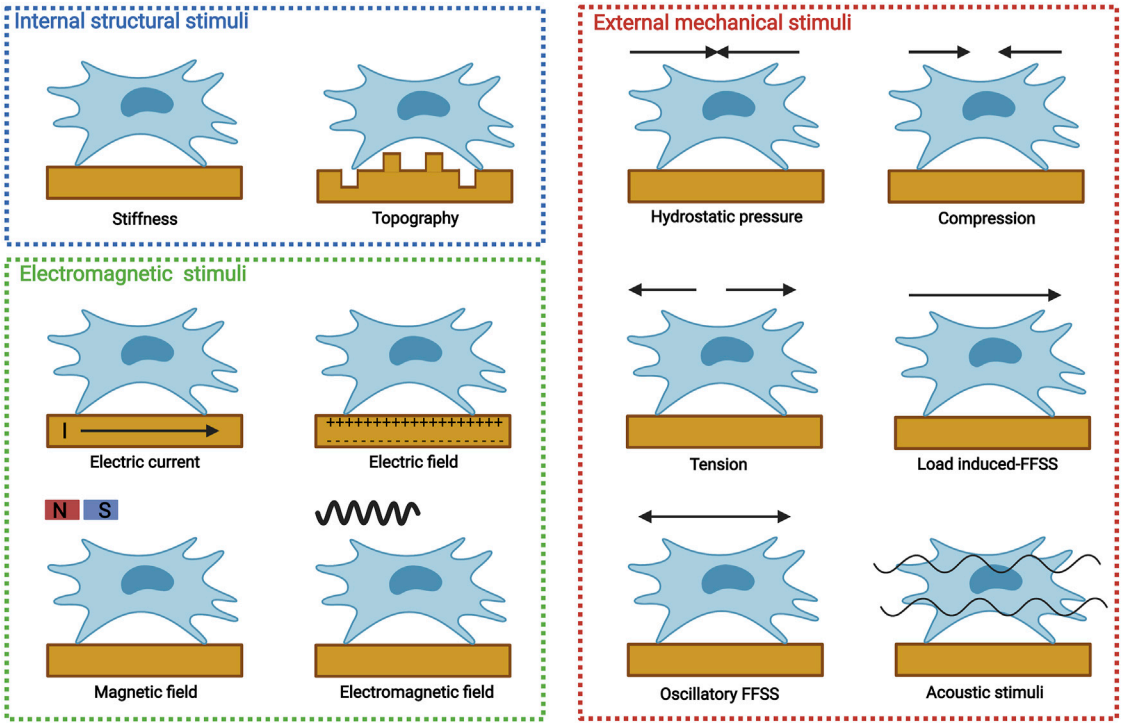

FIGURE 2 | Distinctive biophysical stimuli for bone tissue engineering, including internal structural stimuli (stiffness and topography), external mechanical stimuli [hydrostatic pressure, compression, tension, load induced-fluid flow shear stress (FFSS), oscillatory FFSS without load, and acoustic stimuli], and electromagnetic stimuli (electric current, electric field, magnetic field, and electromagnetic field). Created with BioRender.com.

ligament stem cells (PDLCs). For bone tissue engineering, MSCs are introduced to biomaterials either by direct encapsulation or indirect recruitment. Biophysical stimuli could modulate various MSC processes, including migration, proliferation, and differentiation. Distinctive biophysical stimuli with different parameters may result in different MSC specifications. Biophysical stimuli for osteogenic differentiation should be limited by one or several parameters, which can be termed as osteoinductive windows. Depending on physical properties, biophysical stimuli can be categorized into internal structural stimuli, eternally mechanical stimuli, and electromagnetic stimuli (**Figure 2**).

2.1 Internal Structural Stimuli

Internal structural stimuli are derived from matrix microenvironment where MSCs survive and grow. In human, distinctive tissues show different mechanical properties, among which matrix stiffness and topography determine the fate of MSCs.

2.1.1 Matrix Stiffness

Matrix stiffness is the rigidity or elasticity of the three dimensional (3D) microenvironment. MSCs show different cell shapes when loaded on the surface of collagens with distinctive stiffness (Engler et al., 2006). In specific microenvironment with different matrix stiffness, they transfer from the initially round shape to a branched (0.1–1 kPa), spindle (8–17 kPa), or polygonal (25–40 kPa) shape, which then determines their commitment for neurogenic, myogenic, or osteogenic differentiation (Engler et al., 2006). The results can be also supported by the fact that spread, flattened, and adherent MSCs undergo osteogenic differentiation, whereas unspread and round MSCs undergo adipogenic differentiation (McBeath et al., 2004). However, in a 3D microenvironment, the influence of cell shape transfers to nanoscale integrin binding and the rearrangement of cell adhesion ligands, which could stimulate the osteogenic differentiation of MSCs by contractility (Huebsch et al., 2010). In addition, 3D matrix with a stiffness of 11–30 kPa predominantly stimulates osteogenesis (Huebsch et al., 2010).

2.1.2 Topography

Topography is another mechanical property related to cell adhesion. According to the patterning size, topography exerts effects on different levels, including macroscale colony level (>100 μm), microscale cell level (0.1–100 μm), and nanoscale receptor level (1.0–100 nm), among which nanotopography influences the commitment of MSCs (Prè et al., 2013). Various nanopatterns (such as nanopits, nanorods, nanopillars, or nanocolumns) can be modified on the surface of biomaterials for the osteogenic differentiation of MSCs, and specific osteoinductive parameters (shape, diameter, spacing, height, or depth) vary greatly among these nanopatterns and different fabrication techniques (Dobbenga et al., 2016). However, all osteoinductive windows of different nanotopographies show

nanoscale-controlled disorder, a nanopattern that is not completely random and not highly ordered (Prè et al., 2013). Dalby et al. first fabricated five nanotopographies on the surface of polymethylmethacrylate embossed with nanopits (diameter 120 nm, depth 100 nm): highly ordered hexagonal array (center–center spacing 300 nm), highly ordered square array (center–center spacing 300 nm), disordered square array with a controlled displacement of 20 nm (center–center spacing 300 ± 20 nm), and disordered square array with a controlled displacement of 50 nm (center–center spacing 300 ± 50 nm) (Dalby et al., 2007). All highly ordered groups and completely random groups fail to sufficiently induce the osteogenic differentiation of MSCs, but both disordered nanotopographies with controlled displacement show osteoinductive properties; those with a controlled displacement of 50 nm are superior to those with a controlled displacement of 20 nm in terms of osteocalcin (OCN), osteopontin (OPN), and bone nodule contents (Dalby et al., 2007). Zhang et al. utilized nanorods to explore the osteoinductive properties of nanotopography with controlled disorder (Zhou J. et al., 2016). They fabricated five nanopatterns with different interrod spacings (302.7 ± 10.5, 137.2 ± 7.5, 95.9 ± 3.8, 66.8 ± 4.1, and 32.6 ± 2.7 nm). And they found that the group with interrod spacings over 137 nm impedes MSC osteogenesis, the group with interrod spacings below 96 nm facilitates osteogenic differentiation, and the 66.8 ± 4.1 nm group shows preferable osteoinduction (Zhou X. et al., 2016). The above results suggested that the interspacing of nanopattern determines the osteoinductive windows of nanotopography. And the modification of nonopits may need relatively large interspacing because the spacing area supports cell adhesion, whereas the modification of nanorods or nanopillars needs relatively small interspacing because they support cell adhesion. Although nanopillars with different heights (Sjöström et al., 2009; McNamara et al., 2011; Sjöström et al., 2013) or nanopits with distinctive diameters (Lavenus et al., 2011) show different osteoinductive properties, nanopattern interspacing changes with height. Thus, whether or not the height or diameter of nanopatterns truly controls the osteogenic differentiation of MSCs remains unknown, and further studies should make spacing constant while changing other parameters.

2.2 External Mechanical Stimuli

External mechanical stimuli are derived from external forces, which could exert effects on MSCs continuously or cyclically. External mechanical stimuli that show osteoinductive properties include hydrostatic pressure (HP), compression, tension, load-induced fluid flow shear stress (FFSS), oscillatory FFSS, and acoustic stimuli.

2.2.1 Hydrostatic Pressure

MSCs reside in a fluid-filled microenvironment. Thus, HP affects the fate of MSCs, which may exert homogenous compression to MSCs. Huang et al. used cyclic HP (0.5 MPa, 0.5 Hz) by a perfusion bioreactor and found that the sinusoidal profile could promote osteogenic differentiation, but the proliferation is spoiled (Huang and Ogawa, 2012). HP with high magnitude does not accord with physiological HP; hence, high-magnitude HP may be limited for regenerative medicine. From a physiological perspective, MSCs in the bone marrow are exposed to static intramedullary pressure (approximately 4 kPa), which increases to 50 kPa when exposed to external mechanical stimuli, and stem cells in the perivascular space and Haversian channels may experience 300 kPa pressure. Thus, researchers further compared the osteogenic effects of three HPs (10, 100, and 300 kPa) with different frequencies (0.5, 1, and 2 Hz) and durations (1, 2, and 4 h) and found that HP with 300 kPa and 2 Hz produces the most effective osteoinductive property (Stavenschi et al., 2018). However, the collagen synthesis and mineral deposition are similar among different groups, showing that HP with 10 kPa is sufficient to induce MSC osteogenesis (Stavenschi et al., 2018). Reinwald et al. found that intermittent HP (270 kPa, 1 Hz, 60 min/day, 21 days) promotes the osteogenic differentiation of MSCs when loaded onto poly (E-caprolactone) (PCL) scaffolds (Reinwald and El Haj, 2018). Altogether, cyclic or intermittent HP with magnitude 10–300 kPa induces MSC osteogenesis.

2.2.2 Compression

In addition to HP, compression (physiological strain from 0.2 to 0.4%) is induced on the vertical direction of the force when natural bone is compressed (Al Nazer et al., 2012). Depending on loading pattern, compression can be classified into uniaxial compression and equiaxial compression, both of which could induce the osteogenic differentiation of MSCs when they are limited by specific parameters. The stiffness of biomaterials is enhanced to promote osteogenesis when scaffolds are exposed to compression (Baumgartner et al., 2018). Among parameters describing compression, the magnitude of compression strain determines the fate of compressed MSCs. However, osteoinductive compression strain magnitude varies greatly because of different compression devices, durations, and biomaterials. For relatively high compression strain (≥1.5%), whether or not high-magnitude compression stimulates osteogenesis remains controversial (Haudenschild et al., 2009; Sittichokechaiwut et al., 2010; Aziz et al., 2019; Schreivogel et al., 2019). It was revealed that 5% compression could induce the osteogenic differentiation of MSCs loaded onto polyurethane scaffolds without biochemical cues, which show comparable osteoinduction with dexamethasone (Sittichokechaiwut et al., 2010). However, Horner et al. adopted four compression strains (5, 10, 15, and 20%) and found that osteogenic markers decrease and chondrogenic markers increase in a magnitude-dependent manner (Horner et al., 2018). Haudenschild et al. also found that ±5% bulk strain with 5% offset stimulates chondrogenic differentiation (Haudenschild et al., 2009). Indeed, high compression strain inhibits the expression of Runt-related transcription factor 2 (RUNX2), but the expression of bone Morphogenetic Protein-2 (BMP-2) is interestingly upregulated (Schreivogel et al., 2019). Thus, one potential explanation for this discrepancy is that abundant culture medium blocks the effects of mechanosensitive autocrine factors, which impede osteogenic differentiation. Schreivogel et al. further explored the effects of autocrine

factors by improving the number of scaffolds containing MSCs and reducing the volume of culture medium; results showed that 5 and 10% compression could promote the osteogenic differentiation of MSCs (Schreivogel et al., 2019). Therefore, high-magnitude compression may induce osteogenesis by mechanosensitive autocrine factors, such as BMP-2, and the ratio of cell number and medium volume may determine the fate of MSCs. Compared with high-magnitude compression, low-magnitude compression could directly promote the expression of osteogenic markers. A previous study seeded MSCs to monetite calcium phosphate scaffolds and then subjected them to compression (0.4%, 0.1 Hz) (Gharibi et al., 2013). After 2 h stimulation, some immediate-early response genes are activated, which promote the expression of other genets (such as RUNX-2) to induce the proliferation and osteogenic differentiation of MSCs (Gharibi et al., 2013). Ravichandran et al. adopted low compression strains (0.22, 0.88, and 1.1%) and found that the 0.22% group induces more alkaline phosphatase (ALP) and calcium than the other groups (Ravichandran et al., 2017). These studies indicate that although compression with high magnitude stimulates osteogenesis by mechanosensitive autocrine factors, the precise ratio of cell number to medium volume is difficult to control. Thus, physiological compression (0.2–0.4%) shows great promise for MSC osteogenesis.

2.2.3 Tension

When natural bone is pulled, tension is also induced on the vertical direction of the force. Depending on the loading pattern, tension could be divided into uniaxial compression and equiaxial compression. Different from compression, tension with high strain (such as 5%) promotes osteogenic differentiation and inhibits adipogenic differentiation (Li et al., 2015a). Tensile strain-inducing cell culture plates are generally used to study the effects of tension. In these two dimensional (2D) models, MSCs are initially seeded on the cell culture plates coated with the matrix, and then the plates are subjected to tension strain, which indirectly exerts tension to MSCs. Thus, the matrix should show great ability for cell adhesion, and type I collagen has been widely used for luxuriant arginine–glycine–aspartate (RGD) peptide (Sumanasinghe et al., 2009). Lohberger et al. seeded MSCs on type I collagen-coated cell culture plates, which were then subjected to continuous tension (10%, 0.5 Hz), and the tension-loaded groups show improved expression of osteogenic genes, higher calcium deposition, and more ALP when compared with the unstimulated groups (Lohberger et al., 2014). (Zhao et al., 2010) compared the effects of 0.3 Hz tension with different strains (9, 12, and 15%) and found that the 12% tension group induces robust osteogenic response (Zhao et al., 2021). To explore the effects of tension in a 3D microenvironment, a novel uniaxial tension bioreactor was designed to exert tensile forces (10%, 0.5 Hz for 7 days with 4 h each day) to fibrin hydrogels seeded with MSCs (Carroll et al., 2017). Results show that tension could promote the intramembranous ossification and impede the adipogenic differentiation of MSCs (Carroll et al., 2017). Therefore, the osteoinductive window of tension is mainly determined by tension strain, and 5–15% magnitude could stimulate MSC osteogenesis.

2.2.4 Fluid Flow Shear Stress (Perfusion and Rotation)

FFSS is another external mechanical stimulus generated by the load of compression or tension. Load-induced FFSS could change cell shape. One classic 2D model to explore the effect of load-induced FFSS is parallel-plate flow chamber (Yourek et al., 2010; Dash et al., 2020). Using this model, it was confirmed that short-term continuous FFSS (9 dynes/cm^2) for 24 h could promote the osteogenic differentiation of MSCs without chemically osteoinductive molecules (Yourek et al., 2010). However, for long-term intermittent FFSS, low-magnitude FFSS (such as 10 mPa, namely, 0.1 dynes/cm^2) is sufficient to induce osteogenesis (Dash et al., 2020). However, these strategies fail to emulate the natural ECM microenvironment; thus, various bioreactors, including rotation and perfusion bioreactors, have been developed to generate FFSS. Perfusion bioreactors have been widely used to explore the osteoinductive effects of FFSS (Filipowska et al., 2016). In the absence of biochemical cues (such as dexamethasone), FFSS (1 ml/min) provided by perfusion bioreactors for 16 days could dramatically promote the mineralization of MSCs within decellularized matrix/Ti meshes (Datta et al., 2006). Bjerre et al. (2008) used a perfusion bioreactor to dynamically culture MSCs seeded in silicate-substituted tricalcium phosphate scaffolds and found that FFSS (0.1 ml/min) for 21 days could promote the proliferation and osteogenic differentiation of MSCs. Filipowska et al. established an intermittent model (2.5 ml/min for three times with 2 h per section) by using perfusion bioreactors to stimulate MSCs seeded in gelatin-coated polyurethane scaffolds and found that intermittent protocols can induce MSC osteogenesis (Filipowska et al., 2016). During dynamic perfusion culture, the expression of type X collagen is upregulated, suggesting that endochondral and intramembranous ossification participates in osteogenesis (Moser et al., 2018). Therefore, the osteogenic window of load-induced FFSS is mainly determined by interchangeable pressure or flow rate, and load-induced FFSS with pressure > 0.2 dynes/cm^2 shows osteoinductive properties (Yong et al., 2020).

2.2.5 Oscillatory Fluid Flow Shear Stress (Microvibration and Nanovibration)

Oscillatory FFSS is another FFSS generated by oscillatory displacement without strain, which is the microscale or nanoscale form of vibration (Stewart et al., 2020; Birks and Uzer, 2021). According to amplitude, vibration can be classified into microvibration (≤50 μm) and nanovibration (<100 nm).

Microvibration is vibration with amplitude ≤ 50 μm, magnitude < 1 g, and frequency 1–100 Hz (Wu et al., 2020). Frequency may determine the osteoinductive window of microvibration. Cashion et al. revealed that microvibration with a low frequency (1 Hz) induces chondrogenesis, whereas relatively high frequency (100 Hz) promotes osteogenesis (Cashion et al., 2014). Thus, low-magnitude high-frequency vibration (LMHFV) (magnitude < 1 g, frequency 20–90 Hz) is

generally used for osteogenesis (Steppe et al., 2020). 50 Hz LMHFVs with different magnitudes (0.1, 0.3, 0.6, and 0.9 g) were used to stimulate PDLCs, and it was found that all groups promote osteogenic differentiation, but LMHFV with 0.3 g peaks the osteoinduction (Zhang et al., 2015). Some studies revealed that LMHFV stimulates MSC osteogenesis in a frequency-dependent response. One study revealed that horizontal vibration at 100 Hz causes higher osteoinduction than that at 30 Hz (Pongkitwitoon et al., 2016). A previous study observed that 800 Hz microvibration promotes higher biomineralization and osteogenic marker expression than 0, 30, and 400 Hz, but long-term stimulation of microvibration (30 min/day, 14 days) with frequencies of 30 and 400 Hz inhibits osteogenesis (Chen et al., 2015). Thus, stimulation duration and loading time also influence the osteogenic differentiation of MSCs. One study revealed that microvibration (60 Hz, 1 h/d for 5 days) inhibits the mineralization and osteogenic differentiation of MSCs (Lau et al., 2011), whereas another study showed that microvibration (30 Hz, 45 min/day for 21 or 40 days) could promote MSC osteogenesis (Prè et al., 2013). These results suggest that the osteoinductive window of microvibration can be determined by frequency, duration, and single loading time. For 30 Hz vibration, long-term duration may be effective to osteogenic differentiation. For vibration with frequencies over 60 Hz, single loading time should be limited with 30 min, and short-term duration (<7 days) may be superior for osteogenesis.

Nanovibration refers to vibration with nanoscale amplitude (<100 nm). It was confirmed that nanovibration (frequency 1,000 Hz, amplitude 10–14 nm) could promote the osteogenic differentiation of MSCs in 2D condition (Nikukar et al., 2013). Another study showed that nanovibration (frequency 1,000 Hz, amplitude 10–14 nm) could stimulate the osteogenic differentiation of MSCs seeded in 3D collagen hydrogels (Tsimbouri et al., 2017). Thus, the osteoinductive window of nanovibration is a frequency of approximately 1,000 Hz and amplitude of 10–20 nm.

2.2.6 Acoustic Stimuli

Acoustic stimuli, according to frequency, can be categorized into infrasound (<20 Hz), audible sound (20–20,000 Hz), and ultrasound (>20,000 Hz). Therapeutic acoustic stimuli are generally termed as ultrasound with frequency varying from 0.7 to 3.3 MHz and low or high intensity (Zhang et al., 2017). When loaded to tissue, ultrasound could convert energy to heat via thermal effect, which may cause irreversible damage. Some nonthermal effects induced by ultrasound, including cavitation, acoustic microstreaming, acoustic radiation force, the spread of surface waves, and oscillatory FFSS may modulate the commitment of MSCs. (Esfandiari et al., 2014; Padilla et al., 2014).

Low-intensity pulsed ultrasound (LIPUS) (intensity 30–100 mW/cm^2, frequency 1.5 MHz, and duty cycle 20% or 100%) is a preferential strategy to reduce the thermal effect for regenerative medicine. This strategy has been approved by the United States Food and Drug Administration for the treatment of fresh fractures and established non-union (de Lucas et al., 2020). Depending on duty cycle, continuous LIPUS (100%) can also be used. However, one research revealed that LIPUS with 20% duty cycle shows higher osteoinductive properties toward ADSCs than LIPUS with 50% duty cycle (Yue et al., 2013). Thus, LIPUS may be more effective than cLIPUS. Using PDLCs, the osteoinduction of LIPUS was explored, and it was found that LIPUS could stimulate osteogenic differentiation and upregulate osteocalcin, Runx2, and integrin 1, and that LIPUS with an intensity of 90 mW/cm^2 is more effective for osteoinduction than LIPUS with an intensity of 30 or 60 mW/cm^2 (Hu et al., 2014). Zhou et al. further improved the intensity of LIPUS and found that LIPUS with an intensity of 150 mW/cm^2 is more effective than LIPUS with intensities of 20, 50, 75, and 300 mW/cm^2 (Zhou X. et al., 2016). These results suggest that the osteoinductive window of LIPUS is primarily determined by duty cycle and intensity, and 20% duty cycle and 90–150 mW/cm^2 intensity may be optimal for the osteogenic differentiation of MSCs.

Pulsed focused ultrasound (intensity 133 W/cm^2, frequency 1 MHz, and duty cycle 5%) is another acoustic stimulus model with relatively minimizing thermal effect that is characterized by short term and high intensity (de Lucas et al., 2020). It could induce MSC homing (Burks et al., 2018), but whether or not it induces the osteogenic differentiation of MSCs remains unclear.

2.3 Electromagnetic Stimuli

Electromagnetic stimuli are also important biophysical cues that could exert effects on the fate of MSCs. Depending on physical properties, electromagnetic stimuli can be further classified into magnetic stimuli in the form of magnetic field and electric stimuli in the form of electric field and electric current.

2.3.1 Electric Current

Natural bone physiologically generates electric stimuli on account of non-centrosymmetric collagen after mechanical stress, which supports bone development and repair (Khare et al., 2020). Thus, external electric stimuli can be applied to MSCs for regenerative medicine. Alternating electric current is an effective external electric stimulus that induces the osteogenic differentiation of MSCs (Creecy et al., 2013). In one study, MSCs were seeded on an indium-tin-oxide-coated glass and then subjected to alternating electric current (5–40 μA, 5–10 Hz, 1–24 h/day) for 21 days without exogenous biochemical osteogenic molecules, and results showed that all setups of alternating electric current could stimulate osteogenic differentiation and inhibit chondrogenic and adipogenic differentiation (Wechsler et al., 2016). In addition, alternating electric current (10 μA, 10 Hz, 6 h/day) could reach optimized osteogenic effects (Wechsler et al., 2016). Direct current is another form of electric current, but its osteogenic effects without electric field remain unknown, which needs further research.

2.3.2 Electric Field

Electric field is another effective external electric stimulus to promote MSCs toward osteogenic differentiation. According to the generation pattern, electric field can be categorized into direct current electric field, capacitively coupled electric field, and inductively coupled electric field (Thrivikraman et al., 2018).

When MSCs are exposed to electrical stimuli, the membrane potential could be altered, and hyperpolarization stimulates osteogenesis (Murillo et al., 2017; Bhavsar et al., 2019). In addition, the configuration of plasma receptors could be modulated for osteogenic differentiation (Murillo et al., 2017). Furthermore, cytoskeletal elongation and nuclear orientation could be changed by electric field for osteogenesis (Khaw et al., 2021).

Among various parameters, electric field intensity may determine the osteoinductive windows. Using osteogenic differentiation medium, a previous study applied an electric field (2 mV/mm, 60 kHz, 40 min/day) to induce MSCs and found that the electric field could induce a delayed osteogenic differentiation of MSCs (Esfandiari et al., 2014). However, Hronik-Tupaj et al. reported that a 2 mV/mm, 60 kHz electric field promotes chondrogenesis (Hronik-Tupaj et al., 2011). The discrepancy may be interpreted as the utilization of osteogenic molecules, which could synthetically direct electric field to promote osteogenesis. One research revealed that electric field (0.36 mV/mm, 10 Hz) alone fails to induce osteogenic differentiation but dramatically promotes MSC osteogenesis when osteogenic sulfated hyaluronan derivative is added (Hess et al., 2012). Therefore, electric field with low intensity may not promote MSCs toward osteoblasts but could synthetically improve the osteoinductive properties of biochemical molecules.

Different from low-intensity electric field, high-intensity electric field could directly promote the osteogenic differentiation of MSCs. For instance, when MSCs are subjected to electric field (100 mV/mm, 1 h/day), osteogenic differentiation occurs, and osteoinductive effects could be maintained even when the electric field is removed (Hess et al., 2012; Eischen-Loges et al., 2018). Khaw et al. utilized two electric fields (100 and 200 mV/mm) to MSCs without biochemical osteogenic supplements, and found that both electric fields could promote the osteogenic differentiation of MSCs, and the 200 mV/mm electric field was optimized (Khaw et al., 2021). Ravikumar et al. designed an electric field device where a static potential (15 V) was loaded to parallel electrodes with a space of 15 mm (Ravikumar et al., 2017). MSCs were seeded to HA-$CaTiO_3$ composites and then exposed to electric field for 10 min/day without osteogenic molecules, and results showed that the electric field could dramatically improve the osteogenic markers (Ravikumar et al., 2017). These studies suggest that an electric field with an intensity over 100 mV/mm may be needed for MSC osteogenesis without biochemical osteogenic molecules.

2.3.3 Magnetic Field

Exposure of MSCs to magnetic field may directly deform their plasma membrane, which causes cytoskeleton remodeling, improves cell viability, and promotes differentiation (Santos et al., 2015). Magnetic biomaterials should be introduced to culture systems, including magnetic particles and substrates, to enhance the effects of magnetic field. Boda et al. fabricated a series of hydroxyapatite-Fe_3O_4 magnetic substrates with different magnetization and then applied a periodic magnetic field (100 mT) to these magnetic substrates seeded with MSCs, and they found that all magnetic substrates combined with magnetic field could promote the osteogenic differentiation of MSCs (Boda et al., 2015). Magnetic particles can be also used to transform magnetic stimuli into mechanical stimuli. Magnetic particles coupled with magnetic field (14.7 or 21.6 mT) were used to stimulate ADSCs, and it was found that low-density magnetic field (14.7 mT) with intermittent short-term exposure (2 days) favors adipogenic differentiation, whereas high-density magnetic field (21.6 mT) promotes osteogenesis in all exposure profiles including continuous or intermittent long-term exposure (7 days) and intermittent short-term exposure (2 days) (Labusca et al., 2020). To further control the effects of magnetic particles, magnetic particles are generally functionalized by antibodies or peptides, which could directly exert pico-newton level forces to mechanosensitive plasma membrane receptors under magnetic field, which could then induce the osteogenic differentiation of MSCs (Kanczler et al., 2010; Hu et al., 2013). For example, Henstock et al. used either the antibody of transmembrane ion channel stretch-activated potassium channel (TREK-1) or RGD peptide to functionalize magnetic nanoparticles (Henstock et al., 2014). Then, an oscillating magnetic field (25 mT) was loaded to collagen hydrogels containing MSCs and functionalized magnetic nanoparticles to generate a force of 4 pN, and results showed that functionalized magnetic nanoparticles could promote matrix mineralization (Henstock et al., 2014). The osteogenic window of magnetic field may be determined by magnetic flux density (21.6–100 mT), and the quantity and functionalization of magnetic nanoparticles affect their osteogenic effectiveness.

2.3.4 Electromagnetic Field

Electromagnetic field is a combination of electric and magnetic fields, and pulsed electromagnetic field (PEMF) has been clinically used to delay osteoporosis and bone fracture repair (Sun et al., 2009). When loaded to MSCs, PEMF without osteogenic molecules inherently induces osteogenic differentiation and impedes angiogenic differentiation, and the osteogenic effects can be further enhanced by additional osteogenic molecules (Ongaro et al., 2014; Lu et al., 2015). For example, Arjmand et al. seeded ADSCs to PCL nanofibrous scaffolds, which were then exposed to PEMF (1 mT, 50 Hz) with or without osteogenic medium (Arjmand et al., 2018). Results revealed that the osteogenic effects of PCL scaffolds with PEMF are comparable with those of PCL scaffolds with osteogenic medium and that PCL scaffolds with PEMF and osteogenic medium show enhanced osteogenic differentiation (Arjmand et al., 2018). PEMF has been also verified to stimulate MSC proliferation (Tsai et al., 2009; Sun et al., 2010). Therefore, PEMF shows great promise for bone tissue engineering.

Among various parameters describing PEMF, magnetic flux density and frequency may determine the osteoinductive window of PEMF. For magnetic flux density, Jazayeri et al. compared two PEMFs (0.1 and 0.2 mT) and found that the expression of osteogenic markers, such as RUNX2 and OCN, is higher under 0.2 mT PEGF than under 0.1 mT PEGF (Jazayeri et al., 2017). Esposito et al. used a device that could generate 1.8–3 mT PEGF to induce MSCs and observed osteogenic differentiation (Esposito et al., 2012). Therefore, magnetic flux density is generally limited to 0.1–3 mT, but the optimal density remains

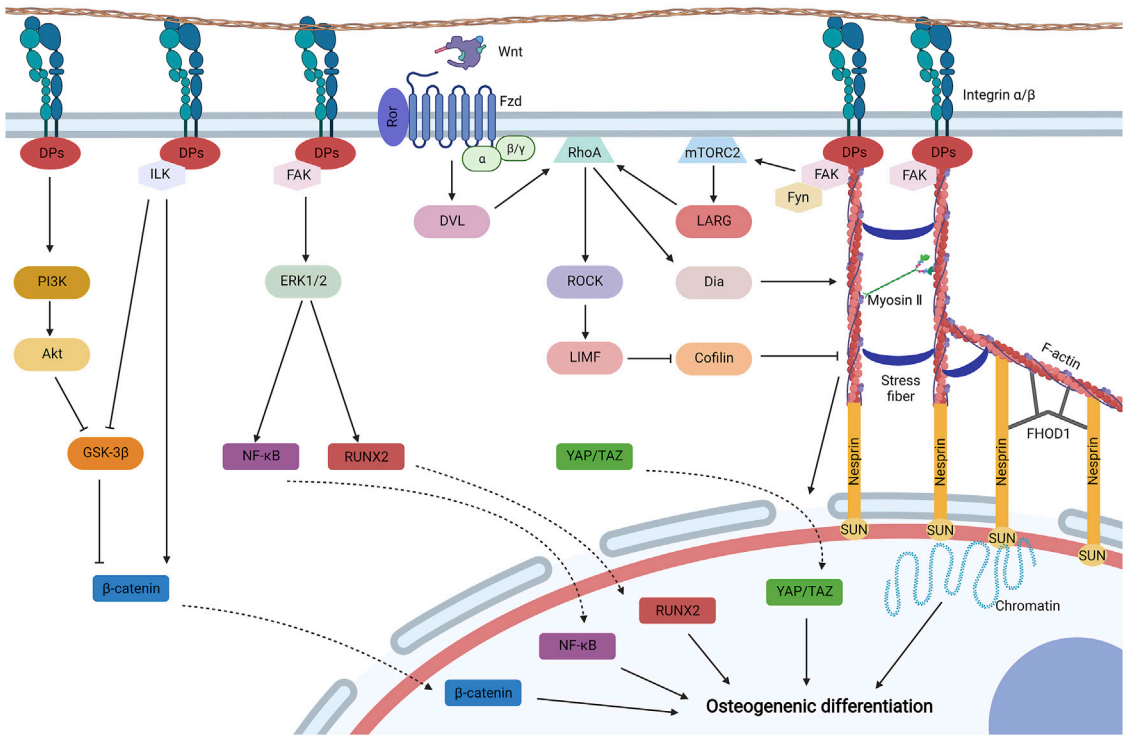

FIGURE 3 | Self-biophysical transduction for mesenchymal stem cell (MSCs) osteogenesis, including biophysical sensitive ion channels, primary cilium, and biophysical sensitive. When MSCs are exposed to biophysical stimuli, various biophysical sensitive ion channels on the plasma membrane may be activated for the influx of Ca^{2+}, which include voltage-gated calcium channels (VGCC), stretch-activated calcium channels (SACCs), Piezo, transient receptor potential vallanoid 1 (TPRV1), and TPRV4. TPRV4 is located at high-strain regions, especially primary cilium. Biophysical stimuli can also stimulate the release of Ca^{2+} from the endoplasmic reticulum to the cytoplasm by uncanonical Wnt-Ca2+ signaling. In specific, Wnt ligand binds to the Frizzled (Fzd)/receptor tyrosine kinase-like orphan receptor (Ror) complex to activate Dishevelled (Dvl), which then activates phospholipase C (PLC) to produce inositol 1,4,5-trisphosphate (IP3). IP3 could activate IP3 receptor for the release of Ca^{2+} from the endoplasmic reticulum. The increased Ca^{2+} in the cytoplasm may promote osteogenic differentiation by activating calcineurin/Nuclear Factor of Activated Cells (NF-AT) signaling and initiating extracellular signal-related kinase 1/2 (ERK1/2) by focal adhesion kinase (FAK) to regulate the activity of β-catenin. Biophysical stimuli could regulate the primary cilium containing intraflagellar transport protein 88 (IFT88) for MSC osteogenesis by regulating length or Gpr161/adenylyl cyclase 6 (AC6) signaling, and the activation of AC6 promotes the synthesis of cyclic adenosine 3′,5′-monophosphate (cAMP), which then promotes the osteogenic differentiation of MSCs by Hedgehog (Hb) signaling and proteinkinase A (PKA) signaling. Biophysical stimuli could also promote some long noncoding RNAs (lncRNAs) to inhibit some microRNAs (miRNAs) for osteogenic differentiation. Created with BioRender.com.

unknown. On the other hand, for frequency, MSCs were exposed to PEMFs with different frequencies (5, 25, 50, 75, 100, and 150 Hz), and all groups showed osteogenic differentiation, but with the increase of frequencies, osteogenic differentiation initially enhanced and then peaked at 50 Hz, which decreased until 150 Hz (Luo et al., 2012). Lim et al. also found that PEMF with 50 Hz shows improved osteogenic differentiation compared with those with 10 and 100 Hz (Lim et al., 2013). Therefore, the frequency of PEMF should be limited to 10–150 Hz, and 50 Hz is preferable.

3 OSTEOINDUCTIVE MECHANISMS OF BIOPHYSICAL STIMULI FOR BONE TISSUE ENGINEERING

When distinctive biophysical stimuli are subjected to MSCs, they will be ultimately loaded by or transferred to either mechanical or electromagnetic stimuli. Thus, mechanotransduction and electrocoupling have been separately proposed to interpret their molecular mechanisms. Considering that both signaling show high comparability and that they simultaneously occur in physiological microenvironment, we propose a new concept of biophysical transduction that integrates mechanotransduction and electrocoupling. Biophysical transduction mainly includes three stages: sensing, transmission, and regulation. According to the sensing pattern of MSCs, biophysical transduction can be further categorized into self-biophysical transduction, cell–matrix biophysical transduction, and cell–cell biophysical transduction.

3.1 Self-Biophysical Transduction

Self-biophysical transduction refers to biophysical sensing coupled with transmission and regulation by structures that do not adhere with biomaterials and adjacent cells, which mainly include biophysical-sensitive ion channels and primary cilium. And some biophysical-sensitive ribose nucleic acids (RNAs) are also upregulated by biophysical stimuli to regulate the osteogenic differentiation of MSCs (**Figure 3**).

3.1.1 Biophysical-Sensitive Ion Channels

A plethora of biophysical-sensitive ion channels exist on the surface of plasma membrane or endoplasmic reticulum, which can be activated by distinctive biophysical stimuli for Ca^{2+} influx to induce the osteogenic differentiation of MSCs. When a sufficiently giant electric field is applied to plasma membrane and generate a large transmembrane potential difference (over 100 mV), voltage-gated calcium channels can be directly activated because of plasma depolarization (Thrivikraman et al., 2018). Electric field and mechanical tension could directly promote the influx of Ca^{2+} by activating stretch-activated calcium channels (Cho et al., 1999; Kearney et al., 2010). In addition, biophysical-sensitive Piezo1 for Ca^{2+} influx could be initiated by mechanical stimuli, such as HP (Sugimoto et al., 2017). Transient receptor potential vallanoid 1 (TRPV1) can be activated by nanovibration (Tsimbouri et al., 2017), whereas TRPV4 can be activated by load-induced FFSS, which is mainly located at high-strain regions (especially primary cilium) (Corrigan et al., 2018; Eischen-Loges et al., 2018). The initiation of these biophysical-sensitive ion channels increases Ca^{2+} concentration in the cytoplasm, which may initiate calmodulin/calcineurin signaling (Kapat et al., 2020). Calcineurin frees the phosphate group from phosphorylated nuclear factor of activated cells (NF-AT), and dephosphorylated NF-AT then shuttles to the nucleus and interacts with other transcription factors to induce the osteogenic differentiation of MSCs (Khare et al., 2020). In addition, increased Ca^{2+} in the cytoplasm initiates protein kinase C and extracellular signal-related kinase 1/2 (ERK1/2), which then regulate the activity of β-catenin to promote MSC osteogenesis (Tsimbouri et al., 2017).

The increase in Ca^{2+} concentration in the cytoplasm can also be mediated by Ca^{2+} release from the endoplasmic reticulum, which may be related to noncanonical Wnt-Ca^{2+} signaling (Bertrand et al., 2020). Biophysical stimuli promote the expression of Wnt (Chen et al., 2019; Fu et al., 2020). Thus, secreted Wnt may interact with a transmembrane receptor Frizzled (Fzd) coupled with receptor tyrosine kinase-like orphan receptor (Ror) to promote the activity of phospholipase C (PLC) by activated Dishevelled (Dvl), and then PLC degrades phosphatidylinositol 4,5-bisphosphate in the cell membrane to obtain inositol 1,4,5-trisphosphate (IP3), which moves to the endoplasmic reticulum and binds to IP3 receptors to promote Ca^{2+} release (Thrivikraman et al., 2018). Moreover, Ca^{2+} channels on the endoplasmic reticulum may be directly modulated by electromagnetic stimuli because of the change in configuration, which also promotes the increase in Ca^{2+} concentration in the cytoplasm (Khare et al., 2020). Therefore, endoplasmic reticulum-derived Ca^{2+} may participate in the osteoinduction of biophysical stimuli.

3.1.2 Primary Cilium

Primary cilium is a biophysical-sensitive organelle based on immotile microtubule and appears from the cytomembrane surface (Delaine-Smith and Reilly, 2012). Primary cilium could sense mechanical and electromagnetic stimuli to induce the osteogenic differentiation of MSCs (Hoey et al., 2012; Chen et al., 2016). The osteoinductive mechanism of primary cilium may be related to its length regulation and ciliary receptors or molecules. One research revealed that topography influences the length of primary, and reduced length promotes the nuclear translocation of β-catenin (McMurray et al., 2013). Thus, specific biophysical stimuli may lower the length of primary cilium for MSC osteogenesis. Gpr161 is a biophysical-sensitive G protein-coupled receptor (GCPR) localized to primary cilium containing intraflagellar transport protein 88 (IFT88), which is essential for cilium formation (Johnson et al., 2021). After being subjected to biophysical stimuli, the GCPR may activate ciliary localized adenylyl cyclase 6 (AC6) for the synthesis of cyclic adenosine 3′,5′-monophosphate (cAMP), which then activates Hedgehog signaling for MSC osteogenesis (Johnson et al., 2018; Johnson et al., 2021). cAMP may also initiate protein kinase A to induce the osteogenic differentiation of MSCs (Johnson et al., 2018). Further studies should focus on other receptors or molecules localized to primary cilium from MSCs and their biophysical transduction and osteoinductive mechanisms.

3.1.3 Biophysical-Sensitive RNAs

After being subjected to biophysical stimuli, MSCs could express some RNAs, including microRNAs (miRNAs) and long noncoding RNAs (lncRNAs), to regulate osteogenic differentiation. One research revealed that tension promotes the expression of lncRNA-MEG3, which then inhibits the expression of miRNA-140-5p for MSC osteogenesis (Zhu et al., 2021). Another research revealed that lncRNA H19 is upregulated to impede miRNA-138, and decreased miRNA-138 may recover the expression of focal adhesion kinase (FAK), which participates in cell–matrix biophysical transduction (Wu et al., 2018). miRNA-132-3p and miR-129-5p are also inhibited when MSCs are subjected to biophysical stimuli for osteogenesis (Hu et al., 2020; Wu et al., 2021). Although biophysical-sensitive RNAs exert critical effects in biophysical regulation, related studies are limited, which need further attention.

3.2 Cell–Matrix Biophysical Transduction

Cell–matrix biophysical transduction refers to biophysical sensing coupled with transmission and regulation by structures that adhere to biomaterials. Cell adhesion is mainly induced and regulated by integrin and focal adhesion (**Figure 4**).

3.2.1 Integrin Signaling

Integrin is a transmembrane heterodimer that serves as a receptor to bind with specific ligands from external microenvironment (Thompson et al., 2012). When MSCs adhere to biomaterials and subjected to biophysical stimuli, multiple integrin signaling can be activated for the osteogenic differentiation of MSCs. FAK, under biophysical stimuli, may be recruited to integrin and undergo autophosphorylation (Bertrand et al., 2020), which then activates mitogen-activated protein kinases (MAPKs), such as ERK1/2 and P38 (Liu et al., 2014; Niu et al., 2017; Chang et al., 2019). Activated or phosphorylated MAPKs then induce the phosphorylation of transcription factors, such as RUNX2, to promote the osteodifferentiation of MSCs (Chang et al., 2019). Activated ERK1/2 also phosphorylates nuclear factor

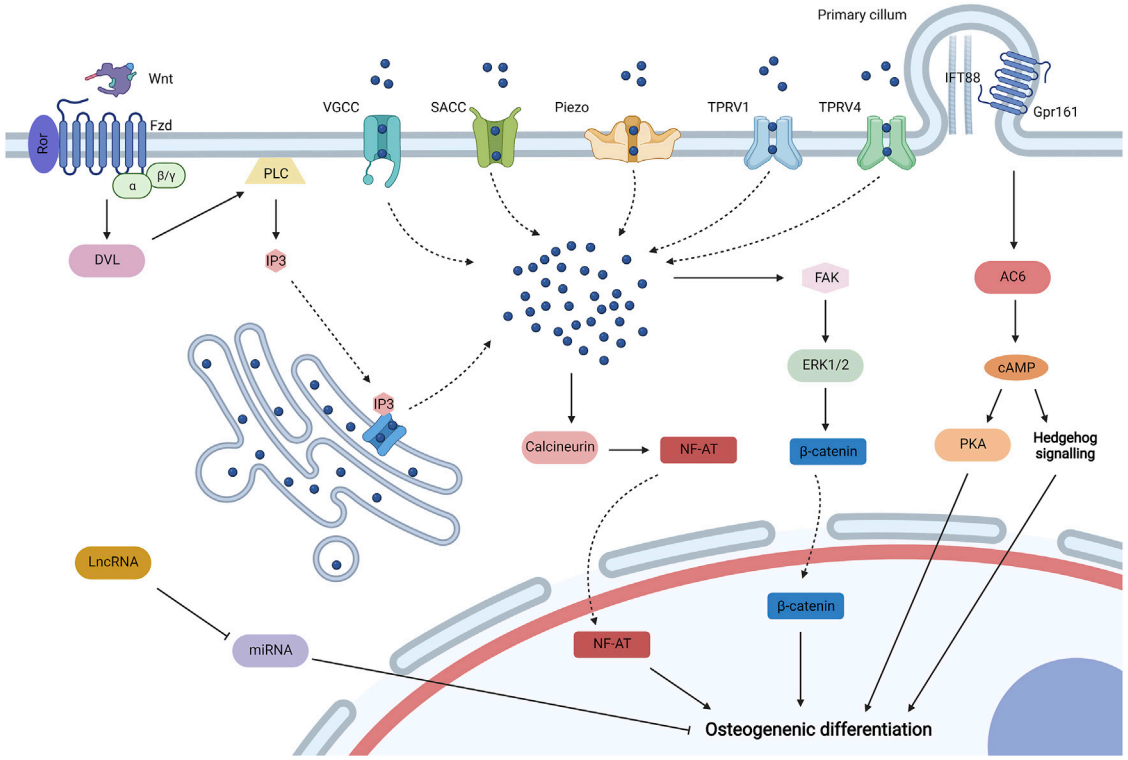

FIGURE 4 | Cell–matrix biophysical transduction for MSC osteogenesis, including integrin signaling and focal adhesion. Integrins generally induce cell adhesion, and integrin signaling may be activated for the osteogenic differentiation of MSCs under biophysical stimuli. Integrin activates phosphatidylinositol 3-kinase (PI3K) to initiate Akt, which then avoids the degradation of β-catenin by inhibiting glycogen synthase kinase-3β (GSK-3β). GSK-3β can be also impeded by integrin linked kinase (ILK) initiated by integrin. Activated ILK can also promote the cytoplastic accumulation of β-catenin by dissociating β-catenin from cadherin. β-catenin is then translocated to the nucleus for osteogenic differentiation. Integrin can also initiate FAK to activate mitogen-activated protein kinase (MAPK) (such as ERK1/2) to phosphorylate transcription factors, such as Runt-related transcription factor 2 (Runx2) and nuclear factor κB (NF-κB), which then shuttles to the nucleus for MSC osteogenesis. Biophysical stimuli can be directly transduced by the structure of focal adhesion-cytoskeleton-nucleus to promote chromatin for gene expression, which is composed of integrin, docking proteins (DPs), recruited FAK, F-actin, myosin II, stress fiber, the Linker of Nucleoskeleton and Cytoskeleton (LINC) complex (nesprin and SUN protein), and formin homology 1/formin homology 2 domain containing protein 1 (FHOD1). The structure is mainly regulated by ras homolog family member A (RhoA) signaling. RhoA can be activated by leukemia-associated Rho guanine nucleotide exchange factor (LARG), which is initiated by the recruitment of Fyn and FAK to initiate mammalian target of rapamycin complex 2 (mTORC2). RhoA can be also activated by initiated Dvl by the binding of Wnt to the Ror/Fzd complex. Activated RhoA initiates LIM kinase (LIMK) by stimulating Rho-associated protein kinase (ROCK), which could inhibit cofilin to avoid F-actin severing. Activated RhoA also promotes the formation and contraction of the structure by initiating Diaphanous (Dia). Furthermore, contracted cytoskeleton may diminish the mechanical resistance for the translocation of Yes-associated protein (YAP) and transcriptional co-activator with PDZ-binding motif (TAZ) to the nucleus for osteogenesis. Created with BioRender.com.

κB (NFκB), which upregulates integrin β1 in a feedback model and promotes the expression of BMP-2 for osteogenesis (Liu et al., 2011; Liu et al., 2014). Another research revealed that activated ERK1/2 inhibits adipogenesis by downregulating the expression of BMP-4 (Lee et al., 2012). Moreover, biophysical stimuli may activate integrin-linked kinase (ILK) by integrin, which inhibits N-cadherin to release β-catenin and glycogen synthase kinase-3β (GSK-3β) to avoid the degradation of β-catenin. Then, β-catenin shuttles to the nucleus to induce the osteogenic differentiation of MSCs (Niu et al., 2017). Furthermore, integrin could be stimulated by biophysical stimuli to activate Akt by phosphatidylinositol 3-kinase (PI3K), which then activates GSK-3β to inhibit the degradation of β-catenin for MSC osteogenesis (Song et al., 2017; Sun et al., 2018). Osteoinductive mechanisms of integrin signaling by biophysical stimuli can be mainly interpreted as FAK/MAPK signaling, ILK/β-catenin signaling, and PI3K/Akt/β-catenin signaling. In addition, crosslinking exists among distinctive integrin signaling.

3.2.2 Focal Adhesion-Cytoskeleton-Nucleus

In addition to indirect integrin signaling to induce osteogenesis, integrins also participate in the formation of focal adhesion to transfer biophysical stimuli directly to contractible cytoskeleton and nucleus, which is generally known as bundles of clustered integrins (Dalby et al., 2014). At the site of focal adhesion, the cytoplasmic tail of integrin is linked to the (F)-actin cytoskeleton by talin and vinculin, which is stabilized by other docking proteins, including zyxin, actinin, and p130Cas (Bertrand et al., 2020). Adjacent actins generate prestress by the bundling of stress fibers (such as α-actinin) and myosin II (Wang et al., 2009). The tail of actin is linked to the nuclear

envelope by the Linker of Nucleoskeleton and Cytoskeleton (LINC) complex, which is composed of nesprin (nesprin1 or nesprin2) and SUN (Bouzid et al., 2019). Moreover, formin homology 1/formin homology 2 domain containing protein 1 binds to multiple sites among nesprin and actin to enhance the association (Birks and Uzer, 2021). Furthermore, SUN proteins bind to lamins to form the lamina, and lamina coupled with G-actin and myosin may assemble into the nucleoskeleton, which connects to chromatin and deoxyribonucleic acid (DNA) (Wang et al., 2009). Therefore, the structure of focal adhesion-cytoskeleton-nucleus allows biophysical stimuli to be transferred from outside to DNA and directly activates gene expression (Wang et al., 2009). When MSCs are subjected to biophysical stimuli, autophosphorylated FAK is recruited to focal adhesion and connects to integrin β by talin and paxillin and promotes cytoskeletal contraction, which then promote MSC osteogenesis (Hao et al., 2015; Bertrand et al., 2020).

Cytoskeletal stabilization and contraction are mainly regulated by biophysical-sensitive ras homolog family member A (RhoA) signaling. And biophysical stimuli could promote the osteogenic differentiation of MSCs by RhoA signaling (Arnsdorf et al., 2009a; Zhao et al., 2015). The activation of RhoA is related to focal adhesion and uncanonical Wnt/RhoA signaling. After biophysical stimuli, kinase Fyn and FAK are recruited to focal adhesion, which synthetically initiate mammalian target of rapamycin complex 2 to activate RhoA, which may be related to the activation of leukemia-associated Rho guanine nucleotide exchange factor (Thompson et al., 2013; Thompson et al., 2018). Moreover, biophysical stimuli could stimulate MSCs to upregulate Wnt5a and Ror2 (Arnsdorf et al., 2009b; Shi et al., 2012). Wnt ligand binds to the complex of Ror and Fzd to initiate Dvl, which could also activate RhoA (Bertrand et al., 2020). The activated RhoA then initiates Rho-associated protein kinase (ROCK) and subsequently LIM kinase (LIMK), which inactivate or phosphorylate cofilin to diminish its effects of severing F-actin (Hayakawa et al., 2011; Bertrand et al., 2020). The structure of focal adhesion-cytoskeleton-nucleus can be also enhanced by the initiation of Diaphanous via RhoA (Bertrand et al., 2020).

Yes-associated protein (YAP) and transcriptional co-activator with PDZ-binding motif (TAZ) are biophysical-sensitive transcriptional activators for MSC osteogenesis. When MSCs are subjected to biophysical stimuli, YAP/TAZ are activated and then translocate to the nucleus, where they interact with various transcription factors to promote osteogenesis (Kim et al., 2014; Qian et al., 2017; Li et al., 2020). The regulation of YAP/TAZ stimulated by biophysical stimuli may undergo a Hippo/LATS-independent signaling pathway (Dupont et al., 2011). Recent studies have revealed that the nuclear translocation of YAP/TAZ is related to the structure of focal adhesion-cytoskeleton-nucleus (Driscoll et al., 2015). When biophysical stimuli are loaded to MSCs, forces cause focal adhesion to the nucleus by the cytoskeleton to open the size of nuclear pores relatively. Thus, the mechanical resistance to transfer molecules is lowered, allowing for YAP/TAZ translocate to the nucleus (Elosegui-Artola et al., 2017).

3.3 Cell–Cell Biophysical Transduction

Cell–cell biophysical transduction refers to biophysical sensing coupled with transmission and regulation by direct contact by structures from adhering with adjacent cells (cadherin and Notch receptor) (**Figure 5**). Bioactive factors under biophysical stimuli by the autocrine and paracrine network could also exert effects via indirect interaction (**Figure 6**).

3.3.1 Adhesion Junction

Intercellular adhesion junction is directed by calcium-dependent cadherins, and MSCs express neural (N-) cadherin and epithelial (E-) cadherin (Qin L. et al., 2020). The classical structure of cadherins can be divided into three domains: an extracellular domain to direct intercellular adhesion, a single-pass transmembrane domain, and a cytoplasmic domain to bind multiple proteins including β-catenin and α-catenin (Leckband and de Rooij, 2014). When MSCs are subjected to mechanical stimuli (such as load-induced FFSS) or electromagnetic stimuli (such as PEMF), β-catenin disassociates from N-cadherin or E-cadherin to the cytoplasm, respectively, which then moves to the nucleus to induce osteogenic differentiation (Arnsdorf et al., 2009b; Zhang et al., 2020).

The β-catenin signaling pathway is generally regulated by canonical Wnt signaling, which shows biophysical sensitivity. When MSCs are subjected to electromagnetic stimuli for osteogenesis, the expression levels of Wnt, low-density lipoprotein receptor-related protein (Lrp), and β-catenin are upregulated, suggesting that canonical Wnt signaling exerts critical effects in osteogenic differentiation (Chen et al., 2019; Fu et al., 2020). Secreted Wnt binds to the complex formed by Fzd and LRP 5/6, which then activates Dvl to impede the phosphorylation and degradation of β-catenin mediated by the axin/adenomatous polyposis coli/GSK-3β/CK1 (Axin/APC/GSK-3β/CK1) complex (Schupbach et al., 2020). Then, β-catenin shuttles to the nucleus to activate osteogenic Runx2 and osterix (Benayahu et al., 2019). The activation of canonical Wnt signaling by biophysical stimuli could also inhibit MSC adipogenesis by downregulating the expression of peroxisome proliferator-activated receptor γ (Sen et al., 2008; Case et al., 2013).

3.3.2 Notch Signaling

Exerting critical effects on stem cell specification and bone development, Notch signaling is an intercellular conversed pathway that is activated by a surface ligand [Delta-like (Dll)1, 3, or 4 and Jagged (JAG)1 or 2] from adjacent cells to bind their Notch receptor (Notch1, 2, 3, or 4) (Bagheri et al., 2018). After initiation, two types of proteases (ADAM-family metalloproteases and presenilin-γ-secretase complex) exert effects at an activated Notch receptor to release the Notch intracellular domain (NICD). The NICD then forms a complex with the DNA-binding CSL protein after translocating to the nucleus, which recruits coactivator Mastermind to transcript related genes. When MSCs are subjected to PEMF, Notch-4 receptor, Dll-4 ligand, and related genes (Hey1, Hes1, and Hes5) are upregulated, and inhibitors of Notch signaling diminish the osteoinducutive effects of PEMG

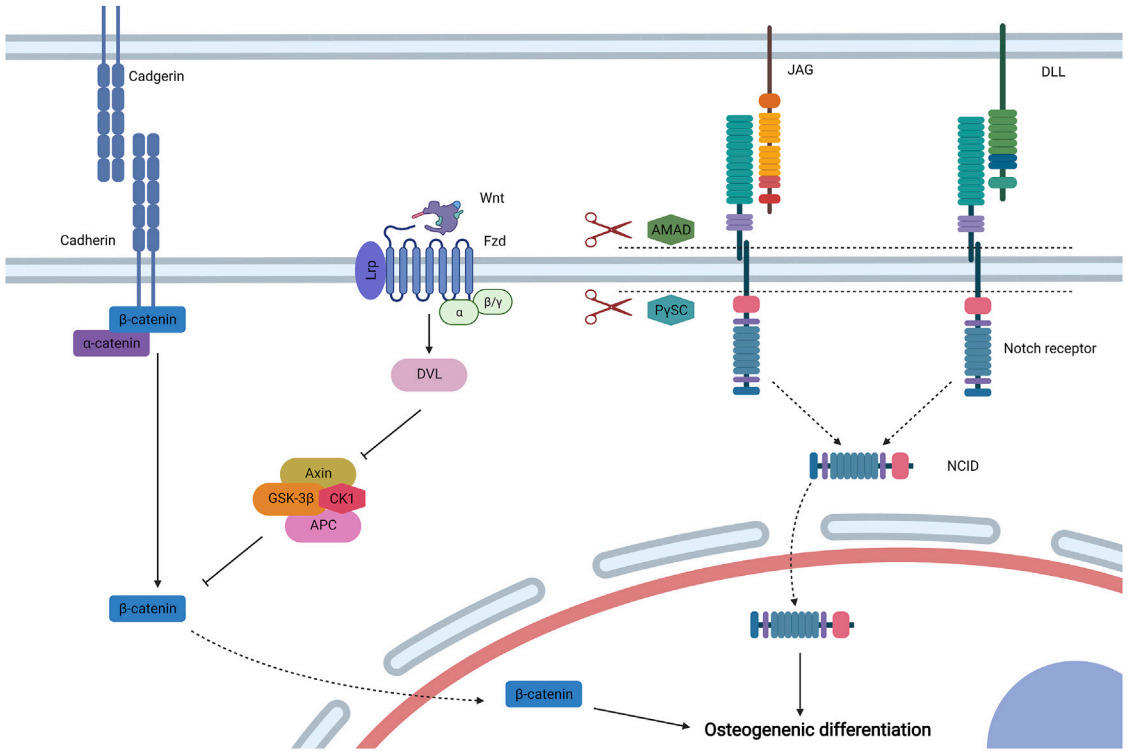

FIGURE 5 | Cell–cell biophysical transduction for MSC osteogenesis: direct interaction. Cadherin is a main molecule to induce direct intercellular interaction, and α-catenin and β-catenin are linked to the cytoplasmic section of cadherin. Under biophysical stimuli, β-catenin dissociates from cadherin to cytoplasm. In addition, β-catenin is mainly regulated by biophysical sensitive canonical Wnt signaling. Wnt binds to the lipoprotein receptor-related protein (Lrp)/Fzd complex and activates Dvl to inhibit the axin/adenomatous polyposis coli/GSK-3β/CK1 (Axin/APC/GSK-3β/CK1) complex to avoid the degradation of β-catenin. Then, β-catenin moves to the nucleus to promote MSC osteogenesis. The osteoinduction of direct cell–cell biophysical transduction can be induced by Notch signaling, which is mediated by Notch receptors and Delta-like (Dll) or Jagged (JAG) ligands. Under biophysical stimuli, two proteases, including ADAM-family metalloproteases and presenilin-γ-secretase complex (PγSC), release Notch intracellular domain (NICD) form Notch receptor, which then moves to the nucleus for osteogenic differentiation. Created with BioRender.com.

(Bagheri et al., 2018). Thus, Notch signaling is involved in the osteogenic differentiation of MSCs stimulated by electromagnetic signaling. Another research also reported that mechanical stimuli could initiate JAG1-mediated Notch signaling to promote MSC osteogenesis, which is controlled by the inhibition of endogenous histone deacetylase 1 (Wang et al., 2016a).

3.3.3 Autocrine and Paracrine Network

After being subjected to biophysical stimuli, MSCs secrete various biophysical-sensitive molecules, including BMP-2 (Liu et al., 2011; Rui et al., 2011), vascular endothelial growth factor (Lee et al., 2017), insulin-like growth factor 1 (Tahimic et al., 2016), transforming growth factor-β (TGF-β) (Li et al., 2015b), and migration inhibitory factor (Yuan et al., 2016), which could biochemically promote MSC osteogenesis by autocrine. In addition, bone regeneration *in vivo* is an extremely complex process that involves osteogenesis, angiogenesis, osteoclastogenesis, neurogenesis, and immune regulation; thus, a paracrine network possibly stimulates osteogenesis among various cells when subjected to biophysical stimuli. Paracrine factors from stimulated osteocytes promote the osteogenic differentiation of MSCs but do not induce the osteogenic differentiation of osteoblasts (Hoey et al., 2011; Brady et al., 2015). Another study found that exosomes containing miRNA181b-5p from stimulated osteocytes enhance the osteogenic differentiation of PDLCs by BMP-2/RUNX2 (Lv et al., 2020). Stimulated osteocytes also secrete nitric oxide and relatively more osteoprotegerin than NF-κB ligand (RANKL) to inhibit osteoclastogenesis (Tan et al., 2007; You et al., 2008). Moreover, exosomes from stimulated MSCs impede osteoclastogenesis by weakening the activity of NF-κB signaling (Xiao et al., 2021). Although paracrine factors from stimulated osteoblasts fail to promote the osteogenic differentiation of MSCs, they inhibit the formation of osteoclasts (Tan et al., 2007). Furthermore, Dong et al. (2021) found that tension could activate macrophages to M2 phenotype, secrete anti-inflammatory factors (such as TGF-β and interleukins-10), and promote the nuclear translocation of YAP to generate BMP-2 for the osteogenic differentiation of MSCs. Altogether, the autocrine and paracrine network may ultimately promote the osteogenic differentiation of MSCs *in vivo*, which further promote bone repair.

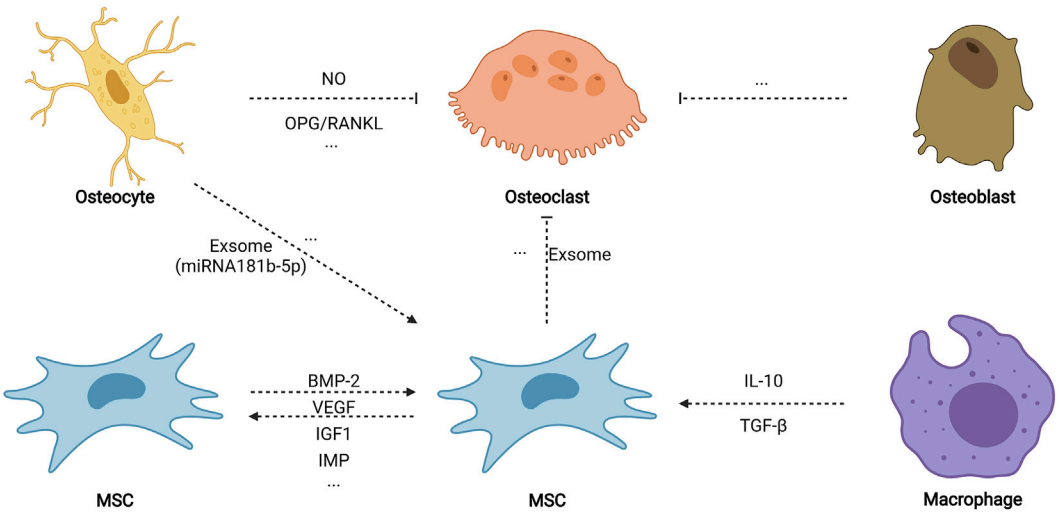

FIGURE 6 | Cell–cell biophysical transduction for MSC osteogenesis: indirect autocrine and paracrine. Indirect cell–cell biophysical transduction is mainly induced by the autocrine and paracrine network. Under biophysical stimuli, MSCs may sensitively secret some autocrine proteins to promote osteogenesis, including BMP-2, VEGF, IGF1, TGF-β, and MIF. MSCs also secrete paracrine factors (such as exosome) to inhibit osteoclastogenesis. Osteocytes release nitric oxide (NO) and relatively more osteoprotegerin (OPG) than NF-κB ligand (RANKL) to impede osteoclastogenesis. Paracrine factors from osteoblasts also diminish osteoclastogenesis. Moreover, paracrine factors (such as exosome containing miRNA181b-5p) stimulate the osteogenic differentiation of MSCs. Biophysical stimuli also stimulate macrophage (phenotype 2) to promote MSC osteogenesis. Created with BioRender.com.

4 APPLICATIONS OF BIOPHYSICAL STIMULI FOR BONE TISSUE ENGINEERING

For critical bone defects, bone tissue engineering is committed to replace or surpass autografts for surgical bone repair. Given their osteoinductive properties, distinctive biophysical stimuli can be used as the fourth pillar to improve traditional bone tissue engineering for bone healing. Biophysical stimuli can be integrated to bone tissue engineering by three methodologies: preconstructed scaffolds with osteoinductive properties, TEBGs, and postoperative biophysical stimuli loading strategies.

4.1 Preconstructed Scaffolds With Osteoinductive Properties

Biomaterial scaffolds comprise an important pillar for bone tissue engineering, but most current scaffolds are used to provide osteoconductivity without osteoinductivity. Thus, most studies focused on the introduction of bioactive molecules to scaffolds by various strategies. However, these methods fail to construct scaffolds with multi-environment for different regenerative purposes. Thus, preconstructed scaffolds by biophysical stimuli show great promise for novel bone tissue engineering because these scaffolds show inherent osteoinductivity, which also support the construction of multi-microenvironment. Preconstructed scaffolds include stiffness-improved scaffolds, topography-modified scaffolds, piezoelectric scaffolds, and magnetically actuated scaffolds.

4.1.1 Stiffness-Improved ECM-like Scaffolds

ECM-like scaffolds are those scaffolds that are structurally analogous to natural nanoscale natural ECM, which can be obtained by electrospinning or hydrogelation. However, the application of ECM-like scaffolds is generally limited by their unsatisfying stiffness. Thus, various strategies, including chemical and physical crosslinking, have been developed to enhance their rigidity. Chemical crosslinking improves stiffness by introducing chemical crosslinkers (such as genipin) and specific chemical groups, whereas physical crosslinking enhances rigidity by constructing an interpenetrating network or physical crosslinkers, such as inorganic particles and graphene (Zhang et al., 2016). When the stiffness of organic scaffolds is improved, these scaffolds could even stimulate the osteogenic differentiation of MSCs without osteogenic molecules. For example, elastin-like polypeptides (ELPs) are recombinant biomaterials that could assemble into organic scaffolds when the temperature reaches over inverse phase transition temperature (Ding et al., 2020). Glassman et al. (2016) utilized telechelic oxidative coupling to chemically interlink or oxidate ELPs containing cysteine, and the stiffness of ELP scaffolds is obviously enhanced, varying from 5 kPa to over 1 MPa. When seeded on the toughened scaffolds, MSCs could be induced to undergo osteogenic differentiation without bioactive molecules. Raftery et al. introduced chitosan to collagen to construct organic scaffolds with an interpenetrating network and found that the modulus is improved and that the interpenetrating scaffold (collagen/chitosan ratio 75/25) could dramatically promote calcium deposition and sulfated glycosaminoglycan production (Raftery et al., 2016). Thus, stiffness-improved scaffolds may be superior to unoptimized organic scaffolds.

4.1.2 Topography-Modified Scaffolds

Modifying topography is another methodology for osteoinductive preconstructed scaffolds. The outer and inner

surfaces can be modified for different regenerative purposes. Outer topography-modified scaffolds are those scaffolds whose outer surface are modified by nanopattern with controlled disorder, which could promote osteointegration and avoid the formation of fibrous tissue at the surface of bone implants (Dobbenga et al., 2016). For example, Silverwood et al. (2016) utilized a block-copolymer templated anodization technique to modify the outer surface of titania scaffolds with nanopillars (height 15 nm) and then transplanted modified titania and polished titania to rabbit femurs. Compared with the flat titania, the outer topography-modified titania with 15 nm nanopillars show higher bone to implant contact (20%) (Silverwood et al., 2016). Meanwhile, inter topography-modified scaffolds are those scaffolds whose porous inner surface are modified by controlled nanotopography. For example, Wang et al. used cold atmospheric plasma to treat or modify the inter topography of 3D printed poly-lactic-acid scaffolds, which could improve nanoscale surface roughness from 1.20 to 10.50 nm (1 min treatment), 22.90 nm (3 min treatment), and 27.60 nm (5 min treatment) (Wang et al., 2016b). And modified scaffolds could improve cell adhesion and proliferation when compared with unmodified scaffolds, showing great potential for bone tissue engineering (Wang M. et al., 2016). Further studies should focus on the osteogenic effects of the modified inter surface, and related treating techniques should also be developed.

4.1.3 Piezoelectric Scaffolds

Natural bone is an electricity-generated tissue because of piezoelectric collagen (Yu et al., 2017). Thus, piezoelectric scaffolds are developed to provide electric stimuli for bone regeneration, which include piezoelectric polymers such as PEDOT (Iandolo et al., 2016) and poly (vinylidene fluoride), piezoelectric ceramics such as $BaTiO_3$ (Polley et al., 2020) and $K_{0.5}Na_{0.5}NbO_3$ (Yu et al., 2017), and scaffolds containing piezoelectric particles such as piezoelectric ceramic particles (Mancuso et al., 2021) and nylon-11 nanoparticles (Ma et al., 2019)). When piezoelectric scaffolds are subjected to external mechanical stimuli (physiologically or additionally), electric stimuli will be induced for bone regeneration (Tang et al., 2017). Osteogenic differentiation can be obtained by high voltage output form piezoelectric scaffolds (Damaraju et al., 2017). However, the piezoelectricity of scaffolds should be optimized for practical applications. For example, Zhang et al. utilized annealing treatment to control β phase contents, thus constructing piezoelectric poly (vinylidene fluoridetrifluoroethylene) [P(VDF-TrFE)] membranes with different surface potentials (−78 and −53 mV) (Zhang et al., 2018). When transplanted to critical calvarial defects of rats, all groups could promote bone regeneration, but P(VDF-TrFE) membrane with −53 mV surface potential is better because it dramatically promotes faster bone regeneration with more mature bone structure than unpolarized group and that with −78 mv surface potential (Zhang et al., 2018). Furthermore, the osteoinductive effects of piezoelectric scaffolds can enhance additional mechanical stimuli. Piezoelectric scaffolds were fabricated by modifying porous Ti6Al4V scaffolds (pTi) with $BaTiO_3$, and then piezoelectric pTi/$BaTiO_3$ or pure pTi were transplanted to rabbit radius bone defects with a length of 13 mm (Fan et al., 2020). Results showed that pTi/$BaTiO_3$ with or without LIPUS promotes more bone regeneration than pure pTi, but LIPUS treatment could further enhance osteointegration and osteogenesis (Fan et al., 2020).

4.1.4 Magnetically Actuated Scaffolds

Magnetically actuated scaffolds are generally constructed by introducing magnetic particles (usually magnetite) to other biomaterial scaffolds (Santos et al., 2015). When magnetically actuated scaffolds are exposed in magnetic field, the deformation of scaffolds stimulates the differentiation of stem cells (Spangenberg et al., 2021). Aldebs et al. (2020) used PEGF (1 mT, 15 Hz) to stimulate ADSCs for 7 days seeded in RADA16 self-assembling peptide hydrogel containing magnetic particles and found that PEGF coupled with magnetic particles could promote the osteogenic differentiation of ADSCs without spoiling cell viability. Moreover, magnetic nanoparticles can be encapsuled to piezoelectric scaffolds, which could provide magnetomechanical and electromagnetic stimuli (Fernandes et al., 2019). Zhang et al. fabricated magnetically actuated scaffolds with magnetic effects by simultaneously incorporating two magnetic particles: positive $CoFe_2O_4$ (CFO) and negative $Tb_xDy_{1-x}Fe_2$ alloy (TD) to piezoelectric P(VDF-TrFE) (Zhang et al., 2020). A CFO/TD ratio of 4:1 could dramatically improve surface potential when scaffolds are exposed to magnetic field. Then, MSCs were seeded on the film for 7 or 14 days, and a magnetic field was applied at the 4^{th} or 8^{th} day. Results showed that magnetic field could dramatically stimulate the osteogenic differentiation of MSCs in the 14-days culture, but osteogenic differentiation was not observed at the 4-days culture, suggesting that magnetic field-coupled magnetic particles could promote osteogenesis, but sufficient exposure time is needed (Zhang et al., 2020). Although magnetically actuated scaffolds show satisfying biocompatibility when transplanted *in vivo*, additional evidence is needed about bone defect repair *in vivo* by magnetically actuated scaffolds coupled with magnetic field.

4.2 Tissue Engineered Bone Grafts by *in vitro* Bioreactors

In addition to prefabricated osteoinductive scaffolds by biophysical stimuli, they can be directly exerted by *in vitro* bioreactors to construct TEBGs, artificial autografts with anatomically matched shape and size (Grayson et al., 2010). TEBGs are generally fabricated by a combination of a biomaterial scaffold, autogenous stem cells, osteogenic supplements, and *in vitro* bioreactors providing biophysical stimuli (Fröhlich et al., 2010).

Among various *in vitro* bioreactors, load-induced FFSS-based bioreactors have been widely used to construct TEBGs, especially perfusion bioreactors. The efficiency of TEBGs for bone tissue engineering was initially verified by ectopic bone formation in animal models. Hosseinkhani et al. mixed MSC suspension with peptide amphiphile (PA) solution to form PA nanofiber hydrogel

containing MSCs, which was then infiltrated to collagen/poly (glycolic acid) sponge for static or prefusion culture (Hosseinkhani et al., 2006). After 3 weeks of *in vitro* culture, both groups were transplanted to the back subcutis of rats for 8 weeks, and results showed that the TEBGs obtained by perfusion culture promote homogenous and robust bone regeneration when compared with those by static culture (Hosseinkhani et al., 2006). Moreover, TEBGs for critical bone defects have been verified in clinically relevant pig bone defect models. An image-guided personalized strategy was utilized to construct TEBGs by 3 weeks of invitro culture (Bhumiratana et al., 2016). TEBGs are constructed by a combination of decellularized bone matrixes (DBMs), autogenous ADSCs, osteogenic medium, and a perfusion-based bioreactor, and immure bone formation is observed after 3 weeks of perfusion culture. Then, TEBGs or acellular DBMs were transplanted to bone defects of mature Yucatán minipigs for 6 weeks, and results revealed that TEBGs show improved bone formation and vascularization compared with untreated defects and acellular scaffolds (Bhumiratana et al., 2016). Therefore, TEBGs show great promise for critical bone defects, which ideally integrate four pillars of bone tissue engineering.

TEBGs may be the second-generation autogenous bone grafts for surgical bone repair. Thus, various methods have been developed to improve the effectiveness of TEBGs, which are based on four hierarchies. The first level is to optimize perfusion profile, which includes perfusion duration and perfusion model. Dynamic culture for at least 2 weeks is needed to fabricate TEBGs (Mitra et al., 2017). In addition, sequential application of continuous perfusion and intermittent perfusion may be better than single model (Correia et al., 2013). The second level is to optimize bioreactor system medium. For example, marine hemoglobin could be incorporated to perfusion medium to deliver sufficient oxygen, which enhances the proliferation and osteogenic differentiation of MSCs in perfusion bioreactors (Le Pape et al., 2018). The third level is to optimize seed cells. For example, BMSCs may be superior to ADSCs because of better potential for osteogenesis (Wu et al., 2015). In addition, co-culture of multiple cells may be superior to single cell culture for the fabrication of TEBGs (Sawyer et al., 2020), but multiple cells must be obtained from autogenous stem cells. Thus, co-culture of osteogenically indued stem cells and angiogenic-induced stem cells shows great promise. Furthermore, the fourth level is to optimize biomaterial scaffolds. Hydrogels can be used to modify other biomaterials because hydrogels could improve cell retention (Yu et al., 2012). In addition, bioactive molecules can be introduced to biomaterial scaffolds to provide sustained-release osteoinductive signaling (Panek et al., 2019).

In addition to perfusion bioreactors, load induced-FFSS-based bioreactors include rotating wall vessel bioreactors, spinner flask bioreactors, and biaxial rotating bioreactors, among which biaxial rotating bioreactors may surpass other uni-axial perfusion bioreactors because they generate homogenous FFSS and promote robust osteogenesis (Singh et al., 2005; Zhang et al., 2010a). TEBGs fabricated by biaxial rotating bioreactors induce ectopic bone regeneration (Zhang et al., 2009) and promote the healing of critical femoral defects of rats (Zhang et al., 2010b).

Other bioreactors include compression bioreactors (Ravichandran et al., 2017), tension bioreactors (Carroll et al., 2017), nanovibration bioreactors (Wu et al., 2020), ultrasound bioreactors (Wang M. et al., 2016), and electromagnetic bioreactors (Fernandes et al., 2019), which show promise to construct TEBGS, but they are limited to transport nitrogen, oxygen, and growth factors. Therefore, other bioreactors can be synthetically used with load induce-FFSS based bioreactors to design multi-biophysical stimuli bioreactors. For example, a multimodal bioreactor was designed which could provide compression and load-induced FFSS, and osteogenic differentiation is improved when compared with static culture and culture with single biophysical stimuli when the system is used to dynamically culture MSCs (Ravichandran et al., 2018). Further evidence is needed about TEBGs fabricated by multimodal bioreactors to repair critical bone defects.

4.3 Postoperative Biophysical Stimuli Loading Strategies

Postoperative biophysical stimuli loading strategies are those methods that use noninvasive methods to generate biophysical stimuli to stimulate bone regeneration after surgery, including distraction osteogenesis (DO) (Shah et al., 2021), LMHFV (Steppe et al., 2020), LIPUS (Hannemann et al., 2014), and PEMF (Wang et al., 2019). These strategies have been clinically used to promote the healing of fractures; thus, their use can be extended to the treatment of critical bone defects. For example, Parmaksiz et al. transplanted DBM and DBM containing magnetic particles to bilateral critical-size cranial defects of rats with or without PEMF exposure, and results revealed that exposed groups of DBM and DBM containing magnetic particles show improved bone regeneration and reduced fibrous formation compared with unexposed groups (Parmaksiz et al., 2021). Yan et al. also verified that postoperative LIPUS could promote the healing of rabbit femurs defects (Yan et al., 2016). Therefore, postoperative biophysical stimuli loading strategies show great promise in bone tissue engineering, but they remain poorly explored. Bone defects are usually limited to local regions. Thus, small loading devices are also highly developed for clinical bone repair. When postoperative biophysical stimuli loading strategies are used in combination of other pillars of bone tissue engineering, their clinical complications or drawbacks may diminish. For example, DO is a long-term treatment that may cause infections or delay, but it shows great promise for bone regeneration when combined with osteoinducive Mg nail, which could reduce the treatment time of traditional DO (Ye et al., 2021).

5 DISCUSSION

Considering the inefficiency of current biomaterials and bioactive molecules, biophysical stimuli are critical to be applied as the

fourth pillar of bone tissue engineering. In addition, biophysical stimuli should not be only limited to external mechanical stimuli, but in a more comprehensive concept, the fourth pillar can also include internal structural stimuli, acoustic stimuli, and electromagnetic stimuli. Although distinctive biophysical stimuli are based on different physical properties, they will be transferred to mechanical or electromagnetic stimuli. Given that both show reminiscent signal pathways for MSC osteogenesis, a novel concept of biophysical transduction is proposed to incorporate mechanotransduction and electrocoupling to interpret the osteoinductive mechanisms of biophysical stimuli for osteogenic differentiation. Biophysical transduction can be divided into three stages: sensing, transmission, and regulation. Depending on sensing pattern, biophysical transduction can be categorized into self-biophysical transduction, cell–matrix biophysical transduction, and cell-cell biophysical transduction. Furthermore, biophysical stimuli, as the fourth pillar of bone tissue engineering, can be used by fabricating preconstructed scaffolds with osteoinductive properties and TEBGs or by employing postoperative biophysical stimuli loading strategies.

While biophysical stimuli show promising potential to be used as the fourth pillar of bone tissue engineering, ideal biophysical stimuli are needed to promote cell recruitment, proliferation, osteogenesis, angiogenesis, neurogenesis, and immune regulation. Osteoinductive windows of biophysical stimuli need to be comprehensively considered and optimized. The synergy effects of multiple biophysical stimuli should be also explored for bone regeneration. Moreover, specific osteoinductive mechanisms of biophysical stimuli need further investigation. The interaction between mechanotransduction and electrocoupling should be probed to interpret their similarity. Whether or not other cell adhesion receptors and ligands participate in cell–matrix biophysical transduction remains unknown. The autocrine and paracrine network of cell–cell biophysical transduction also needs to be refined. *In vivo* preclinical evidence about preconstructed scaffolds may be obtained, especially for piezoelectric scaffolds and magnetically actuated scaffolds. Novel *in vitro* bioreactors may be designed to diminish complexity and volume. Further studies may focus on the application of postoperative biophysical stimuli loading strategies for the treatment of critical bone defects. Specific parameters using model and duration may be established.

AUTHOR CONTRIBUTIONS

ZH, ZX, and XW contributed equally to this work. ZH researched and analyzed the literature, prepared the manuscript, and drew the figures. ZX and XW researched and analyzed the literature, prepared the manuscript. HL and TC researched the literature and modified the manuscript. YH, YW, RC and KH modified the manuscript and figures. JL and CC supervised, administrated and edited the work. All authors have approved for the publication.

FUNDING

We thanks to the funds to support the work, which include the National Natural Science Foundation of China (No: 81871752), Hubei Provincial Natural Science Foundation (No: 2020CFB551), Zhongnan Hospital of Wuhan University Science, Technology and Innovation Seed Fund (No: cxpy2019074), and Translational Medicine and Interdisciplinary Research Joint Fund of Zhongnan Hospital of Wuhan University (No. ZNJC202014).

REFERENCES

Al Nazer, R., Lanovaz, J., Kawalilak, C., Johnston, J. D., and Kontulainen, S. (2012). Direct *In Vivo* Strain Measurements in Human Bone-A Systematic Literature Review. *J. Biomech.* 45, 27–40. doi:10.1016/j.jbiomech.2011.08.004

Aldebs, A. I., Zohora, F. T., Nosoudi, N., Singh, S. P., and Ramirez-Vick, J. E. (2020). Effect of Pulsed Electromagnetic fields on Human Mesenchymal Stem Cells Using 3d Magnetic Scaffolds. *Bioelectromagnetics* 41, 175–187. doi:10.1002/bem.22248

Arjmand, M., Ardeshirylajimi, A., Maghsoudi, H., and Azadian, E. (2018). Osteogenic Differentiation Potential of Mesenchymal Stem Cells Cultured on Nanofibrous Scaffold Improved in the Presence of Pulsed Electromagnetic Field. *J. Cell Physiol* 233, 1061–1070. doi:10.1002/jcp.25962

Arnsdorf, E. J., Tummala, P., and Jacobs, C. R. (2009a). Non-Canonical Wnt Signaling and N-Cadherin Related β-Catenin Signaling Play a Role in Mechanically Induced Osteogenic Cell Fate. *PloS one* 4, e5388. doi:10.1371/journal.pone.0005388

Arnsdorf, E. J., Tummala, P., Kwon, R. Y., and Jacobs, C. R. (2009b). Mechanically Induced Osteogenic Differentiation - the Role of RhoA, ROCKII and Cytoskeletal Dynamics. *J. Cel. Sci.* 122, 546–553. doi:10.1242/jcs.036293

Aziz, A. H., Eckstein, K., Ferguson, V. L., and Bryant, S. J. (2019). The Effects of Dynamic Compressive Loading on Human Mesenchymal Stem Cell Osteogenesis in the Stiff Layer of a Bilayer Hydrogel. *J. Tissue Eng. Regen. Med.* 13, 946–959. doi:10.1002/term.2827

Bagheri, L., Pellati, A., Rizzo, P., Aquila, G., Massari, L., De Mattei, M., et al. (2018). Notch Pathway Is Active during Osteogenic Differentiation of Human Bone Marrow Mesenchymal Stem Cells Induced by Pulsed Electromagnetic fields. *J. Tissue Eng. Regen. Med.* 12, 304–315. doi:10.1002/term.2455

Baumgartner, W., Schneider, I., Hess, S. C., Stark, W. J., Märsmann, S., Brunelli, M., et al. (2018). Cyclic Uniaxial Compression of Human Stem Cells Seeded on a Bone Biomimetic Nanocomposite Decreases Anti-osteogenic Commitment Evoked by Shear Stress. *J. Mech. Behav. Biomed. Mater.* 83, 84–93. doi:10.1016/j.jmbbm.2018.04.002

Benayahu, D., Wiesenfeld, Y., and Sapir-Koren, R. (2019). How Is Mechanobiology Involved in Mesenchymal Stem Cell Differentiation toward the Osteoblastic or Adipogenic Fate? *J. Cell Physiol* 234, 12133–12141. doi:10.1002/jcp.28099

Bertrand, A. A., Malapati, S. H., Yamaguchi, D. T., and Lee, J. C. (2020). The Intersection of Mechanotransduction and Regenerative Osteogenic Materials. *Adv. Healthc. Mater.* 9, 2000709. doi:10.1002/adhm.202000709

Bhavsar, M. B., Cato, G., Hauschild, A., Leppik, L., Costa Oliveira, K. M., Eischen-Loges, M. J., et al. (2019). Membrane Potential (Vmem) Measurements during Mesenchymal Stem Cell (MSC) Proliferation and Osteogenic Differentiation. *PeerJ* 7, e6341. doi:10.7717/peerj.6341

Bhumiratana, S., Bernhard, J. C., Alfi, D. M., Yeager, K., Eton, R. E., Bova, J., et al. (2016). Tissue-engineered Autologous Grafts for Facial Bone Reconstruction. *Sci. Transl. Med.* 8, 343ra83. doi:10.1126/scitranslmed.aad5904

Birks, S., and Uzer, G. (2021). At the Nuclear Envelope of Bone Mechanobiology. *Bone* 151, 116023. doi:10.1016/j.bone.2021.116023

Bjerre, L., Bünger, C. E., Kassem, M., and Mygind, T. (2008). Flow Perfusion Culture of Human Mesenchymal Stem Cells on Silicate-Substituted Tricalcium

Phosphate Scaffolds. *Biomaterials* 29, 2616–2627. doi:10.1016/j.biomaterials.2008.03.003

Boda, S. K., Thrivikraman, G., and Basu, B. (2015). Magnetic Field Assisted Stem Cell Differentiation - Role of Substrate Magnetization in Osteogenesis. *J. Mater. Chem. B* 3, 3150–3168. doi:10.1039/c5tb00118h

Bouzid, T., Kim, E., Riehl, B. D., Esfahani, A. M., Rosenbohm, J., Yang, R., et al. (2019). The Linc Complex, Mechanotransduction, and Mesenchymal Stem Cell Function and Fate. *J. Biol. Eng.* 13, 68. doi:10.1186/s13036-019-0197-9

Brady, R. T., O'Brien, F. J., and Hoey, D. A. (2015). Mechanically Stimulated Bone Cells Secrete Paracrine Factors that Regulate Osteoprogenitor Recruitment, Proliferation, and Differentiation. *Biochem. biophysical Res. Commun.* 459, 118–123. doi:10.1016/j.bbrc.2015.02.080

Burks, S. R., Nagle, M. E., Bresler, M. N., Kim, S. J., Star, R. A., and Frank, J. A. (2018). Mesenchymal Stromal Cell Potency to Treat Acute Kidney Injury Increased by Ultrasound-Activated Interferon-Γ/interleukin-10 axis. *J. Cell Mol Med* 22, 6015–6025. doi:10.1111/jcmm.13874

Carroll, S. F., Buckley, C. T., and Kelly, D. J. (2017). Cyclic Tensile Strain Can Play a Role in Directing Both Intramembranous and Endochondral Ossification of Mesenchymal Stem Cells. *Front. Bioeng. Biotechnol.* 5, 73. doi:10.3389/fbioe.2017.00073

Case, N., Thomas, J., Xie, Z., Sen, B., Styner, M., Rowe, D., et al. (2013). Mechanical Input Restrains PPARγ2 Expression and Action to Preserve Mesenchymal Stem Cell Multipotentiality. *Bone* 52, 454–464. doi:10.1016/j.bone.2012.08.122

Cashion, A. T., Caballero, M., Halevi, A., Pappa, A., Dennis, R. G., and van Aalst, J. A. (2014). Programmable Mechanobioreactor for Exploration of the Effects of Periodic Vibratory Stimulus on Mesenchymal Stem Cell Differentiation. *BioResearch open access* 3, 19–28. doi:10.1089/biores.2013.0048

Chang, Y., Shao, Y., Liu, Y., Xia, R., Tong, Z., Zhang, J., et al. (2019). Mechanical Strain Promotes Osteogenic Differentiation of Mesenchymal Stem Cells on TiO2 Nanotubes Substrate. *Biochem. biophysical Res. Commun.* 511, 840–846. doi:10.1016/j.bbrc.2019.02.145

Chen, J. C., Hoey, D. A., Chua, M., Bellon, R., and Jacobs, C. R. (2016). Mechanical Signals Promote Osteogenic Fate through a Primary Cilia-mediated Mechanism. *FASEB j.* 30, 1504–1511. doi:10.1096/fj.15-276402

Chen, J., Tu, C., Tang, X., Li, H., Yan, J., Ma, Y., et al. (2019). The Combinatory Effect of Sinusoidal Electromagnetic Field and Vegf Promotes Osteogenesis and Angiogenesis of Mesenchymal Stem Cell-Laden Pcl/ha Implants in a Rat Subcritical Cranial Defect. *Stem Cell Res Ther* 10, 379. doi:10.1186/s13287-019-1464-x

Chen, X., He, F., Zhong, D.-Y., and Luo, Z.-P. (20152015). Acoustic-frequency Vibratory Stimulation Regulates the Balance between Osteogenesis and Adipogenesis of Human Bone Marrow-Derived Mesenchymal Stem Cells. *Biomed. Research International* 2015, 1–10. doi:10.1155/2015/540731

Cho, M. R., Thatte, H. S., Silvia, M. T., and Golan, D. E. (1999). Transmembrane Calcium Influx Induced by Ac Electric fields. *FASEB j.* 13, 677–683. doi:10.1096/fasebj.13.6.677

Correia, C., Bhumiratana, S., Sousa, R. A., Reis, R. L., and Vunjak-Novakovic, G. (2013). Sequential Application of Steady and Pulsatile Medium Perfusion Enhanced the Formation of Engineered Bone. *Tissue Eng. A* 19, 1244–1254. doi:10.1089/ten.TEA.2011.0701

Corrigan, M. A., Johnson, G. P., Stavenschi, E., Riffault, M., Labour, M.-N., and Hoey, D. A. (2018). Trpv4-mediates Oscillatory Fluid Shear Mechanotransduction in Mesenchymal Stem Cells in Part via the Primary Cilium. *Sci. Rep.* 8, 3824. doi:10.1038/s41598-018-22174-3

Creecy, C. M., O'Neill, C. F., Arulanandam, B. P., Sylvia, V. L., Navara, C. S., and Bizios, R. (2013). Mesenchymal Stem Cell Osteodifferentiation in Response to Alternating Electric Current. *Tissue Eng. Part A* 19, 467–474. doi:10.1089/ten.TEA.2012.0091

Dalby, M. J., Gadegaard, N., and Oreffo, R. O. C. (2014). Harnessing Nanotopography and Integrin-Matrix Interactions to Influence Stem Cell Fate. *Nat. Mater* 13, 558–569. doi:10.1038/nmat3980

Dalby, M. J., Gadegaard, N., Tare, R., Andar, A., Riehle, M. O., Herzyk, P., et al. (2007). The Control of Human Mesenchymal Cell Differentiation Using Nanoscale Symmetry and Disorder. *Nat. Mater* 6, 997–1003. doi:10.1038/nmat2013

Damaraju, S. M., Shen, Y., Elele, E., Khusid, B., Eshghinejad, A., Li, J., et al. (2017). Three-dimensional Piezoelectric Fibrous Scaffolds Selectively Promote Mesenchymal Stem Cell Differentiation. *Biomaterials* 149, 51–62. doi:10.1016/j.biomaterials.2017.09.024

Dash, S. K., Sharma, V., Verma, R. S., and Das, S. K. (2020). Low Intermittent Flow Promotes Rat Mesenchymal Stem Cell Differentiation in Logarithmic Fluid Shear Device. *Biomicrofluidics* 14, 054107. doi:10.1063/5.0024437

Datta, N., Pham, Q. P., Sharma, U., Sikavitsas, V. I., Jansen, J. A., and Mikos, A. G. (2006). *In Vitro* generated Extracellular Matrix and Fluid Shear Stress Synergistically Enhance 3d Osteoblastic Differentiation. *Proc. Natl. Acad. Sci.* 103, 2488–2493. doi:10.1073/pnas.0505661103

de Lucas, B., Pérez, L. M., Bernal, A., and Gálvez, B. G. (2020). Ultrasound Therapy: Experiences and Perspectives for Regenerative Medicine. *Genes* 11, 1086. doi:10.3390/genes11091086

Delaine-Smith, R. M., and Reilly, G. C. (2012). Mesenchymal Stem Cell Responses to Mechanical Stimuli. *Muscles Ligaments Tendons J.* 2, 169–180.

Ding, X., Zhao, H., Li, Y., Lee, A. L., Li, Z., Fu, M., et al. (2020). Synthetic Peptide Hydrogels as 3d Scaffolds for Tissue Engineering. *Adv. Drug Deliv. Rev.* 160, 78–104. doi:10.1016/j.addr.2020.10.005

Dobbenga, S., Fratila-Apachitei, L. E., and Zadpoor, A. A. (2016). Nanopattern-induced Osteogenic Differentiation of Stem Cells - a Systematic Review. *Acta Biomater.* 46, 3–14. doi:10.1016/j.actbio.2016.09.031

Dong, L., Song, Y., Zhang, Y., Zhao, W., Wang, C., Lin, H., et al. (2021). Mechanical Stretch Induces Osteogenesis through the Alternative Activation of Macrophages. *J. Cell Physiol* 236, 6376–6390. doi:10.1002/jcp.30312

Driscoll, T. P., Cosgrove, B. D., Heo, S.-J., Shurden, Z. E., and Mauck, R. L. (2015). Cytoskeletal to Nuclear Strain Transfer Regulates Yap Signaling in Mesenchymal Stem Cells. *Biophysical J.* 108, 2783–2793. doi:10.1016/j.bpj.2015.05.010

Dupont, S., Morsut, L., Aragona, M., Enzo, E., Giulitti, S., Cordenonsi, M., et al. (2011). Role of Yap/taz in Mechanotransduction. *Nature* 474, 179–183. doi:10.1038/nature10137

Eischen-Loges, M., Oliveira, K. M. C., Bhavsar, M. B., Barker, J. H., and Leppik, L. (2018). Pretreating Mesenchymal Stem Cells with Electrical Stimulation Causes Sustained Long-Lasting Pro-osteogenic Effects. *PeerJ* 6, e4959. doi:10.7717/peerj.4959

Elosegui-Artola, A., Andreu, I., Beedle, A. E. M., Lezamiz, A., Uroz, M., Kosmalska, A. J., et al. (2017). Force Triggers Yap Nuclear Entry by Regulating Transport across Nuclear Pores. *Cell* 171, 1397–1410. e14. doi:10.1016/j.cell.2017.10.008

Engler, A. J., Sen, S., Sweeney, H. L., and Discher, D. E. (2006). Matrix Elasticity Directs Stem Cell Lineage Specification. *Cell* 126, 677–689. doi:10.1016/j.cell.2006.06.044

Esfandiari, E., Roshankhah, S., Mardani, M., Hashemibeni, B., Naghsh, E., Kazemi, M., et al. (2014). The Effect of High Frequency Electric Field on Enhancement of Chondrogenesis in Human Adipose-Derived Stem Cells. *Iran J. Basic Med. Sci.* 17, 571–576.

Esposito, M., Lucariello, A., Riccio, I., Riccio, V., Esposito, V., and Riccardi, G. (2012). Differentiation of Human Osteoprogenitor Cells Increases after Treatment with Pulsed Electromagnetic fields. *In Vivo* 26, 299–304.

Fan, B., Guo, Z., Li, X., Li, S., Gao, P., Xiao, X., et al. (2020). Electroactive Barium Titanate Coated Titanium Scaffold Improves Osteogenesis and Osseointegration with Low-Intensity Pulsed Ultrasound for Large Segmental Bone Defects. *Bioactive Mater.* 5, 1087–1101. doi:10.1016/j.bioactmat.2020.07.001

Fernandes, M. M., Correia, D. M., Ribeiro, C., Castro, N., Correia, V., and Lanceros-Mendez, S. (2019). Bioinspired Three-Dimensional Magnetoactive Scaffolds for Bone Tissue Engineering. *ACS Appl. Mater. Inter.* 11, 45265–45275. doi:10.1021/acsami.9b14001

Filipowska, J., Reilly, G. C., and Osyczka, A. M. (2016). A Single Short Session of media Perfusion Induces Osteogenesis in Hbmscs Cultured in Porous Scaffolds, Dependent on Cell Differentiation Stage. *Biotechnol. Bioeng.* 113, 1814–1824. doi:10.1002/bit.25937

Fröhlich, M., Grayson, W. L., Marolt, D., Gimble, J. M., Kregar-Velikonja, N., and Vunjak-Novakovic, G. (2010). Bone Grafts Engineered from Human Adipose-Derived Stem Cells in Perfusion Bioreactor Culture. *Tissue Eng. Part A* 16, 179–189. doi:10.1089/ten.TEA.2009.0164

Fu, J., Liu, X., Tan, L., Cui, Z., Liang, Y., Li, Z., et al. (2020). Modulation of the Mechanosensing of Mesenchymal Stem Cells by Laser-Induced Patterning for the Acceleration of Tissue Reconstruction through the Wnt/β-Catenin

Signaling Pathway Activation. *Acta Biomater.* 101, 152–167. doi:10.1016/j.actbio.2019.10.041

Gharibi, B., Cama, G., Capurro, M., Thompson, I., Deb, S., Di Silvio, L., et al. (2013). Gene Expression Responses to Mechanical Stimulation of Mesenchymal Stem Cells Seeded on Calcium Phosphate Cement. *Tissue Eng. Part A* 19, 2426–2438. doi:10.1089/ten.tea.2012.0623

Glassman, M. J., Avery, R. K., Khademhosseini, A., and Olsen, B. D. (2016). Toughening of Thermoresponsive Arrested Networks of Elastin-like Polypeptides to Engineer Cytocompatible Tissue Scaffolds. *Biomacromolecules* 17, 415–426. doi:10.1021/acs.biomac.5b01210

Grayson, W. L., Fröhlich, M., Yeager, K., Bhumiratana, S., Chan, M. E., Cannizzaro, C., et al. (2010). Engineering Anatomically Shaped Human Bone Grafts. *Proc. Natl. Acad. Sci. USA* 107, 3299–3304. doi:10.1073/pnas.0905439106

Haffner-Luntzer, M., Liedert, A., and Ignatius, A. (2016). Mechanobiology of Bone Remodeling and Fracture Healing in the Aged Organism. *Innovative Surg. Sci.* 1, 57–63. doi:10.1515/iss-2016-0021

Hannemann, P. F. W., Mommers, E. H. H., Schots, J. P. M., Brink, P. R. G., and Poeze, M. (2014). The Effects of Low-Intensity Pulsed Ultrasound and Pulsed Electromagnetic fields Bone Growth Stimulation in Acute Fractures: A Systematic Review and Meta-Analysis of Randomized Controlled Trials. *Arch. Orthop. Trauma Surg.* 134, 1093–1106. doi:10.1007/s00402-014-2014-8

Hao, J., Zhang, Y., Jing, D., Shen, Y., Tang, G., Huang, S., et al. (2015). Mechanobiology of Mesenchymal Stem Cells: Perspective into Mechanical Induction of Msc Fate. *Acta Biomater.* 20, 1–9. doi:10.1016/j.actbio.2015.04.008

Haudenschild, A. K., Hsieh, A. H., Kapila, S., and Lotz, J. C. (2009). Pressure and Distortion Regulate Human Mesenchymal Stem Cell Gene Expression. *Ann. Biomed. Eng.* 37, 492–502. doi:10.1007/s10439-008-9629-2

Hayakawa, K., Tatsumi, H., and Sokabe, M. (2011). Actin Filaments Function as a Tension Sensor by Tension-dependent Binding of Cofilin to the Filament. *J. Cel. Biol.* 195, 721–727. doi:10.1083/jcb.201102039

Henstock, J. R., Rotherham, M., Rashidi, H., Shakesheff, K. M., and El Haj, A. J. (2014). Remotely Activated Mechanotransduction via Magnetic Nanoparticles Promotes Mineralization Synergistically with Bone Morphogenetic Protein 2: Applications for Injectable Cell Therapy. *Stem Cell translational Med.* 3, 1363–1374. doi:10.5966/sctm.2014-0017

Hess, R., Jaeschke, A., Neubert, H., Hintze, V., Moeller, S., Schnabelrauch, M., et al. (2012). Synergistic Effect of Defined Artificial Extracellular Matrices and Pulsed Electric fields on Osteogenic Differentiation of Human Mscs. *Biomaterials* 33, 8975–8985. doi:10.1016/j.biomaterials.2012.08.056

Hoey, D. A., Kelly, D. J., and Jacobs, C. R. (2011). A Role for the Primary Cilium in Paracrine Signaling between Mechanically Stimulated Osteocytes and Mesenchymal Stem Cells. *Biochem. biophysical Res. Commun.* 412, 182–187. doi:10.1016/j.bbrc.2011.07.072

Hoey, D. A., Tormey, S., Ramcharan, S., O'Brien, F. J., and Jacobs, C. R. (2012). Primary Cilia-Mediated Mechanotransduction in Human Mesenchymal Stem Cells. *Stem Cells* 30, 2561–2570. doi:10.1002/stem.1235

Horner, C. B., Hirota, K., Liu, J., Maldonado, M., Hyle Park, B., and Nam, J. (2018). Magnitude-dependent and Inversely-related Osteogenic/chondrogenic Differentiation of Human Mesenchymal Stem Cells under Dynamic Compressive Strain. *J. Tissue Eng. Regen. Med.* 12, e637–e647. doi:10.1002/term.2332

Hosseinkhani, H., Hosseinkhani, M., Tian, F., Kobayashi, H., and Tabata, Y. (2006). Ectopic Bone Formation in Collagen Sponge Self-Assembled Peptide-Amphiphile Nanofibers Hybrid Scaffold in a Perfusion Culture Bioreactor. *Biomaterials* 27, 5089–5098. doi:10.1016/j.biomaterials.2006.05.050

Hronik-Tupaj, M., Rice, W. L., Cronin-Golomb, M., Kaplan, D. L., and Georgakoudi, I. (2011). Osteoblastic Differentiation and Stress Response of Human Mesenchymal Stem Cells Exposed to Alternating Current Electric fields. *Biomed. Eng. Online* 10, 9. doi:10.1186/1475-925x-10-9

Hu, B., Haj, A., and Dobson, J. (2013). Receptor-targeted, Magneto-Mechanical Stimulation of Osteogenic Differentiation of Human Bone Marrow-Derived Mesenchymal Stem Cells. *Ijms* 14, 19276–19293. doi:10.3390/ijms140919276

Hu, B., Zhang, Y., Zhou, J., Li, J., Deng, F., Wang, Z., et al. (2014). Low-intensity Pulsed Ultrasound Stimulation Facilitates Osteogenic Differentiation of Human Periodontal Ligament Cells. *PloS one* 9, e95168. doi:10.1371/journal.pone.0095168

Hu, Z., Zhang, L., Wang, H., Wang, Y., Tan, Y., Dang, L., et al. (2020). Targeted Silencing of Mirna-132-3p Expression Rescues Disuse Osteopenia by Promoting Mesenchymal Stem Cell Osteogenic Differentiation and Osteogenesis in Mice. *Stem Cell Res Ther* 11, 58. doi:10.1186/s13287-020-1581-6

Huang, C., and Ogawa, R. (2012). Effect of Hydrostatic Pressure on Bone Regeneration Using Human Mesenchymal Stem Cells. *Tissue Eng. Part A* 18, 2106–2113. doi:10.1089/ten.TEA.2012.0064

Huang, J., Lin, D., Wei, Z., Li, Q., Zheng, J., Zheng, Q., et al. (2020). Parathyroid Hormone Derivative with Reduced Osteoclastic Activity Promoted Bone Regeneration via Synergistic Bone Remodeling and Angiogenesis. *Small* 16, 1905876. doi:10.1002/smll.201905876

Huebsch, N., Arany, P. R., Mao, A. S., Shvartsman, D., Ali, O. A., Bencherif, S. A., et al. (2010). Harnessing Traction-Mediated Manipulation of the Cell/matrix Interface to Control Stem-Cell Fate. *Nat. Mater* 9, 518–526. doi:10.1038/nmat2732

Iandolo, D., Ravichandran, A., Liu, X., Wen, F., Chan, J. K. Y., Berggren, M., et al. (2016). Development and Characterization of Organic Electronic Scaffolds for Bone Tissue Engineering. *Adv. Healthc. Mater.* 5, 1505–1512. doi:10.1002/adhm.201500874

Jazayeri, M., Shokrgozar, M. A., Haghighipour, N., Bolouri, B., Mirahmadi, F., and Farokhi, M. (2017). Effects of Electromagnetic Stimulation on Gene Expression of Mesenchymal Stem Cells and Repair of Bone Lesions. *Cell J* 19, 34–44. doi:10.22074/cellj.2016.4870

Johnson, G. P., Fair, S., and Hoey, D. A. (2021). Primary Cilium-Mediated Msc Mechanotransduction Is Dependent on Gpr161 Regulation of Hedgehog Signalling. *Bone* 145, 115846. doi:10.1016/j.bone.2021.115846

Johnson, G. P., Stavenschi, E., Eichholz, K. F., Corrigan, M. A., Fair, S., and Hoey, D. A. (2018). Mesenchymal Stem Cell Mechanotransduction Is Camp Dependent and Regulated by Adenylyl Cyclase 6 and the Primary Cilium. *J. Cel. Sci.* 131. doi:10.1242/jcs.222737

Kanczler, J. M., Sura, H. S., Magnay, J., Green, D., Oreffo, R. O. C., Dobson, J. P., et al. (2010). Controlled Differentiation of Human Bone Marrow Stromal Cells Using Magnetic Nanoparticle Technology. *Tissue Eng. Part A* 16, 3241–3250. doi:10.1089/ten.TEA.2009.0638

Kapat, K., Shubhra, Q. T. H., Zhou, M., and Leeuwenburgh, S. (2020). Piezoelectric Nano-Biomaterials for Biomedicine and Tissue Regeneration. *Adv. Funct. Mater.* 30, 1909045. doi:10.1002/adfm.201909045

Kearney, E. M., Farrell, E., Prendergast, P. J., and Campbell, V. A. (2010). Tensile Strain as a Regulator of Mesenchymal Stem Cell Osteogenesis. *Ann. Biomed. Eng.* 38, 1767–1779. doi:10.1007/s10439-010-9979-4

Khare, D., Basu, B., and Dubey, A. K. (2020). Electrical Stimulation and Piezoelectric Biomaterials for Bone Tissue Engineering Applications. *Biomaterials* 258, 120280. doi:10.1016/j.biomaterials.2020.120280

Khaw, J. S., Xue, R., Cassidy, N. J., and Cartmell, S. H. (2021). Electrical Stimulation of Titanium to Promote Stem Cell Orientation, Elongation and Osteogenesis. *Acta Biomater.*, S1742. doi:10.1016/j.actbio.2021.08.010

Kim, K. M., Choi, Y. J., Hwang, J.-H., Kim, A. R., Cho, H. J., Hwang, E. S., et al. (2014). Shear Stress Induced by an Interstitial Level of Slow Flow Increases the Osteogenic Differentiation of Mesenchymal Stem Cells through Taz Activation. *PloS one* 9, e92427. doi:10.1371/journal.pone.0092427

Krishnan, L., Priddy, L. B., Esancy, C., Klosterhoff, B. S., Stevens, H. Y., Tran, L., et al. (2017). Delivery Vehicle Effects on Bone Regeneration and Heterotopic Ossification Induced by High Dose Bmp-2. *Acta Biomater.* 49, 101–112. doi:10.1016/j.actbio.2016.12.012

Labusca, L., Herea, D.-D., Danceanu, C.-M., Minuti, A. E., Stavila, C., Grigoras, M., et al. (2020). The Effect of Magnetic Field Exposure on Differentiation of Magnetite Nanoparticle-Loaded Adipose-Derived Stem Cells. *Mater. Sci. Eng. C* 109, 110652. doi:10.1016/j.msec.2020.110652

Lau, E., Lee, W. D., Li, J., Xiao, A., Davies, J. E., Wu, Q., et al. (2011). Effect of Low-Magnitude, High-Frequency Vibration on Osteogenic Differentiation of Rat Mesenchymal Stromal Cells. *J. Orthop. Res.* 29, 1075–1080. doi:10.1002/jor.21334

Lavenus, S., Berreur, M., Berreur, M., Trichet, V., Pilet, P., Louarn, G., et al. (2011). Adhesion and Osteogenic Differentiation of Human Mesenchymal Stem Cells on Titanium Nanopores. *eCM* 22, 84–96. doi:10.22203/ecm.v022a07

Le Pape, F., Richard, G., Porchet, E., Sourice, S., Dubrana, F., Férec, C., et al. (2018). Adhesion, Proliferation and Osteogenic Differentiation of Human Mscs Cultured under Perfusion with a marine Oxygen Carrier on an Allogenic

Bone Substitute. *Artif. Cell nanomedicine, Biotechnol.* 46, 95–107. doi:10.1080/21691401.2017.1365724

Leckband, D. E., and de Rooij, J. (2014). Cadherin Adhesion and Mechanotransduction. *Annu. Rev. Cell Dev. Biol.* 30, 291–315. doi:10.1146/annurev-cellbio-100913-013212

Lee, J.-M., Kim, M.-G., Byun, J.-H., Kim, G.-C., Ro, J.-H., Hwang, D.-S., et al. (2017). The Effect of Biomechanical Stimulation on Osteoblast Differentiation of Human Jaw Periosteum-Derived Stem Cells. *Maxillofac. Plast. Reconstr. Surg.* 39, 7. doi:10.1186/s40902-017-0104-6

Lee, J. S., Ha, L., Park, J.-H., and Lim, J. Y. (2012). Mechanical Stretch Suppresses Bmp4 Induction of Stem Cell Adipogenesis via Upregulating Erk but Not through Downregulating Smad or P38. *Biochem. biophysical Res. Commun.* 418, 278–283. doi:10.1016/j.bbrc.2012.01.010

Li, C. W., Lau, Y. T., Lam, K. L., and Chan, B. P. (2020). Mechanically Induced Formation and Maturation of 3d-Matrix Adhesions (3dmas) in Human Mesenchymal Stem Cells. *Biomaterials* 258, 120292. doi:10.1016/j.biomaterials.2020.120292

Li, R., Liang, L., Dou, Y., Huang, Z., Mo, H., Wang, Y., et al. (2015a). Mechanical Strain Regulates Osteogenic and Adipogenic Differentiation of Bone Marrow Mesenchymal Stem Cells. *Biomed. Research International* 2015, 1–10. doi:10.1155/2015/873251

Li, R., Liang, L., Dou, Y., Huang, Z., Mo, H., Wang, Y., et al. (2015b). Mechanical Stretch Inhibits Mesenchymal Stem Cell Adipogenic Differentiation through TGFβ1/Smad2 Signaling. *J. Biomech.* 48, 3656–3662. doi:10.1016/j.jbiomech.2015.08.013

Lim, K., Hexiu, J., Kim, J., Seonwoo, H., Cho, W. J., Choung, P.-H., et al. (2013). Effects of Electromagnetic fields on Osteogenesis of Human Alveolar Bone-Derived Mesenchymal Stem Cells. *Biomed. Research International* 2013, 1–14. doi:10.1155/2013/296019

Liu, L., Shao, L., Li, B., Zong, C., Li, J., Zheng, Q., et al. (2011). Extracellular Signal-Regulated Kinase1/2 Activated by Fluid Shear Stress Promotes Osteogenic Differentiation of Human Bone Marrow-Derived Mesenchymal Stem Cells through Novel Signaling Pathways. *Int. J. Biochem. Cell Biol.* 43, 1591–1601. doi:10.1016/j.biocel.2011.07.008

Liu, L., Zong, C., Li, B., Shen, D., Tang, Z., Chen, J., et al. (2014). The Interaction Betweenβ1 Integrins and ERK1/2 in Osteogenic Differentiation of Human Mesenchymal Stem Cells under Fluid Shear Stress Modelled by a Perfusion System. *J. Tissue Eng. Regen. Med.* 8, 85–96. doi:10.1002/term.1498

Lohberger, B., Kaltenegger, H., Stuendl, N., Payer, M., Rinner, B., and Leithner, A. (20142014). Effect of Cyclic Mechanical Stimulation on the Expression of Osteogenesis Genes in Human Intraoral Mesenchymal Stromal and Progenitor Cells. *Biomed. Research International* 2014, 1–10. doi:10.1155/2014/189516

Lopes, D., Martins-Cruz, C., Oliveira, M. B., and Mano, J. F. (2018). Bone Physiology as Inspiration for Tissue Regenerative Therapies. *Biomaterials* 185, 240–275. doi:10.1016/j.biomaterials.2018.09.028

Lu, T., Huang, Y. X., Zhang, C., Chai, M. X., and Zhang, J. (2015). Effect of Pulsed Electromagnetic Field Therapy on the Osteogenic and Adipogenic Differentiation of Bone Marrow Mesenchymal Stem Cells. *Genet. Mol. Res.* 14, 11535–11542. doi:10.4238/2015.September.28.5

Luo, F., Hou, T., Zhang, Z., Xie, Z., Wu, X., and Xu, J. (2012). Effects of Pulsed Electromagnetic Field Frequencies on the Osteogenic Differentiation of Human Mesenchymal Stem Cells. *Orthopedics* 35, e526–31. doi:10.3928/01477447-20120327-11

Lv, P.-y., Gao, P.-f., Tian, G.-j., Yang, Y.-y., Mo, F.-f., Wang, Z.-h., et al. (2020). Osteocyte-derived Exosomes Induced by Mechanical Strain Promote Human Periodontal Ligament Stem Cell Proliferation and Osteogenic Differentiation via the Mir-181b-5p/pten/akt Signaling Pathway. *Stem Cell Res Ther* 11, 295. doi:10.1186/s13287-020-01815-3

Ma, B., Liu, F., Li, Z., Duan, J., Kong, Y., Hao, M., et al. (2019). Piezoelectric Nylon-11 Nanoparticles with Ultrasound Assistance for High-Efficiency Promotion of Stem Cell Osteogenic Differentiation. *J. Mater. Chem. B* 7, 1847–1854. doi:10.1039/c8tb03321h

Mancuso, E., Shah, L., Jindal, S., Serenelli, C., Tsikriteas, Z. M., Khanbareh, H., et al. (2021). Additively Manufactured BaTiO3 Composite Scaffolds: A Novel Strategy for Load Bearing Bone Tissue Engineering Applications. *Mater. Sci. Eng. C* 126, 112192. doi:10.1016/j.msec.2021.112192

McBeath, R., Pirone, D. M., Nelson, C. M., Bhadriraju, K., and Chen, C. S. (2004). Cell Shape, Cytoskeletal Tension, and Rhoa Regulate Stem Cell Lineage Commitment. *Developmental Cel.* 6, 483–495. doi:10.1016/s1534-5807(04)00075-9

McMurray, R. J., Wann, A. K. T., Thompson, C. L., Connelly, J. T., and Knight, M. M. (2013). Surface Topography Regulates Wnt Signaling through Control of Primary Cilia Structure in Mesenchymal Stem Cells. *Sci. Rep.* 3, 3545. doi:10.1038/srep03545

McNamara, L. E., Sjöström, T., Burgess, K. E. V., Kim, J. J. W., Liu, E., Gordonov, S., et al. (2011). Skeletal Stem Cell Physiology on Functionally Distinct Titania Nanotopographies. *Biomaterials* 32, 7403–7410. doi:10.1016/j.biomaterials.2011.06.063

Mitra, D., Whitehead, J., Yasui, O. W., and Leach, J. K. (2017). Bioreactor Culture Duration of Engineered Constructs Influences Bone Formation by Mesenchymal Stem Cells. *Biomaterials* 146, 29–39. doi:10.1016/j.biomaterials.2017.08.044

Moser, C., Bardsley, K., El Haj, A. J., Alini, M., Stoddart, M. J., and Bara, J. J. (2018). A Perfusion Culture System for Assessing Bone Marrow Stromal Cell Differentiation on Plga Scaffolds for Bone Repair. *Front. Bioeng. Biotechnol.* 6, 161. doi:10.3389/fbioe.2018.00161

Murillo, G., Blanquer, A., Vargas-Estevez, C., Barrios, L., Ibáñez, E., Nogués, C., et al. (2017). Electromechanical Nanogenerator-Cell Interaction Modulates Cell Activity. *Adv. Mater.* 29, 1605048. doi:10.1002/adma.201605048

Nikukar, H., Reid, S., Tsimbouri, P. M., Riehle, M. O., Curtis, A. S. G., and Dalby, M. J. (2013). Osteogenesis of Mesenchymal Stem Cells by Nanoscale Mechanotransduction. *ACS nano* 7, 2758–2767. doi:10.1021/nn400202j

Niu, H., Lin, D., Tang, W., Ma, Y., Duan, B., Yuan, Y., et al. (2017). Surface Topography Regulates Osteogenic Differentiation of MSCs via Crosstalk between FAK/MAPK and ILK/β-Catenin Pathways in a Hierarchically Porous Environment. *ACS Biomater. Sci. Eng.* 3, 3161–3175. doi:10.1021/acsbiomaterials.7b00315

Ongaro, A., Pellati, A., Bagheri, L., Fortini, C., Setti, S., and De Mattei, M. (2014). Pulsed Electromagnetic fields Stimulate Osteogenic Differentiation in Human Bone Marrow and Adipose Tissue Derived Mesenchymal Stem Cells. *Bioelectromagnetics* 35, 426–436. doi:10.1002/bem.21862

Padilla, F., Puts, R., Vico, L., and Raum, K. (2014). Stimulation of Bone Repair with Ultrasound: A Review of the Possible Mechanic Effects. *Ultrasonics* 54, 1125–1145. doi:10.1016/j.ultras.2014.01.004

Panek, M., Antunović, M., Pribolšan, L., Ivković, A., Gotić, M., Vukasović, A., et al. (2019). Bone Tissue Engineering in a Perfusion Bioreactor Using Dexamethasone-Loaded Peptide Hydrogel. *Materials* 12, 919. doi:10.3390/ma12060919

Parmaksiz, M., Lalegül-Ülker, Ö., Vurat, M. T., Elçin, A. E., and Elçin, Y. M. (2021). Magneto-sensitive Decellularized Bone Matrix with or without Low Frequency-Pulsed Electromagnetic Field Exposure for the Healing of a Critical-Size Bone Defect. *Mater. Sci. Eng. C* 124, 112065. doi:10.1016/j.msec.2021.112065

Polley, C., Distler, T., Detsch, R., Lund, H., Springer, A., Boccaccini, A. R., et al. (2020). 3D Printing of Piezoelectric Barium Titanate-Hydroxyapatite Scaffolds with Interconnected Porosity for Bone Tissue Engineering. *Materials* 13, 1773. doi:10.3390/ma13071773

Pongkitwitoon, S., Uzer, G., Rubin, J., and Judex, S. (2016). Cytoskeletal Configuration Modulates Mechanically Induced Changes in Mesenchymal Stem Cell Osteogenesis, Morphology, and Stiffness. *Sci. Rep.* 6, 34791. doi:10.1038/srep34791

Prè, D., Ceccarelli, G., Visai, L., Benedetti, L., Imbriani, M., Cusella De Angelis, M. G., et al. (20132013). High-frequency Vibration Treatment of Human Bone Marrow Stromal Cells Increases Differentiation toward Bone Tissue. *Bone Marrow Res.* 2013, 1–13. doi:10.1155/2013/803450

Qian, W., Gong, L., Cui, X., Zhang, Z., Bajpai, A., Liu, C., et al. (2017). Nanotopographic Regulation of Human Mesenchymal Stem Cell Osteogenesis. *ACS Appl. Mater. Inter.* 9, 41794–41806. doi:10.1021/acsami.7b16314

Qin, E. C., Ahmed, S. T., Sehgal, P., Vu, V. H., Kong, H., and Leckband, D. E. (2020a). Comparative Effects of N-Cadherin Protein and Peptide Fragments on Mesenchymal Stem Cell Mechanotransduction and Paracrine Function. *Biomaterials* 239, 119846. doi:10.1016/j.biomaterials.2020.119846

Qin, L., Liu, W., Cao, H., and Xiao, G. (2020b). Molecular Mechanosensors in Osteocytes. *Bone Res.* 8, 23. doi:10.1038/s41413-020-0099-y

Raftery, R. M., Woods, B., Marques, A. L. P., Moreira-Silva, J., Silva, T. H., Cryan, S.-A., et al. (2016). Multifunctional Biomaterials from the Sea: Assessing the

Effects of Chitosan Incorporation into Collagen Scaffolds on Mechanical and Biological Functionality. *Acta Biomater.* 43, 160–169. doi:10.1016/j.actbio.2016.07.009

Ravichandran, A., Lim, J., Chong, M. S. K., Wen, F., Liu, Y., Pillay, Y. T., et al. (2017). *In Vitro* cyclic Compressive Loads Potentiate Early Osteogenic Events in Engineered Bone Tissue. *J. Biomed. Mater. Res.* 105, 2366–2375. doi:10.1002/jbm.b.33772

Ravichandran, A., Wen, F., Lim, J., Chong, M. S. K., Chan, J. K. Y., and Teoh, S. H. (2018). Biomimetic Fetal Rotation Bioreactor for Engineering Bone Tissues-Effect of Cyclic Strains on Upregulation of Osteogenic Gene Expression. *J. Tissue Eng. Regen. Med.* 12, e2039–e2050. doi:10.1002/term.2635

Ravikumar, K., Boda, S. K., and Basu, B. (2017). Synergy of Substrate Conductivity and Intermittent Electrical Stimulation towards Osteogenic Differentiation of Human Mesenchymal Stem Cells. *Bioelectrochemistry* 116, 52–64. doi:10.1016/j.bioelechem.2017.03.004

Reinwald, Y., and El Haj, A. J. (2018). Hydrostatic Pressure in Combination with Topographical Cues Affects the Fate of Bone Marrow-Derived Human Mesenchymal Stem Cells for Bone Tissue Regeneration. *J. Biomed. Mater. Res.* 106, 629–640. doi:10.1002/jbm.a.36267

Roseti, L., Parisi, V., Petretta, M., Cavallo, C., Desando, G., Bartolotti, I., et al. (2017). Scaffolds for Bone Tissue Engineering: State of the Art and New Perspectives. *Mater. Sci. Eng. C* 78, 1246–1262. doi:10.1016/j.msec.2017.05.017

Rui, Y. F., Lui, P. P. Y., Ni, M., Chan, L. S., Lee, Y. W., and Chan, K. M. (2011). Mechanical Loading Increased Bmp-2 Expression Which Promoted Osteogenic Differentiation of Tendon-Derived Stem Cells. *J. Orthop. Res.* 29, 390–396. doi:10.1002/jor.21218

Santos, L. J., Reis, R. L., and Gomes, M. E. (2015). Harnessing Magnetic-Mechano Actuation in Regenerative Medicine and Tissue Engineering. *Trends Biotechnology* 33, 471–479. doi:10.1016/j.tibtech.2015.06.006

Schreivogel, S., Kuchibhotla, V., Knaus, P., Duda, G. N., and Petersen, A. (2019). Load-induced Osteogenic Differentiation of Mesenchymal Stromal Cells Is Caused by Mechano-regulated Autocrine Signaling. *J. Tissue Eng. Regen. Med.* 13, 1992–2008. doi:10.1002/term.2948

Schupbach, D., Comeau-Gauthier, M., Harvey, E., and Merle, G. (2020). Wnt Modulation in Bone Healing. *Bone* 138, 115491. doi:10.1016/j.bone.2020.115491

Sen, B., Xie, Z., Case, N., Ma, M., Rubin, C., and Rubin, J. (2008). Mechanical Strain Inhibits Adipogenesis in Mesenchymal Stem Cells by Stimulating a Durable β-Catenin Signal. *Endocrinology* 149, 6065–6075. doi:10.1210/en.2008-0687

Shah, H. N., Jones, R. E., Borrelli, M. R., Robertson, K., Salhotra, A., Wan, D. C., et al. (2021). Craniofacial and Long Bone Development in the Context of Distraction Osteogenesis. *Plast. Reconstr. Surg.* 147, 54e–65e. doi:10.1097/prs.0000000000007451

Shi, Y., Fu, Y., Tong, W., Geng, Y., Lui, P. P. Y., Tang, T., et al. (2012). Uniaxial Mechanical Tension Promoted Osteogenic Differentiation of Rat Tendon-Derived Stem Cells (Rtdscs) via the Wnt5a-Rhoa Pathway. *J. Cell. Biochem.* 113, 3133–3142. doi:10.1002/jcb.24190

Silverwood, R. K., Fairhurst, P. G., Sjöström, T., Welsh, F., Sun, Y., Li, G., et al. (2016). Analysis of Osteoclastogenesis/osteoblastogenesis on Nanotopographical Titania Surfaces. *Adv. Healthc. Mater.* 5, 947–955. doi:10.1002/adhm.201500664

Singh, H., Teoh, S. H., Low, H. T., and Hutmacher, D. W. (2005). Flow Modelling within a Scaffold under the Influence of Uni-Axial and Bi-axial Bioreactor Rotation. *J. Biotechnol.* 119, 181–196. doi:10.1016/j.jbiotec.2005.03.021

Sittichokechaiwut, A., Edwards, J. H., Edwards, J., Scutt, A., and Reilly, G. (2010). Short Bouts of Mechanical Loading Are as Effective as Dexamethasone at Inducing Matrix Production by Human Bone Marrow Mesenchymal Stem Cells. *eCM* 20, 45–57. doi:10.22203/ecm.v020a05

Sjöström, T., Dalby, M. J., Hart, A., Tare, R., Oreffo, R. O. C., and Su, B. (2009). Fabrication of Pillar-like Titania Nanostructures on Titanium and Their Interactions with Human Skeletal Stem Cells. *Acta Biomater.* 5, 1433–1441. doi:10.1016/j.actbio.2009.01.007

Sjöström, T., McNamara, L. E., Meek, R. M. D., Dalby, M. J., and Su, B. (2013). 2d and 3d Nanopatterning of Titanium for Enhancing Osteoinduction of Stem Cells at Implant Surfaces. *Adv. Healthc. Mater.* 2, 1285–1293. doi:10.1002/adhm.201200353

Song, F., Jiang, D., Wang, T., Wang, Y., Lou, Y., Zhang, Y., et al. (2017). Mechanical Stress Regulates Osteogenesis and Adipogenesis of Rat Mesenchymal Stem Cells through PI3K/Akt/GSK-3β/β-Catenin Signaling Pathway. *Biomed. Research International* 2017, 1–10. doi:10.1155/2017/6027402

Spangenberg, J., Kilian, D., Czichy, C., Ahlfeld, T., Lode, A., Günther, S., et al. (2021). Bioprinting of Magnetically Deformable Scaffolds. *ACS Biomater. Sci. Eng.* 7, 648–662. doi:10.1021/acsbiomaterials.0c01371

Stavenschi, E., Corrigan, M. A., Johnson, G. P., Riffault, M., and Hoey, D. A. (2018). Physiological Cyclic Hydrostatic Pressure Induces Osteogenic Lineage Commitment of Human Bone Marrow Stem Cells: A Systematic Study. *Stem Cell Res Ther* 9, 276. doi:10.1186/s13287-018-1025-8

Steppe, L., Liedert, A., Ignatius, A., and Haffner-Luntzer, M. (2020). Influence of Low-Magnitude High-Frequency Vibration on Bone Cells and Bone Regeneration. *Front. Bioeng. Biotechnol.* 8, 595139. doi:10.3389/fbioe.2020.595139

Steward, A. J., and Kelly, D. J. (2015). Mechanical Regulation of Mesenchymal Stem Cell Differentiation. *J. Anat.* 227, 717–731. doi:10.1111/joa.12243

Stewart, S., Darwood, A., Masouros, S., Higgins, C., and Ramasamy, A. (2020). Mechanotransduction in Osteogenesis. *Bone Jt. Res.* 9, 1–14. doi:10.1302/2046-3758.91.Bjr-2019-0043.R2

Sugimoto, A., Miyazaki, A., Kawarabayashi, K., Shono, M., Akazawa, Y., Hasegawa, T., et al. (2017). Piezo Type Mechanosensitive Ion Channel Component 1 Functions as a Regulator of the Cell Fate Determination of Mesenchymal Stem Cells. *Sci. Rep.* 7, 17696. doi:10.1038/s41598-017-18089-0

Sumanasinghe, R. D., Osborne, J. A., and Loboa, E. G. (2009). Mesenchymal Stem Cell-seeded Collagen Matrices for Bone Repair: Effects of Cyclic Tensile Strain, Cell Density, and media Conditions on Matrix Contraction *In Vitro*. *J. Biomed. Mater. Res.* 88A, 778–786. doi:10.1002/jbm.a.31913

Sun, L.-Y., Hsieh, D.-K., Lin, P.-C., Chiu, H.-T., and Chiou, T.-W. (2009). Pulsed Electromagnetic fields Accelerate Proliferation and Osteogenic Gene Expression in Human Bone Marrow Mesenchymal Stem Cells during Osteogenic Differentiation. *Bioelectromagnetics* 31, a–n. doi:10.1002/bem.20550

Sun, L.-Y., Hsieh, D.-K., Yu, T.-C., Chiu, H.-T., Lu, S.-F., Luo, G.-H., et al. (2009). Effect of Pulsed Electromagnetic Field on the Proliferation and Differentiation Potential of Human Bone Marrow Mesenchymal Stem Cells. *Bioelectromagnetics* 30, 251–260. doi:10.1002/bem.20472

Sun, M., Chi, G., Xu, J., Tan, Y., Xu, J., Lv, S., et al. (2018). Extracellular Matrix Stiffness Controls Osteogenic Differentiation of Mesenchymal Stem Cells Mediated by Integrin α5. *Stem Cell Res Ther* 9, 52. doi:10.1186/s13287-018-0798-0

Tahimic, C. G. T., Long, R. K., Kubota, T., Sun, M. Y., Elalieh, H., Fong, C., et al. (2016). Regulation of Ligand and Shear Stress-Induced Insulin-like Growth Factor 1 (Igf1) Signaling by the Integrin Pathway. *J. Biol. Chem.* 291, 8140–8149. doi:10.1074/jbc.M115.693598

Tan, S. D., de Vries, T. J., Kuijpers-Jagtman, A. M., Semeins, C. M., Everts, V., and Klein-Nulend, J. (2007). Osteocytes Subjected to Fluid Flow Inhibit Osteoclast Formation and Bone Resorption. *Bone* 41, 745–751. doi:10.1016/j.bone.2007.07.019

Tang, Y., Wu, C., Wu, Z., Hu, L., Zhang, W., and Zhao, K. (2017). Fabrication and *In Vitro* Biological Properties of Piezoelectric Bioceramics for Bone Regeneration. *Sci. Rep.* 7, 43360. doi:10.1038/srep43360

Thompson, W. R., Guilluy, C., Xie, Z., Sen, B., Brobst, K. E., Yen, S. S., et al. (2013). Mechanically Activated Fyn Utilizes Mtorc2 to Regulate Rhoa and Adipogenesis in Mesenchymal Stem Cells. *Stem Cells* 31, 2528–2537. doi:10.1002/stem.1476

Thompson, W. R., Rubin, C. T., and Rubin, J. (2012). Mechanical Regulation of Signaling Pathways in Bone. *Gene* 503, 179–193. doi:10.1016/j.gene.2012.04.076

Thompson, W. R., Yen, S. S., Uzer, G., Xie, Z., Sen, B., Styner, M., et al. (2018). Larg Gef and Arhgap18 Orchestrate Rhoa Activity to Control Mesenchymal Stem Cell Lineage. *Bone* 107, 172–180. doi:10.1016/j.bone.2017.12.001

Thrivikraman, G., Boda, S. K., and Basu, B. (2018). Unraveling the Mechanistic Effects of Electric Field Stimulation towards Directing Stem Cell Fate and Function: A Tissue Engineering Perspective. *Biomaterials* 150, 60–86. doi:10.1016/j.biomaterials.2017.10.003

Tsai, M.-T., Li, W.-J., Tuan, R. S., and Chang, W. H. (2009). Modulation of Osteogenesis in Human Mesenchymal Stem Cells by Specific Pulsed Electromagnetic Field Stimulation. *J. Orthop. Res.* 27, 1169–1174. doi:10.1002/jor.20862

Tsimbouri, P. M., Childs, P. G., Pemberton, G. D., Yang, J., Jayawarna, V., Orapiriyakul, W., et al. (2017). Stimulation of 3d Osteogenesis by Mesenchymal Stem Cells Using a Nanovibrational Bioreactor. *Nat. Biomed. Eng.* 1, 758–770. doi:10.1038/s41551-017-0127-4

Tyrovola, J. B., and Odont, X. (2015). The "mechanostat Theory" of Frost and the Opg/rankl/rank System. *J. Cell. Biochem.* 116, 2724–2729. doi:10.1002/jcb.25265

Wang, J., Tang, N., Xiao, Q., Zhao, L., Li, Y., Li, J., et al. (2016a). The Potential Application of Pulsed Ultrasound on Bone Defect Repair via Developmental Engineering: An *In Vitro* Study. *Artif. organs* 40, 505–513. doi:10.1111/aor.12578

Wang, J., Wang, C. D., Zhang, N., Tong, W. X., Zhang, Y. F., Shan, S. Z., et al. (2016b). Mechanical Stimulation Orchestrates the Osteogenic Differentiation of Human Bone Marrow Stromal Cells by Regulating Hdac1. *Cell Death Dis* 7–e2221. doi:10.1038/cddis.2016.112

Wang, M., Favi, P., Cheng, X., Golshan, N. H., Ziemer, K. S., Keidar, M., et al. (2016c). Cold Atmospheric Plasma (Cap) Surface Nanomodified 3d Printed Polylactic Acid (Pla) Scaffolds for Bone Regeneration. *Acta Biomater.* 46, 256–265. doi:10.1016/j.actbio.2016.09.030

Wang, N., Tytell, J. D., and Ingber, D. E. (2009). Mechanotransduction at a Distance: Mechanically Coupling the Extracellular Matrix with the Nucleus. *Nat. Rev. Mol. Cell Biol* 10, 75–82. doi:10.1038/nrm2594

Wang, T., Yang, L., Jiang, J., Liu, Y., Fan, Z., Zhong, C., et al. (2019). Pulsed Electromagnetic fields: Promising Treatment for Osteoporosis. *Osteoporos. Int.* 30, 267–276. doi:10.1007/s00198-018-04822-6

Wechsler, M. E., Hermann, B. P., and Bizios, R. (2016). Adult Human Mesenchymal Stem Cell Differentiation at the Cell Population and Single-Cell Levels under Alternating Electric Current. *Tissue Eng. C: Methods* 22, 155–164. doi:10.1089/ten.TEC.2015.0324

Wojda, S. J., and Donahue, S. W. (2018). Parathyroid Hormone for Bone Regeneration. *J. Orthop. Res.* 36, 2586–2594. doi:10.1002/jor.24075

W. Sawyer, S., Zhang, K., Zhang, K., A. Horton, J., and Soman, P. (2020). Perfusion-based Co-culture Model System for Bone Tissue Engineering. *AIMS Bioeng.* 7, 91–105. doi:10.3934/bioeng.2020009

Wu, J., Chen, T., Wang, Z., Chen, X., Qu, S., Weng, J., et al. (2020). Joint Construction of Micro-vibration Stimulation and Bcp Scaffolds for Enhanced Bioactivity and Self-Adaptability Tissue Engineered Bone Grafts. *J. Mater. Chem. B* 8, 4278–4288. doi:10.1039/d0tb00223b

Wu, J., Zhao, J., Sun, L., Pan, Y., Wang, H., and Zhang, W.-B. (2018). Long Non-coding Rna H19 Mediates Mechanical Tension-Induced Osteogenesis of Bone Marrow Mesenchymal Stem Cells via Fak by Sponging Mir-138. *Bone* 108, 62–70. doi:10.1016/j.bone.2017.12.013

Wu, W., Le, A. V., Mendez, J. J., Chang, J., Niklason, L. E., and Steinbacher, D. M. (2015). Osteogenic Performance of Donor-Matched Human Adipose and Bone Marrow Mesenchymal Cells under Dynamic Culture. *Tissue Eng. Part A* 21, 1621–1632. doi:10.1089/ten.TEA.2014.0115

Wu, X., Li, Y., Cao, Z., Xie, Y., Fu, C., and Chen, H. (2021). Mechanism of Cyclic Tensile Stress in Osteogenic Differentiation of Human Periodontal Ligament Stem Cells. *Calcif Tissue Int.* 108, 640–653. doi:10.1007/s00223-020-00789-x

Xiao, F., Zuo, B., Tao, B., Wang, C., Li, Y., Peng, J., et al. (2021). Exosomes Derived from Cyclic Mechanical Stretch-Exposed Bone Marrow Mesenchymal Stem Cells Inhibit RANKL-Induced Osteoclastogenesis through the NF-κB Signaling Pathway. *Ann. Transl Med.* 9, 798. doi:10.21037/atm-21-1838

Yan, H., Liu, X., Zhu, M., Luo, G., Sun, T., Peng, Q., et al. (2016). Hybrid Use of Combined and Sequential Delivery of Growth Factors and Ultrasound Stimulation in Porous Multilayer Composite Scaffolds to Promote Both Vascularization and Bone Formation in Bone Tissue Engineering. *J. Biomed. Mater. Res.* 104, 195–208. doi:10.1002/jbm.a.35556

Yang, L., Huang, J., Yang, S., Cui, W., Wang, J., Zhang, Y., et al. (2018). Bone Regeneration Induced by Local Delivery of a Modified Pth-Derived Peptide from Nanohydroxyapatite/chitosan Coated True Bone Ceramics. *ACS Biomater. Sci. Eng.* 4, 3246–3258. doi:10.1021/acsbiomaterials.7b00780

Ye, L., Xu, J., Mi, J., He, X., Pan, Q., Zheng, L., et al. (2021). Biodegradable Magnesium Combined with Distraction Osteogenesis Synergistically Stimulates Bone Tissue Regeneration via Cgrp-Fak-Vegf Signaling axis. *Biomaterials* 275, 120984. doi:10.1016/j.biomaterials.2021.120984

Yong, K. W., Choi, J. R., Choi, J. Y., and Cowie, A. C. (2020). Recent Advances in Mechanically Loaded Human Mesenchymal Stem Cells for Bone Tissue Engineering. *Ijms* 21, 5816. doi:10.3390/ijms21165816

You, L., Temiyasathit, S., Lee, P., Kim, C. H., Tummala, P., Yao, W., et al. (2008). Osteocytes as Mechanosensors in the Inhibition of Bone Resorption Due to Mechanical Loading. *Bone* 42, 172–179. doi:10.1016/j.bone.2007.09.047

Yourek, G., McCormick, S. M., Mao, J. J., and Reilly, G. C. (2010). Shear Stress Induces Osteogenic Differentiation of Human Mesenchymal Stem Cells. *Regenerative Med.* 5, 713–724. doi:10.2217/rme.10.60

Yu, H.-S., Won, J.-E., Jin, G.-Z., and Kim, H.-W. (2012). Construction of Mesenchymal Stem Cell-Containing Collagen Gel with a Macrochanneled Polycaprolactone Scaffold and the Flow Perfusion Culturing for Bone Tissue Engineering. *BioResearch open access* 1, 124–136. doi:10.1089/biores.2012.0234

Yu, P., Ning, C., Zhang, Y., Tan, G., Lin, Z., Liu, S., et al. (2017). Bone-inspired Spatially Specific Piezoelectricity Induces Bone Regeneration. *Theranostics* 7, 3387–3397. doi:10.7150/thno.19748

Yuan, H., Zhou, Y., Lee, M.-S., Zhang, Y., and Li, W.-J. (2016). A Newly Identified Mechanism Involved in Regulation of Human Mesenchymal Stem Cells by Fibrous Substrate Stiffness. *Acta Biomater.* 42, 247–257. doi:10.1016/j.actbio.2016.06.034

Yue, Y., Yang, X., Wei, X., Chen, J., Fu, N., Fu, Y., et al. (2013). Osteogenic Differentiation of Adipose-derived Stem Cells Prompted by Low-intensity Pulsed Ultrasound. *Cell Prolif.* 46, 320–327. doi:10.1111/cpr.12035

Zhang, C., Liu, W., Cao, C., Zhang, F., Tang, Q., Ma, S., et al. (2018). Modulating Surface Potential by Controlling the β Phase Content in Poly(vinylidene Fluoridetrifluoroethylene) Membranes Enhances Bone Regeneration. *Adv. Healthc. Mater.* 7, 1701466. doi:10.1002/adhm.201701466

Zhang, C., Lu, Y., Zhang, L., Liu, Y., Zhou, Y., Chen, Y., et al. (2015). Influence of Different Intensities of Vibration on Proliferation and Differentiation of Human Periodontal Ligament Stem Cells. *aoms* 3, 638–646. doi:10.5114/aoms.2015.52370

Zhang, J., He, X., Chen, X., Wu, Y., Dong, L., Cheng, K., et al. (2020). Enhancing Osteogenic Differentiation of Bmscs on High Magnetoelectric Response Films. *Mater. Sci. Eng. C* 113, 110970. doi:10.1016/j.msec.2020.110970

Zhang, N., Chow, S. K.-H., Leung, K.-S., and Cheung, W.-H. (2017). Ultrasound as a Stimulus for Musculoskeletal Disorders. *J. orthopaedic translation* 9, 52–59. doi:10.1016/j.jot.2017.03.004

Zhang, S., Yang, Q., Zhao, W., Qiao, B., Cui, H., Fan, J., et al. (2016). *In Vitro* and *In Vivo* Biocompatibility and Osteogenesis of Graphene-Reinforced Nanohydroxyapatite Polyamide66 Ternary Biocomposite as Orthopedic Implant Material. *Ijn* 11, 3179–3189. doi:10.2147/ijn.S105794

Zhang, Z.-Y., Teoh, S.-H., Chong, M. S. K., Lee, E. S. M., Tan, L.-G., Mattar, C. N., et al. (2010a). Neo-vascularization and Bone Formation Mediated by Fetal Mesenchymal Stem Cell Tissue-Engineered Bone Grafts in Critical-Size Femoral Defects. *Biomaterials* 31, 608–620. doi:10.1016/j.biomaterials.2009.09.078

Zhang, Z.-Y., Teoh, S. H., Chong, W.-S., Foo, T.-T., Chng, Y.-C., Choolani, M., et al. (2009). A Biaxial Rotating Bioreactor for the Culture of Fetal Mesenchymal Stem Cells for Bone Tissue Engineering. *Biomaterials* 30, 2694–2704. doi:10.1016/j.biomaterials.2009.01.028

Zhang, Z.-Y., Teoh, S. H., Teo, E. Y., Khoon Chong, M. S., Shin, C. W., Tien, F. T., et al. (2010b). A Comparison of Bioreactors for Culture of Fetal Mesenchymal Stem Cells for Bone Tissue Engineering. *Biomaterials* 31, 8684–8695. doi:10.1016/j.biomaterials.2010.07.097

Zhao, L., Weir, M. D., and Xu, H. H. K. (2010). An Injectable Calcium Phosphate-Alginate Hydrogel-Umbilical Cord Mesenchymal Stem Cell Paste for Bone Tissue Engineering. *Biomaterials* 31, 6502–6510. doi:10.1016/j.biomaterials.2010.05.017

Zhao, Y.-H., Lv, X., Liu, Y.-L., Zhao, Y., Li, Q., Chen, Y.-J., et al. (2015). Hydrostatic Pressure Promotes the Proliferation and Osteogenic/chondrogenic Differentiation of Mesenchymal Stem Cells: The Roles of Rhoa and Rac1. *Stem Cel. Res.* 14, 283–296. doi:10.1016/j.scr.2015.02.006

Zhao, Y., Huang, Y., Jia, L., Wang, R., Tan, K., and Li, W. (2021). A Novel Tension Machine Promotes Bone Marrow Mesenchymal Stem Cell Osteoblastic and Fibroblastic Differentiation by Applying Cyclic Tension. *Stem Cell Int.* 2021, 1–15. doi:10.1155/2021/6647651

Zhou, J., Li, B., Han, Y., and Zhao, L. (2016a). The Osteogenic Capacity of Biomimetic Hierarchical Micropore/nanorod-Patterned Sr-Ha Coatings with Different Interrod Spacings. *Nanomedicine: Nanotechnology, Biol. Med.* 12, 1161–1173. doi:10.1016/j.nano.2016.01.011

Zhou, X., Castro, N. J., Zhu, W., Cui, H., Aliabouzar, M., Sarkar, K., et al. (2016b). Improved Human Bone Marrow Mesenchymal Stem Cell Osteogenesis in 3d

Bioprinted Tissue Scaffolds with Low Intensity Pulsed Ultrasound Stimulation. *Sci. Rep.* 6, 32876. doi:10.1038/srep32876

Zhu, G., Zeng, C., Qian, Y., Yuan, S., Ye, Z., Zhao, S., et al. (2021). Tensile Strain Promotes Osteogenic Differentiation of Bone Marrow Mesenchymal Stem Cells through Upregulating Lncrna-Meg3. *Histology and histopathology*, 18365. doi:10.14670/hh-18-365

Zura, R., Xiong, Z., Einhorn, T., Watson, J. T., Ostrum, R. F., Prayson, M. J., et al. (2016). Epidemiology of Fracture Nonunion in 18 Human Bones. *JAMA Surg.* 151, e162775. doi:10.1001/jamasurg.2016.2775

Conflict of Interest: The authors declare that the research was conducted in the absence of any commercial or financial relationships that could be construed as a potential conflict of interest.

Publisher's Note: All claims expressed in this article are solely those of the authors and do not necessarily represent those of their affiliated organizations, or those of the publisher, the editors and the reviewers. Any product that may be evaluated in this article, or claim that may be made by its manufacturer, is not guaranteed or endorsed by the publisher.

frontiers in Cell and Developmental Biology

ORIGINAL RESEARCH
published: 17 December 2021
doi: 10.3389/fcell.2021.802502

Neuraminidase1 Inhibitor Protects Against Doxorubicin-Induced Cardiotoxicity *via* Suppressing Drp1-Dependent Mitophagy

Yating Qin[1], Chao Lv[1], Xinxin Zhang[1], Weibin Ruan[1], Xiangyu Xu[2], Chen Chen[3], Xinyun Ji[1], Li Lu[1,4] and Xiaomei Guo[1]**

[1]Department of Cardiology, Tongji Hospital, Tongji Medical College, Huazhong University of Science and Technology, Wuhan, China, [2]Department of Cardiology, The Second Hospital of Shandong University, Jinan, China, [3]Department of Cardiology, The Third People's Hospital of Hubei Province, Wuhan, China, [4]Department of Cardiology, Renmin Hospital of Wuhan University, Wuhan, China

OPEN ACCESS

Edited by:
Guohui Liu,
Huazhong University of Science and Technology, China

Reviewed by:
Lele Liu,
First Affiliated Hospital of Zhengzhou University, China
Fangzhou Lou,
Shanghai General Hospital, China
Hu Dan,
Xiamen University Affiliated Cardiovascular Hospital, China

***Correspondence:**
Li Lu
docluli@163.com
Xiaomei Guo
xmguo@hust.edu.cn

Specialty section:
This article was submitted to Stem Cell Research, a section of the journal Frontiers in Cell and Developmental Biology

Received: 26 October 2021
Accepted: 18 November 2021
Published: 17 December 2021

Citation:
Qin Y, Lv C, Zhang X, Ruan W, Xu X, Chen C, Ji X, Lu L and Guo X (2021) Neuraminidase1 Inhibitor Protects Against Doxorubicin-Induced Cardiotoxicity via Suppressing Drp1-Dependent Mitophagy. Front. Cell Dev. Biol. 9:802502. doi: 10.3389/fcell.2021.802502

Anthracyclines, such as doxorubicin (DOX), are among the effective chemotherapeutic drugs for various malignancies. However, their clinical use is limited by irreversible cardiotoxicity. This study sought to determine the role of neuraminidase 1 (NEU1) in DOX-induced cardiomyopathy and the potential cardio-protective effects of NEU1 inhibitor oseltamivir (OSE). Male Sprague–Dawley (SD) rats were randomized into three groups: control, DOX, and DOX + OSE. NEU1 was highly expressed in DOX-treated rat heart tissues compared with the control group, which was suppressed by OSE administration. Rats in the DOX + OSE group showed preserved cardiac function and were protected from DOX-induced cardiomyopathy. The beneficial effects of OSE were associated with the suppression of dynamin-related protein 1 (Drp1)-dependent mitochondrial fission and mitophagy. In detail, the elevated NEU1 in cardiomyocytes triggered by DOX increased the expression of Drp1, which subsequently enhanced mitochondrial fission and PINK1/Parkin pathway-mediated mitophagy, leading to a maladaptive feedback circle towards myocardial apoptosis and cell death. OSE administration selectively inhibited the increased NEU1 in myocardial cells insulted by DOX, followed by reduction of Drp1 expression, inhibition of PINK1 stabilization on mitochondria, and Parkin translocation to mitochondria, thus alleviating excessive mitochondrial fission and mitophagy, alleviating subsequent development of cellular apoptotic process. This work identified NEU1 as a crucial inducer of DOX-induced cardiomyopathy by promoting Drp1-dependent mitochondrial fission and mitophagy, and NEU1 inhibitor showed new indications of cardio-protection against DOX cardiotoxicity.

Keywords: doxorubicin, cardiotoxicity, neuraminidase1, oseltamivir, dynamin-related protein 1 (Drp1), mitophagy

1 INTRODUCTION

Doxorubicin (DOX), an extensively prescribed and the most potent chemotherapeutic agent for various malignancies, still remains footstones in oncotherapy combined with emerging targeted drugs. However, its clinical use is limited ascribed to dose-dependent cardiotoxicity, leading to irreversible cardiomyopathy and heart failure ultimately (Swain et al., 2003; Yeh, 2006). Although

clinical evaluation makes it possible to detect cardiotoxicity earlier (Thavendiranathan et al., 2014; Vejpongsa and Yeh, 2014; Cardinale et al., 2015), no consensus has been reached on the best way to prevent DOX-induced cardiotoxicity, emphasizing an immediate need for developing novel therapeutic agents.

Accumulating evidence shows that DOX cardiotoxicity is closely linked to mitochondrial damage. Mitochondria are highly dynamic organelles that undergo successive fusion and fission to maintain an appropriate population for mitochondrial quality control. GTPase dynamin-related protein 1 (Drp1) is an essential regulator of mitochondrial fission (Fonseca et al., 2019), and Drp1-mediated mitochondrial fission has been reported to contribute to various cardiovascular diseases, such as diabetic cardiomyopathy, ischemia/reperfusion cardiac injury, and DOX-induced cardiomyopathy (Xia et al., 2017; Zhou et al., 2017; Ding et al., 2018; Lee et al., 2020; Zhuang et al., 2021). Consistently, mitochondrial fission occurs in coordination with mitophagy (Morales et al., 2020), which is a selective form of autophagy that targets elimination of damaged or unfunctional mitochondria. When excessive mitochondrial fission occurs, the number of functional mitochondria is extensively reduced along with an accumulation of mitochondrial fragmentations. Then, the mitophagy process is triggered to digest and clear those structures, attempting to maintain a healthy mitochondrial network (Palikaras et al., 2018). However, upon prolonged stress, mitophagy can also be detrimental to the heart by aggravating mitochondrial damage and accelerating cellular death *via* excessive self-consumption, resulting in cardiac dysfunction (Morales et al., 2020). A recently published study (Catanzaro et al., 2019) identified that Drp1 knockdown could attenuate DOX-induced accelerated mitophagy flux, and Drp1-deficient mice were protected from DOX-induced cardiac damage, strongly confirming the role of Drp1-dependent mitophagy in DOX cardiotoxicity.

Neuraminidases (NEUs), also called sialidases, are a family of glycosidases responsible for the removal of terminal sialic acid from glycoproteins and glycolipids. In mammals, four types of NEUs (NEU1, NEU2, NEU3, and NEU4), encoded by different genes, have been identified according to their distinct enzymatic properties and subcellular localization (Glanz et al., 2019). Among them, NEU1 is the most highly expressed in the heart, involved in several cardiovascular diseases (Zhang et al., 2021). Researchers discovered that NEU1 was highly expressed in the heart of patients with coronary artery disease, and NEU1 knockdown notably protected cardiomyocytes from ischemic injury (Zhang et al., 2018). Overexpression of NEU1 promoted atherosclerosis development and plaque instability by enhancing pro-inflammatory cytokine expression (Sieve et al., 2018). In addition, in ischemia/reperfusion mice model, NEU1 expression and activity were increased in cardiomyocytes as well as in invading monocytic cells, contributing to stronger inflammation and eventually heart failure (Heimerl et al., 2020). What is more, a recently published study identified that NEU1 acted as a crucial driver in cardiac hypertrophy by interplaying with transcriptional factor GATA4 (Chen et al., 2021). However, there are rare researches exploring the relationship between NEU1 and DOX-induced cardiomyopathy so far. In this study, we proposed the hypothesis that NEU1 was a mediator of DOX-induced cardiomyopathy and NEU1 inhibitor could improve DOX-induced cardiac dysfunction through modulating Drp1-dependent mitochondrial fission and mitophagy.

2 MATERIALS AND METHODS

2.1 Drugs and Materials

DOX (S1208) was purchased from Selleck, and oseltamivir (HY-17016) was obtained from MedChemExpress (MCE). ELISA kits for NEU1 and N-acetylneuraminic acid (Neu5Ac) were purchased from Jingmei Biotechnology (Jiangsu, China). ELISA kits for creatine kinase isoenzyme-MB (CK-MB) and cardiac troponin T (cTnT) were obtained from Meilian Biotechnology. Commercial assay kits of aspartate aminotransferase (AST), lactate dehydrogenase (LDH), superoxide dismutase (SOD), total antioxidant capacity (T-AOC), reduced glutathione (GSH) activities, and hydrogen peroxide (H_2O_2) were purchased from Nanjing Jiancheng Bioengineering Institute (Nanjing, China). Terminal deoxynucleotidyl transferase-mediated dUTP nick end labeling (TUNEL) assay was obtained from Beyotime Biotechnology (Shanghai, China). Cell Mitochondria Isolation Kit was purchased from Beyotime Biotechnology (China). All primary antibodies used in this study are listed in **Supplementary Table S1**.

2.2 Animal Experiment

Adult male Sprague–Dawley (SD) rats (7 weeks old) were purchased from Huazhong University of Science and Technology in a total number of 36. Rats were housed in sterilized filter top cages in a temperature- and humidity-controlled environment (22 ± 2°C) with a 12-h day–night cycle. After adaptive feeding for a week, rats were randomly assigned into three groups as follows. Rats in the DOX group received intraperitoneal injection of DOX in a cumulative dose of 15 mg/kg within 2 weeks (2.5 mg/kg for six times), mimicking the human therapeutic regimens. Rats in the DOX + OSE group received gavage of OSE (20 mg/kg) dissolved in normal saline beginning from 3 days before the first injection of DOX to the end of the experiment. Rats in the control group were given equal volume of saline for intraperitoneal injection or gavage. The scheme of experiment is shown in **Figure 1A**. All animal experiments were approved by the Institutional Animal Care and Use Committee of Tongji Medical College, Huazhong University Science and Technology (IACUC number: 2555), which strictly conformed to the National Institutes of Health Guide for the Care and Use of Laboratory Animals.

2.3 Echocardiography

After the first injection of DOX for a month, transthoracic echocardiography was conducted to evaluate cardiac function. In brief, rats were tied under anesthetization with 100 mg/kg pentobarbital sodium, and their chest hairs were removed.

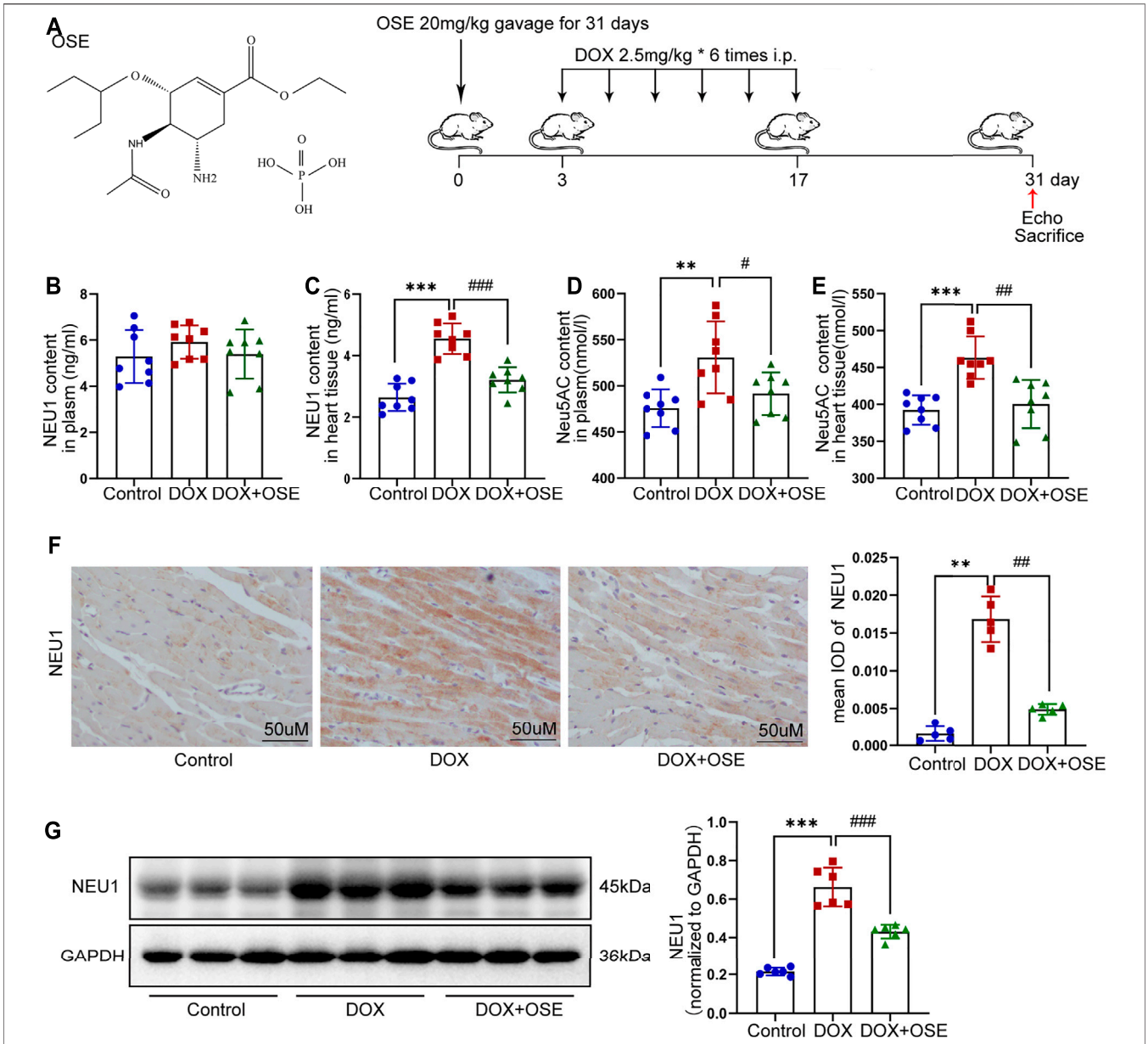

FIGURE 1 | Doxorubicin (DOX) exposure resulted in elevated neuraminidase 1 (NEU1) activity and expression in adult rats. **(A)** The chemical structure of NEU1 inhibitor oseltamivir (OSE) and the schematic diagram of this study. **(B–E)** The content of NEU1 and its regulated downstream metabolite N-acetylneuraminic acid (Neu5AC) in animal plasma or heart tissue measured by commercial ELISA assays (n = 8 per group). **(F)** Representative immunohistochemical images of NEU1 expression in rat hearts (n = 5 per group, scale bar = 50 μm). **(G)** The expression of NEU1 in rat hearts analyzed by western blot (n = 6 per group). (**p < 0.01 vs. control group, ***p < 0.001 vs. control group. #p < 0.05 vs. DOX group, ##p < 0.01 vs. DOX group, ###p < 0.001 vs. DOX group).

M-mode images and echocardiographic parameters were obtained when heart rate was about 450 bpm. Ejection fraction (EF) and Fractional shortening (FS) were calculated as previously described.

2.4 Histopathology Analysis

Hearts were harvested, weighed, and cut into several pieces, and then, samples were either frozen immediately in liquid nitrogen for further biochemistry detection or fixed in 4% paraformaldehyde for histopathological analysis. For histopathological analysis, after being fixed, dehydrated, and embedded in paraffin blocks, heart samples were cut into thin cross sections at 5 μm. To investigate the pathological morphology of the heart, myocardial fibrosis, and cardiomyocyte size, hematoxylin and eosin (HE) staining, Masson's trichrome staining, and wheat germ agglutinin (WGA) staining were conducted strictly following manufacturer's instructions, respectively. All images were obtained by an optical microscope (Olympus, Tokyo, Japan) and analyzed by Image-Pro Plus 6.0 software.

2.5 Biochemical Indexes of Myocardial Injury and Oxidative Stress

Cardiac injury parameters and oxidative stress indexes in adult rat serum were measured. Briefly, blood samples were collected and centrifuged at 3,000 rpm for 10 min at 4°C to obtain the serum, which was directly applied for biochemical detection or stored at −80°C until use. The levels of CK-MB and cTnT were measured by ELISA kits. The levels of AST and LDH were detected by commercial assay kits. Then, the levels of oxidative stress indexes including SOD, T-AOC, GSH, and H_2O_2 were measured by commercially available assay kits too. All detections were strictly in accordance with the manufacturer's instructions.

2.6 Analysis of the Levels of NEU1 and Neu5AC in Rat Hearts and in Serum

The levels of NEU1 and its downregulated metabolite Neu5AC in adult rat hearts and blood serum were measured using ELISA kits. In brief, left ventricular samples were quickly homogenized in PBS on ice (100 mg/ml), and then, homogenate was obtained for later detection after centrifugation at 1,000 g for 10 min at 4°C following manufacturer's protocol.

2.7 Immunohistochemistry and Immunofluorescence Analyses

Formalin-fixed, paraffin-embedded heart sections were deparaffinized, rehydrated in xylene and gradient ethanol, boiled with an antigen retrieval solution for 20 min, and then incubated with 3% hydrogen peroxide for 30 min after cooling down. Next, heart sections were blocked with 5% goat serum in PBS for 1 h at room temperature before incubation with different primary antibodies overnight at 4°C. For immunohistochemical analysis, sections were incubated with secondary antibody prior to staining with diaminobenzidine then counterstaining with hematoxylin; images were obtained by a light microscope (Olympus). For immunofluorescence analysis, after incubation with secondary antibody and counterstaining with DAPI, images were observed and attained by a fluorescent microscope (Olympus). The positive staining areas were calculated and analyzed by Image-Pro Plus 6.0 software.

2.8 Transmission Electron Microscopy Analysis

Hearts were harvested, and left ventricular walls were quickly cut into 1-mm^3 pieces, which were fixed in 2.5% glutaraldehyde with 0.1 M sodium cacodylate buffer for 2 h at room temperature before being stored at 4°C overnight. Heart samples were washed in 0.1 M sodium cacodylate buffer three times for 30 min, then immersed in 1% osmium tetroxide with 0.1 M sodium cacodylate buffer. After being dehydrated, embedded, and counterstained, ultrathin sections were imaged on a transmission electron microscope (Hitachi-151 HT7800, Japan).

2.9 Terminal Deoxynucleotidyl Transferase-Mediated dUTP Nick End Labeling Staining

Paraffin-embedded adult rat heart sections were deparaffinized and rehydrated, then processed for the One-Step TUNEL Apoptosis Assay Detection Kit according to the manufacturer's protocol. The average apoptotic index was defined as the ratio of the number of TUNEL positively stained nuclei to the number of DAPI-stained nuclei.

2.10 Protein Extraction and Immunoblotting

For extraction of the total protein, rat hearts and H9C2 cells were lysed on ice for 15 min in commercial RIPA buffer supplemented with protease inhibitor and phosphatase inhibitor. Lysates were centrifuged at 12,500 rpm for 15 min at 4°C to obtain supernatants. Different from total protein extraction, mitochondrial protein extraction from H9C2 cell was performed using a commercial Cell Mitochondria Isolation Kit. In brief, cells were digested by trypsin, collected in PBS, and centrifuged at 100 g for 5 min at room temperature to obtain sediments. Mitochondria isolation reagent was added, and cells were homogenized several times on ice until the percentage of trypan blue positively stained cells was approximately 50%. Cells were then centrifuged at 600 g for 10 min at 4°C to obtain supernatants, which were centrifuged again at 11,000 g for 10 min at 4°C. Then, the supernatants contained cytosolic protein while the sediments were purified mitochondria. Next, supernatants were centrifuged at 12,500 rpm for 15 min at 4°C to obtain supernatants, which were purified cytosol protein. The purified mitochondria were lysed on ice for 30 min in mitochondria lysis buffer, followed by centrifugation at 12,500 rpm for 15 min at 4°C to obtain supernatants, which were purified mitochondrial protein. Protein concentration was determined by using a bicinchoninic acid assay. Denatured proteins were separated by sodium dodecyl sulfate-polyacrylamide gel electrophoresis and transferred onto polyvinylidene difluoride membranes. Membranes were blocked with 5% bovine serum albumin (BSA) for 1 h at room temperature and subsequently incubated with different primary antibodies at 4°C overnight. After incubation with appropriate peroxidase-conjugated secondary antibodies for 1 h at room temperature, signals were detected with enhanced chemiluminescence.

2.11 Cell Culture and Treatment

H9C2 cell line was purchased from the American Type Culture Collection (ATCC, United States) and was cultured in Dulbecco's modified Eagle's medium, supplemented with 10% fetal bovine serum and 100 U/ml penicillin/streptomycin, at 37°C with 5% CO_2. To investigate the effect of DOX on H9C2 cell line in different times, cells cultured at about 80% confluence were treated with 1 μM DOX for 3, 6, and 12 h, respectively. To study the effect of OSE against DOX-induced myocardial injury, cells were treated as follows: cells in the control group were treated with culture medium only; cells in the DOX group were treated with 1 μM DOX for 12 h; and cells

in the DOX + OSE group were pretreated with 2.5, 5, and 10 μM OSE for 2 h, respectively, followed by incubation with 1 μM DOX for 12 h.

2.12 Statistical Analysis

All data were statistically analyzed using Prism software (GraphPad software 8.0) and shown as Mean ± SEM. Log-rank test was used for survival analysis. p values were calculated with one-way ANOVA or Student's t-test as appropriate. p values <0.05 were considered statistically significant.

3 RESULTS

3.1 Elevated NEU1 Content and Expression in Adult Rats After DOX Exposure

The level of NEU1 in blood serum or left ventricular tissue of adult rats among the three groups was analyzed using a commercial ELISA assay. The level of NEU1 in blood serum tended to be higher in the DOX group in comparison with the other two groups (control vs. DOX: 5.29 ± 1.14 vs. 5.91 ± 0.72 p = 0.21; DOX vs. DOX + OSE: 5.91 ± 0.72 vs. 5.39 ± 1.06 p = 0.27) (**Figure 1B**). As regards to the level of NEU1 in myocardial tissue, a significant increase was observed in the DOX group when compared with the control group ($p < 0.05$), while the increase was dramatically restrained by co-treatment with OSE ($p < 0.05$) (**Figure 1C**). Moreover, DOX exposure resulted in an elevated level of Neu5AC, a kind of metabolite whose generation was predominantly regulated by NEU1, in both blood serum and myocardial tissue compared with the control group, and the elevated level of Neu5AC was significantly attenuated post-OSE treatment (**Figure 1D, E**). What is more, by immunohistochemical staining, it was revealed that NEU1 expression was dramatically increased in myocardial tissues of DOX-treated rats in comparison with the control group, which was significantly attenuated by OSE co-treatment (**Figure 1F**). Western blot analysis revealed that the protein expression of NEU1 in left ventricular tissues was in complete accordance with the results of the immunohistochemical staining (**Figure 1G**). These data indicated that DOX exposure was capable of triggering abnormal activation of NEU1 in adult rat myocardial tissues but not in blood serum, followed by increasing generation of regulated downstream metabolite Neu5AC; however, the abnormally activated processes were substantially prohibited by OSE co-treatment.

3.2 NEU1 Inhibitor Improved DOX-Induced Cardiac Dysfunction in Rats

Based on the hypothesis that abnormally activated NEU1 activity in rat hearts was one of major contributors in DOX-induced cardiac dysfunction, we next investigated whether NEU1 inhibitor OSE could play a protective role against DOX-induced cardiotoxicity. The ratio of body weight to initial body weight (BW/initial BW) analysis showed that rats in the DOX group had a gradually decreasing body weight post-DOX exposure, while NEU1 inhibitor OSE tended to prevent the body weight loss induced by DOX (**Figure 2A**). A survival rate analysis depicted no significant differences among the three groups, indicating that the dose of DOX we used was well tolerated by adult rats (**Figure 2B**). Then, the ratios of heart weight (HW), lung weight (lung W), or liver weight (liver W) to tibial length (TL) among the three groups were assessed. A significant decrease of HW/TL ratio was observed in the DOX group in comparison with the control group, which was prevented by OSE co-treatment (**Supplementary Figure S1A**). No significant difference in lung W/TL ratio or liver W/TL ratio was observed among the three groups (**Supplementary Figure S1B, C**), indicating the absence of lung and liver congestion in these rats, reminiscent of a subclinical myocardial dysfunction, which was observed in chronic DOX-related cardiotoxicity of the clinical practice.

Echocardiographic evaluation at 4 weeks after the first DOX intraperitoneal injection revealed that DOX induced a significant reduction of cardiac contractility (**Figure 2C**), manifested by reduced left ventricular ejection fraction (LVEF) and left ventricular fraction shortening (LVFS), compared with the control group, and the reduction was substantially prevented by OSE treatment (**Figure 2D**). A significant increase of left ventricular end-systolic dimension (LVEDS) but not left ventricular end-diastolic dimension (LVEDD) was observed in DOX-treated rats compared with control rats, and the increase was prevented by OSE co-treatment (**Figure 2D**). Moreover, HE staining, Masson's trichrome staining, and WGA staining uncovered cardiac atrophy, increased fibrosis, and decreased cell sizes in the DOX group hearts, respectively, which were attenuated by OSE treatment (**Figure 2E**). Then, DOX exposure significantly increased the concentrations of cTnT, CK-MB, LDH, and AST in circulation compared the control group, which were alleviated by OSE treatment (**Figure 2F**). The results above strongly confirmed the cardio-protective effects of OSE against DOX-induced cardiomyopathy.

3.3 NEU1 Inhibitor Modulated Autophagy, Mitochondrial Fission, and Mitophagy in DOX-Treated Rat Hearts

Emerging evidence has demonstrated that dysregulation of autophagy in myocardium is critically involved in pathophysiologic processes in cardiovascular disease including DOX cardiotoxicity. The possible link between NEU1 and autophagy was thus investigated in DOX-treated rats. The levels of LC3-II, converting from LC3-I and serving as a specific hallmark of autophagy, were significantly increased in DOX-treated rat hearts by immunofluorescence staining and western blot analysis (**Figure 3A, B**). In contrast, the LC3-II accumulation was dramatically lower in the OSE co-treatment group hearts. Moreover, Beclin 1 and ATG5 are essential components for autophagosome initiation and formation, and we found that, in comparison with the control group, DOX exposure induced much higher protein expressions of these genes, which were effectively suppressed by OSE co-treatment (**Figure 3B**). In addition, p62/SQSTM1, another protein marker

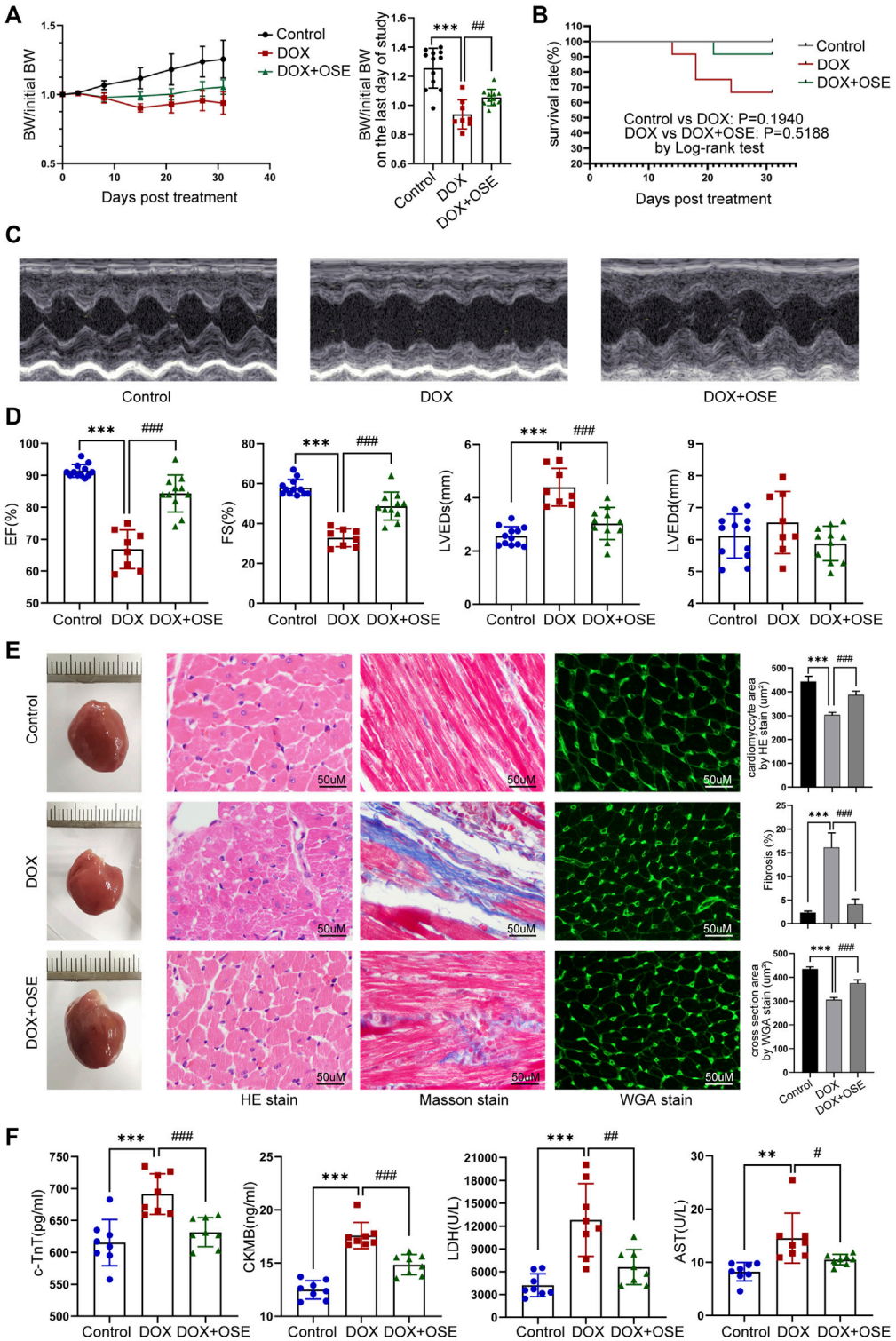

FIGURE 2 | NEU1 inhibitor improved DOX-induced cardiac dysfunction in rats. **(A)** The tendency of body weight change of rats in three groups (n = 12 per group). **(B)** The survival curve of rats in different groups. **(C)** Representative images of M-mode echocardiography in different rat groups at the endpoint of the study. **(D)** Statistical analyses of echocardiographic parameters including ejection fraction (EF), fractional shortening (FS), left ventricular end-systolic dimension (LVEDs), and left ventricular end-diastolic dimension (LVEDD) of rats in the three groups at the end of the study. **(E)** Representative images of hematoxylin and eosin (HE) staining, Masson's trichrome staining, and wheat germ agglutinin (WGA) staining of heart tissues in the three different groups, which display the extent of cardiac atrophy, myocardial fibrosis, and cell sizes, respectively (scale bar = 50 μm). **(F)** Concentrations of cardiac injury markers including cardiac troponin T (cTnT), creatine kinase isoenzyme-MB (CK-MB), lactate dehydrogenase (LDH), and aspartate aminotransferase (AST) in plasma of rats in different groups. (**p < 0.01 vs. control group, ***p < 0.001 vs. control group. #p < 0.05 vs. DOX group, ##p < 0.01 vs. DOX group, ###p < 0.001 vs. DOX group).

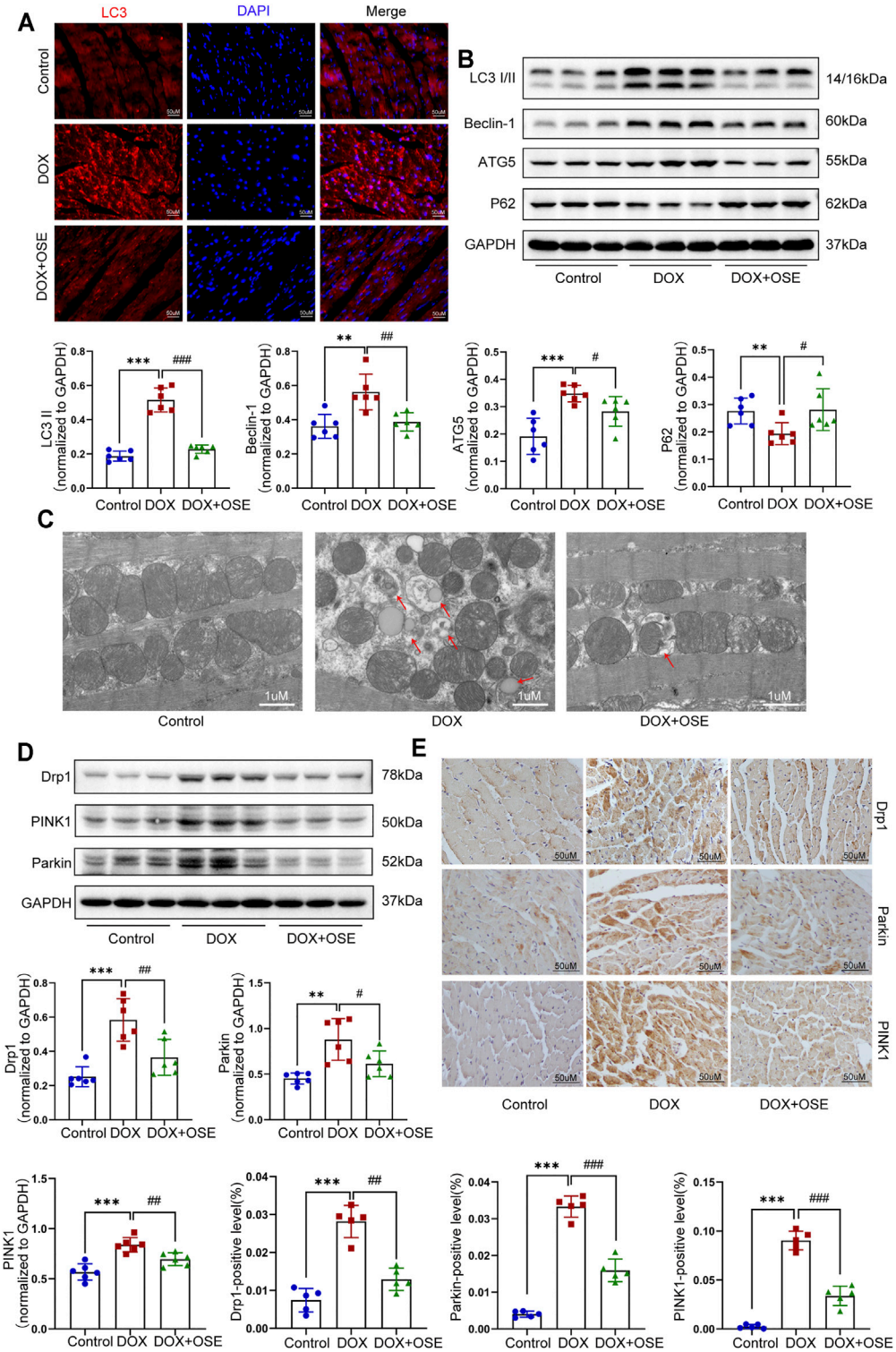

FIGURE 3 | NEU1 inhibitor modulated autophagy, mitochondrial fission, and mitophagy in DOX-treated rat hearts. **(A)** Representative images of LC3II expression in heart tissues of the three groups (scale bar = 50 μm). **(B)** The expression levels of LC3I/II, ATG5, Beclin 1, and P62 in heart tissues of the different groups by western blot (n = 6 per group). **(C)** Representative electron microscopy images of heart tissues in the three groups; the red arrows direct autophagic vacuoles containing cargos (scale bar = 1 μm). **(D)** The expression levels of dynamin-related protein 1 (Drp1), PINK1, and Parkin in heart tissues of the three groups by western blot (n = 6 per group). **(E)** Representative immunohistochemical images of Drp1, PINK1, and Parkin expressions in heart tissues of the three groups (n = 5 per group, scale bar = 50 μm). (**p < 0.01 vs. control group, ***p < 0.001 vs. control group. #p < 0.05 vs. DOX group, ##p < 0.01 vs. DOX group, ###p < 0.001 vs. DOX group).

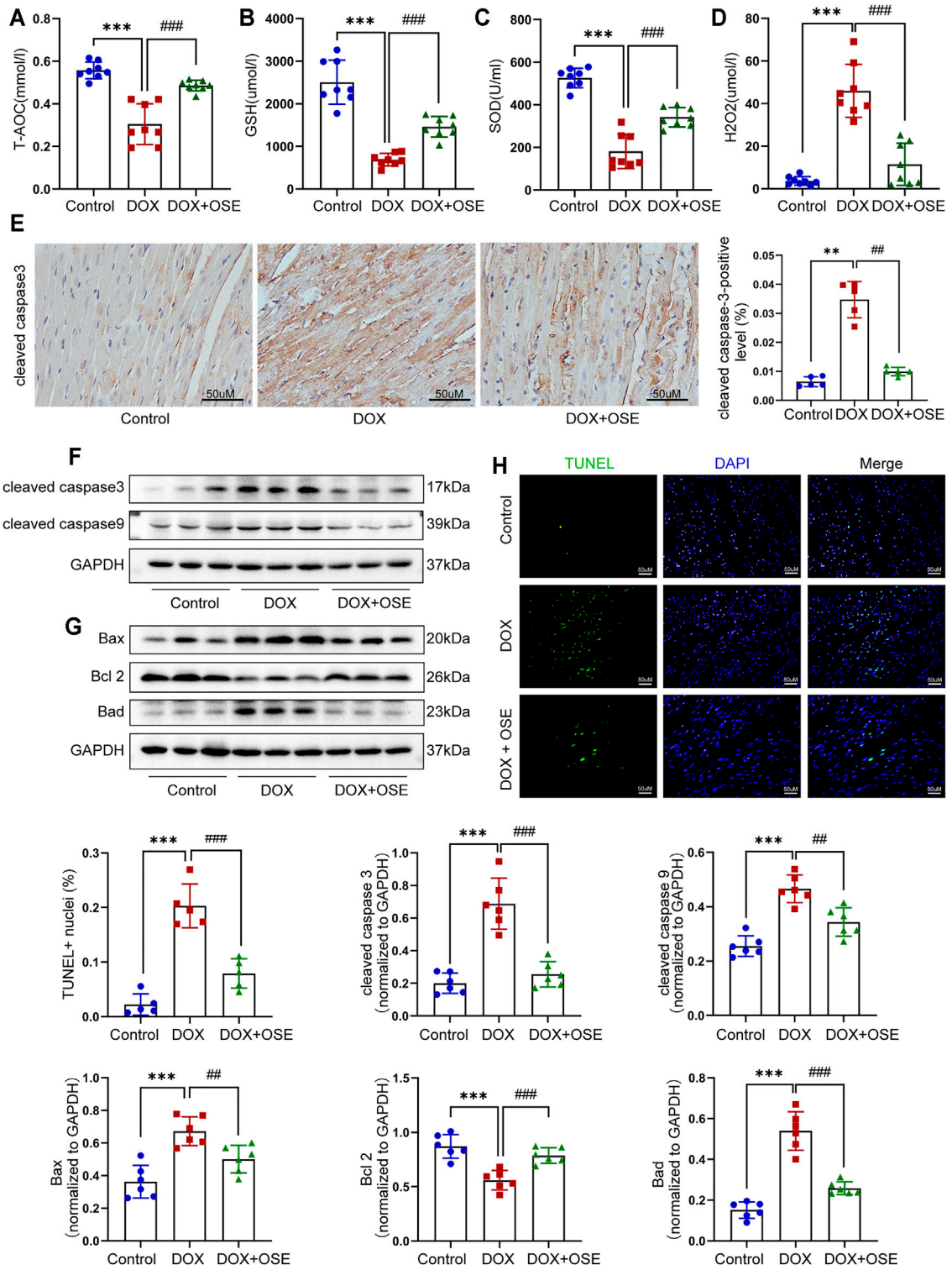

FIGURE 4 | NEU1 inhibitor effectively prevented apoptosis in DOX-treated rat hearts. The concentrations of endogenous antioxidants including total antioxidant capacity (T-AOC) **(A)**, glutathione (GSH) **(B)**, superoxide dismutase (SOD) **(C)**, and endogenous oxidative factor hydrogen peroxide (H_2O_2) **(D)** in blood serum measured by commercial assays. **(E)** Representative immunohistochemical images of cleaved caspase-3 abundance in heart tissues of the three groups (n = 5 per group, scale bar = 50 μm). The expression levels of cleaved caspase-3 and cleaved caspase-9 **(F)** and Bax, Bcl-2, and Bad **(G)** in heart tissues of the three groups by western blot (n = 6 per group). **(H)** Terminal deoxynucleotidyl transferase-mediated dUTP nick end labeling (TUNEL) staining of heart tissues in three groups; positive nuclei were stained in green while nuclei were stained in blue (n = 5 per group, scale bar = 50 μm). (**p < 0.01 vs. control group, ***p < 0.001 vs. control group. ##p < 0.01 vs. DOX group, ###p < 0.001 vs. DOX group).

of autophagy, and western blot analysis showed that the protein expression of p62 was much lower in DOX-treated rat hearts than in the control group, while OSE co-treatment significantly suppressed the effect of DOX on P62 expression (**Figure 3B**). The results above indicate that NEU1 inhibitor OSE may act as a regulator for improving autophagy dysregulation in DOX-induced cardiotoxicity.

Dysregulation of autophagy in myocardium is capable of inducing organelle impairment, especially the mitochondria. Results of transmission electron microscopy revealed an elevated proportion of smaller, fatter, and disorganized mitochondria as well as an increasing number of autophagic vacuoles containing cytosolic cargos including damaged mitochondria in DOX-treated rat hearts compared with the control group (**Figure 3C**), indicating the initiation of mitochondrial autophagy, which was also called mitophagy. However, OSE co-treatment markedly improved the disorders, including maintaining mitochondrial morphology and reducing autophagosome formation. In mammalian cells, mitophagy occurs in coordination with mitochondrial fission. In parallel with the observation from transmission electron microscopy, western blot analysis and immunohistochemical staining both showed that the expression of Drp1, a key protein controlling mitochondrial fission in mammalian cells, was significantly increased in DOX-treated rat hearts compared with the control group, which was attenuated by OSE co-treatment (**Figure 3D, E**). In addition, our findings revealed that mitophagy-related critical proteins including PINK1 and Parkin were dramatically increased in DOX-treated rat hearts compared with the control group, which were reduced by OSE co-treatment (**Figure 3D, E**), indicating that OSE played a protective role against DOX-induced abnormal mitochondrial fission and mitophagy in adult rat hearts.

3.4 NEU1 Inhibitor Effectively Prevented Apoptosis in DOX-Treated Rat Hearts

Abnormal mitochondrial fission and enhanced mitophagy make it hard to maintain a healthy mitochondrial population. Damaged mitochondria not only generate a great deal of reactive oxygen species (ROS) but also have a greater propensity to trigger apoptosis. As shown in **Figure 4**, DOX treatment significantly reduced the concentrations of endogenous antioxidants including SOD, GSH, and T-AOC in blood serum, whereas it dramatically increased the concentrations of endogenous oxidative factors like H_2O_2 compared with the control group, which at least partly indicated that DOX exposure triggered oxidative damage in adult rats, and OSE co-treatment could attenuate the adverse process (**Figure 4A–D**).

In addition, our data showed that the cleaved caspase-3, a critical marker protein of apoptosis, was more abundant in DOX-treated rat hearts than in the control group, which tended to be less abundant after OSE co-treatment, as evidenced by immunohistochemical staining (**Figure 4E**) and western blot analysis (**Figure 4F**). Then, our data demonstrated that DOX exposure resulted in the upregulation of cleaved caspase-9, while OSE co-treatment significantly reversed this phenomenon (**Figure 4F**). B-cell lymphoma 2 (Bcl-2) family proteins, which are located in the outer membrane of mitochondria, are known regulators of mitochondrial-initiated apoptotic events (Dong et al., 2019). Western blot analysis revealed that DOX treatment significantly increased the expression levels of Bax and Bad but decreased Bcl-2 level in adult rat hearts when compared with the control group, which was suppressed by OSE co-treatment (**Figure 4G**). TUNEL staining assay also revealed that myocardial sections in the DOX group had much more amounts of apoptotic cardiomyocytes than in the control group, which tended to be less in the OSE co-treatment group (**Figure 4H**). The results above indicated that the cardio-protective role of OSE against DOX cardiotoxicity was at least partly through inhibiting mitochondrial-mediated myocardial apoptosis.

3.5 DOX Induced the Upregulation of NEU1 and Dysfunction of Autophagy and Mitophagy in H9C2 Cells in a Time-Dependent Manner

The role of NEU1 and its possible relationship with autophagy and mitophagy in DOX-induced cardiotoxicity were further explored in H9C2 cells. As shown in **Figure 5**, the levels of NEU1 and Drp1 in H9C2 cells were gradually increased after DOX exposure for 0, 3, 6, and 12 h, as evidenced by immunofluorescence (**Figure 5A, B**) and western blot analysis (**Figure 5C, D**), indicating that prolonged DOX insult led to the upregulation of NEU1 as well as the increase of mitochondrial fission in H9C2 cells in a time-dependent manner. Our results revealed that DOX insult increased autophagosome formation in H9C2 cells, as evidenced by the gradually increased protein levels of ATG5, Beclin 1, and LC3I/II (**Figure 5E**); meanwhile, DOX exposure promoted the fusion of autophagosome with lysosome in H9C2 cells, as evidenced by the gradually decreased protein level of P62 (**Figure 5E**). Prolonged DOX exposure seemed to enhance mitophagy as well, as evidenced by gradually increased protein levels of PINK1 and Parkin (**Figure 5F**), two critical molecules in the canonical pathway of mitophagy. In addition, the levels of cleaved caspase-9 and cleaved caspase-3 were also observed to increase in a time-dependent manner in H9C2 cells after DOX exposure (**Figure 5G**). These findings strongly suggested that DOX insult was able to upregulate NEU1 expression, enhance mitochondrial fission, and mitophagy in H9C2 cells, followed by myocardial apoptosis.

3.6 OSE and Drp1 Inhibitor Mdivi-1 Effectively Blunted Excessive Mitochondrial Fission and Mitophagy in DOX-Exposed H9C2 Cells

Supposing that the increased mitochondrial fission and mitophagy in DOX-exposed H9C2 cells were ascribed to the upregulation of NEU1, further studies were conducted to investigate whether the NEU1 inhibitor OSE showed protective effects against DOX-induced excessive mitochondrial fission and mitophagy in H9C2 cells. Firstly,

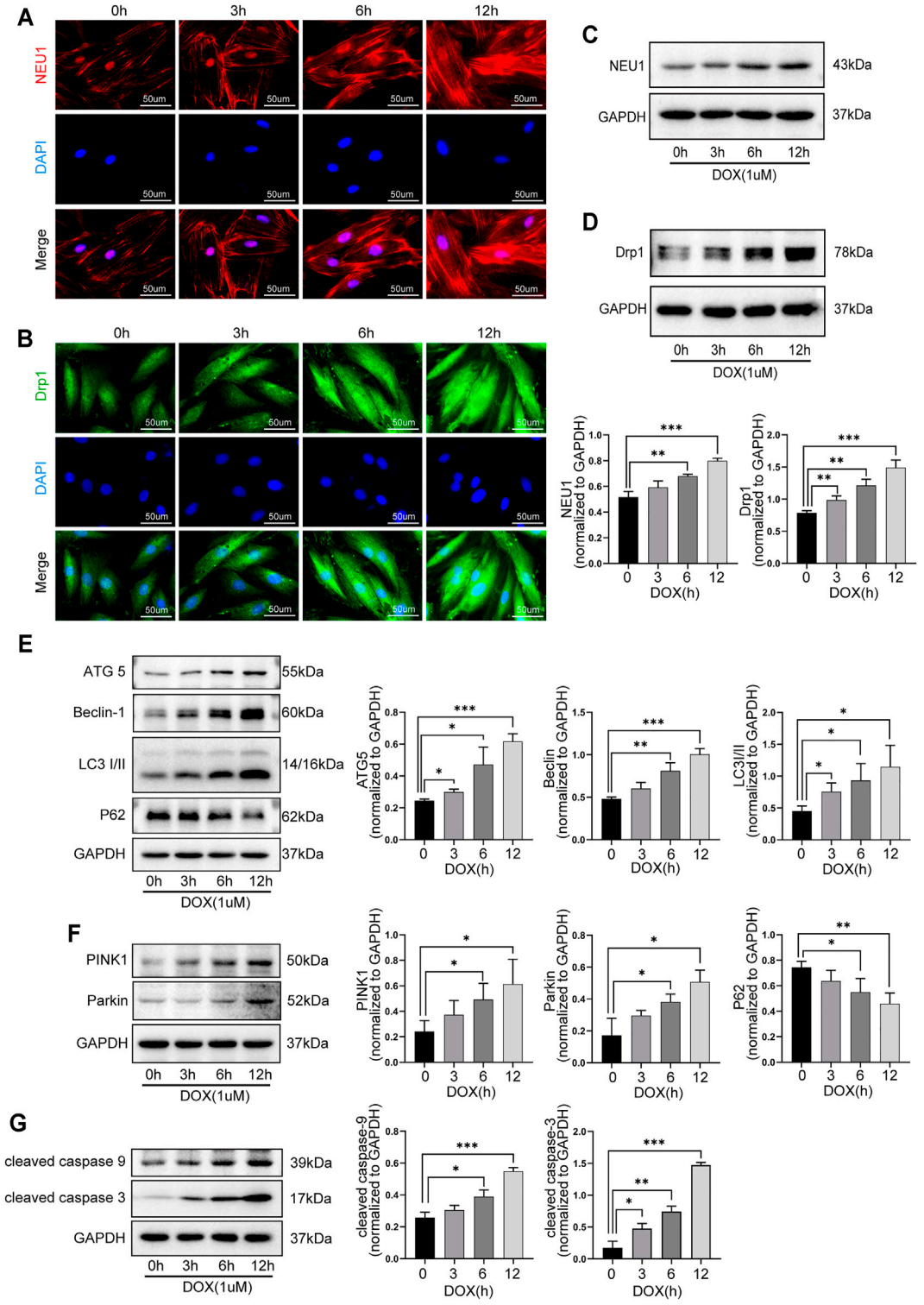

FIGURE 5 | DOX induced the upregulation of NEU1 and dysfunction of autophagy and mitophagy in H9C2 cells in a time-dependent manner. Representative immunofluorescent images of NEU1 **(A)** and Drp1 **(B)** expressions in H9C2 cells that suffered from DOX exposure for 0, 3, 6, and 12 h. Western blot analysis showed that prolonged DOX exposure gradually increased expressions of NEU1 **(C)** and Dpr1 **(D)** in H9C2 cells. **(E)** Prolonged DOX exposure increased the expressions of autophagic markers including ATG5, Beclin 1, and LC3I/II, while it decreased the expression of P62 in H9C2 cells. **(F)** Prolonged DOX exposure enhanced the expressions of mitophagy-related markers like PINK1 and Parkin in H9C2 cells. **(G)** Prolonged DOX exposure activated apoptotic markers including caspase-3 and caspase-9 in H9C2 cells. (*$p < 0.05$, **$p < 0.01$, ***$p < 0.001$).

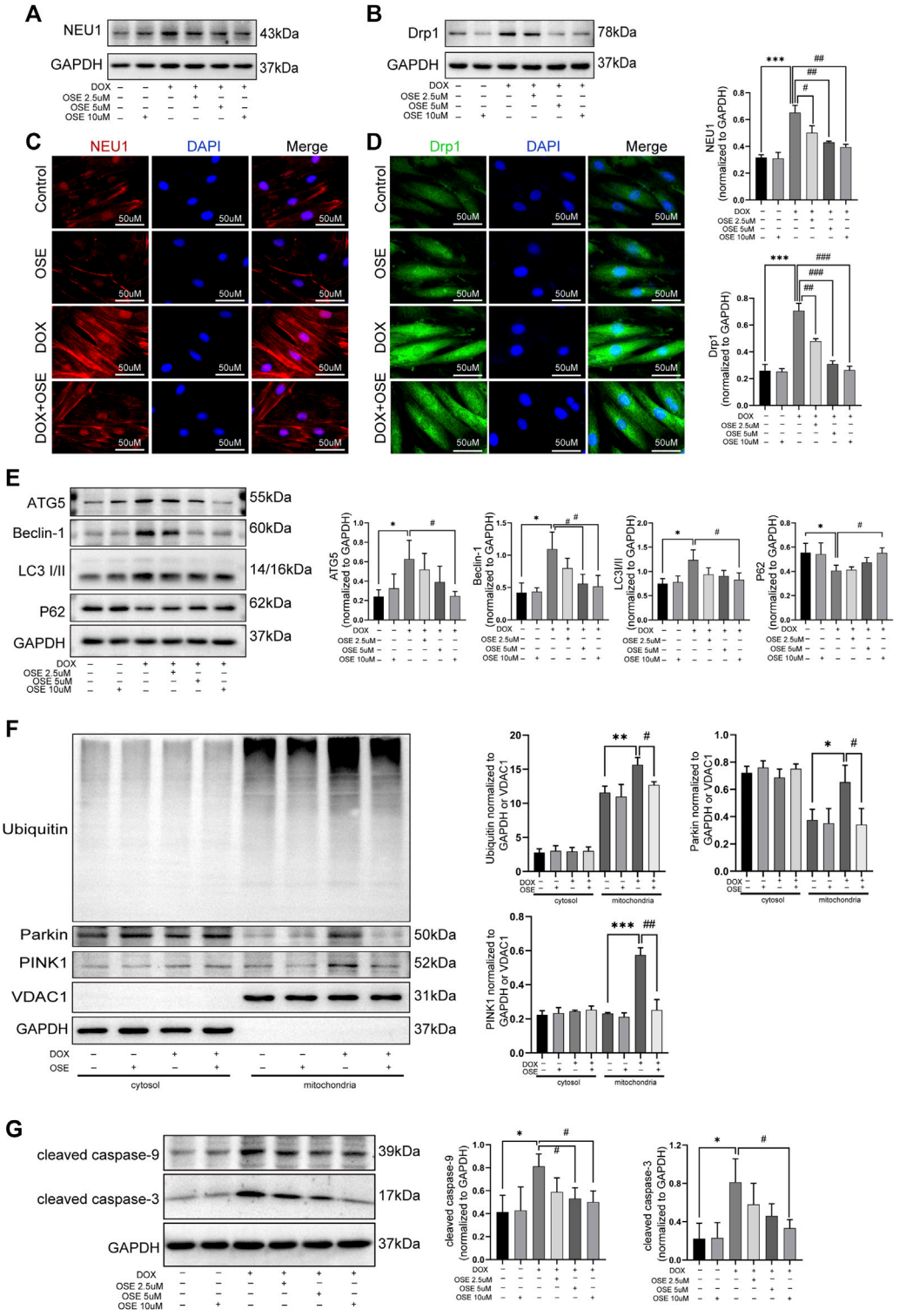

FIGURE 6 | OSE effectively blunted excessive mitochondrial fission and mitophagy in DOX-exposed H9C2 cells. **(A)** OSE suppressed the elevated NEU1 expression induced by DOX in H9C2 cells in a dose-dependent manner. **(B)** OSE suppressed the elevated Drp1 expression induced by DOX in H9C2 cells in a dose-dependent manner. Representative immunofluorescent images of NEU1 expression **(C)** or Drp1 expression **(D)** after OSE treatment in DOX-induced H9C2 cells. **(E)** Western blot analysis revealed that OSE suppressed the excessive autophagy activation induced by DOX in H9C2 cells in a dose-dependent manner. **(F)** Western blot analysis showed that OSE attenuated mitophagy activity in DOX-treated H9C2 cells in a dose-dependent manner through inhibiting PINK1 accumulation, Parkin recruitment, and ubiquitination on mitochondria. **(G)** OSE suppressed apoptotic activity in DOX-treated H9C2 cells in a dose-dependent manner. (*$p < 0.05$ vs. control group, **$p < 0.01$ vs. control group, ***$p < 0.001$ vs. control group. ##$p < 0.01$ vs. DOX group, ###$p < 0.001$ vs. DOX group).

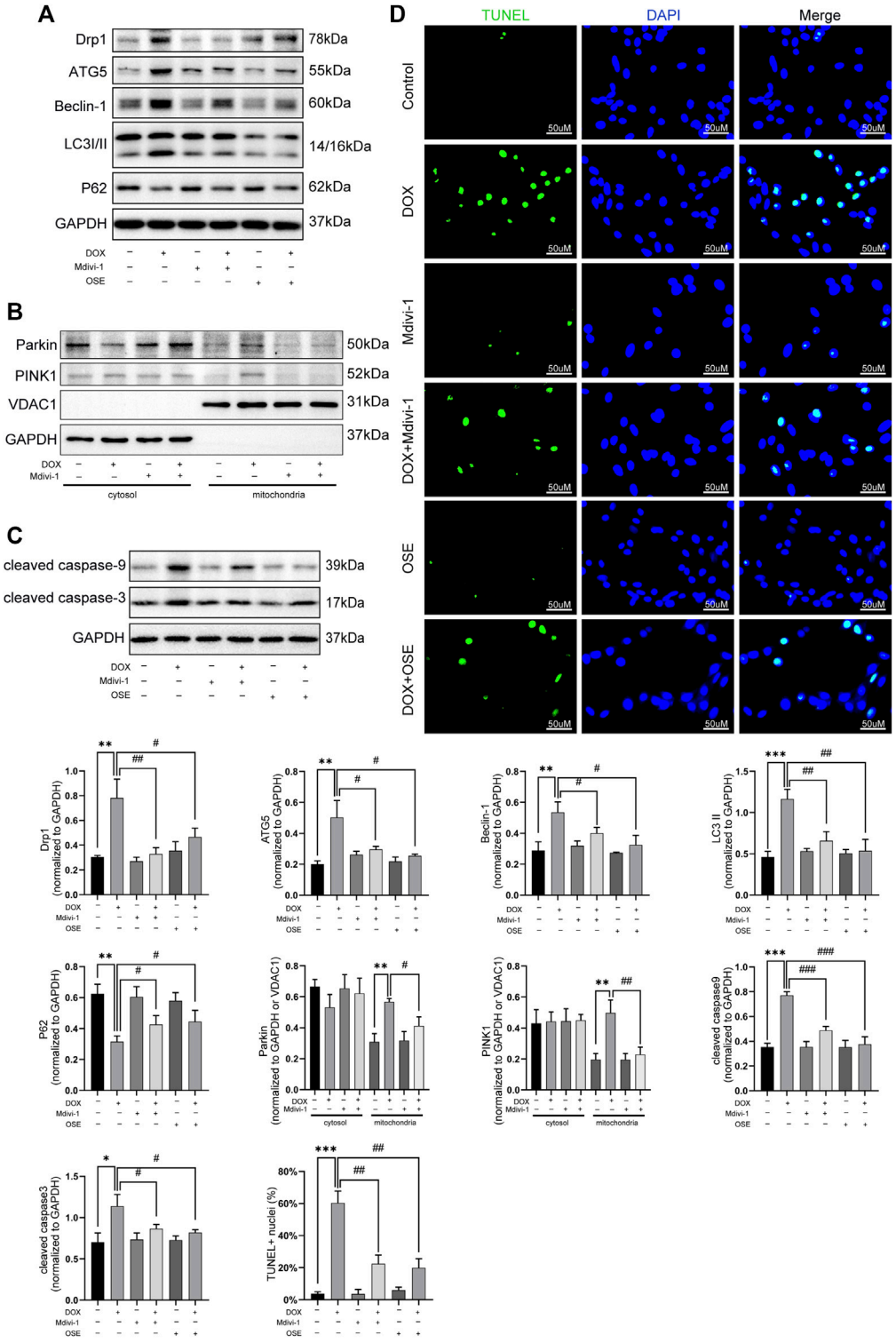

FIGURE 7 | Drp1 inhibitor Mdivi-1 showed similar effects with OSE in DOX-exposed H9C2 cells. **(A)** Mdivi-1 decreased the elevated Drp1 expression and suppressed the enhanced autophagic activity in DOX-treated H9C2 cells, similarly like OSE. **(B)** Mdivi-1 reduced PINK1 accumulation on mitochondria and prevent Parkin translocation from cytosol to mitochondria in DOX-induced H9C2 cells. **(C)** Consistent with the effects of OSE, Mdivi-1 suppressed apoptotic activity in DOX-induced H9C2 cells. **(D)** Representative TUNEL staining images showing that Mdivi-1 suppressed the enhanced apoptosis in DOX-induced H9C2 cells, similarly like OSE.

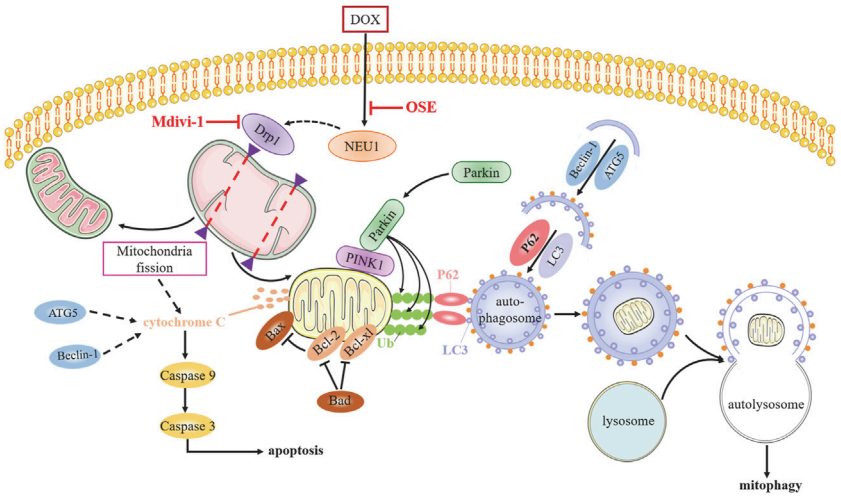

FIGURE 8 | The potential molecular mechanisms of OSE against DOX-induced cardiotoxicity.

western blot analysis revealed that OSE treatment significantly decreased the high expression of NEU1 in DOX-treated H9C2 in a dose-dependent manner (**Figure 6A**), and the most effective dose of OSE was 10 μM, which was used in the later study. Interestingly, the elevated expression of Drp1 caused by DOX was also decreased consistent with NEU1 after OSE treatment (**Figure 6B**). The results above were further evidenced by immunofluorescence assays (**Figure 6C, D**), indicating that the upregulation of Drp1 in DOX-exposed H9C2 cells was ascribed to the elevation of NEU1. What is more, the enhancement of autophagy after DOX insult was suppressed in a dose-dependent manner after OSE treatment, as evidenced by decreased expressions of ATG5, Beclin 1, and LC3II and increased level of P62 (**Figure 6E**).

Then, we explored the effects of OSE on enhanced mitophagy activity in DOX-treated H9C2 cells after extraction and segregation of mitochondrial protein and cytoplasmic protein. Western blot analysis revealed that the level of PINK1, an inducer of mitophagy, was increased in DOX-treated mitochondria (**Figure 6F**), confirming that damaged mitochondria elicited by DOX was deprived of degradation of imported PINK1. Accumulated PINK1 on mitochondria could recruit E3 ubiquitin ligase Parkin from cytosol to mitochondria, which subsequently led to the ubiquitination of mitochondrial substrates. This modification got damaged mitochondria ready for being autophagic removal. In keeping with the increased level of PINK1 on mitochondria, the increased translocation of Parkin from cytosol to mitochondria as well as the increased ubiquitination of mitochondria after DOX exposure were evidenced by western blot analysis (**Figure 6F**), suggesting that DOX treatment enhanced the activity of mitophagy in H9C2 cells. However, the enhanced mitophagy was notably suppressed by the NEU1 inhibitor OSE, as evidenced by less abundant PINK1 accumulation, reduced Parkin recruitment, and decreased ubiquitination on mitochondria after OSE administration (**Figure 6F**). In addition, we further observed that OSE suppressed the processes of mitochondrial fission and mitophagy, accompanied by the inhibition of apoptotic activities in DOX-treated H9C2 cells (**Figure 6G**).

Last but not the least, the role of Drp1 on enhanced mitophagy was further explored in DOX-treated H9C2 cells. As depicted in **Figure 7**, Drp1 inhibitor Mdivi-1 not only blunted the increased expression of Drp1 but also suppressed autophagic activities by decreasing the expressions of ATG5, Beclin 1, and LC3II and increasing the expression of P62 (**Figure 7A**). Consistent with the effects of OSE, Mdivi-1 could also reduce the abundance of PINK1 on mitochondria and prevent the translocation of Parkin from cytosol to mitochondria (**Figure 7B**). Moreover, the increased apoptosis activity caused by DOX was significantly suppressed by Mdivi-1, as evidenced by the results of TUNEL staining and western blot (**Figure 7C, D**).

4 DISCUSSION

Although numerous studies have sought to elucidate the mechanism of anthracycline-induced cardiotoxicity for decades, specific determinants are not yet fully clarified (Renu et al., 2018). The generation of excess ROS and topoisomerase (Top) 2β are most widely accepted contributors facilitating DOX cardiotoxicity progression (Zhang et al., 2012; Rochette et al., 2015); however, neither antioxidants nor iron chelation could completely prevent dilated cardiomyopathy development (Hasinoff et al., 2003; Chow et al., 2015; Ambrosone et al., 2020), indicating multifactorial pathogenic processes responsible for DOX cardiotoxicity. Whether NEU1, a recently identified inducer in various cardiovascular diseases, is involved in DOX cardiotoxicity remains unknown until now. In this study, we uncovered that NEU1 acted as a critical driver of DOX cardiotoxicity, and NEU1 inhibitor had potentials to effectively improve cardiac dysfunction in DOX-induced cardiomyopathy by suppressing Drp1-mediated mitochondrial fission and mitophagy (**Figure 8**).

The role of NEU1 has been studied in different cardiovascular diseases, including atherosclerosis, ischemic/reperfusion injury, cardiac hypertrophy, and heart failure (Heimerl et al., 2020; Chen et al., 2021), (Gökmen et al., 2000; Süer Gökmen et al., 2006; Yang et al., 2012; Gayral et al., 2014; White et al., 2018). In this study, we observed the elevated content as well as the increased protein expression of NEU1 in the hearts of DOX-treated rats, whereas no significant difference in NEU1 level in the plasma of DOX-treated rats was observed when compared with the control group, strongly suggesting that DOX-induced abnormal activation of NEU1 was in the heart and not in blood. We assumed that this may be ascribed to the distribution and subcellular location of NEU1, since NEU1 is highly expressed in the heart (Pshezhetsky et al., 1997) and predominantly distributed in the cell membrane, cytoplasmic vesicles, and lysosomes in mammals (Igdoura et al., 1998). Similar results were also observed in the mice myocardial ischemic model by Zhang et al. (2018). *In vitro* studies further discovered that the expression of NEU1 was increased in a time-dependent manner under DOX exposure in H9C2 cells. Interestingly, NEU1 inhibitor treatment significantly reduced cardiac injury and notably improved cardiac dysfunction in DOX-treated rats, manifested by decreased level of plasma concentrations of cTnT, CKMB, LDH, and AST and improved left ventricular function. Therefore, we conducted advanced studies to investigate the role of NEU1 in DOX-exposed rat hearts and discovered that increased NEU1 content was associated with Drp1-mediated excessive mitochondrial fission and mitophagy, together with an increased risk of myocardial apoptosis.

Although the role of cardiac autophagy and mitophagy in DOX cardiotoxicity has been controversial for decades (Li et al., 2016; Ma et al., 2017; Wang et al., 2019; Liang et al., 2020), our results kept in line with the notion that DOX overstimulated autophagy and mitophagy, and this overstimulation was harmful to the cardiac physiological activities (Catanzaro et al., 2019). Consistent with previous reports (Wang et al., 2014; Yin et al., 2018), our study revealed that DOX exposure induced autophagy activation, as evidenced by elevated levels of autophagy markers including LC3II, Beclin 1, and ATG5, together with a decreased level of autophagosome–autolysosome fusion marker P62 *in vivo* and *in vitro*. Moreover, transmission electron microscopy measure observed small, round, swollen, and disorganized mitochondrial fragmentations as well as increased autophagic vacuoles engulfing cargos like damaged mitochondria in the hearts of DOX-treated rats. Then, we uncovered that NEU1 inhibitor administration dramatically suppressed DOX-induced autophagy activation and mitochondrial damage. It is well known that mitochondrial damage is an apparent hallmark of DOX cardiotoxicity, since DOX accumulates mainly in mitochondria and nucleus (Wallace et al., 2020). Mitochondrial quality control network would segregate damaged mitochondria or mitochondrial fragmentations by mitochondrial fission for autophagic removal, aiming at maintenance of a functional mitochondrial network. However, excessive mitochondrial fission and mitophagy can form a catastrophic feedback loop, disturbing mitochondrial quality control network and resulting in cell death ultimately (Catanzaro et al., 2019). Previous studies have reported that highly expressed Drp1 and Drp1-dependent excessive mitochondrial fission contributed to DOX-induced cardiomyopathy (Xia et al., 2017; Liang et al., 2020; Zhuang et al., 2021), and Drp1 heterozygous knockout mice were protected against DOX-induced cardiotoxicity (Catanzaro et al., 2019), strongly supporting the critical role of Drp1-dependent mitochondrial fission in DOX-related cardiotoxicity. Our results observed highly expressed Drp1 in the hearts of DOX-treated rats; what is more, the expression of Drp1 was demonstrated to increase in a time-dependent manner under continuous DOX insult in H9C2 cells. Given that mitochondrial fission occurs in coordination with mitophagy, we then explored whether and how mitophagy contributes to DOX-stimulated cardiotoxicity.

PINK1/Parkin-mediated mitophagy is the most extensively studied pathway in autophagic elimination of defective mitochondria (Ashrafi and Schwarz, 2013). Under basal conditions, the level of PINK1 is very low since it is imported to the inner mitochondrial membrane for quick degradation by several proteases; however, damaged mitochondria failed to transport and degrade PINK1, thus resulting in accumulation and stabilization of PINK1 on the outer membrane of mitochondria, which subsequently recruited and activated E3 ubiquitin ligase Parkin, leading to Parkin translocation from cytosol to mitochondrial surface. Activated Parkin leads to ubiquitination of mitochondrial substrates readying for autophagic removal (Pickles et al., 2018). However, the role of PINK1/Parkin-mediated mitophagy in DOX-induced cardiomyopathy is still in dispute. Some studies claimed that enhanced mitophagy could protect against DOX cardiotoxicity (Mancilla et al., 2020; Xiao et al., 2020), while others stood on the opposite (Gharanei et al., 2013; Catanzaro et al., 2019). These mixed results might be explained by the different model used, different DOX concentrations, different time of treatment, and different degree of cell damage. Our results showed that mitophagy-related critical proteins including Parkin and PINK1 were notably increased in parallel with the increased expression of Drp1 in the hearts of DOX-treated rats. Whereafter, *in vitro* studies further showed the accumulation of PINK1 on the mitochondria and the translocation of Parkin from cytosol to mitochondria, together with the ubiquitination of mitochondrial substrates in DOX-treated H9C2 cells, confirming the activation of PINK1/Parkin signaling pathway-regulated mitophagy in DOX-induced cardiomyopathy. Then, NEU1 inhibitor administration not only suppressed the increased expression of Drp1 but also reduced PINK1 accumulation on mitochondria and Parkin translocation to mitochondria in DOX-treated hearts as well as in H9C2 cells. Interestingly, Drp1 inhibitor Mdivi-1 exhibited a synergistic effect with NEU1 inhibitor OSE, strongly indicating that NEU1 inhibitor could attenuate DOX-induced cardiotoxicity through suppressing Drp1-dependent mitochondrial fission and mitophagy.

On the other hand, mitochondrial fission could lead to pro-apoptotic protein release from mitochondria to cytosol, triggering apoptosis and finally cell death (Wan et al., 2018). Emerging evidence also demonstrates that mitophagy undergoes abundant crosstalk with apoptosis (Ham et al., 2020). The activation of mitochondrial-dependent apoptotic pathway in DOX-treated cardiomyopathy has been reported by several groups (Hu et al., 2019; Zhang et al., 2020). In line with these studies, our results revealed an increased myocardial apoptosis caused by DOX both *in vivo* and *in vitro*, whereas NEU1 inhibitor OSE and Drp1 inhibitor Mdivi-1 treatment dramatically improved the apoptotic activities, as evidenced by the decreased expression of pro-apoptotic proteins Bax and Bad, the increased expression of anti-apoptotic protein Bcl-2, and the decreased expression of cleaved caspase-3 and cleaved caspase-9. Therefore, we hold the belief that NEU1 inhibitor could suppress myocardial apoptosis through inhibiting Drp1-mediated excessive mitochondrial fission and mitophagy, subsequently delaying the development of DOX-induced cardiomyopathy.

However, there are some limitations existing in this work. First, further investigations are required to clarify how NEU1 was elevated in DOX cardiotoxicity. Second, the mechanisms of how elevated NEU1 induced Drp1 upregulation remain to be further precisely illuminated. Third, although the cardio-protective effect of NEU1 inhibitor against DOX-induced cardiomyopathy was remarkable in animal models, a large number of clinical trials are needed to confirm the efficacy of existing anti-viral drugs like OSE in DOX-induced cardiomyopathy treatment.

5 CONCLUSION

In conclusion, our study confirmed NEU1 as a crucial inducer of DOX cardiotoxicity by enhancing mitochondrial fission and mitophagy, and inhibition of NEU1 could dramatically improve cardiac dysfunction caused by DOX insult, strongly suggesting the clinical potential of targeting NEU1 as a novel strategy for cardiomyopathy treatment.

DATA AVAILABILITY STATEMENT

The original contributions presented in the study are included in the article/**Supplementary Material**, further inquiries can be directed to the corresponding authors.

ETHICS STATEMENT

The animal study was reviewed and approved by the Institutional Animal Care and Use Committee of Tongji Medical College, Huazhong University Science and Technology.

AUTHOR CONTRIBUTIONS

Each author has made significant contributions to this work. YQ conducted the main molecular biology experiments and was a major contributor in writing the manuscript. CL, XZ, and WR helped to perform experiments and collect data. XX, CC, and XJ participated in animal experiments and helped to prepare the figures. LL and XG contributed to the conception and design of the study as well as final revision of the manuscript. All authors contributed to the article and approved the submitted version.

FUNDING

This work was supported by the National Natural Science Foundation of China under Grant (No. 81873518).

SUPPLEMENTARY MATERIAL

The Supplementary Material for this article can be found online at: https://www.frontiersin.org/articles/10.3389/fcell.2021.802502/full#supplementary-material

REFERENCES

Ambrosone, C. B., Zirpoli, G. R., Hutson, A. D., McCann, W. E., McCann, S. E., Barlow, W. E., et al. (2020). Dietary Supplement Use during Chemotherapy and Survival Outcomes of Patients with Breast Cancer Enrolled in a Cooperative Group Clinical Trial (SWOG S0221). *J. Clin. Oncol.* 38 (8), 804–814. doi:10.1200/jco.19.01203

Ashrafi, G., and Schwarz, T. L. (2013). The Pathways of Mitophagy for Quality Control and Clearance of Mitochondria. *Cell Death Differ* 20 (1), 31–42. doi:10.1038/cdd.2012.81

Cardinale, D., Colombo, A., Bacchiani, G., Tedeschi, I., Meroni, C. A., Veglia, F., et al. (2015). Early Detection of Anthracycline Cardiotoxicity and Improvement with Heart Failure Therapy. *Circulation* 131 (22), 1981–1988. doi:10.1161/circulationaha.114.013777

Catanzaro, M. P., Weiner, A., Kaminaris, A., Li, C., Cai, F., Zhao, F., et al. (2019). Doxorubicin-induced Cardiomyocyte Death Is Mediated by Unchecked Mitochondrial Fission and Mitophagy. *FASEB j.* 33 (10), 11096–11108. doi:10.1096/fj.201802663R

Chen, Q.-Q., Ma, G., Liu, J.-F., Cai, Y.-Y., Zhang, J.-Y., Wei, T.-T., et al. (2021). Neuraminidase 1 Is a Driver of Experimental Cardiac Hypertrophy. *Eur. Heart J.* 42, 3770–3782. doi:10.1093/eurheartj/ehab347

Chow, E. J., Asselin, B. L., Schwartz, C. L., Doody, D. R., Leisenring, W. M., Aggarwal, S., et al. (2015). Late Mortality after Dexrazoxane Treatment: A Report from the Children's Oncology Group. *J. Clin. Oncol.* 33 (24), 2639–2645. doi:10.1200/jco.2014.59.4473

Ding, M., Feng, N., Tang, D., Feng, J., Li, Z., Jia, M., et al. (2018). Melatonin Prevents Drp1-Mediated Mitochondrial Fission in Diabetic Hearts through SIRT1-Pgc1α Pathway. *J. Pineal Res.* 65 (2), e12491. doi:10.1111/jpi.12491

Dong, Y., Chen, H., Gao, J., Liu, Y., Li, J., and Wang, J. (2019). Molecular Machinery and Interplay of Apoptosis and Autophagy in Coronary Heart Disease. *J. Mol. Cell Cardiol.* 136, 27–41. doi:10.1016/j.yjmcc.2019.09.001

Fonseca, T. B., Sánchez-Guerrero, Á., Milosevic, I., and Raimundo, N. (2019). Mitochondrial Fission Requires DRP1 but Not Dynamins. *Nature* 570 (7761), E34–E42. doi:10.1038/s41586-019-1296-y

Gayral, S., Garnotel, R., Castaing-Berthou, A., Blaise, S., Fougerat, A., Berge, E., et al. (2014). Elastin-derived Peptides Potentiate Atherosclerosis through the Immune Neu1-Pi3kγ Pathway. *Cardiovasc. Res.* 102 (1), 118–127. doi:10.1093/cvr/cvt336

Gharanei, M., Hussain, A., Janneh, O., and Maddock, H. (2013). Attenuation of Doxorubicin-Induced Cardiotoxicity by Mdivi-1: a Mitochondrial Division/mitophagy Inhibitor. *PLoS One* 8 (10), e77713. doi:10.1371/journal.pone.0077713

Glanz, V. Y., Myasoedova, V. A., Grechko, A. V., and Orekhov, A. N. (2019). Sialidase Activity in Human Pathologies. *Eur. J. Pharmacol.* 842, 345–350. doi:10.1016/j.ejphar.2018.11.014

Gökmen, S. S., Kiliçli, G., Özçelik, F., and Gülen, S. (2000). Serum Total and Lipid-Bound Sialic Acid Levels Following Acute Myocardial Infarction. *Clin. Chem. Lab. Med.* 38 (12), 1249–1255. doi:10.1515/cclm.2000.197

Ham, S. J., Lee, D., Yoo, H., Jun, K., Shin, H., and Chung, J. (2020). Decision between Mitophagy and Apoptosis by Parkin via VDAC1 Ubiquitination. *Proc. Natl. Acad. Sci. USA* 117 (8), 4281–4291. doi:10.1073/pnas.1909814117

Hasinoff, B. B., Patel, D., and Wu, X. (2003). The Oral Iron Chelator ICL670A (Deferasirox) Does Not Protect Myocytes against Doxorubicin. *Free Radic. Biol. Med.* 35 (11), 1469–1479. doi:10.1016/j.freeradbiomed.2003.08.005

Heimerl, M., Sieve, I., Ricke-Hoch, M., Erschow, S., Battmer, K., Scherr, M., et al. (2020). Neuraminidase-1 Promotes Heart Failure after Ischemia/reperfusion Injury by Affecting Cardiomyocytes and Invading Monocytes/macrophages. *Basic Res. Cardiol.* 115 (6), 62. doi:10.1007/s00395-020-00821-z

Hu, C., Zhang, X., Wei, W., Zhang, N., Wu, H., Ma, Z., et al. (2019). Matrine Attenuates Oxidative Stress and Cardiomyocyte Apoptosis in Doxorubicin-Induced Cardiotoxicity via Maintaining AMPKα/UCP2 Pathway. *Acta Pharmaceutica Sinica B* 9 (4), 690–701. doi:10.1016/j.apsb.2019.03.003

Igdoura, S. A., Gafuik, C., Mertineit, C., Saberi, F., Pshezhetsky, A. V., Potier, M., et al. (1998). Cloning of the cDNA and Gene Encoding Mouse Lysosomal Sialidase and Correction of Sialidase Deficiency in Human Sialidosis and Mouse SM/J Fibroblasts. *Hum. Mol. Genet.* 7 (1), 115–120. doi:10.1093/hmg/7.1.115

Lee, T.-L., Lee, M.-H., Chen, Y.-C., Lee, Y.-C., Lai, T.-C., Lin, H. Y.-H., et al. (2020). Vitamin D Attenuates Ischemia/Reperfusion-Induced Cardiac Injury by Reducing Mitochondrial Fission and Mitophagy. *Front. Pharmacol.* 11, 604700. doi:10.3389/fphar.2020.604700

Li, D. L., Wang, Z. V., Ding, G., Tan, W., Luo, X., Criollo, A., et al. (2016). Doxorubicin Blocks Cardiomyocyte Autophagic Flux by Inhibiting Lysosome Acidification. *Circulation* 133 (17), 1668–1687. doi:10.1161/circulationaha.115.017443

Liang, X., Wang, S., Wang, L., Ceylan, A. F., Ren, J., and Zhang, Y. (2020). Mitophagy Inhibitor Liensinine Suppresses Doxorubicin-Induced Cardiotoxicity through Inhibition of Drp1-Mediated Maladaptive Mitochondrial Fission. *Pharmacol. Res.* 157, 104846. doi:10.1016/j.phrs.2020.104846

Ma, Y., Yang, L., Ma, J., Lu, L., Wang, X., Ren, J., et al. (2017). Rutin Attenuates Doxorubicin-Induced Cardiotoxicity via Regulating Autophagy and Apoptosis. *Biochim. Biophys. Acta (Bba) - Mol. Basis Dis.* 1863 (8), 1904–1911. doi:10.1016/j.bbadis.2016.12.021

Mancilla, T. R., Davis, L. R., and Aune, G. J. (2020). Doxorubicin-induced P53 Interferes with Mitophagy in Cardiac Fibroblasts. *PLoS One* 15 (9), e0238856. doi:10.1371/journal.pone.0238856

Morales, P. E., Arias-Durán, C., Ávalos-Guajardo, Y., Aedo, G., Verdejo, H. E., Parra, V., et al. (2020). Emerging Role of Mitophagy in Cardiovascular Physiology and Pathology. *Mol. Aspects Med.* 71, 100822. doi:10.1016/j.mam.2019.09.006

Palikaras, K., Lionaki, E., and Tavernarakis, N. (2018). Mechanisms of Mitophagy in Cellular Homeostasis, Physiology and Pathology. *Nat. Cel Biol* 20 (9), 1013–1022. doi:10.1038/s41556-018-0176-2

Pickles, S., Vigié, P., and Youle, R. J. (2018). Mitophagy and Quality Control Mechanisms in Mitochondrial Maintenance. *Curr. Biol.* 28 (4), R170–R185. doi:10.1016/j.cub.2018.01.004

Pshezhetsky, A. V., Richard, C., Michaud, L., Igdoura, S., Wang, S., Elsliger, M.-A., et al. (1997). Cloning, Expression and Chromosomal Mapping of Human Lysosomal Sialidase and Characterization of Mutations in Sialidosis. *Nat. Genet.* 15 (3), 316–320. doi:10.1038/ng0397-316

Renu, K., Abilash, V. G., Tirupathi Pichiah, P. B., and Arunachalam, S. (2018). Molecular Mechanism of Doxorubicin-Induced Cardiomyopathy - an Update. *Eur. J. Pharmacol.* 818, 241–253. doi:10.1016/j.ejphar.2017.10.043

Rochette, L., Guenancia, C., Gudjoncik, A., Hachet, O., Zeller, M., Cottin, Y., et al. (2015). Anthracyclines/trastuzumab: New Aspects of Cardiotoxicity and Molecular Mechanisms. *Trends Pharmacol. Sci.* 36 (6), 326–348. doi:10.1016/j.tips.2015.03.005

Sieve, I., Ricke-Hoch, M., Kasten, M., Battmer, K., Stapel, B., Falk, C. S., et al. (2018). A Positive Feedback Loop between IL-1β, LPS and NEU1 May Promote Atherosclerosis by Enhancing a Pro-inflammatory State in Monocytes and Macrophages. *Vasc. Pharmacol.* 103-105, 16–28. doi:10.1016/j.vph.2018.01.005

Süer Gökmen, S., Kazezoğlu, C., Sunar, B., Özçelik, F., Güngör, Ö., Yorulmaz, F., et al. (2006). Relationship between Serum Sialic Acids, Sialic Acid-Rich Inflammation-Sensitive Proteins and Cell Damage in Patients with Acute Myocardial Infarction. *Clin. Chem. Lab. Med.* 44 (2), 199–206. doi:10.1515/cclm.2006.037

Swain, S. M., Whaley, F. S., and Ewer, M. S. (2003). Congestive Heart Failure in Patients Treated with Doxorubicin. *Cancer* 97 (11), 2869–2879. doi:10.1002/cncr.11407

Thavendiranathan, P., Poulin, F., Lim, K.-D., Plana, J. C., Woo, A., and Marwick, T. H. (2014). Use of Myocardial Strain Imaging by Echocardiography for the Early Detection of Cardiotoxicity in Patients during and after Cancer Chemotherapy. *J. Am. Coll. Cardiol.* 63 (25 Pt A), 2751–2768. doi:10.1016/j.jacc.2014.01.073

Vejpongsa, P., and Yeh, E. T. H. (2014). Prevention of Anthracycline-Induced Cardiotoxicity. *J. Am. Coll. Cardiol.* 64 (9), 938–945. doi:10.1016/j.jacc.2014.06.1167

Wallace, K. B., Sardão, V. A., and Oliveira, P. J. (2020). Mitochondrial Determinants of Doxorubicin-Induced Cardiomyopathy. *Circ. Res.* 126 (7), 926–941. doi:10.1161/circresaha.119.314681

Wan, Q., Xu, T., Ding, W., Zhang, X., Ji, X., Yu, T., et al. (2018). miR-499-5p Attenuates Mitochondrial Fission and Cell Apoptosis via P21 in Doxorubicin Cardiotoxicity. *Front. Genet.* 9, 734. doi:10.3389/fgene.2018.00734

Wang, P., Wang, L., Lu, J., Hu, Y., Wang, Q., Li, Z., et al. (2019). SESN2 Protects against Doxorubicin-Induced Cardiomyopathy via Rescuing Mitophagy and Improving Mitochondrial Function. *J. Mol. Cell Cardiol.* 133, 125–137. doi:10.1016/j.yjmcc.2019.06.005

Wang, X., Wang, X.-L., Chen, H.-L., Wu, D., Chen, J.-X., Wang, X.-X., et al. (2014). Ghrelin Inhibits Doxorubicin Cardiotoxicity by Inhibiting Excessive Autophagy through AMPK and P38-MAPK. *Biochem. Pharmacol.* 88 (3), 334–350. doi:10.1016/j.bcp.2014.01.040

White, E. J., Gyulay, G., Lhoták, Š., Szewczyk, M. M., Chong, T., Fuller, M. T., et al. (2018). Sialidase Down-Regulation Reduces Non-HDL Cholesterol, Inhibits Leukocyte Transmigration, and Attenuates Atherosclerosis in ApoE Knockout Mice. *J. Biol. Chem.* 293 (38), 14689–14706. doi:10.1074/jbc.RA118.004589

Xia, Y., Chen, Z., Chen, A., Fu, M., Dong, Z., Hu, K., et al. (2017). LCZ696 Improves Cardiac Function via Alleviating Drp1-Mediated Mitochondrial Dysfunction in Mice with Doxorubicin-Induced Dilated Cardiomyopathy. *J. Mol. Cell Cardiol.* 108, 138–148. doi:10.1016/j.yjmcc.2017.06.003

Xiao, D., Chang, W., Ding, W., Wang, Y., Fa, H., and Wang, J. (2020). Enhanced Mitophagy Mediated by the YAP/Parkin Pathway Protects against DOX-Induced Cardiotoxicity. *Toxicol. Lett.* 330, 96–107. doi:10.1016/j.toxlet.2020.05.015

Yang, A., Gyulay, G., Mitchell, M., White, E., Trigatti, B. L., and Igdoura, S. A. (2012). Hypomorphic Sialidase Expression Decreases Serum Cholesterol by Downregulation of VLDL Production in Mice. *J. Lipid Res.* 53 (12), 2573–2585. doi:10.1194/jlr.M027300

Yeh, E. T. H. (2006). Cardiotoxicity Induced by Chemotherapy and Antibody Therapy. *Annu. Rev. Med.* 57, 485–498. doi:10.1146/annurev.med.57.121304.131240

Yin, J., Guo, J., Zhang, Q., Cui, L., Zhang, L., Zhang, T., et al. (2018). Doxorubicin-induced Mitophagy and Mitochondrial Damage Is Associated with Dysregulation of the PINK1/parkin Pathway. *Toxicol. Vitro* 51, 1–10. doi:10.1016/j.tiv.2018.05.001

Zhang, J.-Y., Chen, Q.-Q., Li, J., Zhang, L., and Qi, L.-W. (2021). Neuraminidase 1 and its Inhibitors from Chinese Herbal Medicines: An Emerging Role for Cardiovascular Diseases. *Am. J. Chin. Med.* 49 (4), 843–862. doi:10.1142/S0192415X21500403

Zhang, L., Wei, T.-T., Li, Y., Li, J., Fan, Y., Huang, F.-Q., et al. (2018). Functional Metabolomics Characterizes a Key Role for N -Acetylneuraminic Acid in

Coronary Artery Diseases. *Circulation* 137 (13), 1374–1390. doi:10.1161/CIRCULATIONAHA.117.031139

Zhang, S., Liu, X., Bawa-Khalfe, T., Lu, L.-S., Lyu, Y. L., Liu, L. F., et al. (2012). Identification of the Molecular Basis of Doxorubicin-Induced Cardiotoxicity. *Nat. Med.* 18 (11), 1639–1642. doi:10.1038/nm.2919

Zhang, X., Hu, C., Kong, C.-Y., Song, P., Wu, H.-M., Xu, S.-C., et al. (2020). FNDC5 Alleviates Oxidative Stress and Cardiomyocyte Apoptosis in Doxorubicin-Induced Cardiotoxicity via Activating AKT. *Cel Death Differ* 27 (2), 540–555. doi:10.1038/s41418-019-0372-z

Zhou, H., Zhang, Y., Hu, S., Shi, C., Zhu, P., Ma, Q., et al. (2017). Melatonin Protects Cardiac Microvasculature against Ischemia/reperfusion Injury via Suppression of Mitochondrial Fission-VDAC1-HK2-mPTP-Mitophagy axis. *J. Pineal Res.* 63 (1), e12413. doi:10.1111/jpi.12413

Zhuang, X., Sun, X., Zhou, H., Zhang, S., Zhong, X., Xu, X., et al. (2021). Klotho Attenuated Doxorubicin-Induced Cardiomyopathy by Alleviating Dynamin-Related Protein 1 - Mediated Mitochondrial Dysfunction. *Mech. Ageing Dev.* 195, 111442. doi:10.1016/j.mad.2021.111442

Conflict of Interest: The authors declare that the research was conducted in the absence of any commercial or financial relationships that could be construed as a potential conflict of interest.

frontiers in Cell and Developmental Biology

REVIEW
published: 06 January 2022
doi: 10.3389/fcell.2021.823694

Use of Adipose Stem Cells Against Hypertrophic Scarring or Keloid

*Hongbo Chen†, Kai Hou†, Yiping Wu and Zeming Liu**

Department of Plastic and Cosmetic Surgery, Tongji Hospital, Tongji Medical College, Huazhong University of Science and Technology, Wuhan, China

Hypertrophic scars or keloid form as part of the wound healing reaction process, and its formation mechanism is complex and diverse, involving multi-stage synergistic action of multiple cells and factors. Adipose stem cells (ASCs) have become an emerging approach for the treatment of many diseases, including hypertrophic scarring or keloid, owing to their various advantages and potential. Herein, we analyzed the molecular mechanism of hypertrophic scar or keloid formation and explored the role and prospects of stem cell therapy, in the treatment of this condition.

Keywords: hypertrofic scars, adipose derived stem cell, wound healing, stem cell therapy, mechanism, keloid

OPEN ACCESS

Edited by:
Guohui Liu,
Huazhong University of Science and Technology, China

Reviewed by:
Bo Yin,
Chinese Academy of Medical Sciences and Peking Union Medical College, China
Chanyuan Jiang,
Chinese Academy of Medical Sciences and Peking Union Medical College, China

****Correspondence:***
Zeming Liu
6myt@163.com

†These authors have contributed equally to this work

Specialty section:
This article was submitted to Stem Cell Research, a section of the journal Frontiers in Cell and Developmental Biology

Received: *28 November 2021*
Accepted: *17 December 2021*
Published: *06 January 2022*

Citation:
Chen H, Hou K, Wu Y and Liu Z (2022) Use of Adipose Stem Cells Against Hypertrophic Scarring or Keloid. Front. Cell Dev. Biol. 9:823694. doi: 10.3389/fcell.2021.823694

INTRODUCTION

Hypertrophic scars are abnormal fibroproliferative wound healing reactions (Zouboulis and Orfanos, 1990; Limandjaja et al., 2020), hypertrophic scars can continue to develop into keloids, keloids are lesions that are higher than the skin surface and beyond the original injury range. The texture of the keloid becomes hard and thickened, presenting nodular or flake masses. Hypertrophic scars and keloid are characterized by excessive scar tissue formation and invasive growth beyond the original wound boundary. Hypertrophic scarring is an unpleasant, maladaptive comorbidity that affects most people around the world and imposes a heavy social and economic burden on affected parties.

Scars usually occur on specific body sites, such as the anterior chest, ear-lobe, mandibular border, and the suprapubic region (Huang and Ogawa, 2021). In addition to obvious cosmetic disfigurement, hypertrophic scars can also produce symptoms such as itching, pain, contracture, and movement restriction, resulting in serious impairment of emotional health and reduced quality of life (Bijlard et al., 2017; Balci et al., 2009). Hypertrophic scars can be acquired genetically or pathologically. Histologically, hypertrophic scars are benign hyperplastic disorder caused by excessive accumulation of extracellular matrix (ECM) and other components (Feng et al., 2017).

The incidence of hypertrophic scarring varies widely and is known to correlate with race and ethnicity. Incidence rates are reportedly as low as <1.0% in Taiwanese Chinese and Caucasians (Seifert and Mrowietz, 2009; Sun et al., 2014), and range from 4.5 to 16.0% in the black and Hispanic general population (Rockwell et al., 1989; Hunasgi et al., 2013). More recent data are available for specific subgroups, reporting that the incidence of hypertrophic scar formation increases significantly in African Americans compared to Caucasians, Asians and other groups, after head and neck surgery, and in women, following cesarean section (C-section) (Tulandi et al., 2011; Sun

Abbreviations: ASCs, adipose stem cells; ECM, extracellular matrix; HGF, hepatocyte growth factor; ISCT, International Society for Cell & Gene Therapy; IL-10, interleukin-10; mscMSCs, Mesenchymal stem cells; NO, nitric oxide; PDGF, Platelet-derived growth factor; PGE2, prostaglandin E2; TGF-β, transforming growth factor-β.

et al., 2014). Overcoming the complications, and social and economic burden caused by hypertrophic scarring, has become an important medical research topic.

MECHANISM OF SCAR FORMATION

Scar formation is part of the abnormal wound healing response after non-severe trauma, such as caesarean section incision, chest hair folliculitis, ear piercing and vaccination. The potential mechanism of scar is complicated, involves genetic susceptibility, mechanobiology, endocrine factors, infection, excessive inflammatory response and so on (Huang and Ogawa, 2021; Yu et al., 2021, Riccio et al., 2019b). Scar formation include multiple cell factors and synergy between multiple stages of repair.

The stages of wound healing mainly comprise inflammation, proliferation, and reshaping (Mari et al., 2015; Leavitt et al., 2016; Morikawa et al., 2019; Rodrigues et al., 2019; Tan et al., 2019; De Francesco et al., 2020). When skin lesions occur, the first reaction entails the formation of a platelet plug, followed by clot formation that immediately stems the bleeding. Then, damaged tissue and activated platelets initiate an inflammatory response by recruiting immune cells such as neutrophils and monocytes to fight local infection, engulf localized debris and damaged connective tissue, and subsequently remove fibrin. After the inflammation subsides, the hyperplasia phase begins, during which new blood vessels and connective tissue appear in the wound area. Re-epithelialization, driven by keratinocyte migration, marks the beginning of proliferation. Thereafter, organizational maturity signifies the reshaping phase, which involves the degeneration of neovascularization and concomitant reconstruction of the extracellular matrix (ECM), resulting in development of organized collagen fibrils that serve as the basis of normal scarring (Wang et al., 2020).

Interference with any of these processes can lead to poor or excessive wound healing, resulting in the formation of hypertrophic scars and non-malignant dermal tumors, which share similar phenotypes, cellular bioenergetics, epigenetic methylation, and other characteristics. Platelet-derived growth factor (PDGF), transforming growth factor-β (TGF-β) and other factors can lead to fibroblast dysfunction and phenotypic changes, ECM disorder and repeated deposition, and an unbalanced angiogenesis cascade, ultimately causing excessive scarring (Tan et al., 2019; Wang et al., 2020; Putri and Prasetyono, 2021).

Genetic Variation, Epigenetic Modifications and Scar

Single nucleotide polymorphisms have also been implicated in keloid formation, and genetic studies have identified several SNPS and genes that may contribute to understanding the association with keloid development (Halim et al., 2012, Tsai and Ogawa, 2019). For example, a genome-wide association study (GWAS) by Nakashima et al. found that four SNPS (rs873549, rs1511412, rs940187 and rs8032158) in three chromosomal regions were significantly associated with keloid (Nakashima et al., 2010). In other study, Ogawa et al. also reported that rs8032158 may also influence keloid development (Halim et al., 2012).

Recent studies suggest that epigenetic inheritance may also contribute to keloid formation. For example, DNA methylation can change the structure of DNA, thus affecting cell differentiation and cell phenotype (Bataille et al., 2012). Other epigenetic changes include changes in cell phenotypes by popular non-coding RNA. Epigenetic modifications and DNA methylation caused by non-coding RNA (such as microRNAs and LncRNAs) may also play an important role by inducing sustained activation of keloid fibroblasts (Tsai and Ogawa, 2019).

Mechanical Stress and Scar

The two main anatomical layers of skin, from top to bottom, are the epidermis and dermis. The epidermis consists mainly of epithelial keratinocytes, which are forced together by actin (Harn et al., 2016). These keratinocytes form the skin's barrier and are layered on top of the dermis, acting as building blocks against external shearing and stretching forces. In contrast, the dermis contains mostly ECM, blood vessels, fibroblasts, and other mesenchymal cells, rather than epithelial cells. Mesenchymal cells, such as fibroblasts, exhibit more cell-matrix interactions (Tracy et al., 2016; Harn et al., 2019; Watt and Fujiwara, 2011).

Mechanical forces regulate skin homeostasis and play a role in the pathogenesis of skin diseases (Fu et al., 2021). As mention, the dermis is rich in ECM—especially collagen, secreted by fibroblasts—that provides the bulk of the skin's tension (Hsu et al., 2018). Changes in external tension and the internal mechanical properties of cells are associated with collagen, and scarring is specifically the result of excessive collagen production. To some extent, the mechanical stiffness of the skin environment determines the regenerative ability of wound healing. Strategies that alter mechanical forces or mechanical transduction signals may provide new approaches for treating skin diseases and promoting skin regeneration (Harn et al., 2019).

Immunological Aspects of Scar

Scarring and autoimmune skin disease represent fibrosis events that require a variety of growth factors and result from synergy between immune cells and the medium. These conditions share certain features, such as high infiltration of immune cells and immunoglobulin (Ig), as well as complement deposition in the scar tissue and scar fibroblasts, and medium-high secretion of immune factors, among others (Dong et al., 2013; Jiao et al., 2015; Ogawa, 2017).

Scar can be classified as inflammatory, nodular, and mixed types (Yu et al., 2021). The number and type of immune cells in a patient's scar tissue or peripheral blood may vary by type and stage. Moreover, the formation of a scar may be related to abnormal wound healing and related immune factors, especially in repeatedly recurring scars. Hence, the classification of scar types and stages provides direction for future research. In the process of scar formation, the initial activation of mast cells (MCs) is the key factor inducing chronic inflammation. Further, MCs release mediators that

initiate host defense cascades leading to fibrotic processes. (Hsu et al., 2018; Tsai and Ogawa, 2019).

CURRENT MAINSTREAM STRATEGIES FOR INHIBITING SCAR FORMATION

Therapeutic strategies for treating hypertrophic scars include steroid injection, surgical hypertrophic scar removal, radiotherapy, compression, and cryotherapy, pulsed dye and CO_2 laser, silicone gel, nanoparticles and radiotherapy, among others (Salameh et al., 2021; Ogawa, 2021; Svolacchia et al., 2016; Nicoletti et al., 2013; Riccio et al., 2019a; Jimi et al., 2020; Barrera, 2003; Aoki et al., 2020). However, existing treatments are not guaranteed to reduce recurrence of keloids, due to the high recurrence rate thereof at the hypertrophic scar excision site (Coentro et al., 2019; Kumar and Kamalasanan, 2021).

Scar-free healing is the ultimate goal of scar prevention strategies (Falanga, 2005; Ho Jeong, 2010; Heng, 2011; Leavitt et al., 2016). To develop an optimal combination strategy to this effect, it is necessary to fully reveal the causal relationship between key cells and molecules in scar pathogenesis, thus providing new therapeutic targets for scar-free healing. In addition, advances in stem cell and tissue engineering have brought more alternative therapies closer to reality. Functionalization of biomaterials through various drugs and growth factors, provides a well-controlled approach to scar therapy (Fuller et al., 2016; Rahimnejad et al., 2017; Wang et al., 2022).

MESENCHYMAL STEM CELLS AND ADIPOGENIC STEM CELLS

Mesenchymal stem cells (MSCs) are primarily responsible for the regeneration of damaged cells and can be obtained from a variety of sources, including bone marrow, umbilical cord, and adipose tissue. MSCs are abundant and have recently been attracting increasing research attention as potential treatment options in many diseases. The basic characteristics of MSCs are defined by the International Society for Cell & Gene Therapy (ISCT), as follows: 1) plasticity when cultured under standard conditions; 2) expression of a unique set of surface antigens specified by the ISCT; 3) ability to differentiate into osteoblasts, chondrocytes, and adipose cells (Dominici et al., 2006; De Francesco et al., 2017; Bougioukli et al., 2018).

Adipogenic stem cells (ASCs) are bone marrow MSCs extracted from fat cells (53). Not only do they have the general characteristics of bone marrow MSCs, but they are also easy to obtain. ASCs are found in large numbers in the human body, have high proliferation and self-renewal potential, and other advantages, based on which numerous studies have shown their potential in addressing many diseases, including hypertrophic scarring (Gir et al., 2012; Lee et al., 2012; Strong et al., 2015; O'Halloran et al., 2017; Gardin et al., 2018; Gentile and Garcovich, 2019; Ren et al., 2019; Xiong et al., 2020).

DISCUSSION OF ADIPOGENIC STEM CELLS AND HYPERTROPHIC SCARRING

Existing studies have shown that ASCs' mechanism of action entails secretion of bioactive factors (including growth factors and cytokines, among others), on the one hand, to promote cell proliferation, differentiation, and migration. On the other hand, exosomes derived from ASCs play a role (Hu et al., 2016; Li et al., 2018; Han et al., 2019; Kucharzewski et al., 2019). Moreover, ASCs can play a direct part in disease management, through their multidirectional differentiation ability, by forming complex hybrid systems with novel treatment materials.

Directed Differentiation

ASCs are pluripotent stem cells with the ability of self-renewal and multidirectional differentiation. They are not only the precursors of fat cells, but also capable of differentiating into osteoblasts, chondrocytes, muscle cells, and neuronal cells. ASCs have also been shown to differentiate into keratinocytes. These results suggest that ASCs may also differentiate directly into epidermal and dermal cells to promote tissue regeneration and prevent scarring in an injured area, during wound healing (Joshi et al., 2020; Xiong et al., 2020; Putri and Prasetyono, 2021).

Secretion of Biologically Active Factors

ASCs regulate inflammation facilitated by immune cells, through paracrine bioactive factors, inhibiting scar hyperplasia. Long-term inflammation is a main cause of hypertrophic scar formation. ASCs are known to modulate the activity of inflammatory cells, thereby attenuating periods of excessive and prolonged inflammation. This immunomodulatory activity of ASCs is conducted by paracrine secretion of several anti-fibrotic cytokines, including prostaglandin E2 (PGE2), interleukin (IL)-10, hepatocyte growth factor (HGF), and nitric oxide (NO) (Seo and Jung, 2016). In contrast, mast cells are involved in the regulation of vascular homeostasis and angiogenesis and can upregulate fibroblast proliferation, resulting in excessive collagen synthesis and differentiation of fibroblasts into myofibroblasts. ASCs can further reduce hypertrophic scarring by inhibiting the number and activity of mast cells (Putri and Prasetyono, 2021).

ASCs can also activate various anti-fibrotic molecular pathways through paracrine signaling, regulate the activity of primary fibroblast transforming growth factor, and stabilize the function of fibroblast and keratinocyte receptor sites, to achieve relevant anti-fibrosis goals (Borovikova et al., 2018). In addition, injection of ASCs can reverse the abnormal vascularization pattern of scar tissue and reshape the microvascular structure (Garza et al., 2014; Luan et al., 2016).

Release of Adipogenic Stem Cell-Derived Exosomes (Adipogenic Stem Cell-Exos)

Exosomes are a subset of small, membranous extracellular vesicles (Han et al., 2018; Jing et al., 2018) with a diameter of approximately 30–150 nm, which originate from entosis and are

distributed in many bodily fluids—including blood, urine, cerebrospinal fluid, and bile—under physiological and pathological conditions. Exosomes include a variety of active biological substances such as proteins, DNA, mRNAs, and microRNAs, which can carry complex biological information and release it into target cells (Hessvik et al., 2016; Buratta et al., 2020). In addition, exosomes may exist between MSCs and target cells as paracrine mediators (Valadi et al., 2007; Chiba et al., 2012). Many studies have shown that ASC-derived exosomes (ASC-Exos) play an important role in cell migration, proliferation, and collagen synthesis (Xiong et al., 2020; Putri and Prasetyono, 2021).

For example, characteristics of scarring include collagen receptor rearrangement, activation of myofibroblasts expressing α-smooth muscle actin (α-SMA), and the production and secretion of high levels of TGF-β1 in affected tissues (Beanes et al., 2003). Xu et al. indirectly inhibited PLOD1 levels in ASCs through post-transcriptional regulation, which may significantly improve the anti-corrosion potential of ASCs during wound healing, by changing macrophage polarization and regulating scar formation (Xu et al., 2021). In addition, Wang et al. found that ASC-Exos reduced scar formation mainly by regulating the ratios of type III:type I collagen, TGF-β3:TGF-β1, matrix metalloproteinases-3 (MMP-3):tissue inhibitor of metalloproteinases-1 (TIMP-1), and promoting human dermal fibroblast HDF differentiation. This resulted in improved ECM reconstruction and other implementations (Wang et al., 2017).

Formation of Complex Hybrid Systems

ASCs can play a role in disease management by forming complex hybrid systems with novel materials. For example, Wang et al. proved that ASCs are capable of multi-potential—including lipogenic, osteogenic, and chondrogenic—differentiation, and developed ASC-Exos-delivering collagen/poly (L-lactide-co-caprolactone) (P (LLA-Cl)) nanoyarns, which conform to a material system that mimics the morphological structure of the natural tissue matrix. With sufficient biocompatibility and mechanical properties, it can effectively promote neovascularization, cell proliferation and tissue regeneration, and simultaneously limit scar formation, collagen deposition, and formation of multi-layer epithelium (Wang et al., 2022). Liu et al. showed that hyaluronic acid (HA) can be used as immobilizing agent in a constructed system of ASC-Exos with HA, to retain exosomes in the wound area and effectively play a role in wound repair. The system activated wound-based HDF activity and increased re-epithelialization, which was expected to reduce scar formation (Liu et al., 2019). In addition, Wang et al. developed an FHE hydrogel-carrier system with stimulus-responsive ASC-Exos, which significantly increased the regeneration of skin appendages and reduced scar tissue formation (Wang et al., 2019). Hector et al. also identified three types of ECM-based biomaterials—Integra™ Matrix Wound Dressing, XenoMEM™, and MatriStem™—that serve as human ASC delivery vehicles, which could inhibit scar formation (Capella-Monsonís et al., 2020).

CONCLUSION AND FUTURE DIRECTION

ASCs have the advantages of being derived from a large source, offering abundant availability and high proliferative ability, having low immunogenicity in clinical applications, and being safer and more effective. ASCs histologically promote the regeneration of healthy tissue, reduce fibroblasts, and reconstruct collagen, similar to that of normal skin. At the molecular level, ASCs reduce hypertrophic scarring through direct differentiation and paracrine mechanisms. Clinically, they can improve the color, elasticity, texture, thickness, and size of hypertrophic scars. ASCs have a positive effect on alleviating hypertrophic scarring, indicating their potential as a possible treatment approach in this condition, with broad therapeutic prospect.

AUTHOR CONTRIBUTIONS

All authors contributed to the design of the study and writing of the manuscript. KH and HC undertook the research, YW and HC wrote the main manuscript text and prepared figures. ZL revised the article critically for important intellectual content and final approval of the version to be submitted. All authors reviewed the manuscript.

REFERENCES

Aoki, M., Matsumoto, N. M., Dohi, T., Kuwahawa, H., Akaishi, S., Okubo, Y., et al. (2020). Direct Delivery of Apatite Nanoparticle-Encapsulated siRNA Targeting TIMP-1 for Intractable Abnormal Scars. *Mol. Ther. - Nucleic Acids* 22, 50–61. doi:10.1016/j.omtn.2020.08.005

Balci, D. D., Inandi, T., Dogramaci, C. A., and Celik, E. (2009). DLQI Scores in Patients with Keloids and Hypertrophic Scars: a Prospective Case Control Study. *J. Dtsch Dermatol. Ges* 7 (8), 688–691. doi:10.1111/j.1610-0387.2009.07034.x

Barrera, A. (2003). The Use of Micrografts and Minigrafts in the Aesthetic Reconstruction of the Face and Scalp. *Plast. Reconstr. Surg.* 112 (3), 883–890. doi:10.1097/01.PRS.0000072253.54359.7F

Bataille, V., Lens, M., and Spector, T. D. (2012). The Use of the Twin Model to Investigate the Genetics and Epigenetics of Skin Diseases with Genomic, Transcriptomic and Methylation Data. *J. Eur. Acad. Dermatol. Venereol.* 26 (9), 1067–1073. doi:10.1111/j.1468-3083.2011.04444.x

Beanes, S. R., Dang, C., Soo, C., and Ting, K. (2003). Skin Repair and Scar Formation: the central Role of TGF-β. *Expert Rev. Mol. Med.* 5 (8), 1–22. doi:10.1017/S1462399403005817

Bijlard, E., Kouwenberg, C., Timman, R., Hovius, S., Busschbach, J., and Mureau, M. (2017). Burden of Keloid Disease: A Cross-Sectional Health-Related Quality of Life Assessment. *Acta Derm Venerol* 97 (2), 225–229. doi:10.2340/00015555-2498

Borovikova, A. A., Ziegler, M. E., Banyard, D. A., Wirth, G. A., Paydar, K. Z., Evans, G. R. D., et al. (2018). Adipose-Derived Tissue in the Treatment of Dermal Fibrosis. *Ann. Plast. Surg.* 80 (3), 297–307. doi:10.1097/SAP.0000000000001278

Bougioukli, S., Sugiyama, O., Pannell, W., Ortega, B., Tan, M. H., Tang, A. H., et al. (2018). Gene Therapy for Bone Repair Using Human Cells: Superior Osteogenic Potential of Bone Morphogenetic Protein 2-Transduced Mesenchymal Stem Cells Derived from Adipose Tissue Compared to Bone Marrow. *Hum. Gene Ther.* 29 (4), 507–519. doi:10.1089/hum.2017.097

Buratta, S., Tancini, B., Sagini, K., Delo, F., Chiaradia, E., Urbanelli, L., et al. (2020). Lysosomal Exocytosis, Exosome Release and Secretory Autophagy: The

Autophagic- and Endo-Lysosomal Systems Go Extracellular. *Ijms* 21 (7), 2576. doi:10.3390/ijms21072576

Capella-Monsonís, H., De Pieri, A., Peixoto, R., Korntner, S., and Zeugolis, D. I. (2020). Extracellular Matrix-Based Biomaterials as Adipose-Derived Stem Cell Delivery Vehicles in Wound Healing: a Comparative Study between a Collagen Scaffold and Two Xenografts. *Stem Cel Res Ther* 11 (1), 510. doi:10.1186/s13287-020-02021-x

Chiba, M., Kimura, M., and Asari, S. (2012). Exosomes Secreted from Human Colorectal Cancer Cell Lines Contain mRNAs, microRNAs and Natural Antisense RNAs, that Can Transfer into the Human Hepatoma HepG2 and Lung Cancer A549 Cell Lines. *Oncol. Rep.* 28 (5), 1551–1558. doi:10.3892/or.2012.1967

Coentro, J. Q., Pugliese, E., Hanley, G., Raghunath, M., and Zeugolis, D. I. (2019). Current and Upcoming Therapies to Modulate Skin Scarring and Fibrosis. *Adv. Drug Deliv. Rev.* 146, 37–59. doi:10.1016/j.addr.2018.08.009

De Francesco, F., Busato, A., Mannucci, S., Zingaretti, N., Cottone, G., Amendola, F., et al. (2020). Artificial Dermal Substitutes for Tissue Regeneration: Comparison of the Clinical Outcomes and Histological Findings of Two Templates. *J. Int. Med. Res.* 48 (8), 030006052094550. doi:10.1177/0300060520945508

De Francesco, F., Guastafierro, A., Nicoletti, G., Razzano, S., Riccio, M., and Ferraro, G. (2017). The Selective Centrifugation Ensures a Better *In Vitro* Isolation of ASCs and Restores a Soft Tissue Regeneration *In Vivo*. *Ijms* 18 (5), 1038. doi:10.3390/ijms18051038

Dominici, M., Le Blanc, K., Mueller, I., Slaper-Cortenbach, I., Marini, F. C., Krause, D. S., et al. (2006). Minimal Criteria for Defining Multipotent Mesenchymal Stromal Cells. The International Society for Cellular Therapy Position Statement. *Cytotherapy* 8 (4), 315–317. doi:10.1080/14653240600855905

Dong, X., Mao, S., and Wen, H. (2013). Upregulation of Proinflammatory Genes in Skin Lesions May Be the Cause of Keloid Formation (Review). *Biomed. Rep.* 1 (6), 833–836. doi:10.3892/br.2013.169

Falanga, V. (2005). Wound Healing and its Impairment in the Diabetic Foot. *The Lancet* 366 (9498), 1736–1743. doi:10.1016/S0140-6736(05)67700-8

Feng, J., Xue, S., Pang, Q., Rang, Z., and Cui, F. (2017). miR-141-3p Inhibits Fibroblast Proliferation and Migration by Targeting GAB1 in Keloids. *Biochem. Biophysical Res. Commun.* 490 (2), 302–308. doi:10.1016/j.bbrc.2017.06.040

Fu, S., Panayi, A., Fan, J., Mayer, H. F., Daya, M., Khouri, R. K., et al. (2021). Mechanotransduction in Wound Healing: From the Cellular and Molecular Level to the Clinic. *Adv. Skin Wound Care* 34 (2), 67–74. doi:10.1097/01.ASW.0000725220.92976.a7

Fuller, K. P., Gaspar, D., Delgado, L. M., Pandit, A., and Zeugolis, D. I. (2016). Influence of Porosity and Pore Shape on Structural, Mechanical and Biological Properties of Poly ϵ-caprolactone Electro-Spun Fibrous Scaffolds. *Nanomedicine* 11 (9), 1031–1040. doi:10.2217/nnm.16.21

Gardin, C., Ferroni, L., Bellin, G., Rubini, G., Barosio, S., and Zavan, B. (2018). Therapeutic Potential of Autologous Adipose-Derived Stem Cells for the Treatment of Liver Disease. *Ijms* 19 (12), 4064. doi:10.3390/ijms19124064

Garza, R. M., Paik, K. J., Chung, M. T., Duscher, D., Gurtner, G. C., Longaker, M. T., et al. (2014). Studies in Fat Grafting. *Plast. Reconstr. Surg.* 134 (2), 249–257. doi:10.1097/PRS.0000000000000326

Gentile, P., and Garcovich, S. (2019). Concise Review: Adipose-Derived Stem Cells (ASCs) and Adipocyte-Secreted Exosomal microRNA (A-SE-miR) Modulate Cancer Growth and proMote Wound Repair. *Jcm* 8 (6), 855. doi:10.3390/jcm8060855

Gir, P., Oni, G., Brown, S. A., Mojallal, A., and Rohrich, R. J. (2012). Human Adipose Stem Cells. *Plast. Reconstr. Surg.* 129 (6), 1277–1290. doi:10.1097/PRS.0b013e31824ecae6

Halim, A. S., Emami, A., Salahshourifar, I., and Kannan, T. P. (2012). Keloid Scarring: Understanding the Genetic Basis, Advances, and Prospects. *Arch. Plast. Surg.* 39 (3), 184–189. doi:10.5999/aps.2012.39.3.184

Han, Y., Jia, L., Zheng, Y., and Li, W. (2018). Salivary Exosomes: Emerging Roles in Systemic Disease. *Int. J. Biol. Sci.* 14 (6), 633–643. doi:10.7150/ijbs.25018

Han, Y., Sun, T., Han, Y., Lin, L., Liu, C., Liu, J., et al. (2019). Human Umbilical Cord Mesenchymal Stem Cells Implantation Accelerates Cutaneous Wound Healing in Diabetic Rats via the Wnt Signaling Pathway. *Eur. J. Med. Res.* 24 (1), 10. doi:10.1186/s40001-019-0366-9

Harn, H. I. C., Hsu, C. K., Wang, Y. K., Huang, Y. W., Chiu, W. T., Lin, H. H., et al. (2016). Spatial Distribution of Filament Elasticity Determines the Migratory Behaviors of a Cell. *Cell Adhes. Migration* 10 (4), 368–377. doi:10.1080/19336918.2016.1156825

Harn, H. I. C., Ogawa, R., Hsu, C. K., Hughes, M. W., Tang, M. J., and Chuong, C. M. (2019). The Tension Biology of Wound Healing. *Exp. Dermatol.* 28 (4), 464–471. doi:10.1111/exd.13460

Heng, M. C. Y. (2011). Wound Healing in Adult Skin: Aiming for Perfect Regeneration. *Int. J. Dermatol.* 50 (9), 1058–1066. doi:10.1111/j.1365-4632.2011.04940.x

Hessvik, N. P., Øverbye, A., Brech, A., Torgersen, M. L., Jakobsen, I. S., Sandvig, K., et al. (2016). PIKfyve Inhibition Increases Exosome Release and Induces Secretory Autophagy. *Cell. Mol. Life Sci.* 73 (24), 4717–4737. doi:10.1007/s00018-016-2309-8

Ho Jeong, J. (2010). Adipose Stem Cells and Skin Repair. *Cscr* 5 (2), 137–140. doi:10.2174/157488810791268690

Hsu, C. K., Lin, H. H., Harn, H. I. C., Hughes, M. W., Tang, M. J., and Yang, C. C. (2018). Mechanical Forces in Skin Disorders. *J. Dermatol. Sci.* 90 (3), 232–240. doi:10.1016/j.jdermsci.2018.03.004

Hu, L., Wang, J., Zhou, X., Xiong, Z., Zhao, J., Yu, R., et al. (2016). Exosomes Derived from Human Adipose Mensenchymal Stem Cells Accelerates Cutaneous Wound Healing via Optimizing the Characteristics of Fibroblasts. *Sci. Rep.* 6, 32993. doi:10.1038/srep32993

Huang, C., and Ogawa, R. (2021). Keloidal Pathophysiology: Current Notions. *Scars, Burns & Healing* 7, 205951312098032. doi:10.1177/2059513120980320

Hunasgi, S., Koneru, A., Vanishree, M., and Shamala, R. (2013). Keloid: A Case Report and Review of Pathophysiology and Differences between Keloid and Hypertrophic Scars. *J. Oral Maxillofac. Pathol.* 17 (1), 116–120. doi:10.4103/0973-029X.110701

Jiao, H., Fan, J., Cai, J., Pan, B., Yan, L., Dong, P., et al. (2015). Analysis of Characteristics Similar to Autoimmune Disease in Keloid Patients. *Aesth Plast. Surg.* 39 (5), 818–825. doi:10.1007/s00266-015-0542-4

Jimi, S., Takagi, S., De Francesco, F., Miyazaki, M., and Saparov, A. (2020). Acceleration of Skin Wound-Healing Reactions by Autologous Micrograft Tissue Suspension. *Medicina* 56 (7), 321. doi:10.3390/medicina56070321

Jing, H., He, X., and Zheng, J. (2018). Exosomes and Regenerative Medicine: State of the Art and Perspectives. *Translational Res.* 196, 1–16. doi:10.1016/j.trsl.2018.01.005

Joshi, A., Xu, Z., Ikegami, Y., Yamane, S., Tsurashima, M., and Ijima, H. (2020). Co-culture of Mesenchymal Stem Cells and Human Umbilical Vein Endothelial Cells on Heparinized Polycaprolactone/gelatin Co-spun Nanofibers for Improved Endothelium Remodeling. *Int. J. Biol. Macromolecules* 151, 186–192. doi:10.1016/j.ijbiomac.2020.02.163

Kucharzewski, M., Rojczyk, E., Wilemska-Kucharzewska, K., Wilk, R., Hudecki, J., and Los, M. J. (2019). Novel Trends in Application of Stem Cells in Skin Wound Healing. *Eur. J. Pharmacol.* 843, 307–315. doi:10.1016/j.ejphar.2018.12.012

Kumar, A. S., and Kamalasanan, K. (2021). Drug Delivery to Optimize Angiogenesis Imbalance in Keloid: A Review. *J. Controlled Release* 329, 1066–1076. doi:10.1016/j.jconrel.2020.10.035

Leavitt, T., Hu, M. S., Marshall, C. D., Barnes, L. A., Lorenz, H. P., and Longaker, M. T. (2016). Scarless Wound Healing: Finding the Right Cells and Signals. *Cell Tissue Res* 365 (3), 483–493. doi:10.1007/s00441-016-2424-8

Lee, S. H., Jin, S. Y., Song, J. S., Seo, K. K., and Cho, K. H. (2012). Paracrine Effects of Adipose-Derived Stem Cells on Keratinocytes and Dermal Fibroblasts. *Ann. Dermatol.* 24 (2), 136–143. doi:10.5021/ad.2012.24.2.136

Li, X., Xie, X., Lian, W., Shi, R., Han, S., Zhang, H., et al. (2018). Exosomes from Adipose-Derived Stem Cells Overexpressing Nrf2 Accelerate Cutaneous Wound Healing by Promoting Vascularization in a Diabetic Foot Ulcer Rat Model. *Exp. Mol. Med.* 50 (4), 1–14. doi:10.1038/s12276-018-0058-5

Limandjaja, G. C., Niessen, F. B., Scheper, R. J., and Gibbs, S. (2020). The Keloid Disorder: Heterogeneity, Histopathology, Mechanisms and Models. *Front. Cel Dev. Biol.* 8, 360. doi:10.3389/fcell.2020.00360

Liu, K., Chen, C., Zhang, H., Chen, Y., and Zhou, S. (2019). Adipose Stem Cell-derived Exosomes in Combination with Hyaluronic Acid Accelerate Wound Healing through Enhancing Re-epithelialization and Vascularization. *Br. J. Dermatol.* 181 (4), 854–856. doi:10.1111/bjd.17984

Luan, A., Duscher, D., Whittam, A. J., Paik, K. J., Zielins, E. R., Brett, E. A., et al. (2016). Cell-Assisted Lipotransfer Improves Volume Retention in Irradiated Recipient Sites and Rescues Radiation-Induced Skin Changes. *Stem Cells* 34 (3), 668–673. doi:10.1002/stem.2256

Mari, W., Alsabri, S. G., Tabal, N., Younes, S., Sherif, A., and Simman, R. (2015). Novel Insights on Understanding of Keloid Scar: Article Review. *J. Am. Coll. Clin. Wound Specialists* 7 (1-3), 1–7. doi:10.1016/j.jccw.2016.10.001

Morikawa, S., Iribar, H., Gutiérrez-Rivera, A., Ezaki, T., and Izeta, A. (2019). Pericytes in Cutaneous Wound Healing. *Adv. Exp. Med. Biol.* 1147, 1–63. doi:10.1007/978-3-030-16908-4_1

Nakashima, M., Chung, S., Takahashi, A., Kamatani, N., Kawaguchi, T., Tsunoda, T., et al. (2010). A Genome-wide Association Study Identifies Four Susceptibility Loci for Keloid in the Japanese Population. *Nat. Genet.* 42 (9), 768–771. doi:10.1038/ng.645

Nicoletti, G., De Francesco, F., Mele, C. M., Cataldo, C., Grella, R., Brongo, S., et al. (2013). Clinical and Histologic Effects from CO2 Laser Treatment of Keloids. *Lasers Med. Sci.* 28 (3), 957–964. doi:10.1007/s10103-012-1178-0

Ogawa, R. (2017). Keloid and Hypertrophic Scars Are the Result of Chronic Inflammation in the Reticular Dermis. *Ijms* 18 (3), 606. doi:10.3390/ijms18030606

Ogawa, R. (2021). The Most Current Algorithms for the Treatment and Prevention of Hypertrophic Scars and Keloids: A 2020 U36pdate of the Algorithms Published 10 Years Ago. *Plast. Reconstr. Surg.* 125, 557–568. doi:10.1097/PRS.0000000000008667

O'Halloran, N., Courtney, D., Kerin, M. J., and Lowery, A. J. (2017). Adipose-Derived Stem Cells in Novel Approaches to Breast Reconstruction: Their Suitability for Tissue Engineering and Oncological Safety. *Breast Cancer(Auckl)* 11, 117822341772677. doi:10.1177/1178223417726777

Putri, K. T., and Prasetyono, T. O. H. (2021). A Critical Review on the Potential Role of Adipose-derived Stem Cells for Future Treatment of Hypertrophic Scars. *J. Cosmet. Dermatol.* doi:10.1111/jocd.14385

Rahimnejad, M., Derakhshanfar, S., and Zhong, W. (2017). Biomaterials and Tissue Engineering for Scar Management in Wound Care. *Burns Trauma* 5, 4. doi:10.1186/s41038-017-0069-9

Ren, S., Chen, J., Duscher, D., Liu, Y., Guo, G., Kang, Y., et al. (2019). Microvesicles from Human Adipose Stem Cells Promote Wound Healing by Optimizing Cellular Functions via AKT and ERK Signaling Pathways. *Stem Cel Res Ther* 10 (1), 47. doi:10.1186/s13287-019-1152-x

Riccio, M., Marchesini, A., Senesi, L., Skrami, E., Gesuita, R., and De Francesco, F. (2019a). Managing Pathologic Scars by Injecting Auto-Cross-Linked Hyaluronic Acid: A Preliminary Prospective Clinical Study. *Aesth Plast. Surg.* 43 (2), 480–489. doi:10.1007/s00266-018-01303-3

Riccio, M., Marchesini, A., Zingaretti, N., Carella, S., Senesi, L., Onesti, M. G., et al. (2019b). A Multicentre Study: The Use of Micrografts in the Reconstruction of Full-Thickness Posttraumatic Skin Defects of the Limbs-A Whole Innovative Concept in Regenerative Surgery. *Stem Cell Int.* 2019, 1–10. doi:10.1155/2019/5043518

Rockwell, W. B., Cohen, I. K., and Ehrlich, H. P. (1989). Keloids and Hypertrophic Scars. *Plast. Reconstr. Surg.* 84 (5), 827–837. doi:10.1097/00006534-198911000-00021

Rodrigues, M., Kosaric, N., Bonham, C. A., and Gurtner, G. C. (2019). Wound Healing: A Cellular Perspective. *Physiol. Rev.* 99 (1), 665–706. doi:10.1152/physrev.00067.2017

Salameh, F., Shumaker, P. R., Goodman, G. J., Spring, L. K., Seago, M., Alam, M., et al. (2021). Energy-based Devices for the Treatment of Acne Scars: 2022 International Consensus Recommendations. *Lasers Surg. Med.* doi:10.1002/lsm.23484

Seifert, O., and Mrowietz, U. (2009). Keloid Scarring: Bench and Bedside. *Arch. Dermatol. Res.* 301 (4), 259–272. doi:10.1007/s00403-009-0952-8

Seo, B. F., and Jung, S. N. (2016). The Immunomodulatory Effects of Mesenchymal Stem Cells in Prevention or Treatment of Excessive Scars. *Stem Cell Int.* 2016, 1–8. doi:10.1155/2016/6937976

Strong, A. L., Burow, M. E., Gimble, J. M., and Bunnell, B. A. (2015). Concise Review: The Obesity Cancer Paradigm: Exploration of the Interactions and Crosstalk with Adipose Stem Cells. *Stem Cells* 33 (2), 318–326. doi:10.1002/stem.1857

Sun, L. M., Wang, K. H., and Lee, Y. C. G. (2014). Keloid Incidence in Asian People and its Comorbidity with Other Fibrosis-Related Diseases: a Nationwide Population-Based Study. *Arch. Dermatol. Res.* 306 (9), 803–808. doi:10.1007/s00403-014-1491-5

Svolacchia, F., De Francesco, F., Trovato, L., Graziano, A., and Ferraro, G. A. (2016). An Innovative Regenerative Treatment of Scars with Dermal Micrografts. *J. Cosmet. Dermatol.* 15 (3), 245–253. doi:10.1111/jocd.12212

Tan, S., Khumalo, N., and Bayat, A. (2019). Understanding Keloid Pathobiology from a Quasi-Neoplastic Perspective: Less of a Scar and More of a Chronic Inflammatory Disease with Cancer-like Tendencies. *Front. Immunol.* 10, 1810. doi:10.3389/fimmu.2019.01810

Tracy, L. E., Minasian, R. A., and Caterson, E. J. (2016). Extracellular Matrix and Dermal Fibroblast Function in the Healing Wound. *Adv. Wound Care* 5 (3), 119–136. doi:10.1089/wound.2014.0561

Tsai, C. H., and Ogawa, R. (2019). Keloid Research: Current Status and Future Directions. *Scars, Burns & Healing* 5, 205951311986865. doi:10.1177/2059513119868659

Tulandi, T., Al-Sannan, B., Akbar, G., Ziegler, C., and Miner, L. (2011). Prospective Study of Intraabdominal Adhesions Among Women of Different Races with or without Keloids. *Am. J. Obstet. Gynecol.* 204 (2), e1–132. doi:10.1016/j.ajog.2010.09.005

Valadi, H., Ekström, K., Bossios, A., Sjöstrand, M., Lee, J. J., and Lötvall, J. O. (2007). Exosome-mediated Transfer of mRNAs and microRNAs Is a Novel Mechanism of Genetic Exchange between Cells. *Nat. Cel Biol* 9 (6), 654–659. doi:10.1038/ncb1596

Wang, C., Wang, M., Xu, T., Zhang, X., Lin, C., Gao, W., et al. (2019). Engineering Bioactive Self-Healing Antibacterial Exosomes Hydrogel for Promoting Chronic Diabetic Wound Healing and Complete Skin Regeneration. *Theranostics* 9 (1), 65–76. doi:10.7150/thno.29766

Wang, L., Cheng, W., Zhu, J., Li, W., Li, D., Yang, X., et al. (2022). Electrospun Nanoyarn and Exosomes of Adipose-Derived Stem Cells for Urethral Regeneration: Evaluations *In Vitro* and *In Vivo*. *Colloids Surf. B: Biointerfaces* 209 (Pt 2), 112218. doi:10.1016/j.colsurfb.2021.112218

Wang, L., Hu, L., Zhou, X., Xiong, Z., Zhang, C., Shehada, H. M. A., et al. (2017). Exosomes Secreted by Human Adipose Mesenchymal Stem Cells Promote Scarless Cutaneous Repair by Regulating Extracellular Matrix Remodelling. *Sci. Rep.* 7 (1), 13321. doi:10.1038/s41598-017-12919-x

Wang, Z. C., Zhao, W. Y., Cao, Y., Liu, Y. Q., Sun, Q., Shi, P., et al. (2020). The Roles of Inflammation in Keloid and Hypertrophic Scars. *Front. Immunol.* 11, 603187. doi:10.3389/fimmu.2020.603187

Watt, F. M., and Fujiwara, H. (2011). Cell-extracellular Matrix Interactions in normal and Diseased Skin. *Cold Spring Harbor Perspect. Biol.* 3 (4)), a005124. doi:10.1101/cshperspect.a005124

Xiong, M., Zhang, Q., Hu, W., Zhao, C., Lv, W., Yi, Y., et al. (2020). Exosomes from Adipose-Derived Stem Cells: The Emerging Roles and Applications in Tissue Regeneration of Plastic and Cosmetic Surgery. *Front. Cel Dev. Biol.* 8, 574223. doi:10.3389/fcell.2020.574223

Xu, M., Fang, S., and Xie, A. (2021). Posttranscriptional Control of PLOD1 in Adipose-Derived Stem Cells Regulates Scar Formation through Altering Macrophage Polarization. *Ann. Transl Med.* 9 (20), 1573. doi:10.21037/atm-21-4978

Yu, Y., Wu, H., Zhang, Q., Ogawa, R., and Fu, S. (2021). Emerging Insights into the Immunological Aspects of Keloids. *J. Dermatol.* 48 (12), 1817–1826. doi:10.1111/1346-8138.16149

Zouboulis, C. C., and Orfanos, C. E. (1990). Cryosurgical Treatment of Hypertrophic Scars and Keloids. *Hautarzt* 41 (12), 683–688.

Conflict of Interest: The authors declare that the research was conducted in the absence of any commercial or financial relationships that could be construed as a potential conflict of interest.

Publisher's Note: All claims expressed in this article are solely those of the authors and do not necessarily represent those of their affiliated organizations, or those of the publisher, the editors and the reviewers. Any product that may be evaluated in this article, or claim that may be made by its manufacturer, is not guaranteed or endorsed by the publisher.

frontiers in Cell and Developmental Biology

REVIEW
published: 11 January 2022
doi: 10.3389/fcell.2021.821652

Adipose Stem Cell-Based Treatments for Wound Healing

Ning Zeng†, *Hongbo Chen*†, *Yiping Wu and Zeming Liu* *

Department of Plastic and Cosmetic Surgery, Tongji Hospital, Tongji Medical College, Huazhong University of Science and Technology, Wuhan, China

Wound healing is one of the most complex physiological regulation mechanisms of the human body. Stem cell technology has had a significant impact on regenerative medicine. Adipose stem cells (ASCs) have many advantages, including their ease of harvesting and high yield, rich content of cell components and cytokines, and strong practicability. They have rapidly become a favored tool in regenerative medicine. Here, we summarize the mechanism and clinical therapeutic potential of ASCs in wound repair.

Keywords: adipose stem cells, wound healing, regenerative medicine, skin regeneration, inflammation

OPEN ACCESS

Edited by:
Guohui Liu,
Huazhong University of Science and Technology, China

Reviewed by:
Ke Jiang,
Sun Yat-sen University Cancer Center (SYSUCC), China
Antonio Casado Díaz,
Centro de Investigación Biomédica en Red sobre Fragilidad y Envejecimiento Saludable (CIBERFES), Spain

***Correspondence:**
Zeming Liu
6myt@163.com

†*These authors have contributed equally to this work*

Specialty section:
This article was submitted to Stem Cell Research, a section of the journal Frontiers in Cell and Developmental Biology

Received: *24 November 2021*
Accepted: *23 December 2021*
Published: *11 January 2022*

Citation:
Zeng N, Chen H, Wu Y and Liu Z (2022) Adipose Stem Cell-Based Treatments for Wound Healing. Front. Cell Dev. Biol. 9:821652. doi: 10.3389/fcell.2021.821652

INTRODUCTION

The skin is the largest organ of the body. It is a key structure that protects internal tissues from mechanical damage, microbial infection, ultraviolet radiation, and extreme temperatures (Falanga, 2005; Ren et al., 2019; Rodrigues et al., 2019; Yang et al., 2020). In the United States, the annual medical cost of adverse wounds, including surgical incisions and scars, is $12 billion (Fife and Carter, 2012; Leavitt et al., 2016). Wound healing is a highly complex physiological regulation mechanism (Rodrigues et al., 2019) and a sophisticated multicellular process involving the coordination of various cell types and cytokines (Ho Jeong, 2010). Interactions involving epidermal and dermal cells, extracellular matrix (ECM), cytokines, and growth factors coordinate the entire repair process, which can be roughly divided into three stages: inflammation, new tissue formation, and reconstruction (Heublein et al., 2015; Rodrigues et al., 2019). The inflammatory stage includes neutrophil and monocyte recruitment and macrophage activation (Park and Barbul, 2004; Larouche et al., 2018). New tissue formation mainly refers to the proliferation, migration, and recombination of endothelial cells to form new blood vessels. When new blood vessels are formed, resident fibroblasts proliferate and invade fibrin clots to form contractile granulation tissue and produce collagen (Heng, 2011; Ansell and Izeta, 2015; Morikawa et al., 2019). This is followed by the proliferation of epidermal stem cells to rebuild the epidermis and stem cells from sebaceous glands, sweat glands, and hair follicles to form epidermal attachments.

Routine Treatment of Wounds

In view of the complex, multi-stage, physiological and pathological processes of acute and chronic skin wound healing, efficient targeted wound healing treatment methods have been studied and applied. Thorough surgical debridement, prevention of infection, and elimination of dead spaces can minimize the risk of poor wound healing. Emerging technologies, such as those based on growth factors, bioactive molecules, and gene modification, can also overcome the limitations of wound healing technology to some extent and serve as personalized therapeutic strategies (Tottoli et al., 2020).

Abbreviations: ASCs, adipose stem cells; ECM, extracellular matrix; IGF, insulin-like growth factor; IL-10, interleukin-10; MVs, microvesicles; PDGF, platelet derived growth factor; SVFs, stromal vascular fragments; TGF-β, transforming growth factor-β.

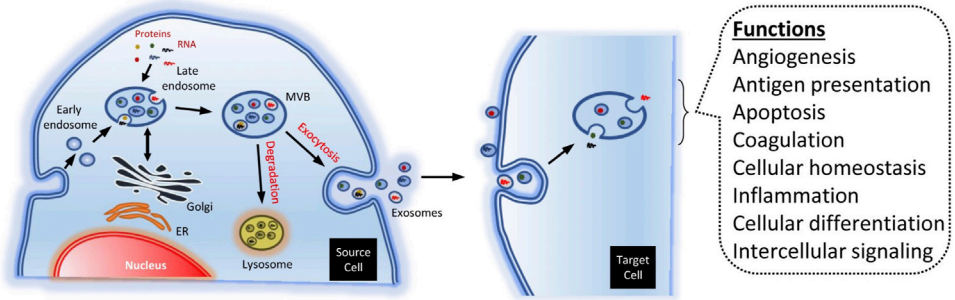

FIGURE 1 | Biogenesis and function of exosomes (Casado-Díaz et al., 2020).

However, despite these efforts, existing interventions for wound healing have not been sufficiently effective. While there are several treatments available for both acute and chronic wounds, traditional approaches have had limited success. Due to the limitations of traditional methods, such as drug-based therapy, more effective treatments are needed. Skin regeneration therapy strategies and experimental techniques for cell and tissue engineering have also emerged. Stem cell-based therapy has opened a new door for wound repair and has attracted extensive attention in the field of regenerative medicine.

Stem Cells

There are thousands of cells undergoing constant daily dynamic changes, such as loss and self-renewal, to maintain tissue homeostasis. Self-renewal is mainly driven by stem cells. Stimulation from regeneration signals, such as the accumulation of crosstalk with niche factors or environmental changes at the time of injury, can disrupt tissue homeostasis, change stem cell behavior, induce self-renewal, and promote tissue growth (Hsu et al., 2011; Cosgrove et al., 2014; Porpiglia et al., 2017). When homeostasis is restored, differentiated progeny can return to their niche, preventing further proliferation and tissue regeneration, and this process is regulated by a careful balance of time-coordinated cell interactions and molecular feedback loops (Fuchs and Blau, 2020).

Stem cells can be divided into embryonic and adult stem cells according to their developmental stage. Embryonic stem cells refer to cells derived from the embryonic inner cell mass or primordial germ cells *in vitro*. Embryonic stem cells have developmental totipotency and can differentiate into any type of cell. Embryonic stem cells can be extensively amplified, screened, frozen, and resuspended *in vitro* without them losing their original characteristics (VanOudenhove et al., 2017; Wang et al., 2019; Sun et al., 2021). Adult stem cells, which are found in various tissues and organs of the body, are undifferentiated cells in a differentiated tissue that can self-renew and differentiate into the specialized cells composing that tissue. These stem cells include hematopoietic stem cells, bone marrow mesenchymal stem cells, neural stem cells, muscle satellite cells, epidermal stem cells, and adipose stem cells (ASCs) (Cinat et al., 2021; Menche and Farin, 2021). In this review, we focus on ASCs.

Sources and Applications of ASCs

Adipose tissue is a multifunctional tissue that contains a variety of cell types, such as the stromal vascular fraction and mature adipose cells. Stromal vascular fragments (SVFs) are a rich source of ASCs that can be easily isolated from human fat (Whiteside, 2008; O'Halloran et al., 2017). The Mesenchymal and Tissue Stem Cell Committee of the International Society for Cellular Therapy (ISCT MSC) proposes minimal criteria to define human MSC follows: First, MSC must be plastic-adherent when maintained in standard culture conditions. Second, MSC must express CD105, CD73 and CD90, and lack expression of CD45, CD34, CD14 or CD11b, CD79alpha or CD19 and HLA-DR surface molecules. Third, MSC must differentiate to osteoblasts, adipocytes and chondroblasts *in vitro*. ASCs conform to most of the mesenchymal criteria of ISCT MSC, defined as $CD45^{-}CD235a^{-}CD31^{-}CD34^{+}$. The phenotype of cultured ASCs is $CD13^{+}CD73^{+}CD90^{+}CD105^{+}CD31^{-}CD45^{-}CD235a^{-}$ (Dominici et al., 2006; Bourin et al., 2013).

ASCs have many advantages. They can be directly extracted from the adipose layer of a patient. Adipose tissue has a high frequency of stem cells, and ASCs can be used immediately with primary cells without the need for culture amplification. In addition, ASCs provide not only cellular components, but also a large number of cytokines. Currently, ASCs have various clinical applications, including in scar reshaping and tissue repair, regeneration, and reconstruction, which are treatments often associated with cancer and metabolic diseases (Brayfield et al., 2010; Gir et al., 2012; Rodrigues et al., 2014; Strong et al., 2015; Clevenger et al., 2016; Gentile and Garcovich, 2019; Sabol et al., 2019; Qin et al., 2020). Skin repair/regeneration is one of the most common clinical applications of ASCs, which has a positive therapeutic effect when used to treat skin wounds in patients with diabetes, vascular dysfunction, radiation history, or burn history.

Mechanism of ASCs in Wound Healing

Factors Secreted by ASCs

The mechanisms of wound healing by ASCs are complex and diverse. ASCs are involved throughout the entire process of wound healing, including inflammation, proliferation, and remodeling (Hyldig et al., 2017). During inflammation, ASCs may induce the transformation of the macrophage phenotype

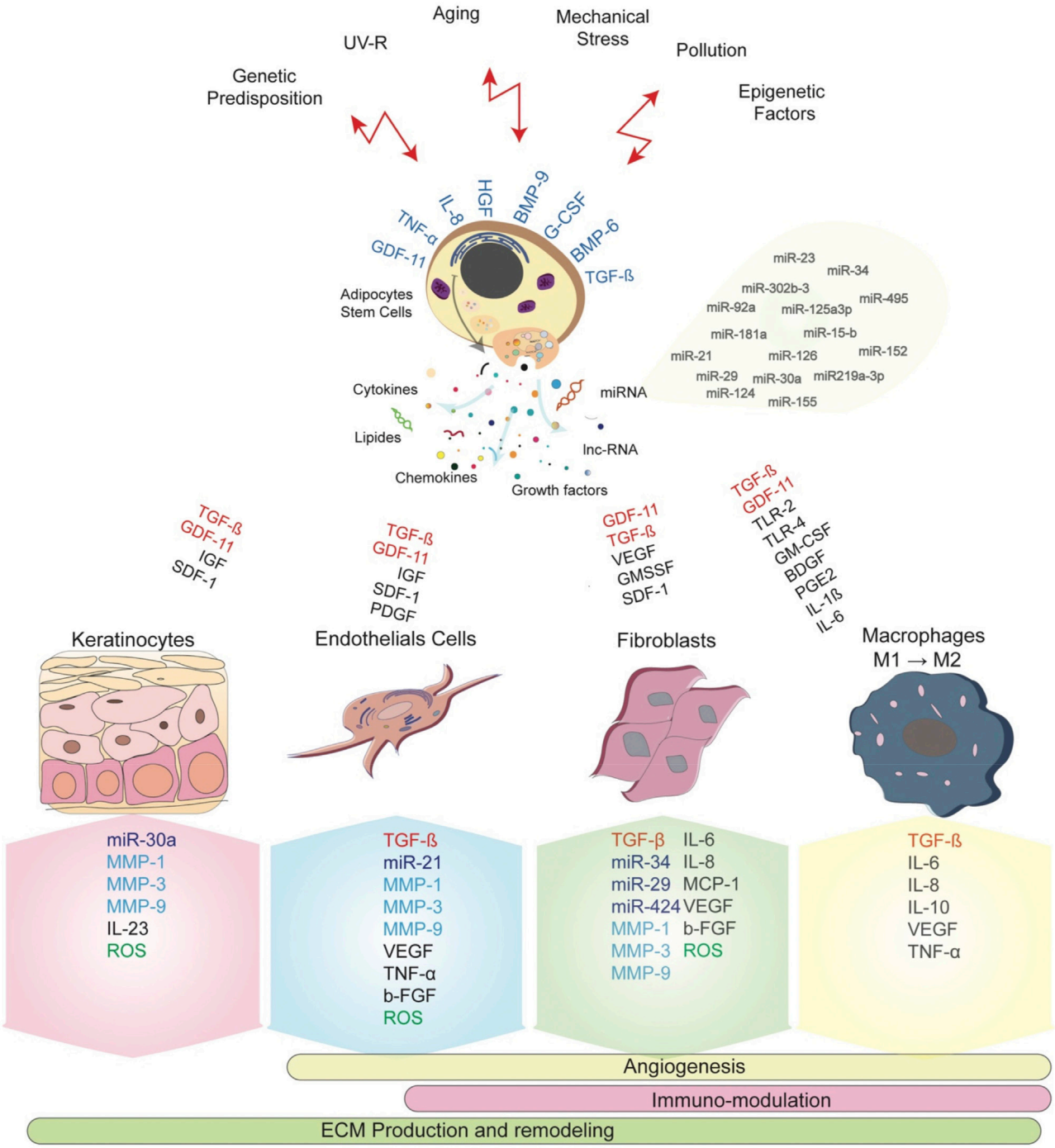

FIGURE 2 | ASCs serve as effective immunomodulators in inflammatory environments to promote wound healing and regeneration (Mazini et al., 2021).

from pro-inflammatory M1 to anti-inflammatory M2 to regulate inflammation (Lo Sicco et al., 2017). During proliferation and remodeling, ASCs secrete biological factors such as VEGF, HGF, IGF, PDGF, and TGF-β, which promote the proliferation and migration of fibroblasts, the growth of new blood vessels, and the synthesis of collagen and other ECM proteins, which have beneficial effects on the skin (Rehman et al., 2004; Ho Jeong, 2010; Rodrigues et al., 2014; Na et al., 2017). For example, radiation damage to the skin can cause progressive occlusive endarteritis in local tissues, leading to severe tissue ischemia. Mesenchymal stem cells can be used to repair cellular damage and regenerate new blood vessels in ischemic tissues in patients with radioactive skin injury (Bensidhoum et al., 2005; François et al., 2006). ASC replacement after radiotherapy may reduce the incidence of radiation-related skin

complications and is used for the prevention and treatment of skin injury related to tumor radiotherapy (Rigotti et al., 2007).

In addition, ASCs inhibit ECM degradation by increasing the binding of matrix metalloproteinases and secreting tissue metalloproteinase inhibitors (Lozito et al., 2014). Proteins in the ECM, in turn, protect against degradation of growth factors and cytokines produced by activated platelets and macrophages, such as PDGF and TGF-β (Barrientos et al., 2008). Finally, *in vitro* studies have confirmed that ASCs may promote re-epithelialization by regulating keratinocyte proliferation and migration (Riis et al., 2017). In summary, ASCs can promote wound healing by reducing inflammation, inducing angiogenesis, promoting the growth of fibroblasts and keratinocytes, and generating ECM.

ASC-Derived Extracellular Vesicles

Recent studies have shown that paracrine factors significantly promote the effect of stem cells during tissue repair and that extracellular vesicles may play an important role. Extracellular vesicles include exosomes and microvesicles, which play an important role in and are considered mediators of intercellular communication (Shao et al., 2018; Théry et al., 2018). The differences between exosomes and microvesicles in terms of physical function are yet to be clarified. Microvesicles are large vesicles (50–1000 nm in diameter) that germinate outward from the plasma membrane, whereas exosomes are small vesicles (50–150 nm in diameter), and their secretion requires the fusion of multiple vesicles with the plasma membrane.

In recent years, there has been extensive research on different types of cells, such as fibroblasts, endothelial progenitor cells, and human umbilical cord mesenchymal stem cells, that are involved in tissue repair by regulating cell function and promoting angiogenesis and wound healing (Zhang et al., 2015a; Li et al., 2016; Geiger et al., 2015; Zhang et al., 2015b). ASC-derived exosomes have also been shown to accelerate wound healing by optimizing fibroblast function (**Figure 1**) (Ren et al., 2019; Casado-Díaz et al., 2020). Studies have found that ASC-derived microvesicles (ASC-MVs) are easily internalized by human umbilical vein endothelial cells (HUVECs), HaCaTs, and fibroblasts, suggesting that ASC-MVs can serve as a suitable vector for delivering a variety of biomolecules and signals to these targeted cells. ASC-MVs can enhance the migration and proliferation of HUVECs, HaCaTs, and fibroblasts through internalization (Zhang et al., 2018; Bi et al., 2019; Ren et al., 2019). Cell cycle progression can be accelerated in a variety of ways, including by increasing the expression of genes related to cyclin D1, cyclin D2, cyclin A1, and cyclin A2, ultimately promoting wound healing (Bretones et al., 2015).

The migration of HUVECs and angiogenesis play an important role in promoting wound healing. ASC-MVs can significantly upregulate the gene expression of integrin β1 and CXCL16 and regulate migration of HUVECs (Hattermann et al., 2008; Tang et al., 2017). ASC-MVs can also accelerate the wound healing process by promoting angiogenesis (Zhang et al., 2018).

ASCs Serve as Effective Immunomodulators in Inflammatory Environments to Promote Wound Healing and Regeneration

Adipose tissue has an immune function because it contains many immune cells and immunomodulatory cells, including ASCs. ASCs regulate mechanisms related to cell differentiation, proliferation, and migration through exosomes by upregulating genes involved in different functions, including skin barrier, immune regulation, cell proliferation, and epidermal regeneration (58). In addition, there are several populations of stromal and immune cells in heterogeneous products obtained after the digestion of adipose tissue, including SVFs. These properties make ASCs effective immune modulators in inflammatory environments (DelaRosa et al., 2012; Gardin et al., 2018; Li and Guo, 2018).

ADSCs directly interact with their microenvironment and specifically the immune cells, including macrophages, NK cell, T cells and B cells, resulting in differential inflammatory and anti-inflammatory effect (**Figure 2**) (Mazini et al., 2021). The immune regulatory function of ASCs is manifested as regulation of the Th1/Th2 balance and promotion of Tregs to restore immune tolerance. ASCs secrete the anti-inflammatory cytokine interleukin-10 (IL-10), which enhances Treg activity, and Tregs respond by further secreting IL-10 and amplifying IL-10 signaling (Chaudhry et al., 2011). Tregs and IL-10 attenuate Th1 and Th17 activity, thereby reducing the aggregation of additional pro-inflammatory immune cells at pathological sites (Skapenko et al., 2005; Chaudhry et al., 2011). Additionally, the low expression of NK-activated receptor ligands increases human ASC resistance to NK-mediated recognition, which enables them to remain in the host for longer period. Furthermore, the mechanism by which human ASCs develop NK cell tolerance may be mediated by soluble factors (Spaggiari et al., 2008; DelaRosa et al., 2012). The role of these anti-inflammatory and immunomodulatory effects of ASCs in wound healing needs to be further confirmed.

DISCUSSION

Although ASCs are fundamental to the tissue regeneration process, the clinical transformation of ASC-based therapies remains problematic. Due to the variation in donor age, sex, body mass index, clinical condition, and cell sampling location, ASCs are heterogeneous. Transplanted cells in severe trauma cases have only a limited ability to survive, which can affect their phenotypic features and functions, including proliferation, differentiation potential, immune phenotype, and paracrine activity (Prieto González, 2019). Therefore, future studies on the role of ASCs in regenerative medicine, especially dermatology, are still needed. Nevertheless, ASCs have promising applications in regenerative medicine, including the development of lipogenic potential and the construction of artificial skin by replacing dermal fibroblasts (Trottier et al., 2008; Tartarini and Mele, 2015), which will be the direction of our future research.

AUTHOR CONTRIBUTIONS

All authors contributed to the design of the study and writing of the manuscript. NZ and HC undertook the research, YW and HC wrote the main manuscript text and prepared figures. ZL revised the article critically for important intellectual content and final approval of the version to be submitted. All authors reviewed the manuscript.

REFERENCES

Ansell, D. M., and Izeta, A. (2015). Pericytes in Wound Healing: Friend or Foe? *Exp. Dermatol.* 24 (11), 833–834. doi:10.1111/exd.12782

Barrientos, S., Stojadinovic, O., Golinko, M. S., Brem, H., and Tomic-Canic, M. (2008). PERSPECTIVE ARTICLE: Growth Factors and Cytokines in Wound Healing. *Wound Repair Regen.* 16 (5), 585–601. doi:10.1111/j.1524-475X.2008.00410.x

Bensidhoum, M., Gobin, S., Chapel, A., Lemaitre, G., Bouet, S., Waksman, G., et al. (2005). Potentiel thérapeutique des cellules souches mésenchymateuses humaines dans les lésions cutanées radioinduites. *J. Soc. Biol.* 199 (4), 337–341. doi:10.1051/jbio:2005035

Bi, H., Li, H., Zhang, C., Mao, Y., Nie, F., Xing, Y., et al. (2019). Stromal Vascular Fraction Promotes Migration of Fibroblasts and Angiogenesis Through Regulation of Extracellular Matrix in the Skin Wound Healing Process. *Stem Cel Res Ther* 10 (1), 302. doi:10.1186/s13287-019-1415-6

Bourin, P., Bunnell, B. A., Casteilla, L., Dominici, M., Katz, A. J., March, K. L., et al. (2013). Stromal Cells from the Adipose Tissue-Derived Stromal Vascular Fraction and Culture Expanded Adipose Tissue-Derived Stromal/stem Cells: A Joint Statement of the International Federation for Adipose Therapeutics and Science (IFATS) and the International Society for Cellular Therapy (ISCT). *Cytotherapy* 15 (6), 641–648. doi:10.1016/j.jcyt.2013.02.006

Brayfield, C., Marra, K., and Rubin, J. P. (2010). Adipose Stem Cells for Soft Tissue Regeneration. *Handchir Mikrochir Plast. Chir* 42 (2), 124–128. doi:10.1055/s-0030-1248269

Bretones, G., Delgado, M. D., and León, J. (2015). Myc and Cell Cycle Control. *Biochim. Biophys. Acta (Bba) - Gene Regul. Mech.* 1849 (5), 506–516. doi:10.1016/j.bbagrm.2014.03.013

Casado-Díaz, A., Quesada-Gómez, J. M., and Dorado, G. (2020). Extracellular Vesicles Derived from Mesenchymal Stem Cells (MSC) in Regenerative Medicine: Applications in Skin Wound Healing. *Front. Bioeng. Biotechnol.* 8, 146. doi:10.3389/fbioe.2020.00146

Chaudhry, A., Samstein, R. M., Treuting, P., Liang, Y., Pils, M. C., Heinrich, J.-M., et al. (2011). Interleukin-10 Signaling in Regulatory T Cells Is Required for Suppression of Th17 Cell-Mediated Inflammation. *Immunity* 34 (4), 566–578. doi:10.1016/j.immuni.2011.03.018

Cinat, D., Coppes, R. P., and Barazzuol, L. (2021). DNA Damage-Induced Inflammatory Microenvironment and Adult Stem Cell Response. *Front. Cel Dev. Biol.* 9, 729136. doi:10.3389/fcell.2021.729136

Clevenger, T. N., Luna, G., Fisher, S. K., and Clegg, D. O. (2016). Strategies for Bioengineered Scaffolds That Support Adipose Stem Cells in Regenerative Therapies. *Regenerative Med.* 11 (6), 589–599. doi:10.2217/rme-2016-0064

Cosgrove, B. D., Gilbert, P. M., Porpiglia, E., Mourkioti, F., Lee, S. P., Corbel, S. Y., et al. (2014). Rejuvenation of the Muscle Stem Cell Population Restores Strength to Injured Aged Muscles. *Nat. Med.* 20 (3), 255–264. doi:10.1038/nm.3464

DelaRosa, O., Sánchez-Correa, B., Morgado, S., Ramírez, C., del Río, B., Menta, R., et al. (2012). Human Adipose-Derived Stem Cells Impair Natural Killer Cell Function and Exhibit Low Susceptibility to Natural Killer-Mediated Lysis. *Stem Cell Dev.* 21 (8), 1333–1343. doi:10.1089/scd.2011.0139

Dominici, M., Le Blanc, K., Mueller, I., Slaper-Cortenbach, I., Marini, F. C., Krause, D. S., et al. (2006). Minimal Criteria for Defining Multipotent Mesenchymal Stromal Cells. The International Society for Cellular Therapy Position Statement. *Cytotherapy* 8 (4), 315–317. doi:10.1080/14653240600855905

Falanga, V. (2005). Wound Healing and its Impairment in the Diabetic Foot. *The Lancet* 366 (9498), 1736–1743. doi:10.1016/S0140-6736(05)67700-8

Fife, C. E., and Carter, M. J. (2012). Wound Care Outcomes and Associated Cost Among Patients Treated in US Outpatient Wound Centers: Data from the US Wound Registry. *Wounds* 24 (1), 10–17.

François, S., Mouiseddine, M., Mathieu, N., Semont, A., Monti, P., Dudoignon, N., et al. (2006). Human Mesenchymal Stem Cells Favour Healing of the Cutaneous Radiation Syndrome in a Xenogenic Transplant Model. *Ann. Hematol.* 86 (1), 1–8. doi:10.1007/s00277-006-0166-5

Fuchs, E., and Blau, H. M. (2020). Tissue Stem Cells: Architects of Their Niches. *Cell Stem Cell* 27 (4), 532–556. doi:10.1016/j.stem.2020.09.011

Gardin, C., Ferroni, L., Bellin, G., Rubini, G., Barosio, S., and Zavan, B. (2018). Therapeutic Potential of Autologous Adipose-Derived Stem Cells for the Treatment of Liver Disease. *Int. J. Mol. Sci.* 19 (12), 4064. doi:10.3390/ijms19124064

Geiger, A., Walker, A., and Nissen, E. (2015). Human Fibrocyte-Derived Exosomes Accelerate Wound Healing in Genetically Diabetic Mice. *Biochem. Biophysical Res. Commun.* 467 (2), 303–309. doi:10.1016/j.bbrc.2015.09.166

Gentile, P., and Garcovich, S. (2019). Concise Review: Adipose-Derived Stem Cells (ASCs) and Adipocyte-Secreted Exosomal microRNA (A-SE-miR) Modulate Cancer Growth and proMote Wound Repair. *J. Clin. Med.* 8 (6), 855. doi:10.3390/jcm8060855

Gir, P., Oni, G., Brown, S. A., Mojallal, A., and Rohrich, R. J. (2012). Human Adipose Stem Cells. *Plast. Reconstr. Surg.* 129 (6), 1277–1290. doi:10.1097/PRS.0b013e31824ecae6

Hattermann, K., Ludwig, A., Gieselmann, V., Held-Feindt, J., and Mentlein, R. (2008). The Chemokine CXCL16 Induces Migration and Invasion of Glial Precursor Cells via its Receptor CXCR6. *Mol. Cell Neurosci.* 39 (1), 133–141. doi:10.1016/j.mcn.2008.03.009

Heng, M. C. Y. (2011). Wound Healing in Adult Skin: Aiming for Perfect Regeneration. *Int. J. Dermatol.* 50 (9), 1058–1066. doi:10.1111/j.1365-4632.2011.04940.x

Heublein, H., Bader, A., and Giri, S. (2015). Preclinical and Clinical Evidence for Stem Cell Therapies as Treatment for Diabetic Wounds. *Drug Discov. Today* 20 (6), 703–717. doi:10.1016/j.drudis.2015.01.005

Ho Jeong, J. (2010). Adipose Stem Cells and Skin Repair. *Curr. Stem Cel Res.* 5 (2), 137–140. doi:10.2174/157488810791268690

Hsu, Y.-C., Pasolli, H. A., and Fuchs, E. (2011). Dynamics Between Stem Cells, Niche, and Progeny in the Hair Follicle. *Cell* 144 (1), 92–105. doi:10.1016/j.cell.2010.11.049

Hyldig, K., Riis, S., Pennisi, C., Zachar, V., and Fink, T. (2017). Implications of Extracellular Matrix Production by Adipose Tissue-Derived Stem Cells for Development of Wound Healing Therapies. *Int. J. Mol. Sci.* 18 (6), 1167. doi:10.3390/ijms18061167

Larouche, J., Sheoran, S., Maruyama, K., and Martino, M. M. (2018). Immune Regulation of Skin Wound Healing: Mechanisms and Novel Therapeutic Targets. *Adv. Wound Care* 7 (7), 209–231. doi:10.1089/wound.2017.0761

Leavitt, T., Hu, M. S., Marshall, C. D., Barnes, L. A., Lorenz, H. P., and Longaker, M. T. (2016). Scarless Wound Healing: Finding the Right Cells and Signals. *Cell Tissue Res* 365 (3), 483–493. doi:10.1007/s00441-016-2424-8

Li, P., and Guo, X. (2018). A Review: Therapeutic Potential of Adipose-Derived Stem Cells in Cutaneous Wound Healing and Regeneration. *Stem Cel Res Ther* 9 (1), 302. doi:10.1186/s13287-018-1044-5

Li, X., Jiang, C., and Zhao, J. (2016). Human Endothelial Progenitor Cells-Derived Exosomes Accelerate Cutaneous Wound Healing in Diabetic Rats by Promoting Endothelial Function. *J. Diabetes its Complications* 30 (6), 986–992. doi:10.1016/j.jdiacomp.2016.05.009

Lo Sicco, C., Reverberi, D., Balbi, C., Ulivi, V., Principi, E., Pascucci, L., et al. (2017). Mesenchymal Stem Cell-Derived Extracellular Vesicles as Mediators of Anti-inflammatory Effects: Endorsement of Macrophage Polarization. *STEM CELLS Translational Med.* 6 (3), 1018–1028. doi:10.1002/sctm.16-0363

Lozito, T. P., Jackson, W. M., Nesti, L. J., and Tuan, R. S. (2014). Human Mesenchymal Stem Cells Generate a Distinct Pericellular Zone of MMP Activities via Binding of MMPs and Secretion of High Levels of TIMPs. *Matrix Biol.* 34, 132–143. doi:10.1016/j.matbio.2013.10.003

Mazini, L., Rochette, L., Hamdan, Y., and Malka, G. (2021). Skin Immunomodulation During Regeneration: Emerging New Targets. *J. Personalized Med.* 11 (2), 85. doi:10.3390/jpm11020085

Menche, C., and Farin, H. F. (2021). Strategies for Genetic Manipulation of Adult Stem Cell-Derived Organoids. *Exp. Mol. Med.* 53 (10), 1483–1494. doi:10.1038/s12276-021-00609-8

Morikawa, S., Iribar, H., Gutiérrez-Rivera, A., Ezaki, T., and Izeta, A. (2019). Pericytes in Cutaneous Wound Healing. *Adv. Exp. Med. Biol.* 1147, 1–63. doi:10.1007/978-3-030-16908-4_1

Na, Y. K., Ban, J.-J., Lee, M., Im, W., and Kim, M. (2017). Wound Healing Potential of Adipose Tissue Stem Cell Extract. *Biochem. Biophysical Res. Commun.* 485 (1), 30–34. doi:10.1016/j.bbrc.2017.01.103

O'Halloran, N., Courtney, D., Kerin, M. J., and Lowery, A. J. (2017). Adipose-Derived Stem Cells in Novel Approaches to Breast Reconstruction: Their Suitability for Tissue Engineering and Oncological Safety. *Breast Cancer (Auckl)* 11, 117822341772677. doi:10.1177/1178223417726777

Park, J. E., and Barbul, A. (2004). Understanding the Role of Immune Regulation in Wound Healing. *Am. J. Surg.* 187 (5A), 11S–16S. doi:10.1016/S0002-9610(03)00296-4

Porpiglia, E., Samusik, N., Ho, A. T. V., Cosgrove, B. D., Mai, T., Davis, K. L., et al. (2017). High-resolution Myogenic Lineage Mapping by Single-Cell Mass Cytometry. *Nat. Cel Biol* 19 (5), 558–567. doi:10.1038/ncb3507

Prieto González, E. A. (2019). Heterogeneity in Adipose Stem Cells. *Adv. Exp. Med. Biol.* 1123, 119–150. doi:10.1007/978-3-030-11096-3_8

Qin, F., Huang, J., Zhang, W., Zhang, M., Li, Z., Si, L., et al. (2020). The Paracrine Effect of Adipose-Derived Stem Cells Orchestrates Competition Between Different Damaged Dermal Fibroblasts to Repair UVB-Induced Skin Aging. *Stem Cell Int.* 2020, 1–19. doi:10.1155/2020/8878370

Rehman, J., Traktuev, D., Li, J., Merfeld-Clauss, S., Temm-Grove, C. J., Bovenkerk, J. E., et al. (2004). Secretion of Angiogenic and Antiapoptotic Factors by Human Adipose Stromal Cells. *Circulation* 109 (10), 1292–1298. doi:10.1161/01.CIR.0000121425.42966.F1

Ren, S., Chen, J., Duscher, D., Liu, Y., Guo, G., Kang, Y., et al. (2019). Microvesicles from Human Adipose Stem Cells Promote Wound Healing by Optimizing Cellular Functions via AKT and ERK Signaling Pathways. *Stem Cel Res Ther* 10 (1), 47. doi:10.1186/s13287-019-1152-x

Rigotti, G., Marchi, A., Gali, M., Baroni, G., Benati, D., Krampera, M., et al. (2007). Clinical Treatment of Radiotherapy Tissue Damage by Lipoaspirate Transplant: A Healing Process Mediated by Adipose-Derived Adult Stem Cells. *Plast. Reconstr. Surg.* 119 (5), 1409–1422. doi:10.1097/01.prs.0000256047.47909.71

Riis, S., Newman, R., Ipek, H., Andersen, J. I., Kuninger, D., Boucher, S., et al. (2017). Hypoxia Enhances the Wound-Healing Potential of Adipose-Derived Stem Cells in a Novel Human Primary Keratinocyte-Based Scratch Assay. *Int. J. Mol. Med.* 39 (3), 587–594. doi:10.3892/ijmm.2017.2886

Rodrigues, C., de Assis, A. M., Moura, D. J., Halmenschlager, G., Saffi, J., Xavier, L. L., et al. (2014). New Therapy of Skin Repair Combining Adipose-Derived Mesenchymal Stem Cells with Sodium Carboxymethylcellulose Scaffold in a Pre-clinical Rat Model. *PLoS One* 9 (5), e96241. doi:10.1371/journal.pone.0096241

Rodrigues, M., Kosaric, N., Bonham, C. A., and Gurtner, G. C. (2019). Wound Healing: A Cellular Perspective. *Physiol. Rev.* 99 (1), 665–706. doi:10.1152/physrev.00067.2017

Sabol, R. A., Giacomelli, P., Beighley, A., and Bunnell, B. A. (2019). Adipose Stem Cells and Cancer: Concise Review. *Stem Cells* 37 (10), 1261–1266. doi:10.1002/stem.3050

Shao, H., Im, H., Castro, C. M., Breakefield, X., Weissleder, R., and Lee, H. (2018). New Technologies for Analysis of Extracellular Vesicles. *Chem. Rev.* 118 (4), 1917–1950. doi:10.1021/acs.chemrev.7b00534

Skapenko, A., Leipe, J., Lipsky, P. E., and Schulze-Koops, H. (2005). The Role of the T Cell in Autoimmune Inflammation. *Arthritis Res. Ther.* 7 (Suppl. 2), S4–S14. doi:10.1186/ar1703

Spaggiari, G. M., Capobianco, A., Abdelrazik, H., Becchetti, F., Mingari, M. C., and Moretta, L. (2008). Mesenchymal Stem Cells Inhibit Natural Killer-Cell Proliferation, Cytotoxicity, and Cytokine Production: Role of Indoleamine 2,3-dioxygenase and Prostaglandin E2. *Blood* 111 (3), 1327–1333. doi:10.1182/blood-2007-02-074997

Strong, A. L., Burow, M. E., Gimble, J. M., and Bunnell, B. A. (2015). Concise Review: The Obesity Cancer Paradigm: Exploration of the Interactions and Crosstalk with Adipose Stem Cells. *Stem Cells* 33 (2), 318–326. doi:10.1002/stem.1857

Sun, L., Fu, X., Ma, G., and Hutchins, A. P. (2021). Chromatin and Epigenetic Rearrangements in Embryonic Stem Cell Fate Transitions. *Front. Cel Dev. Biol.* 9, 637309. doi:10.3389/fcell.2021.637309

Tang, D., Yan, T., Zhang, J., Jiang, X., Zhang, D., and Huang, Y. (2017). Notch1 Signaling Contributes to Hypoxia-Induced High Expression of Integrin β1 in Keratinocyte Migration. *Sci. Rep.* 7, 43926. doi:10.1038/srep43926

Tartarini, D., and Mele, E. (2015). Adult Stem Cell Therapies for Wound Healing: Biomaterials and Computational Models. *Front. Bioeng. Biotechnol.* 3, 206. doi:10.3389/fbioe.2015.00206

Théry, C., Witwer, K. W., Aikawa, E., Alcaraz, M. J., Anderson, J. D., Andriantsitohaina, R., et al. (2018). Minimal Information for Studies of Extracellular Vesicles 2018 (MISEV2018): A Position Statement of the International Society for Extracellular Vesicles and Update of the MISEV2014 Guidelines. *J. Extracell Vesicles* 7 (1), 1535750. doi:10.1080/20013078.2018.1535750

Tottoli, E. M., Dorati, R., Genta, I., Chiesa, E., Pisani, S., and Conti, B. (2020). Skin Wound Healing Process and New Emerging Technologies for Skin Wound Care and Regeneration. *Pharmaceutics* 12 (8), 735. doi:10.3390/pharmaceutics12080735

Trottier, V., Marceau-Fortier, G., Germain, L., Vincent, C., and Fradette, J. (2008). IFATS Collection: Using Human Adipose-Derived Stem/Stromal Cells for the Production of New Skin Substitutes. *Stem Cells* 26 (10), 2713–2723. doi:10.1634/stemcells.2008-0031

VanOudenhove, J. J., Grandy, R. A., Ghule, P. N., Lian, J. B., Stein, J. L., Zaidi, S. K., et al. (2017). Unique Regulatory Mechanisms for the Human Embryonic Stem Cell Cycle. *J. Cel. Physiol.* 232 (6), 1254–1257. doi:10.1002/jcp.25567

Wang, D., Bu, F., and Zhang, W. (2019). The Role of Ubiquitination in Regulating Embryonic Stem Cell Maintenance and Cancer Development. *Int. J. Mol. Sci.* 20 (11), 2667. doi:10.3390/ijms20112667

Whiteside, T. L. (2008). The Tumor Microenvironment and its Role in Promoting Tumor Growth. *Oncogene* 27 (45), 5904–5912. doi:10.1038/onc.2008.271

Yang, S., Gu, Z., Lu, C., Zhang, T., Guo, X., Xue, G., et al. (2020). Neutrophil Extracellular Traps Are Markers of Wound Healing Impairment in Patients with Diabetic Foot Ulcers Treated in a Multidisciplinary Setting. *Adv. Wound Care* 9 (1), 16–27. doi:10.1089/wound.2019.0943

Zhang, B., Wang, M., Gong, A., Zhang, X., Wu, X., Zhu, Y., et al. (2015). HucMSC-Exosome Mediated-Wnt4 Signaling Is Required for Cutaneous Wound Healing. *Stem Cells* 33 (7), 2158–2168. doi:10.1002/stem.1771

Zhang, J., Guan, J., Niu, X., Hu, G., Guo, S., Li, Q., et al. (2015). Exosomes Released from Human Induced Pluripotent Stem Cells-Derived MSCs Facilitate Cutaneous Wound Healing by Promoting Collagen Synthesis and Angiogenesis. *J. Transl Med.* 13, 49. doi:10.1186/s12967-015-0417-0

Zhang, W., Bai, X., Zhao, B., Li, Y., Zhang, Y., Li, Z., et al. (2018). Cell-free Therapy Based on Adipose Tissue Stem Cell-Derived Exosomes Promotes Wound Healing via the PI3K/Akt Signaling Pathway. *Exp. Cel Res.* 370 (2), 333–342. doi:10.1016/j.yexcr.2018.06.035

Conflict of Interest: The authors declare that the research was conducted in the absence of any commercial or financial relationships that could be construed as a potential conflict of interest.

frontiers in Cell and Developmental Biology

MINI REVIEW
published: 07 February 2022
doi: 10.3389/fcell.2022.817877

Role of Lysosomal Acidification Dysfunction in Mesenchymal Stem Cell Senescence

Weijun Zhang[1,2†], *Jinwu Bai*[1,2†], *Kai Hang*[1,2], *Jianxiang Xu*[1,2], *Chengwei Zhou*[1,2], *Lijun Li*[1,2], *Zhongxiang Wang*[1,2], *Yibo Wang*[1,2], *Kanbin Wang*[1,2] *and Deting Xue*[1,2]*

[1]*Department of Orthopaedics, Second Affiliated Hospital, Zhejiang University School of Medicine, Zhejiang University, Hangzhou, China,* [2]*Institute of Orthopaedics, School of Medicine, Zhejiang University, Hangzhou, China*

Mesenchymal stem cell (MSC) transplantation has been widely used as a potential treatment for a variety of diseases. However, the contradiction between the low survival rate of transplanted cells and the beneficial therapeutic effects has affected its clinical use. Lysosomes as organelles at the center of cellular recycling and metabolic signaling, play essential roles in MSC homeostasis. In the first part of this review, we summarize the role of lysosomal acidification dysfunction in MSC senescence. In the second part, we summarize some of the potential strategies targeting lysosomal proteins to enhance the therapeutic effect of MSCs.

Keywords: mesenchymal stem cells, senescence, lysosomal acidification, V-ATPase, pH

OPEN ACCESS

Edited by:
Guohui Liu,
Huazhong University of Science and Technology, China

Reviewed by:
Marisa Brini,
University of Padua, Italy
Tang Liu,
Central South University, China

****Correspondence:***
Deting Xue
blueskine@zju.edu.cn

[†]These authors have contributed equally to this work

Specialty section:
This article was submitted to Stem Cell Research, a section of the journal Frontiers in Cell and Developmental Biology

Received: *18 November 2021*
Accepted: *14 January 2022*
Published: *07 February 2022*

Citation:
Zhang W, Bai J, Hang K, Xu J, Zhou C, Li L, Wang Z, Wang Y, Wang K and Xue D (2022) Role of Lysosomal Acidification Dysfunction in Mesenchymal Stem Cell Senescence. Front. Cell Dev. Biol. 10:817877. doi: 10.3389/fcell.2022.817877

INTRODUCTION

Mesenchymal stem cells (MSCs) are pluripotent stem cells with self-renewal (Pittenger et al., 1999), immunosuppressive (Bartholomew et al., 2002), and anti-inflammatory capabilities (Uccelli et al., 2008). MSCs were first extracted from mouse bone marrow by Friedenstein in 1976 when he referred to them as clonogenic fibroblast precursor cells (CFU-F) (Friedenstein et al., 1976). It was not until 1991 that Caplan first defined these cells as mesenchymal stem cells (MSCs) (Caplan, 1991). In 1995, Lazarus et al. completed the world's first clinical trial of MSCs therapy (Lazarus et al., 1995). As of November 2020, 1,025 clinical trials based on MSC therapies have been registered at FDA. gov (Zhang et al., 2021) (clinicaltrials.gov). However, the therapeutic effects of MSCs given to humans are not as robust as preclinical studies have shown, and most clinical-stage MSC therapies fail to meet the primary efficacy endpoint. To date, only 10 MSC-based products have been approved by regulatory authorities worldwide (Levy et al., 2020).

In vitro aging of stem cells severely affects its therapeutic efficacy. These "*in vitro* aged" cells exhibit abnormal morphology, skewed differentiation potential, diminished expression of surface markers, downward migration and antioxidant capacity (Wagner et al., 2008; Geissler et al., 2012; Lunyak et al., 2017; Yang et al., 2018). Diminished autophagic activity and lysosomal function play an important role in these age-related manifestations (Cuervo et al., 2005). With recent advances in the understanding of lysosomal function, new opportunities for treatment by specifically targeting lysosomes are beginning to emerge (Bonam et al., 2019). Lysosomes degrade intracellular pathogens, as well as damaged organelles and proteins, through the autophagic pathway. Lysosomes must be able to respond rapidly with enhanced or diminished function to a variety of metabolic conditions (Ballabio and Bonifacino, 2020). Therefore, depending on the disease context, activation, or inhibition of different components of the lysosome may represent potential pharmacological strategies.

Regulation of lysosomal acidification is an emerging direction in MSCs-based therapy (Ruckenstuhl et al., 2014). Therapeutic strategies targeting lysosomes in autoimmune disorders and neurodegenerative diseases have been described in great detail by Srinivasa Reddy Bonam et al. (Bonam et al., 2019). In this paper, we focus on the relationship between lysosomal acidification and senescence. We assemble information from relevant studies to demonstrate the association between lysosomal acidity and the aging process, as well as highlight the most recent research on lysosomal acidification control, in the hopes of providing some insight into the entire MSC aging process.

MECHANISM OF LYSOSOMAL ACIDIFICATION

Lysosome was first discovered in the 1950s by Christian de Duve et al. (De Duve et al., 1955). It is a membrane-bound vesicle containing more than 60 hydrolytic enzymes that break down proteins, lipids, nucleic acids, and polysaccharides. In addition to degradation, lysosomes are involved in many other cellular processes, including nutrient sensing (Shin and Zoncu, 2020), metabolic signaling (Sancak et al., 2010), chromatin processing (Ivanov et al., 2013), and plasma membrane repair (Morgan et al., 2011). Each of these behaviors is influenced by the internal pH of the lysosome, which is maintained in the 4.5–5 pH range by the vacuolar H^+-ATPases (V-ATPases) and the counterion transporter, which can be either a cation (moving out of the lysosome) or an anion (moving into the lysosome) (Steinberg et al., 2010; Mindell, 2012).

Vacuolar H^+-ATPases are ATP-driven pH-regulated proton pumps. V-ATPase was first found in the vesicles of microsomal membrane fractions of maize coleoptiles in 1980 by A Hager et al. (Hager et al., 1980). S Ohkuma et al. first identified v-ATPase on mammalian cell lysosomes in 1982 (Ohkuma et al., 1982). V-ATPase consists of two functional domains, V0 embedded in the lysosome membrane, responsible for proton translocation, and V1 in the cytoplasm, responsible for ATP hydrolysis. Membrane-bound V0 consists of six subunits (a, c, c', c'', d, e) and intracellular V1 consists of eight subunits (A, B, C, D, E, F, G, H), several of these subunits are present in multiple copies. Subunit a of V0 accepts and expels protons with the help of a central proteolipid ring consisting of the c, c', and c'' subunits. Subunits A, B, and D of V1 form a catalytic core that is involved in the binding and hydrolysis of ATP, while the other subunits play structural and regulatory roles. ATP-driven V1V0 proton transport maintains organelle, cellular and extracellular pH homeostasis (**Figure 1**). Recently, overexpression of v-ATPase components has been reported to increase lifespan (Hughes and Gottschling, 2012; Ruckenstuhl et al., 2014). However, these were found experimentally in yeast, and whether this is the case in mammals needs further study.

Lysosomal ion channels and transport proteins play a crucial role in lysosomal homeostasis. Lysosomal function requires the maintenance of intraluminal ion homeostasis and membrane potential $\Delta\Psi$ (defined as $V_{cytosol}—V_{lumen}$) (Bertl et al., 1992). But it is not well known how ionic conductance determines $\Delta\Psi$. Studies have revealed several lysosomal channels/transporters Cl−, H+, Ca2+, and Na+,K+. Among the counterion channels, CIC and TRPML are the most thoroughly studied. Shigekuni Hosogi et al. found that lowering the level of Cl-leads to lysosomal acidification disruption and dysfunctional autophagy (Hosogi et al., 2014). Mihyun Bae et al. stimulated TRPM1 with agonists, resulting in increased calcium efflux, luminal acidification, and a clear increase in sphingomyelin and Aβ in lysosomes (Bae et al., 2014). Chunlei Cang et al. identified the K+ channel protein TMEM175 on the lysosome, and the stabilization of K+ helps maintain the pH stability of the lysosome during cell starvation (Cang et al., 2015).

Lysosomal biogenesis is mainly regulated by TFEB (Sardiello et al., 2009; Settembre et al., 2011). Translocation of TFEB from the cytoplasm to the nucleus upregulates v-ATPase and lysosomal gene expression. Because of its physiological importance, V-ATPase is seen as the product of housekeeping genes expressed continuously (Wechser and Bowman, 1995). V-ATPase activity can be regulated in a variety of ways. V-ATPase transcription can be enhanced through TFEB-dependent (Peña-Llopis et al., 2011) and non-TFEB-dependent pathways (Zhu et al., 2017). V-ATPase reversible catabolism and recombination have been reported to be regulated by many factors. The formation of disulfide bonds between cysteine residues at the catalytic site of the V-ATPase is another mechanism proposed for regulating the activity of the V-ATPase *in vivo* (Forgac, 1999). Finally, because V-ATPases are electrogenic, parallel ion conductance must accompany proton transport for significant acidification to occur. The regulation of these ion channels to achieve lysosome acidification represents a very comprehensive method that has not been studied. Lysosomal acidification is essential to maintain normal cellular function. Defective lysosomal acidification is a pathophysiological mechanism in a variety of diseases including virus infection (Jouve et al., 2007; Singh et al., 2021), autoimmune disorders (Monteith et al., 2016), neurodegeneration diseases (Lee et al., 2010) and tumor drug resistance (Chauhan et al., 2003). Pathogens avoid phagocytosis by preventing vacuolar acidification (Pujol et al., 2009). Recently, lysosome pH elevation has been found in and MSCs (Wang et al., 2014; Wang et al., 2018a), Lihong Wang and Fang-Wu Wang et al. use acridine orange and Lysosensor™ Green DND-189 to identify the lysosome acidity and activity. Under a confocal laser scanning microscope, they both down-regulated in senescent MSCs.

ROLE OF LYSOSOMAL ACIDIFICATION DYSFUNCTION IN CELLULAR SENESCENCE

The proliferative potential of bone marrow MSCs cultured *in vitro* is very limited (Stenderup, 2003), and the presence of aging stem cells severely limits their clinical therapeutic effects. The causes of aging are very complicated, and many studies are still at the hypothetical stage. They include genetic determination theory (Larsson, 2011), oxidative free radical damage theory

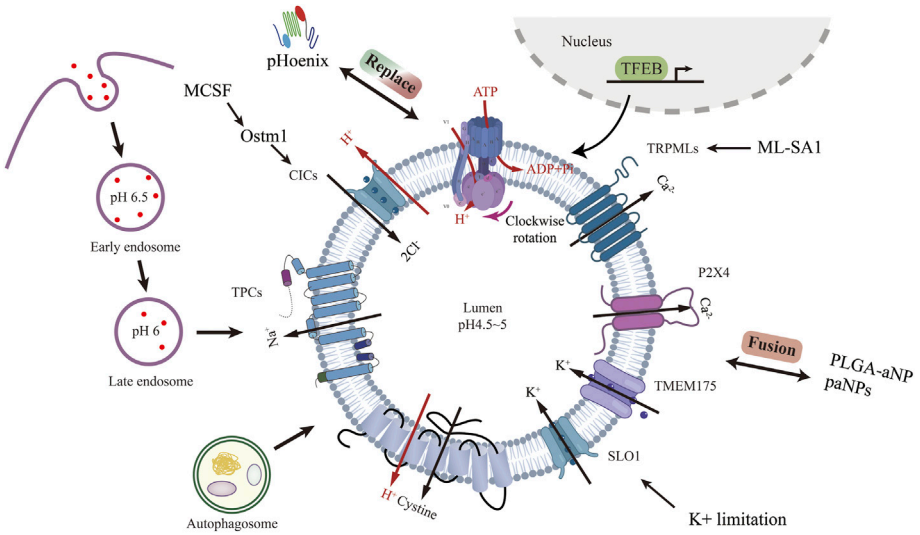

FIGURE 1 | Lysosomal acidification process and regulatory strategies targeting channel proteins other than V-ATPase. Created with BioRender.com.

(Harman, 1956), telomere clock theory (Olovnikov, 1996), metabolic waste accumulation theory (Benveniste et al., 2019), inflamm-aging theory (Franceschi et al., 2000), and so on. In recent years, the relationship between cellular senescence and lysosomal function has received increasing attention (Ansari et al., 2021). Hui Sun et al. found that many lysosomal genes showed differences in aging MSCs (Sun et al., 2021). During aging, lysosomes undergo various modifications that weaken their degradability and increase their susceptibility to metabolic conditions. Impaired lysosomal acidification during cellular senescence is a phenomenon that has been studied and confirmed (Colacurcio and Nixon, 2016). However, whether in turn lysosomal acidification impairment is a determinant of aging remains an open question. Lysosomal acidification disorders have many negative effects on cells, and these effects are highly consistent with the oxidative free radical damage theory of aging and the metabolic waste accumulation theory.

Defective Cellular Clearance and Accumulation of Toxic Proteins

An abnormal increase in lysosomal pH can have a broad impact on lysosomal digestion. Lysosome alkalization inhibits acidic hydrolases and increases the activity of neutral hydrolases. This shift promotes poor digestion and atypical cleavage of the substrate, which may produce toxic digestion products. Impaired substrate clearance is one of the key lysosomal functions that may be affected by acidification defects (Colacurcio and Nixon, 2016). Altered lysosomal pH may also promote lipid oxidation and ROS generation (Yokomakura et al., 2012). Dan L. Li et al. use dihydroethidium (DHE) staining revealed that knocking down the V-ATPase subunit ATP6V0D1 or ATP6V1B2 in neonatal rat ventricular myocytes (NRVMs) increased cellular reactive oxygen species (Li et al., 2016). This further weaken the integrity of lysosomal membranes (Kurz et al., 2008a), increase the release of cathepsins, leading ultimately a "lysosomal pathway of apoptosis" (Guicciardi et al., 2004) or "lysosomal cell death" (Gómez-Sintes et al., 2016) (**Figure 2**). The degree of oxidative stress determines the degree of lysosomal membrane instability (Kurz et al., 2008b). In addition, ROS may promote lysosome membrane permeabilization (LMP) by activating lysosomal Ca2+ channels (Sumoza-Toledo and Penner, 2011) or by altering the activity of lysosomal enzymes such as phospholipase A2 (PLA2). Mild LMP activates apoptotic pathways, while extensive LMP can lead to uncontrollable necrosis (Kågedal et al., 2001). Decreased cellular component turnover and accumulation of abnormal intracellular macromolecules are common features of all aging cells. Lysosome-mediated activation of selective-autophagy actively inhibits cellular senescence through degradation of the senescence regulator GATA4 (Kang and Elledge, 2016). Autophagy includes nucleation, autophagosome formation, and fusion with lysosomes (Ktistakis and Tooze, 2016). Each step can be regulated to enhance the autophagy flux and new evidence suggests that autophagic activity can be enhanced by enhancing lysosomal acidification to delay cellular degeneration (Zhu et al., 2017).

Decreased Mitophagy and ROS Accumulation

During aging, changes in mitochondrial structure and function are evident in most eukaryotes (Seo et al., 2010), but how this occurs is unclear. Adam L. Hughes et al. identified a functional link between lysosome-like vacuoles and mitochondria in *Saccharomyces cerevisiae*, and showed that mitochondrial dysfunction in replicative senescent yeast is caused by altered vesicle PH. Preventing the vacuolar acidity decrease inhibits mitochondrial dysfunction and extends lifespan (Hughes and Gottschling, 2012). In addition, Mikako Yagi et al. found that HIF1α-Nmnat3-mediated NAD (+) levels affected by

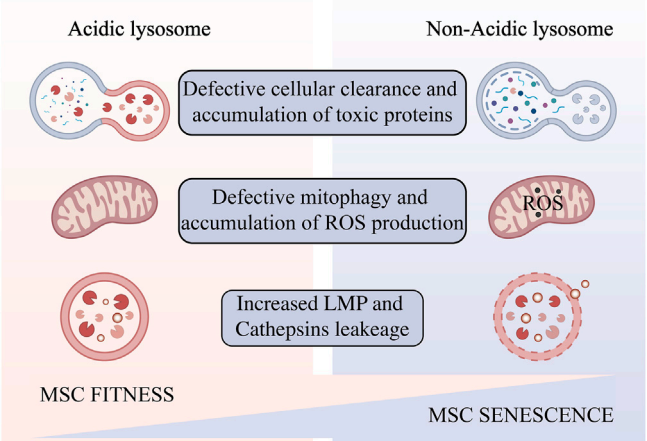

FIGURE 2 | Impaired lysosomal acidification occurs in aging MSCs amplified *in vitro*. Lysosomal alkalinization leads to reduced autophagic flux and accumulation of toxic products, resulting in oxidative stress and increased lysosomal permeability, and ultimately cell senescence and death. Created with BioRender.com.

mitochondrial dysfunction are essential for lysosomal maintenance (Yagi et al., 2021). Mitochondrial ROS production damages lysosomes (Demers-Lamarche et al., 2016). King Faisal Yambire et al. showed that inhibition of lysosomal acidification triggers cellular iron deficiency, which leads to impaired mitochondrial function and cell death (Yambire, 2019). Interplay between lysosome and mitochondrial play an important role in cellular senescence in multiple ways.

PREVENTING LYSOSOMAL ACIDIFICATION DYSFUNCTION AND SENESCENCE IN MSCS

Pretreatment of MSCs with hypoxia (Lan et al., 2015; Martinez et al., 2017; Sivanathan et al., 2017), oxidative stress (Sharma et al., 2008; Pendergrass et al., 2013), heat shock (Wang et al., 2009; Bolhassani et al., 2019), starvation (Moya et al., 2017), or inflammatory biological agents (Klinker et al., 2017; Boland et al., 2018) has been reported to potentially improve their survival and potency. However, less attention has been paid so far to investigate the potential of directly targeting the lysosomes of MSCs with small molecules, peptide drugs, and nanomaterials. Vacuolar H^+-ATPase (v-ATPase) defects are the underlying cause of several human diseases (Haggie and Verkman, 2009; Halcrow et al., 2021). New studies have shown v-ATPase activity is altered, and lysosomal pH regulation is dysregulated during cellular senescence and apoptosis (Nilsson et al., 2006). Regulation of lysosomal acidification is an emerging direction in MSCs-based therapy.

Coupling Efficiency of V-ATPase Pump

Coupling efficiency of the V-ATPase pump is thought to regulate intracellular acidification (Kane, 2006). Interestingly, the assembly of the V0 and V1 structural domains is dependent on the nutrient (Cotter et al., 2015). Amino acid starvation has been shown to promote v-ATPase assembly (Onishi et al., 2019) by inactivating mTORC1 in a TFEB-dependent manner (Peña-Llopis et al., 2011). AKT1, AKT3 isoforms are required to maintain V-ATPase activity in a state of amino acid starvation (Collins et al., 2020). Ju-Hyun Lee et al. showed that presenilin-1 (PS1) knockout impairs the orientation of v-ATPase V0a1 subunit to the lysosome (Lee et al., 2010). Michael C. Jaskolka et al. found that the prokaryotic RAVE and eukaryotic Rabconnectin-3 complexes facilitate the recombination of V1 with V0 during glucose recovery and consequently restore ATP-driven proton transport (Jaskolka et al., 2021). Qing Tang et al. reported the absence of the N-deacetylase and N-sulfotransferase 3 (NDST3) promotes the assembly of the V-ATPase holoenzyme on the lysosomal membrane (Tang et al., 2021). Limor Avrahami et al. found that treatment with a novel substrate competitive GSK-3 inhibitor, L803-mts, restored N-glycosylation of the V-ATPase V0a1 subunit and the impairment caused by dysfunctional presenilin-1 in Alzheimer disease patients (Avrahami and Eldar-Finkelman, 2013; Avrahami et al., 2013). Ju-Hyun Lee et al. reported that isoproterenol (ISO) and related β2-adrenergic agonists re-acidify lysosomes in PSEN1 knockout (KO) cells by restore delivery of vATPaseV0a1 to lysosome (Lee et al., 2020). Youn-Sang Jung et al. found that transmembrane protein 9 (TMEM9), a regulator of vesicle acidification, binds to V-ATPase and promotes its assembly, leading to enhanced vacuolar acidification and trafficking (Jung et al., 2018).

Dan L Li et al. found that Doxorubicin obstructs proton translocation of the V-ATPase V0 domain and impaires lysosomal acidification in cardiomyocytes (Li et al., 2016). Yoshinori Tanaka et al. found that Progranulin (PGRN), a secreted lysosomal protein, promoted lysosomal acidification by enhancing the function of V-ATPase rather than its amount (Tanaka et al., 2017). Limor Avrahami et al. found that inhibition of glycogen synthase kinase-3 (GSK-3) and activation of tuberous sclerosis complex (TSC) promotes lysosomal acidification through the mTORC1/autophagy axis and endocytic trafficking pathways (Avrahami et al., 2020). In contrast, some clinical agents have been found to inhibit lysosomal acidification. Yong Lin et al. shown that GlcN, a dietary supplement widely used to promote joint health and effectively treat osteoarthritis, inhibits the acidification of lysosomes through its amino group (Lin et al., 2020). Modulation of V-ATPase activity is by far the most used method to alter lysosomal acidity (**Figure 3**).

Expression and Amount of V-ATPase Pump

A second method to increase lysosomal acidification is to modulate V-ATPase expression. Simon Wheeler et al. reported that inhibition of non-lysosomal glucocerebrosidase2 (GBA2) increased expression of ATP6V0a1 subunit in Niemann-Pick type C disease (NPCD) fibroblasts (Wheeler et al., 2019). Joo-Yong Jung et al. reported that providing IL-12 and neutralizing IL-27 increases lysosomal acidification by increasing V-ATPase expression (Jung and Robinson, 2014). The use of imatinib and siRNA to inhibit the expression of Abelson (Abl) tyrosine kinase

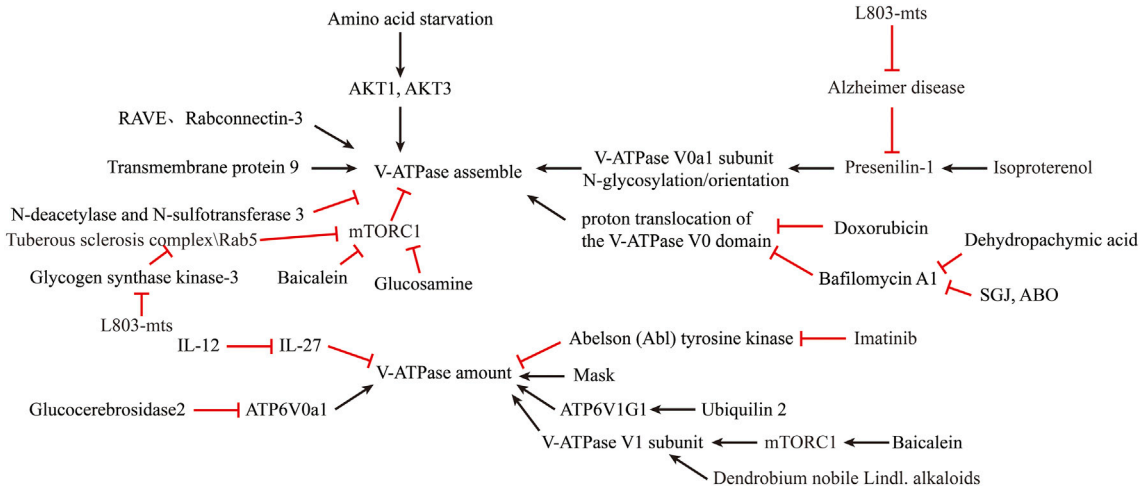

FIGURE 3 | Reversal of lysosomal acidification in *in-vitro* amplified senescent MSCs by regulating V-ATPase activity.

increased the transcription and expression of v-ATPase and decreased the pH of lysosomes in human macrophages (Bruns et al., 2012). Traditional Chinese medicine is an emerging source for exploring new treatments for lysosomal acidification disorders. Xinhong Zhu et al. showed that supplementation with Baicalein increased the expression of V-ATPase V1 subunit and co-localization of V1 subunit in mouse lysosomes via the mTOR pathway (Zhu et al., 2020). Jing Nie et al. found that Dendrobium nobile Lindl. alkaloids (DN LA) could increase the expression of the A1 subunit of v-ATPase to promote lysosomal acidification (Nie et al., 2018). Mengyao Yu et al. found that Dehydropachymic acid (DPA) treatment restored the bafilomycin A1-induced increase in lysosomal pH (Yu et al., 2017). Mingwei Zhu et al. found that Mask, an Ankyrin-repeat and KH-domain containing protein, enhance lysosomal acidification by promoting V-ATPase expression levels in a TFEB-independent manner (Zhu et al., 2017). Josephine J Wu et al. identified UBQLN2 as an important regulator of ATP6V1G1 expression and stability, and overexpression of UBQLN2 increased acidification of autophagosomes (Wu et al., 2020).

Nanomaterials and Artificial Small Molecule Compounds

Nanomaterials and artificial small molecule compounds also have great potential in promoting lysosomal acidification. Most of the nanomaterials taken up by cells are concentrated on lysosomes, making the lysosomal compartment the most common intracellular site for nanoparticle sequestration and degradation (Stern et al., 2012). Lihong Wang et al. invented a novel small molecule, 3-butyl-1-chloro imidazo (Caplan, 1991, Pittenger et al., 1999 pyridine-7-carboxylic acid (SGJ), which can promote lysosomal acidification and inhibit hBMSCs senescence (Wang et al., 2018b). Fang-Wu Wang et al. identified a small molecule compound 6-amino-3,4-dihydro-2H-3-hydroxymethyl-1,4-benzoxazine (ABO), which could promote the expression of Annexin A7 (ANXA7) to counteract the damage of lysosomes by Baf-A1, and inhibit the senescence of MSCs (Wang et al., 2014). Mathieu Bourdenx et al. showed that added poly (DL-lactide-co-glycolide) (PLGA) acidic nanoparticles (aNP) (PLGA-aNP) were transported to the lysosomes in human dopaminergic neuroblastoma BE-M17 cells within 24 h, lowering the lysosomal pH. After PLGA-aNP treatment, defective lysosomes are re-acidified and lysosomal function is restored (Bourdenx et al., 2016). Kyle M Trudeau et al. described a photoactivatable acidified nanoparticle (paNPs) that were taken up by lysosomes in INS1 and mouse β-cells and lysosomal acidity and function was enhanced (Trudeau et al., 2016). Jialiu Zeng et al. reported that biodegradable poly (lactic acid-glycolic acid) (PLGA) nanoparticles (NPs) can be localized to the lysosome to reduce luminal pH and restore autophagic flux in insulin-secreting (INS1) β-cells (Zeng et al., 2019). Benjamin R Ros et al. have proposed a new tool, pHoenix, could functionally replace the endogenous proton pump with the light-driven proton pump Arch3, enabling optogenetic control of lysosomal acidification and neurotransmitter accumulation (Rost et al., 2015).

Other Ion Channels in Lysosome Membrane

In addition to V-ATPase, targeting other channel proteins can also regulate lysosomal acidification. Amitabha Majumdar et al. found that resting microglia expressed only low levels of osteopetrosis-associated transmembrane protein 1 (Ostm1), which impaired lysosomal transport of voltage-gated chloride channel-7 (ClC-7) protein (Lange et al., 2006). Activation of microglia with MCSF increased lysosomal ClC-7 and Ostm1 transcription, leading to increased lysosomal acidification (Majumdar et al., 2011). Anke Di et al. found that the cystic fibrosis transmembrane conductance regulator Cl–channel (CFTR) contributes to lysosomal acidification (Di et al., 2006). Zhiqiang Xia et al. found that ML-SA1, a TRPML agonist, inhibits dengue virus (DENV) and Zika virus (ZIKV) *in vitro* by promoting lysosomal acidification (Xia et al., 2020). Liang Hui

et al. found that TRPML1 agonist ML-SA1 blocked LDL-induced increases in intra-neuronal and secretory levels of Aβ and the accumulation of Aβ in endolysosomes and increase lysosomal acidification (Hui et al., 2019). Huikyong Lee et al. reported that ZnT3/H+/K + -ATPase is another pathway for lysosomal acidification, cAMP activation of PKA increased the overall level and proportion of H+/K + - atpase in lysosomes when v-ATPase is blocked, indicate a potential strategy to overcome this lysosomal dysfunction (Lee and Koh, 2021). Arjun N Sasikumar et al. used a yeast model to show that potassium limitation enhances lysosomal acidity and brings health benefits early in life (Sasikumar et al., 2019).

DISCUSSION

In this review, we summarize the effects of lysosomal acidification disorders that can further cause cellular senescence and summarize existing strategies for controlling lysosomal acidification disorders. During aging, lysosomal acidification becomes impaired and the luminal pH increases. To begin, a rise in luminal pH decreases acidic hydrolase activity while increasing neutral hydrolase activity. This shift causes inefficient substrate degradation and a rise in hazardous metabolites, as well as a decrease in mitophagy and an increase in ROS generation. ROS accumulation further causes LMP and cathepsins leakage, ultimately leads to cellular senescence and apoptosis. In the next place, we summarize current studies that promote lysosomal acidification in the hope of providing some insights into reversing aging of MSCs. Genetic engineering, traditional Chinese medicine, nanomaterials, and small molecule compounds all have potential to be strategies for lysosomal acidification therapy.

However, the current understanding of lysosomes may still be only the tip of the iceberg. Lysosomal membranes contain hundreds of integrins and peripheral proteins, many of which have unknown functions (Ballabio and Bonifacino, 2020). The upregulation of V-ATPase activity and lysosomal acidification can be beneficial in some diseases as well as harmful in others. Activating only the V-ATPase activity in specific cells without affecting others is also a major difficulty in the clinical transformation process. For all these reasons, the study of lysosomes remains a highly specialized field. More research is needed in the future to focus on the translation of lysosomal biology to clinical applications.

AUTHOR CONTRIBUTIONS

WZ and JB contributed equally to this article. WZ and JB collected literature, prepared the manuscript, and drew figures. KH, JX and CZ analyzed the literature and revised the manuscript. LL and ZW revised the manuscript and remade the figures. YW and KW provided ideas and revised the manuscript. DX supervised, managed, and edited the work.

FUNDING

This research was supported by the Joint Funds of the Zhejiang Provincial Natural Science Foundation of China (No. LBY21H060004), the Zhejiang Provincial Natural Science Foundation of China (No. LY18H060003), the National Natural Science Foundation of China (Nos 81871759 and 82172189).

REFERENCES

Ansari, M. Y., Ball, H. C., Wase, S. J., Novak, K., and Haqqi, T. M. (2021). Lysosomal Dysfunction in Osteoarthritis and Aged Cartilage Triggers Apoptosis in Chondrocytes through BAX Mediated Release of Cytochrome C. *Osteoarthritis and Cartilage* 29 (1), 100–112. doi:10.1016/j.joca.2020.08.014

Avrahami, L., and Eldar-Finkelman, H. (2013). GSK-3 and Lysosomes Meet in Alzheimer's Disease. *Communicative Integr. Biol.* 6 (5), e25179. doi:10.4161/cib.25179

Avrahami, L., Farfara, D., Shaham-Kol, M., Vassar, R., Frenkel, D., and Eldar-Finkelman, H. (2013). Inhibition of Glycogen Synthase Kinase-3 Ameliorates β-Amyloid Pathology and Restores Lysosomal Acidification and Mammalian Target of Rapamycin Activity in the Alzheimer Disease Mouse Model. *J. Biol. Chem.* 288 (2), 1295–1306. doi:10.1074/jbc.m112.409250

Avrahami, L., Paz, R., Dominko, K., Hecimovic, S., Bucci, C., and Eldar-Finkelman, H. (2020). GSK-3-TSC axis Governs Lysosomal Acidification through Autophagy and Endocytic Pathways. *Cell Signal.* 71, 109597. doi:10.1016/j.cellsig.2020.109597

Bae, M., Patel, N., Xu, H., Lee, M., Tominaga-Yamanaka, K., Nath, A., et al. (2014). Activation of TRPML1 Clears Intraneuronal A in Preclinical Models of HIV Infection. *J. Neurosci.* 34 (34), 11485–11503. doi:10.1523/jneurosci.0210-14.2014

Ballabio, A., and Bonifacino, J. S. (2020). Lysosomes as Dynamic Regulators of Cell and Organismal Homeostasis. *Nat. Rev. Mol. Cel Biol* 21 (2), 101–118. doi:10.1038/s41580-019-0185-4

Bartholomew, A., Sturgeon, C., Siatskas, M., Ferrer, K., McIntosh, K., Patil, S., et al. (2002). Mesenchymal Stem Cells Suppress Lymphocyte Proliferation *In Vitro* and Prolong Skin Graft Survival *In Vivo*. *Exp. Hematol.* 30 (1), 42–48. doi:10.1016/s0301-472x(01)00769-x

Benveniste, H., Liu, X., Koundal, S., Sanggaard, S., Lee, H., and Wardlaw, J. (2019). The Glymphatic System and Waste Clearance with Brain Aging: A Review. *Gerontology* 65 (2), 106–119. doi:10.1159/000490349

Bertl, A., Blumwald, E., Coronado, R., Eisenberg, R., Findlay, G., Gradmann, D., et al. (1992). Electrical Measurements on Endomembranes. *Science* 258 (5084), 873–874. doi:10.1126/science.1439795

Boland, L., Burand, A. J., Brown, A. J., Boyt, D., Lira, V. A., and Ankrum, J. A. (2018). IFN-γ and TNF-α Pre-licensing Protects Mesenchymal Stromal Cells from the Pro-inflammatory Effects of Palmitate. *Mol. Ther.* 26 (3), 860–873. doi:10.1016/j.ymthe.2017.12.013

Bolhassani, A., Shahbazi, S., Agi, E., Haghighipour, N., Hadi, A., and Asgari, F. (2019). Modified DCs and MSCs with HPV E7 Antigen and Small Hsps: Which One Is the Most Potent Strategy for Eradication of Tumors? *Mol. Immunol.* 108, 102–110. doi:10.1016/j.molimm.2019.02.016

Bonam, S. R., Wang, F., and Muller, S. (2019). Lysosomes as a Therapeutic Target. *Nat. Rev. Drug Discov.* 18 (12), 923–948. doi:10.1038/s41573-019-0036-1

Bourdenx, M., Daniel, J., Genin, E., Soria, F. N., Blanchard-Desce, M., Bezard, E., et al. (2016). Nanoparticles Restore Lysosomal Acidification Defects: Implications for Parkinson and Other Lysosomal-Related Diseases. *Autophagy* 12 (3), 472–483. doi:10.1080/15548627.2015.1136769

Bruns, H., Stegelmann, F., Fabri, M., Döhner, K., van Zandbergen, G., Wagner, M., et al. (2012). Abelson Tyrosine Kinase Controls Phagosomal Acidification

Required for Killing ofMycobacterium Tuberculosisin Human Macrophages. *J.I.* 189 (8), 4069–4078. doi:10.4049/jimmunol.1201538

Cang, C., Aranda, K., Seo, Y.-j., Gasnier, B., and Ren, D. (2015). TMEM175 Is an Organelle K + Channel Regulating Lysosomal Function. *Cell* 162 (5), 1101–1112. doi:10.1016/j.cell.2015.08.002

Caplan, A. I. (1991). Mesenchymal Stem Cells. *J. Orthop. Res.* 9 (5), 641–650. doi:10.1002/jor.1100090504

Chauhan, S. S., Liang, X. J., Su, A. W., Pai-Panandiker, A., Shen, D. W., Hanover, J. A., et al. (2003). Reduced Endocytosis and Altered Lysosome Function in Cisplatin-Resistant Cell Lines. *Br. J. Cancer* 88 (8), 1327–1334. doi:10.1038/sj.bjc.6600861

Colacurcio, D. J., and Nixon, R. A. (2016). Disorders of Lysosomal Acidification-The Emerging Role of V-ATPase in Aging and Neurodegenerative Disease. *Ageing Res. Rev.* 32, 75–88. doi:10.1016/j.arr.2016.05.004

Collins, M. P., Stransky, L. A., and Forgac, M. (2020). AKT Ser/Thr Kinase Increases V-ATPase-dependent Lysosomal Acidification in Response to Amino Acid Starvation in Mammalian Cells. *J. Biol. Chem.* 295 (28), 9433–9444. doi:10.1074/jbc.ra120.013223

Cotter, K., Stransky, L., McGuire, C., and Forgac, M. (2015). Recent Insights into the Structure, Regulation, and Function of the V-ATPases. *Trends Biochem. Sci.* 40 (10), 611–622. doi:10.1016/j.tibs.2015.08.005

Cuervo, A. M., Bergamini, E., Brunk, U. T., Dröge, W., Ffrench, M., and Terman, A. (2005). Autophagy and Aging: The Importance of Maintaining "Clean" Cells. *Autophagy* 1 (3), 131–140. doi:10.4161/auto.1.3.2017

De Duve, C., Pressman, B. C., Gianetto, R., Wattiaux, R., and Appelmans, F. (1955). Tissue Fractionation Studies. 6. Intracellular Distribution Patterns of Enzymes in Rat-Liver Tissue. *Biochem. J.* 60 (4), 604–617. doi:10.1042/bj0600604

Demers-Lamarche, J., Guillebaud, G., Tlili, M., Todkar, K., Bélanger, N., Grondin, M., et al. (2016). Loss of Mitochondrial Function Impairs Lysosomes. *J. Biol. Chem.* 291 (19), 10263–10276. doi:10.1074/jbc.m115.695825

Di, A., Brown, M. E., Deriy, L. V., Li, C., Szeto, F. L., Chen, Y., et al. (2006). CFTR Regulates Phagosome Acidification in Macrophages and Alters Bactericidal Activity. *Nat. Cel Biol* 8 (9), 933–944. doi:10.1038/ncb1456

Forgac, M. (1999). Structure and Properties of the Vacuolar (H+)-ATPases. *J. Biol. Chem.* 274 (19), 12951–12954. doi:10.1074/jbc.274.19.12951

Franceschi, C., Bonafè, M., Valensin, S., Olivieri, F., De Luca, M., Ottaviani, E., et al. (2000). Inflamm-aging. An Evolutionary Perspective on Immunosenescence. *Ann. N. Y Acad. Sci.* 908, 244–254. doi:10.1111/j.1749-6632.2000.tb06651.x

Friedenstein, A. J., Gorskaja, J. F., and Kulagina, N. N. (1976). Fibroblast Precursors in normal and Irradiated Mouse Hematopoietic Organs. *Exp. Hematol.* 4 (5), 267–274.

Geissler, S., Textor, M., Kühnisch, J., Könnig, D., Klein, O., Ode, A., et al. (2012). Functional Comparison of Chronological and *In Vitro* Aging: Differential Role of the Cytoskeleton and Mitochondria in Mesenchymal Stromal Cells. *PLoS One* 7 (12), e52700. doi:10.1371/journal.pone.0052700

Gómez-Sintes, R., Ledesma, M. D., and Boya, P. (2016). Lysosomal Cell Death Mechanisms in Aging. *Ageing Res. Rev.* 32, 150–168. doi:10.1016/j.arr.2016.02.009

Guicciardi, M. E., Leist, M., and Gores, G. J. (2004). Lysosomes in Cell Death. *Oncogene* 23 (16), 2881–2890. doi:10.1038/sj.onc.1207512

Hager, A., Frenzel, R., and Laible, D. (1980). ATP-dependent Proton Transport into Vesicles of Microsomal Membranes of Zea mays Coleoptiles. *Z. Naturforsch C Biosci.* 35 (9-10), 783–793. doi:10.1515/znc-1980-9-1021

Haggie, P. M., and Verkman, A. S. (2009). Defective Organellar Acidification as a Cause of Cystic Fibrosis Lung Disease: Reexamination of a Recurring Hypothesis. *Am. J. Physiology-Lung Cell Mol. Physiol.* 296 (6), L859–L867. doi:10.1152/ajplung.00018.2009

Halcrow, P. W., Lakpa, K. L., Khan, N., Afghah, Z., Miller, N., Datta, G., et al. (2021). HIV-1 Gp120-Induced Endolysosome De-acidification Leads to Efflux of Endolysosome Iron, and Increases in Mitochondrial Iron and Reactive Oxygen Species. *J. Neuroimmune Pharmacol.* doi:10.1007/s11481-021-09995-2

Harman, D. (1956). Aging: a Theory Based on Free Radical and Radiation Chemistry. *J. Gerontol.* 11 (3), 298–300. doi:10.1093/geronj/11.3.298

Hosogi, S., Kusuzaki, K., Inui, T., Wang, X., and Marunaka, Y. (2014). Cytosolic Chloride Ion Is a Key Factor in Lysosomal Acidification and Function of Autophagy in Human Gastric Cancer Cell. *J. Cel. Mol. Med.* 18 (6), 1124–1133. doi:10.1111/jcmm.12257

Hughes, A. L., and Gottschling, D. E. (2012). An Early Age Increase in Vacuolar pH Limits Mitochondrial Function and Lifespan in Yeast. *Nature* 492 (7428), 261–265. doi:10.1038/nature11654

Hui, L., Soliman, M. L., Geiger, N. H., Miller, N. M., Afghah, Z., Lakpa, K. L., et al. (2019). Acidifying Endolysosomes Prevented Low-Density Lipoprotein-Induced Amyloidogenesis. *Jad* 67 (1), 393–410. doi:10.3233/jad-180941

Ivanov, A., Pawlikowski, J., Manoharan, I., van Tuyn, J., Nelson, D. M., Rai, T. S., et al. (2013). Lysosome-mediated Processing of Chromatin in Senescence. *J. Cel Biol.* 202 (1), 129–143. doi:10.1083/jcb.201212110

Jaskolka, M. C., Winkley, S. R., and Kane, P. M. (2021). RAVE and Rabconnectin-3 Complexes as Signal Dependent Regulators of Organelle Acidification. *Front. Cel Dev. Biol.* 9, 698190. doi:10.3389/fcell.2021.698190

Jouve, M., Sol-Foulon, N., Watson, S., Schwartz, O., and Benaroch, P. (2007). HIV-1 Buds and Accumulates in "nonacidic" Endosomes of Macrophages. *Cell Host & Microbe* 2 (2), 85–95. doi:10.1016/j.chom.2007.06.011

Jung, J.-Y., and Robinson, C. M. (2014). IL-12 and IL-27 Regulate the Phagolysosomal Pathway in Mycobacteria-Infected Human Macrophages. *Cell Commun. Signaling* 12, 16. doi:10.1186/1478-811x-12-16

Jung, Y.-S., Jun, S., Kim, M. J., Lee, S. H., Suh, H. N., Lien, E. M., et al. (2018). TMEM9 Promotes Intestinal Tumorigenesis through Vacuolar-ATPase-Activated Wnt/β-Catenin Signalling. *Nat. Cel Biol* 20 (12), 1421–1433. doi:10.1038/s41556-018-0219-8

Kågedal, K., Zhao, M., Svensson, I., and Brunk, U. T. (2001). Sphingosine-induced Apoptosis Is Dependent on Lysosomal Proteases. *Biochem. J.* 359 (2), 335–343. doi:10.1042/bj3590335

Kane, P. M. (2006). The where, when, and How of Organelle Acidification by the Yeast Vacuolar H + -ATPase. *Microbiol. Mol. Biol. Rev.* 70 (1), 177–191. doi:10.1128/mmbr.70.1.177-191.2006

Kang, C., and Elledge, S. J. (2016). How Autophagy Both Activates and Inhibits Cellular Senescence. *Autophagy* 12 (5), 898–899. doi:10.1080/15548627.2015.1121361

Klinker, M. W., Marklein, R. A., Lo Surdo, J. L., Wei, C.-H., and Bauer, S. R. (2017). Morphological Features of IFN-γ-Stimulated Mesenchymal Stromal Cells Predict Overall Immunosuppressive Capacity. *Proc. Natl. Acad. Sci. USA* 114 (13), E2598–E2607. doi:10.1073/pnas.1617933114

Ktistakis, N. T., and Tooze, S. A. (2016). Digesting the Expanding Mechanisms of Autophagy. *Trends Cel Biol.* 26 (8), 624–635. doi:10.1016/j.tcb.2016.03.006

Kurz, T., Terman, A., Gustafsson, B., and Brunk, U. T. (2008). Lysosomes and Oxidative Stress in Aging and Apoptosis. *Biochim. Biophys. Acta (Bba) - Gen. Subjects* 1780 (11), 1291–1303. doi:10.1016/j.bbagen.2008.01.009

Kurz, T., Terman, A., Gustafsson, B., and Brunk, U. T. (2008). Lysosomes in Iron Metabolism, Ageing and Apoptosis. *Histochem. Cel Biol* 129 (4), 389–406. doi:10.1007/s00418-008-0394-y

Lan, Y.-W., Choo, K.-B., Chen, C.-M., Hung, T.-H., Chen, Y.-B., Hsieh, C.-H., et al. (2015). Hypoxia-preconditioned Mesenchymal Stem Cells Attenuate Bleomycin-Induced Pulmonary Fibrosis. *Stem Cel Res Ther* 6, 97. doi:10.1186/s13287-015-0081-6

Lange, P. F., Wartosch, L., Jentsch, T. J., and Fuhrmann, J. C. (2006). ClC-7 Requires Ostm1 as a β-subunit to Support Bone Resorption and Lysosomal Function. *Nature* 440 (7081), 220–223. doi:10.1038/nature04535

Larsson, L.-G. (2011). Oncogene- and Tumor Suppressor Gene-Mediated Suppression of Cellular Senescence. *Semin. Cancer Biol.* 21 (6), 367–376. doi:10.1016/j.semcancer.2011.10.005

Lazarus, H. M., Haynesworth, S. E., Gerson, S. L., Rosenthal, N. S., and Caplan, A. I. (1995). *Ex Vivo* expansion and Subsequent Infusion of Human Bone Marrow-Derived Stromal Progenitor Cells (Mesenchymal Progenitor Cells): Implications for Therapeutic Use. *Bone Marrow Transpl.* 16 (4), 557–564.

Lee, H., and Koh, J. Y. (2021). Roles for H +/K + - ATPase and Zinc Transporter 3 in cAMP -mediated Lysosomal Acidification in Bafilomycin A1 -treated Astrocytes. *Glia* 69 (5), 1110–1125. doi:10.1002/glia.23952

Lee, J.-H., Wolfe, D. M., Darji, S., McBrayer, M. K., Colacurcio, D. J., Kumar, A., et al. (2020). β2-adrenergic Agonists Rescue Lysosome Acidification and Function in PSEN1 Deficiency by Reversing Defective ER-To-Lysosome Delivery of ClC-7. *J. Mol. Biol.* 432 (8), 2633–2650. doi:10.1016/j.jmb.2020.02.021

Lee, J.-H., Yu, W. H., Kumar, A., Lee, S., Mohan, P. S., Peterhoff, C. M., et al. (2010). Lysosomal Proteolysis and Autophagy Require Presenilin 1 and Are Disrupted

by Alzheimer-Related PS1 Mutations. *Cell* 141 (7), 1146–1158. doi:10.1016/j.cell.2010.05.008

Levy, O., Kuai, R., Siren, E. M. J., Bhere, D., Milton, Y., Nissar, N., et al. (2020). Shattering Barriers toward Clinically Meaningful MSC Therapies. *Sci. Adv.* 6 (30), eaba6884. doi:10.1126/sciadv.aba6884

Li, D. L., Wang, Z. V., Ding, G., Tan, W., Luo, X., Criollo, A., et al. (2016). Doxorubicin Blocks Cardiomyocyte Autophagic Flux by Inhibiting Lysosome Acidification. *Circulation* 133 (17), 1668–1687. doi:10.1161/circulationaha.115.017443

Lin, Y., Wu, C., Wang, X., Liu, S., Zhao, K., Kemper, T., et al. (2020). Glucosamine Promotes Hepatitis B Virus Replication through its Dual Effects in Suppressing Autophagic Degradation and Inhibiting MTORC1 Signaling. *Autophagy* 16 (3), 548–561. doi:10.1080/15548627.2019.1632104

Lunyak, V. V., Amaro-Ortiz, A., and Gaur, M. (2017). Mesenchymal Stem Cells Secretory Responses: Senescence Messaging Secretome and Immunomodulation Perspective. *Front. Genet.* 8, 220. doi:10.3389/fgene.2017.00220

Majumdar, A., Capetillo-Zarate, E., Cruz, D., Gouras, G. K., and Maxfield, F. R. (2011). Degradation of Alzheimer's Amyloid Fibrils by Microglia Requires Delivery of ClC-7 to Lysosomes. *MBoC* 22 (10), 1664–1676. doi:10.1091/mbc.e10-09-0745

Martinez, V. G., Ontoria-Oviedo, I., Ricardo, C. P., Harding, S. E., Sacedon, R., Varas, A., et al. (2017). Overexpression of Hypoxia-Inducible Factor 1 Alpha Improves Immunomodulation by Dental Mesenchymal Stem Cells. *Stem Cel Res Ther* 8 (1), 208. doi:10.1186/s13287-017-0659-2

Mindell, J. A. (2012). Lysosomal Acidification Mechanisms. *Annu. Rev. Physiol.* 74 (1), 69–86. doi:10.1146/annurev-physiol-012110-142317

Monteith, A. J., Kang, S., Scott, E., Hillman, K., Rajfur, Z., Jacobson, K., et al. (2016). Defects in Lysosomal Maturation Facilitate the Activation of Innate Sensors in Systemic Lupus Erythematosus. *Proc. Natl. Acad. Sci. USA* 113 (15), E2142–E2151. doi:10.1073/pnas.1513943113

Morgan, A. J., Platt, F. M., Lloyd-Evans, E., and Galione, A. (2011). Molecular Mechanisms of Endolysosomal Ca2+ Signalling in Health and Disease. *Biochem. J.* 439 (3), 349–378. doi:10.1042/bj20110949

Moya, A., Larochette, N., Paquet, J., Deschepper, M., Bensidhoum, M., Izzo, V., et al. (2017). Quiescence Preconditioned Human Multipotent Stromal Cells Adopt a Metabolic Profile Favorable for Enhanced Survival under Ischemia. *Stem Cells* 35 (1), 181–196. doi:10.1002/stem.2493

Nie, J., Jiang, L.-S., Zhang, Y., Tian, Y., Li, L.-S., Lu, Y.-L., et al. (2018). Dendrobium Nobile Lindl. Alkaloids Decreases the Level of Intracellular β-Amyloid by Improving Impaired Autolysosomal Proteolysis in APP/PS1 Mice. *Front. Pharmacol.* 9, 1479. doi:10.3389/fphar.2018.01479

Nilsson, C., Johansson, U., Johansson, A.-C., Kågedal, K., and Öllinger, K. (2006). Cytosolic Acidification and Lysosomal Alkalinization during TNF-α Induced Apoptosis in U937 Cells. *Apoptosis* 11 (7), 1149–1159. doi:10.1007/s10495-006-7108-5

Ohkuma, S., Moriyama, Y., and Takano, T. (1982). Identification and Characterization of a Proton Pump on Lysosomes by Fluorescein-Isothiocyanate-Dextran Fluorescence. *Proc. Natl. Acad. Sci.* 79 (9), 2758–2762. doi:10.1073/pnas.79.9.2758

Olovnikov, A. M. (1996). Telomeres, Telomerase, and Aging: Origin of the Theory. *Exp. Gerontol.* 31 (4), 443–448. doi:10.1016/0531-5565(96)00005-8

Onishi, K., Shibutani, S., Goto, N., Maeda, Y., and Iwata, H. (2019). Amino Acid Starvation Accelerates Replication of Ibaraki Virus. *Virus. Res.* 260, 94–101. doi:10.1016/j.virusres.2018.10.008

Peña-Llopis, S., Vega-Rubin-de-Celis, S., Schwartz, J. C., Wolff, N. C., Tran, T. A. T., Zou, L., et al. (2011). Regulation of TFEB and V-ATPases by mTORC1. *EMBO J.* 30 (16), 3242–3258. doi:10.1038/emboj.2011.257

Pendergrass, K. D., Boopathy, A. V., Seshadri, G., Maiellaro-Rafferty, K., Che, P. L., Brown, M. E., et al. (2013). Acute Preconditioning of Cardiac Progenitor Cells with Hydrogen Peroxide Enhances Angiogenic Pathways Following Ischemia-Reperfusion Injury. *Stem Cell Develop.* 22 (17), 2414–2424. doi:10.1089/scd.2012.0673

Pittenger, M. F., Mackay, A. M., Beck, S. C., Jaiswal, R. K., Douglas, R., Mosca, J. D., et al. (1999). Multilineage Potential of Adult Human Mesenchymal Stem Cells. *Science* 284 (5411), 143–147. doi:10.1126/science.284.5411.143

Pujol, C., Klein, K. A., Romanov, G. A., Palmer, L. E., Cirota, C., Zhao, Z., et al. (2009). *Yersinia pestis* Can Reside in Autophagosomes and Avoid Xenophagy in Murine Macrophages by Preventing Vacuole Acidification. *Infect. Immun.* 77 (6), 2251–2261. doi:10.1128/iai.00068-09

Rost, B. R., Schneider, F., Grauel, M. K., Wozny, C., G Bentz, C., Blessing, A., et al. (2015). Optogenetic Acidification of Synaptic Vesicles and Lysosomes. *Nat. Neurosci.* 18 (12), 1845–1852. doi:10.1038/nn.4161

Ruckenstuhl, C., Netzberger, C., Entfellner, I., Carmona-Gutierrez, D., Kickenweiz, T., Stekovic, S., et al. (2014). Lifespan Extension by Methionine Restriction Requires Autophagy-dependent Vacuolar Acidification. *Plos Genet.* 10 (5), e1004347. doi:10.1371/journal.pgen.1004347

Sancak, Y., Bar-Peled, L., Zoncu, R., Markhard, A. L., Nada, S., and Sabatini, D. M. (2010). Ragulator-Rag Complex Targets mTORC1 to the Lysosomal Surface and Is Necessary for its Activation by Amino Acids. *Cell* 141 (2), 290–303. doi:10.1016/j.cell.2010.02.024

Sardiello, M., Palmieri, M., di Ronza, A., Medina, D. L., Valenza, M., Gennarino, V. A., et al. (2009). A Gene Network Regulating Lysosomal Biogenesis and Function. *Science* 325 (5939), 473–477. doi:10.1126/science.1174447

Sasikumar, A. N., Killilea, D. W., Kennedy, B. K., and Brem, R. B. (2019). Potassium Restriction Boosts Vacuolar Acidity and Extends Lifespan in Yeast. *Exp. Gerontol.* 120, 101–106. doi:10.1016/j.exger.2019.02.001

Seo, A. Y., Joseph, A. M., Dutta, D., Hwang, J. C., Aris, J. P., and Leeuwenburgh, C. (2010). New Insights into the Role of Mitochondria in Aging: Mitochondrial Dynamics and More. *J. Cel Sci* 123 (Pt 15), 2533–2542. doi:10.1242/jcs.070490

Settembre, C., Di Malta, C., Polito, V. A., Arencibia, M. G., Vetrini, F., Erdin, S., et al. (2011). TFEB Links Autophagy to Lysosomal Biogenesis. *Science* 332 (6036), 1429–1433. doi:10.1126/science.1204592

Sharma, R. K., Zhou, Q., and Netland, P. A. (2008). Effect of Oxidative Preconditioning on Neural Progenitor Cells. *Brain Res.* 1243, 19–26. doi:10.1016/j.brainres.2008.08.025

Shin, H. R., and Zoncu, R. (2020). The Lysosome at the Intersection of Cellular Growth and Destruction. *Develop. Cel* 54 (2), 226–238. doi:10.1016/j.devcel.2020.06.010

Singh, K., Chen, Y.-C., Hassanzadeh, S., Han, K., Judy, J. T., Seifuddin, F., et al. (2021). Network Analysis and Transcriptome Profiling Identify Autophagic and Mitochondrial Dysfunctions in SARS-CoV-2 Infection. *Front. Genet.* 12, 599261. doi:10.3389/fgene.2021.599261

Sivanathan, K. N., Gronthos, S., Grey, S. T., Rojas-Canales, D., and Coates, P. T. (2017). Immunodepletion and Hypoxia Preconditioning of Mouse Compact Bone Cells as a Novel Protocol to Isolate Highly Immunosuppressive Mesenchymal Stem Cells. *Stem Cell Develop.* 26 (7), 512–527. doi:10.1089/scd.2016.0180

Steinberg, B. E., Huynh, K. K., Brodovitch, A., Jabs, S., Stauber, T., Jentsch, T. J., et al. (2010). A Cation Counterflux Supports Lysosomal Acidification. *J. Cel Biol* 189 (7), 1171–1186. doi:10.1083/jcb.200911083

Stenderup, K. (2003). Aging Is Associated with Decreased Maximal Life Span and Accelerated Senescence of Bone Marrow Stromal Cells,. *Bone* 33 (6), 919–926. doi:10.1016/j.bone.2003.07.005

Stern, S. T., Adiseshaiah, P. P., and Crist, R. M. (2012). Autophagy and Lysosomal Dysfunction as Emerging Mechanisms of Nanomaterial Toxicity. *Part. Fibre Toxicol.* 9 (1), 20. doi:10.1186/1743-8977-9-20

Sumoza-Toledo, A., and Penner, R. (2011). TRPM2: a Multifunctional Ion Channel for Calcium Signalling. *J. Physiol.* 589 (7), 1515–1525. doi:10.1113/jphysiol.2010.201855

Sun, H., Sun, Y., Yu, X., Gao, X., Wang, H., Zhang, L., et al. (2021). Analysis of Age-Related Circular RNA Expression Profiles in Mesenchymal Stem Cells of Rat Bone Marrow. *Front. Genet.* 12, 600632. doi:10.3389/fgene.2021.600632

Tanaka, Y., Suzuki, G., Matsuwaki, T., Hosokawa, M., Serrano, G., Beach, T. G., et al. (2017). Progranulin Regulates Lysosomal Function and Biogenesis through Acidification of Lysosomes. *Hum. Mol. Genet.* 26, 969–988. doi:10.1093/hmg/ddx011

Tang, Q., Liu, M., Liu, Y., Hwang, R.-D., Zhang, T., Wang, J., et al. (2021). NDST3 Deacetylates α-tubulin and Suppresses V-ATPase Assembly and Lysosomal Acidification. *EMBO J.* 40 (19), e107204. doi:10.15252/embj.2020107204

Trudeau, K. M., Colby, A. H., Zeng, J., Las, G., Feng, J. H., Grinstaff, M. W., et al. (2016). Lysosome Acidification by Photoactivated Nanoparticles Restores Autophagy under Lipotoxicity. *J. Cel Biol* 214 (1), 25–34. doi:10.1083/jcb.201511042

Uccelli, A., Moretta, L., and Pistoia, V. (2008). Mesenchymal Stem Cells in Health and Disease. *Nat. Rev. Immunol.* 8 (9), 726–736. doi:10.1038/nri2395

Wagner, W., Horn, P., Castoldi, M., Diehlmann, A., Bork, S., Saffrich, R., et al. (2008). Replicative Senescence of Mesenchymal Stem Cells: a Continuous and Organized Process. *PLoS One* 3 (5), e2213. doi:10.1371/journal.pone.0002213

Wang, F.-W., Zhao, F., Qian, X.-Y., Yu, Z.-Z., Zhao, J., Su, L., et al. (2014). Identification of a Small Molecule Preventing BMSC Senescence *In Vitro* by Improving Intracellular Homeostasis via ANXA7 and Hmbox1. *RSC Adv.* 4 (100), 56722–56730. doi:10.1039/c4ra10404h

Wang, L., Han, X., Qu, G., Su, L., Zhao, B., and Miao, J. (2018). A pH Probe Inhibits Senescence in Mesenchymal Stem Cells. *Stem Cel Res Ther* 9 (1), 343. doi:10.1186/s13287-018-1081-0

Wang, L., Han, X., Qu, G., Su, L., Zhao, B., and Miao, J. (2018). A pH Probe Inhibits Senescence in Mesenchymal Stem Cells. *Stem Cel Res Ther* 9 (1), 343. doi:10.1186/s13287-018-1081-0

Wang, X., Zhao, T., Huang, W., Wang, T., Qian, J., Xu, M., et al. (2009). Hsp20-Engineered Mesenchymal Stem Cells Are Resistant to Oxidative Stress via Enhanced Activation of Akt and Increased Secretion of Growth Factors. *Stem Cells* 27 (12), 3021–3031. doi:10.1002/stem.230

Wechser, M. A., and Bowman, B. J. (1995). Regulation of the Expression of Three Housekeeping Genes Encoding Subunits of the Neurospora Crassa Vacuolar ATPase. *Mol. Gen. Genet.* 249 (3), 317–327. doi:10.1007/bf00290533

Wheeler, S., Haberkant, P., Bhardwaj, M., Tongue, P., Ferraz, M. J., Halter, D., et al. (2019). Cytosolic Glucosylceramide Regulates Endolysosomal Function in Niemann-Pick Type C Disease. *Neurobiol. Dis.* 127, 242–252. doi:10.1016/j.nbd.2019.03.005

Wu, J. J., Cai, A., Greenslade, J. E., Higgins, N. R., Fan, C., Le, N. T. T., et al. (2020). ALS/FTD Mutations in UBQLN2 Impede Autophagy by Reducing Autophagosome Acidification through Loss of Function. *Proc. Natl. Acad. Sci. USA* 117 (26), 15230–15241. doi:10.1073/pnas.1917371117

Xia, Z., Wang, L., Li, S., Tang, W., Sun, F., Wu, Y., et al. (2020). ML-SA1, a Selective TRPML Agonist, Inhibits DENV2 and ZIKV by Promoting Lysosomal Acidification and Protease Activity. *Antiviral Res.* 182, 104922. doi:10.1016/j.antiviral.2020.104922

Yagi, M., Toshima, T., Amamoto, R., Do, Y., Hirai, H., Setoyama, D., et al. (2021). Mitochondrial Translation Deficiency Impairs NAD+ -mediated Lysosomal Acidification. *Embo j* 40 (8), e105268. doi:10.15252/embj.2020105268

Yambire, K. F. (2019). Impaired Lysosomal Acidification Triggers Iron Deficiency and Inflammation *In Vivo*. *Elife* 8. doi:10.7554/elife.51031

Yang, Y.-H. K., Ogando, C. R., Wang See, C., Chang, T.-Y., and Barabino, G. A. (2018). Changes in Phenotype and Differentiation Potential of Human Mesenchymal Stem Cells Aging *In Vitro*. *Stem Cel Res Ther* 9 (1), 131. doi:10.1186/s13287-018-0876-3

Yokomakura, A., Hong, J., Ohuchi, K., Oh, S.-E., Lee, J.-Y., Mano, N., et al. (2012). Increased Production of Reactive Oxygen Species by the Vacuolar-type (H+)-ATPase Inhibitors Bafilomycin A1 and Concanamycin A in RAW 264 Cells. *J. Toxicol. Sci.* 37 (5), 1045–1048. doi:10.2131/jts.37.1045

Yu, M., Xu, X., Jiang, N., Wei, W., Li, F., He, L., et al. (2017). Dehydropachymic Acid Decreases Bafilomycin A1 Induced β-Amyloid Accumulation in PC12 Cells. *J. Ethnopharmacology* 198, 167–173. doi:10.1016/j.jep.2017.01.007

Zeng, J., Shirihai, O. S., and Grinstaff, M. W. (2019). Degradable Nanoparticles Restore Lysosomal pH and Autophagic Flux in Lipotoxic Pancreatic Beta Cells. *Adv. Healthc. Mater.* 8 (12), e1801511. doi:10.1002/adhm.201801511

Zhang, Y., Ravikumar, M., Ling, L., Nurcombe, V., and Cool, S. M. (2021). Age-Related Changes in the Inflammatory Status of Human Mesenchymal Stem Cells: Implications for Cell Therapy. *Stem Cel Rep.* 16 (4), 694–707. doi:10.1016/j.stemcr.2021.01.021

Zhu, M., Zhang, S., Tian, X., and Wu, C. (2017). Mask Mitigates MAPT- and FUS-Induced Degeneration by Enhancing Autophagy through Lysosomal Acidification. *Autophagy* 13 (11), 1924–1938. doi:10.1080/15548627.2017.1362524

Zhu, X., Yao, P., Liu, J., Guo, X., Jiang, C., and Tang, Y. (2020). Baicalein Attenuates Impairment of Hepatic Lysosomal Acidification Induced by High Fat Diet via Maintaining V-ATPase Assembly. *Food Chem. Toxicol.* 136, 110990. doi:10.1016/j.fct.2019.110990

Conflict of Interest: The authors declare that the research was conducted in the absence of any commercial or financial relationships that could be construed as a potential conflict of interest.

Publisher's Note: All claims expressed in this article are solely those of the authors and do not necessarily represent those of their affiliated organizations, or those of the publisher, the editors, and the reviewers. Any product that may be evaluated in this article, or claim that may be made by its manufacturer, is not guaranteed or endorsed by the publisher.

frontiers in Cell and Developmental Biology

BRIEF RESEARCH REPORT
published: 09 February 2022
doi: 10.3389/fcell.2022.830928

Circulating TGF-β Pathway in Osteogenesis Imperfecta Pediatric Patients Subjected to MSCs-Based Cell Therapy

Arantza Infante[1†], *Leire Cabodevilla*[1], *Blanca Gener*[1,2†] *and Clara I. Rodríguez*[1*†]

[1]Stem Cells and Cell Therapy Laboratory, Biocruces Bizkaia Health Research Institute, Cruces University Hospital, Barakaldo, Spain, [2]Service of Genetics, Cruces University Hospital, Barakaldo, Spain

OPEN ACCESS

Edited by:
Guohui Liu,
Huazhong University of Science and Technology, China

Reviewed by:
Cecilia Götherström,
Karolinska Institutet (KI), Sweden
Nikolaos A. Afratis,
National and Kapodistrian University of Athens, Greece

***Correspondence:**
Clara I. Rodríguez
cirodriguez@osakidetza.eus

†ORCID:
Arantza Infante
0000-0002-1625-2865
Blanca Gener
0000-0001-8945-812X
Clara Clara I. Rodríguez
0000-0002-6749-6288

Specialty section:
This article was submitted to Stem Cell Research, a section of the journal Frontiers in Cell and Developmental Biology

Received: 07 December 2021
Accepted: 24 January 2022
Published: 09 February 2022

Citation:
Infante A, Cabodevilla L, Gener B and Rodríguez CI (2022) Circulating TGF-β Pathway in Osteogenesis Imperfecta Pediatric Patients Subjected to MSCs-Based Cell Therapy. Front. Cell Dev. Biol. 10:830928. doi: 10.3389/fcell.2022.830928

Osteogenesis Imperfecta (OI) is a rare genetic disease characterized by bone fragility, with a wide range in the severity of clinical manifestations. The majority of cases are due to mutations in *COL1A1* or *COL1A2*, which encode type I collagen. There is no cure for OI, and real concerns exist for current therapeutic approaches, mainly antiresorptive drugs, regarding their effectiveness and security. Safer and effective therapeutic approaches are demanded. Cell therapy with mesenchymal stem cells (MSCs), osteoprogenitors capable of secreting type I collagen, has been tested to treat pediatric OI with encouraging outcomes. Another therapeutic approach currently under clinical development focuses on the inhibition of TGF-β pathway, based on the excessive TGF-β signaling found in the skeleton of severe OI mice models, and the fact that TGF-β neutralizing antibody treatment rescued bone phenotypes in those OI murine models. An increased serum expression of TGF-β superfamily members has been described for a number of bone pathologies, but still it has not been addressed in OI patients. To delve into this unexplored question, in the present study we investigated serum TGF-β signalling pathway in two OI pediatric patients who participated in TERCELOI, a phase I clinical trial based on reiterative infusions of MSCs. We examined not only the expression and bioactivity of circulating TGF-β pathway in TERCELOI patients, but also the effects that MSCs therapy could elicit. Strikingly, basal serum from the most severe patient showed an enhanced expression of several TGF-β superfamily members and increased TGF-β bioactivity, which were modulated after MSCs therapy.

Keywords: stem cells, cell therapy, TGF-β, osteogenesis imperfecta, mesenchymal stem cells

INTRODUCTION

Osteogenesis Imperfecta (OI), a rare skeletal dysplasia with a high degree of genetic and phenotypic heterogeneity, is characterized by bone fragility, due to low bone mass and abnormalities in bone material properties. Accordingly, OI patients manifest an increased risk of fractures and skeletal deformities with a broad range of clinical severities: mild, moderate, severe and even lethal (Marini et al., 2017). OI is currently considered a collagen-related disorder, caused mainly by autosomal dominant mutations in type I collagen, the main bone extracellular matrix (ECM) protein (approximately 85% of all cases), or by mutations (autosomal dominant or recessive) in genes playing key roles in collagen homeostasis (around 15%) (Jovanovic et al., 2021). OI patients with

TABLE 1 | Characteristics of TERCELOI pediatric patients.

	Gender	Age (years)	OI type	Disease Severity	Affected Gene	Mutation	Molecular consequence
P01	Male	6	III	Severe	*COL1A1*	c.1031G > A	Glycine substitution p.Gly344Asp
P02	Female	8	IV	Moderate	*COL1A2*	c.2133+6T > A	Skipping of exon 35

mutations in *COL1A1* or *COL1A2* genes, who have a mixture of normal and abnormal collagen fibrils, can exhibit a wide range of OI severities, depending on the mutated α-chain and the type and position of the mutation along the triple helix (Marini et al., 2007). Thus, mutations that disrupt the structure of type I collagen (usually glycine substitutions) lead to severe OI, manifested in multiple low-trauma fractures throughout patient's lifetime, short height, long-bone deformities, reduced mobility and chronic pain.

Currently, there is no effective treatment for OI. Since OI bones exhibit an increased bone remodeling, with a higher bone resorption at the expenses of bone formation, inhibitors of bone resorption, mainly bisphosphonates (BPs), are the first-line therapy in pediatric OI (Tauer et al., 2019). However, although BPs increase bone mineral density (BMD) in most OI patients, their efficacy in reducing long bones fractures and pain is controversial. Moreover, the associated adverse events (such as delayed bone healing of osteotomy site) and the safety about long-term use (BPs are retained in bone for extended periods after discontinuation of therapy) are a matter of concern. Hence, the development of new therapeutic strategies exploring novel safer and more effective approaches to address the pathological OI bone phenotypes is an actual and urgent need. In this line, the cell therapy based on MSCs emerged as a possible therapeutic option, with the assumption that MSCs would engraft in host bone and differentiate into osteoblasts, the collagen-producing cells, ameliorating the symptoms associated with OI (Pereira et al., 1995). Thus, MSCs therapy was first addressed by Horwitz and coworkers, who administered allogenic MSCs in immunosuppressed OI pediatric patients (Horwitz et al., 1999; Horwitz et al., 2002). One or two MSCs infusions were demonstrated to be feasible and safe, exerting clinical improvements of OI phenotypes, in spite of being short-lived with transitory beneficial effects, mainly because the expected cell engraftment into bone was utterly low (Horwitz et al., 1999; Horwitz et al., 2002; Götherström et al., 2014). The existence of a paracrine mediation of MSCs was then considered as underlying mechanism responsible for the observed clinical benefits in OI patients (Horwitz et al., 2002; Otsuru et al., 2018; Infante et al., 2021).

In order to overcome the transitory effect of MSCs therapy in OI pediatric patients, we conducted an independent, multi-center cell therapy phase I clinical trial based on reiterative infusions of allogenic MSCs applied to two OI pediatric patients (TERCELOI) (Infante et al., 2021). Moreover, to avoid a possible alloimmunization of non-immunosuppressed patients after repeated exposure to non-self MSCs, the need of human leukocyte antigen (HLA)-identical or histocompatible (5 shared out of six HLA antigens) not affected sibling donor was mandatory to enroll in TERCELOI. In fact, only two domestic patients fulfilled all the restricted inclusion criteria, P01 and P02 (**Table 1**). P01, a 6-year-old boy affected by severe Type III OI, carried a *de novo* heterozygous missense mutation in exon 16 of *COL1A1*, leading to a glycine substitution in the α1(I) chain of type I collagen. P02 (8-year-old girl affected by moderate Type IV OI), carried a *de novo* heterozygous variant in exon 35 of *COL1A2*, leading to the skipping of exon 35, in the α2(I) chain of type I collagen. We demonstrated that the reiterative cell therapy was safe and both patients showed durable improvements regarding the reduction of the number of bone fractures and enhancement in morphometric bone parameters, leading to a better quality of life. In TERCELOI, we also addressed for the first time, the possibility of a paracrine mechanism exerted by MSCs in OI patients' context. Intriguingly, the clinical beneficial effects were especially noticeable in the most severe patient, P01, and after the first MSCs infusion, coupled with the molecular and cellular significances characterized by enhanced serum response in terms of global protein expression and pro-osteogenic capabilities among others (Infante et al., 2021). Moreover, P01, but not P02 basal serum also showed a clear upregulation of several bone-fracture associated miRNAs, which were gradually downregulated during the cell therapy.

Other completely different therapeutic strategy for OI, currently under clinical development, attempts to inhibit the transforming growth factor (TGF-β) signaling, a key pathway for bone homeostasis (MacFarlane et al., 2017). The *rationale* for this approach stands on the excessive TGF-β signaling found in the skeleton of three severe OI mouse models (*Col1a2*$^{+/G61°C}$, *Crtap*$^{-/-}$ and *Col1a1*$^{Jrt/+}$), and the concomitant rescue of the pathological bone phenotypes by using 1D11, a specific anti-TGF-β monoclonal antibody in two of them, *Col1a2*$^{+/G61°C}$, *Crtap*$^{-/-}$ (Grafe et al., 2014; Greene et al., 2021). Interestingly, the inhibition of TGF-β signaling by 1D11 was not effective in *Col1a1*$^{Jrt/+}$ mice (Tauer et al., 2018), suggesting that the different response to anti-TGF-β treatment depends on the severity of the OI mouse model, which in turn, is determined by the mutation type leading to OI. Thus, *Col1a1*$^{Jrt/+}$ mice carry a splice mutation in *Col1a1* leading to an 18-amino acid deletion in the collagen I alpha I chain, exhibiting the most severe phenotype within these three OI mice models (Tauer et al., 2018).

Surprisingly, the knowledge about the status of TGF-β pathway activation in OI patients is quite scarce, although some evidences, such as an increased expression of TGF-β receptors in human OI osteoblasts, point also to an increased TGF-β signaling in OI patients (Gebken et al., 2000). In this line, the pathogenic excessive TGF-β activation in OI could be correlated with increased circulating TGF-β levels, although to the best of our knowledge, this possibility has not been described in OI population. Supporting this assumption, correlations between increased circulating TGF-β levels and other

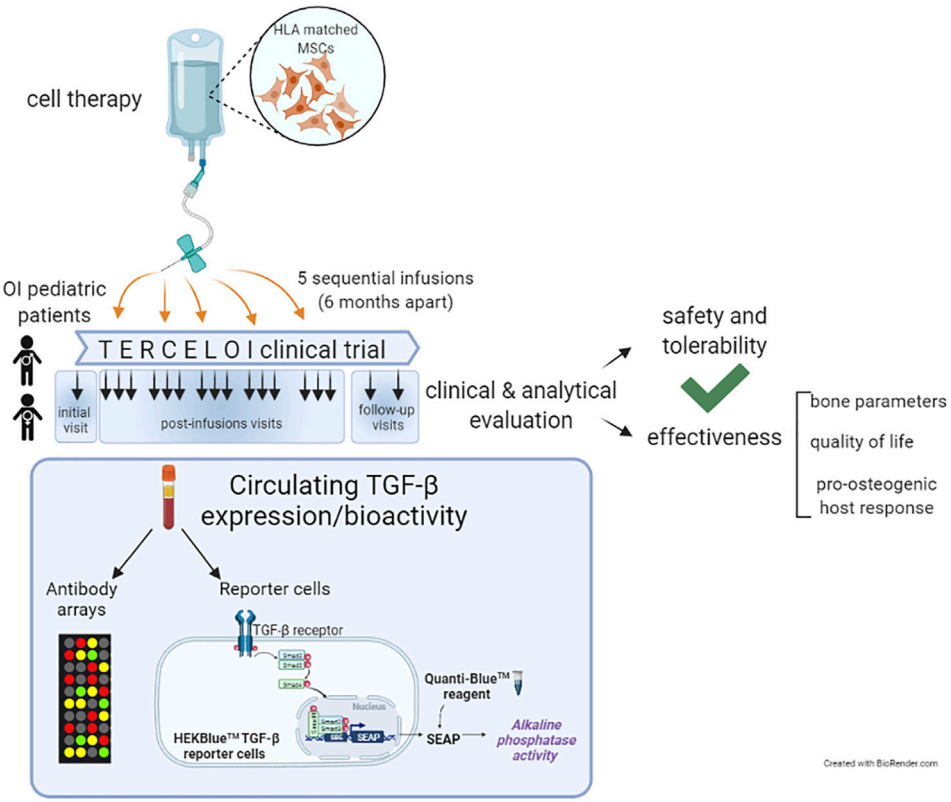

FIGURE 1 | Schematic diagram illustrating TERCELOI clinical trial cellular infusions and the current study of circulating TGF-β expression and bioactivity in patients' sera collected before (basal serum) and after the five consecutive MSCs infusions. The post-infusions sera included those collected 1 week (1w), 1 month (1 m) and 4 months (4 m) after each cell infusion, as well as the follow-up sera, collected 1 year and 2 years after the last cell infusion.

pathologies with causative alterations in ECM components which lead to TGF-β dysregulation have been described, such as in Marfan syndrome, a genetic disease caused by mutations in *FBN1*, encoding fibrillin-1, an ECM protein that binds to latent TGF-β. Thus, mutations in fibrillin-1 leads to an increased pool of active TGF-β and therefore to an enhanced TGF-β signalling (Matt et al., 2009; Franken et al., 2013). Moreover, increased TGF-β circulating levels have also been observed in conditions altering bone homeostasis, such as extensive exercise and bone fractures healing (Hering et al., 2001; Hering et al., 2002; Zimmermann et al., 2005; Sarahrudi et al., 2011). In addition, evidences of a positive correlation between increasing circulating TGF-β levels and a decreased bone mineral density in osteoporosis, a low bone mass disease, have been also described (Grainger et al., 1999; Wu et al., 2013; Faraji et al., 2016).

Considering these previous evidences, in this work we have delved into TERCELOI, exploring the circulating expression levels and functional activity (bioactivity), of TGF-β superfamily in OI patients before and after being subjected to the cell therapy (Infante et al., 2021). For this, we re-analyzed the sera proteomic data obtained in TERCELOI, based on antibody arrays which covered multiple members of the TGF-β superfamily such as structurally related ligands, TGF-β transmembrane receptors, and effectors. In order to elucidate the resultant bioactivity regarding TGF-β signaling, we also examined the ability of OI sera samples in activating TGF-β pathway, by using a TGF-β reporter cell line (**Figure 1**).

To the best of our knowledge, the current study is the first to address the circulating TGF-β pathway in the context of OI patients. Our results, which are indeed supported by the aforementioned molecular and cellular findings obtained from TERCELOI, show an increased expression and activation of TGF-β pathway in the basal serum from the most severe patient. Moreover, in the most severe patient, TGF-β signaling was modulated after MSCs therapy. These results suggest that different circulating TGF-β pathway activation could be occurring depending on OI mutation and its corresponding severity. Even more, MSCs therapy could modulate the enhanced TGF-β bioactivity in the case of the severe patient.

MATERIALS AND METHODS

Ethics Statement

The study was in accordance with the ethical standards formulated in the Helsinki Declaration and was approved by

the Basque Ethics Committee for Clinical Research and the Spanish Agency of Medicines and Medical Devices (AEMPS).

Patients and Sera Samples

TERCELOI is a clinical trial Mesenchymal Stem Cell Therapy for the Treatment of Osteogenesis Imperfecta, registered at clinicaltrials.gov (NCT02172885) and eudract. ema.europa.eu (2012-002553-38). TERCELOI is an independent multi-center phase I clinical trial to evaluate the feasibility, safety and potential efficacy of infused sibling HLA-matched MSCs in non-immunosuppressed children with OI. Due to the highly restrictive eligibility criteria, especially limited by the need of having an HLA-matched unaffected sibling susceptible to donate, only two patients enrolled: P01, male, 6 years 1 month of age affected by severe OI and P02, female, 8 years and 1 month of age with a moderate OI. Patients' characteristics are reported in **Table 1**.

Blood samples were collected in clot activator tubes (BD Vacutainer) and left undisturbed for 40 min at RT to allow the blood to clot. Then, blood samples were centrifuged at 1,300 g at RT during 15 min to remove the clot. The resulting serum supernatant was immediately aliquoted, frozen and stored at-80°C until analysis.

Antibody Arrays

RayBio® biotin label-based (L-Series) Human Antibody Array 1,000 kit (AAH-BLG-1000), including a total of 1,000 soluble proteins, were used to perform sera hybridizations according to the manufacturer's instructions (RayBiotech, United States) and as previously described(Infante et al., 2021). Sera from P01 and P02 collected before the cell therapy (basal serum) and 1 week, 1 month and 4 months after the first MSCs infusion were use. In order to be comparable, each array was processed under the same conditions and signals were scanned using an Axon GenePix laser scanner and data normalized with RayBiotech analysis tool. Fluorescent intensities were obtained by taking the mean of the two spots specific to each target protein, and all protein intensities on each array were normalized against the negative control, representing non-specific binding of the Cy3-conjugated streptavidin, and positive control spots, standardized amounts of biotinylated IgGs printed directly onto the array. Thus, after *subtracting background* signals spot intensities from each array, fluorescent signal intensities were normalized to *positive* controls, allowing the comparison among different arrays.

In this work, after normalization and to ensure the detection of a positive, real binding of target proteins to array antibodies, only the spots with a fluorescent intensity ≥300 above background were considered, as previously described by other studies using the same technology(Wang et al., 2020). To compare the TGF-β superfamily member expression after and before the cell therapy, any ≥1.5-fold increase or ≤0.65-fold decrease in signal intensity for a single protein between samples was considered a significant difference in expression.

TGF-β Reporter Cell Line

The ability of patients' sera to activate the TGF-β pathway was determined using the HEK-Blue-TGF-β^{TM} reporter cells (Invivogen) according to the manufacturer's protocol. Briefly, 180 µL of HEK-Blue-TGF-β^{TM} reporter cells at a concentration of 280,000 cells/mL were seeded in p96 plates in test medium (DMEM 4.5 g/L glucose, 2 mM L-glutamine, 10% FBS heat inactivated, Pen-Strep 100 U/mL) in the presence of 20 µL of patient's serum (10% v/v) for 24 h at 37°C and 5% CO_2. Then, 20 µL of the cell culture supernantant were removed from each well and transferred to a transparent p96 plate containing 180 µL of prewarmed QUANTI-Blue solution and incubated at 37°C (in the dark) during 30 min. The QUANTI-Blue is a colorimetric enzymatic assay in which the presence of alkaline phosphatase changes the media color from pink to blue and can be quantified at 655 nm using a microplate reader. 20 µL of test medium and 20 µL of human recombinant TGF-β at 10 ng/ml were used as negative and positive controls, respectively. For each serum, the HEK-Blue-TGF-β^{TM} reporter cells were seeded in octuplicates. Two independent experiments were performed for each serum. Data are mean ± standard deviation obtained from the two independent experiments. Induced SEAP data for each serum is expressed normalized versus the values obtained for the negative control in each experiment.

RESULTS

Increased Circulating TGF-β-Related Members Expression in Severe OI Patient

The study scheme is illustrated in **Figure 1**. First, we explored the global protein expression of basal OI serum (before the cell therapy), by using antibody array technology, which allows the simultaneous determination of over 1,000 proteins (**Figures 2A,B**). After detecting the expressed proteins in each basal serum (showing a fluorescent intensity of at least 300 above the background), we compared the total number of proteins expressed in the sera from P01 and P02 patients (**Figure 2A**, left heatmap). Interestingly, we observed a very different trend in terms of number and expression level between the two OI patients. Thus, 746 of the 1,000 proteins evaluated were detected as expressed in P01 (more than 70% of the total target proteins) *versus* the only 228 detected proteins in P02 (the ≈25% of total target proteins) (**Figure 2A**, left heatmap). Moreover, the fluorescent intensity of the detected proteins in P01 was in general higher than that exhibited by detected proteins in P02 basal serum, indicating a higher expression of circulating proteins in P01. Therefore, after grouping expressed proteins depending on fluorescent intensities, P01 basal serum showed 451 proteins with low signal intensities (signal between 300 and 2,000), 246 with medium signal intensity group (between 2,000 and 10,000) and 40 proteins with a high signal intensity (over 10,000). In the case of P02, the majority of the detected proteins, 218, exhibited a low signal intensity, whereas only eight and two proteins displayed medium and high signal intensities respectively

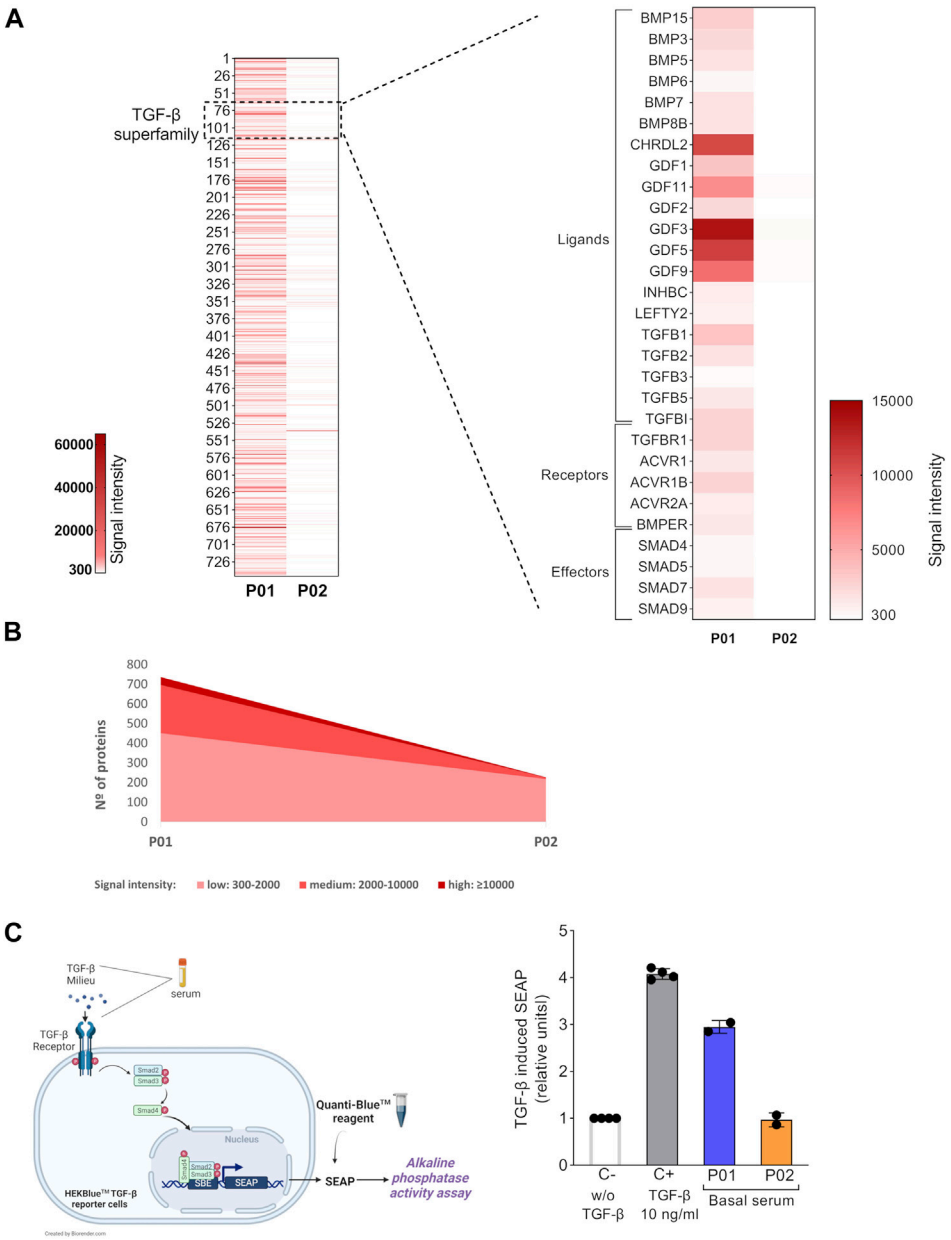

FIGURE 2 | Basal circulating TGF-β superfamily members' expression and bioactivity in OI patients. **(A)** Left heatmap shows the fluorescent signal intensities for target proteins expressed in P01 and P02 basal sera samples. Only the spots with a fluorescent intensity cutoff ≥300 above the background were considered. Right heatmap magnified shows the fluorescent intensities of the TGF-β superfamily members present in basal P01 and P02 sera are shown (right heatmap). **(B)** Graph showing the total number of expressed proteins in P01 and P02 basal sera, grouped according to their fluorescent signal intensity: low (300-2,000), medium (2,000-10,000) and high (>10,000). **(C)** Left, schematic representation of the HEK-Blue-TGF-β^{TM} reporter cell line assay. Right, Scatter plot with bars showing TGF-β-induced SEAP in HEK-Blue-TGF-β^{TM} cells. The TGF-β induced SEAP from patients' sera samples is shown normalized *versus* that shown by the negative control (C-; w/o TGF-β). C+ stands for the positive control, cells stimulated with TGF-β (10 ng/ml). The experiments were performed in octuplicates for each condition and repeated two independent times. Data are mean ± standard deviation obtained from the two independent experiments. Each dot represents an independent experiment.

(**Figure 2B**). Further analysis identified a quite high expression of a number of TGF-β-relevant members, including ligands (activators and inhibitors), receptors and effectors in P01 basal serum, contrarily to P02 basal serum (**Figure 2A**, right heatmap). These results point to the existence of a global higher expression of circulating TGF-β superfamily members in P01, finding that could be due to the highest OI severity exhibited by this patient.

Increased TGF-β Bioactivity in Basal Serum From Severe OI Patient

The circulating TGF-β-enriched milieu in basal P01 serum, showed a coexistence of several TGF-β superfamily ligands (activators and inhibitors which can bind the same receptors and compete with each other for binding) and soluble receptors (able to bind to ligands and therefore to modulate the downstream TGF-β signaling) (Wang et al., 2017; Nickel et al., 2018; Martinez-Hackert et al., 2021). This mixture of activating and inhibiting signals led us to interrogate for the final TGF-β bioactivity of P01 (and P02) basal serum. For this, we used the HEK-Blue-TGF-β^{TM} reporter cell line which expresses TGFBRI, Smad3 and Smad4 genes and a secreted embryonic alkaline phosphatase (SEAP) reporter gene under the control of the *ß*-globin minimal promoter fused to three Smad3/4-binding elements (SBE). Stimulation of HEK-Blue-TGF-β^{TM} cells with TGF-β induces the activation of the TGF-β/Smad signaling pathway leading to the formation of a Smad3/Smad4 complex, which enters the nucleus and binds SBE sites inducing the production of SEAP. The secreted SEAP can be measured using QUANTI-Blue™ solution, a SEAP detection reagent (**Figure 2C**, left image). We first validated the functionality of this reporter system by stimulating the HEK-Blue-TGF-β^{TM} cells with the manufacturer's recommended concentration of recombinant human TGF-β, which led to a high TGF-β pathway activation (**Figure 2C**, right). Concerning TERCELOI sera samples, we found that the TGF-β bioactivity of P01 basal serum was three times higher than that exhibited by P02, consistently with the TGF-β superfamily enrichment detected in P01 basal serum. In fact, P02 basal serum was unable to activate TGF-β pathway, showing similar activation levels to that obtained by the negative control (w/o TGF-β). Interestingly, P01 basal serum showed almost similar levels of TGF-β signaling activation as the positive control (**Figure 2C**, right). These data suggest that in the TGF-β enriched milieu of P01 basal serum, the TGF-β pro-activating factors prevailed over those inhibiting this pathway.

The Circulating TGF-β Pathway in the Severe OI Patient Was Modulated After the MSCs Therapy

Next, we interrogated whether a modulation of the circulating TGF-β pathway could be occurring after the MSCs therapy in P01 and P02. Thus, we focused on the sera collected after the 1st MSCs infusion, which, in the case of P01, showed in TERCELOI the most significant molecular findings in terms of global protein and miRNAs expression (Infante et al., 2021). We studied the antibody arrays's signal intensities of TGF-β superfamily members in P01 and P02 sera collected 1 week, 1 month and 4 months after the 1st cell infusion, and compared them to those of their respective basal sera. Interestingly, we found in P01 a profound upregulation of the expression level of most TGF-β superfamily members analyzed, especially in the sera collected 1 and 4 months after the 1st cell infusion (**Figure 3A**). On the contrary, we did not observe this effect in the expression of TGF-β superfamily members in P02 sera (**Figure 3A**).

Then, we analyzed the TGF-β bioactivity of P01's and P02's sera after the 1st cell infusion, and compared them to that showed by the basal serum of each patient. Intriguingly, the TGF-β bioactivity of P01's sera collected after the 1st cell infusion showed a diminished trend when compared to that showed by P01's basal serum, in spite of the enhanced expression of TGF-β superfamily members found in these sera (**Figure 3B**). Regarding P02, the sera collected after the 1st cell infusion showed no TGF-β bioactivity (similar to the negative control), as occurred with the basal serum. These results were consistent with the absence of significant expression of TGF-β superfamily members in P02 sera before and after the 1st cell infusion, (**Figure 3B**). Given that only the P01's sera showed a modulation of TGF-β pathway after the 1st cell infusion, we wondered if those sera collected after the successive MSCs administrations (second, third, fourth, fifth infusions) and in the follow-up visits (1 year and 2 years since the last cell infusion) in P01 exhibited also a reduction in the TGF-β bioactivity. Strikingly, we observed that the reduced TGF-β bioactivity of P01 sera was maintained with a similar trend during the consecutive MSCs infusions and follow-up visits (**Figure 3C**). These results suggest that, after the cell therapy, the circulating TGF-β inhibiting factors prevailed over those activating this pathway in P01.

DISCUSSION

The present study addresses, for the first time, the circulating TGF-β pathway in OI pediatric patients before and after receiving MSCs therapy. Our results should be interpreted in the context of certain limitations derived from the inherent nature of TERCELOI clinical trial. First, and the most important, the low number of pediatric patients included in this study, determined by the low prevalence of a rare disorder as OI and the restrictive inclusion criteria of TERCELOI such as the need of a HLA compatible sibling donor. Second, the fact that our patients were pediatric and third, the absence of a population of healthy pediatric controls. Thus, our findings need further confirmation in larger cohorts of OI patients, encompassing different OI severities and ages, along with age-matched healthy controls. Nevertheless, the present study provides new insights into the pathophysiology of OI, specifically concerning the circulating TGF-β pathway before and after MSCs therapy. Moreover, our observations shed light about the possibility of increased circulating levels of TGF-β superfamily members and TGF-β bioactivity correlating with OI severity.

Thus, to the best of our knowledge, this is the first time that an enhanced TGF-β expression and bioactivity has been reported in the serum of a severe OI pediatric patient when compared to a moderate OI one. These results are in line with previous findings in the skeleton of severe OI mice models and in osteoblasts isolated from OI patients (Gebken et al., 2000; Grafe et al., 2014; Tauer et al., 2018).

We speculate that the basal overactivation of circulating TGF-β pathway in the severe patient when compared to the moderate

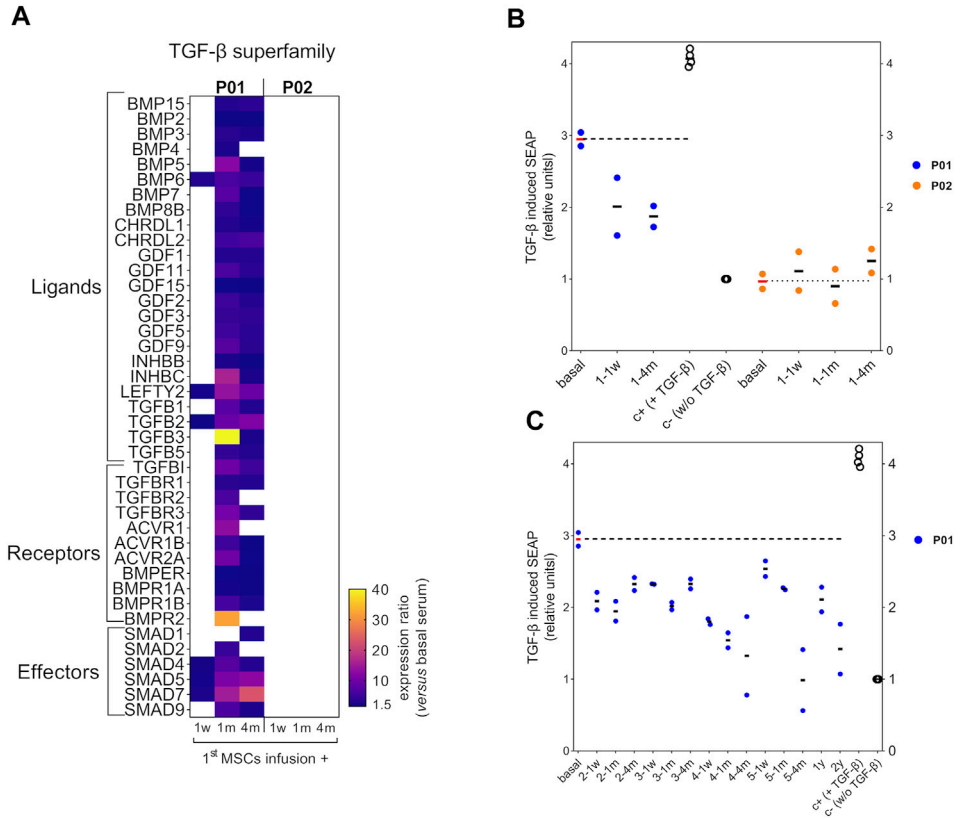

FIGURE 3 | Circulating TGF-β superfamily members expression and bioactivity after MSCs therapy in OI patients. **(A)** Heatmap showing the expression ratio of TGF-β superfamily members after the 1st MSCs infusion in P01 and P02, calculated as the fluorescent signal intensity of target proteins after the MSCs therapy, 1 week (1w), 1 month (1 m) or 4 months (4 m) *versus* the fluorescent intensity of target proteins from each patient's basal serum. To be considered, a cutoff ratio of ±1.5 was established. **(B)** Scatter plot showing TGF-β induced SEAP of HEK-Blue-TGF-β^{TM} cells exposed to P01 and P02 sera collected after the first MSCs infusion and compared to the results obtained with basal serum for each patient. The TGF-β induced SEAP is shown normalized *versus* the negative control. **(C)** Scatter plot showing TGF-β induced SEAP of HEK-Blue-TGF-β^{TM} cells exposed to the sera from P01 obtained during the 2nd, 3rd, 4th, 5th infusions and follow-up visits, and compared to the results obtained with basal serum. Two independent experiments were performed with P01 and P02 sera, each of one with their respective positive (c+) and negative controls (c-). Within each independent experiment, each condition was performed in octuplicates. Data are mean ± standard deviation obtained from the two independent experiments. Each dot represents an independent experiment.Dashed horizontal lines illustrate the TGF-β bioactivity level of basal P01 and P02 sera.

one could be due to the different phenotypic severities that these patients show, which in turn depends not only on the affected gene, but also on the type and the position of the mutation in the gene. In this line, mutations leading to a glycine substitution, such as that present in the severe patient, have been associated to most severe, and even perinatal lethal, phenotypes (Maioli et al., 2019). Thus, the enrichment of TGF-β superfamily members in the serum of the most severe patient could be reflecting the intense alteration in bone homeostasis that this patient exhibits. There are two evidences supporting this observation. First, the existence of increased circulating TGF-β1 activity and concentration in other connective tissue disorders such as heterotopic ossification, characterized by ectopic bone formation in extraskeletal tissues and Marfan syndrome, caused by mutations in fibrillin-1, an ECM protein (Matt et al., 2009; Franken et al., 2013; Wang et al., 2018). Second, as previously reported in TERCELOI, we also found striking molecular changes in basal serum from the most severe OI patient, which we also linked to the OI severity of this patient: an enhanced expression of circulating miRNAs known to be associated with osteoporotic bone fractures which was not observed in the moderate OI patient (Infante et al., 2021).

Interestingly, after the MSCs therapy we detected a general increase in the expression of several circulating TGF-β superfamily members only in the severe OI patient, but not in the moderate one. Surprisingly, TGF-β bioactivity of these sera was decreased when compared to that exerted by P01 basal serum. We speculate that this effect could be driven by the prevalence of ligands that function as inhibitors and compete with activators for the same TGF-β receptors, and the existence of more soluble TGF-β receptors (which can bind to ligands and therefore modulate the downstream TGF-β signaling) in the sera after cell therapy (Wang et al., 2017; Martinez-Hackert et al., 2021). Supporting our assumption, a previous study using the HEK-Blue-TGF-β^{TM} reporter cell line showed that not only the three TGF-β isoforms were able to activate the downstream TGF-β signaling, but also activin A, a member of the TGF-β superfamily binding to activing type I and II receptors, different from TGF-β receptors. Moreover, the concomitant

addition of soluble chimeric TGF-β receptors inhibited this activation (Takahashi et al., 2020).

Importantly, our work shows that increased TGF-β bioactivity of basal serum from the severe OI patient can be modulated along the MSCs treatment, correlating with the beneficial effects exhibited by this patient (at clinical, molecular and cellular levels) after the cell therapy (Infante et al., 2021). Interestingly, the increased miRNA expression previously found in the basal serum of this patient, was also downregulated after the MSCs infusions.

The moderately affected patient exhibited low expression and bioactivity levels of circulating TGF-β, that were not modulated after the cell therapy. The specific mutation of this patient, an exon skipping of exon 35 in *COL1A2*, which leads to moderate OI, could be responsible for its lack of impact on the homeostasis of TGF-β pathway.

Assuming the limitations of the present study, our hypothesis linking OI disease severity with the activation of TGF-β pathway is in line with the increased skeleton TGF-β activation that mice models resembling severe OI, Col1a2$^{+/G61°C}$, Crtap$^{-/-}$, and Col1a1$^{Jrt/+}$ exhibit (Grafe et al., 2014; Tauer et al., 2018). Interestingly, TGF-β inhibition was efficient in Col1a2$^{+/G61°C}$, and Crtap$^{-/-}$ mice, but not in Col1a1$^{Jrt/+}$ ones, suggesting different effects of the antibody in different OI types or even different TGF-β activation levels in these OI murine models. Thus, OI severity should be a point of especial interest to take into account when addressing a TGF-β targeting approach.

On the other hand, it is worth mentioning that the inhibition of TGF-β has been also shown to be effective in mice models exhibiting skeletal pathologies and elevated TGF-β signaling, such as heterotopic ossification (HO), and osteoarthritis (Zhen et al., 2013; Wang et al., 2018). Moreover, and supporting our finding in the most severe patient, significantly elevated circulating levels of active TGF-β were found in HO patients (Wang et al., 2018). Denoting the interest in exploring the inhibition of TGF-β pathway in OI, a phase I clinical trial evaluating the safety and efficacy of fresolimumab, a human monoclonal antibody, that recognizes all TGF-β isoforms, is currently being assessed in adult patients (NCT03064074).

Overall, further studies involving representative cohorts of OI patients with different severities are needed to clarify the status of circulating TGF-β pathway activation in OI. Our study suggests that mainly severe OI patients would show increased circulating TGF-β signaling, and therefore could benefit from treatment approaches aiming to inhibit the excessive TGF-β activation.

The identification of those OI patients with excessive TGF-β would be crucial to select patients who may benefit from TGF-β targeting therapies.

CONCLUSION

Osteogenesis Imperfecta (OI) is a rare collagen-related disorder with no current curative treatment. New therapeutic approaches have been tested with encouraging results, such as MSCs therapy. The inhibition of TGF-β signaling, effective in some severe murine OI models showing increased TGF-β activation in the skeleton, is also currently undergoing clinical evaluation for OI. This study examined for the first time the TGF-β pathway in the serum of two OI pediatric patients. These patients previously participated in TERCELOI clinical trial, and showed clinical improvements after receiving MSCs therapy. We found elevated basal TGF-β levels and bioactivity in the serum of the most severely affected patient, which were modulated after the MSCs therapy. The outcomes suggest that the specific mutation of the severe patient could be mediating the TGF-β overactivation. The current investigation provides a foundation for further exploring the circulating TGF-β pathway in a bigger cohort of OI patients encompassing different disease severities. The identification of OI patients with excessive TGF-β activation would be crucial to identify those patients who could benefit from TGF-β targeted therapies.

DATA AVAILABILITY STATEMENT

The raw data supporting the conclusion of this article will be made available by the authors, without undue reservation.

ETHICS STATEMENT

The studies involving human participants were reviewed and approved by the Basque Ethics Committee for Clinical Research and the Spanish Agency of Medicines and Medical Devices (AEMPS). Written informed consent to participate in this study was provided by the participants' legal guardian/next of kin.

AUTHOR CONTRIBUTIONS

AI, BG, and CR conceived the original idea and designed the experiments. AI collected the serum samples. CR performed the antibody arrays experiments. AI and LC carried out the reporter cell line experiments. LC, AI, BG, and CR analyzed the data. AI wrote the original manuscript. AI and CR wrote, reviewed and edited the final manuscript. CR obtained funding support. All authors: approved the final version of the manuscript.

FUNDING

This study was funded by the Spanish Ministry of Health through the call for independent clinical trials projects "EC10-219", Instituto de Salud Carlos III through the projects "PI15/00820" and "PI21/00077" (Co-funded by European Regional Development Fund; "A way to make Europe"), Bioef-EiTB maratoia (BIO14/TP/007) and the AHUCE Foundation.

ACKNOWLEDGMENTS

We are truly grateful to the patients and families affected by OI, and to the AHUCE Foundation, especially to its director Julia Piniella, for her invaluable and tireless support.

REFERENCES

Faraji, A., Abtahi, S., Ghaderi, A., and Samsami Dehaghani, A. (2016). Transforming Growth Factor β1 (TGF-B1) in the Sera of Postmenopausal Osteoporotic Females. *Int. J. Endocrinol. Metab.* 14 (4), e36511. doi:10.5812/ijem.36511

Franken, R., Den Hartog, A. W., De Waard, V., Engele, L., Radonic, T., Lutter, R., et al. (2013). Circulating Transforming Growth Factor-β as a Prognostic Biomarker in Marfan Syndrome. *Int. J. Cardiol.* 168 (3), 2441–2446. doi:10.1016/j.ijcard.2013.03.033

Gebken, J., Brenner, R., Feydt, A., Notbohm, H., Brinckmann, J., Müller, P. K., et al. (2000). Increased Cell Surface Expression of Receptors for Transforming Growth Factor-β on Osteoblasts from Patients with Osteogenesis Imperfecta. *Pathobiology* 68 (3), 106–112. doi:10.1159/000055910

Götherström, C., Westgren, M., Shaw, S. W., Aström, E., Biswas, A., Byers, P. H., et al. (2014). Pre- and Postnatal Transplantation of Fetal Mesenchymal Stem Cells in Osteogenesis Imperfecta: a Two-center Experience. *Stem Cell Transl Med* 3 (2), 255–264. doi:10.5966/sctm.2013-0090

Grafe, I., Yang, T., Alexander, S., Homan, E. P., Lietman, C., Jiang, M. M., et al. (2014). Excessive Transforming Growth Factor-β Signaling Is a Common Mechanism in Osteogenesis Imperfecta. *Nat. Med.* 20 (6), 670–675. doi:10.1038/nm.3544

Grainger, D. J., Percival, J., Chiano, M., and Spector, T. D. (1999). The Role of Serum TGF-β Isoforms as Potential Markers of Osteoporosis. *Osteoporos. Int.* 9 (5), 398–404. doi:10.1007/s001980050163

Greene, B., Russo, R. J., Dwyer, S., Malley, K., Roberts, E., Serrielo, J., et al. (2021). Inhibition of TGF-β Increases Bone Volume and Strength in a Mouse Model of Osteogenesis Imperfecta. *JBMR Plus* 5 (9), e10530. doi:10.1002/jbm4.10530

Hering, S., Isken, E., Knabbe, C., Janott, J., Jost, C., Pommer, A., et al. (2001). TGFbeta1 and TGFbeta2 mRNA and Protein Expression in Human Bone Samples. *Exp. Clin. Endocrinol. Diabetes* 109 (4), 217–226. doi:10.1055/s-2001-15109

Hering, S., Jost, C., Schulz, H., Hellmich, B., Schatz, H., and Pfeiffer, H. (2002). Circulating Transforming Growth Factor Beta1 (TGFbeta1) Is Elevated by Extensive Exercise. *Eur. J. Appl. Physiol.* 86 (5), 406–410. doi:10.1007/s00421-001-0537-5

Horwitz, E. M., Gordon, P. L., Koo, W. K. K., Marx, J. C., Neel, M. D., Mcnall, R. Y., et al. (2002). Isolated Allogeneic Bone Marrow-Derived Mesenchymal Cells Engraft and Stimulate Growth in Children with Osteogenesis Imperfecta: Implications for Cell Therapy of Bone. *Proc. Natl. Acad. Sci.* 99 (13), 8932–8937. doi:10.1073/pnas.132252399

Horwitz, E. M., Prockop, D. J., Fitzpatrick, L. A., Koo, W. W. K., Gordon, P. L., Neel, M., et al. (1999). Transplantability and Therapeutic Effects of Bone Marrow-Derived Mesenchymal Cells in Children with Osteogenesis Imperfecta. *Nat. Med.* 5 (3), 309–313. doi:10.1038/6529

Infante, A., Gener, B., Vázquez, M., Olivares, N., Arrieta, A., Grau, G., et al. (2021). Reiterative Infusions of MSCs Improve Pediatric Osteogenesis Imperfecta Eliciting a Pro-osteogenic Paracrine Response: TERCELOI Clinical Trial. *Clin. Transl Med.* 11 (1), e265. doi:10.1002/ctm2.265

Jovanovic, M., Guterman-Ram, G., and Marini, J. C. (2021). Osteogenesis Imperfecta: Mechanisms and Signaling Pathways Connecting Classical and Rare OI Types. *Endocr. Rev.* 43 (1), 61–90. doi:10.1210/endrev/bnab017

MacFarlane, E. G., Haupt, J., Dietz, H. C., and Shore, E. M. (2017). TGF-β Family Signaling in Connective Tissue and Skeletal Diseases. *Cold Spring Harb Perspect. Biol.* 9 (11), a022269. doi:10.1210/endrev/bnab017

Maioli, M., Gnoli, M., Boarini, M., Tremosini, M., Zambrano, A., Pedrini, E., et al. (2019). Genotype-phenotype Correlation Study in 364 Osteogenesis Imperfecta Italian Patients. *Eur. J. Hum. Genet.* 27 (7), 1090–1100. doi:10.1038/s41431-019-0373-x

Marini, J. C., Forlino, A., Bächinger, H. P., Bishop, N. J., Byers, P. H., Paepe, A. D., et al. (2017). Osteogenesis Imperfecta. *Nat. Rev. Dis. Primers* 3, 17052. doi:10.1038/nrdp.2017.52

Marini, J. C., Forlino, A., Cabral, W. A., Barnes, A. M., San Antonio, J. D., Milgrom, S., et al. (2007). Consortium for Osteogenesis Imperfecta Mutations in the Helical Domain of Type I Collagen: Regions Rich in Lethal Mutations Align with Collagen Binding Sites for Integrins and Proteoglycans. *Hum. Mutat.* 28 (3), 209–221. doi:10.1002/humu.20429

Martinez-Hackert, E., Sundan, A., and Holien, T. (2021). Receptor Binding Competition: A Paradigm for Regulating TGF-β Family Action. *Cytokine Growth Factor. Rev.* 57, 39–54. doi:10.1016/j.cytogfr.2020.09.003

Matt, P., Schoenhoff, F., Habashi, J., Holm, T., Van Erp, C., Loch, D., et al. (2009). Circulating Transforming Growth Factor-β in Marfan Syndrome. *Circulation* 120 (6), 526–532. doi:10.1161/circulationaha.108.841981

Nickel, J., Ten Dijke, P., and Mueller, T. D. (2018). TGF-β Family Co-receptor Function and Signaling. *Acta Biochim. Biophys. Sin (Shanghai)* 50 (1), 12–36. doi:10.1093/abbs/gmx126

Otsuru, S., Desbourdes, L., Guess, A. J., Hofmann, T. J., Relation, T., Kaito, T., et al. (2018). Extracellular Vesicles Released from Mesenchymal Stromal Cells Stimulate Bone Growth in Osteogenesis Imperfecta. *Cytotherapy* 20 (1), 62–73. doi:10.1016/j.jcyt.2017.09.012

Pereira, R. F., Halford, K. W., O'hara, M. D., Leeper, D. B., Sokolov, B. P., Pollard, M. D., et al. (1995). Cultured Adherent Cells from Marrow Can Serve as Long-Lasting Precursor Cells for Bone, Cartilage, and Lung in Irradiated Mice. *Proc. Natl. Acad. Sci.* 92 (11), 4857–4861. doi:10.1073/pnas.92.11.4857

Sarahrudi, K., Thomas, A., Mousavi, M., Kaiser, G., Köttstorfer, J., Kecht, M., et al. (2011). Elevated Transforming Growth Factor-Beta 1 (TGF-B1) Levels in Human Fracture Healing. *Injury* 42 (8), 833–837. doi:10.1016/j.injury.2011.03.055

Takahashi, K., Akatsu, Y., Podyma-Inoue, K. A., Matsumoto, T., Takahashi, H., Yoshimatsu, Y., et al. (2020). Targeting All Transforming Growth Factor-β Isoforms with an Fc Chimeric Receptor Impairs Tumor Growth and Angiogenesis of Oral Squamous Cell Cancer. *J. Biol. Chem.* 295 (36), 12559–12572. doi:10.1074/jbc.ra120.012492

Tauer, J. T., Abdullah, S., and Rauch, F. (2018). Effect of Anti-TGF-β Treatment in a Mouse Model of Severe Osteogenesis Imperfecta. *J. Bone Miner Res.* 34 (2), 207–214. doi:10.1002/jbmr.3617

Tauer, J. T., Robinson, M. E., and Rauch, F. (2019). Osteogenesis Imperfecta: New Perspectives from Clinical and Translational Research. *JBMR Plus* 3 (8), e10174. doi:10.1002/jbm4.10174

Wang, X., Li, F., Xie, L., Crane, J., Zhen, G., Mishina, Y., et al. (2018). Inhibition of Overactive TGF-β Attenuates Progression of Heterotopic Ossification in Mice. *Nat. Commun.* 9 (1), 551. doi:10.1038/s41467-018-02988-5

Wang, Y., Chen, Q., Zhao, M., Walton, K., Harrison, C., and Nie, G. (2017). Multiple Soluble TGF-β Receptors in Addition to Soluble Endoglin Are Elevated in Preeclamptic Serum and They Synergistically Inhibit TGF-β Signaling. *J. Clin. Endocrinol. Metab.* 102 (8), 3065–3074. doi:10.1210/jc.2017-01150

Wang, Z., Li, Y., Hou, B., Pronobis, M. I., Wang, M., Wang, Y., et al. (2020). An Array of 60,000 Antibodies for Proteome-Scale Antibody Generation and Target Discovery. *Sci. Adv.* 6 (11), eaax2271. doi:10.1126/sciadv.aax2271

Wu, X. Y., Peng, Y. Q., Zhang, H., Xie, H., Sheng, Z. F., Luo, X. H., et al. (2013). Relationship between Serum Levels of OPG and TGF- β with Decreasing Rate of BMD in Native Chinese Women. *Int. J. Endocrinol.* 2013, 727164. doi:10.1155/2013/727164

Zhen, G., Wen, C., Jia, X., Li, Y., Crane, J. L., Mears, S. C., et al. (2013). Inhibition of TGF-β Signaling in Mesenchymal Stem Cells of Subchondral Bone Attenuates Osteoarthritis. *Nat. Med.* 19 (6), 704–712. doi:10.1038/nm.3143

Zimmermann, G. G., Kusswetter, M., Küsswetter, A., Moghaddam, S., Wentzensen, A., Richter, W., et al. (2005). TGF-β1 as a Marker of Delayed Fracture Healingg. *Bone* 36 (5), 779–785. doi:10.1016/j.bone.2005.02.011

Conflict of Interest: The authors declare that the research was conducted in the absence of any commercial or financial relationships that could be construed as a potential conflict of interest.

frontiers in Genetics

ORIGINAL RESEARCH
published: 15 February 2022
doi: 10.3389/fgene.2022.782750

Comprehensive Analysis of LncRNA AC010789.1 Delays Androgenic Alopecia Progression by Targeting MicroRNA-21 and the Wnt/β-Catenin Signaling Pathway in Hair Follicle Stem Cells

Jiachao Xiong[1], Baojin Wu[2], Qiang Hou[1], Xin Huang[3], Lingling Jia[1], Yufei Li[1] and Hua Jiang[1]**

[1]Department of Plastic Surgery, Shanghai East Hospital, Tongji University School of Medicine, Shanghai, China, [2]Department of Plastic Surgery, Huashan Hospital, Fudan University, Shanghai, China, [3]Department of Dermatology, Tongji Hospital, Tongji University School of Medicine, Shanghai, China

OPEN ACCESS

Edited by:
Jiacan Su,
Second Military Medical University, China

Reviewed by:
Yong Miao,
Southern Medical University, China
Lie Zhu,
Shanghai Changzheng Hospital, China
Yingying Jing,
Shanghai University, China

***Correspondence:**
Yufei Li
lufylee@hotmail.com
Hua Jiang
dosjh@126.com

Specialty section:
This article was submitted to Stem Cell Research, a section of the journal Frontiers in Genetics

Received: 24 September 2021
Accepted: 11 January 2022
Published: 15 February 2022

Citation:
Xiong J, Wu B, Hou Q, Huang X, Jia L, Li Y and Jiang H (2022) Comprehensive Analysis of LncRNA AC010789.1 Delays Androgenic Alopecia Progression by Targeting MicroRNA-21 and the Wnt/β-Catenin Signaling Pathway in Hair Follicle Stem Cells. Front. Genet. 13:782750. doi: 10.3389/fgene.2022.782750

Background: Androgen alopecia (AGA), the most common type of alopecia worldwide, has become an important medical and social issue. Accumulating evidence indicates that long noncoding RNAs (lncRNAs) play crucial roles in the progression of various human diseases, including AGA. However, the potential roles of lncRNAs in hair follicle stem cells (HFSCs) and their subsequent relevance for AGA have not been fully elucidated. The current study aimed to explore the function and molecular mechanism of the lncRNA AC010789.1 in AGA progression.

Methods: We investigated the expression levels of AC010789.1 in AGA scalp tissues compared with that in normal tissues and explored the underlying mechanisms using bioinformatics. HFSCs were then isolated from hair follicles of patients with AGA, and an AC010789.1-overexpressing HFSC line was produced and verified. Quantitative real-time polymerase chain reaction (qRT-PCR) and Western blotting were performed to verify the molecular mechanisms involved.

Results: AC010789.1 overexpression promoted the proliferation and differentiation of HFSCs. Mechanistically, we demonstrated that AC010789.1 overexpression promotes the biological function of HFSCs by downregulating miR-21-5p and TGF-β1 expression but upregulating the Wnt/β-catenin signaling pathway.

Conclusion: These results reveal that overexpression of AC010789.1 suppresses AGA progression via downregulation of hsa-miR-21-5p and TGF-β1 and promotion of the Wnt/β-catenin signaling pathway, highlighting a potentially promising strategy for AGA treatment.

Keywords: androgen alopecia, hair follicle stem cells, AC010789.1, Wnt/β-catenin, TGF-1

INTRODUCTION

Alopecia, a common disorder occurring worldwide, characterized by hair loss, can be caused by multiple factors, such as heredity, hormonal disorders, immune inflammation, malnutrition, environmental factors, mental disorders, and aging (Ho and Shapiro, 2019). Androgen alopecia (AGA) is the most common type of alopecia and has become an important medical and social issue due to its high incidence; increasingly young onset age; and associated psychological problems, such as depression, anxiety, and emotional disorders (Bas et al., 2015; Molina-Leyva et al., 2016; Katzer et al., 2019; Ding et al., 2020). Currently, finasteride and minoxidil are the only therapeutic drugs approved by the Food and Drug Administration for AGA treatment (Chen et al., 2020a). Finasteride, a specific inhibitor of type II 5α reductase, inhibits the metabolic conversion of testosterone to highly active dihydrotestosterone, reducing the effect of active androgens on hair follicles (Spinucci and Pasquali, 1996). However, finasteride is associated with a risk of sexual dysfunction and depression during treatment (Motofei et al., 2020). Minoxidil treats AGA by predominantly promoting hair growth but can cause side effects, such as contact dermatitis, skin irritation, and dizziness during treatment, and on treatment cessation, alopecia generally recurs (Goren et al., 2017; Jimenez-Cauhe et al., 2019). Hair transplantation is the gold standard for AGA treatment, but the limited number of active hair follicles in the donor site makes it impossible to apply to large areas of baldness (Chouhan et al., 2019a; Chouhan et al., 2019b). Hence, new methods for the treatment of AGA need to be developed urgently.

The three phases of periodic hair follicle growth are resting, growth, and degenerative periods, and cessation of this regeneration cycle is the main mechanism contributing to AGA (Baker and Murray, 2012). Previous studies report that the periodic growth of hair follicles depends on the hair follicle stem cells (HFSCs) located in the bulge area of the hair follicle (Cotsarelis et al., 1990; Fu and Hsu, 2013). HFSCs are a group of adult stem cells with self-renewal ability that specifically express surface markers such as CD34 and CK15 (Morris et al., 2004; Owczarczyk-Saczonek et al., 2018). In normal conditions or during wound repair, HFSCs in the bulge area activate and differentiate into various hair follicle cell types for hair follicle regeneration (Oshima et al., 2001; Yang et al., 2017). However, there is evidence that the scalp hair follicles in patients with AGA are impaired in HFSC activation, thereby preventing their differentiation into hair follicle precursors. Garza et al. (2011) found that, although patients with AGA had a similar quantity of hair follicles in the alopecia scalp area as in nonalopecia areas, the HFSCs in the alopecia areas were in a static state and did not actively differentiate into hair follicle precursors. Thus, activation of HFSC proliferation and differentiation may be an effective breakthrough for the treatment of AGA.

Long noncoding RNAs (lncRNAs), a type of noncoding RNA over 200 nt in length, have attracted considerable interest in recent years. Functional data suggest that they play essential regulatory roles in multiple biological processes, such as cell development, differentiation, disease, subcellular localization, and cell structure maintenance (Yao et al., 2019). Intriguingly, genome analyses comparing AGA scalp tissues with adjacent normal tissues (defined as 5 cm from the margin of the AGA areas with a follicle density >325/cm^2) in patients with AGA found a large number of differentially expressed lncRNAs, indicating that the dysregulation of lncRNA expression profiles may be involved in AGA progression (Chew et al., 2016; Bao et al., 2017). Moreover, several lines of evidence demonstrate a novel lncRNA regulatory mechanism in promoting hair follicle regeneration. Zhu et al. (2020) demonstrate that overexpression of lncRNA H19 can directly downregulate the expression of Wnt pathway inhibitors, including DKK1, Kremen2, and sFRP2, which activates Wnt signaling, thereby maintaining the hair follicle regeneration potential of dermal papilla cells (DPCs). Likewise, Lin et al. (2020a); Lin et al. (2020b) found that lncRNA XIST targets miR-424 and PCAT1 targets miR-329 to activate Wnt and hedgehog signaling, respectively, and maintain the regeneration characteristics of DPCs. To date, many molecular mechanisms of DPC-mediated hair follicle regeneration have been investigated. However, the role of the potential connection between lncRNAs and HFSCs in AGA has not been fully elucidated.

The current study aimed to explore the potential function of the lncRNA AC010789.1 in AGA progression. We demonstrate that AC010789.1 expression was downregulated in AGA scalp tissues, and overexpression of AC010789.1 promoted the proliferation and differentiation of HFSCs. Mechanistically, overexpression of AC010789.1 was shown to delay AGA progression by interacting with miR-21 and activating Wnt/β-catenin signaling. Therefore, this study provides insights into the mechanisms underlying AC010789.1 regulation of AGA progression to provide a new theoretical and experimental basis for the prevention and treatment of AGA.

MATERIALS AND METHODS

Tissue Collection and Ethics Statement

Hair follicle tissues extracted from patients with AGA were obtained from the Shanghai East Hospital affiliated with the Tongji University School of Medicine, and informed consent was obtained from all patients. Ethical approval was obtained from the Shanghai East Hospital Ethics Committee. Tissue specimens were snap-frozen and stored in liquid nitrogen until further use.

Microarray Data Acquisition

Gene expression microarray data sets (GSE84839 and GSE36169) were downloaded from the Gene Expression Omnibus (GEO) database (https://www.ncbi.nlm.nih.gov/geo). The GSE84839 data set was based on the GPL21827 platform (Agilent-079487 Arraystar Human LncRNA microarray V4) and included three pairs of male AGA scalp tissues and adjacent normal tissues. The GSE36169 data set was based on the GPL96 platform (Affymetrix Human Genome U133A Array) and contained AGA and adjacent normal scalp tissues from five individuals. The

lncRNA and mRNA expression data in the AGA and adjacent normal tissues were downloaded and used for this study.

Differential Analysis of lncRNA and mRNA Expression

Differential analysis of lncRNA and mRNA expression between AGA and adjacent normal scalp tissues was performed using the GEO2R analysis tool. The platform data were converted using R language software and standardized using the limma array function within the R package (http://www.bioconductor.org/). A p-value < .05, and a base-2 logarithm of fold change (log FC) < −1 or >1 were used as selection criteria to screen differentially expressed lncRNAs and mRNAs (Xiong et al., 2020).

Functional and Pathway Enrichment Analysis

Database for Annotation, Visualization, and Integrated Discovery (DAVID) v6.8 (https://david.ncifcrf.gov/) provides a comprehensive annotation tool to help investigators better clarify the biological function of the submitted genes (Dennis et al., 2003). In this study, DAVID v6.8 was used for gene ontology (GO) annotation and Kyoto Encyclopedia of Genes and Genomes (KEGG) pathway enrichment analysis. GO annotation analysis revealed biological processes (BPs), cellular components (CCs), and molecular functions (MFs) of the genes. Statistical significance was set at $p < 0.05$. Then, XTalkDB (http://www.xtalkdb.org/home), a database that documents scientific literature supporting crosstalk between pairs of signaling pathways, was used to explore the relationship between pathways.

Integrated Analysis of Interaction Network

GeneMANIA (http://genemania.org/) is a data set that provides a series of functional association information to identify the relation between genes of the submitted set in terms of their genetic interactions, pathways, expression patterns, localization, and protein domain similarity. In this study, protein-protein interaction (PPI) networks were analyzed using the GeneMANIA data set, and Cytoscape (version 3.7.2) was used to visualize the PPI networks.

Isolation and Cultivation of HFSC

Isolation of HFSCs was performed as previously described (Aran et al., 2020). Follicular unit extraction was performed to collect and isolate hair follicle tissues from 20 patients with AGA under a stereomicroscope. A needle was used to separate the hair shaft and papilla, and only the bulge areas were reserved. The bulge areas were treated with dispase II (2.5 mg/ml, Sigma, United States) and collagenase I (1 mg/ml, Gibco, United States) for 60 min, and 0.25% trypsin-ethylene diamine tetra acetic acid (EDTA; Gibco, Grand Island, NY, United States) for 15 min. The obtained cells were cultured in a keratinocyte serum-free medium (K-SFM, Gibco) in a 5% CO_2 humidified incubator at 37°C, and the medium was changed every 2–3 days. The third passage (P3) of HFSCs was characterized by immunofluorescence with an anti-K15 antibody (Santa Cruz Biotechnology, TX, United States) and was used for follow-up studies.

Cell Proliferation Assay

Cell Counting Kit 8 (CCK8) assays (Beyotime Biotechnology Company, Jiangsu, China) and 5-ethynyl-2 deoxyuridine (EdU) assays (RiboBio, Guangzhou, China) were performed to assess the cell proliferation ability. For CCK8 assays, cells were seeded at approximately 2×10^3 cells/well in 96-well plates, and cell attachment was allowed for 12 h. Then, a 10 μl CCK8 test solution was added to each well at 24, 48, 72, and 96 h, and the cells were incubated in a humidified incubator with 5% CO_2 at 37°C for 2 h at each time point to evaluate the cell growth viability. The optical density (OD) was measured at 450 nm with a microplate reader (Tecan, Thermo Scientific, United States). For EdU assays, the experiments were performed according to the manufacturer's instructions (Xiong et al., 2019). Then, the cells were observed under a fluorescence microscope (Zeiss HLA100, Shanghai, China) and analyzed by using ImageJ software (Bethesda, MD, United States). The data shown are representative of three independent experiments.

Quantitative Real-Time Polymerase Chain Reaction

Total RNA was isolated from tissues or cells using Trizol® Reagent (Life Technologies, United States) and reverse transcribed into cDNA using a cDNA synthesis kit (Thermo Scientific) according to the manufacturer's instructions. qRT-PCR was performed as previously reported (Xiong et al., 2019). Melt curves were established for the reactions, and the normalized fold expression was calculated using the $2^{-\Delta\Delta\ Ct}$ method. The primer sequences are listed in **Table 1**.

Western Blotting

The cells from each sample were collected and lysed in radioimmunoprecipitation (RIPA) buffer (Thermo Scientific), followed by centrifugation at 1,200×g for 10 min and subsequent collection of the supernatant. Western blotting was performed as previously described (Xiong et al., 2019). The primary antibodies were GAPDH (1:20,000, Proteintech, China), Lgr5 (1:1,000, Abcam, United States), TGF-β1 (1:1,000, Santa Cruz Biotechnology, United States), and β-catenin (1:1,000, Cell Signaling Technology, United States), and the secondary antibody was horseradish peroxidase-conjugated goat antimouse (1:10,000, Abcam, United States). Protein expression was observed and visualized by chemiluminescence using an Alpha Imager scanner (Tecan, Thermo Scientific).

Statistical Analysis

All data are expressed as the mean ± standard deviation, and statistical significance was determined using Student's t-test. All statistical analyses were performed using SPSS (version 17.0). Statistical significance was set at $p < 0.05$.

TABLE 1 | Primers used for qRT-PCR.

Gene	Forward primer (5′-3′)	Reverse primer (5′-3′)
GAPDH	AGAAGGCTGGGGCTCATT	TGCTAAGCAGTTGGTGGTG
AC010789.1	TGCATCCCTGGCAATACTCAG	GGAGTGCTGTGCATTCATTGG
U6	CGATACAGAGAAGATTAGCATGGC	AACGCTTCACGAATTTGCGT
hsa-miR-21-5p	GCAGTAGCTTATCAGACTGATG	AGTGCGTGTCGTGGAGTCG
TGF-β1	ATGGAGAGAGGACTGCGGAT	GTAGTGTTCCCCACTGGTCC
K6hf	TTGTAGCCCTGAAAAAGGACG	CAGCTCTGCATCAAAGACTGAG
WNT10b	CATCCAGGCACGAATGCGA	CGGTTGTGGGTATCAATGAAGA
DKK-1	GAGTACTGCGCTAGTCCCAC	TTTGCAGTAATTCCCGGGGC

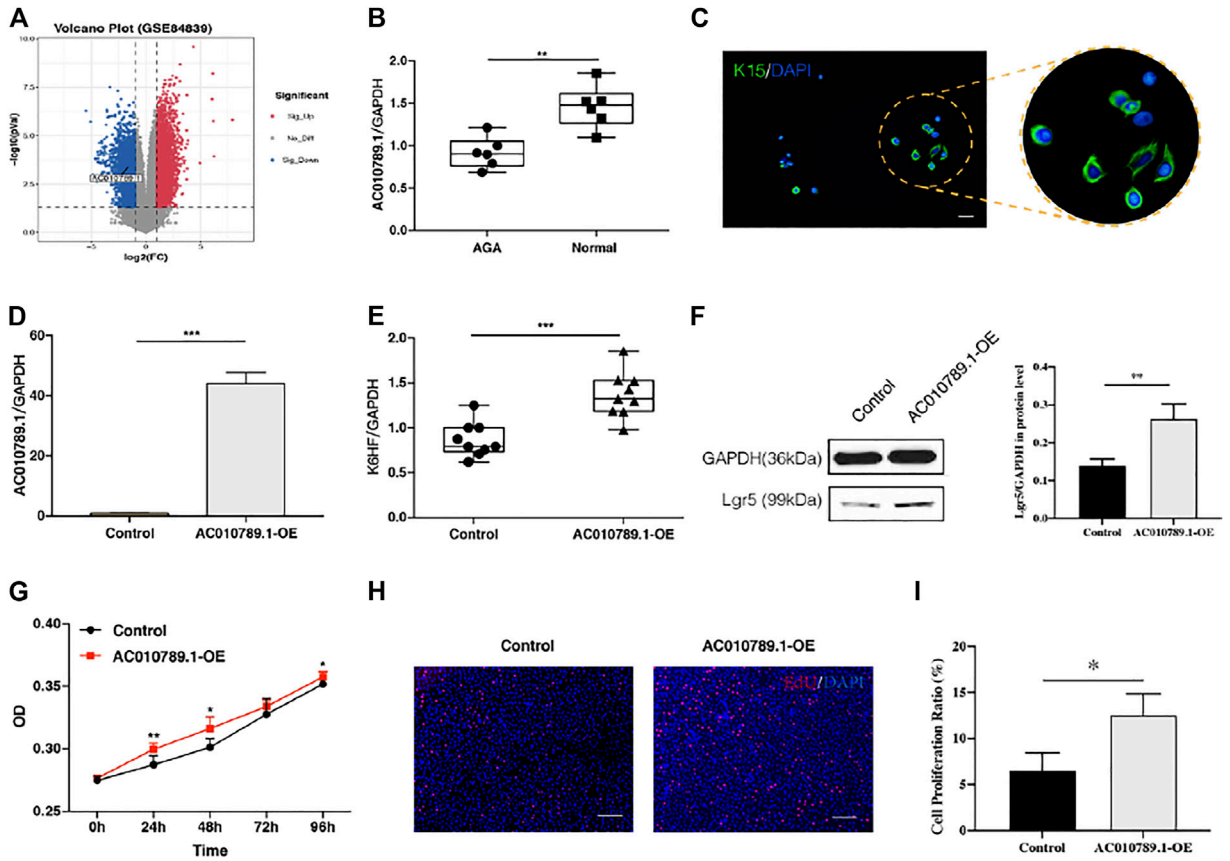

FIGURE 1 | AC010789.1 is downregulated in patients with AGA, and its overexpression promotes proliferation and differentiation of HFSCs. **(A)** Volcano plot of the GSE84839 microarray data set. **(B)** AC010789.1 was downregulated in scalp tissues compared with adjacent normal tissues of AGA patients. $n = 6$ **(C)** The HFSCs highly express K15. HFSCs were stained with green fluorescence, and all nuclei were stained with blue fluorescence. Scale bars indicate 100 μm. **(D)** The AC010789.1 overexpression HFSC cell lines were successfully constructed. **(E–I)** Overexpression of AC010789.1 increased cell abilities of differentiation and proliferation. Scale bars indicate 100 μm $n = 3$ $^{*}p < 0.05$, $^{**}p < 0.01$ and $^{***}p < 0.001$.

RESULTS

AC010789.1 Expression is Downregulated in Patients With AGA

To investigate the role of lncRNAs in AGA, we used the gene expression microarray data set GSE84839, which included the data of three pairs of male scalp AGA and adjacent normal tissues. Analysis using the screening criteria of $p < 0.05$ and $|\log FC| > 1$ revealed a total of 4,939 differentially expressed lncRNAs (4,239 upregulated and 700 downregulated). A volcano map was used to show the distribution of all differentially expressed lncRNAs (**Figure 1A**). AC010789.1, whose expression was significantly reduced in AGA scalp tissues compared with adjacent normal tissues, was selected for further analysis. To validate the results from the GSE84839 data set, we examined the expression level of AC010789.1 in clinical AGA scalp and

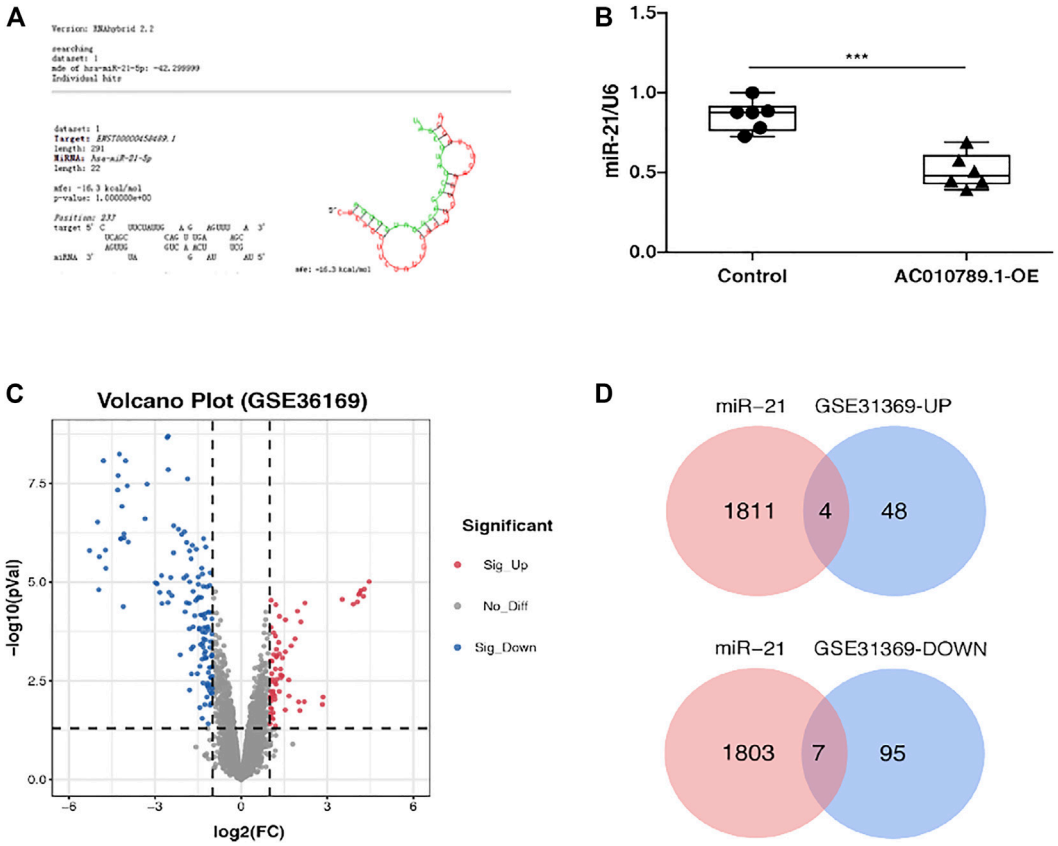

FIGURE 2 | AC010789.1 interacts with miR-21 to participate in AGA progress and exploration on the pathogenesis of AGA. **(A)** RNAhybrid v2.2 showed the putative binding sites of miR-21-5p on AC010789.1. **(B)** Relative expression of miR-21-5p in AC010789.1-OE. $n = 6$ **(C)** Volcano plot of the GSE36169 microarray data set. **(D)** Venn diagram of upregulated and downregulated DEGs among the mRNA expression profiling sets GSE36169 and hsa-miR-21-5p targeted genes. $^{*}p < 0.05$, $^{**}p < 0.01$ and $^{***}p < 0.001$.

adjacent normal tissues. The results showed that AC010789.1 expression was indeed downregulated in the AGA scalp tissues of patients (**Figure 1B**). These results strongly indicate that AC010789.1 expression is significantly downregulated in AGA scalp tissues and might be an essential predictive factor for patients with AGA.

Overexpression of AC010789.1 Promotes Proliferation and Differentiation of HFSCs

HFSCs were isolated from normal hair follicle tissues, and immunofluorescence was performed to detect the hair follicle stem cell marker K15. As shown in **Figure 1C**, the HFSCs displayed a high expression of K15. To better understand the biological effects of AC010789.1 on AGA development, we constructed an AC010789.1 overexpression plasmid, which was subsequently transfected into HFSCs. The qRT-PCR results in **Figure 1D** show that AC010789.1 was successfully overexpressed, and the resulting HFSC line (AC010789.1-OE) was used for further study. The qRT-PCR analysis showed that overexpression of AC010789.1 significantly upregulated the expression of HFSC differentiation markers K6HF and Lgr5 (**Figures 1E,F**). Subsequently, CCK8 and EdU assays revealed that AC010789.1 upregulation also resulted in increased cell proliferation (**Figures 1G–I**). Taken together, these experiments reveal that AC010789.1 has important functions in regulating the proliferation and differentiation of HFSCs.

AC010789.1 Interacts With miR-21 to Participate in AGA Progression

LncRNAs can act as miRNA sponges to regulate downstream targets. Therefore, we predicted putative candidate AC010789.1-binding miRNAs using RNAhybrid v2.2 and identified hsa-miR-21-5p as a potential candidate (**Figure 2A**). Next, we demonstrated that the expression level of hsa-miR-21-5p negatively correlated with that of AC010789.1 in AC010789.1-OE samples (**Figure 2B**). Hence, we considered hsa-miR-21-5p to be a potential target of AC010789.1.

To further evaluate the mechanism by which AC010789.1 interacts with hsa-miR-21-5p in the pathogenesis of AGA, we analyzed the gene expression microarray data set GSE36169, which contained data of AGA and adjacent normal scalp tissues from five individuals. Analysis using the same

TABLE 2 | Common genes crossed by DEGs and hsa-miR-21-5p target genes.

Gene name	Regulated
ENPP4	Upregulated
JCHAIN	Upregulated
PLP1	Upregulated
P2RY14	Upregulated
LEF1	Downregulated
BNC2	Downregulated
SPOCK1	Downregulated
THBS1	Downregulated
TIMP3	Downregulated
VSNL1	Downregulated
FGF18	Downregulated

screening criteria described above revealed a total of 198 differentially expressed genes (DEGs; 68 upregulated and 300 downregulated), which were represented on a volcano map (**Figure 2C**). Subsequently, we used the databases miRWalk and miRDB to predict the target genes of hsa-miR-21-5p and Venn diagram software to identify the genes that were common to both sets of analyses (**Figure 2D**). A total of 11 common genes (four upregulated and nine downregulated) were detected (**Table 2**).

GO Annotation and KEGG Pathway Enrichment Analysis of DEGs

To further explore the pathogenesis of AGA, we performed GO and KEGG enrichment analyses to further reveal the enrichment status of the DEGs in terms of their MFs, BPs, CCs, and pathways. With regard to BPs (**Figures 3A,E**), the upregulated DEGs were mainly involved in GO:0050776 (regulation of immune response), GO:0030199 (collagen fibril organization), and GO: 0006954 (inflammatory response), and the downregulated DEGs were mainly involved in GO:0008544 (*epidermis* development), GO:0001942 (hair follicle development), and GO:0007010 (cytoskeleton organization). In terms of CCs (**Figures 3B,F**), the majority of upregulated DEGs were components of GO: 0005576 (extracellular region), GO:0005615 (extracellular space), and GO:0072562 (blood microparticles), and the downregulated DEGs were mainly components of GO:0005882 (intermediate filament), GO:0045095 (keratin filament), and GO: 0005615 (extracellular space). For the MFs (**Figures 3C,G**), the upregulated DEGs were mainly involved in GO:0031720 (haptoglobin binding), GO:0004252 (serine-type endopeptidase activity), and GO:0048407 (platelet-derived growth factor binding), and the downregulated DEGs were mainly involved in GO:0005198 (structural molecule activity), GO:0005509 (calcium ion binding), and GO:0008013 (beta-catenin binding). KEGG pathway analysis was used to explore pathway enrichment of the DEGs (**Figures 3D,H**). The most upregulated DEGs were significantly enriched in hsa05143 (African trypanosomiasis), hsa05144 (malaria), and hsa05150 (*Staphylococcus aureus* infection), and the downregulated DEGs were mainly enriched in hsa05144 (malaria), hsa04151 (PI3K-Akt signaling pathway), and hsa04350 (TGF-beta signaling pathway).

Comprehensive Analysis of the Common DEGs

Next, the PPI networks of the common DEGs were analyzed using GeneMANIA, and the 20 most relevant genes were identified. GPM6B, SOX10, MBP, PIM2, CDH19, PMP2, GPM6A, PTPRN, MAG, TNFRSF17, ENPP6, ENPP2, SP2, ITGAV, SPI1, PIGO, CD79A, ENPP7, PIGG, and ENPP5 were primarily associated with the PPI network of the upregulated

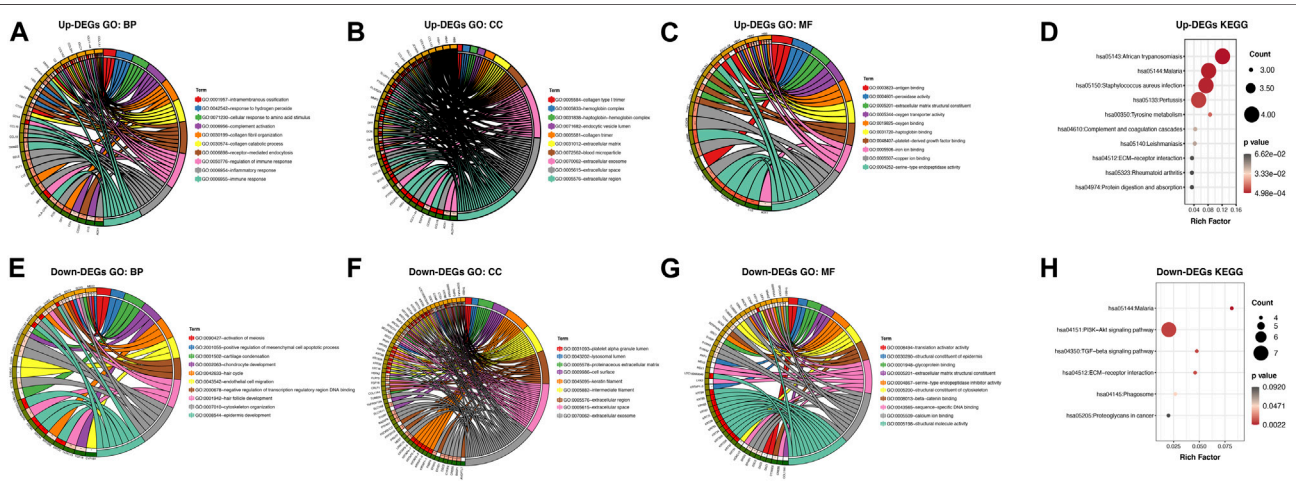

FIGURE 3 | GO annotation and KEGG pathway enrichment analysis of the DEGs through the DAVID database. **(A,E)** The category of "biological process" of upregulated DEGs and downregulated DEGs, respectively. **(B,F)** The category of "cellular component" of upregulated DEGs and downregulated DEGs, respectively. **(C,G)** The category of "molecular function" of the predicted TG of upregulated DEGs and downregulated DEGs, respectively. **(D,H)** The category of "KEGG" of upregulated DEGs and downregulated DEGs, respectively.

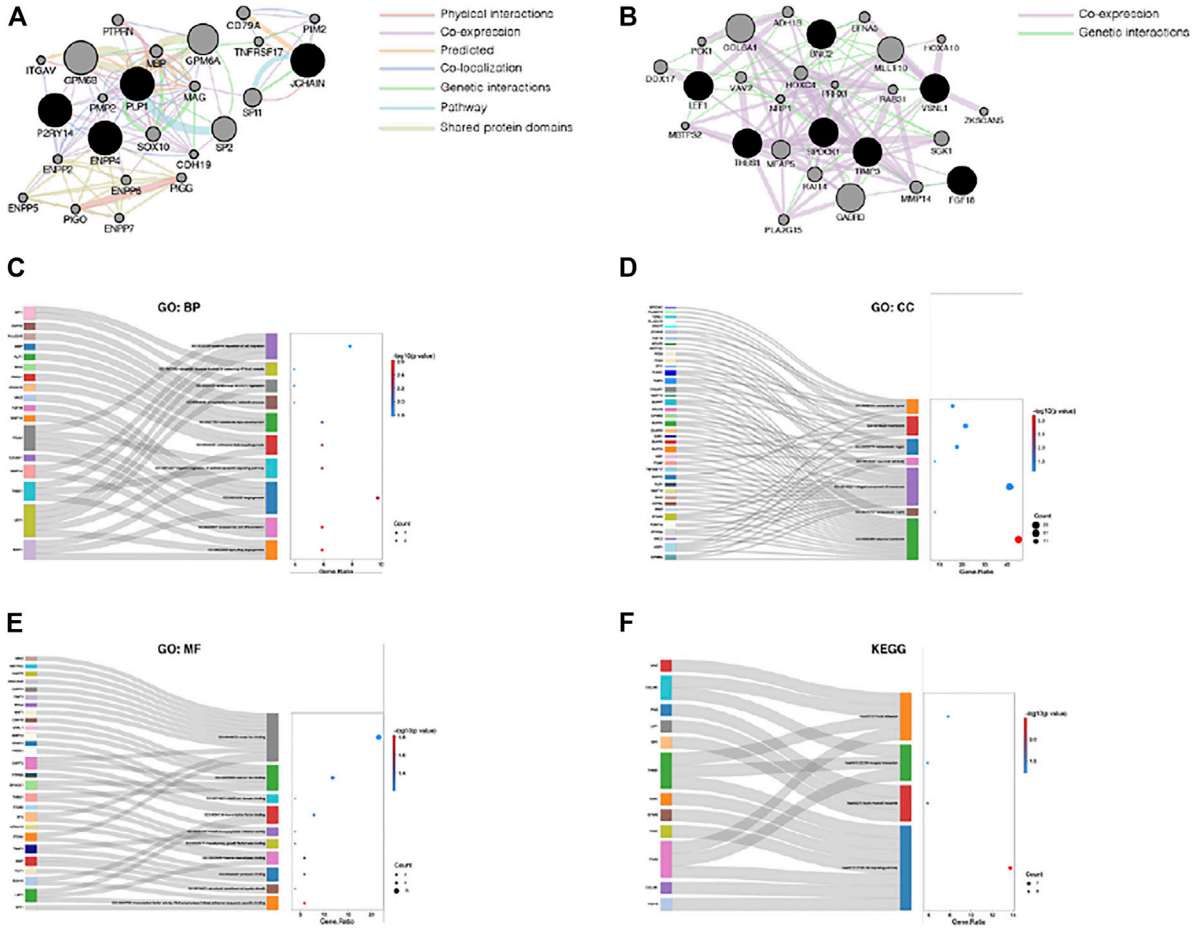

FIGURE 4 | Comprehensive analysis of the common DEGs. **(A)** PPI network of the upregulated common DEGs. **(B)** PPI network of the downregulated common DEGs. **(C)** The category of "biological process" of the common DEGs and their most relevant genes. **(D)** The category of "cellular component" of the common DEGs and their most relevant genes. **(E)** The category of "molecular function" of the common DEGs and their most relevant genes. **(F)** The category of "KEGG" of the common DEGs and their most relevant genes.

common genes (**Figure 4A**), and COL6A1, GABRD, MLLT10, MFAP5, SGK1, RAI14, DDX17, HOXC4, MMP14, ADH1B, VAV2, EFNA5, PLA2G15, RAB31, PCK1, HOXA10, NRP1, ZKSCAN5, MBTPS2, and PRRX1 were primarily associated with the PPI network of the downregulated common genes (**Figure 4B**). Furthermore, all the common DEGs and their 20 most relevant network genes were analyzed by GO and KEGG enrichment analysis. For BP (**Figure 4C**), most of the genes were involved in GO:0002040 (sprouting angiogenesis), GO:0035987 (endodermal cell differentiation), and GO:0001525 (angiogenesis). For CC (**Figure 4D**), the genes were mainly components of GO:0005886 (plasma membrane) and GO: 0031012 (extracellular matrix). With regard to MF (**Figure 4E**), a majority of the genes were involved in GO: 0003705 (transcription factor activity, RNA polymerase II distal enhancer sequence-specific binding), GO:0019911 (structural constituent of myelin sheath), and GO:0002020 (protease binding). KEGG pathway enrichment analysis results showed that hsa04151 (PI3K-Akt signaling pathway) and hsa05221 (acute myeloid leukemia) were the most significantly enriched pathways of the genes (**Figure 4F**).

AC010789.1 Targets the Wnt/β-Catenin Signaling Pathway to Regulate AGA Progression

According to the results of KEGG pathway enrichment analysis, a majority of the enriched pathways were highly associated with Wnt/β-catenin signaling (**Figures 5A,B**). Thus, we analyzed the mRNA and protein expression levels of several key genes of the Wnt/β-catenin pathway, including DKK-1, TGF-β1, Wnt10b, and β-catenin in AC010789.1-OE. The results showed that the expression of DKK-1 and TGF-β1 was significantly downregulated, whereas the expression of Wnt10b and β-catenin was significantly upregulated in AC010789.1-OE compared with control cells (**Figures 5C–F**). These data suggest that AC010789.1 may participate in AGA progression by regulating the Wnt/β-catenin pathway.

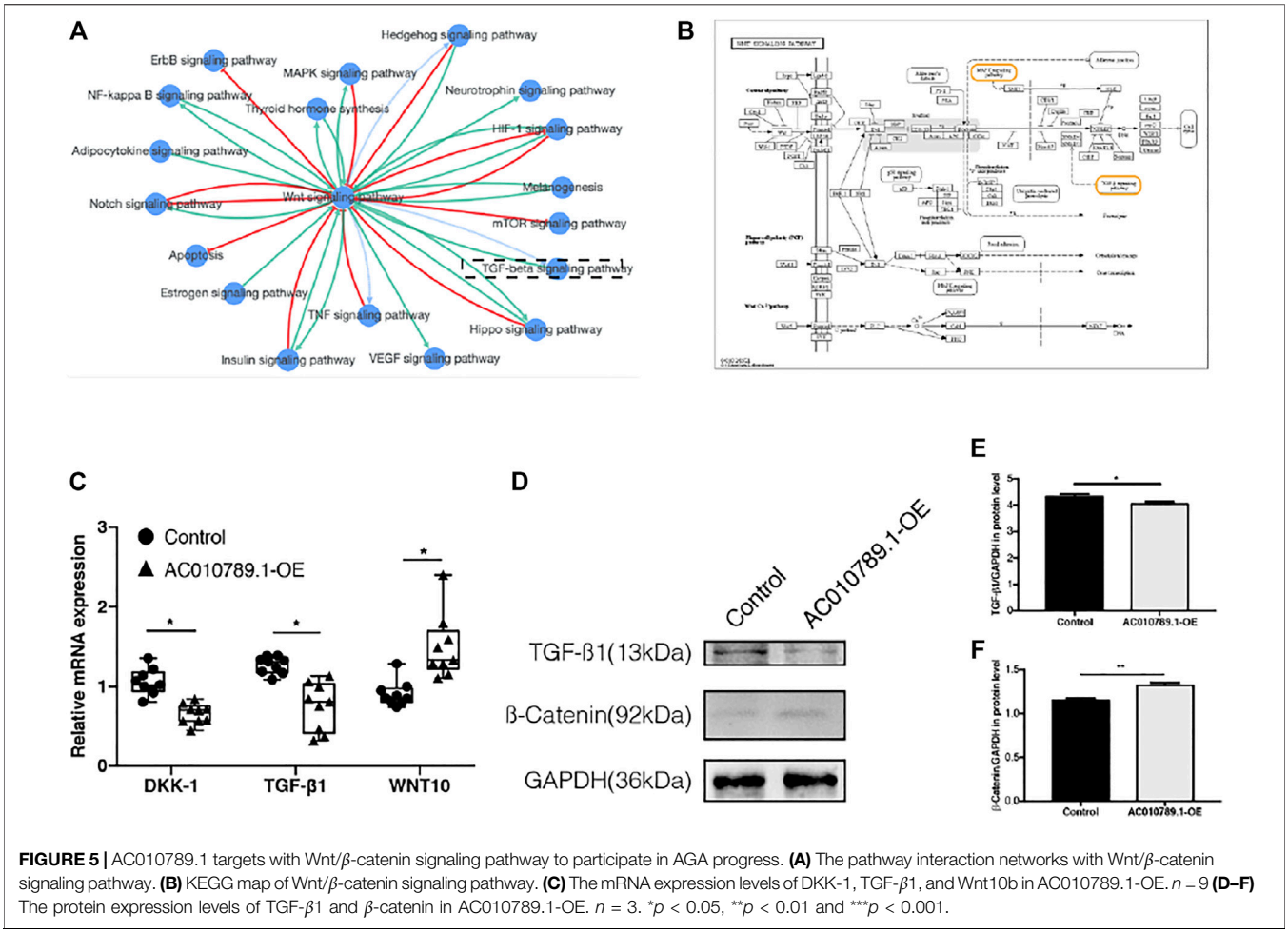

FIGURE 5 | AC010789.1 targets with Wnt/β-catenin signaling pathway to participate in AGA progress. **(A)** The pathway interaction networks with Wnt/β-catenin signaling pathway. **(B)** KEGG map of Wnt/β-catenin signaling pathway. **(C)** The mRNA expression levels of DKK-1, TGF-β1, and Wnt10b in AC010789.1-OE. $n = 9$ **(D–F)** The protein expression levels of TGF-β1 and β-catenin in AC010789.1-OE. $n = 3$. $^{*}p < 0.05$, $^{**}p < 0.01$ and $^{***}p < 0.001$.

DISCUSSION

AGA is an androgen-dependent genetic hair loss disorder characterized by progressive microencapsulation of hair follicles and continuous shortening of the hair follicle growth period (Randall et al., 2000; Rathnayake and Sinclair, 2010). It is currently the most common clinical type of alopecia and can seriously affect a patient's appearance, mental health, and social behavior. The most common first-line treatments for AGA currently include finasteride and minoxidil, but their application is hindered by limited efficacy, the need for long-term treatment, and inevitable complications. Hair transplant surgery, which involves hair follicle redistribution, is an effective method to improve the appearance of patients; however, as hair follicles cannot be regenerated, AGA patients with large areas of alopecia often have insufficient donor site hair follicles (Rogers, 2015). Therefore, it is necessary to explore the potential molecular mechanisms of AGA onset, progression, and hair follicle regeneration to design more effective treatments.

Several studies indicate that lncRNAs play essential roles in the occurrence and progression of various diseases and that they could be used as new diagnostic and treatment markers. For example, Wang et al. (2018) report that lncHOXA-AS2 promotes the progression of various human tumors by inducing epithelial–mesenchymal transition by directly inhibiting Bax expression, promoting c-Myc and Bcl-2 expression, and activating the Akt-MMP signaling pathway. Accumulating evidence now indicates that the deregulation of the expression of lncRNAs is strongly correlated with the onset and development of AGA (Bao et al., 2017; Zhu et al., 2020). In this study, we used the GSE84839 microarray data set from the GEO database and found that AC010789.1 was expressed to a lower level in AGA scalp tissues than in adjacent normal tissues, which was verified using clinical AGA samples. This suggests that low expression of AC010789.1 is associated with the progression of AGA.

HFSC aging, characterized by a reduction in stemness signatures and a concomitant increase in epidermal commitment, leads to a progressive miniaturization of hair follicles and ultimately, to the hair loss characteristic of AGA (Matsumura et al., 2016). Recently, accumulating evidence indicates that activating HFSCs could be an effective treatment for AGA. Zhang et al. (2020) found that vascular endothelial growth factor significantly reduced 5α-dihydrotestosterone-induced HFSC apoptosis by inhibiting the PI3K-Akt pathway, thereby delaying the progression of AGA. Kubo et al. (2020) used fisetin to induce a telogen-to-anagen transition in hair follicles by inducing the proliferation of HFSCs,

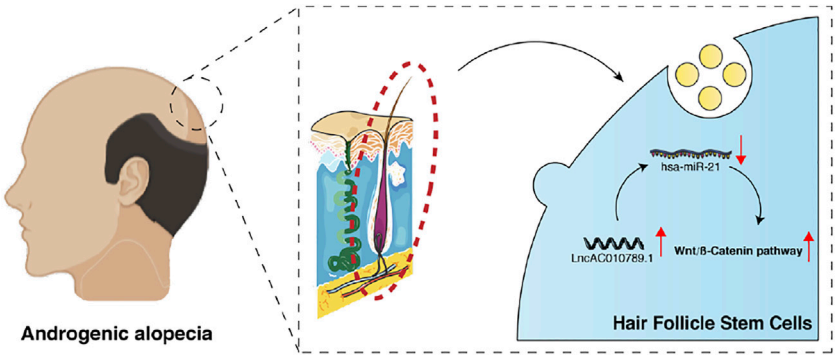

FIGURE 6 | A schematic diagram shows how AC010789.1 delays AGA progression by targeting microRNA-21 and the Wnt/β-catenin signaling pathway.

thus promoting hair growth. Therefore, we hypothesized that AC010789.1 may promote hair growth by promoting the proliferation and differentiation of HFSCs. In the current study, we successfully isolated K15-positive HFSCs from hair follicles of patients with AGA and constructed an AC010789.1-overexpressing HFSC line. K6HF and Lgr5 are shown to be particularly good markers of hair differentiation and proliferation (Roh et al., 2004; Chen et al., 2020b), and we found that the expression of both marker genes as well as the cell proliferation rate were significantly higher in AC010789.1-OE than in the control group, indicating an important role of AC010789.1 in regulating HFSC functions.

Emerging evidence indicates that a large number of lncRNAs participate in a variety of biological functions by interacting with miRNAs and regulating their target genes (Huang, 2018). In this study, we found that AC010789.1 interacts with miR-21 to participate in the progression of AGA. Many reports show that miR-21 plays an essential role in the regulation of several diseases (Lakhter et al., 2018; Wang et al., 2020). To further explore how the interaction between AC010789.1 and hsa-miR-21-5p regulates the pathogenesis of AGA, the GSE36169 microarray data were downloaded, and the genes targeted by hsa-miR-21-5p were identified. A total of 198 AGA-related DEGs, including 11 common genes intersecting with hsa-miR-21-5p target genes, were identified by differential analysis with adjacent normal controls. GO annotation enrichment analysis was performed to explore the biological functions of the AGA-associated DEGs. The upregulated DEGs were primarily enriched in the BP category of immune and inflammatory responses. Previous studies show that an abundance of immune inflammatory cells in the bulge area of the hair follicle leads to the deregulation of the hair follicle microenvironment, thus impairing the normal function of HFSCs and resulting in alopecia (Wang and Higgins, 2020). Interestingly, the downregulated DEGs were directly related to hair follicle development (GO:0001942) and the hair cycle (GO:0042633). Subsequently, we extended the PPI network of the common genes and performed annotated enrichment analysis. Notably, the most downregulated common genes and their most relevant network genes were enriched in angiogenesis. Vascularization is closely related to hair growth (Gentile and Garcovich, 2019). The vascular system plays a vital role in maintaining the HFSC microenvironment, and angiogenesis helps to increase the blood supply of DPCs and promote hair growth. These findings enhance our understanding of the pathogenesis of AGA and the potential mechanism of interaction between AC010789.1 and miR-21-5p to delay the progression of AGA.

The TGF-β1 and Wnt signaling pathways are the most crucial pathways for maintaining a quiescent niche and regulating the proliferation and differentiation of HFSCs (Yang and Peng, 2010; Ge et al., 2019). Previous studies report that TGF-β1 promotes telogen-to-anagen transition in hair follicles, whereas the transition from anagen to telogen is significantly delayed in the hair follicles of TGF-β1 knockout mice (Foitzik et al., 2000; Daszczuk et al., 2020). The Wnt signaling pathway is the main regulatory pathway of biological development and a key driving factor for stem cells in most tissues (Nusse and Clevers, 2017). In the hair follicle, the Wnt signaling pathway plays a key role in starting the hair follicle cycle by initiating the proliferation response of HFSCs in the bulge area; HFSCs treated with Wnt pathway activator can quickly enter the proliferation period (Greco et al., 2009; Hawkshaw et al., 2020). Moreover, Leirós et al. (2017) found that Wnt pathway inhibitors (DKK-1) impair the differentiation of HFSCs, and the addition of promoters (Wnt10b) can reverse this effect in AGA. In addition, miR-21 is closely related to the Wnt/β-catenin signaling pathway. Previous studies reveal that inhibiting the expression of miR-21 can lead to upregulation of the Wnt/β-catenin pathway, thereby promoting cell activity (Hao et al., 2019; Liu et al., 2019). A recent study also reveals that lncRNA GAS5 competitively combined with miR-21 to regulate the epithelial–mesenchymal transition of human peritoneal mesothelial cells via activation of Wnt/β-catenin signaling (Fan et al., 2021). In this study, we conducted a comprehensive pathway analysis of the DEGs, common genes, and the genes most closely related in the PPI network to help us understand the molecular mechanisms underlying AGA progression. In line with our results, we found that the upregulated DEGs were highly enriched in the TGF-β signaling pathway, and a majority of the pathways were highly correlated with the Wnt/β-catenin signaling pathway. Further analysis showed that AC010789.1 overexpression induced the upregulation of Wnt10b and β-catenin, and downregulation of DKK-1 and TGF-β1. In summary, our results suggest that AC010789.1 regulates Wnt/β-catenin pathway activation,

thereby enhancing the proliferation and differentiation of HFSCs and participating in AGA progression.

In summary, our data shows that AC010789.1 overexpression delayed AGA progression through the downregulation of hsa-miR-21-5p and promotion of the Wnt/β-catenin signaling pathway (**Figure 6**). Our findings provide a novel insight into the mechanism by which AC010789.1 promotes the proliferation and differentiation of HFSCs, which sheds light on the future development of lncRNA-based AGA therapies.

DATA AVAILABILITY STATEMENT

All datasets generated for this study are included in the article/Supplementary Material, further inquiries can be directed to the corresponding authors.

AUTHOR CONTRIBUTIONS

HJ and YL designed the study; JX performed and drafted the experiment; BW and XH revised manuscript, and all authors approved the final version of the manuscript.

FUNDING

This work was supported by the east hospital affiliated to tongji university introduced talent research startup fund (grant no. DFRC2019008), clinical expansion foundation of PLA (Key Program) (grant no. 18KS1643), tongji hospital affiliated to tongji university excellent talent training program (grant no. HBRC2002), and featured clinical discipline project of shanghai pudong (grant no. PWYts2021-07).

REFERENCES

Aran, S., Zahri, S., Asadi, A., Khaksar, F., and Abdolmaleki, A. (2020). Hair Follicle Stem Cells Differentiation into Bone Cells on Collagen Scaffold. *Cell Tissue Bank* 21 (2), 181–188. doi:10.1007/s10561-020-09812-9

Baker, R. E., and Murray, P. J. (2012). Understanding Hair Follicle Cycling: a Systems Approach. *Curr. Opin. Genet. Dev.* 22 (6), 607–612. doi:10.1016/j.gde.2012.11.007

Bao, L., Yu, A., Luo, Y., Tian, T., Dong, Y., Zong, H., et al. (2017). Genomewide Differential Expression Profiling of Long Non-coding RNAs in Androgenetic Alopecia in a Chinese Male Population. *J. Eur. Acad. Dermatol. Venereol.* 31 (8), 1360–1371. doi:10.1111/jdv.14278

Bas, Y., Seckin, H. Y., Kalkan, G., Takci, Z., Citil, R., Önder, Y., et al. (2015). Prevalence and Types of Androgenetic Alopecia in north Anatolian Population: A Community-Based Study. *J. Pak Med. Assoc.* 65 (8), 806–809.

Chen, L., Zhang, J., Wang, L., Wang, H., and Chen, B. (2020a). The Efficacy and Safety of Finasteride Combined with Topical Minoxidil for Androgenetic Alopecia: A Systematic Review and Meta-Analysis. *Aesth Plast. Surg.* 44 (3), 962–970. doi:10.1007/s00266-020-01621-5

Chen, P., Miao, Y., Zhang, F., Huang, J., Chen, Y., Fan, Z., et al. (2020b). Nanoscale Microenvironment Engineering Based on Layer-By-Layer Self-Assembly to Regulate Hair Follicle Stem Cell Fate for Regenerative Medicine. *Theranostics* 10 (25), 11673–11689. doi:10.7150/thno.48723

Chew, E. G. Y., Tan, J. H. J., Bahta, A. W., Ho, B. S.-Y., Liu, X., Lim, T. C., et al. (2016). Differential Expression between Human Dermal Papilla Cells from Balding and Non-balding Scalps Reveals New Candidate Genes for Androgenetic Alopecia. *J. Invest. Dermatol.* 136 (8), 1559–1567. doi:10.1016/j.jid.2016.03.032

Chouhan, K., Kota, R. S., Kumar, A., and Gupta, J. (2019a). Assessment of Safe Donor Zone of Scalp and Beard for Follicular Unit Extraction in Indian Men: A Study of 580 Cases. *J. Cutan. Aesthet. Surg.* 12 (1), 31–35. doi:10.4103/jcas.jcas_142_18

Chouhan, K., Roga, G., Kumar, A., and Gupta, J. (2019b). Approach to Hair Transplantation in Advanced Grade Baldness by Follicular Unit Extraction: A Retrospective Analysis of 820 Cases. *J. Cutan. Aesthet. Surg.* 12 (4), 215–222. doi:10.4103/jcas.jcas_173_18

Cotsarelis, G., Sun, T.-T., and Lavker, R. M. (1990). Label-retaining Cells Reside in the Bulge Area of Pilosebaceous Unit: Implications for Follicular Stem Cells, Hair Cycle, and Skin Carcinogenesis. *Cell* 61 (7), 1329–1337. doi:10.1016/0092-8674(90)90696-c

Daszczuk, P., Mazurek, P., Pieczonka, T. D., Olczak, A., Boryń, Ł. M., and Kobielak, K. (2020). An Intrinsic Oscillation of Gene Networks inside Hair Follicle Stem Cells: An Additional Layer that Can Modulate Hair Stem Cell Activities. *Front. Cell Dev. Biol.* 8, 595178. doi:10.3389/fcell.2020.595178

Dennis, G., Jr., Sherman, B. T., Hosack, D. A., Yang, J., Gao, W., Lane, H. C., et al. (2003). DAVID: Database for Annotation, Visualization, and Integrated Discovery. *Genome Biol.* 4 (5), P3. doi:10.1186/gb-2003-4-5-p3

Ding, Q., Xu, Y.-X., Sun, W.-L., Liu, J.-J., Deng, Y.-Y., Wu, Q.-F., et al. (2020). Early-onset Androgenetic Alopecia in China: a Descriptive Study of a Large Outpatient Cohort. *J. Int. Med. Res.* 48 (3), 030006051989719. doi:10.1177/0300060519897190

Fan, Y., Zhao, X., Ma, J., and Yang, L. (2021). LncRNA GAS5 Competitively Combined with miR-21 Regulates PTEN and Influences EMT of Peritoneal Mesothelial Cells via Wnt/β-Catenin Signaling Pathway. *Front. Physiol.* 12, 654951. doi:10.3389/fphys.2021.654951

Foitzik, K., Lindner, G., Mueller-Roever, S., Maurer, M., Botchkareva, N., Botchkarev, V., et al. (2000). Control of Murine Hair Follicle Regression (Catagen) by TGF-β1 *In Vivo*. *FASEB j.* 14 (5), 752–760. doi:10.1096/fasebj.14.5.752

Fu, J., and Hsu, W. (2013). Epidermal Wnt Controls Hair Follicle Induction by Orchestrating Dynamic Signaling Crosstalk between the Epidermis and Dermis. *J. Invest. Dermatol.* 133 (4), 890–898. doi:10.1038/jid.2012.407

Garza, L. A., Yang, C.-C., Zhao, T., Blatt, H. B., Lee, M., He, H., et al. (2011). Bald Scalp in Men with Androgenetic Alopecia Retains Hair Follicle Stem Cells but Lacks CD200-Rich and CD34-Positive Hair Follicle Progenitor Cells. *J. Clin. Invest.* 121 (2), 613–622. doi:10.1172/jci44478

Ge, M., Liu, C., Li, L., Lan, M., Yu, Y., Gu, L., et al. (2019). miR-29a/b1 Inhibits Hair Follicle Stem Cell Lineage Progression by Spatiotemporally Suppressing WNT and BMP Signaling. *Cell Rep.* 29 (8), 2489–2504. doi:10.1016/j.celrep.2019.10.062

Gentile, P., and Garcovich, S. (2019). Advances in Regenerative Stem Cell Therapy in Androgenic Alopecia and Hair Loss: Wnt Pathway, Growth-Factor, and Mesenchymal Stem Cell Signaling Impact Analysis on Cell Growth and Hair Follicle Development. *Cells* 8 (5), 466. doi:10.3390/cells8050466

Goren, A., Naccarato, T., Situm, M., Kovacevic, M., Lotti, T., and McCoy, J. (2017). Mechanism of Action of Minoxidil in the Treatment of Androgenetic Alopecia Is Likely Mediated by Mitochondrial Adenosine Triphosphate Synthase-Induced Stem Cell Differentiation. *J. Biol. Regul. Homeost Agents* 31 (4), 1049–1053.

Greco, V., Chen, T., Rendl, M., Schober, M., Pasolli, H. A., Stokes, N., et al. (2009). A Two-step Mechanism for Stem Cell Activation during Hair Regeneration. *Cell Stem Cell* 4 (2), 155–169. doi:10.1016/j.stem.2008.12.009

Hao, L., Wang, J., and Liu, N. (2019). Long Noncoding RNA TALNEC2 Regulates Myocardial Ischemic Injury in H9c2 Cells by Regulating miR-21/PDCD4-medited Activation of Wnt/β-catenin Pathway. *J. Cell Biochem* 120 (8), 12912–12923. doi:10.1002/jcb.28562

Hawkshaw, N. J., Hardman, J. A., Alam, M., Jimenez, F., and Paus, R. (2020). Deciphering the Molecular Morphology of the Human Hair Cycle: Wnt

Signalling during the Telogen-Anagen Transformation. *Br. J. Dermatol.* 182 (5), 1184–1193. doi:10.1111/bjd.18356

Ho, A., and Shapiro, J. (2019). Medical Therapy for Frontal Fibrosing Alopecia: A Review and Clinical Approach. *J. Am. Acad. Dermatol.* 81 (2), 568–580. doi:10.1016/j.jaad.2019.03.079

Huang, Y. (2018). The Novel Regulatory Role of lncRNA-miRNA-mRNA axis in Cardiovascular Diseases. *J. Cell Mol Med* 22 (12), 5768–5775. doi:10.1111/jcmm.13866

Jimenez-Cauhe, J., Saceda-Corralo, D., Rodrigues-Barata, R., Hermosa-Gelbard, A., Moreno-Arrones, O. M., Fernandez-Nieto, D., et al. (2019). Effectiveness and Safety of Low-Dose Oral Minoxidil in Male Androgenetic Alopecia. *J. Am. Acad. Dermatol.* 81 (2), 648–649. doi:10.1016/j.jaad.2019.04.054

Katzer, T., Leite Junior, A., Beck, R., and da Silva, C. (2019). Physiopathology and Current Treatments of Androgenetic Alopecia: Going beyond Androgens and Anti-androgens. *Dermatol. Ther.* 32 (5), e13059. doi:10.1111/dth.13059

Kubo, C., Ogawa, M., Uehara, N., and Katakura, Y. (2020). Fisetin Promotes Hair Growth by Augmenting TERT Expression. *Front. Cell Dev. Biol.* 8, 566617. doi:10.3389/fcell.2020.566617

Lakhter, A. J., Pratt, R. E., Moore, R. E., Doucette, K. K., Maier, B. F., DiMeglio, L. A., et al. (2018). Beta Cell Extracellular Vesicle miR-21-5p Cargo Is Increased in Response to Inflammatory Cytokines and Serves as a Biomarker of Type 1 Diabetes. *Diabetologia* 61 (5), 1124–1134. doi:10.1007/s00125-018-4559-5

Leirós, G. J., Ceruti, J. M., Castellanos, M. L., Kusinsky, A. G., and Balañá, M. E. (2017). Androgens Modify Wnt Agonists/antagonists Expression Balance in Dermal Papilla Cells Preventing Hair Follicle Stem Cell Differentiation in Androgenetic Alopecia. *Mol. Cell Endocrinol.* 439, 26–34. doi:10.1016/j.mce.2016.10.018

Lin, B.-J., Lin, G.-Y., Zhu, J.-Y., Yin, G.-Q., Huang, D., and Yan, Y.-Y. (2020a). LncRNA-PCAT1 Maintains Characteristics of Dermal Papilla Cells and Promotes Hair Follicle Regeneration by Regulating miR-329/Wnt10b axis. *Exp. Cell Res.* 394 (1), 112031. doi:10.1016/j.yexcr.2020.112031

Lin, B.-J., Zhu, J.-Y., Ye, J., Lu, S.-D., Liao, M.-D., Meng, X.-C., et al. (2020b). LncRNA-XIST Promotes Dermal Papilla Induced Hair Follicle Regeneration by Targeting miR-424 to Activate Hedgehog Signaling. *Cell Signal.* 72, 109623. doi:10.1016/j.cellsig.2020.109623

Liu, X. G., Zhang, Y., Ju, W. F., Li, C. Y., and Mu, Y. C. (2019). MiR-21 Relieves Rheumatoid Arthritis in Rats via Targeting Wnt Signaling Pathway. *Eur. Rev. Med. Pharmacol. Sci.* 23 (3 Suppl. l), 96–103. doi:10.26355/eurrev_201908_18635

Matsumura, H., Mohri, Y., Binh, N. T., Morinaga, H., Fukuda, M., Ito, M., et al. (2016). Hair Follicle Aging Is Driven by Transepidermal Elimination of Stem Cells via COL17A1 Proteolysis. *Science* 351 (6273), aad4395. doi:10.1126/science.aad4395

Molina-Leyva, A., Caparros-Del Moral, I., Gomez-Avivar, P., Alcalde-Alonso, M., and Jimenez-Moleon, J. J. (2016). Psychosocial Impairment as a Possible Cause of Sexual Dysfunction Among Young Men with Mild Androgenetic Alopecia: A Cross-Sectional Crowdsourcing Web-Based Study. *Acta Dermatovenerol Croat.* 24 (1), 42–48.

Morris, R. J., Liu, Y., Marles, L., Yang, Z., Trempus, C., Li, S., et al. (2004). Capturing and Profiling Adult Hair Follicle Stem Cells. *Nat. Biotechnol.* 22 (4), 411–417. doi:10.1038/nbt950

Motofei, I. G., Rowland, D. L., Tampa, M., Sarbu, M.-I., Mitran, M.-I., Mitran, C.-I., et al. (2020). Finasteride and Androgenic Alopecia; from Therapeutic Options to Medical Implications. *J. Dermatol. Treat.* 31 (4), 415–421. doi:10.1080/09546634.2019.1595507

Nusse, R., and Clevers, H. (2017). Wnt/β-Catenin Signaling, Disease, and Emerging Therapeutic Modalities. *Cell* 169 (6), 985–999. doi:10.1016/j.cell.2017.05.016

Oshima, H., Rochat, A., Kedzia, C., Kobayashi, K., and Barrandon, Y. (2001). Morphogenesis and Renewal of Hair Follicles from Adult Multipotent Stem Cells. *Cell* 104 (2), 233–245. doi:10.1016/s0092-8674(01)00208-2

Owczarczyk-Saczonek, A., Krajewska-Włodarczyk, M., Kruszewska, A., Banasiak, Ł., Placek, W., Maksymowicz, W., et al. (2018). Therapeutic Potential of Stem Cells in Follicle Regeneration. *Stem Cell Int.* 2018, 1–16. doi:10.1155/2018/1049641

Randall, V. A., Hibberts, N. A., Thornton, M. J., Hamada, K., Merrick, A. E., Kato, S., et al. (2000). The Hair Follicle: a Paradoxical Androgen Target Organ. *Horm. Res. Paediatr.* 54 (5-6), 243–250. doi:10.1159/000053266

Rathnayake, D., and Sinclair, R. (2010). Male Androgenetic Alopecia. *Expert Opin. Pharmacother.* 11 (8), 1295–1304. doi:10.1517/14656561003752730

Rogers, N. (2015). Hair Transplantation Update. *Sem Cutan. Med. Surg.* 34 (2), 89–94. doi:10.12788/j.sder.2015.0131

Roh, C., Tao, Q., and Lyle, S. (2004). Dermal Papilla-Induced Hair Differentiation of Adult Epithelial Stem Cells from Human Skin. *Physiol. Genomics* 19 (2), 207–217. doi:10.1152/physiolgenomics.00134.2004

Spinucci, G., and Pasquali, R. (1996). Finasteride: a New Drug for the Treatment of Male Hirsutism and Androgenetic Alopecia? *Clin. Ter* 147 (6), 305–315.

Wang, E. C. E., and Higgins, C. A. (2020). Immune Cell Regulation of the Hair Cycle. *Exp. Dermatol.* 29 (3), 322–333. doi:10.1111/exd.14070

Wang, G., Zhou, Y., Chen, W., Yang, Y., Ye, J., Ou, H., et al. (2020). miR-21-5p Promotes Lung Adenocarcinoma Cell Proliferation, Migration and Invasion via Targeting WWC2. *Cbm* 28 (4), 549–559. doi:10.3233/cbm-201489

Wang, J., Su, Z., Lu, S., Fu, W., Liu, Z., Jiang, X., et al. (2018). LncRNA HOXA-AS2 and its Molecular Mechanisms in Human Cancer. *Clinica Chim. Acta* 485, 229–233. doi:10.1016/j.cca.2018.07.004

Xiong, J., Ji, B., Wang, L., Yan, Y., Liu, Z., Fang, S., et al. (2019). Human Adipose-Derived Stem Cells Promote Seawater-Immersed Wound Healing by Activating Skin Stem Cells via the EGFR/MEK/ERK Pathway. *Stem Cell Int.* 2019, 1–16. doi:10.1155/2019/7135974

Xiong, J., Xue, Y., Xia, Y., Zhao, J., and Wang, Y. (2020). Identification of Key microRNAs of Plasma Extracellular Vesicles and Their Diagnostic and Prognostic Significance in Melanoma. *Open Med. (Wars)* 15 (1), 464–482. doi:10.1515/med-2020-0111

Yang, H., Adam, R. C., Ge, Y., Hua, Z. L., and Fuchs, E. (2017). Epithelial-Mesenchymal Micro-niches Govern Stem Cell Lineage Choices. *Cell* 169 (3), 483–496. doi:10.1016/j.cell.2017.03.038

Yang, L., and Peng, R. (2010). Unveiling Hair Follicle Stem Cells. *Stem Cell Rev Rep* 6 (4), 658–664. doi:10.1007/s12015-010-9172-z

Yao, R.-W., Wang, Y., and Chen, L.-L. (2019). Cellular Functions of Long Noncoding RNAs. *Nat. Cell Biol* 21 (5), 542–551. doi:10.1038/s41556-019-0311-8

Zhang, X., Zhou, D., Ma, T., and Liu, Q. (2020). Vascular Endothelial Growth Factor Protects CD200-Rich and CD34-Positive Hair Follicle Stem Cells against Androgen-Induced Apoptosis through the Phosphoinositide 3-Kinase/Akt Pathway in Patients with Androgenic Alopecia. *Ds* 46 (3), 358–368. doi:10.1097/dss.0000000000002091

Zhu, N., Lin, E., Zhang, H., Liu, Y., Cao, G., Fu, C., et al. (2020). LncRNA H19 Overexpression Activates Wnt Signaling to Maintain the Hair Follicle Regeneration Potential of Dermal Papilla Cells. *Front. Genet.* 11, 694. doi:10.3389/fgene.2020.00694

Conflict of Interest: The authors declare that the research was conducted in the absence of any commercial or financial relationships that could be construed as a potential conflict of interest.

Publisher's Note: All claims expressed in this article are solely those of the authors and do not necessarily represent those of their affiliated organizations, or those of the publisher, the editors and the reviewers. Any product that may be evaluated in this article, or claim that may be made by its manufacturer, is not guaranteed or endorsed by the publisher.

frontiers in Cell and Developmental Biology

REVIEW
published: 23 February 2022
doi: 10.3389/fcell.2022.824812

Recent Advances in Enhancement Strategies for Osteogenic Differentiation of Mesenchymal Stem Cells in Bone Tissue Engineering

Kangkang Zha[1,2†], *Yue Tian*[3†], *Adriana C. Panayi*[4], *Bobin Mi*[1,2*] *and Guohui Liu*[1,2*]

[1]Department of Orthopaedics, Union Hospital, Tongji Medical College, Huazhong University of Science and Technology, Wuhan, China, [2]Hubei Province Key Laboratory of Oral and Maxillofacial Development and Regeneration, Wuhan, China, [3]Department of Military Patient Management, The Second Medical Center & National Clinical Research Center for Geriatric Diseases, Institute of Orthopaedics, Chinese PLA General Hospital, Beijing, China, [4]Division of Plastic Surgery, Brigham and Women's Hospital and Harvard Medical School, Boston, MA, United States

OPEN ACCESS

Edited by:
Selim Kuci,
University Hospital Frankfurt, Germany

Reviewed by:
Dirk Henrich,
University Hospital Frankfurt, Germany
Janos Kanczler,
University of Southampton,
United Kingdom

***Correspondence:**
Bobin Mi
mibobin@hust.edu.cn
Guohui Liu
liuguohui@hust.edu.cn

†These authors have contributed equally to this work and share first authorship

Specialty section:
This article was submitted to Stem Cell Research, a section of the journal Frontiers in Cell and Developmental Biology

Received: 29 November 2021
Accepted: 08 February 2022
Published: 23 February 2022

Citation:
Zha K, Tian Y, Panayi AC, Mi B and Liu G (2022) Recent Advances in Enhancement Strategies for Osteogenic Differentiation of Mesenchymal Stem Cells in Bone Tissue Engineering. Front. Cell Dev. Biol. 10:824812. doi: 10.3389/fcell.2022.824812

Although bone is an organ that displays potential for self-healing after damage, bone regeneration does not occur properly in some cases, and it is still a challenge to treat large bone defects. The development of bone tissue engineering provides a new approach to the treatment of bone defects. Among various cell types, mesenchymal stem cells (MSCs) represent one of the most promising seed cells in bone tissue engineering due to their functions of osteogenic differentiation, immunomodulation, and secretion of cytokines. Regulation of osteogenic differentiation of MSCs has become an area of extensive research over the past few years. This review provides an overview of recent research progress on enhancement strategies for MSC osteogenesis, including improvement in methods of cell origin selection, culture conditions, biophysical stimulation, crosstalk with macrophages and endothelial cells, and scaffolds. This is favorable for further understanding MSC osteogenesis and the development of MSC-based bone tissue engineering.

Keywords: mesenchymal stem cell, osteogenesis, bone defect, bone healing, tissue engineering

INTRODUCTION

Bone is an important organ that serves a wide range of functions, including preserving vital internal organs and structures, providing the levers for muscles, maintaining mineral homeostasis, secreting growth factors and cytokines, and providing the environment for hematopoietic cell development (Clarke, 2008). It is mainly comprised of osteocytes, osteoblasts, osteoclasts and extracellular matrix (ECM), which maintains a dynamic balance between bone resorption and bone formation (Yang and Liu, 2021). Bone is a vascularized organ that can undergo self-healing after less severe damage. However, it is still a challenge for orthopedists to treat large segmental bone defects (Gage et al., 2018). In addition, an increasing number of people are suffering osteoporosis as the population ages, in which bone quality is decreased and adversely affects the treatment of bone injury (Tarantino et al., 2011). Thus, the development of strategies for bone healing and regeneration represents an area that is of great significance to improve patients' function and quality of life (Guda et al., 2014).

Over the past few decades, increasing attention has been given to bone tissue engineering for the treatment of bone damage. Multiple factors are essential in bone tissue engineering, such as an ideal microenvironment, appropriate scaffolds, and viable cell populations (Li J. J. et al., 2018; Zhao et al.,

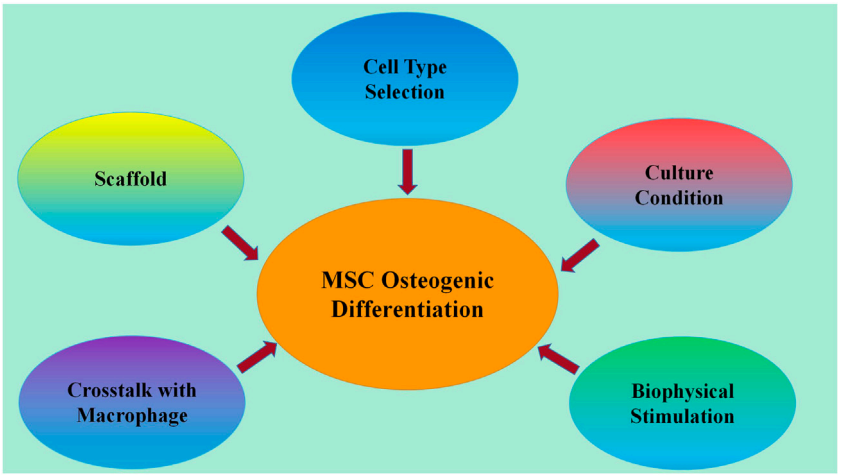

FIGURE 1 | Developed methods for enhancing MSC osteogenic differentiation. Recent research progress on strategies for enhancing MSC osteogenic differentiation includes improvement of methods in cell origin selection, culture conditions, biophysical stimulation, crosstalk with macrophages and endothelial cells, and scaffolds.

2020). Mesenchymal stem cells (MSCs) are adult stem cells with self-renewal, multiple differentiation and immunomodulation functions and are regarded as promising seed cells for bone tissue engineering (Seong et al., 2010; Wang et al., 2013). MSCs reside in a variety of tissues, such as bone marrow, peripheral blood, adipose tissue, umbilical cord, and placenta (Hass et al., 2011). MSCs are multipotent cells that are able to differentiate into a determined mesenchymal lineage under specific conditions, such as osteoblasts, chondrocytes, adipocytes, muscle cells, neural cells and keratinocytes (Han et al., 2019). The cell fate and differentiation direction of MSCs depend on various factors, including the cell origin and viability, extracellular environment, and physical stimulation (Chen et al., 2016; Halim et al., 2020). The identification of appropriate approaches that support the osteogenic differentiation of MSCs is important for bone tissue engineering.

Several clinical trials have proven that MSC-based bone tissue engineering is safe and effective in promoting bone healing and leading to functional outcomes in patients, but the long-term therapeutic effect cannot be guaranteed (Giannotti et al., 2013; Morrison et al., 2018; Garcia de Frutos et al., 2020). It has been proposed that MSCs contribute to bone healing through three different approaches: differentiation and replacement (Garg et al., 2017), secretion of cytokines and extracellular vesicles (Marolt Presen et al., 2019; Tsiapalis and O'Driscoll, 2020), and immunomodulatory activity (Medhat et al., 2019; Weiss and Dahlke, 2019). It is still difficult to judge which is the most important way for MSCs to improve bone regeneration. Nevertheless, the regulation of MSC osteogenesis is conducive to improving the therapeutic effect of MSC-based bone tissue engineering. How to make MSCs differentiate into osteocytes or osteoblasts and maintain their physiological function has become a field of extensive research.

In this review, we overviewed the recent research progress in enhancement strategies for MSC osteogenesis, including improvement of methods in cell origin selection, culture conditions, biophysical stimulation, crosstalk with macrophages and endothelial cells, and scaffolds (**Figure 1**). This will aid the further development of MSC-based bone tissue engineering.

OSTEOGENIC DIFFERENTIATION OF MSCS

A thorough understanding of the regulation of MSC osteogenesis requires familiarity with the normal osteogenic differentiation process of MSCs. It is indicated that MSCs are prone to give rise to preosteoblasts for the first step instead of directly differentiating into osteocytes. Preosteoblasts develop into mature osteoblasts, which synthesize bone matrix and then become entombed in the matrix as osteocytes (James, 2013). The whole process is regulated by numerous signaling pathways, such as transforming growth factor-β (TGF-β)/bone morphogenetic protein (BMP) signaling, Wingless-type MMTV integration site (Wnt) signaling, and Sonic Hedgehog (SHH) signaling (**Figure 2**). As the targets of these signaling pathways, runt-related transcription factor 2 (Runx2) and osterix (Osx) are key transcription factors in the process of MSC osteogenic differentiation (Pokrovskaya et al., 2020). BMPs are members of the TGF-β superfamily, of which BMP-2 (Hu et al., 2017), -4 (Querques et al., 2019), -6 (Friedman et al., 2006), -7 (Kim Y. et al., 2018), and -9 (Wu et al., 2021) are involved in the promotion of MSC osteogenesis. BMP-2 is the most widely studied BMP in MSC osteogenic differentiation, and its function is achieved through the activation of downstream signaling, including in Drosophila mothers against decapentaplegic protein (Smad)1/5/8 (Li et al., 2014; Aquino-Martinez et al., 2017) and mitogen-activated protein kinase (MAPK) (Kong et al., 2012). Wnt signaling is considered another central signaling pathway in the regulation of MSC osteogenesis. The proosteogenic effect of Wnt signaling on MSCs can be achieved

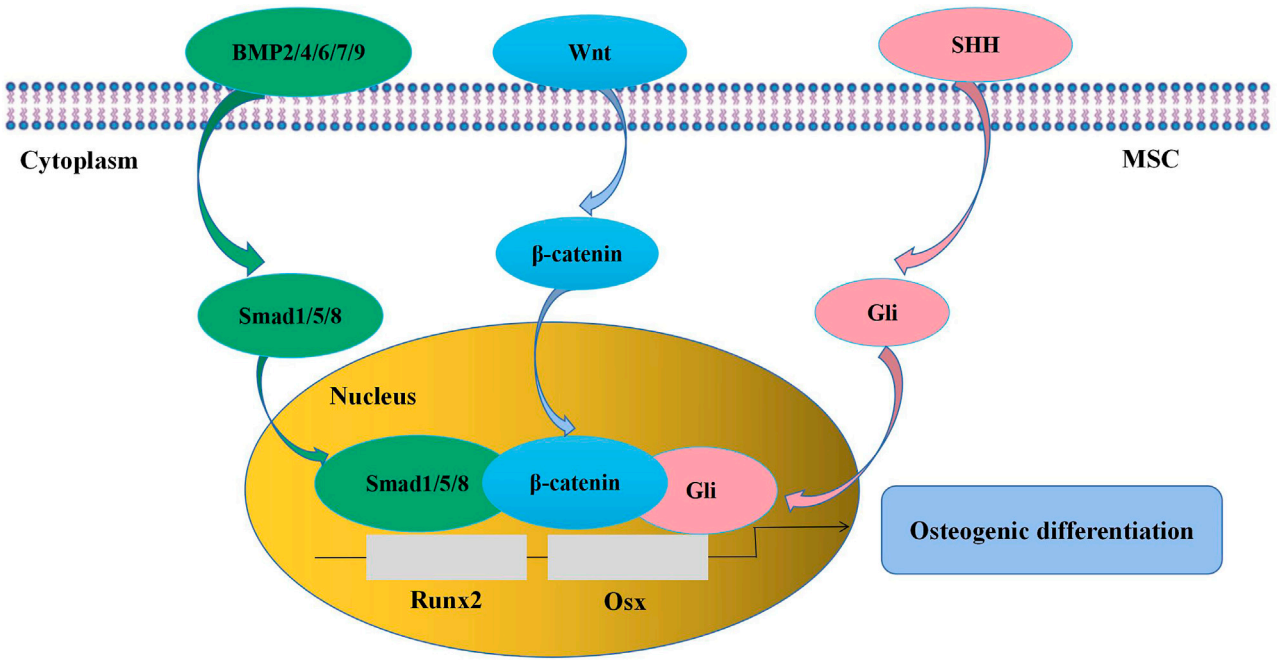

FIGURE 2 | Signaling pathways in the regulation of MSC osteogenic differentiation. BMP signaling, Wnt signaling, and SHH signaling pathways are involved in the modulation of MSC osteogenesis, and the targets are the transcription factors Runx2 and Osx. MSC, mesenchymal stem cell; BMP, bone morphogenetic protein; Wnt, wingless-type MMTV integration site; SHH, sonic hedgehog; Runx2, runt-related transcription factor 2; Osx, osterix.

through both β-catenin-dependent and β-catenin-independent signaling pathways (Fakhry et al., 2013; James, 2013; Li Y. et al., 2018). It is reported that Wnt/β-catenin activity is involved in the regulation of bone development and bone remodeling (Little et al., 2002; Day et al., 2005; Chen and Long, 2013). Meanwhile, inactivation of Wnt/β-catenin in MSCs *in vitro* causes significant inhibition of osteogenic differentiation and promotion of adipogenic or chondrogenic differentiation, indicating that Wnt/β-catenin signaling is important in determining whether MSCs will differentiate toward osteoblasts (Day et al., 2005; Zhou et al., 2019). The SHH signaling pathway also has a well-established effect on MSC osteogenesis at an early stage *via* the activity of the Gli transcription factor (James, 2013). The addition of SHH protein significantly stimulated MSC osteogenic differentiation and reduced MSC adipogenic differentiation (James et al., 2012). Interestingly, SHH signaling and BMP-2 signaling can interact with each other and synergistically promote osteogenic differentiation by regulating Smad activity in the murine MSC line C3H10T1/2 (Spinella-Jaegle et al., 2001; Yuasa et al., 2002).

HETEROGENEITY IN MSC OSTEOGENIC DIFFERENTIATION POTENTIAL

The International Society for Cellular Therapy has provided the following standard criteria for human MSCs: 1) must be plastic-adherent in standard culture conditions; 2) must have the capacity to differentiate into adipocytes, osteoblasts and chondroblasts; and 3) must express CD105, CD73 and CD90 and lack the expression of CD45, CD34, CD14 or CD11b, CD79α or CD19 and HLA-DR (Dominici et al., 2006). In recent years, increasing research has identified that MSCs are heterogeneous populations. It is well acknowledged that MSCs from different individual donors and tissue sources have different biological properties (Wang and Han, 2019). Moreover, MSCs can be divided into different subpopulations according to their expression of cell surface markers, which also exhibit unique characteristics and cellular functions. Thus, the selection and utilization of superior MSCs is fundamental to improve the therapeutic effect of bone tissue engineering.

Characteristics of Donors

The osteogenic differentiation potential of MSCs from donors of different ages has been studied. Gene expression analysis revealed that bone marrow-derived MSCs (BMSCs) from 3- and 6-month-old mice expressed similar levels of osteogenic differentiation-related genes (Bragdon et al., 2015). Tokalov et al. (2007) isolated BMSCs from rats of 2–48 weeks of age and reported that MSC osteogenesis was independent of donor age, as revealed by similar levels of calcium accumulation after osteogenic induction *in vitro*. Lee et al. (2021) demonstrated that the osteogenic differentiation potential of human BMSCs was not impaired in older donors, as shown by alizarin red staining. Similar results were found by Ding and his coworkers, who revealed that the osteogenic differentiation capacities of human adipose tissue-derived MSCs (ADSCs) between old age individuals and young age individuals were the same (Ding et al., 2013). These results

suggest that MSC osteogenesis is independent of donor age, indicating that MSCs from elderly donors are eligible for bone tissue engineering in terms of osteogenic differentiation potential. However, Yang et al. (2014) analyzed the cellular properties of ADSCs isolated from 66 human donors (age: 10–70 years). Although they observed a trend in which the osteogenic differentiation ability of ADSCs declined as the donor age rose, it failed to reach statistical significance. Carvalho et al. (2021) found that the osteogenic differentiation potential of BMSCs from older fracture patients (60 and 80 years old) was inferior to that from younger fracture patients (30 and 45 years old), as evidenced by alkaline phosphatase (ALP) activity, calcium deposition, and osteogenic gene expression assays after 21 days under osteogenic differentiation conditions. The conflicting results obtained by these researchers might be due to the different cell sources, culture conditions, and evaluation methods used. The effect of donor age on the osteogenic differentiation capacity of MSCs remains controversial, and more related research is still needed.

Since bone formation and development are different between males and females, it is necessary to determine whether MSC osteogenesis was also sexually dimorphic. Leonardi et al. demonstrated that the osteogenic differentiation potential of human BMSCs was not affected by donor sex after 14 days of induction culture (Leonardi et al., 2008). Interestingly, Bragdon et al. (2015) revealed that the expression of bone-related genes in BMSCs derived from male mice and female mice was similar at 3 and 9 months, while at 6 months, BMSCs from female mice expressed these genes twofold greater than those from male mice. This suggests that at certain ages, MSC osteogenesis is different between males and females.

Tissue Sources

In bone tissue engineering, bone marrow, adipose tissue, dental pulp, and umbilical cord are widely used as tissue sources of MSCs (Seong et al., 2010). The osteogenic differentiation abilities of MSCs from these tissues are heterogeneous. Above all, comparisons are often made between the osteogenesis of BMSCs and ADSCs. Lotfy et al. (2014) compared the characteristics of rat-derived BMSCs and ADSCs and found that BMSCs were more prone to differentiate into osteocytes after 2–3 weeks of induction culture than ADSCs. Similarly, Zaminy et al. (2008) studied the effects of melatonin on the osteogenic differentiation of rat-derived MSCs and concluded that BMSCs had greater potential for osteogenic differentiation than ADSCs, as determined by ALP activity and matrix mineralization assays. In addition, Lee et al. (2017) seeded dog-derived BMSCs and ADSCs on three-dimensional (3D)-printed polycaprolactone/tricalcium phosphate (PCL/TCP) scaffolds. When the composites were subjected to an *in vitro* osteogenic differentiation assay, the expression of genes associated with ossification was higher in BMSCs. These results indicate that BMSCs may represent a better candidate for bone tissue engineering than ADSCs regarding MSC osteogenesis. Dental pulp-derived MSCs (DPSCs), originating in the neural crest, are characterized by a fast proliferation rate and the capacity to differentiate into multiple cell lineages and have been widely used in the regeneration of periodontal bone defects (Ferro et al., 2014; Amghar-Maach et al., 2019; Lorusso et al., 2020). Pettersson et al. (2017) compared the osteogenic differentiation potential of DPSCs with jawbone-derived MSCs (JBMSCs) *in vitro* and reported no significant difference in osteogenesis between them. In other studies, it was demonstrated that DPSCs possessed a stronger ability to differentiate into osteoblasts than BMSCs both *in vitro* and *in vivo* (Ito et al., 2011; Jensen et al., 2016; Kumar et al., 2018). Wharton's jelly derived MSCs (WJMSCs) appear to be another good choice for bone regeneration (Liu et al., 2017; Ansari et al., 2018; Kosinski et al., 2020). The osteogenic commitment in WJMSCs has been identified and was reported to be poorer than that in BMSCs and ADSCs (Zajdel et al., 2017; Cabrera-Perez et al., 2019). On the other hand, WJMSCs have reached a more advanced stage of immunomodulation action and proliferation ability, which deserves to be taken into account for bone tissue engineering (Kalaszczynska and Ferdyn, 2015; Vieira Paladino et al., 2019).

Expression of Surface Markers

In recent years, increasing evidence has suggested that MSCs derived from the same tissue source express different surface markers, which reflect their different origins, statuses, and osteogenic differentiation potential (**Table 1**). CD73 is a well-known surface marker for MSCs in humans and mice. $CD73^+$ mouse BMSCs were proposed to have increased "stemness" and greater osteogenic differentiation potential *in vitro* than $CD73^-$ mouse BMSCs. When used to repair bone fractures in mice, $CD73^+$ BMSCs also displayed an enhanced ability to promote fracture healing (Kimura et al., 2021). Gullo and De Bari (2013) used the combination of CD73 and CD39 (ectonucleoside triphosphate diphosphohydrolase 1, ENTPD1) to purify human synovial membrane-derived MSCs (SMSCs) and confirmed that $CD73^+CD39^+$ SMSCs exhibited significantly greater chondro-osteogenic potency than $CD73^+CD39^-$ SMSCs. CD200 is another potential new marker of BMSCs. Kim H. J. et al. (2018) evaluated the effect of CD200 on the cellular function of human BMSCs and found that CD200 overexpression significantly enhanced the osteogenic differentiation potential of BMSCs. In addition, Kouroupis et al. (2020) revealed that the expression of CD10 was associated with improved differentiation potential of human ADSCs. Ding et al. (2020) demonstrated that both $CD10^+$ and $CD10^-$ human adventitial cells exhibited phenotypic features of MSCs. Compared with their $CD10^-$ counterparts, $CD10^+$ adventitial cells showed higher proliferation ability and osteogenic differentiation potential. CD271, also known as low-affinity nerve growth factor receptor (LNGFR), has been regarded as an important surface protein of MSCs (Zha et al., 2021). Quirici et al. (2002) investigated the expression and function of CD271 in human BMSCs and demonstrated that $CD271^+$ BMSCs exhibited greater CFU-F activity and adipogenic and osteogenic differentiation abilities, indicating that CD271 might be a "stemness" marker of BMSCs. Similar results were found in mouse and human ADSCs (Yamamoto et al.,

TABLE 1 | Osteogenic differentiation potential different MSC subpopulations.

MSC subpopulations	Control	Species	Analysis methods	Results	References
BMSCs transfected with CD200	BMSCs transfected without interposed gene	human	ALP staining and gene expression and protein production of Runx2	CD200 expression increased the levels of ALP activity and Runx2 expression in BMSCs	Kim et al. (2018a)
$CD73^+$ BMSCs	$CD73^-$ BMSCs	mouse	Alizarin red staining, bone fracture repair *in vivo*	$CD73^+$ BMSCs exhibited enhanced potentials for osteogenic differentiation *in vitro* and fracture repair *in vivo*	Kimura et al. (2021)
$CD73^+$ $CD39^+$ SMSCs	$CD73^+$ $CD39^-$ SMSCs	human	Alizarin red staining and expression of osteoblast genes	$CD73^+$ $CD39^+$ SMSCs showed increase in calcium accumulation and gene expression of *Runx2*	Gullo and De Bari, (2013)
$CD10^{High}$ ADSCs	ADSCs	human	Alizarin red staining	$CD10^{High}$ ADSCs exhibited higher level of calcium accumulation	Kouroupis et al. (2020)
$CD271^+$ BMSCs	PA BMSCs	human	Alizarin red S staining	$CD271^+$ BMSCs had a larger mineralized area	Quirici et al. (2002)
$CD271^+$ ADSCs	$CD271^-$ ADSCs	mouse	Alizarin red S staining	$CD271^+$ ADSCs were more prone to form calcium nodule after osteogenic differentiation	Yamamoto et al. (2007)
		human			Barilani et al. (2018)
$CD271^+$ DPSCs	$CD271^-$ DPSCs	human	ALP staining, Ca^{2+} level, and genes expression of *Runx2*, *Osterix*, *Osteocalcin*, and *Nestin*	ALP activity and Ca^{2+} levels were lower in $CD271^+$ DPSCs; no difference in the expression level of osteogenic genes was detected	Mikami et al. (2011)
$CD146^+$ PDSCs	$CD146^-$ PDSCs	human	von Kossa staining	$CD146^+$ PDSCs exhibited a higher level of spontaneous ossification	Ulrich et al. (2015)
$CD146^{Low}$ PCy-MSCs	$CD146^{High}$ PCy-MSCs	human	Alizarin red staining and expression of osteoblast genes	calcium accumulation and genes expression of *Runx2* and *Osteopontin* were greater in the $CD146^{Low}$ than in $CD146^{High}$ PCy-MSCs	Paduano et al. (2016)

BMSCs, *bone marrow-derived mesenchymal stem cells;* ALP, *alkaline phosphatase;* SMSCs, *synovial membrane-derived mesenchymal stem cells;* ADSCs, *adipose tissue-derived mesenchymal stem cells,* PA, *plastic adherent;* DPSCs, *dental pulp-derived mesenchymal stem cells;* PDSCs, *placenta-derived mesenchymal stem cells;* PCy-MSCs, *periapical cyst mesenchymal stem cells.*

2007; Barilani et al., 2018). However, it was challenged by Mikami and his colleagues, who found that the expression of CD271 could inhibit multipotential differentiation of DPSCs, including osteogenic differentiation (Mikami et al., 2011). These findings indicate that the effects of CD271 on different types of MSCs might be different or even opposite. In addition, CD271 expression is not consistently detectable in MSCs from fetal tissues, such as Wharton's jelly, umbilical cord blood, and amniotic fluid, indicating that CD271 might not be an appropriate marker for the identification of functional subpopulations in fetal tissue-derived MSCs (Barilani et al., 2018). CD146, also known as melanoma cell adhesion molecule, is an adhesion molecule belonging to the immunoglobulin superfamily and is expressed in various types of MSCs. Ulrich et al. (2015) investigated the effect of CD146 on osteogenic differentiation of human placenta-derived MSCs (PDSCs) and demonstrated that $CD146^+$ PDSCs had higher osteogenic differentiation and mineralized extracellular matrix production abilities than $CD146^-$ PDSCs *in vitro*, indicating that $CD146^+$ PDSCs might present a PDSC subpopulation that was predetermined to differentiate into osteoblasts. However, Paduano et al. (2016) found that $CD146^{Low}$ human periapical cyst MSCs (PCy-MSCs) displayed stronger osteogenic differentiation potential than $CD146^{High}$ PCy-MSCs. This variation might be attributed to the different types of MSCs they used. The role of CD146 in MSC osteogenesis requires more comprehensive and accurate research.

CULTURE CONDITIONS

In general, MSCs isolated from tissues need to be cultured and expanded *in vitro* before *in vivo* transplantation. The improvement of culture conditions might be an efficient approach to enhance MSC osteogenesis. It is well recognized that conventional 2D culture is unable to mimic the *in vivo* 3D MSC niche, which is characterized by cell-cell and cell-ECM interactions. The drawback of 2D culturing methods has currently promoted the development of 3D MSC culture. In an effort to more closely recapitulate the *in vivo* microenvironment, both cellular properties and functions of MSCs, such as phenotype, differentiation ability and immunomodulatory action, can be preserved or enhanced by 3D culturing technologies (Kouroupis and Correa, 2021). Recent studies have compared the osteogenic differentiation abilities of MSCs in 2D monolayers and 3D culture systems. It was demonstrated that MSCs in 3D culture systems (e.g., scaffolds and microcarriers) exhibited spread morphology and were more prone to differentiate into osteoblasts than MSCs in 2D cultures, indicating that 3D cultures might be more suitable for bone tissue engineering (Brennan et al., 2015; Shekaran et al., 2015). In addition, flow perfusion culture has been shown to enhance osteoblastic differentiation and ECM deposition of MSCs compared to static culture (Holtorf et al., 2005). Mitra et al. (2017) cultured human BMSCs in macroporous scaffolds in direct perfusion bioreactors and found that continuous dynamic culture conditions could significantly promote BMSC

osteogenic differentiation, as shown by enhanced osteogenic gene expression and ectopic bone formation. In addition, MSC 3D spheroids have shown increased osteogenic differential potential compared to monolayer cultured MSCs (Griffin et al., 2017; Kim et al., 2019). Saleh et al. (2016) revealed that Wnt signaling was activated in MSC spheroids but not 2D cultured MSCs during osteogenic differentiation. Interestingly, Sankar et al. (2019) used a 3D double strategy for osteogenic differentiation of human ADSC spheroids on patterned poly (lactic-co-glycolic acid) (PLGA)/collagen/hydroxyapatite (HA) electrospun fiber mats and found that the osteogenic differentiation of ADSCs was significantly enhanced even in the absence of osteogenic induction culture medium.

Several studies have shown that aged MSCs after long-term *in vitro* expansion exhibit decreased osteogenic differential potential (Yu et al., 2014; Bertolo et al., 2016; Yang et al., 2018). Senescence is associated with the impaired differentiation ability of late-passage MSCs, which show decreased colony-forming unit (CFU) activity, reduced proliferation capacity, and increased senescence-associated β-galactosidase activity and gene expression (Bertolo et al., 2016; Grotheer et al., 2021). Thus, it is suggested that MSCs at early passages are more appropriate candidates for bone tissue engineering. Oxidative stress is another factor that could impact the behaviors of MSCs, including their proliferation, differentiation and immunomodulation functions. Increased reactive oxygen species (ROS) usually promote MSC adipogenesis but impair MSC osteogenesis (Denu and Hematti, 2016). Binder et al. (2015) indicated that reduced serum (5%) and hypoxic conditions (5%) in culture medium could enhance osteogenic differentiation in human BMSCs. Similar effects of hypoxia were also found in human PDSCs (Gu et al., 2016) and ADSCs (Fotia et al., 2015). However, MSCs exposed to excessively low oxygen content (1%) demonstrated decreased osteogenic differentiation capacity, which is associated with increased expression of *hypoxia inducible factors* (*HIFs*) and *Notch1* (Tamama et al., 2011; Yang et al., 2019). In addition, it has been proposed that MSC osteogenesis is influenced by the glucose content in the culture medium. Aswamenakul et al. (2020) confirmed that human BMSC osteogenesis was reduced under high glucose conditions (10, 25, and 40 mM), as revealed by Alizarin red S staining and ALP activity assays.

BIOPHYSICAL STIMULATION

Physical stimulation has been proposed to affect MSC fate and differentiation by initiating or strengthening biochemical signaling (Wang and Chen, 2013; Huang et al., 2015). The effects of mechanical stimulation, electric field, and electromagnetic field on MSC osteogenesis have been widely investigated over the past few years.

Mechanical Stimulation

Since the promotion of exercise on bone repair and reconstruction in clinical settings is well recognized, the effect of mechanical stimulation on MSC osteogenesis is worth exploring. Hu et al. (2013) conducted a study in which they delivered noninvasive dynamic hydraulic stimulation (DHS) to rat mid-tibiae and found that BMSCs in the stimulated tibiae were induced into osteoblasts in a time-dependent manner. In addition, Gharibi et al. (2013) seeded human BMSCs onto calcium phosphate scaffolds and subjected the composite to an appropriate pulsating compressive force (5.5 ± 4.5 N at a frequency of 0.1 Hz). Gene expression analysis showed that *Runx2* was significantly upregulated after 22 h of loading. Kang et al. (2012) examined the impact of mechanical strain on the osteogenic differentiation of human umbilical cord-derived MSCs (UCMSCs) and revealed that mechanical strain (5% or 10% strain magnitude, 5 s of stretch and 15 s of relaxation) decreased the protein expression of MSC surface antigens, such as CD73, CD90, and CD105, while increasing the gene expression of osteogenic markers, such as *osteopontin* (*OPN*), *osteonectin* (*ON*), and *type I collagen (COL I)*. Similar results were reported by Li and his coworkers in rat BMSCs, who demonstrated that the gene expression of *Runx2* and *Osx* and the production of COL I were more strongly induced in cells subjected to mechanical strain (5% strain magnitude, 6 h/day, 10 times/min) compared to those in unstrained groups (Li et al., 2015). The underlying mechanism by which mechanical stimulation regulates MSC osteogenesis has been investigated. It has been proposed that cell–cell and cell-ECM adhesion is the major structure for MSCs to sense mechanical stimulation. Integrin is a transmembrane protein on MSCs and acts as a bridge between the ECM and intracellular actomyosin cytoskeleton in mechanical transmission, resulting in the activation of downstream signaling pathways (Sun et al., 2021). Qi et al. (2008) indicated that mechanical strain was able to promote BMSC osteogenesis through upregulation of the transcription factors core binding factor alpha 1 (Cbfa1) and v-ets erythroblastosis virus E26 oncogene homolog 1 (Ets-1). In addition, Chen et al. (2018) demonstrated that mechanical stretching could improve MSC osteogenic differentiation through activation of the AMP-activated protein kinase (AMPK)-silent information regulator type 1 (SIRT1) signaling pathway.

Electrical Stimulation

Electrical stimulation has emerged as a useful tool to enhance MSC osteogenic differentiation and bone healing. It was found that exposing human BMSCs to an appropriate electrical current (10 or 40 mA, 10 Hz, sinusoidal waveform, 6 h/day) resulted in enhanced osteogenic differentiation, as evidenced by significantly increased expression of the osteogenic marker genes *Runx2*, *Osx*, *OPN* and *osteocalcin* (*OCN*) (Creecy et al., 2013). Similar findings were achieved by Zhang and his coworkers in human ADSCs (Zhang et al., 2018). Eischen-Loges et al. (2018) reported that treatment with electrical stimulation (100 mV/mm, 1 h/day) significantly promoted rat BMSC osteogenic differentiation, and this effect lasted a maximum of 7 days after electrical stimulation was discontinued. Furthermore, Leppik et al. (2018) combined ADSCs, β-TCP scaffolds and electrical stimulation (1.2 V, 80 mAh) to treat large bone defects in rats and found that bone healing was more strongly improved in the electrically stimulated group than in the control group.

Interestingly, Hou et al. efficiently initiated the process of MSC osteogenic differentiation by optimizing electrical stimulation parameters based on the calcium spike patterns of MSCs (Hou et al., 2019). The effects of electrical stimulation on cellular properties and functions are known to be achieved through induction of conformational changes in voltage-sensitive proteins, reversible pore formation in plasma membranes, Ca^{2+} influx, and activation of various signaling pathways (Thrivikraman et al., 2018; Ning et al., 2019). It has been demonstrated that electric fields were able to induce activation of the wnt/β-catenin signaling pathway and BMP signaling pathway (Zhang et al., 2014; Kwon et al., 2016). However, how electrical cues are transferred into intracellular molecular signals that result in MSC osteogenic differentiation remains unclear and needs further investigation.

Magnetic Stimulation

Magnetic stimulation is another physical approach to regulate MSC osteogenic differentiation. Kim et al. (2015) evaluated the effects of static magnetic field treatment on the osteogenic differentiation of human BMSCs. Their results demonstrated that a moderate intensity (15 mT) magnetic field promoted osteoblastic differentiation in BMSCs, as determined by increased ALP activity, mineralized nodule formation, calcium content, and expression of osteogenic markers, such as *Run×2*, *Osx*, *OCN*, *ON*, *OPN*, *COL I* and *bone sialoprotein 2* (*BSP2*) In another study, Ceccarelli et al. investigated the effects of pulse electromagnetic field (PEMF) (magnetic field intensity: 2—0.2 mT, electric tension amplitude: 5—1 mV, 75—2 Hz, pulse duration: ~1.3 msec) exposure on the osteogenic differentiation of human BMSCs and ADSCs. Bone-related ECM deposition was more strongly induced in BMSCs than in ADSCs, indicating that the promoting effect of PEMFs might be more efficient in BMSCs (Ceccarelli et al., 2013). It has been proposed that cells respond to magnetic stimulation with changes in cytoskeleton remodeling, membrane potential, ion channel gating, and targeted gene expression (Zablotskii et al., 2018). However, the underlying mechanism by which magnetic stimulation promotes MSC osteogenic differentiation has not been revealed and needs to be studied in the future.

CROSSTALK WITH MACROPHAGES AND ENDOTHELIAL CELLS

Macrophages, key cells of innate immunity, can be found in nearly all tissues during inflammation and infection. The important roles of macrophages in the secretion of anti-inflammatory factors and the recruitment and regulation of the differentiation of MSCs during bone healing have been revealed in recent years (Pajarinen et al., 2019). In response to environmental signals, macrophages can undergo polarization into the M1 phenotype (related to the inflammatory response) and M2 phenotype (related to inflammation resolution and tissue regeneration) (Sinder et al., 2015; Pajarinen et al., 2019). Gong et al. utilized cocultures of mouse macrophages and BMSCs to investigate the effects of macrophages with different phenotypes on mediating MSC osteogenic differentiation. They found that osteogenic markers, ALP activity, and bone mineralization were increased in MSCs cocultured with M2 macrophages but decreased in MSCs cocultured with M1 macrophages. The effects might be regulated by M2 macrophage-derived pro-regenerative cytokines, such as TGF-β, VEGF, and IFG-1, and M1 macrophage-derived inflammatory cytokines, such as IL-6, IL-12, and TNF-α (Gong et al., 2016). Similar results were obtained by Zhang and his coworkers in human ADSCs (Zhang et al., 2017). It was suggested that the soluble proteins BMP-2, -6 and oncostatin M (OSM) produced by M2 macrophages and related signaling pathways might be involved in the promotion of MSC osteogenic differentiation (Zhang et al., 2017; Wang et al., 2021). In addition, Luo et al. (2020) indicated that macrophages stimulated BMSC osteogenesis by reducing intracellular ROS, which was increased during osteogenic differentiation. However, researchers found that in a 3D coculture system, both M1 and M2 macrophages inhibited the osteogenic differentiation of human ADSCs (Tang et al., 2019). The conflicting conclusions might be due to the use of different cell ratios, culture times and means, and polarization methods for macrophages. Therefore, the role of macrophages in the osteogenic differentiation of MSCs needs to be investigated more comprehensively and accurately.

It is well recognized that angiogenesis is mandatory for successful bone repair. The crosstalk between endothelial cells and MSCs has been studied in the past decade. The coculture of endothelial progenitor cells and MSCs is proposed to have a synergistic effect in terms of angiogenesis and bone formation, in which endothelial progenitor cells promote osteogenesis, and conversely, MSCs foster angiogenesis (Bouland et al., 2021). Gershovich et al. (2013) evaluated the effects of coculturing BMSCs and human umbilical vein endothelial cells on BMSC osteogenic differentiation and found that ALP activity, collagen production, and calcium nodule formation were significantly promoted. Chen et al. cocultured rabbit endothelial progenitor cells and peripheral blood-derived MSCs (PBSCs) on a 3D calcium phosphate bioceramic scaffold and found that the expression of osteogenic- and vascular-related genes was increased *in vitro*. When the cell-scaffold construct was used to repair large bone defects in rabbits, both new bone and promoted vascularization were observed *in vivo* (Chen et al., 2019). Similar results were obtained by Liang et al. (2016), who utilized cocultures of rat EPCs and BMSCs to treat alveolar bone defects in rats. The underlying mechanism by which endothelial cells regulate MSC osteogenic differentiation has been partly revealed. It has been proposed that endothelial cells directly interact with MSCs and regulate MSC osteogenesis *via* gap and adherence junctions (Bouland et al., 2021). In addition, endothelial cells can promote MSC osteogenic differentiation through the secretion of growth factors, such as BMP-2, endothelin-1 (ET-1), and insulin-like growth factor (IGF), which interact with specific membrane receptors on MSCs (Grellier et al., 2009). Xu et al. (2020) indicated that the MAPK signaling pathway was involved in the regulation of endothelial progenitor cells on MSC osteogenic differentiation. They found that silencing the expression of p38 resulted in

TABLE 2 | The effects of scaffolds on MSC osteogenic differentiation.

Aspects	Scaffold features	MSCs	Effects on MSC osteogenic differentiation	References
composition	nanoHA/collagen scaffold modified with phosphorylated amino acids	human BMSCs	BMSCs underwent osteogenic differentiation *in vitro* in the absence of osteogenic inductor and ectopic bone formation *in vivo*	Salgado et al. (2019)
	collagen/glycosaminoglycan scaffold incorporated with a calcium phosphate mineral phase	human BMSCs	the scaffold promoted osteogenic differentiation and mineral deposition of BMSCs within osteogenic induction media	Caliari and Harley, (2014)
	PCL scaffold coated with human BMSCs derived ECM	human BMSCs	BMSCs seeded on the scaffold exhibited an increase in calcium deposition and expression of bone-specific genes	Silva et al. (2020)
	gelatin scaffold incorporated with magnesium calcium phosphate	rat BMSCs	BMSCs exhibited enhanced osteogenic differentiation, as shown by increased ALP activity	Hussain et al. (2014)
	PLGA microspheres with tunable Mg^{2+} release	rat BMSCs	the scaffold promoted BMSC osteogenic differentiation *in vitro* and resulted in significant bone regeneration in rats with critical-sized calvarial defects	Yuan et al. (2019)
structure	calcium phosphate scaffolds with hemispherical concavities of various sizes	human ADSCs	ADSCs seeded on scaffolds with 440 and 800 μm concavities, but not with 1800 μm concavities, showed enhanced osteogenic differentiation	Urquia Edreira et al. (2016)
	3D printed PPF porous scaffolds	human BMSCs	scaffolds with ordered cubic pores were more suitable for the promotion of BMSC osteogenic differentiation than that with cylindrical pores	Ferlin et al. (2016)
	3D printed PCL/DCM scaffolds with micro/nanosurface pores	human BMSCs	BMSCs displayed increased ALP activity and osteocalcin production in osteogenic medium	Prasopthum et al. (2019)
	barium titanate nanoparticle/alginate scaffold	human DPSCs	DPSCs exhibited higher levels of *BMP-2* and *ALP* genes expression	Amaral et al. (2019)
bioactive molecule delivery	chitosan oligosaccharide/heparin nanoparticles-modified chitosan-agarose-gelatin scaffold with sustainable BMP-2 release	mouse BMSCs	the scaffold induced BMSC differentiation towards osteoblasts in the absence of osteogenic media	Wang et al. (2018)
	titanium dioxide scaffold with alginate hydrogel containing simvastatin	human ADSCs	ADSCs seeded on the scaffold showed increased expression of osteogenic genes and proteins	Pullisaar et al. (2014)
	β-TCP scaffold containing human-induced pluripotent stem cell-derived MSC-derived exosomes	human BMSCs	the scaffold increased the levels of ALP activity and calcium deposition of BMSCs in osteogenic media	Zhang et al. (2016)

HA, *hydroxyapatite;* BMSCs, *bone marrow-derived mesenchymal stem cells;* PCL, *polycaprolactone; ECM, extracellular matrix;* ALP, *alkaline phosphatase; PLGA, poly (lactic-co-glycolic acid),* ADSCs, *adipose tissue-derived mesenchymal stem cells;* PPF, *Poly Propylene Fumarate),* DCM, *dichloromethane;* DPSCs, *dental pulp-derived mesenchymal stem cells;* BMP-2, *bone morphogenetic protein-2,* β-TCP *β-tricalcium phosphate.*

decreased osteogenic gene expression, ALP activity, and calcium deposition in cocultured MSCs.

SCAFFOLD

The scaffold is an essential component of bone tissue regeneration, which supports MSC adhesion and survival by providing a 3D structure and forming the cell niche. In addition, both the composition and structure of scaffolds can regulate MSC fate and behaviors, such as cell migration, proliferation and differentiation (Garcia-Sanchez et al., 2019). Thus, culturing MSCs onto scaffolds may be an efficient approach to improve the engraftment of MSCs and the therapeutic effects of MSC-based bone tissue engineering. Designing an appropriate scaffold for bone healing has been a focus of research in bone tissue engineering, in which the stimulatory effect on MSC osteogenesis is an important aspect (**Table 2**).

The composition is a key factor that needs to be taken into account when designing scaffolds to enhance MSC osteogenesis. Many different materials have been applied to fabricate scaffolds in bone tissue engineering, including natural and synthetic materials. Natural materials, such as collagen, ECM, calcium phosphate, chitosan, hyaluronic acid, silk fibroin and alginate, are widely used due to their high biocompatibility and biodegradability (Tang et al., 2021). Of these, collagen, ECM and calcium phosphate are probably most commonly used because of their abilities to replicate the properties of the bone microenvironment and to promote MSC osteogenic differentiation (Curry et al., 2016; Dong and Lv, 2016). For example, Salgado et al. (2019) developed an HA/collagen scaffold that was modified with phosphorylated amino acids. The results of ectopic bone formation analysis showed that the scaffold could promote osteogenic differentiation and bone-related ECM deposition of human BMSCs. In another study, Caliari and Harley (2014) endowed the collagen/glycosaminoglycan scaffold with the ability to promote osteogenic differentiation of human BMSCs by incorporation of a calcium phosphate mineral phase. However, their applications in bone tissue engineering are limited by unsatisfactory mechanical strength and rapid degradation rate. Thus, they are often used in conjunction with synthetic polymers, which possess low biocompatibility but sufficient mechanical strength. For example, Silva et al. (2020) coated human BMSC-derived ECM on a 3D polycaprolactone (PCL) scaffold and demonstrated that the composite scaffold was able to

modulate BMSC behavior in favor of differentiation into osteoblasts. Recently, the application of biodegradable metals and their alloys has shown broad prospects in bone fracture healing. Increasing evidence demonstrates that calcium (Ca) and magnesium (Mg) ions are able to promote the osteogenic differentiation of MSCs (Park et al., 2019; Hohenbild et al., 2021). Hussain et al. (2014) found that rat BMSCs seeded on gelatin scaffolds incorporating magnesium calcium phosphate exhibited enhanced osteogenic differentiation, as shown by increased ALP activity. Yuan et al. (2019) developed injectable PLGA microspheres with tunable Mg^{2+} release and confirmed that they were able to promote rat BMSC osteogenic differentiation *in vitro* and result in significant bone regeneration *in vivo*.

In addition, the microstructure of the scaffold is also proposed to have an impact on the osteogenic differentiation of MSCs. The porosity and appropriate pore size of the scaffold were considered influencing factors for MSC osteogenesis (Kasten et al., 2008). Urquia Edreira et al. (2016) conducted a study in which they cultured human ADSCs on calcium phosphate scaffolds with hemispherical concavities of various sizes (440, 800 or 1800 μm). They revealed that ADSCs seeded on scaffolds with 440 and 800 μm concavities, but not with 1800 μm concavities, exhibited enhanced osteogenic differentiation. Ferlin et al. (2016) investigated the impact of pore geometries on human BMSC osteogenic differentiation and found that osteogenic marker expression at early timepoints was increased in BMSCs cultured on scaffolds with cylindrical pores, while BMSCs cultured in scaffolds with ordered cubic pores expressed late osteogenic markers, suggesting that ordered cubic pores might be more suitable for the promotion of MSC osteogenic differentiation. However, the underlying mechanism is not fully understood and needs further investigation. In addition, based on the advancement of manufacturing technology, 3D printing technology has been applied to fabricate porous scaffolds with 3D architecture, good biocompatibility, and bone induction function (Wang et al., 2020). For example, Prasopthum et al. fabricated 3D printed polymer scaffolds with micro/nanosurface pores (0.2–2.4 μm) and found that they were able to promote human BMSC osteogenic differentiation in the absence of soluble differentiation factors (Prasopthum et al., 2019). Recently, the application of nanomaterial-based scaffolds in bone tissue engineering has also received much attention, showing improved bone regeneration effects compared with conventional scaffolds. It has been proposed that nanomaterials can promote MSC osteogenic differentiation due to their specific chemical, physical and mechanical properties (Zhang et al., 2021). The commonly used nanomaterials in bone tissue engineering include metals and their derivatives, bioactive ceramics, carbon nanomaterials and polymers (Ye et al., 2020). For example, Las Amaral et al. (2019) designed a barium titanate nanoparticle/alginate scaffold that exhibited highly interconnected pores and surface nanotopography. The osteogenic differentiation of human DPSCs seeded on it was enhanced, as indicated by upregulated gene expression of BMP-2 and ALP.

Another strategy for inducing MSCs into osteoblasts is to design scaffolds containing spatially graded bioactive molecules. For example, Wang et al. (2018) constructed a chitosan-agarose-gelatin scaffold that was modified with chitosan oligosaccharide/heparin nanoparticles, which could sustainably release BMP-2 and induce mouse BMSC differentiation towards osteoblasts. Pullisaar et al. (2014) coated a titanium dioxide (TiO_2) scaffold with alginate hydrogel containing simvastatin and found that human ADSCs seeded on it were more strongly induced into osteoblasts, as demonstrated by increased expression of osteogenic genes and proteins, compared with TiO_2 scaffolds without simvastatin. Recently, exosomes have been introduced into bone tissue engineering, which also shows an osteogenic induction effect on MSCs (Qi et al., 2016; Yahao and Xinjia, 2021). Zhang et al. (2016) loaded human-induced pluripotent stem cell-derived MSC-derived exosomes on β-TCP scaffolds and confirmed that the composite was able to efficiently enhance the osteogenic differentiation of human BMSCs.

CONCLUSION AND PERSPECTIVE

MSCs represent one of the most promising cell types in bone tissue engineering, in which researchers are always making efforts to guide MSCs to efficiently differentiate toward osteoblasts. In the present review, we provide an overview of recently developed strategies for enhancing osteogenic differentiation of MSCs, including selection of optimal cell origin, improvement of culture conditions, application of biophysical stimulations, crosstalk with M2 macrophages and endothelial cells, and fabrication of appropriate scaffolds. Although significant advances in the development of methods for promotion of MSC osteogenic differentiation have been achieved, there are still some issues that need to be resolved. First, numerous strategies display positive effects in promoting MSC osteogenic differentiation. However, the efficiency of different methods has not yet been compared. In addition, the safety and ease of applying these approaches also need to be considered before making a choice. Second, the in vivo microenvironment is quite different from that in vitro. Thus, the efficiency and safety of these methods should be evaluated in vivo. Third, the underlying mechanisms by which several methods regulate MSC osteogenic differentiation, such as how the presence of macrophages and magnetic fields increase MSC osteogenesis, remain unclear. Future research should focus on the signaling pathways leading to the response of MSCs to osteogenic stimulation.

AUTHOR CONTRIBUTIONS

KZ: collection and assembly of data, manuscript writing; YT: conception of figures, manuscript writing; AP: conception and design; BM and GL: conception and design, final approval of the manuscript.

FUNDING

This work was supported by the National Science Foundation of China (No. 82002313, No. 82072444), the National Key Research and Development Program of China (No. 2018YFC2001502, 2021YFA1101500); the Department of Science and Technology of Hubei Province (No. 2020BCB004), Hubei Province Key Laboratory of Oral and Maxillofacial Development and Regeneration (No. 2020kqhm008), the Health Commission of Hubei Province (No. WJ 2019Z009), and the Wuhan Union Hospital "Pharmaceutical Technology nursing" special fund (No.2019xhyn021).

ACKNOWLEDGMENTS

We thank members of the Liu lab for constructive suggestions.

REFERENCES

Amaral, D. L., Zanette, R. S., Almeida, C. G., Almeida, L. B., Oliveira, L. F. d., Marcomini, R. F., et al. (2019). *In Vitro* evaluation of Barium Titanate Nanoparticle/alginate 3D Scaffold for Osteogenic Human Stem Cell Differentiation. *Biomed. Mater.* 14, 035011. doi:10.1088/1748-605X/ab0a52

Amghar-Maach, S., Gay-Escoda, C., and Sanchez-Garces, M. (2019). Regeneration of Periodontal Bone Defects with Dental Pulp Stem Cells Grafting: Systematic Review. *J. Clin. Exp. Dent* 11, e373–e381. doi:10.4317/jced.55574

Ansari, A. S., Yazid, M. D., Sainik, N. Q. A. V., Razali, R. A., Saim, A. B., and Idrus, R. B. H. (2018). Osteogenic Induction of Wharton's Jelly-Derived Mesenchymal Stem Cell for Bone Regeneration: A Systematic Review. *Stem Cell Int.* 2018, 1–17. doi:10.1155/2018/2406462

Aquino-Martínez, R., Artigas, N., Gámez, B., Rosa, J. L., and Ventura, F. (2017). Extracellular Calcium Promotes Bone Formation from Bone Marrow Mesenchymal Stem Cells by Amplifying the Effects of BMP-2 on SMAD Signalling. *PLoS One* 12, e0178158. doi:10.1371/journal.pone.0178158

Aswamenakul, K., Klabklai, P., Pannengpetch, S., Tawonsawatruk, T., Isarankura-Na-Ayudhya, C., Roytrakul, S., et al. (2020). Proteomic Study of *In Vitro* Osteogenic Differentiation of Mesenchymal Stem Cells in High Glucose Condition. *Mol. Biol. Rep.* 47, 7505–7516. doi:10.1007/s11033-020-05811-x

Barilani, M., Banfi, F., Sironi, S., Ragni, E., Guillaumin, S., Polveraccio, F., et al. (2018). Low-affinity Nerve Growth Factor Receptor (CD271) Heterogeneous Expression in Adult and Fetal Mesenchymal Stromal Cells. *Sci. Rep.* 8, 9321. doi:10.1038/s41598-018-27587-8

Bertolo, A., Mehr, M., Janner-Jametti, T., Graumann, U., Aebli, N., Baur, M., et al. (2016). Anin Vitroexpansion Score for Tissue-Engineering Applications with Human Bone Marrow-Derived Mesenchymal Stem Cells. *J. Tissue Eng. Regen. Med.* 10, 149–161. doi:10.1002/term.1734

Binder, B. Y. K., Sagun, J. E., and Leach, J. K. (2015). Reduced Serum and Hypoxic Culture Conditions Enhance the Osteogenic Potential of Human Mesenchymal Stem Cells. *Stem Cel Rev Rep* 11, 387–393. doi:10.1007/s12015-014-9555-7

Bouland, C., Philippart, P., Dequanter, D., Corrillon, F., Loeb, I., Bron, D., et al. (2021). Cross-Talk between Mesenchymal Stromal Cells (MSCs) and Endothelial Progenitor Cells (EPCs) in Bone Regeneration. *Front. Cel Dev. Biol.* 9, 674084. doi:10.3389/fcell.2021.674084

Bragdon, B., Burns, R., Baker, A. H., Belkina, A. C., Morgan, E. F., Denis, G. V., et al. (2015). Intrinsic Sex-Linked Variations in Osteogenic and Adipogenic Differentiation Potential of Bone Marrow Multipotent Stromal Cells. *J. Cel. Physiol.* 230, 296–307. doi:10.1002/jcp.24705

Brennan, M. Á., Renaud, A., Gamblin, A.-l., D'Arros, C., Nedellec, S., Trichet, V., et al. (2015). 3D Cell Culture and Osteogenic Differentiation of Human Bone Marrow Stromal Cells Plated onto Jet-Sprayed or Electrospun Micro-fiber Scaffolds. *Biomed. Mater.* 10, 045019. doi:10.1088/1748-6041/10/4/045019

Cabrera-Pérez, R., Monguió-Tortajada, M., Gámez-Valero, A., Rojas-Márquez, R., Borràs, F. E., Roura, S., et al. (2019). Osteogenic Commitment of Wharton's Jelly Mesenchymal Stromal Cells: Mechanisms and Implications for Bioprocess Development and Clinical Application. *Stem Cel Res Ther* 10, 356. doi:10.1186/s13287-019-1450-3

Caliari, S. R., and Harley, B. A. C. (2014). Structural and Biochemical Modification of a Collagen Scaffold to Selectively Enhance MSC Tenogenic, Chondrogenic, and Osteogenic Differentiation. *Adv. Healthc. Mater.* 3, 1086–1096. doi:10.1002/adhm.201300646

Carvalho, M. S., Alves, L., Bogalho, I., Cabral, J. M. S., and da Silva, C. L. (2021). Impact of Donor Age on the Osteogenic Supportive Capacity of Mesenchymal Stromal Cell-Derived Extracellular Matrix. *Front. Cel Dev. Biol.* 9, 747521. doi:10.3389/fcell.2021.747521

Ceccarelli, G., Bloise, N., Mantelli, M., Gastaldi, G., Fassina, L., Cusella De Angelis, M. G., et al. (2013). A Comparative Analysis of theIn VitroEffects of Pulsed Electromagnetic Field Treatment on Osteogenic Differentiation of Two Different Mesenchymal Cell Lineages. *BioResearch Open Access* 2, 283–294. doi:10.1089/biores.2013.0016

Chen, J., and Long, F. (2013). β-Catenin Promotes Bone Formation and Suppresses Bone Resorption in Postnatal Growing Mice. *J. Bone Miner Res.* 28, 1160–1169. doi:10.1002/jbmr.1834

Chen, L., Wu, J., Wu, C., Xing, F., Li, L., He, Z., et al. (2019). Three-Dimensional Co-culture of Peripheral Blood-Derived Mesenchymal Stem Cells and Endothelial Progenitor Cells for Bone Regeneration. *J. Biomed. Nanotechnol* 15, 248–260. doi:10.1166/jbn.2019.2680

Chen, Q., Shou, P., Zheng, C., Jiang, M., Cao, G., Yang, Q., et al. (2016). Fate Decision of Mesenchymal Stem Cells: Adipocytes or Osteoblasts? *Cell Death Differ* 23, 1128–1139. doi:10.1038/cdd.2015.168

Chen, X., Yan, J., He, F., Zhong, D., Yang, H., Pei, M., et al. (2018). Mechanical Stretch Induces Antioxidant Responses and Osteogenic Differentiation in Human Mesenchymal Stem Cells through Activation of the AMPK-SIRT1 Signaling Pathway. *Free Radic. Biol. Med.* 126, 187–201. doi:10.1016/j.freeradbiomed.2018.08.001

Clarke, B. (2008). Normal Bone Anatomy and Physiology. *Cjasn* 3 (Suppl. 3), S131–S139. doi:10.2215/CJN.04151206

Creecy, C. M., O'Neill, C. F., Arulanandam, B. P., Sylvia, V. L., Navara, C. S., and Bizios, R. (2013). Mesenchymal Stem Cell Osteodifferentiation in Response to Alternating Electric Current. *Tissue Eng. A* 19, 467–474. doi:10.1089/ten.TEA.2012.0091

Curry, A. S., Pensa, N. W., Barlow, A. M., and Bellis, S. L. (2016). Taking Cues from the Extracellular Matrix to Design Bone-Mimetic Regenerative Scaffolds. *Matrix Biol.* 52-54, 397–412. doi:10.1016/j.matbio.2016.02.011

Day, T. F., Guo, X., Garrett-Beal, L., and Yang, Y. (2005). Wnt/β-Catenin Signaling in Mesenchymal Progenitors Controls Osteoblast and Chondrocyte Differentiation during Vertebrate Skeletogenesis. *Developmental Cel* 8, 739–750. doi:10.1016/j.devcel.2005.03.016

Denu, R. A., and Hematti, P. (20162016). Effects of Oxidative Stress on Mesenchymal Stem Cell Biology. *Oxidative Med. Cell Longevity* 2016, 1–9. doi:10.1155/2016/2989076

Ding, D.-C., Chou, H.-L., Hung, W.-T., Liu, H.-W., and Chu, T.-Y. (2013). Human Adipose-Derived Stem Cells Cultured in Keratinocyte Serum Free Medium: Donor's Age Does Not Affect the Proliferation and Differentiation Capacities. *J. Biomed. Sci.* 20, 59. doi:10.1186/1423-0127-20-59

Ding, L., Vezzani, B., Khan, N., Su, J., Xu, L., Yan, G., et al. (2020). CD10 Expression Identifies a Subset of Human Perivascular Progenitor Cells with High Proliferation and Calcification Potentials. *Stem Cells* 38, 261–275. doi:10.1002/stem.3112

Dominici, M., Le Blanc, K., Mueller, I., Slaper-Cortenbach, I., Marini, F. C., Krause, D. S., et al. (2006). Minimal Criteria for Defining Multipotent Mesenchymal Stromal Cells. The International Society for Cellular Therapy Position Statement. *Cytotherapy* 8, 315–317. doi:10.1080/14653240600855905

Dong, C., and Lv, Y. (2016). Application of Collagen Scaffold in Tissue Engineering: Recent Advances and New Perspectives. *Polymers* 8, 42. doi:10.3390/polym8020042

Eischen-Loges, M., Oliveira, K. M. C., Bhavsar, M. B., Barker, J. H., and Leppik, L. (2018). Pretreating Mesenchymal Stem Cells with Electrical Stimulation Causes Sustained Long-Lasting Pro-osteogenic Effects. *PeerJ* 6, e4959. doi:10.7717/peerj.4959

Fakhry, M., Hamade, E., Badran, B., Buchet, R., and Magne, D. (2013). Molecular Mechanisms of Mesenchymal Stem Cell Differentiation towards Osteoblasts. *Wjsc* 5, 136–148. doi:10.4252/wjsc.v5.i4.136

Ferlin, K. M., Prendergast, M. E., Miller, M. L., Kaplan, D. S., and Fisher, J. P. (2016). Influence of 3D Printed Porous Architecture on Mesenchymal Stem Cell Enrichment and Differentiation. *Acta Biomater.* 32, 161–169. doi:10.1016/j.actbio.2016.01.007

Ferro, F., Spelat, R., and Baheney, C. S. (2014). Dental Pulp Stem Cell (DPSC) Isolation, Characterization, and Differentiation. *Methods Mol. Biol.* 1210, 91–115. doi:10.1007/978-1-4939-1435-7_8

Fotia, C., Massa, A., Boriani, F., Baldini, N., and Granchi, D. (2015). Prolonged Exposure to Hypoxic Milieu Improves the Osteogenic Potential of Adipose Derived Stem Cells. *J. Cel. Biochem.* 116, 1442–1453. doi:10.1002/jcb.25106

Friedman, M. S., Long, M. W., and Hankenson, K. D. (2006). Osteogenic Differentiation of Human Mesenchymal Stem Cells Is Regulated by Bone Morphogenetic Protein-6. *J. Cel. Biochem.* 98, 538–554. doi:10.1002/jcb.20719

Gage, J., Liporace, A., Egol, A., and McLaurin, M. (2018). Management of Bone Defects in Orthopedic Trauma. *Bull. Hosp. Jt. Dis. (2013)* 76, 4–8.

García de Frutos, A., González-Tartière, P., Coll Bonet, R., Ubierna Garcés, M. T., Del Arco Churruca, A., Rivas García, A., et al. (2020). Randomized Clinical Trial: Expanded Autologous Bone Marrow Mesenchymal Cells Combined with Allogeneic Bone Tissue, Compared with Autologous Iliac Crest Graft in Lumbar Fusion Surgery. *Spine J.* 20, 1899–1910. doi:10.1016/j.spinee.2020.07.014

Garcia-Sanchez, D., Fernandez, D., Rodríguez-Rey, J. C., and Perez-Campo, F. M. (2019). Enhancing Survival, Engraftment, and Osteogenic Potential of Mesenchymal Stem Cells. *Wjsc* 11, 748–763. doi:10.4252/wjsc.v11.i10.748

Garg, P., Mazur, M. M., Buck, A. C., Wandtke, M. E., Liu, J., and Ebraheim, N. A. (2017). Prospective Review of Mesenchymal Stem Cells Differentiation into Osteoblasts. *Orthop. Surg.* 9, 13–19. doi:10.1111/os.12304

Gershovich, J. G., Dahlin, R. L., Kasper, F. K., and Mikos, A. G. (2013). Enhanced Osteogenesis in Cocultures with Human Mesenchymal Stem Cells and Endothelial Cells on Polymeric Microfiber Scaffolds. *Tissue Eng. Part A* 19, 2565–2576. doi:10.1089/ten.TEA.2013.0256

Gharibi, B., Cama, G., Capurro, M., Thompson, I., Deb, S., Di Silvio, L., et al. (2013). Gene Expression Responses to Mechanical Stimulation of Mesenchymal Stem Cells Seeded on Calcium Phosphate Cement. *Tissue Eng. Part A* 19, 2426–2438. doi:10.1089/ten.tea.2012.0623

Giannotti, S., Trombi, L., Bottai, V., Ghilardi, M., D'Alessandro, D., Danti, S., et al. (2013). Use of Autologous Human Mesenchymal Stromal Cell/fibrin Clot Constructs in Upper Limb Non-unions: Long-Term Assessment. *PLoS One* 8, e73893. doi:10.1371/journal.pone.0073893

Gong, L., Zhao, Y., Zhang, Y., and Ruan, Z. (2016). The Macrophage Polarization Regulates MSC Osteoblast Differentiation *In Vitro*. *Ann. Clin. Lab. Sci.* 46, 65–71.

Grellier, M., Bordenave, L., and Amédée, J. (2009). Cell-to-cell Communication between Osteogenic and Endothelial Lineages: Implications for Tissue Engineering. *Trends Biotechnol.* 27, 562–571. doi:10.1016/j.tibtech.2009.07.001

Griffin, F. E., Schiavi, J., McDevitt, T. C., McGarry, J. P., and McNamara, L. M. (2017). The Role of Adhesion Junctions in the Biomechanical Behaviour and Osteogenic Differentiation of 3D Mesenchymal Stem Cell Spheroids. *J. Biomech.* 59, 71–79. doi:10.1016/j.jbiomech.2017.05.014

Grotheer, V., Skrynecki, N., Oezel, L., Windolf, J., and Grassmann, J. (2021). Osteogenic Differentiation of Human Mesenchymal Stromal Cells and Fibroblasts Differs Depending on Tissue Origin and Replicative Senescence. *Sci. Rep.* 11, 11968. doi:10.1038/s41598-021-91501-y

Gu, Q., Gu, Y., Shi, Q., and Yang, H. (2016). Hypoxia Promotes Osteogenesis of Human Placental-Derived Mesenchymal Stem Cells. *Tohoku J. Exp. Med.* 239, 287–296. doi:10.1620/tjem.239.287

Guda, T., Labella, C., Chan, R., and Hale, R. (2014). Quality of Bone Healing: Perspectives and Assessment Techniques. *Wound Repair Regen.* 22 (Suppl. 1), 39–49. doi:10.1111/wrr.12167

Gullo, F., and De Bari, C. (2013). Prospective Purification of a Subpopulation of Human Synovial Mesenchymal Stem Cells with Enhanced Chondro-Osteogenic Potency. *Rheumatology (Oxford)* 52, 1758–1768. doi:10.1093/rheumatology/ket205

Halim, A., Ariyanti, A. D., Luo, Q., and Song, G. (2020). Recent Progress in Engineering Mesenchymal Stem Cell Differentiation. *Stem Cel Rev Rep* 16, 661–674. doi:10.1007/s12015-020-09979-4

Han, Y., Li, X., Zhang, Y., Han, Y., Chang, F., and Ding, J. (2019). Mesenchymal Stem Cells for Regenerative Medicine. *Cells* 8, 886. doi:10.3390/cells8080886

Hass, R., Kasper, C., Böhm, S., and Jacobs, R. (2011). Different Populations and Sources of Human Mesenchymal Stem Cells (MSC): A Comparison of Adult and Neonatal Tissue-Derived MSC. *Cell Commun Signal* 9, 12. doi:10.1186/1478-811X-9-12

Hohenbild, F., Arango Ospina, M., Schmitz, S. I., Moghaddam, A., Boccaccini, A. R., and Westhauser, F. (2021). An *In Vitro* Evaluation of the Biological and Osteogenic Properties of Magnesium-Doped Bioactive Glasses for Application in Bone Tissue Engineering. *Ijms* 22, 12703. doi:10.3390/ijms222312703

Holtorf, H. L., Jansen, J. A., and Mikos, A. G. (2005). Flow Perfusion Culture Induces the Osteoblastic Differentiation of Marrow Stromal Cell-Scaffold Constructs in the Absence of Dexamethasone. *J. Biomed. Mater. Res.* 72A, 326–334. doi:10.1002/jbm.a.30251

Hou, J., Luo, T., Chen, S., Lin, S., Yang, M. M., Li, G., et al. (2019). Calcium Spike Patterns Reveal Linkage of Electrical Stimulus and MSC Osteogenic Differentiation. *IEEE Trans.on Nanobioscience* 18, 3–9. doi:10.1109/TNB.2018.2881004

Hu, K., Sun, H., Gui, B., and Sui, C. (2017). Gremlin-1 Suppression Increases BMP-2-Induced Osteogenesis of Human Mesenchymal Stem Cells. *Mol. Med. Rep.* 15, 2186–2194. doi:10.3892/mmr.2017.6253

Hu, M., Yeh, R., Lien, M., Teeratananon, M., Agarwal, K., and Qin, Y.-X. (2013). Dynamic Fluid Flow Mechanical Stimulation Modulates Bone Marrow Mesenchymal Stem Cells. *Bone Res.* 1, 98–104. doi:10.4248/BR201301007

Huang, C., Dai, J., and Zhang, X. A. (2015). Environmental Physical Cues Determine the Lineage Specification of Mesenchymal Stem Cells. *Biochim. Biophys. Acta (Bba) - Gen. Subjects* 1850, 1261–1266. doi:10.1016/j.bbagen.2015.02.011

Hussain, A., Bessho, K., Takahashi, K., and Tabata, Y. (2014). Magnesium Calcium Phosphate/β-Tricalcium Phosphate Incorporation into Gelatin Scaffold: Anin Vitrocomparative Study. *J. Tissue Eng. Regen. Med.* 8, 919–924. doi:10.1002/term.1596

Ito, K., Yamada, Y., Nakamura, S., and Ueda, M. (2011). Osteogenic Potential of Effective Bone Engineering Using Dental Pulp Stem Cells, Bone Marrow Stem Cells, and Periosteal Cells for Osseointegration of Dental Implants. *Int. J. Oral Maxillofac. Implants* 26, 947–954.

James, A. W., Pang, S., Askarinam, A., Corselli, M., Zara, J. N., Goyal, R., et al. (2012). Additive Effects of Sonic Hedgehog and Nell-1 Signaling in Osteogenic versus Adipogenic Differentiation of Human Adipose-Derived Stromal Cells. *Stem Cell Development* 21, 2170–2178. doi:10.1089/scd.2011.0461

James, A. W. (20132013). Review of Signaling Pathways Governing MSC Osteogenic and Adipogenic Differentiation. *Scientifica* 2013, 1–17. doi:10.1155/2013/684736

Jensen, J., Tvedesøe, C., Rölfing, J. H. D., Foldager, C. B., Lysdahl, H., Kraft, D. C. E., et al. (2016). Dental Pulp-Derived Stromal Cells Exhibit a Higher Osteogenic Potency Than Bone Marrow-Derived Stromal Cells *In Vitro* and in a Porcine Critical-Size Bone Defect Model. *SICOT-J* 2, 16. doi:10.1051/sicotj/2016004

Kalaszczynska, I., and Ferdyn, K. (2015). Wharton's Jelly Derived Mesenchymal Stem Cells: Future of Regenerative Medicine? Recent Findings and Clinical Significance. *Biomed. Res. Int.* 2015, 1–11. doi:10.1155/2015/430847

Kang, M.-N., Yoon, H.-H., Seo, Y.-K., and Park, J.-K. (2012). Effect of Mechanical Stimulation on the Differentiation of Cord Stem Cells. *Connect. Tissue Res.* 53, 149–159. doi:10.3109/03008207.2011.619284

Kasten, P., Beyen, I., Niemeyer, P., Luginbühl, R., Bohner, M., and Richter, W. (2008). Porosity and Pore Size of β-tricalcium Phosphate Scaffold Can Influence Protein Production and Osteogenic Differentiation of Human Mesenchymal Stem Cells: An *In Vitro* and *In Vivo* Study. *Acta Biomater.* 4, 1904–1915. doi:10.1016/j.actbio.2008.05.017

Kim, E.-C., Leesungbok, R., Lee, S.-W., Lee, H.-W., Park, S. H., Mah, S.-J., et al. (2015). Effects of Moderate Intensity Static Magnetic fields on Human Bone Marrow-Derived Mesenchymal Stem Cells. *Bioelectromagnetics* 36, 267–276. doi:10.1002/bem.21903

Kim, H.-J., Sung, I.-Y., Cho, Y.-C., Kang, M.-S., Rho, G.-J., Byun, J.-H., et al. (2019). Three-Dimensional Spheroid Formation of Cryopreserved Human Dental Follicle-Derived Stem Cells Enhances Pluripotency and Osteogenic Induction Properties. *Tissue Eng. Regen. Med.* 16, 513–523. doi:10.1007/s13770-019-00203-0

Kim, H. J., Kim, K.-W., Kwon, Y.-R., Kim, B.-M., and Kim, Y.-J. (2018a). Forced Expression of CD200 Improves the Differentiation Capability and Immunoregulatory Functions of Mesenchymal Stromal Cells. *Biotechnol. Lett.* 40, 1425–1433. doi:10.1007/s10529-018-2561-0

Kim, Y., Kang, B.-J., Kim, W., Yun, H.-s., and Kweon, O.-k. (2018b). Evaluation of Mesenchymal Stem Cell Sheets Overexpressing BMP-7 in Canine Critical-Sized Bone Defects. *Ijms* 19, 2073. doi:10.3390/ijms19072073

Kimura, K., Breitbach, M., Schildberg, F. A., Hesse, M., and Fleischmann, B. K. (2021). Bone Marrow CD73+ Mesenchymal Stem Cells Display Increased Stemness *In Vitro* and Promote Fracture Healing *In Vivo*. *Bone Rep.* 15, 101133. doi:10.1016/j.bonr.2021.101133

Kosinski, M., Figiel-Dabrowska, A., Lech, W., Wieprzowski, L., Strzalkowski, R., Strzemecki, D., et al. (2020). Bone Defect Repair Using a Bone Substitute Supported by Mesenchymal Stem Cells Derived from the Umbilical Cord. *Stem Cell Int.* 2020, 1–15. doi:10.1155/2020/1321283

Kouroupis, D., Bowles, A. C., Best, T. M., Kaplan, L. D., and Correa, D. (2020). CD10/Neprilysin Enrichment in Infrapatellar Fat Pad-Derived Mesenchymal Stem Cells under Regulatory-Compliant Conditions: Implications for Efficient Synovitis and Fat Pad Fibrosis Reversal. *Am. J. Sports Med.* 48, 2013–2027. doi:10.1177/0363546520917699

Kouroupis, D., and Correa, D. (2021). Increased Mesenchymal Stem Cell Functionalization in Three-Dimensional Manufacturing Settings for Enhanced Therapeutic Applications. *Front. Bioeng. Biotechnol.* 9, 621748. doi:10.3389/fbioe.2021.621748

Kumar, A., Kumar, V., Rattan, V., Jha, V., and Bhattacharyya, S. (2018). Secretome Proteins Regulate Comparative Osteogenic and Adipogenic Potential in Bone Marrow and Dental Stem Cells. *Biochimie* 155, 129–139. doi:10.1016/j.biochi.2018.10.014

Kwon, H. J., Lee, G. S., and Chun, H. (2016). Electrical Stimulation Drives Chondrogenesis of Mesenchymal Stem Cells in the Absence of Exogenous Growth Factors. *Sci. Rep.* 6, 39302. doi:10.1038/srep39302

Lee, H.-J., Lee, H., Na, C.-B., Song, I.-S., Ryu, J.-J., and Park, J.-B. (2021). Evaluation of the Age- and Sex-Related Changes of the Osteogenic Differentiation Potentials of Healthy Bone Marrow-Derived Mesenchymal Stem Cells. *Medicina* 57, 520. doi:10.3390/medicina57060520

Lee, J., Chu, S., Kim, H., Choi, K., Oh, E., Shim, J.-H., et al. (2017). Osteogenesis of Adipose-Derived and Bone Marrow Stem Cells with Polycaprolactone/Tricalcium Phosphate and Three-Dimensional Printing Technology in a Dog Model of Maxillary Bone Defects. *Polymers* 9, 450. doi:10.3390/polym9090450

Leonardi, E., Devescovi, V., Perut, F., Ciapetti, G., and Giunti, A. (2008). Isolation, Characterisation and Osteogenic Potential of Human Bone Marrow Stromal Cells Derived from the Medullary Cavity of the Femur. *Chir Organi Mov* 92, 97–103. doi:10.1007/s12306-008-0057-0

Leppik, L., Zhihua, H., Mobini, S., Thottakkattumana Parameswaran, V., Eischen-Loges, M., Slavici, A., et al. (2018). Combining Electrical Stimulation and Tissue Engineering to Treat Large Bone Defects in a Rat Model. *Sci. Rep.* 8, 6307. doi:10.1038/s41598-018-24892-0

Li, A., Xia, X., Yeh, J., Kua, H., Liu, H., Mishina, Y., et al. (2014). PDGF-AA Promotes Osteogenic Differentiation and Migration of Mesenchymal Stem Cell by Down-Regulating PDGFRα and Derepressing BMP-Smad1/5/8 Signaling. *PLoS One* 9, e113785. doi:10.1371/journal.pone.0113785

Li, J. J., Ebied, M., Xu, J., and Zreiqat, H. (2018a). Current Approaches to Bone Tissue Engineering: The Interface between Biology and Engineering. *Adv. Healthc. Mater.* 7, 1701061. doi:10.1002/adhm.201701061

Li, R., Liang, L., Dou, Y., Huang, Z., Mo, H., Wang, Y., et al. (2015). Mechanical Strain Regulates Osteogenic and Adipogenic Differentiation of Bone Marrow Mesenchymal Stem Cells. *Biomed. Res. Int.* 2015, 1–10. doi:10.1155/2015/873251

Li, Y., Jin, D., Xie, W., Wen, L., Chen, W., Xu, J., et al. (2018b). PPAR-γ and Wnt Regulate the Differentiation of MSCs into Adipocytes and Osteoblasts Respectively. *Cscr* 13, 185–192. doi:10.2174/1574888X12666171012141908

Liang, Y., Wen, L., Shang, F., Wu, J., Sui, K., and Ding, Y. (2016). Endothelial Progenitors Enhanced the Osteogenic Capacities of Mesenchymal Stem Cells *In Vitro* and in a Rat Alveolar Bone Defect Model. *Arch. Oral Biol.* 68, 123–130. doi:10.1016/j.archoralbio.2016.04.007

Little, R. D., Folz, C., Manning, S. P., Swain, P. M., Zhao, S.-C., Eustace, B., et al. (2002). A Mutation in the LDL Receptor-Related Protein 5 Gene Results in the Autosomal Dominant High-Bone-Mass Trait. *Am. J. Hum. Genet.* 70, 11–19. doi:10.1086/338450

Liu, S., Jia, Y., Yuan, M., Guo, W., Huang, J., Zhao, B., et al. (2017). Repair of Osteochondral Defects Using Human Umbilical Cord Wharton's Jelly-Derived Mesenchymal Stem Cells in a Rabbit Model. *Biomed. Res. Int.* 2017, 1–12. doi:10.1155/2017/8760383

Lorusso, F., Inchingolo, F., Dipalma, G., Postiglione, F., Fulle, S., and Scarano, A. (2020). Synthetic Scaffold/Dental Pulp Stem Cell (DPSC) Tissue Engineering Constructs for Bone Defect Treatment: An Animal Studies Literature Review. *Ijms* 21, 9765. doi:10.3390/ijms21249765

Lotfy, A., Salama, M., Zahran, F., Jones, E., Badawy, A., and Sobh, M. (2014). Characterization of Mesenchymal Stem Cells Derived from Rat Bone Marrow and Adipose Tissue: a Comparative Study. *Int. J. Stem Cell* 7, 135–142. doi:10.15283/ijsc.2014.7.2.135

Luo, M.-l., Jiao, Y., Gong, W.-p., Li, Y., Niu, L.-n., Tay, F. R., et al. (2020). Macrophages Enhance Mesenchymal Stem Cell Osteogenesis via Down-Regulation of Reactive Oxygen Species. *J. Dentistry* 94, 103297. doi:10.1016/j.jdent.2020.103297

Marolt Presen, D., Traweger, A., Gimona, M., and Redl, H. (2019). Mesenchymal Stromal Cell-Based Bone Regeneration Therapies: From Cell Transplantation and Tissue Engineering to Therapeutic Secretomes and Extracellular Vesicles. *Front. Bioeng. Biotechnol.* 7, 352. doi:10.3389/fbioe.2019.00352

Medhat, D., Rodríguez, C. I., and Infante, A. (2019). Immunomodulatory Effects of MSCs in Bone Healing. *Ijms* 20, 5467. doi:10.3390/ijms20215467

Mikami, Y., Ishii, Y., Watanabe, N., Shirakawa, T., Suzuki, S., Irie, S., et al. (2011). CD271/p75NTRInhibits the Differentiation of Mesenchymal Stem Cells into Osteogenic, Adipogenic, Chondrogenic, and Myogenic Lineages. *Stem Cell Development* 20, 901–913. doi:10.1089/scd.2010.0299

Mitra, D., Whitehead, J., Yasui, O. W., and Leach, J. K. (2017). Bioreactor Culture Duration of Engineered Constructs Influences Bone Formation by Mesenchymal Stem Cells. *Biomaterials* 146, 29–39. doi:10.1016/j.biomaterials.2017.08.044

Morrison, D. A., Kop, A. M., Nilasaroya, A., Sturm, M., Shaw, K., and Honeybul, S. (2018). Cranial Reconstruction Using Allogeneic Mesenchymal Stromal Cells: A Phase 1 First-in-human Trial. *J. Tissue Eng. Regen. Med.* 12, 341–348. doi:10.1002/term.2459

Ning, T., Zhang, K., Zhang, K., Chin Heng, B., and Ge, Z. (2019). Diverse Effects of Pulsed Electrical Stimulation on Cells - with a Focus on Chondrocytes and Cartilage Regeneration. *eCM* 38, 79–93. doi:10.22203/eCM.v038a07

Paduano, F., Marrelli, M., Palmieri, F., and Tatullo, M. (2016). CD146 Expression Influences Periapical Cyst Mesenchymal Stem Cell Properties. *Stem Cel Rev Rep* 12, 592–603. doi:10.1007/s12015-016-9674-4

Pajarinen, J., Lin, T., Gibon, E., Kohno, Y., Maruyama, M., Nathan, K., et al. (2019). Mesenchymal Stem Cell-Macrophage Crosstalk and Bone Healing. *Biomaterials* 196, 80–89. doi:10.1016/j.biomaterials.2017.12.025

Park, J.-W., Hanawa, T., and Chung, J.-H. (2019). The Relative Effects of Ca and Mg Ions on MSC Osteogenesis in the Surface Modification of Microrough Ti Implants. *Ijn* 14, 5697–5711. doi:10.2147/IJN.S214363

Pettersson, L. F., Kingham, P. J., Wiberg, M., and Kelk, P. (2017). *In Vitro* Osteogenic Differentiation of Human Mesenchymal Stem Cells from Jawbone Compared with Dental Tissue. *Tissue Eng. Regen. Med.* 14, 763–774. doi:10.1007/s13770-017-0071-0

Pokrovskaya, L. A., Nadezhdin, S. V., Zubareva, E. V., Burda, Y. E., and Gnezdyukova, E. S. (2020). Expression of RUNX2 and Osterix in Rat Mesenchymal Stem Cells during Culturing in Osteogenic-Conditioned Medium. *Bull. Exp. Biol. Med.* 169, 571–575. doi:10.1007/s10517-020-04931-5

Prasopthum, A., Cooper, M., Shakesheff, K. M., and Yang, J. (2019). Three-Dimensional Printed Scaffolds with Controlled Micro-/Nanoporous Surface Topography Direct Chondrogenic and Osteogenic Differentiation of Mesenchymal Stem Cells. *ACS Appl. Mater. Inter.* 11, 18896–18906. doi:10.1021/acsami.9b01472

Pullisaar, H., Reseland, J. E., Haugen, H. J., Brinchmann, J. E., and Østrup, E. (2014). Simvastatin Coating of TiO2 Scaffold Induces Osteogenic Differentiation of Human Adipose Tissue-Derived Mesenchymal Stem Cells. *Biochem. Biophysical Res. Commun.* 447, 139–144. doi:10.1016/j.bbrc.2014.03.133

Qi, M.-C., Hu, J., Zou, S.-J., Chen, H.-Q., Zhou, H.-X., and Han, L.-C. (2008). Mechanical Strain Induces Osteogenic Differentiation: Cbfa1 and Ets-1 Expression in Stretched Rat Mesenchymal Stem Cells. *Int. J. Oral Maxillofacial Surg.* 37, 453–458. doi:10.1016/j.ijom.2007.12.008

Qi, X., Zhang, J., Yuan, H., Xu, Z., Li, Q., Niu, X., et al. (2016). Exosomes Secreted by Human-Induced Pluripotent Stem Cell-Derived Mesenchymal Stem Cells Repair Critical-Sized Bone Defects through Enhanced Angiogenesis and Osteogenesis in Osteoporotic Rats. *Int. J. Biol. Sci.* 12, 836–849. doi:10.7150/ijbs.14809

Querques, F., D'Agostino, A., Cozzolino, C., Cozzuto, L., Lombardo, B., Leggiero, E., et al. (2019). Identification of a Novel Transcription Factor Required for Osteogenic Differentiation of Mesenchymal Stem Cells. *Stem Cell Development* 28, 370–383. doi:10.1089/scd.2018.0152

Quirici, N., Soligo, D., Bossolasco, P., Servida, F., Lumini, C., and Deliliers, G. L. (2002). Isolation of Bone Marrow Mesenchymal Stem Cells by Anti-nerve Growth Factor Receptor Antibodies. *Exp. Hematol.* 30, 783–791. doi:10.1016/s0301-472x(02)00812-3

Saleh, F., Carstairs, A., Etheridge, S. L., and Genever, P. (2016). Real-Time Analysis of Endogenous Wnt Signalling in 3D Mesenchymal Stromal Cells. *Stem Cell Int.* 2016, 1–9. doi:10.1155/2016/7132529

Salgado, C. L., Teixeira, B. I. B., and Monteiro, F. J. M. (2019). Biomimetic Composite Scaffold with Phosphoserine Signaling for Bone Tissue Engineering Application. *Front. Bioeng. Biotechnol.* 7, 206. doi:10.3389/fbioe.2019.00206

Sankar, S., Sharma, C. S., and Rath, S. N. (2019). Enhanced Osteodifferentiation of MSC Spheroids on Patterned Electrospun Fiber Mats - an Advanced 3D Double Strategy for Bone Tissue Regeneration. *Mater. Sci. Eng. C* 94, 703–712. doi:10.1016/j.msec.2018.10.025

Seong, J. M., Kim, B.-C., Park, J.-H., Kwon, I. K., Mantalaris, A., and Hwang, Y.-S. (2010). Stem Cells in Bone Tissue Engineering. *Biomed. Mater.* 5, 062001. doi:10.1088/1748-6041/5/6/062001

Shekaran, A., Sim, E., Tan, K. Y., Chan, J. K. Y., Choolani, M., Reuveny, S., et al. (2015). Enhanced *In Vitro* Osteogenic Differentiation of Human Fetal MSCs Attached to 3D Microcarriers versus Harvested from 2D Monolayers. *BMC Biotechnol.* 15, 102. doi:10.1186/s12896-015-0219-8

Silva, J. C., Carvalho, M. S., Udangawa, R. N., Moura, C. S., Cabral, J. M. S., L. da Silva, C., et al. (2020). Extracellular Matrix Decorated Polycaprolactone Scaffolds for Improved Mesenchymal Stem/stromal Cell Osteogenesis towards a Patient-tailored Bone Tissue Engineering Approach. *J. Biomed. Mater. Res.* 108, 2153–2166. doi:10.1002/jbm.b.34554

Sinder, B. P., Pettit, A. R., and McCauley, L. K. (2015). Macrophages: Their Emerging Roles in Bone. *J. Bone Miner Res.* 30, 2140–2149. doi:10.1002/jbmr.2735

Spinella-Jaegle, S., Rawadi, G., Kawai, S., Gallea, S., Faucheu, C., Mollat, P., et al. (2001). Sonic Hedgehog Increases the Commitment of Pluripotent Mesenchymal Cells into the Osteoblastic Lineage and Abolishes Adipocytic Differentiation. *J. Cel Sci* 114, 2085–2094. doi:10.1242/jcs.114.11.2085

Sun, Y., Yuan, Y., Wu, W., Lei, L., and Zhang, L. (2021). The Effects of Locomotion on Bone Marrow Mesenchymal Stem Cell Fate: Insight into Mechanical Regulation and Bone Formation. *Cell Biosci* 11, 88. doi:10.1186/s13578-021-00601-9

Tamama, K., Kawasaki, H., Kerpedjieva, S. S., Guan, J., Ganju, R. K., and Sen, C. K. (2011). Differential Roles of Hypoxia Inducible Factor Subunits in Multipotential Stromal Cells under Hypoxic Condition. *J. Cel. Biochem.* 112, 804–817. doi:10.1002/jcb.22961

Tang, G., Liu, Z., Liu, Y., Yu, J., Wang, X., Tan, Z., et al. (2021). Recent Trends in the Development of Bone Regenerative Biomaterials. *Front. Cel Dev. Biol.* 9, 665813. doi:10.3389/fcell.2021.665813

Tang, H., Husch, J. F. A., Zhang, Y., Jansen, J. A., Yang, F., and Beucken, J. J. J. P. (2019). Coculture with Monocytes/macrophages Modulates Osteogenic Differentiation of Adipose-derived Mesenchymal Stromal Cells on Poly(lactic-co-glycolic) Acid/polycaprolactone Scaffolds. *J. Tissue Eng. Regen. Med.* 13, 785–798. doi:10.1002/term.2826

Tarantino, U., Cerocchi, I., Scialdoni, A., Saturnino, L., Feola, M., Celi, M., et al. (2011). Bone Healing and Osteoporosis. *Aging Clin. Exp. Res.* 23, 62–64.

Thrivikraman, G., Boda, S. K., and Basu, B. (2018). Unraveling the Mechanistic Effects of Electric Field Stimulation towards Directing Stem Cell Fate and Function: A Tissue Engineering Perspective. *Biomaterials* 150, 60–86. doi:10.1016/j.biomaterials.2017.10.003

Tokalov, S. V., Gruener, S., Schindler, S., Iagunov, A. S., Baumann, M., and Abolmaali, N. D. (2007). A Number of Bone Marrow Mesenchymal Stem Cells but Neither Phenotype Nor Differentiation Capacities Changes with Age of Rats. *Mol. Cell* 24, 255–260.

Tsiapalis, D., and O'Driscoll, L. (2020). Mesenchymal Stem Cell Derived Extracellular Vesicles for Tissue Engineering and Regenerative Medicine Applications. *Cells* 9, 991. doi:10.3390/cells9040991

Ulrich, C., Abruzzese, T., Maerz, J. K., Ruh, M., Amend, B., Benz, K., et al. (2015). Human Placenta-Derived CD146-Positive Mesenchymal Stromal Cells Display a Distinct Osteogenic Differentiation Potential. *Stem Cell Development* 24, 1558–1569. doi:10.1089/scd.2014.0465

Urquia Edreira, E. R., Hayrapetyan, A., Wolke, J. G. C., Croes, H. J. E., Klymov, A., Jansen, J. A., et al. (2016). Effect of Calcium Phosphate Ceramic Substrate Geometry on Mesenchymal Stromal Cell Organization and Osteogenic Differentiation. *Biofabrication* 8, 025006. doi:10.1088/1758-5090/8/2/025006

Vieira Paladino, F., de Moraes Rodrigues, J., da Silva, A., and Goldberg, A. C. (2019). The Immunomodulatory Potential of Wharton's Jelly Mesenchymal Stem/Stromal Cells. *Stem Cell Int.* 2019, 1–7. doi:10.1155/2019/3548917

Wang, B., Guo, Y., Chen, X., Zeng, C., Hu, Q., Yin, W., et al. (2018). Nanoparticle-modified Chitosan-Agarose-Gelatin Scaffold for Sustained Release of SDF-1 and BMP-2. *Ijn* 13, 7395–7408. doi:10.2147/IJN.S180859

Wang, C., Huang, W., Zhou, Y., He, L., He, Z., Chen, Z., et al. (2020). 3D Printing of Bone Tissue Engineering Scaffolds. *Bioactive Mater.* 5, 82–91. doi:10.1016/j.bioactmat.2020.01.004

Wang, Q., Xu, L., Willumeit-Römer, R., and Luthringer-Feyerabend, B. J. C. (2021). Macrophage-derived Oncostatin M/bone Morphogenetic Protein 6 in Response to Mg-Based Materials Influences Pro-osteogenic Activity of Human Umbilical Cord Perivascular Cells. *Acta Biomater.* 133, 268–279. doi:10.1016/j.actbio.2020.12.016

Wang, W., and Han, Z. C. (2019). Heterogeneity of Human Mesenchymal Stromal/Stem Cells. *Adv. Exp. Med. Biol.* 1123, 165–177. doi:10.1007/978-3-030-11096-3_10

Wang, X., Wang, Y., Gou, W., Lu, Q., Peng, J., and Lu, S. (2013). Role of Mesenchymal Stem Cells in Bone Regeneration and Fracture Repair: a Review. *Int. Orthopaedics (Sicot)* 37, 2491–2498. doi:10.1007/s00264-013-2059-2

Wang, Y. K., and Chen, C. S. (2013). Cell Adhesion and Mechanical Stimulation in the Regulation of Mesenchymal Stem Cell Differentiation. *J. Cel. Mol. Med.* 17, 823–832. doi:10.1111/jcmm.12061

Weiss, A. R. R., and Dahlke, M. H. (2019). Immunomodulation by Mesenchymal Stem Cells (MSCs): Mechanisms of Action of Living, Apoptotic, and Dead MSCs. *Front. Immunol.* 10, 1191. doi:10.3389/fimmu.2019.01191

Wu, J.-q., Mao, L.-b., Liu, L.-f., Li, Y., Wu, J., Yao, J., et al. (2021). Identification of Key Genes and Pathways of BMP-9-Induced Osteogenic Differentiation of Mesenchymal Stem Cells by Integrated Bioinformatics Analysis. *J. Orthop. Surg. Res.* 16, 273. doi:10.1186/s13018-021-02390-w

Xu, C., Liu, H., He, Y., Li, Y., and He, X. (2020). Endothelial Progenitor Cells Promote Osteogenic Differentiation in Co-cultured with Mesenchymal Stem Cells via the MAPK-dependent Pathway. *Stem Cel Res Ther* 11, 537. doi:10.1186/s13287-020-02056-0

Yahao, G., and Xinjia, W. (2021). The Role and Mechanism of Exosomes from Umbilical Cord Mesenchymal Stem Cells in Inducing Osteogenesis and Preventing Osteoporosis. *Cel Transpl.* 30, 096368972110574. doi:10.1177/09636897211057465

Yamamoto, N., Akamatsu, H., Hasegawa, S., Yamada, T., Nakata, S., Ohkuma, M., et al. (2007). Isolation of Multipotent Stem Cells from Mouse Adipose Tissue. *J. Dermatol. Sci.* 48, 43–52. doi:10.1016/j.jdermsci.2007.05.015

Yang, H. J., Kim, K.-J., Kim, M. K., Lee, S. J., Ryu, Y. H., Seo, B. F., et al. (2014). The Stem Cell Potential and Multipotency of Human Adipose Tissue-Derived Stem Cells Vary by Cell Donor and Are Different from Those of Other Types of Stem Cells. *Cells Tissues Organs* 199, 373–383. doi:10.1159/000369969

Yang, M., Liu, H., Wang, Y., Wu, G., Qiu, S., Liu, C., et al. (2019). Hypoxia Reduces the Osteogenic Differentiation of Peripheral Blood Mesenchymal Stem Cells by Upregulating Notch-1 Expression. *Connect. Tissue Res.* 60, 583–596. doi:10.1080/03008207.2019.1611792

Yang, N., and Liu, Y. (2021). The Role of the Immune Microenvironment in Bone Regeneration. *Int. J. Med. Sci.* 18, 3697–3707. doi:10.7150/ijms.61080

Yang, Y.-H. K., Ogando, C. R., Wang See, C., Chang, T.-Y., and Barabino, G. A. (2018). Changes in Phenotype and Differentiation Potential of Human Mesenchymal Stem Cells Aging *In Vitro*. *Stem Cel Res Ther* 9, 131. doi:10.1186/s13287-018-0876-3

Ye, G., Bao, F., Zhang, X., Song, Z., Liao, Y., Fei, Y., et al. (2020). Nanomaterial-based Scaffolds for Bone Tissue Engineering and Regeneration. *Nanomedicine* 15, 1995–2017. doi:10.2217/nnm-2020-0112

Yu, Y., Park, Y. S., Kim, H. S., Kim, H. Y., Jin, Y. M., Jung, S.-C., et al. (2014). Characterization of Long-Term *In Vitro* Culture-Related Alterations of Human Tonsil-Derived Mesenchymal Stem Cells: Role for CCN1 in Replicative Senescence-Associated Increase in Osteogenic Differentiation. *J. Anat.* 225, 510–518. doi:10.1111/joa.12229

Yuan, Z., Wei, P., Huang, Y., Zhang, W., Chen, F., Zhang, X., et al. (2019). Injectable PLGA Microspheres with Tunable Magnesium Ion Release for Promoting Bone Regeneration. *Acta Biomater.* 85, 294–309. doi:10.1016/j.actbio.2018.12.017

Yuasa, T., Kataoka, H., Kinto, N., Iwamoto, M., Enomoto-Iwamoto, M., Iemura, S.-i., et al. (2002). Sonic Hedgehog Is Involved in Osteoblast Differentiation by Cooperating with BMP-2. *J. Cel. Physiol.* 193, 225–232. doi:10.1002/jcp.10166

Zablotskii, V., Polyakova, T., and Dejneka, A. (2018). Cells in the Non-uniform Magnetic World: How Cells Respond to High-Gradient Magnetic Fields. *Bioessays* 40, 1800017. doi:10.1002/bies.201800017

Zajdel, A., Kałucka, M., Kokoszka-Mikołaj, E., and Wilczok, A. (2017). Osteogenic Differentiation of Human Mesenchymal Stem Cells from Adipose Tissue and Wharton's Jelly of the Umbilical Cord. *Acta Biochim. Pol.* 64, 365–369. doi:10.18388/abp.2016_1488

Zaminy, A., Ragerdi Kashani, I., Barbarestani, M., Hedayatpour, A., Mahmoudi, R., and Farzaneh Nejad, A. (2008). Osteogenic Differentiation of Rat Mesenchymal Stem Cells from Adipose Tissue in Comparison with Bone Marrow Mesenchymal Stem Cells: Melatonin as a Differentiation Factor. *Iran Biomed. J.* 12, 133–141.

Zha, K., Yang, Y., Tian, G., Sun, Z., Yang, Z., Li, X., et al. (2021). Nerve Growth Factor (NGF) and NGF Receptors in Mesenchymal Stem/stromal Cells: Impact on Potential Therapies. *Stem Cell Transl Med* 10, 1008–1020. doi:10.1002/sctm.20-0290

Zhang, J., Liu, X., Li, H., Chen, C., Hu, B., Niu, X., et al. (2016). Exosomes/tricalcium Phosphate Combination Scaffolds Can Enhance Bone Regeneration by Activating the PI3K/Akt Signaling Pathway. *Stem Cel Res Ther* 7, 136. doi:10.1186/s13287-016-0391-3

Zhang, J., Neoh, K. G., and Kang, E. T. (2018). Electrical Stimulation of Adipose-derived Mesenchymal Stem Cells and Endothelial Cells Co-cultured in a Conductive Scaffold for Potential Orthopaedic Applications. *J. Tissue Eng. Regen. Med.* 12, 878–889. doi:10.1002/term.2441

Zhang, K., Guo, J., Ge, Z., and Zhang, J. (2014). Nanosecond Pulsed Electric Fields (nsPEFs) Regulate Phenotypes of Chondrocytes through Wnt/β-Catenin Signaling Pathway. *Sci. Rep.* 4, 5836. doi:10.1038/srep05836

Zhang, R., Niu, Y. B., Song, X. M., Zhao, D. D., Wang, J., Wu, X. L., et al. (2012). Astragaloside II Induces Osteogenic Activities of Osteoblasts through the Bone Morphogenetic Protein-2/MAPK and Smad1/5/8 Pathways. *Int. J. Mol. Med.* 29, 1090–1098. doi:10.3892/ijmm.2012.941

Zhang, T., Gao, Y., Cui, W., Li, Y., Xiao, D., and Zhou, R. (2021). Nanomaterials-based Cell Osteogenic Differentiation and Bone Regeneration. *Cscr* 16, 36–47. doi:10.2174/1574888X15666200521083834

Zhang, Y., Böse, T., Unger, R. E., Jansen, J. A., Kirkpatrick, C. J., and van den Beucken, J. J. J. P. (2017). Macrophage Type Modulates Osteogenic Differentiation of Adipose Tissue MSCs. *Cell Tissue Res* 369, 273–286. doi:10.1007/s00441-017-2598-8

Zhao, B., Peng, Q., Zhou, R., Liu, H., Qi, S., and Wang, R. (2020). Precision Medicine in Tissue Engineering on Bone. *Methods Mol. Biol.* 2204, 207–215. doi:10.1007/978-1-0716-0904-0_18

Zhou, X., Liu, Z., Huang, B., Yan, H., Yang, C., Li, Q., et al. (2019). Orcinol Glucoside Facilitates the Shift of MSC Fate to Osteoblast and Prevents Adipogenesis via Wnt/β-Catenin Signaling Pathway. *Ddt* 13, 2703–2713. doi:10.2147/DDDT.S208458

Conflict of Interest: The authors declare that the research was conducted in the absence of any commercial or financial relationships that could be construed as a potential conflict of interest.

Publisher's Note: All claims expressed in this article are solely those of the authors and do not necessarily represent those of their affiliated organizations, or those of the publisher, the editors and the reviewers. Any product that may be evaluated in this article, or claim that may be made by its manufacturer, is not guaranteed or endorsed by the publisher.

frontiers | Frontiers in Cell and Developmental Biology

ORIGINAL RESEARCH
published: 04 April 2022
doi: 10.3389/fcell.2022.826023

SHIP1 Activator AQX-1125 Regulates Osteogenesis and Osteoclastogenesis Through PI3K/Akt and NF-κb Signaling

Xudong Xie[1,2†], Liangcong Hu[1,2†], Bobin Mi[1,2†], Adriana C. Panayi[3], Hang Xue[1,2], Yiqiang Hu[1,2], Guodong Liu[4], Lang Chen[1,2], Chenchen Yan[1,2], Kangkang Zha[1,2], Ze Lin[1], Wu Zhou[1,2], Fei Gao[1,2]* and Guohui Liu[1,2]**

[1]Department of Orthopedics, Union Hospital, Tongji Medical College, Huazhong University of Science and Technology, Wuhan, China, [2]Hubei Province Key Laboratory of Oral and Maxillofacial Development and Regeneration, Wuhan, China, [3]Division of Plastic Surgery, Brigham and Women's Hospital, Harvard Medical School, Boston, MA, United States, [4]Medical Center of Trauma and War Injuries, Daping Hospital, Army Medical University, Chongqing, China

OPEN ACCESS

Edited by:
Thimios Mitsiadis,
University of Zurich, Switzerland

Reviewed by:
Gemma Di Pompo,
Rizzoli Orthopedic Institute (IRCCS), Italy
Sofia Avnet,
University of Bologna, Italy

***Correspondence:**
Wu Zhou
2016XH0120@hust.edu.cn
Fei Gao
docgaofei@foxmail.com
Guohui Liu
liuguohui@hust.edu.cn

[†]These authors have contributed equally to this work

Specialty section:
This article was submitted to Stem Cell Research, a section of the journal Frontiers in Cell and Developmental Biology

Received: 30 November 2021
Accepted: 08 March 2022
Published: 04 April 2022

Citation:
Xie X, Hu L, Mi B, Panayi AC, Xue H, Hu Y, Liu G, Chen L, Yan C, Zha K, Lin Z, Zhou W, Gao F and Liu G (2022) SHIP1 Activator AQX-1125 Regulates Osteogenesis and Osteoclastogenesis Through PI3K/Akt and NF-κb Signaling. Front. Cell Dev. Biol. 10:826023. doi: 10.3389/fcell.2022.826023

With the worldwide aging population, the prevalence of osteoporosis is on the rise, particularly the number of postmenopausal women with the condition. However, the various adverse side effects associated with the currently available treatment options underscore the need to develop novel therapies. In this study, we investigated the use of AQX-1125, a novel clinical-stage activator of inositol phosphatase-1 (SHIP1), in ovariectomized (OVX) mice, identifying a protective role. We then found that the effect was likely due to increased osteogenesis and mineralization and decreased osteoclastogenesis caused by AQX-1125 in a time- and dose-dependent manner. The effect against OVX-induced bone loss was identified to be SHIP1-dependent as pretreatment of BMSCs and BMMs with SHIP1 RNAi could greatly diminish the osteoprotective effects. Furthermore, SHIP1 RNAi administration *in vivo* induced significant bone loss and decreased bone mass. Mechanistically, AQX-1125 upregulated the expression level and activity of SHIP1, followed upregulating the phosphorylation levels of PI3K and Akt to promote osteoblast-related gene expressions, including Alp, cbfa1, Col1a1, and osteocalcin (OCN). NF-κB signaling was also inhibited through suppression of the phosphorylation of IκBα and P65 induced by RANKL, resulting in diminished osteoclastogenesis. Taken together, our results demonstrate that AQX-1125 may be a promising candidate for preventing and treating bone loss.

Keywords: AQX-1125, SHIP1, bone loss, osteoblast, osteoclast

INTRODUCTION

Bone homeostasis requires osteoclast-mediated removal of old or damaged bones and osteoblast-mediated formation of new bones. An imbalanced process, either due to excessive bone resorption and/or decreased bone formation, can lead to bone quality deterioration (Recker et al., 2004; Tranquilli Leali et al., 2009) and result in various bone conditions, including osteoporosis. Furthermore, the worldwide prevalence of osteoporosis is on the rise due to the aging population, which has also resulted in a growing number of postmenopausal women with osteoporosis (Looker et al., 2012). However, given the various severe side effects associated with currently available treatments, it is crucial to develop novel therapies to treat such conditions (Brumsen et al., 1997; Knopp-Sihota et al., 2013; Compston et al., 2019).

Increased bone formation, decreased bone resorption, or a combination of both effects may be a crucial therapeutic target for the treatment of osteoporosis. Osteoclasts, which are responsible for bone resorption, are tissue-specific multinucleated giant and cooperatively induced by the nuclear factor-κB ligand (RANKL) and the macrophage colony-stimulating factor (M-CSF) (Teitelbaum and Ross, 2003). The association of RANKL and its receptor RANKL recruits tumor necrosis factor receptor-associated factor 6 (TRAF6) and subsequent activation of downstream signaling molecules, including nuclear factor kappa-B (NF-κB), fos proto-oncogene (c-Fos), and mitogen-activated protein kinase (MAPK), leading to expression of osteoclast-related genes, such as the nuclear factor of activated T cells c1 (NFATc1) and tartrate-resistant acid phosphatase (TRAP) (Kim and Kim, 2016). Osteoblasts, the bone-forming cells, are derived from bone marrow mesenchymal stem cells (BMSCs) under the control of several transcription factors and signaling cascades. It has been shown that the Wnt/β-catenin pathway is involved in bone formation (Krishnan et al., 2006; Maupin et al., 2013), which promotes osteogenic differentiation of BMSCs through activation of Runt-related transcription factor 2 (Runx2) and inhibits peroxisome proliferator-activated receptor-γ (PPARγ) transcription to inhibit adipogenic differentiation of BMSCs (Bennett et al., 2005).

Studies have demonstrated that inositol phosphatase-1 (SHIP1) is strongly associated with the development of osteoporosis (Iyer et al., 2013). Specifically, $SHIP^{-/-}$ mice exhibit severe osteoporosis, which is considered to be the result of excessive osteoclast activity (Takeshita et al., 2002). Mechanistically, src homology 2 (SH2) domain–containing inositol phosphatase-1 (SHIP1) can suppress TREM2- and DAP12-induced signaling *via* connection with DAP12 in an SH2 domain–dependent manner and restrict the recruitment of PI3K to DAP12 (Peng et al., 2010). Furthermore, hematopoietic stem cells (HSCs) from SHIP-deficient mice exhibit defective repopulating and self-renewal capacity upon transfer to SHIP-competent hosts (Desponts et al., 2006). In addition, lower alkaline phosphatase (Alp) activity, which is required for bone formation mediated by osteoblasts, has been noted in bone marrow–derived $SHIP1^{-/-}$ osteoblasts, suggesting that osteoblast development and function might be directly impaired by SHIP1 deficiency (Hazen et al., 2009). Nonetheless, the aforementioned findings strongly indicate that SHIP1 is critical to maintain the balance between bone formation and bone resorption.

AQX-1125, also known as (1S,3S,4R)-4-[(3aS,4R,5S,7aS)-4-(aminomethyl)-7a–methyl-1-methylidene-octahydro-1H-inden-5-yl]-3-(hydroxymethyl)-4-methylcyclohexan-1-ol; acetic acid salt, is a novel, clinical-stage, low molecular weight activator of SHIP1, which has exhibited promising anti-inflammatory effects in a number of animal models of pulmonary inflammation (Stenton et al., 2013). Furthermore, oral AQX-1125 treatment of women with moderate to severe interstitial cystitis/bladder pain syndrome showed no serious adverse events, displaying a good tolerance profile (Nickel et al., 2016). As the effect of AQX-1125 on osteogenesis or/and osteoclastogenesis is yet to be established, in this study, we first carried out experiments *in vitro* to observe the molecule effect on osteogenesis or/and osteoclastogenesis, followed by *in vivo* demonstration of its protective functions in OVX-induced bone loss model.

MATERIALS AND METHODS

Reagents

AQX-1125 was purchased from MedChemExpress (MCE). The primary antibodies of GAPDH, PI3K, p-PI3K, Akt, p-AKT, P65, p-P65, IκBα, p- IκBα, SHIP1, Runx2, Alp, NFATc1, and c-Fos were acquired from ABclonal (Wuhan, China). Phalloidin and 4, 6-diamidino-2-phenylindole (DAPI) were purchased from Solarbio (Beijing, China). RANKL (the receptor activator of the nuclear factor kappa-B ligand) and M-CSF (macrophage colony-stimulating factor) were obtained from R&D Systems (Minnesota, USA). Cell culturing plates were purchased from NEST (Jiangsu, China). Minimum Essential Medium Alpha (α-MEM), Dulbecco's Modified Eagle Medium: F-12 (DMEM/F-12), fetal bovine serum (FBS), penicillin, streptomycin, and trypsin were purchased from Gibco (Grand Island, NY, United States). The TRAP staining kit was obtained from Solarbio (Beijing, China).

Animal Model and Treatment

The ovariectomized mouse model was performed in specific pathogen-free (SPF) facilities, as previously described (Chen et al., 2017). All animal studies were performed according to protocols approved by the Laboratory Animal Center, Tongji Medical College, Huazhong University of Science and Technology, and were carried out as regulated by the Tongji Medical College Animal Care and Use Committee. Eight-week-old female C57BL/6 mice were randomly distributed into three groups ($n = 3$): the sham group (served as controls), model group (mice subjected to bilateral OVX and treated with vehicle), and treatment group (mice underwent bilateral OVX and treated with AQX-1125).

Briefly, mice were weighed and given general anesthesia with 1% pentobarbital by intraperitoneal injection and then subjected to bilateral OVX or a sham operation. Four weeks later, mice were treated with AQX-1125 (10 mg/kg) through intraperitoneal administration in the treatment group three times per week for 4 weeks. SHIP1-RNAi (5 nmol/20 g) was administrated through the tail vein to the mice in the treatment group twice a week for 4 weeks.

Preparation and Culture of BMSCs

Human bone marrow specimens were collected from the iliac crests of healthy volunteer donors. All samples were attained with signed informed consent. BMSCs were isolated by density gradient centrifugation, and adherent cells were harvested. Cells were cultured in DMEM/F12 medium containing 10% FBS and 1% penicillin–streptomycin solution. The cells from the third passage were used in subsequent experiments.

Preparation and Culture of Osteoclasts

Five-week-old male C57BL/6 mice were obtained from the Center of Experimental Animal, Tongji Medical College, Huazhong University of Science and Technology. Bone marrow–derived macrophages (BMMs) were prepared, as previously described (Xie et al., 2014). Briefly, bone marrow cells were obtained from mouse femurs and

tibias. After elimination of red blood cells (RBCs) using RBC lysis buffer (Servicebio; Wuhan, China), the cells were incubated overnight in α-MEM medium (Gibco; Grand Island, NY, United States) supplemented with 10% FBS (Gibco) and 1% penicillin–streptomycin solution (Gibco). Nonadherent cells (stroma-free bone marrow cells) were incubated with 30 ng/ml M-CSF for 5 days to differentiate into osteoclast precursors (BMMs), which were then seeded into a 96-well culture plate at 1×10^4 cells/0.2 ml/well and differentiated into mature osteoclasts with 30 ng/ml M-CSF and 50 ng/ml RANKL.

Cell Counting Kit 8

For BMSCs, cells were seeded at a density of 5×10^3 cells per well in 96-well plates and cultured overnight. Then, cell viability was tested 3 days after AQX-1125 treatment. For the BMMs, approximately 1×10^4 cells were seeded in 96-well plates and cultured overnight. Then, cells were incubated with various concentrations of AQX-1125 for 5 days in the presence of 30 ng/ml M-CSF and 50 ng/ml RANKL. The medium was replaced with serum-free medium containing the CCK-8 reagent and incubated for 2 h, followed by detection of absorbance at 450 nm.

Osteoclastogenesis Assay *In Vitro*

Approximately 1×10^4 BMMs were seeded into each well of a 96-well plate and cultured overnight. A differentiation medium (α-MEM medium, 10% fetal bovine serum, 1% penicillin–streptomycin solution, 30 ng/ml M-CSF, and 50 ng/ml RANKL) with or without AQX-1125 was used to induce osteoclast differentiation. After 5 days, TRAP staining was performed following the manufacturer's instructions. TRAP-positive cells with more than three nuclei were regarded as osteoclasts. The osteoclastogenic ability was determined by analyzing the TRAP-positive area compared with the total area.

Pit Formation Assay

Approximately 1 × 104 BMMs were seeded into each well of a 96-well plate and cultured overnight. Then, cells were incubated without AQX-1125 in the presence of 30 ng/ml M-CSF and 50 ng/ml RANKL and the medium was changed every 2 days. After 5 days, TRAP staining was performed to detect the osteoclast formation. Then, osteoclasts were digested with collagenase and seeded into a Corning® Osteo Assay Surface 96-well Plate, and cultured for 4 days with AQX-1125 in the presence of 30 ng/ml M-CSF and 50 ng/ml RANKL. The culture medium was replaced and the surface was washed with 0.5% sodium hypochlorite. The plate was washed twice with PBS and left to dry at room temperature for 3 h. Finally, the resorbing area was visualized using a digital microscope system and analyzed with the ImageJ software.

Western Blotting

Cells (4×10^5 cells per well) were seeded into six-well plates and cultured overnight. After treatment, total protein was extracted using a RIPA lysis buffer (50 mM Tris, 150 mM NaCl, 1% NP-40, and 0.5% sodium deoxycholate) with a proteinase inhibitor cocktail. Subsequently, 10 μg protein was subjected to 10% or 12.5% SDS-PAGE and electrophoretically transferred onto polyvinylidene fluoride (PVDF) membranes. After blocking with nonfat milk for 2 h, the PVDF membranes were incubated with specific antibodies at 4°C overnight. Next, the membranes were washed three times, each time for 10 min with TBS-T, and incubated with anti-rabbit secondary antibodies for 1 h at room temperature. After washing thrice with TBS-T, the membranes were incubated in a chemiluminescent substrate and visualized using the Bio-Rad Image Capture system.

TABLE 1 | Primer sequences.

Gene name	Primer sequence (5′ to 3′)
NFATc1-forward	5′-GGAGCGGAGAAACTTTGCG-3′
NFATc1-reverse	5′-GTGACACTAGGGGACACATAACT-3′
c-Fos	5′-CGGGTTTCAACGCCGACTA-3′
c-Fos	5′-TTGGCACTAGAGACGGACAGA-3′
CTSK-forward	5′-CTCGGCGTTTAATTTGGGAGA-3′
CTSK-reverse	5′-TCGAGAGGGAGGTATTCTGAGT-3′
ACP5-forward	5′-CACTCCCACCCTGAGATTTGT-3′
ACP5-reverse	5′-AAGTAGTGCAGCCCGGAGTA-3′
Alp-forward	5′-ACCACCACGAGAGTGAACCA-3′
Alp-reverse	5′-CGTTGTCTGAGTACCAGTCCC-3′
Cbfa1-forward	5′-TGGTTACTGTCATGGCGGGTA-3′
Cbfa1-reverse	5′-TCTCAGATCGTTGAACCTTGCTA-3′
Col1a1-forward	5′-GTGCGATGACGTGATCTGTGA-3′
Col1a1-reverse	5′-CGGTGGTTTCTTGGTCGGT-3′
Osteocalcin-forward	5′-GGCGCTACCTGTATCAATGG-3′
Osteocalcin-reverse	5′-GTGGTCAGCCAACTCGTCA-3′
Mouse GAPDH-forward	5′-ACCCAGAAGACTGTGGATGG-3′
Mouse GAPDH-reverse	5′-CACATTGGGGGTAGGAACAC-3′
Human GAPDH-forward	5′-ACAACTTTGGTATCGTGGAAGG-3′
Human GAPDH-reverse	5′-GCCATCACGCCACAGTTTC-3′
Mouse SHIP1-forward	5′-GCCCCTGCATGGGAAATCAA-3′
Mouse SHIP1-reverse	5′-TGGGTAGCTGGTCATAACTCC-3′
Human SHIP1-forward	5′-GCGTGCTGTATCGGAATTGC-3′
Human SHIP1-reverse	5′-TGGTGAAGAACCTCATGGAGAC-3′

Real-Time PCR

Total RNA was extracted using TRIzol (Invitrogen), according to standard protocols. The concentration and purity of RNA were measured at an optical density of 260 nm/280 nm. One microgram of total RNA was used to synthesize cDNA (Vazyme; Nanjing, China). Equal quantities of cDNA were subjected to qRT-PCR using the 2×AceQ qPCR SYBR Green Master Mix (Vazyme; Nanjing, China), while GAPDH was used as the control. The cycle threshold (Ct) values were collected. The ΔΔCt method was used to calculate the relative mRNA levels of each target gene. The primers are listed in **Table 1**.

Immunofluorescence Staining

Approximately 1×10^4 BMMs were seeded into each well of a 96-well plate and cultured overnight. For the actin ring formation assay, α-MEM medium supplemented with 10% FBS, 1% penicillin–streptomycin solution, 30 ng/ml M-CSF, and AQX-1125 (0, 50, 100, 200 nM) in the presence/absence of 50 ng/ml RANKL was used to induce osteoclast differentiation for 5 days. The cells were fixed in 4% paraformaldehyde (PFA) for 20 min at room temperature. Then, the cells were washed at least four times with PBS and stained with phalloidin (proteintech; Wuhan, China) for 1 h,

followed by DAPI staining for 5 min. Finally, the cells were observed using a digital microscope system (IX81; Olympus, Japan).

For immunofluorescence staining of OCN, the femurs were collected from mice and fixed in 4% PFA for 4 days. The samples were subsequently decalcified for 2 weeks using 10% tetracycline-EDTA (Servicebio, Wuhan, China), and 4-μm-thick paraffin-embedded sections were prepared. Subsequently, the slices were dewaxed in xylene for 20 min and rehydrated with a graded series of alcohol for 5 min, followed by antigen recovery in the 10 mM citrate buffer. Endogenous peroxidase was quenched using 3% hydrogen peroxide for 15 min, and then, sections were blocked with 10% unimmunized donkey serum for 30 min after washing three times with PBS. After that, the slices were incubated with the OCN rabbit polyclonal antibody (1:100; ABcolonal, China) at 4°C overnight. The slices were washed three times with PBS and incubated with the horseradish peroxidase-conjugated secondary antibody (1:200; proteintech) at room temperature for 1 h, followed by DAPI staining for 5 min.

SHIP1 Small Interfering RNA Transfection

BMMs and BMSCs were incubated with SHIP1 small interfering RNA (siRNA; GENE; Shanghai, China) or nontarget control (NTC) siRNA (GENE; Shanghai, China) using the transfection reagents for 48 h, according to the manufacturer's instructions. We verified the SHIP1 knockdown efficiency using qRT-PCR and Western blotting, followed by testing the differentiation capacity of BMSCs into osteoblasts and BMMs into osteoclasts. To enhance stability in serums and transfection efficiency, cholesterol, and methylation-modified siRNA, *in vivo* experiments were performed.

Micro-CT Analysis

Micro-computed tomography (micro-CT; Bruker SkyScan 1176 scanner mCT system) was used to analyze the femur structure. Setting the analysis conditions to 37 kV and 121 mA, 300 section planes were scanned. For the morphometric analysis, we obtained the following trabecular parameters, bone mineral density (BMD), bone volume/tissue volume (BV/TV), trabecular bone surface area/total value (BS/TV) and trabecular number (Tb. N).

Hematoxylin and Eosin Staining and TRAP Staining

The femurs were collected from mice and fixed in 4% PFA for 4 days. The samples were subsequently decalcified for 2 weeks using 10% tetracycline-EDTA (Servicebio), and 4-μm-thick paraffin-embedded sections were prepared for H&E staining and TRAP staining for further analysis. H&E and TRAP staining were carried out according to the kit instructions (Solarbio, Beijing, China). The images were obtained using a microscope, and histological analyses were performed by ImageJ software.

Alkaline Phosphatase and Alizarin Red S Staining

Osteogenic induction was performed by culturing cells in an osteogenic differentiation medium (Cyagen Biosciences) containing 10% (v/v) FBS, 1% (v/v) penicillin–streptomycin, 2 mM l-glutamine, 50 μM ascorbate, 10 mM β-glycerophosphate, and 100 nM dexamethasone. The culture medium was changed every 2–3 days. The BMSCs were induced in the osteogenic differentiation medium for 14 days. Cells were washed thrice with PBS, and then fixed with 4% PFA for 15 min. Finally, cells were stained with an Alkaline Phosphatase Assay Kit (Alp; Beyotime, Shanghai, China, #C3206), according to the manufacturer's instructions.

Alizarin Red S staining was performed after 21 days of induction. After fixing with 4% PFA, each well was treated with Alizarin Red S solution (Cyagen Biosciences) and incubated in the dark for 30 min. Then, the images were obtained by microscopy. Finally, quantification of calcium deposition was performed by elution of AR-S with 10% (W/V) cetylpyridinium chloride in 10 mM sodium phosphate (PH 7.0) for 1 h at room temperature, and absorbance of the eluted dye was measured at 570 nm.

Statistical Analysis

All experiments were performed at least three times and are presented as the mean ± standard deviation (SD). One-way analysis of variance for three groups and Student's t-test for two groups were performed using GraphPad Prism 5.0 (GraphPad Software). A value of $p < 0.05$ was considered statistically significant.

RESULTS

AQX-1125 Alleviates OVX-Induced Bone Loss *In Vivo*

To investigate whether AQX-1125 has protective effects in osteoporosis, we performed an ovariectomized mouse model mimicking postmenopausal osteoporosis. We observed extensive bone loss in the OVX groups using micro-CT. Intraperitoneal injection of AQX-1125 (10 mg/kg) for 4 weeks was shown to reduce the OVX-induced bone loss in the distal femur (**Figure 1A**). BMD, BV/TV, BS/TV and Tb.N were measured, and an increase in BMD, BV/TV, BS/TV, and Tb.N in the OVX + AQX-1125 group was observed compared to the OVX group (**Figure 1B**), as confirmed by H&E staining (**Figures 1C,D**). To investigate whether AQX-1125's bone protective effects occurred through enhanced osteoblast differentiation and/or decreased osteoclast formation and activity, we performed immunofluorescence analysis of the levels of the OCN expression and TRAP staining in the femurs. As seen in **Figures 1E,F**, the OCN expression level was downregulated in OVX mice, while reduced level of the OCN expression was partly restored upon AQX-1125 stimulation. In addition, we also found that AQX-1125 administration could reduce the number of TRAP-positive cells in the femurs of ovariectomized mice (**Figures 1G,H**). Together, these results demonstrated that AQX-1125 could effectively rescue OVX-induced bone loss potentially *via* regulation of osteogenesis and osteoclastogenesis.

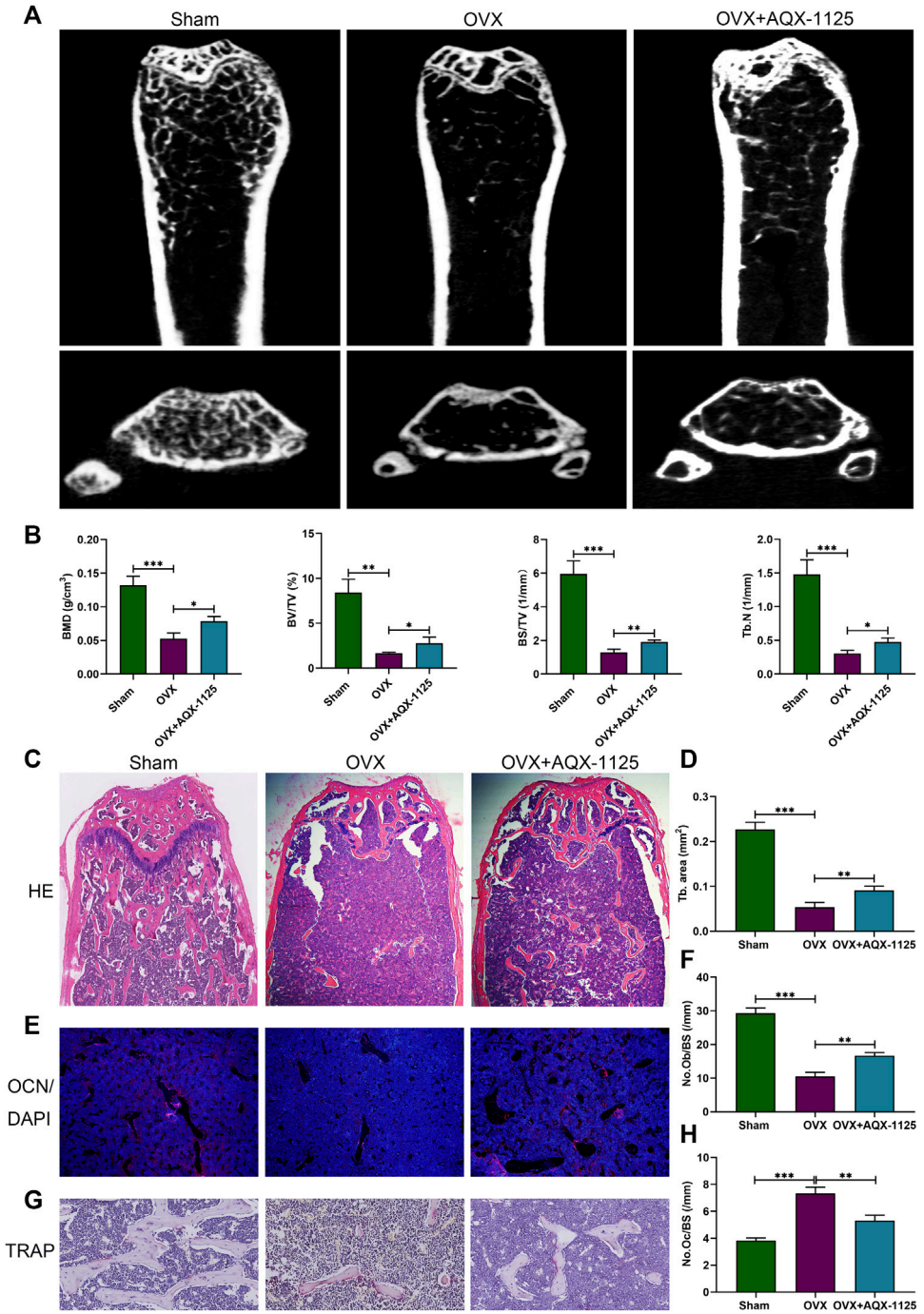

FIGURE 1 | AQX-1125 alleviates OVX-induced bone loss *in vivo*. **(A)** Micro-CT analysis of the distal femurs from three groups ($n = 3$): sham, OVX, and OVX + AQX-1125 (10 mg/kg/bw). **(B)** Quantitative analysis of BMD, BV/TV, BS/TV and Tb. N. **(C)** Representative images of HE staining of the distal femur sections. Scale bars = 200 μm. **(D)** Quantitative analysis of trabecular (Tb) bone area in **(C)**. **(E)** Representative immunofluorescence images of OCN in femurs from different groups. Blue: DAPI; red: OCN. Scale bars = 100 μm. **(F)** Quantification of the osteoblast number in **(E)**. **(G)** Representative images of femurs stained with TRAP. Scale bars = 50 μm. **(H)** Histomorphometric analysis of the osteoclast number in **(G)**. Data are presented as means ± SD from three independent experiments (*$p < 0.05$; **$p < 0.01$; and ***$p < 0.001$).

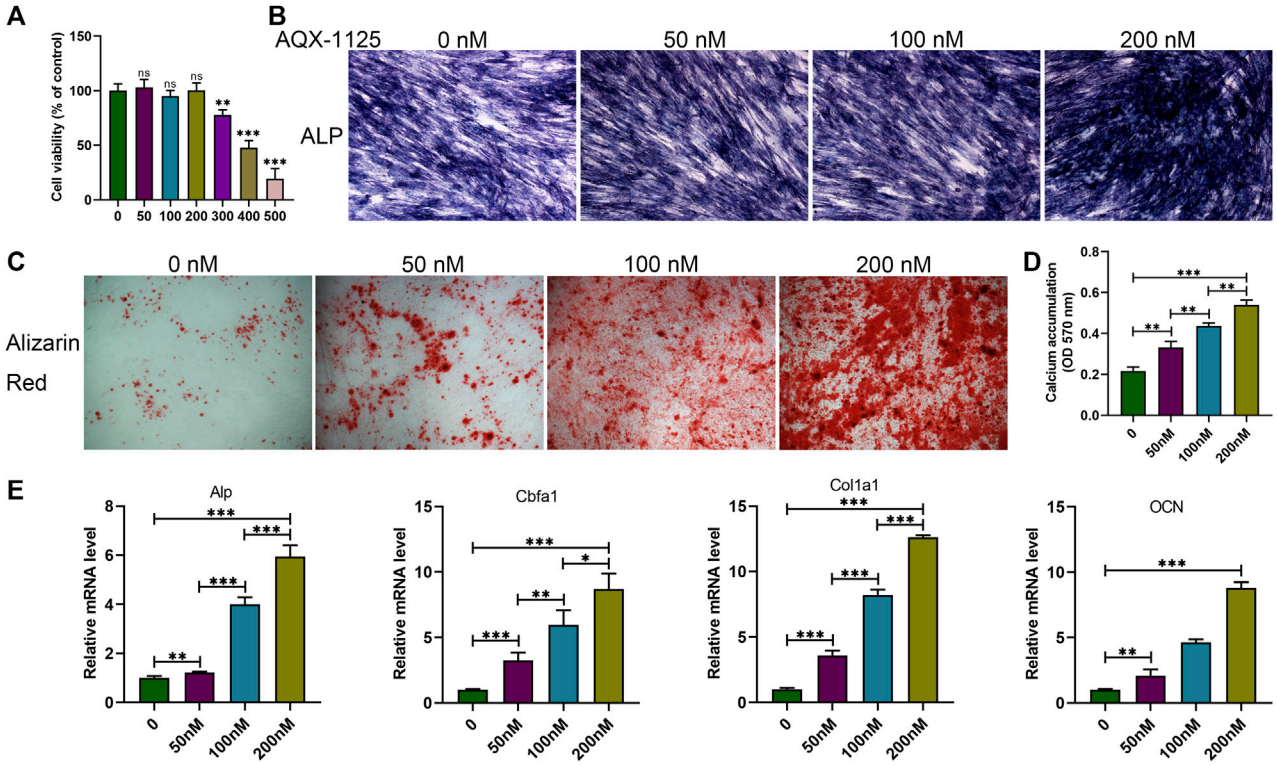

FIGURE 2 | AQX-1125 facilitates osteoblast differentiation. **(A)** Effect of AQX-1125 on BMSCs viability. **(B,C)** BMSCs were cultured in osteogenic differentiation medium with various concentrations of AQX-1125, as indicated for 14 days (B, Alp staining) or 21 days (C, alizarin red staining. scale bars = 100 μm). **(D)** Matrix mineralization was assessed by quantitative analysis of alizarin red S staining in **(C)**. **(E)** Relative mRNA expression level of Alp, Cbfa1, Col1a1, and OCN in BMSCs treated with AQX-1125, as indicated for 24 h. Data are presented as means ± SD from three independent experiments (*$p < 0.05$; **$p < 0.01$; and ***$p < 0.001$).

AQX-1125 Facilitates Osteoblast Differentiation

We first investigated the influence of AQX-1125 on osteoblast formation *in vitro*. Before the study, a CCK-8 analysis was performed to determine the appropriate assay concentration of AQX-11125. As seen in **Figure 2A**, no toxic effects were observed after incubation with an AQX-1125 concentration lower than 200 nM. Alp and alizarin red S staining were performed to detect osteoblast differentiation and mineralization. Alp- and alizarin red S–positive cells increased in the presence of AQX-1125 in a dose-dependent manner, which demonstrated that AQX-1125 could enhance osteoblast differentiation and mineralization (**Figures 2B–D**). Consistently, the osteogenic markers, including Alp, Cbfa1, Col1a1, and OCN genes were also markedly upregulated after induction with AQX-1125 (**Figure 2E**). These data showed that BMSCs after exposure to AQX-1125 were in a state of enhanced osteogenesis.

AQX-1125 Inhibits RANKL-Induced Osteoclast Differentiation *In Vitro*

To explore the effect of AQX-1125 on osteoclast formation *in vitro*, bone marrow macrophages (BMMs), a standard *in vitro* osteoclast differentiation model, were used. We performed CCK-8 assay to explore the effect of AQX-1125 on BMMs viability, suggesting that cell viability was comparable to that of the vehicle-treated cultures at lower doses below 200 nM (**Figure 3A**). After RANKL induction for 5 days, we observed significantly increased numbers of TRAP-positive cells. BMMs were then treated with AQX-1125 at various concentrations (0, 50, 100, 200 nM) in the presence of 30 ng/ml M-CSF and 50 ng/ml RANKL and we found that addition of AQX-1125 sharply suppressed osteoclast differentiation in a dose-dependent manner, as demonstrated by TRAP staining (**Figure 3B**). Osteoclasts with smaller size and fewer than eight nuclei were observed upon treatment with 200 nM AQX-1125 (**Figure 3C**), which was consistent with the qRT-PCR results (**Figure 3D**). Then, to evaluate the osteoclast activity, we detected actin ring formation of osteoclasts, which is considered to be a key process during the formation of mature osteoclasts. After treatment with various concentrations of AQX-1125, the actin ring became smaller in a dose-dependent manner, showing that AQX-1125 could impede actin ring formation in mature osteoclasts (**Figure 3E**). Furthermore, to verify the direct effect of AQX-1125 on osteoclast activity, we cultured BMMs in differentiation medium for 5 days in the absence of AQX-1125 and then verified osteoclast differentiation by TRAP staining (**Figures 3F,G**), which suggested that BMMs differentiated into osteoclasts, and no difference was seen in the osteoclast number and size in the

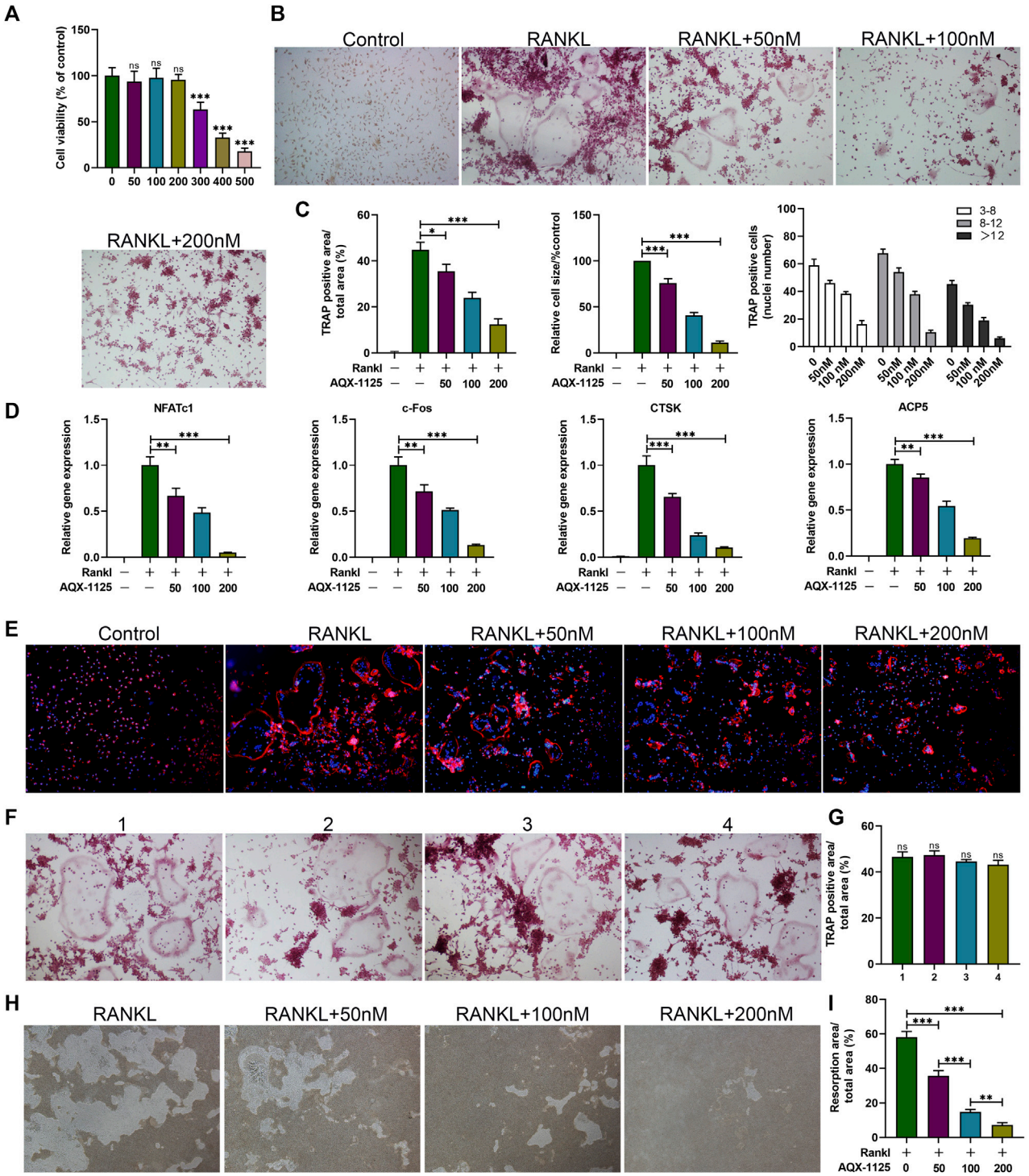

FIGURE 3 | AQX-1125 inhibits RANKL-induced osteoclast differentiation *in vitro*. **(A)** Effect of AQX-1125 on BMMs viability. **(B)** BMMs were cultured in α-MEM medium with 30 ng/ml M-CSF and 50 ng/ml RANKL in the presence of various concentrations of AQX-1125, as indicated for 5 days. TRAP-staining and quantification of TRAP-positive cells. Scale bars = 100 μm. **(C)** Quantitative analysis was performed to assess TRAP-positive cells/total area, relative TRAP-positive cell size, and the number of nuclei in TRAP-positive cells. **(D)** BMMs were cultured for 24 h in the presence of different concentrations of AQX-1125 (0, 50, 100, 200 nM). The mRNA expression levels of NFATc1, c-Fos, Ctsk, and ACP5 were detected with qRT-PCR. **(E)** F-Actin ring formation assays were carried out to detect the effect of AQX-1125 on the generation of mature osteoclasts. The actin rings were detected using phalloidin by fluorescence microscopy following treatment with various concentrations of AQX-1125. Scale bars = 100 μm. **(F)** TRAP-staining and quantitation of TRAP-positive cells. BMMs were cultured for 5 days to differentiate into mature osteoclasts in differentiation medium in the absence of AQX-1125. Scale bars = 100 μm. **(G)** Quantitative analysis was performed to test TRAP-positive cells/total area. **(H,I)** Pit

(*Continued*)

FIGURE 3 | formation assay of osteoclasts and quantification of the pits area. The images were captured with a microscope. Scale bars = 100 μm. Data are presented as means ± SD from three independent experiments (*p < 0.05; **p < 0.01; ***p < 0.001).

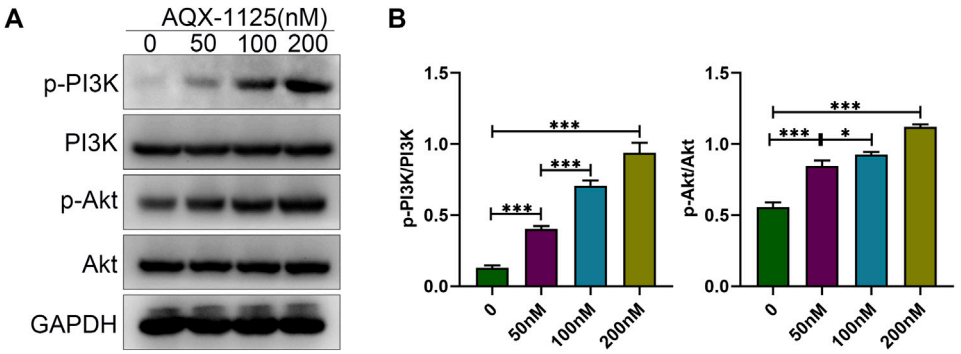

FIGURE 4 | AQX-1125 promotes osteoblast differentiation *via* the PI3K/Akt signaling pathway. **(A)** Protein expression levels of PI3K, p-PI3K, Akt and p-Akt in BMSCs were detected by Western blotting after treatment with various concentration of AQX-1125 for 4 days. **(B)** Quantitative analysis of each immunoblot in **(A)**. Data are presented as means ± SD from three independent experiments (*p < 0.05; **p < 0.01; ***p < 0.001).

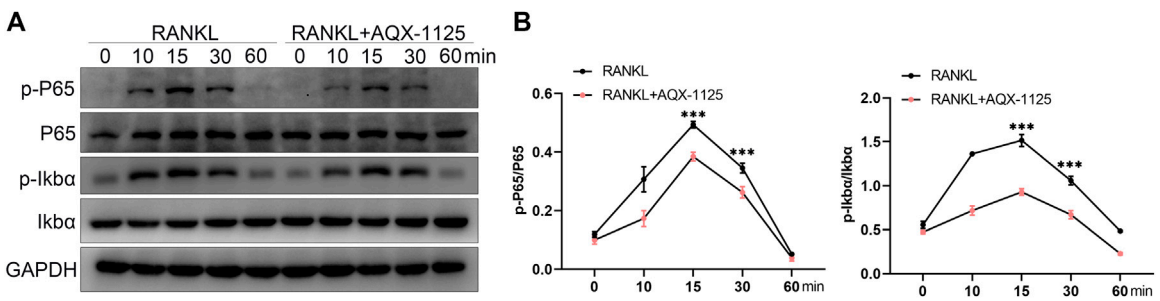

FIGURE 5 | AQX-1125 suppresses the NF-κB pathway in osteoclastogenesis. **(A)** Western blotting was used to test the phosphorylation levels of IκBα and P65 in the presence of 50 ng/ml RANKL after pretreatment with AQX-1125 for the indicated time. **(B)** Quantitative analysis of the Western blotting results. Data are presented as means ± SD from three independent experiments (*p < 0.05; **p < 0.01; ***p < 0.001).

absence of AQX-1125. Then, mature osteoclasts were cultured for 4 additional days with AQX-1125, and the bone resorption pits were analyzed to evaluate AQX-1125's effect on the resorption activity of mature osteoclasts. The results indicated that treatment with AQX-1125 decreased the bone resorption area significantly compared with vehicle treatment (**Figures 3H,I**).

AQX-1125 Promotes Osteoblast Differentiation *via* the PI3K/Akt Signaling Pathway

Studies have indicated that PI3K plays a central role in osteoblast differentiation and survival (Guntur and Rosen, 2011), and PI3K/Akt signaling activation by Wnt3a and heparin exhibits increased osteoblast differentiation (Ling et al., 2010). Therefore, we tested whether AQX-1125 increased osteoblast differentiation through activation of the PI3K/Akt signaling pathway. As shown in **Figures 4A,B**, Western blotting showed that treatment with AQX-1125 facilitated the phosphorylation of p-PI3K and p-Akt in BMSCs, which suggested that AQX-1125 significantly activated PI3K/Akt signaling pathway.

AQX-1125 Suppresses the NF-κB Pathway during Osteoclastogenesis

In the last decade, studies have established that NF-κB signaling is involved in RANKL–induced osteoclastogenesis, and it has been proven that inhibition of NF-κB signaling is an effective strategy to suppress osteoclast formation and bone resorption activity (Abu-Amer, 2013). Therefore, NF-κB signaling plays a predominant function in osteoclast differentiation and activity. To investigate whether AQX-1125 inhibited osteoclastogenesis *via* the NF-κB signaling mechanism, we performed Western blotting assays of the NF-κB signaling pathway. In BMMs, we observed that AQX-1125 suppressed the RANKL-induced

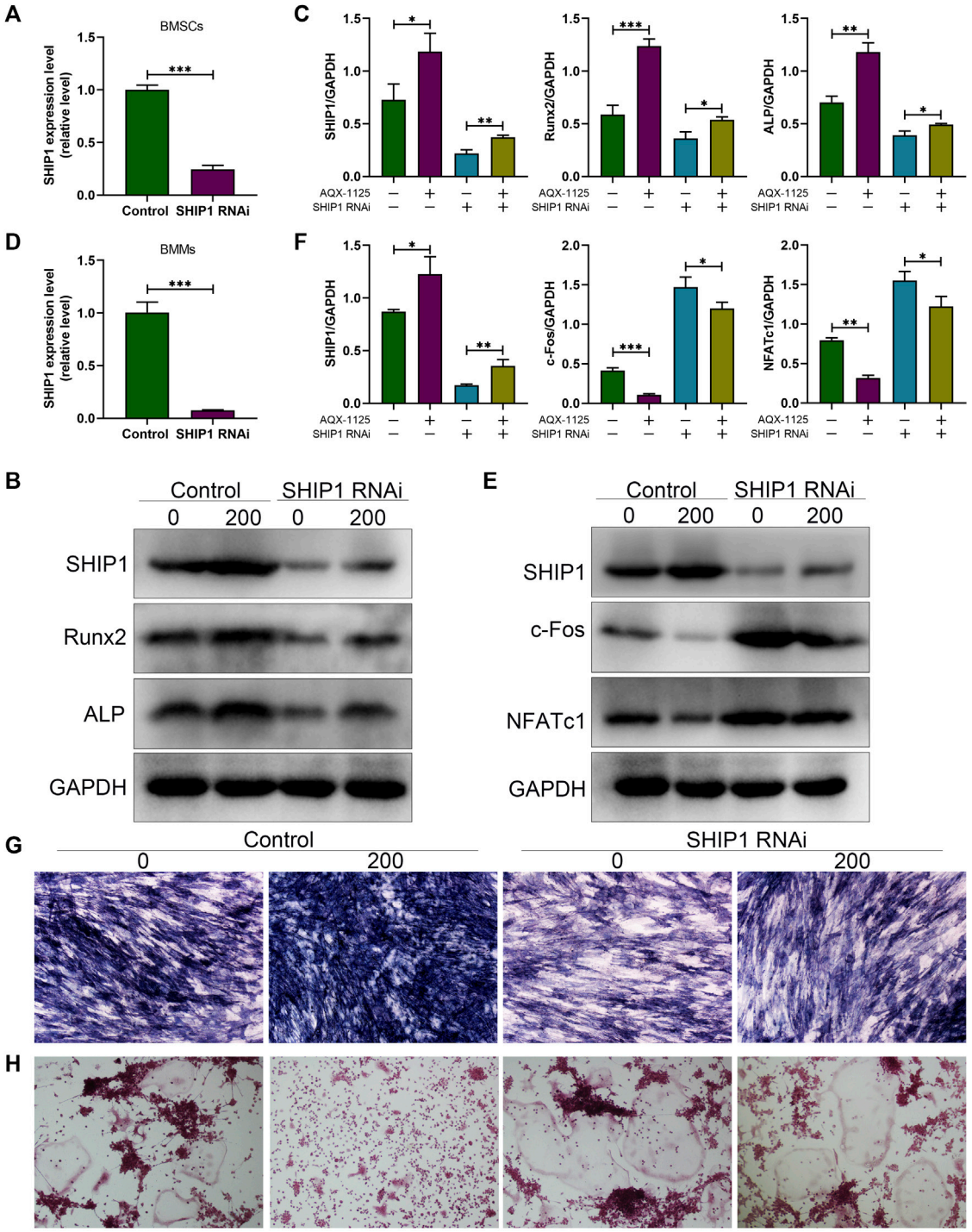

FIGURE 6 | Increased osteogenesis and decreased osteoclastogenesis induced by AQX-1125 are SHIP1-dependent. **(A)** Gene expression level of SHIP1 in BMSCs after transfection with SHIP1 RNAi. **(B)** Protein expression levels of SHIP1, Runx2, and Alp in BMSCs with or without AQX-1125, were detected 4 days following transfection with SHIP1 RNAi. **(C)** Quantitative analysis of each immunoblot in **(B)**. **(D)** Gene expression level of SHIP1 in BMMs after transfection with SHIP1 RNAi. **(E)** BMMs were treated with or without AQX-1125 for 3 days in the presence of M-CSF and RANKL. The expression levels of SHIP1, NFATc1, and c-Fos was measured with Western blotting. **(F)** Quantitative analysis of each immunoblot in **(E)**. **(G)** BMSCs were transfected with SHIP1 RNAi for 48 h, and then, Alp staining was performed 14 days after osteogenic induction in the absence or presence of AQX-1125. Scale bars = 100 μm. **(H)** BMMs were incubated with SHIP1 RNAi for 48 h, and then TRAP staining was used to test the effect of SHIP1 RNAi on AQX-1125-mediated osteoclastogenesis after 5-days incubation with differentiation medium in the absence or presence of AQX-1125. TRAP staining was used to test the effect of SHIP1 RNAi on AQX-1125-mediated osteoclastogenesis. Scale bars = 100 μm. Data are presented as means ± SD from three independent experiments (*$p < 0.05$; **$p < 0.01$; and ***$p < 0.001$).

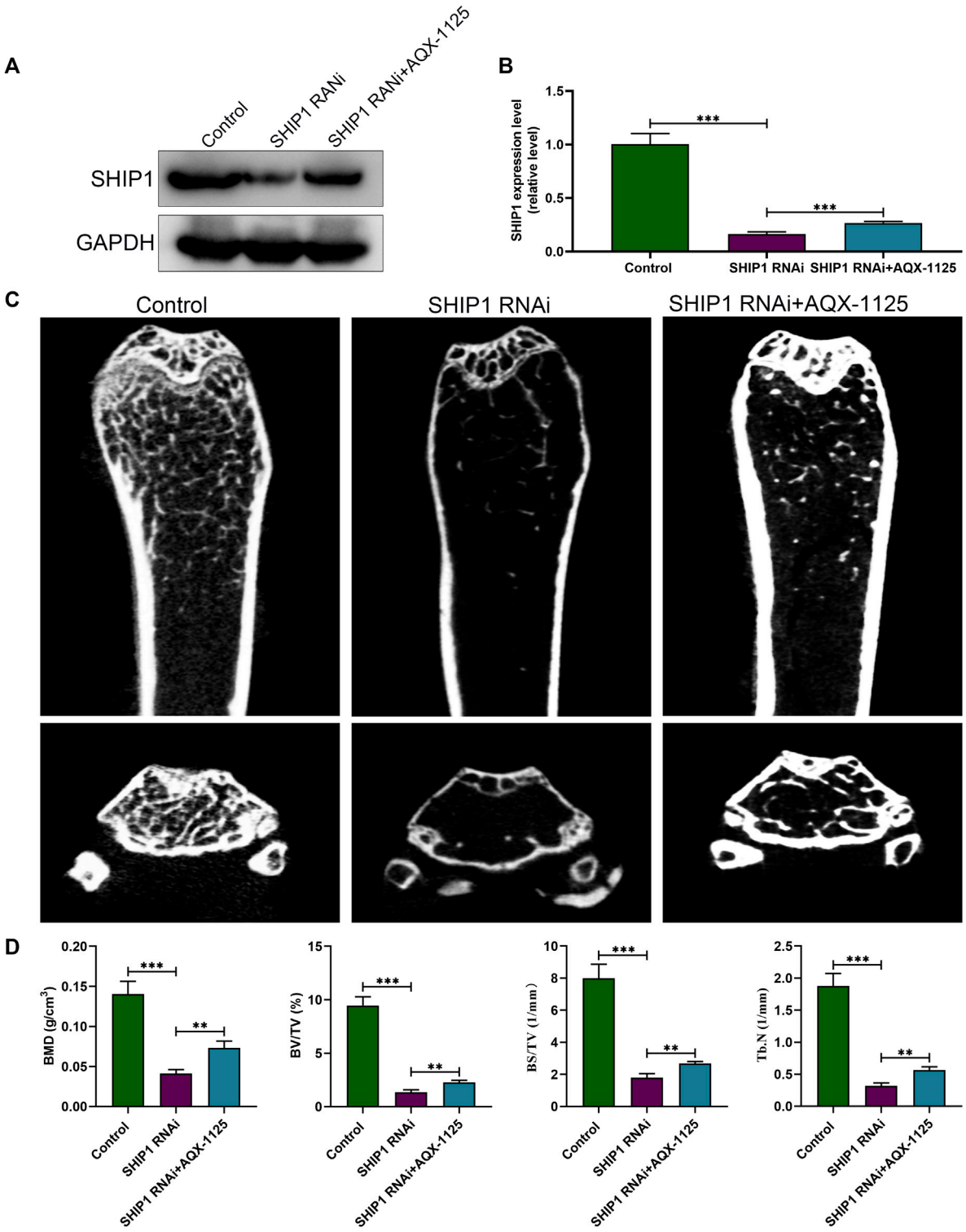

FIGURE 7 | SHIP1 RNAi administration induces bone loss. **(A)** Protein expression level of SHIP1 in femurs after exposure to treatment. Eight-week-old male C57 mice were retreated with vehicle (control group), SHIP1 RNAi (5 nm/20 g), and SHIP1 RNAi (5 nm/20 g) +AQX-1125 (10 mg/kg) for 4 weeks. Total protein was isolated from femurs of each group, and Western blotting was performed. **(B)** Quantitative analysis of each immunoblot in **(A)**. **(C)** Micro CT analysis of the distal femurs from the control, SHIP1 RNAi, and SHIP1 RNAi + AQX-1125 group. **(D)** Calculation of the BMD, BV/TV, BS/TV and Tb.N. Data are presented as means ± SD from three independent experiments (*$p < 0.05$; **$p < 0.01$; ***$p < 0.001$).

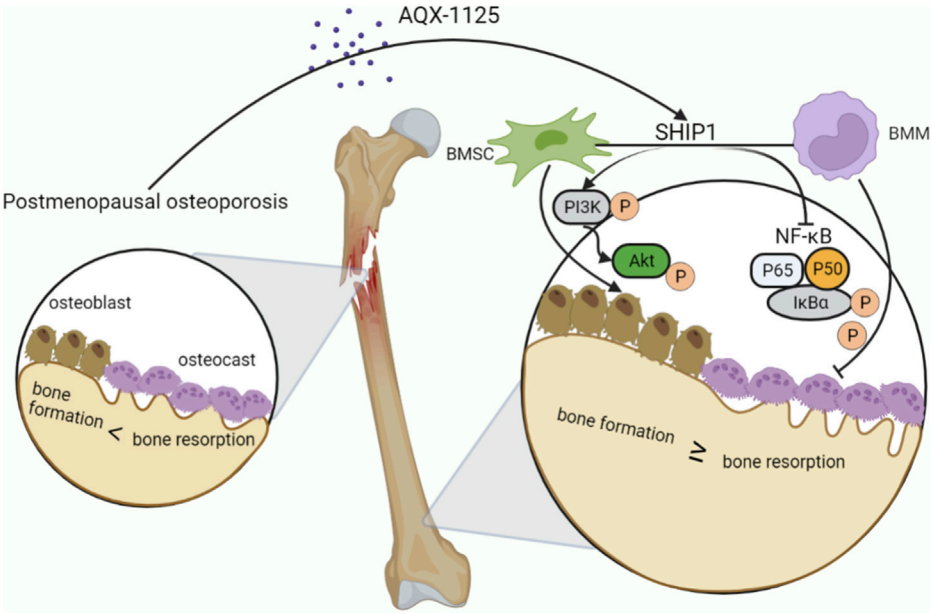

FIGURE 8 | AQX-1125 positively regulates osteogenesis through PI3K/Akt signaling and inhibits osteoclastogenesis through NF-κb signaling *via* activation of SHIP1. Upon AQX-1125 stimulation, SHIP1 was activated in the BMSCs and BMMs. The activated SHIP1 facilitates the phosphorylation of PI3K and Akt in BMSCs, followed by acceleration of the differentiation of BMSCs into osteoblasts. In addition, activated SHIP1 inhibits the NF-κb signaling pathway, which reduces the phosphorylation of p65 and IkBα in BMMs, followed by suppression of the differentiation of BMMs into osteoclasts and the activity of osteoclasts. Overall, AQX-1125 alleviates OVX-induced bone loss.

phosphorylation of IκBα and P65 (**Figures 5A,B**). These data showed that the AQX-1125 treatment suppressed RANKL-mediated NF-κB signaling activation.

Increased Osteogenesis and Decreased Osteoclastogenesis Induced by AQX-1125 are SHIP1-Dependent

To demonstrate that AQX-1125 predominantly exerted its effects through activation of SHIP1, BMSCs and BMMs were first transfected with either control siRNA or siRNA against SHIP1. To verify the transfection efficiency, the expression of the SHIP1 expression levels in BMSCs and BMMs were detected. These results showed that SHIP1 RNAi (SHIP1 siRNA) significantly decreased the SHIP1 mRNA level in BMSCs (**Figure 6A**) and BMMs (**Figure 6D**). Subsequently, Western blotting showed that AQX-1125 significantly activated the SHIP1 expression, followed by an increase in the Runx2 and Alp expression level in BMSCs (**Figures 6B,C**) and a diminished NFATc1 and c-Fos expression level in BMMs (**Figures 6E,F**), while the effects could be markedly reversed after pretreatment with SHIP1 RNAi (**Figures 6B,C,E,F**). Furthermore, after pretreatment with SHIP1 RNAi, reduced Alp activity and staining and increased osteoclast formation were observed compared with the control group, which had received no treatment with SHIP1 RNAi (**Figures 6G,H**). The results highlighted that the protective role against OVX-induced bone loss was likely to be SHIP1-dependent.

SHIP1 RNAi Administration Causes Bone Loss

After demonstrating that the protective effect of AQX-1125 against bone loss is SHIP1-dependent, we investigated whether SHIP1 RNAi administration could cause bone loss or deteriorate osteoporosis. Western blotting verified efficient knockdown of SHIP1 in femurs, following treatment with SHIP1 RNAi *via* the tail vein for 4 weeks, while AQX-1125 only partly reversed the effect of SHIP1 RNAi (**Figures 7A,B**). Furthermore, SHIP1 RNAi–treated mice displayed deteriorated trabecular bone microarchitecture in their femurs compared with the vehicle-treated group (**Figure 7C**). Morphometric analyses of trabecular parameters confirmed the decreased bone mass in BMD, BS/TV, BV/TV, and Tb.N in SHIP1 RNAi–treated mice, and the SHIP1 RNAi–induced deterioration of the trabecular microarchitecture was only partly reversed with AQX-1125 (**Figure 7D**). Together, AQX-1125, as an activator of SHIP1, is highly likely to exhibit the bone protective roles.

DISCUSSION

In this study, our data demonstrate that AQX-1125 facilitates osteogenesis and inhibits osteoclastogenesis *in vitro* through SHIP1-dependent PI3K/Akt and NF-κB signaling pathway (**Figure 8**). Moreover, AQX-1125 rescued OVX-induced osteoporosis *in vivo*, while SHIP1 RNAi administration led to bone loss. Together, these findings indicate that AQX-1125 has promising potential as a novel drug for the treatment of osteoporosis.

Studies have demonstrated that AQX-1125 can exhibit a variety of biological effects, including inhibition of bleomycin-induced pulmonary fibrosis (Cross et al., 2017), relief of allergic and pulmonary inflammation *in vivo* (Stenton et al., 2013), and improvement of moderate to severe interstitial cystitis/bladder pain syndrome (Nickel et al., 2016), but no such evidence has been shown in bones. Therefore, we first explored the ability of AQX-1125 to treat osteoporosis. Here, AQX-1125 was used in OVX-induced osteoporosis model, and the results highlighted that the compound could sharply attenuate bone loss *in vivo*.

The balance between bone regeneration and resorption is dependent on the osteoblast and osteoclast population (Jakob et al., 2015). Disruption of the balance, for example, increased osteoclastogenesis and decreased osteogenesis under certain conditions, such as the estrogen deficiency, aging, and inflammation, results in bone loss or osteoporosis (Chen et al., 2016; Seo et al., 2016; Wang et al., 2016). Inhibition of osteoclastogenesis or/and promotion of osteogenesis can counteract bone loss under these conditions. To further investigate the mechanism of increased bone mass caused by AQX-1125, we performed *in vitro* experiments. We found that AQX-1125 could facilitate osteogenesis and mineralization in a dose-dependent manner. Additionally, treatment with AQX-1125 was associated with upregulation of osteoblast-related genes, including *Alp*, *cbfa1*, *Col1a1*, and OCN. The PI3K/Akt signaling pathway plays a crucial role in bone tissue not only by facilitating proliferation and differentiation but also by suppressing apoptosis in osteoblasts (Ling et al., 2010; Guntur and Rosen, 2011). We demonstrated that the compound might activate the PI3K/Akt signaling pathway to accelerate osteoblast differentiation and mineralization by Western blot assay, which exhibited that treatment with AQX-1125 significantly increased the phosphorylation of PI3K and subsequently increased the phosphorylation of Akt in a dose-dependent manner.

Additionally, we also observed that AQX-1125 suppressed RANKL-induced osteoclast differentiation and bone resorption in a dose-dependent manner *in vitro*. Osteoclast-related genes, such as *NFATc1*, *c-Fos*, *CTSK*, and *ACP5*, were downregulated following treatment with AQX-1125. From these, NFATc1 is considered to be a central regulator of osteoclast differentiation (Takayanagi et al., 2002). Mechanistically, we found that AQX-1125 could suppress the activation of RANKL-induced NF-κB signaling by inhibiting the phosphorylation of p65 and IκBα. These results show that AQX-1125-mediated inhibition of osteoclastogenesis might be involved in the NF-κB signaling pathway.

It is well established that PI3K/Akt and NF-κB are downstream signaling molecules in this process. Hence, we hypothesized the existence of an upstream molecule that regulates the effects upon stimulation with AQX-1125. Given that the compound is a novel, clinical-stage activator of SHIP1, we identified SHIP1 as the crucial upstream molecule. Moreover, prior research has shown that SHIP1 is associated with osteogenesis and osteoclastogenesis (Peng et al., 2010; Iyer et al., 2013). In our study, treatment with AQX-1125 markedly upregulated SHIP1 protein level, followed by an increase in the Alp and Runx2 expression levels and a concurrent decrease in the NFATc1 and c-Fos expression levels. Pretreatment with SHIP1 RNAi could reverse the effects. Accordingly, increased Alp activity and staining and decreased TRAP staining were observed with the use of AQX-1125, while SHIP1 RNAi significantly weakened the effects of stimulation of AQX-1125. Furthermore, SHIP1 RNAi administration *in vivo* resulted in bone loss. Our results highlight that the AQX-1125–induced protection against bone loss was SHIP1-dependent.

CONCLUSION

Taken together, our results demonstrate that AQX-1125 promotes osteogenesis and suppresses osteoclastogenesis *in vitro* and attenuates OVX-induced bone loss *in vivo* through SHIP1-dependent PI3K/Akt and NF-κB signaling. Therefore, regulating the expression of SHIP1 with AQX-1125 could be a promising option for the treatment of osteoporosis in the future. However, our findings are based solely on the ovarectomized mouse model, with more clinical research warranted.

DATA AVAILABILITY STATEMENT

The raw data supporting the conclusion of this article will be made available by the authors, without undue reservation.

ETHICS STATEMENT

The studies involving human participants were reviewed and approved by the Ethics Committee of Tongji Medical College, Huazhong University of Science and Technology. The patients/participants provided their written informed consent to participate in this study. The animal study was reviewed and approved by the Tongji Medical College Animal Care and Use Committee, Huazhong University of Science and Technology. Written informed consent was obtained from the individual(s) for the publication of any potentially identifiable images or data included in this article.

AUTHOR CONTRIBUTIONS

XX, LH, and BM performed most of the experiments, wrote the manuscript, and analyzed the data. HX, YH, GL, and LC performed the data extraction and analysis. CY, KZ, AP, and ZL wrote and proofread the manuscript. WZ, FG, and GL designed and directed the study. All authors read and approved the final manuscript.

FUNDING

This work was supported by the National Science Foundation of China (Nos 82002313 and 82072444), the National Key Research & Development Program of China (Nos 2018YFC2001502 and 2018YFB1105705), the Hubei Province Key Laboratory of Oral and Maxillofacial Development and Regeneration (No. 2020kqhm008), and the Wuhan Union Hospital "Pharmaceutical Technology nursing" special fund (No. 2019xhyn021).

REFERENCES

Abu-Amer, Y. (2013). NF-κB Signaling and Bone Resorption. *Osteoporos. Int.* 24 (9), 2377–2386. doi:10.1007/s00198-013-2313-x

Bennett, C. N., Longo, K. A., Wright, W. S., Suva, L. J., Lane, T. F., Hankenson, K. D., et al. (2005). Regulation of Osteoblastogenesis and Bone Mass by Wnt10b. *Proc. Natl. Acad. Sci. U.S.A.* 102 (9), 3324–3329. doi:10.1073/pnas.0408742102

Brumsen, C., Hamdy, N. A., and Papapoulos, S. E. (1997). Long-Term Effects of Bisphosphonates on the Growing Skeleton: Studies of Young Patients with Severe Osteoporosis. *Medicine* 76 (4), 266–283. doi:10.1097/00005792-199707000-00005

Chen, X., Wang, C., Zhang, K., Xie, Y., Ji, X., Huang, H., et al. (2016). Reduced Femoral Bone Mass in Both Diet-Induced and Genetic Hyperlipidemia Mice. *Bone* 93, 104–112. doi:10.1016/j.bone.2016.09.016

Chen, X., Zhi, X., Pan, P., Cui, J., Cao, L., Weng, W., et al. (2017). Matrine Prevents Bone Loss in Ovariectomized Mice by Inhibiting RANKL-induced Osteoclastogenesis. *FASEB j.* 31 (11), 4855–4865. doi:10.1096/fj.201700316r

Compston, J. E., Mcclung, M. R., and Leslie, W. D. (2019). Osteoporosis. *The Lancet* 393 (10169), 364–376. doi:10.1016/s0140-6736(18)32112-3

Cross, J., Stenton, G. R., Harwig, C., Szabo, C., Genovese, T., Di Paola, R., et al. (2017). AQX-1125, Small Molecule SHIP1 Activator Inhibits Bleomycin-Induced Pulmonary Fibrosis. *Br. J. Pharmacol.* 174 (18), 3045–3057. doi:10.1111/bph.13934

Desponts, C., Ninos, J. M., and Kerr, W. G. (2006). s-SHIP Associates with Receptor Complexes Essential for Pluripotent Stem Cell Growth and Survival. *Stem Cell Dev.* 15 (5), 641–646. doi:10.1089/scd.2006.15.641

Guntur, A. R., and Rosen, C. J. (2011). The Skeleton: a Multi-Functional Complex Organ. New Insights into Osteoblasts and Their Role in Bone Formation: the central Role of PI3Kinase. *J. Endocrinol.* 211 (2), 123–130. doi:10.1530/joe-11-0175

Hazen, A. L., Smith, M. J., Desponts, C., Winter, O., Moser, K., and Kerr, W. G. (2009). SHIP Is Required for a Functional Hematopoietic Stem Cell Niche. *Blood* 113 (13), 2924–2933. doi:10.1182/blood-2008-02-138008

Iyer, S., Margulies, B. S., and Kerr, W. G. (2013). Role of SHIP1 in Bone Biology. *Ann. N.Y. Acad. Sci.* 1280, 11–14. doi:10.1111/nyas.12091

Jakob, F., Genest, F., Baron, G., Stumpf, U., Rudert, M., and Seefried, L. (2015). Regulation des Knochenstoffwechsels bei Osteoporose. *Unfallchirurg* 118 (11), 925–932. doi:10.1007/s00113-015-0085-9

Kim, J. H., and Kim, N. (2016). Signaling Pathways in Osteoclast Differentiation. *Chonnam Med. J.* 52 (1), 12–17. doi:10.4068/cmj.2016.52.1.12

Knopp-Sihota, J. A., Cummings, G. G., Homik, J., and Voaklander, D. (2013). The Association between Serious Upper Gastrointestinal Bleeding and Incident Bisphosphonate Use: a Population-Based Nested Cohort Study. *BMC Geriatr.* 13, 36. doi:10.1186/1471-2318-13-36

Krishnan, V., Bryant, H. U., and Macdougald, O. A. (2006). Regulation of Bone Mass by Wnt Signaling. *J. Clin. Invest.* 116 (5), 1202–1209. doi:10.1172/jci28551

Ling, L., Dombrowski, C., Foong, K. M., Haupt, L. M., Stein, G. S., Nurcombe, V., et al. (2010). Synergism between Wnt3a and Heparin Enhances Osteogenesis via a Phosphoinositide 3-kinase/Akt/RUNX2 Pathway. *J. Biol. Chem.* 285 (34), 26233–26244. doi:10.1074/jbc.m110.122069

Looker, A. C., Borrud, L. G., Dawson-Hughes, B., Shepherd, J. A., and Wright, N. C. (2012). Osteoporosis or Low Bone Mass at the Femur Neck or Lumbar Spine in Older Adults: United States, 2005-2008. *NCHS Data Brief* 93 (93), 1–8.

Maupin, K. A., Droscha, C. J., and Williams, B. O. (2013). A Comprehensive Overview of Skeletal Phenotypes Associated with Alterations in Wnt/β-Catenin Signaling in Humans and Mice. *Bone Res.* 1 (1), 27–71. doi:10.4248/br201301004

Nickel, J. C., Egerdie, B., Davis, E., Evans, R., Mackenzie, L., and Shrewsbury, S. B. (2016). A Phase II Study of the Efficacy and Safety of the Novel Oral SHIP1 Activator AQX-1125 in Subjects with Moderate to Severe Interstitial Cystitis/Bladder Pain Syndrome. *J. Urol.* 196 (3), 747–754. doi:10.1016/j.juro.2016.03.003

Peng, Q., Malhotra, S., Torchia, J. A., Kerr, W. G., Coggeshall, K. M., and Humphrey, M. B. (2010). TREM2- and DAP12-dependent Activation of PI3K Requires DAP10 and Is Inhibited by SHIP1. *Sci. Signal.* 3 (122), ra38. doi:10.1126/scisignal.2000500

Recker, R., Lappe, J., Davies, K. M., and Heaney, R. (2004). Bone Remodeling Increases Substantially in the Years after Menopause and Remains Increased in Older Osteoporosis Patients. *J. Bone Miner Res.* 19 (10), 1628–1633. doi:10.1359/jbmr.040710

Seo, B.-K., Ryu, H.-K., Park, Y.-C., Huh, J.-E., and Baek, Y.-H. (2016). Dual Effect of WIN-34B on Osteogenesis and Osteoclastogenesis in Cytokine-Induced Mesenchymal Stem Cells and Bone Marrow Cells. *J. Ethnopharmacol.* 193, 227–236. doi:10.1016/j.jep.2016.07.022

Stenton, G. R., Mackenzie, L. F., Tam, P., Cross, J. L., Harwig, C., Raymond, J., et al. (2013). Characterization of AQX-1125, a Small-Molecule SHIP1 Activator. *Br. J. Pharmacol.* 168 (6), 1519–1529. doi:10.1111/bph.12038

Takayanagi, H., Kim, S., Koga, T., Nishina, H., Isshiki, M., Yoshida, H., et al. (2002). Induction and Activation of the Transcription Factor NFATc1 (NFAT2) Integrate RANKL Signaling in Terminal Differentiation of Osteoclasts. *Develop. Cel* 3 (6), 889–901. doi:10.1016/s1534-5807(02)00369-6

Takeshita, S., Namba, N., Zhao, J. J., Jiang, Y., Genant, H. K., Silva, M. J., et al. (2002). SHIP-deficient Mice Are Severely Osteoporotic Due to Increased Numbers of Hyper-Resorptive Osteoclasts. *Nat. Med.* 8 (9), 943–949. doi:10.1038/nm752

Teitelbaum, S. L., and Ross, F. P. (2003). Genetic Regulation of Osteoclast Development and Function. *Nat. Rev. Genet.* 4 (8), 638–649. doi:10.1038/nrg1122

Tranquilli Leali, P., Doria, C., Zachos, A., Ruggiu, A., Milia, F., and Barca, F. (2009). Bone Fragility: Current Reviews and Clinical Features. *Clin. Cases Miner Bone Metab.* 6 (2), 109–113.

Wang, Y.-g., Han, X.-g., Yang, Y., Qiao, H., Dai, K.-r., Fan, Q.-m., et al. (2016). Functional Differences between AMPK α1 and α2 Subunits in Osteogenesis, Osteoblast-Associated Induction of Osteoclastogenesis, and Adipogenesis. *Sci. Rep.* 6, 32771. doi:10.1038/srep32771

Xie, H., Cui, Z., Wang, L., Xia, Z., Hu, Y., Xian, L., et al. (2014). PDGF-BB Secreted by Preosteoclasts Induces Angiogenesis during Coupling with Osteogenesis. *Nat. Med.* 20 (11), 1270–1278. doi:10.1038/nm.3668

Conflict of Interest: The authors declare that the research was conducted in the absence of any commercial or financial relationships that could be construed as a potential conflict of interest.

frontiers | Frontiers in Cell and Developmental Biology

ORIGINAL RESEARCH
published: 11 April 2022
doi: 10.3389/fcell.2022.820922

Hesperidin Ameliorates Dexamethasone-Induced Osteoporosis by Inhibiting p53

Meng Zhang[1,2†], Delong Chen[3†], Ning Zeng[4†], Zhendong Liu[2,5], Xiao Chen[1,2], Hefang Xiao[1,2], Likang Xiao[1,2], Zeming Liu[4], Yonghui Dong[1,2]* and Jia Zheng[1]**

[1]Department of Orthopedics, Henan Provincial People's Hospital, People's Hospital of Zhengzhou University, Henan University People's Hospital, Zhengzhou, China, [2]Microbiome Laboratory, Henan Provincial People's Hospital, People's Hospital of Zhengzhou University, Zhengzhou, China, [3]Department of Orthopaedics, Erasmus University Medical Center, Rotterdam, Netherlands, [4]Department of Plastic and Cosmetic Surgery, Tongji Hospital, Tongji Medical College, Huazhong University of Science and Technology, Wuhan, China, [5]Department of Surgery of Spine and Spinal Cord, Henan Provincial People's Hospital, People's Hospital of Zhengzhou University, Henan University People's Hospital, Zhengzhou, China

OPEN ACCESS

Edited by:
Guohui Liu,
Huazhong University of Science and Technology, China

Reviewed by:
Jun Zhou,
Brigham and Women's Hospital and Harvard Medical School, United States
Xing Li,
Guangzhou University of Chinese Medicine, China

***Correspondence:**
Zeming Liu
6myt@163.com
Yonghui Dong
dongyh@zzu.edu.cn
Jia Zheng
zhengjia90180@sina.com

[†]These authors have contributed equally to this work

Specialty section:
This article was submitted to Stem Cell Research, a section of the journal Frontiers in Cell and Developmental Biology

Received: 23 November 2021
Accepted: 16 March 2022
Published: 11 April 2022

Citation:
Zhang M, Chen D, Zeng N, Liu Z, Chen X, Xiao H, Xiao L, Liu Z, Dong Y and Zheng J (2022) Hesperidin Ameliorates Dexamethasone-Induced Osteoporosis by Inhibiting p53. Front. Cell Dev. Biol. 10:820922. doi: 10.3389/fcell.2022.820922

Osteoporosis is one of the most frequent skeletal disorders and a major cause of morbidity and mortality in the expanding aging population. Evidence suggests that hesperidin may have a therapeutic impact on osteoporosis. Nevertheless, little is known about the role of hesperidin in the development of osteoporosis. Bioinformatics analyses were carried out to explore the functions and possible molecular mechanisms by which hesperidin regulates osteogenic differentiation. In the present study, we screened and harvested 12 KEGG pathways that were shared by hesperidin-targeted genes and osteoporosis. The p53 signaling pathway was considered to be a key mechanism. Our *in vitro* results showed that hesperidin partially reversed dexamethasone-induced inhibition of osteogenic differentiation by suppressing the activation of p53, and suggest that hesperidin may be a promising candidate for the treatment against dexamethasone-induced osteoporosis.

Keywords: hesperidin, osteoporosis, bioinformatics, KEGG, p53

INTRODUCTION

Millions of individuals suffer from skeletal disorders each year, which result in severe morbidity and mortality in the elderly (Kannegaard et al., 2010; Marrinan et al., 2015). Osteoporosis is one of the most frequent skeletal disorders characterized by decreased bone mass and deteriorated bone microarchitecture, leading to skeletal fragility and increased susceptibility to fractures (Golob and Laya, 2015; Qiu et al., 2021). Globally, more than 200 million individuals are affected with osteoporosis, impairing quality of life and imposing a heavy economic burden on individuals and society (Johnell and Kanis, 2006). With the expanding aging population, osteoporotic fractures increase dramatically each year. Currently, the approaches to treat osteoporosis work primarily through inhibiting bone absorption and promoting bone formation (Langdahl, 2021). However, the side effects of anti-osteoporosis drugs pose a huge challenge to the prevention and treatment of osteoporosis in clinical practice (Cuzick, 2001; McClung et al., 2019). As a result, it is extremely important to explore new treatment strategies for osteoporosis.

Hesperidin (hesperetin-7-O-rutinoside), a flavanone glycoside highly abundant in citrus fruits, particularly in oranges, has gained considerable attention in recent years due to its diverse

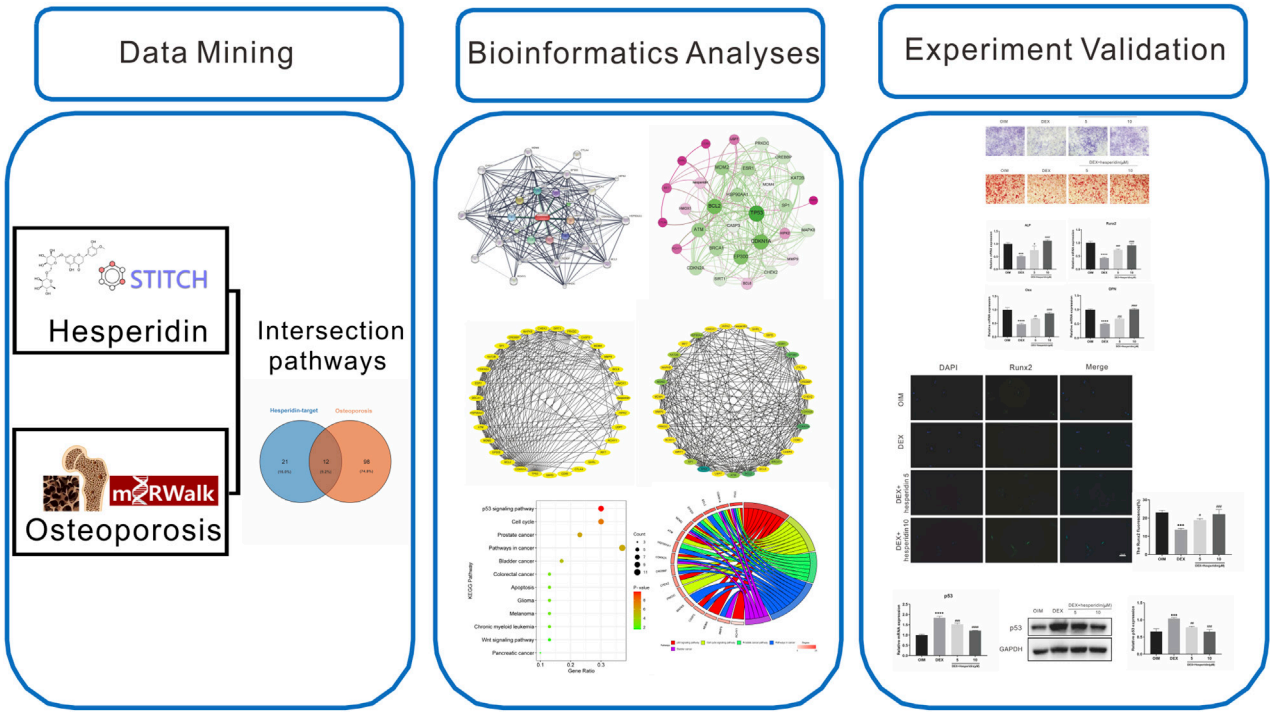

FIGURE 1 | Flowchart of the bioinformatics analyses and experimental validation in this study.

bioactivities (Gattuso et al., 2007). Hesperidin exhibits a variety of potential positive benefits, including antioxidant, anti-inflammatory, anti-atherogenic, and neuroprotective properties, therefore may serve as a promising therapeutic approach for a wide range of disorders (Li et al., 2008; Yamamoto et al., 2013; Semis et al., 2021). Accumulating evidence suggests that hesperidin plays an important role in regulating bone metabolism and bone formation, which may contribute to ameliorate or prevent the onset of osteoporosis. It has been found that hesperidin appears to regulate cell differentiation through Wnt/β-catenin signaling pathway while also influence the mineralization process by increasing the expression of osteogenic gene (ALP, OCN, Osx, and Runx2) in human alveolar osteoblasts (Hong and Zhang, 2020). In a previous study, hesperidin protected bone mass loss by alleviating oxidative stress and inflammation in an ovariectomy rat model (Zhang et al., 2021). Hesperidin could upregulate the expression of osteogenic markers and promote the maturation of bone organic matrix, thus exerting anti-osteoporosis effects *in vitro* and *in vivo* (Miguez et al., 2021). In an experimental rat model, hesperidin intake resulted in bone mass gain in young rats and protected against ovariectomy-induced bone loss in adult rats, as well as reduced oxidative stress and total lipid content (Horcajada et al., 2008). However, the molecular and cellular mechanisms underlying the osteogenic effect of hesperidin are still largely unknown.

In the present study, we identified the targets genes of hesperidin using the STITCH database, followed by the construction of protein–protein interaction (PPI) network to investigate the protein interactions. In addition, Kyoto Encyclopedia of Genes and Genomes (KEGG) enrichment analysis was carried out to identify pathways that are involved in hesperidin targeted genes and osteoporosis. According to the bioinformatics analyses results, we finally conducted *in vitro* experiments to further investigate the potential molecular mechanisms underlying hesperidin's anti-osteoporosis effects. The schematic flow chart of this work is shown in **Figure 1**.

MATERIALS AND METHODS

Regents

Hesperidin was purchased from Herbpurify (Chengdu, China) and dissolved in dimethyl sulphoxide (DMSO). Ascorbic acid phosphate, β-glycerophosphate, and dexamethasone used in this study were purchased from Sigma-Aldrich.

Cell Culture and Treatment

Bone marrow mesenchymal stem cells (BMSCs) were harvested from C57BL/6 mice and were kept in α-MEM supplemented with 10% fetal bovine serum (FBS) and 1% penicillin/streptomycin according to a previous work (Case et al., 2010). The third to sixth generations of BMSCs were used for our subsequent experiments. To induce osteogenic differentiation, the medium was changed to osteogenic induction medium (OIM) containing 20 mM β-glycerophosphate, 100 nM dexamethasone (DEX), and 50 μM ascorbic acid phosphate once the cells reached subconfluence. BMSCs were co-incubated with DEX (1 μM)

and different concentrations of hesperidin (5 and 10 μM) for 7 days or 14 days for further analysis.

Alkaline Phosphatase and Alizarin Red S Staining

BMSCs were seeded and cultured in OIM on indicated days, then washed with PBS and fixed with 4% paraformaldehyde for 15 min. After 7 days of osteogenic differentiation, alkaline phosphatase (ALP) staining was performed using a BCIP/NBT Kit (C3206, Beyotime) following the manufacturer's instructions. After 14 days of osteogenic differentiation, alizarin red S (ARS) staining was performed to evaluate the mineralized matrix formation.

Quantitative Real-Time Polymerase Chain Reaction

The BMSCs were seeded into and cultured in 6-well plates, co-incubated with DEX and different concentrations of hesperidin for 7 days. Total RNA was extracted from the cells using the NucleoZOL Reagent (Machery-Nagel GmbH, Düren, Germany). Next, 1 μg of total RNA from each sample was reverse transcribed into cDNA using the Hifair® II 1st Strand cDNA Synthesis SuperMix for qPCR (YEASON, Shanghai, China). Quantitative real-time polymerase chain reaction (qRT-PCR) was performed on an ABI Stepone plus real-time PCR system (Applied Biosystems, Foster City, CA) with Hieff® qPCR SYBR Green Master Mix (YEASON, Shanghai, China). Relative expression of each gene was analyzed using the $2^{-\Delta\Delta Ct}$ method. The primer sequences were listed in **Supplementary Table S1**.

Western Blot

The BMSCs were seeded into and cultured in 6-well plates, co-incubated with DEX and different concentrations of hesperidin for 7 days. Total cell lysates from BMSCs were extracted using RIPA lysis buffer supplemented with protease inhibitors. The protein concentrations were measured with the use of a BCA protein assay kit (Beyotime, Shanghai, China) according to the manufacturer's protocol. Equal amounts of protein from each sample were then separated by SDS-PAGE gel and subjected to standard western blot procedures. Protein bands were visualized using an ECL kit (BeyoECL Plus, Beyotime Biotechnology) and quantitatively analyzed with Image Lab 3.0 software (Bio-Rad). The antibodies against P53 and GAPDH were purchased from Proteintech (Wuhan, China).

Immunofluorescence

For immunofluorescence, BMSCs were washed and fixed with 4% paraformaldehyde at room temperature for 30 min, followed by permeabilization with 0.3% Triton X-100 for 10 min. After blocking with 3% BSA for 30 min, the cells were incubated with anti-Runx2 antibody overnight at 4°C. Subsequently, the cells were washed with PBS and incubated with corresponding secondary antibody for 1 h at room temperature, then mounted with DAPI contained fluorescent mounting solution (F6057, Sigma-Aldrich). All images were viewed and photoed with a fluorescence microscope (Olympus).

Identification of Hesperidin-Targeted Genes and Construction of Protein–Protein Interaction Network

Target genes related to hesperidin were obtained from STITCH (http://stitch.embl.de/) based on the following settings: three shells with a maximum interaction number of 10 for each shell, while the parameter organism was limited to "Homo sapiens" (Szklarczyk et al., 2016). Then, the interactive network map of hesperidin and its targeted genes was constructed, while the degree value in the protein–protein interaction (PPI) network was calculated with the help of the Cytoscape 3.7.2 software. Furthermore, Gephi software was used to establish and visualize a weighted network between hesperidin and targeted genes.

Identification of Shared KEGG Pathways Involved Both in Osteoporosis and Hesperidin-Targeted Genes

Hesperidin-targeted genes were imported into DAVID database (https://david.ncifcrf.gov/) (Huang et al., 2007), and the KEGG pathway enrichment analysis was carried out to explore the most significantly enriched pathways with a p-value of ≤0.05. The miRWalk2.0 database was used to identify KEGG pathways associated with human osteoporosis (Dweep and Gretz, 2015). Subsequently, the overlapping KEGG pathways between osteoporosis and hesperidin-targeted genes were displayed by using Venn diagram webtool (http://bioinformatics.psb.ugent.be/webtools/Venn/).

Identification of Hub Genes and KEGG Pathways Related to Hesperidin-Targeted Genes

The top five shared KEGG pathways ranked by the smallest p values calculated in the KEGG pathway analysis were screened out, followed by graphically visualizing the enrichment information using the bioinformatics platform (http://www.bioinformatics.com.cn/). Hub genes were defined as those genes included in each of the top five shared KEGG pathways.

Data Analysis

The data was displayed as mean ± standard deviation (SD) and statistically analyzed with GraphPad Prism 8.0 (GraphPad). Statistically differences between two groups were evaluated by Student's t-test, while comparisons among multiple groups were estimated by one-way analyses of variance (ANOVA). A p-value of less than 0.05 indicated statistical significance.

RESULTS

Bioinformatics Analyses of Hesperidin-Targeted Genes

Based on a three shell limit screening criteria, a total of 30 hesperidin-targeted genes were obtained from online

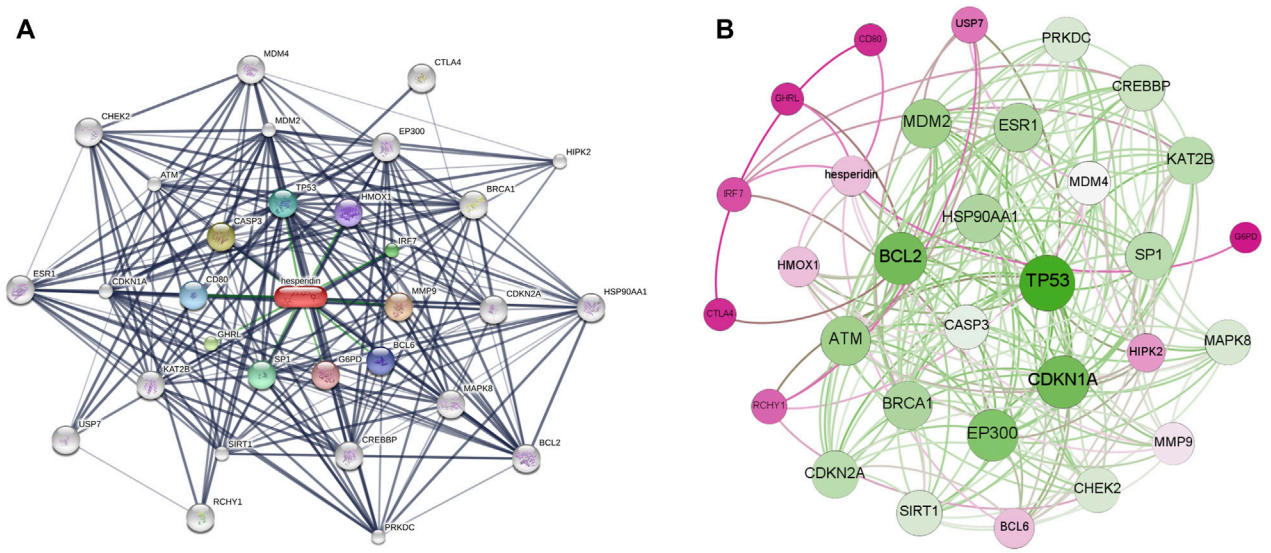

FIGURE 2 | The interaction networks of hesperidin-targeted genes **(A)** Interaction network constructed by Cytoscape **(B)** Weighted interaction network constructed by Gephi.

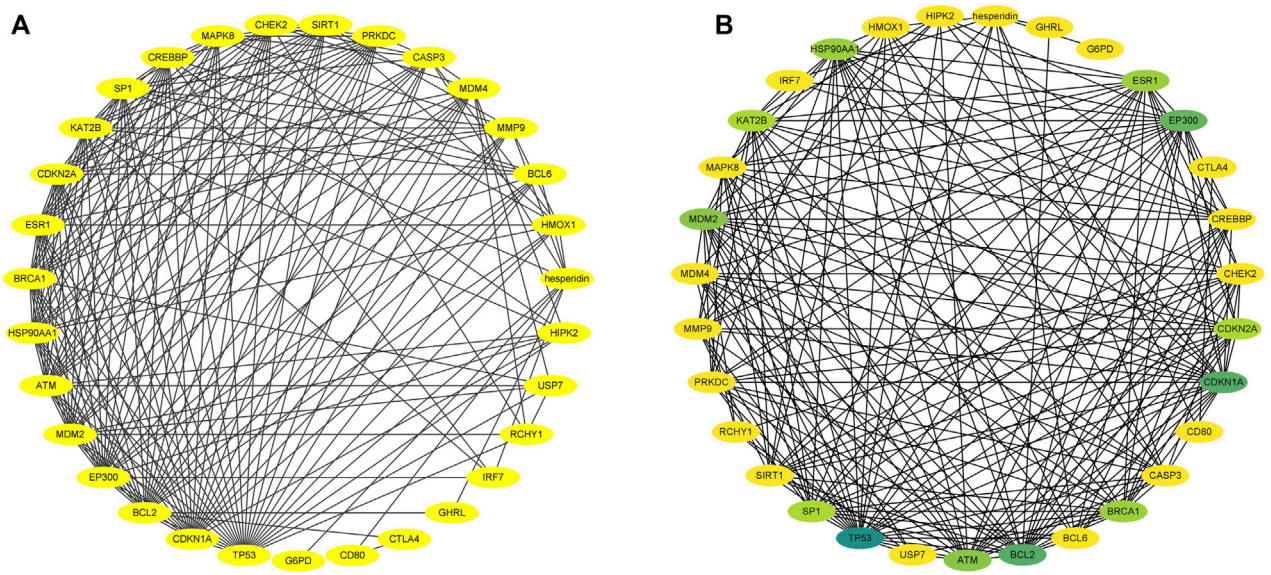

FIGURE 3 | PPI network of hesperidin-targeted genes **(A)** PPI network of hesperidin-targeted genes was constructed by Cytoscape **(B)** PPI network of hesperidin-targeted genes was shown according to degree connectivity. The top ten hesperidin-targeted genes ranked by degree connectivity were displayed as green color.

database STITCH. Subsequently, a network map of the interactions between hesperidin and the targeted genes was constructed the STITCH online tool (**Figure 2A**). Members in the first shell (chemical-protein), including NOS3, PPARG, PTGS2, SIRT1, SIRT3, TP53, AKT1, PTGS1, ESR1 and SIRT5, were considered to be closely related to hesperidin. The second shell (protein-protein) were composed of ATM, BRCA1, EP300, FOXO1, RICTOR, KAT2B, FOXO3, MTOR, CDKN1A, and MDM2, whereas HSP90AA1, CDKN2A, HIPK2, SRC, RCHY1, NCOA3, MAPK8, CREBBP, USP7, and SP1 were found in the third shell (protein-protein and chemical). To facilitate exploration and comprehension of the complicated connections between targeted genes, a visual network based on interaction weights was established (**Figure 2B**). Further analysis revealed that TP53 was the most highly weighted gene, making it a significant part of the network.

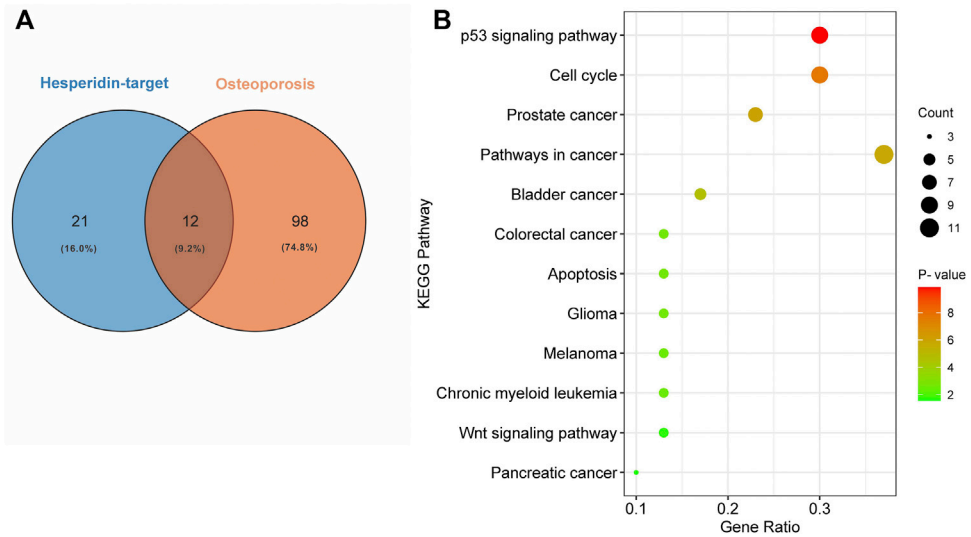

FIGURE 4 | Enrichment analysis of KEGG pathways **(A)** Common shared KEGG pathways between hesperidin-targeted genes and osteoporosis was showed by Venn diagram **(B)** Enrichment information of hesperidin-related KEGG pathways involved in 12 KEGG pathways.

TABLE 1 | Top five KEGG pathways and related genes.

Term	KEGG Pathway	Hesperidin-Targeted Genes	*p*-Value
hsa04115	p53 signaling pathway	CDKN1A, CDKN2A, TP53, MDM2, RCHY1, ATM	1.40E-10
hsa04110	Cell cycle signaling pathway	CDKN1A, CDKN2A, EP300, CREBBP, TP53, MDM2, ATM	2.04E-08
hsa05215	Prostate cancer pathway	AKT1, CDKN1A, HSP90AA1, EP300, CREBBP, TP53, FOXO1, MDM2, MTOR	1.11E-06
hsa05200	Pathways in cancer	FOXO1, AKT1, CDKN1A, EP300, CDKN2A, MDM2, MAPK8, MTOR	1.71E-06
hsa05219	Bladder cancer	CDKN1A, CDKN2A, MDM2, TP53, MMP9	2.01E-05

PPI Network of Hesperidin-Targeted Genes

A visualized PPI network of hesperidin-targeted genes was constructed by using Cytoscape (**Figure 3A**). Subsequently, the hesperidin-targeted genes were ranked according to degree values (**Figure 3B**). Due to the fact that CDKN2A, KAT2B and SP1 had the same degree value, the top 10 genes were TP53, CDKN1A, BCL2, EP300, MDM2, ATM, ESR1, HSP90AA1, BRCA1, CDKN2A, KAT2B, and SP1.

Enrichment Analysis of KEGG Pathways and Identification of Shared KEGG Pathways Between Hesperidin-Targeted Genes and Osteoporosis

We used DAVID to perform KEGG pathway enrichment analysis. 39 hesperidin-related KEGG pathways were obtained, and 33 KEGG pathways with p-value < 0.05 were finally selected. Additionally, 110 KEGG pathways associated with osteoporosis were identified using the miRwalk database. With the help of a Venn Diagram, we were able to identify 12 KEGG pathways that were shared by hesperidin-targeted genes and osteoporosis (**Figure 4A**). The enrichment information of hesperidin-related KEGG pathways involved in 12 KEGG pathways was shown in **Figure 4B**. As shown in **Table 1**, the top five shared KEGG pathways were prostate cancer signaling pathway, pathways in cancer, glioma signaling pathway, p53 signaling pathway, and cell cycle signaling pathway.

Identification of Hesperidin-Targeted Hub Genes

Among the 30 hesperidin-targeted genes, TP53, CDKN1A, BCL2, EP300, MDM2, ATM, HSP90AA1, CDKN2A, CREBBP, CHEK2, PRKDC, MAPK8, CASP3, MDM4, MMP9, and RCHY1 were involved in the top five shared KEGG pathways. The enrichment analysis results of these genes were shown in **Figure 5**. Importantly, TP53, CDKN1A, and MDM2 were involved in all top five KEGG pathways and were considered as hub genes.

Hesperidin Partially Reverses Dexamethasone-Induced Inhibition of Osteogenic Differentiation

ALP staining and ARS staining results showed that dexamethasone exposure significantly inhibited the osteogenic differentiation of

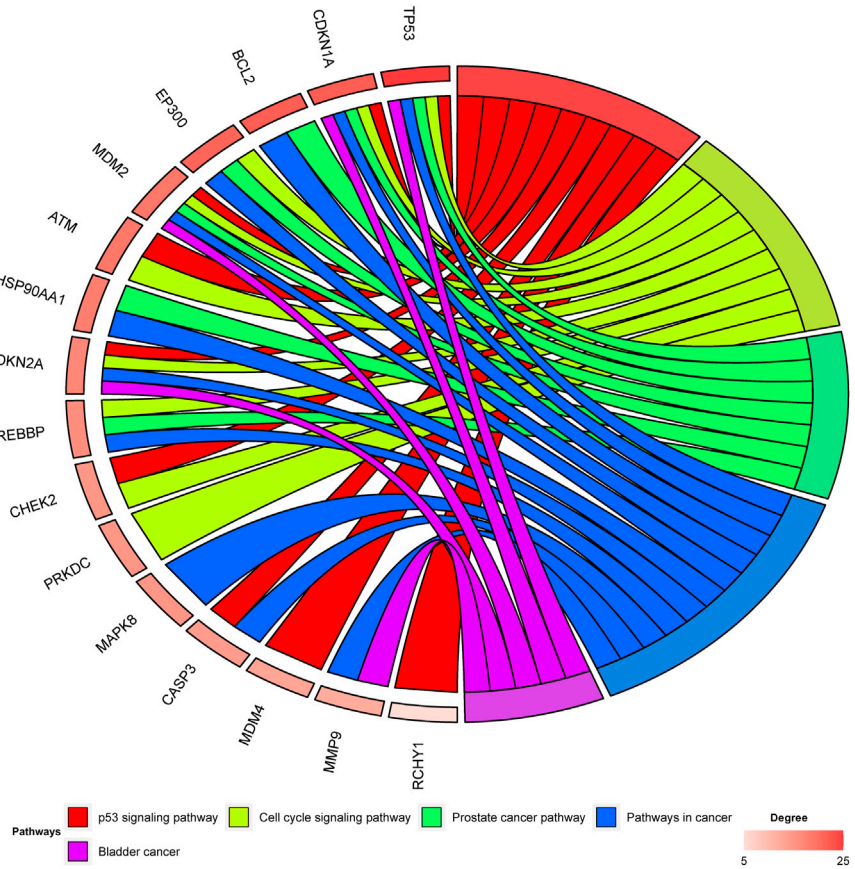

FIGURE 5 | Enrichment analysis of hesperidin-targeted genes. TP53, CDKN1A, and MDM2 were involved in all five shared KEGG pathways. The top three genes by degree were TP53, CDKN1A, and BCL2.

BMSCs, whereas hesperidin partially promoted nodule formation against dexamethasone treatment (**Figure 5A** and **Figure 6B**). Furthermore, qRT-PCR analysis results showed that the dexamethasone treatment dramatically downregulated the mRNA levels of osteogenic genes such as ALP, Runx2, Osx, and OPN in BMSCs, but further incubation with hesperidin partially reversed the inhibitory effect of dexamethasone (**Figure 6C**).

Hesperidin Partially Reverses Dexamethasone-Induced Osteoporosis by Inhibiting p53 Expression

Immunofluorescence staining results demonstrated that dexamethasone dramatically inhibited the protein levels of Runx2 during the osteogenic differentiation of BMSCs, while higher levels of Runx2 protein expression were observed after hesperidin treatment (**Figure 7A**). Besides, treated with dexamethasone significantly increased the mRNA level of p53 compared with OIM group, but hesperidin partially inhibited the p53 activation in the dexamethasone group in a dose-dependent manner (**Figure 7B**). Similar results were also observed regarding the protein expression of p53 detected by Western blot (**Figure 7C**). Thus, it can be assumed that downregulation of p53 expression alleviated dexamethasone-induced osteogenic reduction.

DISCUSSION

Osteoporosis is a chronic metabolic bone disorder associated with aging, resulting in functional disability and a decrease in quality of life. As the population ages, a rising number of people currently suffer from osteoporosis substantially. Up to date, there is still no effective treatment for osteoporosis. Furthermore, the mechanisms responsible for osteoporosis remain largely unknown. In the present study, the molecular mechanisms behind hesperidin's anti-osteoporosis benefits were explored using bioinformatics analyses and *in vitro* studies.

Hesperidin, a flavanone glycoside with a wide range of biological activities, is widely used in the treatment of various diseases. In recent years, emerging studies highlight the importance of hesperidin in the regulation and bone metabolism. Hesperidin has been shown to protect male

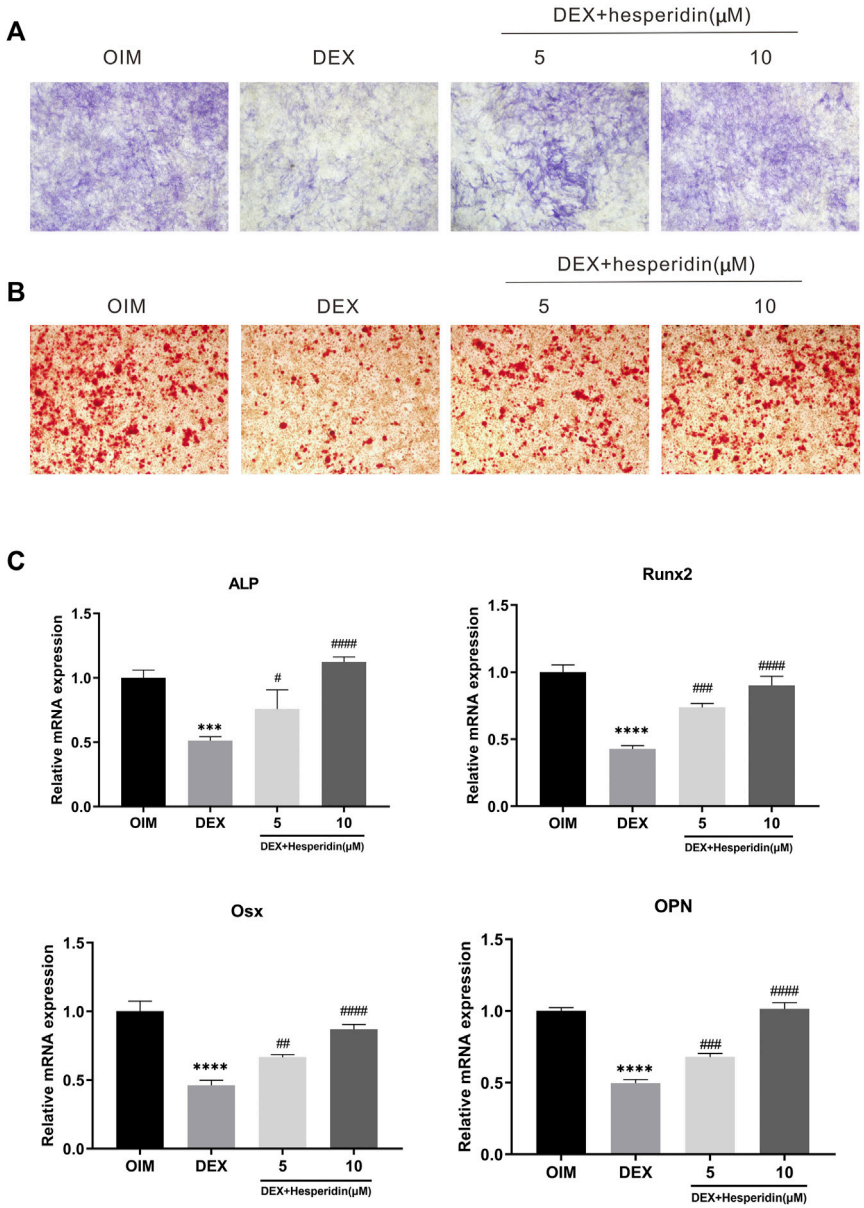

FIGURE 6 | The effect of hesperidin on DEX-induced osteogenic differentiation of BMSCs **(A)** ALP staining was conducted on day 7 **(B)** ARS staining was conducted on day 14 **(C)** The mRNA expression of ALP, Runx2, Osx and OPN were detected by qRT-PCR on day 7. $^{***}p < 0.001$, $^{****}p < 0.0001$ vs OIM; $^{\#}p < 0.05$, $^{\#\#}p < 0.01$, $^{\#\#\#}p < 0.001$, $^{\#\#\#\#}p < 0.0001$ vs DEX.

mice against androgen deficiency-induced bone loss by inhibiting bone resorption and hyperlipidemia (Chiba et al., 2014). It has been reported that hesperidin alleviated diabetic osteoporosis via reducing the expression level of TNF-α and NF-κB in rat bone and increasing the expression of OPN and OCN in serum (Shehata et al., 2017). In addition, calcium supplementation along with hesperidin was effective to improve bone health in postmenopausal women (Martin et al., 2016). However, the exact mechanisms through which hesperidin exerts its anti-osteoporosis effects are still needed to be explored.

In this study, 110 KEGG pathways associated with osteoporosis and 33 KEGG pathways associated with hesperidin-targeted genes were screened out by KEGG pathway enrichment analysis. A total of 13 KEGG pathways were commonly shared by these two groups. Among them, the top five KEGG pathways with the smallest *p*-values were the p53 signaling pathway, Cell cycle signaling pathway, Prostate cancer pathway, Pathways in cancer, and Bladder cancer. The hub genes involved in all five KEGG pathways were TP53, CDKN1A, and MDM2. These findings suggested that hesperidin may exert its biological activity by regulating the p53 signaling pathway.

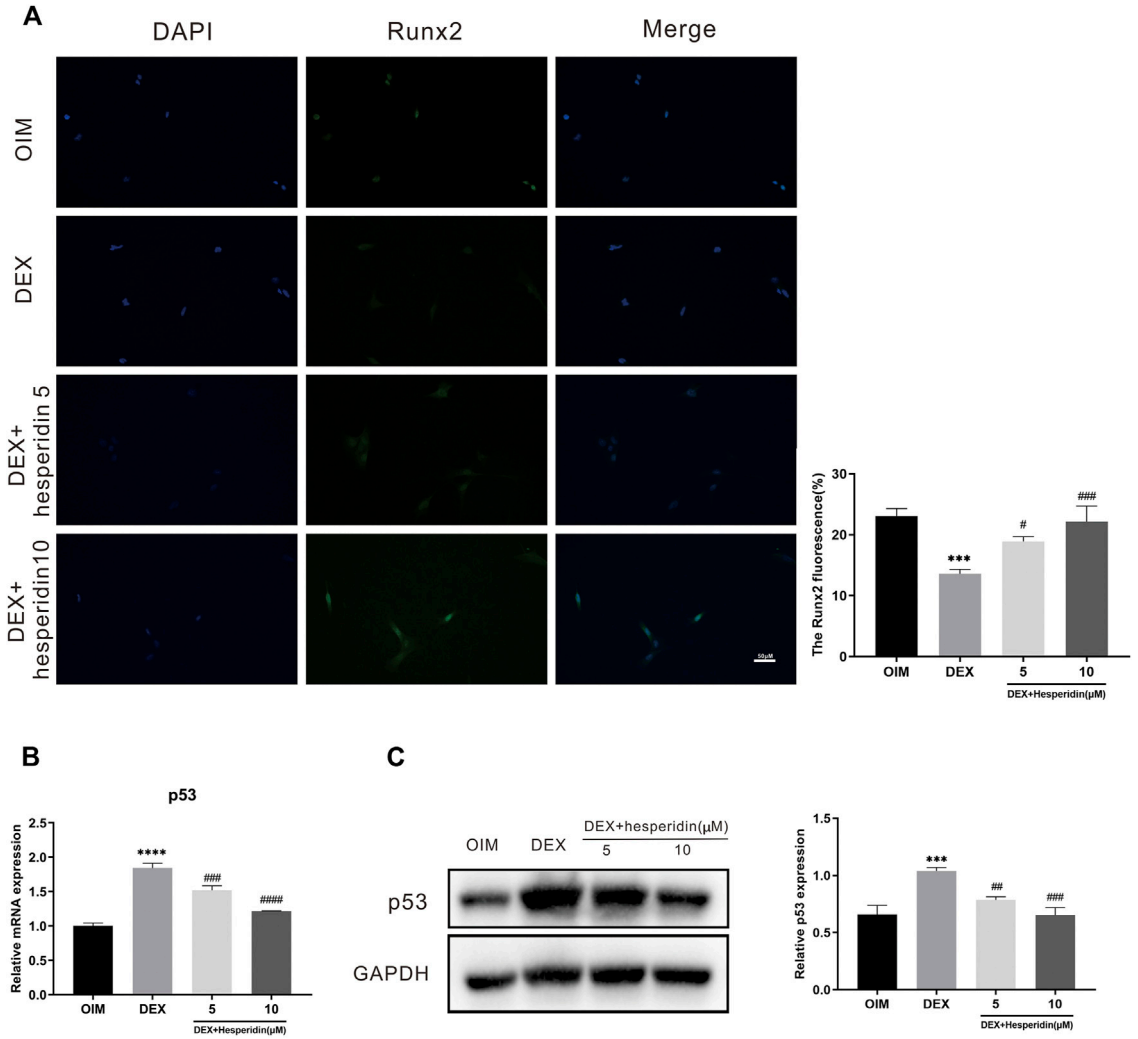

FIGURE 7 | Involvement of the p53 signaling pathway in the regulation of hesperidin **(A)** The typical image of immunofluorescence staining of Runx2. Scale bars = 50 μm **(B)** The relative expression of p53 in the different groups. $^{***}p < 0.001$, $^{****}p < 0.0001$ vs OIM; $^{\#}p < 0.05$, $^{\#\#}p < 0.01$, $^{\#\#\#}p < 0.001$, $^{\#\#\#\#}p < 0.0001$ vs DEX **(C)** The level of p53 was detected by western blot.

Glucocorticoids, most commonly dexamethasone, have been widely used to treat a variety of diseases due to their significant anti-inflammatory, immunosuppressive, and metabolic regulator effects (Schacke et al., 2002; Giles et al., 2018). It has been well accepted that there is a strong correlation between long-term glucocorticoids therapy and the development of osteoporosis (Ding et al., 2015; Liu et al., 2018). Growing evidence from *in vitro* and *in vivo* studies shows that glucocorticoids can inhibit osteoblast proliferation and promote its apoptosis, subsequently resulting in the suppression of bone production and growth (Wang Y. et al., 2020; Wang L. et al., 2020).

Consistent with previous findings, the results of the present study suggest that dexamethasone treatment significantly inhibited the osteogenic differentiation of BMSCs following ALP Staining and ARS Staining, as well as downregulated the expression of osteogenic genes such as ALP and Runx2, implying that dexamethasone inhibited osteogenic differentiation of BMSCs *in vitro*. Notably, hesperidin treatment partially alleviated the dexamethasone-induced suppression of osteogenic differentiation, showing the positive effect of hesperidin on dexamethasone-induced bone deterioration.

The p53 tumor suppressor has long been recognized as critical in cancer prevention (Vogelstein et al., 2000; Qin et al., 2018). In recent years, increasing attention has been paid to the role of p53 in skeletal disorders. Several studies conducted *in vitro* have demonstrated that p53 plays a negative role in the differentiation of MSCs(Molchadsky et al., 2010). It was observed that the expression of p53 was increased in patients with osteoporosis, and upregulation of p53 was associated with a decrease bone mass (Yu et al., 2020). Emerging evidence suggests that glucocorticoids can lead to upregulation of p53, causing

activation of the p53 signaling pathway (Li et al., 2012; Zhen et al., 2014). Therefore, we investigated whether hesperidin could exert its anti-osteoporosis effects via the p53 signaling pathway. In this study, p53 was identified as the hub gene with the highest degree value in the PPI network. qRT-PCR and western blot analysis confirmed that the expression of p53 was upregulated in BMSCs during osteogenic differentiation after dexamethasone's treatment. The results indicated that dexamethasone treatment activated the p53 signaling pathway, leading to inhibition of osteogenic differentiation *in vitro*. However, treated with hesperidin partially inhibited both the mRNA and protein level of p53. Thus, when combined with our findings, this evidence suggests that hesperidin may protect against dexamethasone-induced osteoporosis by inhibiting the p53 signaling pathway.

Some concerns and limitations in this study should be acknowledged. Firstly, we did not perform quantitative analysis of the ALP and ARS staining results. Second, the effects of hesperidin on osteogenic differentiation were not investigated while activating or inhibiting the p53 signaling pathway. Furthermore, no *in vivo* evidence was presented regarding the beneficial effects of hesperidin on osteoporosis.

CONCLUSION

In summary, our study determined that dexamethasone activated the p53 signaling pathway in BMSCs, causing downregulation of osteogenic markers and suppression of extracellular matrix mineralization during osteogenic differentiation, while hesperidin exerted anti-osteoporosis effects by inhibiting the p53 signaling pathway. Collectively, our study demonstrated that hesperidin could be a potential candidate for the treatment against dexamethasone-induced osteoporosis.

DATA AVAILABILITY STATEMENT

The original contributions presented in the study are included in the article/**Supplementary Material**, further inquiries can be directed to the corresponding authors.

ETHICS STATEMENT

The animal study was reviewed and approved by Henan Provincial People's Hospital Medical Ethics Committee.

AUTHOR CONTRIBUTIONS

MZ conceived and designed the study. JZ, YD, and ZL supervised the study. MZ and DC prepared the manuscript. MZ, NZ and ZD performed the bioinformatics analyses and *in vitro* experiments. MZ, XF, XQ, NZ, and LX analyzed the data and prepared all the figures. All authors approved the final manuscript.

FUNDING

This study was supported by the Joint Construction Project of Henan Provincial Health Committee and Ministry of Health (LHGJ20210035).

SUPPLEMENTARY MATERIAL

The Supplementary Material for this article can be found online at: https://www.frontiersin.org/articles/10.3389/fcell.2022.820922/full#supplementary-material

REFERENCES

Case, N., Xie, Z., Sen, B., Styner, M., Zou, M., O'Conor, C., et al. (2010). Mechanical Activation of β-catenin Regulates Phenotype in Adult Murine Marrow-Derived Mesenchymal Stem Cells. *J. Orthop. Res.* 28 (11), 1531–1538. doi:10.1002/jor.21156

Chiba, H., Kim, H., Matsumoto, A., Akiyama, S., Ishimi, Y., Suzuki, K., et al. (2014). Hesperidin Prevents Androgen Deficiency-Induced Bone Loss in Male Mice. *Phytother. Res.* 28 (2), 289–295. doi:10.1002/ptr.5001

Cuzick, J. (2001). Is Hormone Replacement Therapy Safe for Breast Cancer Patients? *JNCI J. Natl. Cancer Inst.* 93 (10), 733. doi:10.1093/jnci/93.10.733

Ding, H., Wang, T., Xu, D., Cha, B., Liu, J., and Li, Y. (2015). Dexamethasone-induced Apoptosis of Osteocytic and Osteoblastic Cells Is Mediated by TAK1 Activation. *Biochem. Biophysical Res. Commun.* 460 (2), 157–163. doi:10.1016/j.bbrc.2015.02.161

Dweep, H., and Gretz, N. (2015). miRWalk2.0: a Comprehensive Atlas of microRNA-Target Interactions. *Nat. Methods* 12 (8), 697. doi:10.1038/nmeth.3485

Gattuso, G., Barreca, D., Gargiulli, C., Leuzzi, U., and Caristi, C. (2007). Flavonoid Composition of Citrus Juices. *Molecules* 12 (8), 1641–1673. doi:10.3390/12081641

Giles, A. J., Hutchinson, M.-K. N. D., Sonnemann, H. M., Jung, J., Fecci, P. E., Ratnam, N. M., et al. (2018). Dexamethasone-induced Immunosuppression: Mechanisms and Implications for Immunotherapy. *J. Immunotherapy Cancer* 6 (1), 51. doi:10.1186/s40425-018-0371-5

Golob, A. L., and Laya, M. B. (2015). Osteoporosis. *Med. Clin. North America* 99 (3), 587–606. doi:10.1016/j.mcna.2015.01.010

Hong, W., and Zhang, W. (2020). Hesperidin Promotes Differentiation of Alveolar Osteoblasts via Wnt/β-Catenin Signaling Pathway. *J. Receptors Signal Transduction* 40 (5), 442–448. doi:10.1080/10799893.2020.1752718

Horcajada, M. N., Habauzit, V., Trzeciakiewicz, A., Morand, C., Gil-Izquierdo, A., Mardon, J., et al. (20081985). Hesperidin Inhibits Ovariectomized-Induced Osteopenia and Shows Differential Effects on Bone Mass and Strength in Young and Adult Intact Rats. *J. Appl. Physiol.* 104 (3), 648–654. doi:10.1152/japplphysiol.00441.2007

Huang, D. W., Sherman, B. T., Tan, Q., Kir, J., Liu, D., Bryant, D., et al. (2007). DAVID Bioinformatics Resources: Expanded Annotation Database and Novel Algorithms to Better Extract Biology from Large Gene Lists. *Nucleic Acids Res.* 35, W169–W175. Web Server issue. doi:10.1093/nar/gkm415

Johnell, O., and Kanis, J. A. (2006). An Estimate of the Worldwide Prevalence and Disability Associated with Osteoporotic Fractures. *Osteoporos. Int.* 17 (12), 1726–1733. doi:10.1007/s00198-006-0172-4

Kannegaard, P. N., van der Mark, S., Eiken, P., and Abrahamsen, B. (2010). Excess Mortality in Men Compared with Women Following a Hip Fracture. National Analysis of Comedications, Comorbidity and Survival. *Age and Ageing* 39 (2), 203–209. doi:10.1093/ageing/afp221

Langdahl, B. L. (2021). Overview of Treatment Approaches to Osteoporosis. *Br. J. Pharmacol.* 178 (9), 1891–1906. doi:10.1111/bph.15024

Li, H., Qian, W., Weng, X., Wu, Z., Li, H., Zhuang, Q., et al. (2012). Glucocorticoid Receptor and Sequential P53 Activation by Dexamethasone Mediates

Apoptosis and Cell Cycle Arrest of Osteoblastic MC3T3-E1 Cells. *PLoS One* 7 (6), e37030. doi:10.1371/journal.pone.0037030

Li, R., Li, J., Cai, L., Hu, C. M., and Zhang, L. (2008). Suppression of Adjuvant Arthritis by Hesperidin in Rats and its Mechanisms. *J. Pharm. Pharmacol.* 60 (2), 221–228. doi:10.1211/jpp.60.2.0011

Liu, S., Yang, L., Mu, S., and Fu, Q. (2018). Epigallocatechin-3-Gallate Ameliorates Glucocorticoid-Induced Osteoporosis of Rats *In Vivo* and *In Vitro*. *Front. Pharmacol.* 9, 447. doi:10.3389/fphar.2018.00447

Marrinan, S., Pearce, M. S., Jiang, X. Y., Waters, S., and Shanshal, Y. (2015). Admission for Osteoporotic Pelvic Fractures and Predictors of Length of Hospital Stay, Mortality and Loss of independence. *Age Ageing* 44 (2), 258–261. doi:10.1093/ageing/afu123

Martin, B. R., McCabe, G. P., McCabe, L., Jackson, G. S., Horcajada, M. N., Offord-Cavin, E., et al. (2016). Effect of Hesperidin with and without a Calcium (Calcilock) Supplement on Bone Health in Postmenopausal Women. *J. Clin. Endocrinol. Metab.* 101 (3), 923–927. doi:10.1210/jc.2015-3767

McClung, M. R., O'Donoghue, M. L., Papapoulos, S. E., Bone, H., Langdahl, B., Saag, K. G., et al. (2019). Odanacatib for the Treatment of Postmenopausal Osteoporosis: Results of the LOFT Multicentre, Randomised, Double-Blind, Placebo-Controlled Trial and LOFT Extension Study. *Lancet Diabetes Endocrinol.* 7 (12), 899–911. doi:10.1016/S2213-8587(19)30346-8

Miguez, P. A., Tuin, S. A., Robinson, A. G., Belcher, J., Jongwattanapisan, P., Perley, K., et al. (2021). Hesperidin Promotes Osteogenesis and Modulates Collagen Matrix Organization and Mineralization *In Vitro* and *In Vivo*. *Ijms* 22 (6), 3223. doi:10.3390/ijms22063223

Molchadsky, A., Rivlin, N., Brosh, R., Rotter, V., and Sarig, R. (2010). p53 Is Balancing Development, Differentiation and De-differentiation to Assure Cancer Prevention. *Carcinogenesis* 31 (9), 1501–1508. doi:10.1093/carcin/bgq101

Qin, J.-J., Li, X., Hunt, C., Wang, W., Wang, H., and Zhang, R. (2018). Natural Products Targeting the P53-MDM2 Pathway and Mutant P53: Recent Advances and Implications in Cancer Medicine. *Genes Dis.* 5 (3), 204–219. doi:10.1016/j.gendis.2018.07.002

Qiu, Y., Zhao, Y., Long, Z., Song, A., Huang, P., Wang, K., et al. (2021). Liquiritigenin Promotes Osteogenic Differentiation and Prevents Bone Loss via Inducing Auto-Lysosomal Degradation and Inhibiting Apoptosis. *Genes Dis.* doi:10.1016/j.gendis.2021.06.008

Schacke, H., Docke, W. D., and Asadullah, K. (2002). Mechanisms Involved in the Side Effects of Glucocorticoids. *Pharmacol. Ther.* 96 (1), 23–43. doi:10.1016/s0163-7258(02)00297-8

Semis, H. S., Kandemir, F. M., Kaynar, O., Dogan, T., and Arikan, S. M. (2021). The Protective Effects of Hesperidin against Paclitaxel-Induced Peripheral Neuropathy in Rats. *Life Sci.* 287, 120104. doi:10.1016/j.lfs.2021.120104

Shehata, A. S., Amer, M. G., Abd El-Haleem, M. R., and Karam, R. A. (2017). The Ability of Hesperidin Compared to that of Insulin for Preventing Osteoporosis Induced by Type I Diabetes in Young Male Albino Rats: A Histological and Biochemical Study. *Exp. Toxicologic Pathol.* 69 (4), 203–212. doi:10.1016/j.etp.2017.01.008

Szklarczyk, D., Santos, A., von Mering, C., Jensen, L. J., Bork, P., and Kuhn, M. (2016). STITCH 5: Augmenting Protein-Chemical Interaction Networks with Tissue and Affinity Data. *Nucleic Acids Res.* 44 (D1), D380–D384. doi:10.1093/nar/gkv1277

Vogelstein, B., Lane, D., and Levine, A. J. (2000). Surfing the P53 Network. *Nature* 408 (6810), 307–310. doi:10.1038/35042675

Wang, L., Li, Q., Yan, H., Jiao, G., Wang, H., Chi, H., et al. (2020b). Resveratrol Protects Osteoblasts against Dexamethasone-Induced Cytotoxicity through Activation of AMP-Activated Protein Kinase. *Dddt* Vol. 14, 4451–4463. doi:10.2147/dddt.s266502

Wang, Y., Chen, J., Chen, J., Dong, C., Yan, X., Zhu, Z., et al. (2020a). Daphnetin Ameliorates Glucocorticoid-Induced Osteoporosis via Activation of Wnt/GSK-3β/β-Catenin Signaling. *Toxicol. Appl. Pharmacol.* 409, 115333. doi:10.1016/j.taap.2020.115333

Yamamoto, M., Jokura, H., Hashizume, K., Ominami, H., Shibuya, Y., Suzuki, A., et al. (2013). Hesperidin Metabolite Hesperetin-7-O-Glucuronide, but Not Hesperetin-3'-O-Glucuronide, Exerts Hypotensive, Vasodilatory, and Anti-inflammatory Activities. *Food Funct.* 4 (9), 1346–1351. doi:10.1039/c3fo60030k

Yu, T., Wu, Q., You, X., Zhou, H., Xu, S., He, W., et al. (2020). Tomatidine Alleviates Osteoporosis by Downregulation of P53. *Med. Sci. Monit.* 26, e923996. doi:10.12659/MSM.923996

Zhang, Q., Song, X., Chen, X., Jiang, R., Peng, K., Tang, X., et al. (2021). Antiosteoporotic Effect of Hesperidin against Ovariectomy-induced Osteoporosis in Rats via Reduction of Oxidative Stress and Inflammation. *J. Biochem. Mol. Toxicol.* 35 (8), e22832. doi:10.1002/jbt.22832

Zhen, Y.-f., Wang, G.-d., Zhu, L.-q., Tan, S.-p., Zhang, F.-y., Zhou, X.-z., et al. (2014). P53 Dependent Mitochondrial Permeability Transition Pore Opening Is Required for Dexamethasone-Induced Death of Osteoblasts. *J. Cel. Physiol* 229 (10), 1475–1483. doi:10.1002/jcp.24589

Conflict of Interest: The authors declare that the research was conducted in the absence of any commercial or financial relationships that could be construed as a potential conflict of interest.

Publisher's Note: All claims expressed in this article are solely those of the authors and do not necessarily represent those of their affiliated organizations, or those of the publisher, the editors and the reviewers. Any product that may be evaluated in this article, or claim that may be made by its manufacturer, is not guaranteed or endorsed by the publisher.

Advantages of publishing in Frontiers

OPEN ACCESS
Articles are free to read for greatest visibility and readership

FAST PUBLICATION
Around 90 days from submission to decision

HIGH QUALITY PEER-REVIEW
Rigorous, collaborative, and constructive peer-review

TRANSPARENT PEER-REVIEW
Editors and reviewers acknowledged by name on published articles

Frontiers
Avenue du Tribunal-Fédéral 34
1005 Lausanne | Switzerland

Visit us: www.frontiersin.org
Contact us: frontiersin.org/about/contact

REPRODUCIBILITY OF RESEARCH
Support open data and methods to enhance research reproducibility

DIGITAL PUBLISHING
Articles designed for optimal readership across devices

FOLLOW US
@frontiersin

IMPACT METRICS
Advanced article metrics track visibility across digital media

EXTENSIVE PROMOTION
Marketing and promotion of impactful research

LOOP RESEARCH NETWORK
Our network increases your article's readership